



Technische Universität München

TUM School of Engineering and Design

Assessment of Vehicle-to-X concepts based on investigations of stationary and mobile battery storage applications

Benedikt Josef Schroeder, M.Sc.

Vollständiger Abdruck der von der TUM School of Engineering and Design der Technischen Universität München zur Erlangung eines

Doktors der Ingenieurwissenschaften (Dr.-Ing.)

genehmigten Dissertation.

Vorsitz: Prof. Dr. Reinaldo Tonkoski Junior
Prüfende der Dissertation: 1. Prof. Dr.-Ing. Andreas Jossen
2. Prof. Dr. rer. nat. Holger Hesse
3. Associate Professor Mattia Marinelli Ph.D.

Die Dissertation wurde am 09.01.2024 bei der Technischen Universität München eingereicht und durch die TUM School of Engineering and Design am 30.05.2024 angenommen.

Abstract

Driven by the energy transition and the increasing decentralized generation of renewable, electrical energy, storage capacities are needed to balance the volatile generation and variable demand. Stationary battery storage systems offer one way of providing the necessary flexibility. Electric vehicles offer a further opportunity for flexibility. Electric cars, electric buses or electric boats are purchased for the primary purpose of mobility of people and goods, but are not used during part of the time. If they are idle and connected to the electricity grid, the potential of the vehicles can be used for Vehicle-to-X use cases, for example Vehicle-to-Grid or Vehicle-to-Home. Vehicle-to-X concepts are developed and investigated in this thesis. For this purpose, battery storage systems in stationary applications are first identified, simulated and representative battery load profiles in these applications are determined. The drive-related usage patterns of the means of transport are then investigated using simulation and field data. The usage profiles of mobile batteries are also compared with those of stationary batteries. In addition, a method of gradually anonymizing electrical load profiles is developed to enable the anonymization and subsequent open-access use of otherwise non-shareable data. A Python-based tool is developed for this purpose and made available for usage in the community. Based on real commercial driving data, power capability profiles are also developed that indicate the power electric vehicles could provide for Vehicle-to-X at any given time. With the help of these profiles, an aggregator concept is developed that optimizes electric vehicle pools for various electricity markets in terms of pool revenues. These vehicle pools are then evaluated with regard to battery size and economic sector. Finally, Vehicle-to-X is simulated with a simulation tool for the various vehicle types and electricity markets and the effects on the vehicle batteries are examined. Overall, this work shows the financial and temporal potential of using various means of electric transportation for Vehicle-to-X services during idle times.

Kurzfassung

Getrieben durch die Energiewende und die zunehmende dezentrale Erzeugung erneuerbarer, elektrischer Energie, werden Speicherkapazitäten benötigt, um die volatile Erzeugung und die variable Nachfrage auszugleichen. Stationäre Batteriespeicher bieten hier eine Möglichkeit, die notwendige Flexibilität bereitzustellen. Elektrofahrzeuge bieten eine weitere Möglichkeit der Flexibilität. Elektroautos, Elektrobusse oder Elektroboote werden für die Mobilität von Personen und Gütern angeschafft, werden jedoch einen Teil der Zeit nicht genutzt. Sind diese geparkt und an das Stromnetz angeschlossen, kann das Potential der Fahrzeuge für Vehicle-to-X, beispielsweise Vehicle-to-Grid oder Vehicle-to-Home genutzt werden. In dieser Arbeit werden Vehicle-to-X-Konzepte entwickelt und untersucht. Dazu werden zunächst typische stationäre Batteriespeicheranwendungen identifiziert, simuliert und repräsentative Batteriebelastungsprofile in diesen Anwendungen ermittelt. Anschließend wird das Fahrverhalten von Transportmitteln anhand von Simulations- und Felddaten untersucht. Dabei wird auch die Belastung der mobilen Batterien mit stationär eingesetzten Batterien verglichen. Darüber hinaus wird eine Methode entwickelt, elektrische Lastprofile graduell zu anonymisieren, um die Anonymisierung und anschließende open-access Nutzung von ansonsten nicht teilbaren Daten zu ermöglichen. Dazu wird ein Python-basiertes Tool entwickelt, das öffentlich verfügbar ist. Auf Basis realer gewerblicher Fahrdaten werden außerdem Leistungs-Potential-Profile entwickelt, die angeben, welche Leistung Elektrofahrzeuge zu welcher Zeit für Vehicle-to-X bereitstellen könnten. Mithilfe dieser Profile wird ein Aggregatorkonzept entwickelt, das Elektrofahrzeugpools für verschiedene Elektrizitätsmärkte hinsichtlich Einnahmen optimiert zusammenstellt. Anschließend werden diese Fahrzeugpools bezüglich Batteriegröße und ökonomischem Sektor ausgewertet. Zuletzt wird die Vehicle-to-X-Nutzung mit einem Simulationstool für die verschiedenen Fahrzeugtypen und Elektrizitätsmärkte simuliert und die Auswirkungen auf die Fahrzeugbatterien untersucht. Insgesamt zeigt diese Arbeit das finanzielle und zeitliche Potential, verschiedene elektrische Transportmittel während Standzeiten für Vehicle-to-X-Services zu nutzen.

Contents

Abstract	c
Kurzfassung	e
List of Publications	III
Abbreviations	V
1 Introduction	1
1.1 Motivation and scope of this work	1
1.2 Thesis outline	3
2 Fundamentals of battery storage systems and Vehicle-to-X	7
2.1 Lithium-ion battery basics and relevant parameters	7
2.2 Battery Storage in stationary applications	9
2.2.1 Self-consumption increase	11
2.2.2 Peak shaving	13
2.2.3 Frequency containment reserve	14
2.2.4 Spot market trading	15
2.2.5 Further stationary applications and multi-use	16
2.3 Battery storage in mobile applications	17
2.3.1 Electric Cars	17
2.3.2 Electric Buses	19
2.3.3 Electric Boats	19
2.3.4 Further transportation means	19
2.4 Usage profiles	20
2.4.1 Basics and forms of profiles	20
2.4.2 Profile analysis, clustering and anonymization	22
2.5 Vehicle-to-X (V2X)	23
2.5.1 Forms of V2X	24
2.5.2 V2X opportunities and barriers	25
2.5.3 Aggregator role and pool composition	27
2.5.4 Economic potential in balancing markets	27
2.5.5 From research to industry	29
2.5.6 V2X with further means of electric transportation	30
3 Battery applications and load profile anonymization	31
3.1 Investigation of stationary battery storage systems in various applications	31
3.2 Investigation of mobile battery storage systems in various applications	53
3.3 Feature-conserving gradual anonymization of electrical load profiles	73

4	Vehicle-to-Grid provision with electric vehicle pools	97
4.1	Provision of frequency containment reserve using pools of electric vehicles	97
4.2	Optimal pool composition of electric vehicles in various vehicle-to-grid applications . . .	121
4.3	Analysis of optimally composed pools regarding battery sizes and economic sectors . . .	142
5	Vehicle-to-X provision in various applications using three modes of e-transportation	153
6	Conclusion and Outlook	167
6.1	Conclusion	167
6.2	Potential future research	169
	References	171
	Supervised Student Theses	193
	Acknowledgment	195

List of Publications

Peer-reviewed journal paper contributions (lead author)

- a Kucevic, D.¹; Tepe, B.¹; Englberger, S.; Parlikar, A.; Mühlbauer, M.; Bohlen, O.; Jossen, A.; Hesse, H.: *Standard battery energy storage system profiles: Analysis of various applications for stationary energy storage systems using a holistic simulation framework*, in: *Journal of Energy Storage* 28, p.101077, doi: [10.1016/j.est.2019.101077](https://doi.org/10.1016/j.est.2019.101077), 2020 [1]
- b Tepe, B.; Figgenger, J.; Englberger, S.; Sauer, D.; Jossen, A.; Hesse, H.: *Optimal pool composition of commercial electric vehicles in V2G fleet operation of various electricity markets*, in: *Applied Energy* 308 p.118351, doi: [10.1016/j.apenergy.2021.118351](https://doi.org/10.1016/j.apenergy.2021.118351), 2022 [2]
- c Tepe, B.; Haberschusz, D.; Figgenger, J.; Hesse, H.; Sauer, D.; Jossen, A.: *Feature-conserving gradual anonymization of load profiles and the impact on battery storage systems*, in: *Applied Energy* 343, p. 121191, doi: [10.1016/j.apenergy.2023.121191](https://doi.org/10.1016/j.apenergy.2023.121191), 2023 [3]
- d Tepe, B.; Jablonski, S.; Hesse, H.; Jossen, A.: *Lithium-ion battery utilization in various modes of e-transportation*, in: *eTransportation* 18, p. 100274, doi: [10.1016/j.etrans.2023.100274](https://doi.org/10.1016/j.etrans.2023.100274), 2023 [4]

Peer-reviewed conference paper contributions (lead author)

- a Tepe, B.; Jablonski, S.; Parlikar, A.; Hesse, H.; Jossen, A.: *Vehicle-to-X Service Provision for Various Modes of e-Transportation With Consideration of the Influence on Lithium-Ion Battery Utilization*, in: *15th International Conference on Applied Energy, Qatar*, accepted, 2023 [5]

Self-written sections of lead author journal/conference paper contributions are partially contained in this doctoral thesis without further reference in the text.

Non-peer reviewed paper contributions (lead author)

- a Tepe, B.; Collath, N.; Hesse, H.; Rosenthal, M.; Windelen, U: *Stationäre Batteriespeicher in Deutschland: Aktuelle Entwicklungen und Trends in 2021*, in: *Energiewirtschaftliche Tagesfragen* 71, 3, p.23-27, 2021 [6]
- b Tepe, B.; Figgenger, J.; Englberger, S.; Sauer, D.; Jossen, A.; Hesse, H.: *Analysis of optimally composed EV pools for the aggregated provision of frequency containment reserve and energy arbitrage trading*, in: *5th E-Mobility Power System Integration Symposium (EMOB 2021)*, p.175-180, doi: [10.1049/icp.2021.2521](https://doi.org/10.1049/icp.2021.2521), 2021 [7]

Peer-reviewed journal paper contributions (co-author)

- a Kucevic, D.; Englberger, S.; Sharma, A.; Trivedi, A.; Tepe, B.; Schachler, B.; Hesse, H.; Srinivasan, D., Jossen, A.: *Reducing grid peak load through the coordinated control of battery energy storage systems located at electric vehicle charging parks*, in: *Applied Energy* 295, p. 116936, doi: [10.1016/j.apenergy.2021.116936](https://doi.org/10.1016/j.apenergy.2021.116936), 2021 [8]

¹ These authors contributed equally to this work.

- b Englberger, S.; Abo Gamra, K.; Tepe, B.; Schreiber, M.; Jossen, A.; Hesse, H.: *Electric vehicle multi-use: Optimizing multiple value streams using mobile storage systems in a vehicle-to-grid context*, in: *Applied Energy* 304, p. 117862, doi: [10.1016/j.apenergy.2021.117862](https://doi.org/10.1016/j.apenergy.2021.117862), 2021 [9]
- c Möller, M.; Kucevic, D.; Collath, N.; Parlikar, A.; Dotzauer, P.; Tepe, B.; Englberger, S.; Jossen, A.; Hesse, H.: *SimSES: A holistic simulation framework for modeling and analyzing stationary energy storage systems*, in: *Journal of Energy Storage* 49, p. 103743, doi: [10.1016/j.est.2021.103743](https://doi.org/10.1016/j.est.2021.103743), 2022 [10]
- d Figgenger, J.; Tepe, B.; Rücker, F.; Schöneberger, I.; Hecht, Christopher; Jossen, A.; Sauer, D.: *The Influence of Frequency Containment Reserve Flexibilization on the Economics of Electric Vehicle Fleet Operation*, in: *Journal of Energy Storage* 53, p. 105138, doi: [10.1016/j.est.2022.105138](https://doi.org/10.1016/j.est.2022.105138), 2022 [11]
- e Collath, N.; Tepe, B.; Englberger, S.; Jossen, A.; Hesse, H.: *Aging aware operation of lithium-ion battery energy storage systems: A review*, in: *Journal of Energy Storage* 55, p. 105634, doi: [10.1016/j.est.2022.105634](https://doi.org/10.1016/j.est.2022.105634), 2022 [12]
- f Luque, J.; Tepe, B.; Larios, D.; León, C.; Hesse, H.: *Machine Learning Estimation of Battery Efficiency and Related Key Performance Indicators in Smart Energy Systems*, in: *Energies* 2023, 16(14), p. 5548, doi: [10.3390/en16145548](https://doi.org/10.3390/en16145548), 2023 [13]
- g Moyassari, E.; Zheng, L.; Tepe, B.; Streck, L.; Jossen, A.: *Cycle Characterization of SiO-based Lithium-Ion-Batteries using Real Load Profiles*, in: *Journal of The Electrochemical Society* 170(10), p. 100510, doi: [10.1149/1945-7111/acf9e](https://doi.org/10.1149/1945-7111/acf9e), 2023 [14]
- h Parlikar, A.; Tepe, B.; Möller, M.; Hesse, H.; Jossen, A.: *Quantifying the carbon footprint of energy storage applications with a python-based energy system simulation framework - Energy System Network*, submitted to: *Energy Conversion and Management*, under review, 2023

Peer-reviewed conference contributions (co-author)

- a Jablonski, S.; Tepe, B.; Zhao, Y.; Jossen, A.: *Analysis and Characterization of the Energy Consumption in an Electric Bus Fleet*, in: *NEIS Conference, Hamburg*, 2023 [15]

Selection of conference contributions

- a Tepe, B.; Kucevic, D.; Dotzauer, P.; Hesse, H.; Jossen, A.: *Modeling framework for Simulating Energy Storage Systems in Grid Applications*, in: *Jahrestreffen Forschungsnetzwerk Energiesystemanalyse*, Aachen, Poster, 2019
- b Tepe, B.; Kucevic, D.; Englberger, S.; Hesse, H.; Jossen, A.: *Development of Reference Storage Profiles for Electrical Grid Applications*, in: *NEIS Conference on Sustainable Energy Supply and Energy Storage Systems*, Hamburg, Poster, 2019
- c Tepe, B.; Müller, F.; Hesse, H.; Jossen, A.: *Possibilities for Efficiency Improvements of Large Scale Storage Systems using Field Data*, in: *IRES 2021*, Online Conference, Poster, 2021
- d Tepe, B.; Hesse, H.; Jossen, A.: *EV fleet operation with V2G: Potential and optimization in different markets*, in: *Advanced Battery Power 2022*, Münster, Presentation, 2022
- e Tepe, B.; Jablonski, S.; Hesse, H.; Jossen, A.: *Battery usage in electric transportation means and influence of the charging strategy*, in: *Advanced Battery Power 2023*, Aachen, Poster, 2023
- f Tepe, B.; Hesse, H.; Jossen, A.: *Evaluation of the V2G Potential of Electric Cars, Electric Buses and Electric Boats* in: *The Smarter E - Power2Drive Conference*, München, Presentation, 2023

Abbreviations

Please note that the list below is based on the main part of this thesis and does not fully cover the abbreviations used in the papers. Each paper itself includes an individual list.

AC	alternating current
aFRR	frequency restoration reserve with automatic activation
BSS	battery storage system
BTM	behind-the-meter
C-rate	charging rate
DC	direct current
DFT	discrete fourier transformation
DoC	depth-of-cycle
DoD	depth-of-discharge
DSO	distribution system operator
e-Boat	electric boat
e-Bus	electric bus
e-Car	electric car
e-Truck	electric truck
EES	Chair of Electrical Energy Storage Technology
EFC	equivalent full cycle
ESS	energy storage system
EU	European Union
EV	electric vehicle
FCR	frequency containment reserve
FEC	full-equivalent cycle
FTM	front-of-the-meter
HSS	home storage system
LFP	lithium iron phosphate
LIB	lithium-ion battery
LTO	lithium titanate oxide
mFRR	frequency restoration reserve with manual activation

NiCd	nickel-cadmium battery
NiMH	nickel-metal hydride battery
NMC	nickel manganese cobalt oxide
PS	peak shaving
PV	photovoltaic
ROI	return on investment
SCI	self-consumption increase
SCR	self-consumption rate
SEI	solid electrolyte interphase
SimSES	simulation of stationary energy storage systems
SoC	state-of-charge
SoE	state-of-energy
SoH	state-of-health
SSR	self-sufficiency rate
SUV	sports utility vehicle
TSO	transmission system operator
TUM	Technical University of Munich
V2B	Vehicle-to-Building
V2G	Vehicle-to-Grid
V2H	Vehicle-to-Home
V2L	Vehicle-to-Load
V2V	Vehicle-to-Vehicle
V2X	Vehicle-to-X
WLTP	worldwide harmonized light vehicles test procedure

1 Introduction

1.1 Motivation and scope of this work

In order to achieve the European Union (EU) climate targets, a decarbonization of society is necessary [16]. This includes various areas such as energy supply and transport sector. In the area of energy supply, not only improved energy efficiency, but also the increased usage of renewable energy systems are seen as suitable measures [16, 17]. As of 2023, the EU target is to achieve a 45% share of renewable energies in the energy mix by 2030 [18]. This target corresponds to a doubling of the renewable share in nine years, as it was 21.8 % in 2021 [19]. At increased shares of renewable energy systems, flexibility in the electricity grid is also required to compensate for fluctuations in generation [20]. Stationary energy storage systems (ESSs) provide one way to supply this flexibility [20]. At times of excessive power generation, ESSs can charge energy, and at times of insufficient generation, they can discharge. Another area to be decarbonized is the transport sector. The road transport sector, for example, was responsible for 740 million tonnes of carbon dioxide emissions in the EU in 2021 [21]. To reduce emissions from cars, the EU requires new cars to have zero carbon dioxide emissions from 2035 [22]. Here, electrically powered vehicles are seen as a possibility for decarbonization [20]. When charged with renewable energy, they produce fewer greenhouse gas emissions over their entire service life than comparable vehicles with internal combustion engines [23].

Alongside the increased interest in decarbonization in recent years, the lithium-ion battery (LIB), which was introduced in the 1990s, has been further enhanced [24]. Compared to other battery technologies such as lead-acid batteries or nickel-metal hydride batteries, LIBs offer advantages in several categories. For example, they have a relatively high gravimetric and volumetric energy density combined with a high lifetime [25]. In addition, a variety of usable material combinations exist for the cathode and anode of LIBs [24, 25]. Due to economy of scale effects in recent years, LIBs are now also cost competitive compared to other battery technologies in various applications [25, 26].

Along with consumer electronics applications such as smartphones and laptops, LIBs are increasingly being deployed in stationary battery storage systems (BSSs), which are a subgroup of ESSs [26, 27]. When installed together with wind farms or photovoltaic (PV) parks, BSSs can provide the necessary flexibility for temporal fluctuations of generated electricity [28, 29]. In addition, there are other applications for stationary BSSs: Small-scale BSSs of up to 30 kWh are installed in combination with household PV systems to increase the self-consumption rate and the self-sufficiency [27, 30, 31]. Companies install medium sized industrial BSSs of 30 to 1000 kWh also for solar self-consumption increase or to cover the peaks in their electrical load profile, which is called peak shaving [27, 32, 33]. Furthermore, large-scale BSSs of up to 3 GWh provide balancing power to compensate for fluctuations between power generation and power consumption [34–36] or support renewable energy integration [27].

The main driver for the further development of LIBs in recent years has been the rise of electromobility [24, 37, 38]. In political and social terms, interest in electric vehicles (EVs) increased. Accordingly, the number of electric cars (e-Cars) sold worldwide grew from one million in 2017 to ten million in

2022 [38]. In Europe every fifth car sold in 2022 was an e-Car [38]. In Germany, the federal government's goal is to reach 15 million e-Cars on German roads by 2030 [39]. But it is not only the number of e-Cars that has increased in recent years. Other electrically powered vehicles, such as electric buses (e-Buses) and electric boats (e-Boats), are also gaining relevance [40–42]. From 2020 to 2021, sales of e-Buses increased by 40% worldwide, although the global bus market remained constant [40]. In addition, the global market for e-Boats is expected to double in volume from 2022 to 2028 [42].

The increasing number of EVs entails large battery capacities. If Germany, for example, reaches its goal of 15 million e-Cars in 2030, those cars are estimated to have 750 GWh of total capacity assuming an average battery capacity of 50 kWh. Studies on the mobility of German households show that private cars are parked 97% of the time [43]. If these cars were connected to the electricity grid with bidirectional 11 kW chargers, 165 GW could theoretically be discharged for a short period of time assuming the grid was designed for that power. This is about twice as much as the annual load peak in Germany, which corresponded to about 81 GW in 2021 and just under 79 GW in 2022 [44]. Accordingly, e-Cars can contribute significantly to stabilizing the electricity grid in the future or take on other tasks, such as shifting the consumption of solar energy into the nighttime hours. Even unidirectional vehicles can provide flexibility for the electricity grid through controlled smart charging. However, the potential is greater if the e-Cars and other types of EVs are bidirectional in the future, i.e., they must not only be able to charge from, but also to discharge into the grid [45, 46]. Depending on how the EVs are used, this concept is called Vehicle-to-Grid (V2G), Vehicle-to-Home (V2H) or Vehicle-to-Building (V2B). These terms are summarized under the general term Vehicle-to-X (V2X) [47].

EVs are used for the mobility of people and goods and are therefore only temporarily connected to the electricity grid. Furthermore, the vehicle batteries with their mostly 30 to 100 kWh large batteries are often smaller than industrial and large scale stationary BSSs. However, minimum power and capacities of 1 MW and 1 MWh, respectively, are often required to provide balancing power [36] and minimum bid sizes also exist for spot market trading on the day-ahead and intraday market [48]. For these reasons, EVs must be pooled in virtual power plants and controlled by aggregators if they are to provide V2G [49]. Relevant questions arise for aggregators about how pools should be composed and how required power should be allocated to the EVs.

In general, the stationary and mobile applications place varying demands on the batteries. In EVs, gravimetric and volumetric energy density are relevant in order to have the smallest and lightest possible battery system. In addition, the battery system should be able to be charged at high power to enable short-term fast charging on longer journeys. In stationary applications, the above properties are less relevant compared to others [28]. Depending on the requirements of the application, LIBs can be improved in the future in terms of relevant characteristics and the system design can be adapted to meet the requirements. This demands a specification of the requirements and representative or exemplary publicly available data of the various applications.

This thesis follows up on this requirement. Stationary and mobile battery applications are examined and the load on the batteries is investigated. The respective storage load profiles are published open-source and thus available to the general public. In addition, the financial V2G potential of EVs in frequency containment reserve (FCR) and arbitrage applications is examined and a methodology is developed to optimize vehicle pool compositions according to various V2G markets. Finally, e-Cars, e-Buses and e-Boats are simulated in various V2X applications and the battery stress is quantified.

1.2 Thesis outline

This publication-based dissertation is based on seven contributions. An outline of the thesis is shown in Figure 1.1. After the introduction and motivation, chapter 2 explains the fundamentals of stationary and mobile BSSs and of V2X provision. Here, the general BSS applications are described based on the state of the art and the concept of V2X is explained. Furthermore, previous work on the topics is elaborated, research gaps are identified, and concepts and terms introduced in the context of the dissertation are explained.

Chapter 3 contains three journal publications on the topics of battery applications and load profiles [1, 3, 4]. In section 3.1, the three stationary storage applications self-consumption increase (SCI), FCR, and peak shaving (PS) are simulated [1]. The simulation of stationary energy storage systems (SimSES) tool developed at the Chair of Electrical Energy Storage Technology (EES) of the Technical University of Munich (TUM), is used for this purpose. Furthermore, a methodology is presented to extract representative storage load profiles from a set of profiles using six key characteristics. Section 3.2 then discusses the three mobile storage applications, e-Car, e-Bus, and e-Boat, and evaluates the impact of the applications on the vehicle batteries [4]. For the e-Cars, data was simulated using the python based open-source tool *emobpy* [50]. For the e-Buses and e-Boats, real field data was collected from Hamburger Hochbahn AG respectively Torqeedo. The battery-relevant parameters of the mobile applications are also determined using SimSES. This involves simulating and comparing various unidirectional charging strategies for the vehicles. The stationary and mobile application data is made available open-access in consultation with the industry partners so that industry and research can use them in their own developments and simulations. In an exchange with other industry partners on data from various applications, the research question arose as to whether electrical load profiles could be anonymized before sharing or publishing. The requirement was that the load profiles could

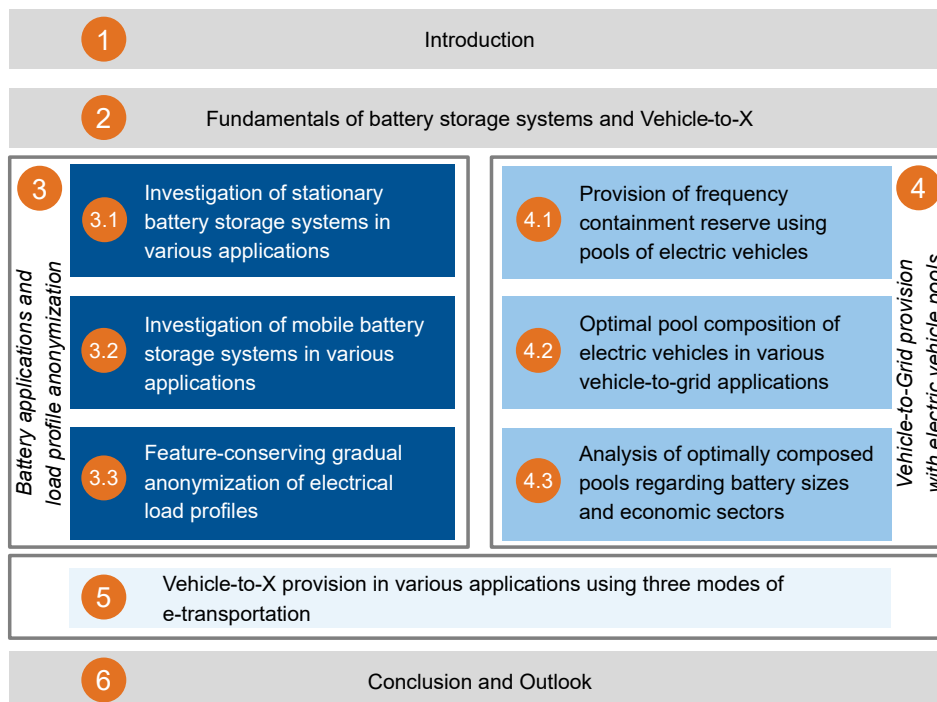


Figure 1.1: Structure of this thesis. The chapter and section numbers are shown in the orange circles.

be changed gradually, i.e. to different degrees, depending on the preferences of the owning entity of the data. Since no publicly available tool met these requirements, a python-based open-source tool was developed and published as part of this thesis. Section 3.3 presents the methodology of the gradual electrical load profile anonymization and determines the impact on BSS relevant parameters for two stationary battery applications [3].

In chapter 4, V2G provision with fleets of commercial EVs is subsequently investigated. The results were published in two journal and one conference publications that form the three sections of this chapter [2, 7, 11]. Section 4.1 includes the generation of "power and energy capability profiles" of commercial EVs and the monetary potential of the EV pool in the German FCR market [11]. For this purpose, publicly available data from commercial vehicles with internal combustion engines is used to simulate the driving of these vehicles as EVs. Afterwards, power and energy capability profiles of each EV are determined. The profiles are then aggregated and the potential for the FCR application in Germany is determined. In addition, potential changes in FCR market regulations and impacts on aggregate pool revenues are evaluated. Section 4.2 then presents the concept of the optimized profile combination using the power and energy capability profiles from section 4.1 [2]. A methodology based on genetic algorithms is presented to optimize the composition of the pool in order to maximize revenue per participating vehicle in various V2G markets. The optimized vehicle pools are then analyzed in terms of their composition in section 4.3 [7]. Here, vehicle battery sizes and economic sectors are

Table 1.1: Main research questions of the thesis and chapter numbers.

Research question	Chapter/ Section
What are typical stationary applications of BSSs and how are LIBs utilized in these applications? How can representative profiles be determined from a set of stationary BSS load profiles?	3.1
What are typical mobile applications of BSSs and how are BSSs utilized in these applications? To what extent are battery-relevant parameters in mobile applications similar to stationary applications and could therefore similar LIBs be used in those applications?	3.2
How can electrical load profiles be anonymized gradually and how could an open-source tool look like that allows anonymization? How much may an original electrical load profile be modified to maintain parameters critical to a storage application?	3.3
How much power can commercial EV fleets offer for the market of FCR over different time periods? How much money can commercial EVs expect to earn through FCR in Germany?	4.1
Can aggregators of EV pools gain a competitive advantage through smart selection of vehicles? How large are potential revenues in various electricity markets for random and for optimized pools?	4.2
Which EV battery sizes are explicitly suitable for providing balancing power or arbitrage trading in energy markets? EVs of which economic sectors are particularly attractive for the considered markets?	4.3
How predictably do e-Cars, e-Buses, and e-Boats behave and what is their temporal V2X-ready ratio over the week? How do battery-relevant parameters change due to the provision of V2X and what are the effects in terms of battery aging?	5

evaluated.

In chapter 5, the topics of chapter 3 and chapter 4 are linked in a conference publication [5]. Here, the data from the stationary and mobile applications are used to simulate various types of vehicles in SimSES. Beyond unidirectional charging strategies, V2X-based charging strategies are simulated. Subsequently, effects of V2X provision on battery-relevant parameters are quantified and battery aging is simulated.

Lastly, Chapter 6 presents a summary and outlook. The latter presents potential future research questions and connecting points to this thesis. Table 1.1 shows an overview of the research questions dealt with in the respective chapters and sections. At the beginning of each chapter, the individual topics are presented in more detail and the research questions are explained.

2 Fundamentals of battery storage systems and Vehicle-to-X

This chapter introduces the relevant topics of the dissertation. It thus lays the foundations for the following chapters, which deal with stationary and mobile applications of BSSs and the topic of V2X. Each individual paper in the following chapters also presents the individual topics in detail and provides literature reviews. First, section 2.1 explains the basics of LIBs and introduces battery parameters relevant for the thesis. Subsequently, stationary applications of BSSs are explained in section 2.2. Section 2.3 then explains mobile BSS applications and the driving behavior in these applications. Section 2.4 deals with the topic of load and usage profiles, before section 2.5 finally introduces the topic of V2X.

2.1 Lithium-ion battery basics and relevant parameters

The fact that LIBs have gained popularity in many different applications is due to a number of advantageous properties over other battery technologies [24, 25, 51]. Lead-acid batteries have been in use for over 150 years and have the lowest cost per kWh as a comparison of different battery technologies showed in 2021 [51, 52]. But LIBs outperform lead-acid batteries in terms of lifetime, power density, energy density and efficiency [51]. Other technologies such as nickel-cadmium battery (NiCd) (usable in wide temperature range) and nickel-metal hydride battery (NiMH) (high safety) have individual advantages [51], but the overall package offered by LIBs led to a focus on this technology for mobile and stationary applications [24, 25].

Basically, there is no single LIB technology. Instead, various anode and cathode materials, electrolyte compositions and additives are employed in commercial cells [24]. The two cathode materials with the largest market share are lithium nickel manganese cobalt oxide (NMC) and lithium iron phosphate (LFP), often combined with a graphite anode [24]. LIBs with NMC cathode offer high energy and power density, which is why they are often used in e-Cars [53]. LFP cathode-based LIBs have the advantage of high cycling stability and thus relatively long lifetime and high safety [24, 53]. The disadvantage is a lower energy density compared to NMC [24, 53]. On the anode side, apart from graphite, lithium titanate and silicon-graphite composites show advantages and are therefore being further researched [54, 55].

For this thesis, several parameters of LIBs are relevant. They will be explained in the following. The first parameter is the state-of-charge (SoC), which describes the currently remaining available capacity of a battery in relation to the nominal capacity. The SoC can be calculated according to equation 2.1, which is based on reference [56]. Here, $SoC(t_0)$ describes the start SoC, $I(t)$ the current at each point in time, η_c the coulombic efficiency and Q_n the nominal capacity of the battery [56]. The sign convention in this representation is that during charging the current is positive and during discharging it is negative [56]. An SoC of 0% describes a fully discharged battery and an SoC of 100% a fully

charged battery.

$$SoC(t) = SoC(t_0) + \frac{\int_{t_0}^t I(\tau) \cdot \eta_c d\tau}{Q_n} \quad (2.1)$$

The second relevant parameter is the state-of-energy (SoE). This parameter describes the currently remaining available energy of a battery in relation to the nominal energy [56]. For this purpose the power is integrated over time and divided by the nominal energy, as shown in equation 2.2, which is based on reference [56] and extended by the energy efficiency η_e [57]. Analogous to the *SoC* calculation, *SoE*(t_0) describes the start *SoE*.

$$SoE(t) = SoE(t_0) - \frac{\int_{t_0}^t P(\tau) \cdot \eta_e d\tau}{E_n} \quad (2.2)$$

Due to various aging mechanisms, a battery loses capacity over the course of its life. For this reason, the state-of-health (SoH) was introduced, which indicates the currently available capacity when fully charged relative to the initial nominal capacity [58]. The calculation of the SoH is shown in equation 2.3. Here, $Q_{discharge}(t)$ describes the capacity that can be discharged in the fully charged state at time t and at nominal discharge conditions. At the beginning of its life, a battery has an SoH of 100 %.

$$SoH(t) = \frac{Q_{discharge}(t)}{Q_n} \quad (2.3)$$

Another important parameter for charging and discharging LIBs is the depth-of-discharge (DoD). This parameter describes the depth to which a battery is discharged (see equation 2.4). For this purpose, the SoC at the end of a discharge cycle is subtracted from the SoC at the beginning of the cycle. In the laboratory, batteries are often cycled with a fixed DoD to test battery behavior [59, 60]. In the field, the DoD varies depending on the application and the energy management strategy. In addition to the expression DoD, the expressions depth-of-cycle (DoC) and ΔSOC are also used to take account of the DoC_{dis} in the discharging direction and DoC_{cha} in the charging direction [59, 61]. In chapter 3.1 of this thesis the expression DoC_{dis} is used as a synonym for the DoD.

$$DoD = SoC_{cycle,start} - SoC_{cycle,end} \quad (2.4)$$

Furthermore, the charging rate (C-rate) is a relevant parameter for LIBs. The C-rate describes the current at which a battery is charged or discharged relative to its nominal (or rated) capacity [12]. The calculation of the C-rate is shown in equation 2.5. For example, if a battery with a rated capacity of 2 Ah is charged with 1 A, the C-rate is $0.5 h^{-1}$ and the battery would be fully charged after 2 hours. Battery cell manufacturers also often specify maximum charge and discharge C-rates for their batteries.

$$C_{rate}(t) = \frac{I(t)}{Q_n} \quad (2.5)$$

The number of equivalent full cycles (EFCs) is also relevant for the degradation of batteries [62, 63]. The EFCs experienced by a LIB can be calculated by dividing the energy throughput E_{tp} by two times the rated energy of a battery, as displayed in equation 2.6. Alternatively, the energy throughput in one direction can be divided by the rated energy content. While some research works call the term EFC [9, 62, 64], others use the term full-equivalent cycle (FEC) [12, 59, 63, 65].

$$EFC = \frac{E_{tp}}{2 * E_{rated}} \quad (2.6)$$

LIBs are subject to aging processes that can be categorized into calendar and cyclic aging. The former occurs over time independently of charging and discharging processes of the battery. The latter depends on the cyclization of the battery. The aging of LIBs is apparent on the one hand by a decrease in the available capacity, which is often quantified by the SoH, and on the other hand by an increase in the internal resistance. Reduced available capacity means reduced range in e-Cars, for example. A higher internal resistance, in contrast, means that losses during charging and discharging increase and an e-Car can no longer be charged with the same high power. Critical to the aging of LIBs are stress factors that trigger chemical reactions and processes in LIBs that reduce capacity or increase internal resistance [12]. For instance, higher battery cell temperatures and SoCs typically lead to accelerated calendar aging [12]. Cyclic aging, conversely, is enhanced by higher C-rates, higher DoCs, high or low temperature, and more EFCs [12]. The aforementioned stress factors then lead to effects in the battery cell such as the growth of a solid electrolyte interphase (SEI) and lithium plating at the anode and particle cracking at the cathode [12]. These effects cause lithium inventory and anode and cathode active material to be lost, reducing capacity and increasing internal resistance [12].

The end of life of a battery is often defined as 70 % or 80 % SoH, i.e. 70 % respectively 80 % of the initial capacity [66–68]. These values are used because the available capacity, which decreases slowly at the beginning, may eventually reach a knee point and decrease rapidly [68, 69]. If this knee point is exceeded, the performance of a battery drops quickly and safety-relevant problems can occur.

Aging models have been developed to quantify the aging of LIBs in calculations and simulations. Physicochemical aging models, on the one hand, directly represent the physicochemical aging effects, such as SEI growth in differential equations. Semi-empirical aging models, on the other hand, such as those by Naumann et al. [59, 70] and Schmalstieg et al. [60], quantify the decrease of capacity and the increase in internal resistance on the basis of stress factors like SoC and DoD. In this thesis, these semi-empirical aging models are used in chapters 4.2 and 5.

2.2 Battery Storage in stationary applications

Electricity grids traditionally consisted of generators, transmission elements such as cables and transformers, and consumers. In the days when the electricity grids were built, generators were often large power plants that produced electricity for a large number of households or businesses from coal, for

example. Today, many decentralized generators exist in electricity grids, often producing electricity from renewable sources. For instance, PV systems are transforming households from consumers to so-called prosumers that consume and generate electricity. The increasing importance of renewable generators is also evident in numbers: The share of renewable-generated electricity in net electricity generation in Germany nearly doubled from 25.8% to 49.8% between 2012 and 2022 [44]. Worldwide, the share rose from 21.25% to just under 30% in the same period [71]. However, renewable generators such as wind and PV are subject to natural volatility due to variable wind conditions and day-night cycles. Here, ESSs offer the opportunity to store energy during periods of high generation and make it available again during periods of low generation.

The principle of ESSs has been used for more than two centuries. As early as 1795, a mill in New York used the tidal range to generate mechanical energy from stored water flowing downhill [72]. In the second half of the 19th century, the first pumped hydro storage power plants were built in Europe [72]. Later, other energy storage technologies were developed, such as the flywheel, which stores energy in kinetic form, and compressed air energy storage, which stores energy in the form of compressed air [73, 74]. The development and technical advances of batteries have enabled another energy storage technology: BSSs, which store energy in electrochemical form.

Various technologies exist as possible battery types for BSSs, such as lead-acid batteries or redox flow batteries [73, 74]. In the last 10 years, however, LIBs have become the most popular battery technology in BSSs [27, 75]. The development of LIBs was originally driven by mobile electronics such as camcorders and later cell phones and smartphones [24]. However, the potential of using LIBs in transportation and the associated further development led to them also being increasingly used in stationary BSSs [37, 75]. In 2012, the global share of LIBs in stationary BSSs was 30% and increased to almost 90% by 2016 [75]. Battery technologies such as lead-acid, which also had a 30% share in 2012, have largely been displaced from the market [75]. The areas of application for stationary BSSs are described subsequently.

A variety of applications exist for stationary BSSs. The applications can be divided into behind-the-meter (BTM) and front-of-the-meter (FTM). In the former, battery storage is installed behind the electricity meter. Subsequently, they can be used for intermediate storage of locally generated energy or to help balance the load profile to prevent peaks in grid energy consumption. The latter are installed in front of the electricity meter and therefore act on the side of the electricity grid. There they can stabilize the electricity grid by balancing out fluctuations between total generation and total consumption, or they can trade on the electricity market.

The open-source simulation tool SimSES developed at the TUM allows to perform time series simulations of stationary ESS in various applications [10]. The modular python-based tool enables users to evaluate ESS technologies technically and economically. Various topologies, system components and storage technologies can be simulated in a storage application. SimSES includes a variety of energy management strategies for different applications. For the SCI application, which is explained in the following section a household load profile and a PV generation profile are required as input. The energy management system then decides at each simulation step how the ESS should behave. The ESS itself consists of one or more alternating current (AC) systems, which in turn consist of one or more direct current (DC) systems connected by power electronic elements. These contain the energy storage technologies, for example LIBs. A large number of LIB models, including degradation models, can be selected in SimSES. There are also thermal and auxiliary models. Following the simulation, the ESS behavior is evaluated technically and economically. As part of this thesis, SimSES is extended to

mobile applications, bidirectional charging strategies are developed and V2X simulations are carried out.

The stationary storage applications relevant to this thesis are explained in the following. An overview of the applications with the corresponding section numbers is shown in Figure 2.1.

2.2.1 Self-consumption increase

A typical BTM application of stationary BSSs is the SCI of self-generated energy. In private households with PV systems, home storage systems (HSSs) are often used to temporarily store the energy generated during the day and use it in the evening or at night. HSSs enable households to use a larger share of their self-generated electricity and thus increase their self-consumption rate (SCR) r_{SCR} [76, 77]. The SCR describes the proportion of PV energy that is used by the household itself and not fed into the grid (see equation 2.7). In addition, HSSs reduce the amount of electricity purchased from the grid, increasing the household's self-sufficiency rate (SSR) r_{SSR} [77, 78]. This indicator shows what proportion of the load can be covered by self-generated energy, i.e. how independent a household is from the electricity grid (see equation 2.8). The storage capacity of HSSs is typically below 30 kWh and averaged 8.8 kWh in Germany in 2022 [27].

$$r_{SCR} = \frac{E_{PV}^{direct} + E_{BSS}^{charged}}{E_{PV}} \quad (2.7)$$

$$r_{SSR} = \frac{E_{PV}^{direct} + E_{BSS}^{discharged}}{E_{Load}} \quad (2.8)$$

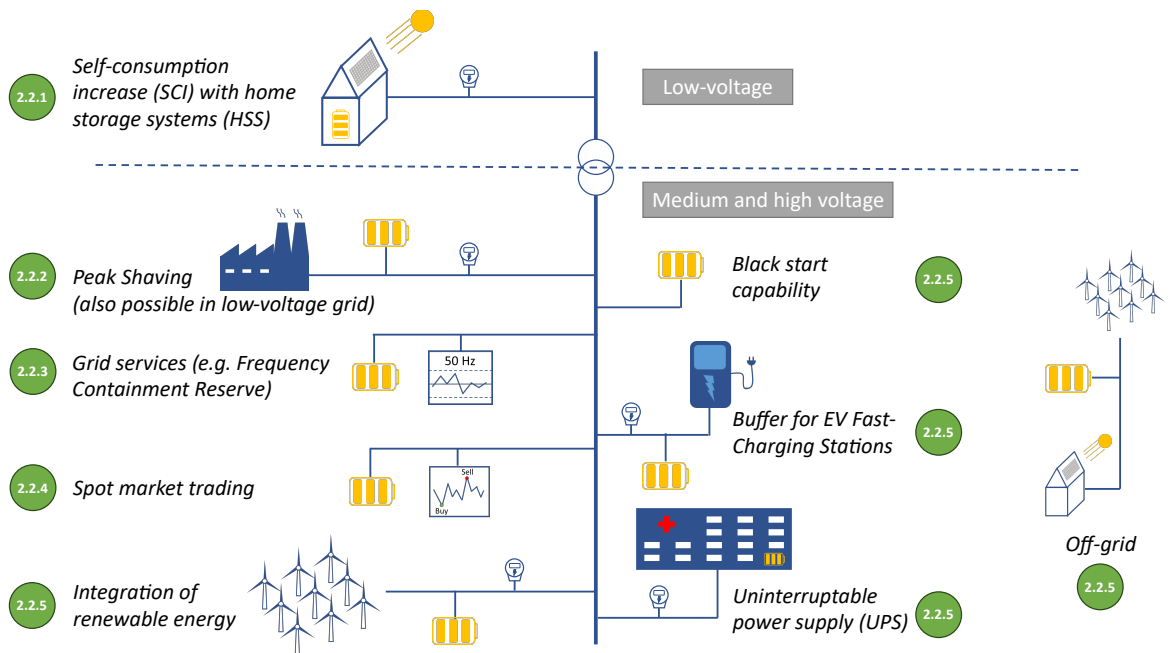


Figure 2.1: Graphical overview of stationary battery storage applications. The green circles represent the section of the thesis in which the application is addressed.

The business model of HSSs results from the fact that the feed-in tariff of PV electricity is often lower than the electricity purchase costs [79]. In Germany, as of June 2023, the 20-year fixed feed-in tariff for PV electricity from systems smaller than 10 kWp that feed in only a portion of their generated energy was 0.086 €/kWh [80], while the average electricity price was 0.4627 €/kWh [81]. This means that every kilowatt hour charged and discharged improves the economics of a HSS and reduces the electricity bill of the household. However, this only applies if the battery and power electronics efficiency is sufficiently high. Nevertheless, a survey of the HSS market in Germany showed that monetary investment was not a primary reason for purchasing the HSS in 2018 [82]. In contrast, the main reasons were a hedge against rising electricity prices and wanting to make a contribution to the energy transition [82]. Other reasons for installing HSSs are protection against power outages, as some models can provide an emergency power supply, and general interest in technology [82].

In 2016, Truong et al. identified the gap between feed-in tariff and electricity purchase costs, storage investment costs, and usable battery capacity as the three factors that most affect the economics of an HSS [79]. They showed that in 2016, with German electricity prices and feed-in tariffs at that time, the return on investment (ROI) was negative in most scenarios considered [79]. The same conclusion was reached in 2017 by Uddin et al. for a household considered in the UK [31]. They developed an aging model for the battery of a HSS in the field and used it to estimate battery aging costs. The result was that the HSS had no economic benefit. The conditions for the profitability of HSSs have improved due to the rise in electricity prices in Germany in recent years and the simultaneous fall in battery prices and feed-in tariffs. However, whether a specific HSS is profitable depends on the individual load and generation profile.

Despite the lack of profitability at the start of the ramp-up of the HSS market in Germany, the number of installed HSSs has increased strongly [27]. While only 10,000 HSSs were installed in Germany in 2014, their number was already 220,000 in 2022 [27]. This makes Germany the largest HSS market in Europe with a market share of 59 % in 2021 [83]. Furthermore the numbers in other European countries such as Italy, Austria and UK are also increasing [83]. In Europe as a whole, the HSS market grew by 107 % from 2020 to 2021 [83]. The market for HSS is also growing steadily in the US [84] and other countries worldwide [85, 86].

The operation of HSSs can be carried out according to a variety of operation strategies. Relevant for almost all operation strategies is the residual load, which results from the current energy generated by the renewable source (mostly PV) and the current load according to equation 2.9 [78, 87].

$$P_{Res}(t) = P_{Load}(t) - P_{PV}(t) \quad (2.9)$$

The simplest and most primitive charging strategy of a HSS is to charge the BSS directly as soon as the residual load is negative, i.e. PV generation exceeds the load [78, 88]. In chapter 3.1, this strategy is applied and called *greedy*. In the literature, the strategy is also called *direct charging* or *increased self-consumption* [78, 88]. If HSSs are operated with the *greedy* strategy, they often charge up to an SoC of 100 % in the morning, especially in the summer months, and then remain in this SoC for several hours. On the battery side, this long stay in the high SoC range leads to accelerated battery aging, as described in chapter 2.1. On the distribution grid side, stopping the HSS from charging at 100 % SoC can cause the PV energy fed into the grid to ramp up significantly and peak around noon [88]. For the above reasons, smarter operation strategies for HSS have been developed. First, the grid feed-in

could be limited to a fixed value and the HSS would only be charged above this value [88]. This would reduce the impact on the distribution grid, but the HSS would then only be charged insufficiently on cloudy days. The SCR would consequently decrease. Second, grid feed-in could also be dynamically limited depending on weather and load forecasts [88]. This strategy would reduce the maximum grid feed-in and at the same time not reduce the SCR or only reduce it slightly in the case of forecast errors. In chapter 3.1, this strategy is called *feed-in damping*. The strategy chooses the daily grid feed-in limit based on the last time of PV generation of the day and is based on a work by Zeh and Witzmann [89]. During the course of the day the battery charging power is then increased depending on the spare battery capacity in order to achieve an SoC of 100 % by sunset [89]. More advanced operation strategies of HSSs include multi-objective optimization [77, 90], more comprehensive prediction models for PV generation and load profile [76, 91], and machine learning approaches [92–94]. In addition to HSS, SCI applications can also take place in company buildings having a PV system installed. The strategies can be basically identical to those described above, but the BSSs are often larger dimensioned due to the higher power consumption and larger PV systems. Moreover, the economic incentives are different due to other electricity tariffs.

The SCI application is discussed in more detail in chapters 3.1 and 3.3 of this thesis. In chapter 3.1, representative storage load parameters of HSS in SCI applications are determined. In chapter 3.3, household load profiles are anonymized, which are subsequently used and evaluated for SCI simulations.

2.2.2 Peak shaving

In Germany, for example, the price of electricity for private households is calculated on the basis of the energy consumed in addition to a base price [81, 95]. The peak load of the household is not taken into account. However, this does not apply to companies whose electricity consumption exceeds 100,000 kWh per year [95]. These companies must pay grid fees for the annual load peak in addition to the energy-based price. This is because the electricity grid has to be designed and possibly expanded for this load peak. There are also special regulations for end consumers with a temporary high power consumption [95]. Electricity grid operators must offer these consumers an individual grid fee based on monthly power charges [95]. The amount of the grid fees is then based on the number of hours the electricity is consumed [95]. If, for example, an industrial customer in Germany with a consumption of over 10 GWh uses the electricity for at least 8,000 hours, the grid fee has to be at least 10 % of the regular published grid fee [95]. Due to these load-peak-dependent grid fees, PS has also emerged as a BTM application for industrial companies [27, 96]. In this application, load peaks that occur are covered by discharging the BSS instead of drawing from the grid. The PS performing BSS in the industrial customer sector often have capacities between 30 and 1000 kWh [27]. Analogous to the HSS, the number of industrial BSS in Germany has increased in recent years [27]. This also applies to industrial storage capacities worldwide [97].

The simplest operation strategy of PS is to constantly maintain 100 % SoC and discharge as soon as a load peak exceeds a defined threshold [98]. The BSS is then fully charged again as soon as the load is below the threshold without exceeding the threshold [98]. This strategy can cause the BSS to stand idle for a long time at high SoC, which is critical for the calendar aging of the batteries, as described in chapter 2.1. For this reason, more sophisticated operation strategies have been developed to predict peak loads [98, 99]. This allows the BSS to be kept at a medium SoC range and only charged to 100 % SoC when a load peak is expected. Further research on PS is focused on optimal battery capacity and power design [98, 100].

In addition to the conventional BTM application of PS where the load peak at a single grid connection point is reduced, PS can also be performed on the distribution grid side [8, 32, 33]. For instance, decentralized HSS can be used to significantly reduce the load peak at low voltage substations in residential areas [32]. Furthermore, companies can use stationary BSSs that communicate with each other to operate PS at the point of common coupling instead of locally [8, 33].

The PS application is addressed in chapters 3.1, 3.3 and 5 of this thesis. As for the SCI application, representative storage load parameters are determined for the PS application in chapter 3.1. Likewise, an anonymization of e-Car charging station load profiles is performed with subsequent evaluation of the impact on a PS application in chapter 3.3. Chapter 5 examines the PS application with bidirectional e-Cars and quantifies the impact of the V2X provision on battery-relevant parameters.

2.2.3 Frequency containment reserve

One FTM application for stationary BSS is the provision of frequency regulation [28, 75]. In principle, generation and consumption must always be balanced in an electricity grid. However, since there are forecast errors in load and (renewable) generation, storage capacity is needed to balance these fluctuations, charging when there is excessive generation and discharging when there is excessive consumption [75]. The grid frequency serves as an indicator for the mismatch between generation and consumption. In Europe, where the nominal grid frequency is 50 Hz, the transmission system operators (TSOs) are responsible for the electricity balancing [101, 102]. Accordingly, the four German TSOs invite tenders for balancing capacities on a public platform, for which pre-qualified storage entities can apply over different time periods [103].

The three product types frequency containment reserve (FCR), frequency restoration reserve with automatic activation (aFRR) and frequency restoration reserve with manual activation (mFRR) can be distinguished [104]. Storage offering FCR must be able to activate the marketed power within 30 seconds and provide it for 15 minutes [104]. aFRR offering storage systems replace FCR storage after 5 minutes [104]. After 15 minutes, mFRR offering storage systems replace aFRR storage systems [104]. As of the end of 2023, the offer time sections are four hours each [105]. This means that stationary BSSs must hold the marketed power ready over these four hours. In the FCR application, the provision is bidirectional [106]. It must therefore be possible to charge and discharge the storage system with the marketed power. In addition, only multiples of 1 MW can be offered on the FCR market [105]. In Germany, 570 MW are currently being tendered to cover the fluctuations for all four hour slots, for which pre-qualified energy storage entities can apply [103]. Possible FCR-providing ESSs are pumped hydro power plants or gas power plants. In the meantime, however, 630 MW of large-scale BSSs have also been prequalified for the provision of FCR [27, 107]. In this context, large-scale BSSs are storage systems that have more than 1000 kWh of battery capacity.

In contrast to the SCI and PS application, the operation strategy of FCR BSSs is relatively constrained by the TSOs. First, there are prequalification conditions that dictate the dimensioning of the BSS [108]. Second, the ramping up of power in case of frequency deviations is predetermined and an allowed operating range is defined [108]. However, there are also degrees of freedom in the provision of FCR with BSSs. For instance, an overfulfillment of up to 120% of the required power can take place [108]. Moreover, there is a dead band between 49.99 Hz and 50.01 Hz in which charging and discharging can take place [109]. Additionally, schedule transactions are allowed to recharge or discharge the storage system to reach the allowed SoC range [109].

Due to the cost degression of BSSs, the FCR application became the focus of not only BSS operators but also research institutions in the 2010s. In 2013, Swierczynski et al. described the operation of a stationary BSS to provide FCR in Denmark with a focus on the battery degradation [110]. Zeh et al. studied the impact of newly published TSO frameworks on BSS profitability in 2016 [36]. Moreover, Zeh et al. and Thien et al. published control algorithms that met the new regulatory framework [35, 36]. Other research studies investigated the economics [111], bidding strategies [112] and efficiencies [113] of FCR BSSs. In addition to these single-BSS considerations, Hollinger et al. published an approach for FCR provision with distributed HSSs of 10 kWh each [114].

Stationary BSSs can generate revenue by participating in the FCR market. In 2016, Zeh et al. calculated possible revenues of 130 € per kWh and year in Germany if the power had to be kept available for 15 minutes (so called 15-min criterion) [36]. Filippa et al. investigated the participation of BSSs in the FCR-N market in Eastern Denmark in 2019 [115]. This publication showed that no scenario considered was profitable, taking into account the battery ageing and the tax regime at the time, and that regulation is the determining factor. In 2018, there were already 46 large-scale BSS projects in Germany that planned to participate in the FCR market [116]. However, as German FCR prices fell in 2019, market growth in this area slowed [117]. Market growth picked up again in 2022 due to increased FCR prices [27].

In this thesis, the FCR application is covered in chapters 3.1, 4.1, 4.2, 4.3 and 5. In chapter 3.1, analogous to the SCI and PS applications, the FCR application is investigated and the representative load on the batteries is determined. The provision of FCR with pools of commercial EVs is investigated in chapter 4.1. Then, the power capability profiles defined there are used in chapter 4.2 to assemble optimized vehicle pools. These optimized pools are examined in chapter 4.3 before the impact of FCR provision with various modes of transportation on battery-relevant parameter is examined in chapter 5.

2.2.4 Spot market trading

Another FTM application is spot market trading, where electricity is traded on wholesale markets. In Central Europe, the European Power Exchange EPEX Spot SE exists for this purpose. A total of 621 TWh of electricity was traded on EPEX in 2021 [48]. The order of magnitude of the electricity traded there becomes apparent when comparing it with Germany's gross electricity generation, which was 587.1 TWh in 2021 [118]. The large amount of electricity traded is due to the fact that a kilowatt-hour can be virtually traded several times before it is executed. Electricity can essentially be traded on EPEX in two forms. One is day-ahead trading, where electricity is traded in the form of blind auctions for each hour of the following day [48]. It is also possible to trade block orders for several hours with the same price. The other form is intraday trading, where electricity can be traded in smaller time segments (intraday auction) and continuously (intraday continuous) [48]. For Germany, Austria, Belgium and the Netherlands, trading is possible up to five minutes before delivery [48]. Intraday trading is further subdivided into the two products auction and continuous trading. In addition to hourly products, half-hourly and 15-minute products can also be traded here [48].

The approach of spot market trading with BSSs is based on arbitrage trading. Electricity is purchased at times of relatively low prices and the BSS is charged. At times of high prices, the BSS is discharged again and the electricity is sold. In principle, arbitrage trading is also possible with other ESS types [119]. While the idea is simple, some points should be considered when performing arbitrage trading with BSSs: First, BSS efficiencies during charging and discharging and self-discharge of the

storage technology have to be taken into account [119]. If the losses are high, the price spread must be correspondingly higher. Second, a good prediction of the price development on the respective market is required [120]. For this purpose, optimization models and bidding strategies have been researched and published [120–122]. Third, battery degradation plays an important role in the profit of the BSS [123, 124]. If the BSS is frequently charged and discharged at a high C-rate, this leads to accelerated aging, as described in chapter 2.1 [123]. To account for degradation in the optimization models, penalty costs are often introduced into the objective function to prevent trading at small price spreads [123, 124]. Fourth, regulation affects the profitability of arbitrage trading. Higher taxes and fees on electricity purchases and sales lead to lower attractiveness of arbitrage trading in a country [125, 126]. Finally, a larger number of arbitrage trading BSSs leads to reduced attractiveness of the arbitrage trading due to increased market saturation [127]. Underestimating this effect may lead to overestimating the economic value of BSSs [128].

Spot market trading in the form of arbitrage trading is examined in more detail in chapters 4.2, 4.3 and 5 of this thesis. In chapter 4.2, a simple arbitrage algorithm with perfect foresight is used to estimate the revenues of pools of commercial e-Cars on the day-ahead and intraday market. The optimized vehicle pools determined are then evaluated in chapter 4.3 in terms of vehicle size and economic sector. In chapter 5, data from reference [124] are used to evaluate the stress of arbitrage trading with pools of e-Cars, e-Buses and e-Boats on the LIBs.

2.2.5 Further stationary applications and multi-use

In addition to the extensively presented applications for stationary BSSs, there are a number of other applications that are less relevant to this thesis. Another BTM application is to ensure **uninterruptible power supply** [73, 129]. Stationary BSSs are installed in hospitals, for example, and kept in a charged state in order to continue to meet power requirements in the event of power failures. Large scale BSSs can also be installed BTM side by side with PV or wind farms to prevent large feed-in peaks and to smooth the feed-in [130–132]. This would also prevent shutdown when there is excessive wind or solar radiation. In this way, the **integration of renewable energy** into the electricity grid would be supported. Another exemplary FTM application is BSSs providing **black start capability** to rebuild the electricity grid in case of outages [28, 133]. In addition, BSSs can be applied **off-grid** using renewable generators and BSSs, where the BSS covers the load at times of insufficient generation, similar to the SCI application [28, 134]. An application of stationary BSSs associated with the ramp-up of electromobility, is **buffer storage placed at fast charging stations** for EVs [135–137]. With the help of buffer storage, EVs can be charged simultaneously with high power. If the charging stations are subsequently no longer occupied, the buffer storage can be recharged with lower power. This means that the electricity grid does not have to be expanded, or only to a lesser extent, in order to install the fast charging stations at the location [137]. Buffer storage can be provided by flywheels, hydrogen storage or, due to their low cost and high efficiency, batteries [136].

In addition to the individual applications described, concepts have been developed to combine them in **multi-use** operations [64, 138, 139]. Multi-use can be executed sequentially, in parallel or dynamically [140, 141]. In sequential multi-use, different applications are executed one after the other [140]. For instance, a stationary BSS can provide FCR at night and be used for PS during the day. Parallel multi-use is defined by the simultaneous provision of different applications [140]. In this case, a certain fraction of the power and energy of the BSS is allocated to each application. In dynamic multi-use, the allocated fractions of power and energy vary so that more or less power and energy is allocated

to the applications depending on factors relevant to the application [140]. Research has shown that combining applications can increase the profitability of BSSs [140, 142]. However, regulatory hurdles must be overcome for implementation of multi-use [142, 143]. A special form of sequential multi-use is the combination of mobile applications and stationary applications. Batteries of e-Cars that are temporarily used for mobility can either be used in stationary applications after the mobile usage time in second-life or second-use scenarios. Alternatively, mobile applications and stationary applications can alternate by using the vehicles for stationary applications during idle times. This V2X use is introduced in section 4.1 of this thesis as "dual use".

The topic of stationary BSS applications runs throughout the whole thesis. The focus is on the applications SCI, PS, FCR and spot market trading, as these are the dominant stationary applications with already existing markets [27]. These applications will therefore be interesting for the V2X use of EVs in the future. In chapter 3.1, the questions of what typical stationary applications are and how LIBs are used in these applications are answered. The LIB stress is compared with mobile applications in chapter 3.2. In chapter 3.3, load profiles are anonymized and then the impact on the load of stationary BSSs in different applications is evaluated. Subsequently, in chapters 4.1 to 4.3, the provision of typical stationary applications with commercial EVs is simulated and optimal vehicle pools are formed. Therein, various research questions on the potential of providing stationary applications with pools of EVs are answered. Lastly, chapter 5 then answers research questions on the V2X impact on e-Cars, e-Buses, and e-Boats in various stationary applications.

2.3 Battery storage in mobile applications

In addition to the stationary applications described, LIBs are also used in mobile applications. Camcorders and cell phones were the first portable applications for LIBs in the 1990s [24]. Other portable electronics applications today include tablets, laptops, wearables and power tools [53]. The focus of this thesis is on transportation means that have also been gradually electrified over the last 30 years [24, 53]. In contrast to the stationary battery applications, the purpose of using batteries in transportation means is self-explanatory: transporting people and cargo. Chapter 3.2 of this thesis addresses research questions related to mobile applications. One focus is on the energy consumption of e-Cars and e-Buses. Another focus is on the battery stress in the e-Cars, e-Buses and e-Boats applications. A comparison to the stress in stationary applications will be made and the influence of the charging strategy will be discussed. In the following, the markets and characteristics of e-Cars, e-Buses and e-Boats are explained, as these three means of transport are relevant for this thesis. Subsequently, other means of transport will be briefly presented. In chapter 2.5, the link to the V2X use of the means of transport is then drawn.

2.3.1 Electric Cars

In Germany, approximately 48,750,000 passenger cars were registered as of 01.01.2023 [144]. This corresponds to an increase of 6% in the last five years [145]. But not only the total number of cars has increased in recent years. The number of pure battery electric cars increased by a factor of 19 from 54,000 in 2018 to 1 million cars in 2023 [144, 146]. Together with hybrid vehicles, the stock of passenger cars with alternative drives was 3.75 million at the beginning of 2023 [144]. The number of electric vehicles is also on the rise worldwide. As described in section 1.1, the number of e-Cars sold

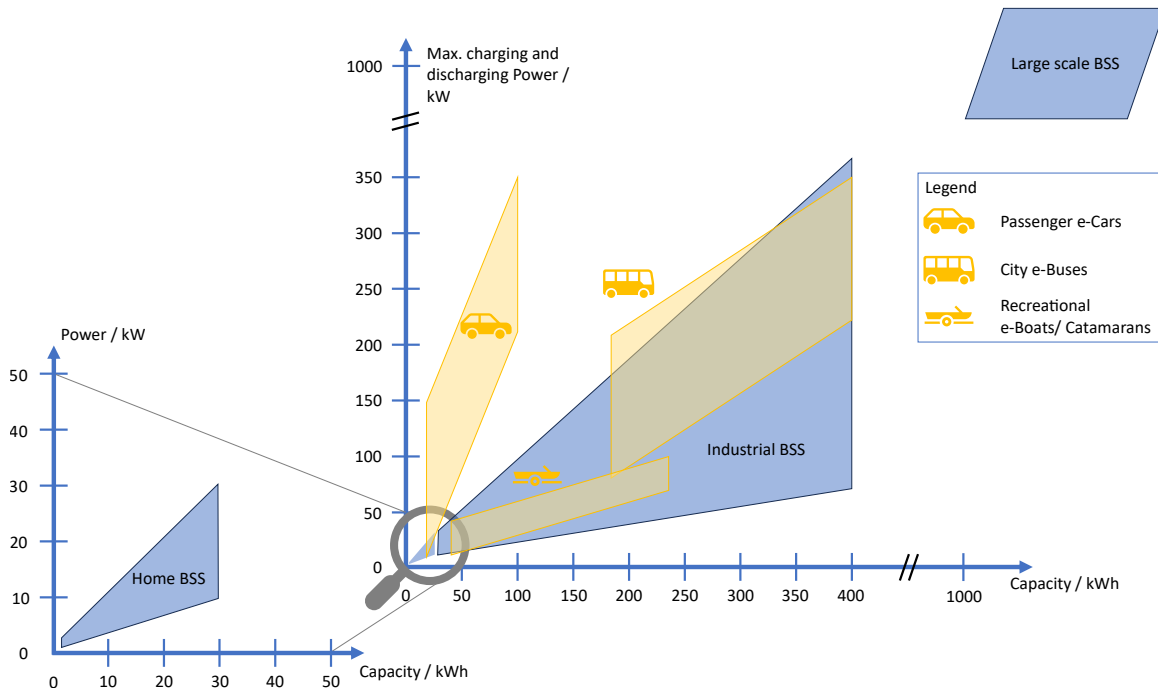


Figure 2.2: Power and capacity ranges of stationary and mobile BSSs. The areas of the stationary BSSs are marked according to Figgenger et al. [27, 149]. The ranges for mobile applications are own estimations based on data from industry partners. The electric boats are on the scale of catamarans, while large electric ferries can have capacities of over 1000 kWh.

worldwide rose from 1 million in 2017 to 10 million in 2022 [38]. Sorting the available models worldwide by vehicle size, it is noticeable that almost 60% of the models are sports utility vehicles (SUVs) or large cars (E and F segments) [38]. The average battery capacities of e-Cars depend on the vehicle size and the country considered. In 2022, small e-Cars had a sales-weighted average of 25 kWh in China, 35 kWh in Germany and 60 kWh in the USA [38]. For SUVs and large e-Cars, on the other hand, the sales-weighted average in the countries named was 70 to 90 kWh [38]. Compared with the average 8.8 kWh HSS in Germany (see section 2.2.1), e-Cars therefore have an average battery capacity that is three to ten times higher. Figure 2.2 compares the capacities and possible charging and discharging power of the transportation means with the dimensions of stationary BSSs. Large e-Cars typically have capacities of up to 100 kWh. The power with which e-Cars are connected to the electricity grid corresponds to up to 22 kW in a domestic context and up to 350 kW with fast charging stations. With the battery capacities mentioned, the e-Cars achieve ranges of 220 to 600 km [38]. However, a study on mobility behavior in Germany showed that private cars (not specifically e-Cars) have an annual mileage of 14,700 km, driving an average of only 40 km per day [43]. For e-Cars, studies showed even lower annual mileage. A study from Belgium showed annual mileages of 5,000 to 6,000 km [147] and a study in Shanghai almost 12,000 km [148]. The study on mobility behavior in Germany further showed that private cars are parked on average 97% of the time, and at home over 84% of the time [43]. In e-Cars, NMC LIBs are often used due to their advantages in terms of energy density [38]. Their market share was 60% in 2022 [38]. However, the share of LFP LIBs in e-Cars has increased in recent years, mainly driven by China's car manufacturers, so that their share amounted to 30% in 2022 [38].

2.3.2 Electric Buses

Alongside e-Cars, electrically powered buses are also gaining in popularity. From 2020 to 2021, the number of e-Buses sold worldwide increased by 40 %, while the total number of sales remained constant [40]. In 2022, the global share of e-Buses in all buses sold was already 4.5 % [38]. For example, in Finland, where the government aims to reduce emissions in public transport, the share was already 65 % [38]. A leading country in the field of e-Buses is China, which accounted for 80 % of all e-Buses sold worldwide in 2022 [38]. Figure 2.2 ranks the capacities and power ranges of e-Buses in comparison to e-Cars and stationary BSSs. Compared to e-Cars, e-Buses have larger battery capacities. Depending on the application of the e-Buses, for instance as a school bus or transit bus, average capacities are between 137 and 345 kWh [38]. Hochbahn Hamburg operates e-Buses with a capacity of up to almost 400 kWh, as will be shown in chapter 3.2. This means that the capacities of e-Buses are a factor of five to 14 higher than those of small e-Cars (with 25 kWh) and in the range of industry BSSs. The charging power is typically between 100 and 350 kW. The driving ranges of e-Buses vary depending on the manufacturer and battery capacity. A study of the Chinese e-Buses market showed average ranges of approximately 440 km for 2021 [150]. Despite the lower volumetric and gravimetric energy density, 95 % of e-Buses sold in China in 2021 were based on LFP batteries [150]. The reasons for this are the lower cost, higher durability and higher safety compared to NMC batteries [150].

2.3.3 Electric Boats

The third mobile BSS application relevant to the thesis are e-Boats. While the market for e-Boats is generally smaller than that for e-Cars and e-Buses, it is also forecasted to grow. Thus, the market volume is expected to double from 2022 to 2028 [42]. In general, a distinction can be made between different types of boats. The EU defines a recreational boat as a boat used for sports and leisure purposes that is between 2.5 and 24 meters long [151]. Catamarans, which are currently tested as autonomous electric passenger ferries in Helsinki, for example, are often of a similar size [152]. Figure 2.2 compares the capacity and power of e-Boats with the other means of transportation and stationary BSSs. The battery capacities of catamarans range from 60 to 240 kWh [153]. The electric boat propulsion manufacturer Torqeedo, who provided data for the results obtained in chapter 3.2 of this thesis, develops drives for boats of a similar and smaller size [154]. Torqeedo uses NMC and LFP batteries as cell chemistry [154]. An order of magnitude above the catamarans are ferries. These can also be powered by batteries. Since May 2015 an electric car ferry has been operating in Norway, covering a distance of 5.7 km with its 1090 kWh battery [155]. There are also some hybrid concepts with battery and diesel in the field of ferries [155]. For international shipping, i.e. ships of larger size driving larger distances, LIBs are not yet seen as an option for decarbonization [156]. Batteries do not play a role as propulsion systems here, in contrast to biofuels and e-fuels [156]. However, battery applications on international ships do exist, for instance as backup power, spinning reserves and for load optimization [157].

2.3.4 Further transportation means

In addition to the three mobile applications for BSSs described in detail, a variety of other applications exist where batteries are still a niche market. **Trucks** are also gradually being converted to alternative propulsion systems [38]. Depending on the distance to be driven by the trucks, batteries in combination with electric motors offer a possibility of propulsion [158]. Fast-charging or battery swapping

stations enable operation with few interruptions [158]. In 2022, 1.2 % of all trucks sold worldwide were electrically powered trucks [38]. The average battery capacities of electric trucks in 2022 were between 92 and 311 kWh, depending on the truck size [38]. In addition, individual models reach capacities of up to 800 kWh [38]. Another mobile application is **trains** powered by batteries [159]. In Germany, 36 % of rail passenger traffic was carried by diesel trains in 2017 [160]. Worldwide, a quarter of passenger rail transport was powered by diesel in 2019 [159]. Train manufacturers such as Bombardier and Siemens are developing battery-electric trains to cover the routes without overhead lines, which could replace diesel trains [160, 161]. Depending on the model, these trains have battery capacities of 300 to 700 kWh and achieve battery-powered ranges of 35 to 80 km [160, 161]. Bombardier and Siemens rely on LIBs with NMC cathodes and graphite or lithium titanate oxide (LTO) anodes for their 2020 models [160, 161]. Flight applications, such as **drones**, **electric vertical take-off and landing aircraft** and small battery-powered **aircraft**, are other mobile applications of BSSs [162]. For these applications, the specific energy density is most relevant [162]. While battery-powered drones are already in use, electric vertical take-off and landing aircraft are still in development [163, 164]. Battery-powered regional aircraft are not expected until after 2030, and commercial aircraft with more than 70 seats are not expected until between 2040 and 2050 [165].

2.4 Usage profiles

A key focus of this thesis are time-series power demand profiles in various forms. Profiles are temporal courses of values, which can have different temporal resolutions. Figure 2.3 provides an overview of the forms of profiles relevant to this work. In this chapter, section 2.4.1 deals with the basics and forms of profiles and section 2.4.2 with the analysis, processing and anonymization of load profiles.

2.4.1 Basics and forms of profiles

In this thesis, a distinction is made between various types of profiles, which are shown in simplified form in Figure 2.3. One form of profiles are electrical load profiles, which describe the energy consumption of devices, households or companies over time. In Germany, standard load profiles exist for households, agriculture and commerce, which aim to describe the behavior of these entities in a representative manner [166]. The standard load profiles have a resolution of 15 minutes and are often used in energy system simulations and calculations where detailed, individual, measured load profiles are missing [89, 167, 168]. Household load profiles of 74 households with a resolution of 1 second were measured by the HTW Berlin and published open-access [169]. These household load profiles are referenced in chapter 3.1. In general, household load profiles change due to the increasing electrification of vehicles and heat generation [170]. A simplified example of a load profile is shown in Figure 2.3 a).

Generation profiles can be measured from renewable generation units such as PV systems or wind turbines. The profiles describe the power that is generated at the selected location and with the dimensioned system at any given time. For Munich, for example, a PV generation profile with a resolution of 1 second was measured at the Technical University of Munich and has been used in several publications [79, 89, 171]. Figure 2.3 b) shows a simplified generation profile of a PV system on a cloudless day. Residual load profiles can be generated as a result of load and generation profiles, as explained in chapter 2.2.1. Figure 2.3 c) shows an example of a residual load profile. While load and generation profiles always have a constant sign or are zero, residual profiles can have positive and

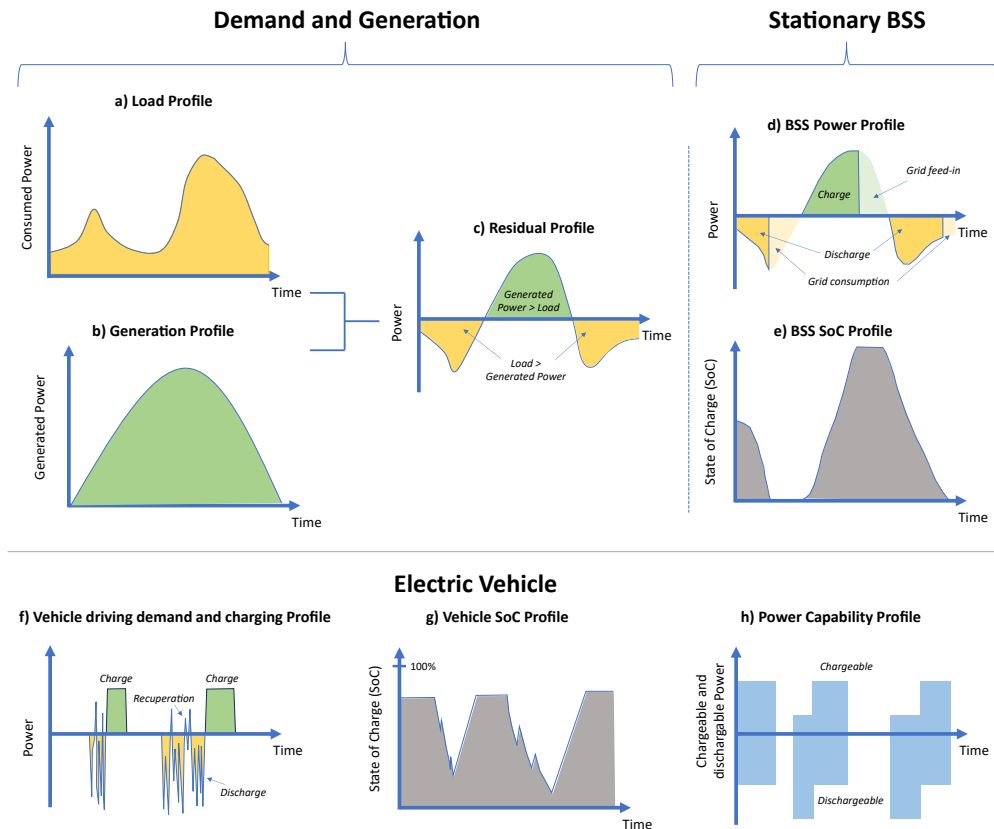


Figure 2.3: Forms of Profiles relevant to this thesis.

negative values.

In addition to those demand and generation based profiles, BSS power profiles and BSS SoC profiles can also be measured for storage facilities. Figure 2.3 d) shows a simplified BSS power profile where the BSS is discharged in the morning, charged around noon and discharged again in the evening. As shown in the exemplary figure, the residual load is not always reproduced in the BSS power profile due to energy management decisions or voltage limits. Furthermore, SoC profiles can be measured for storage systems using the battery voltage, indicating the SoC between 0 and 100% at any time (see Figure 2.3 e)). In chapters 3.1 and 3.2 of this thesis, batteries are simulated in various applications and the power and SoC profiles are published open-access.

Chapter 3.1 also develops a methodology for determining representative candidates from a data set of BSS power profiles. One approach would be to simply determine the mean value of all profiles at all times. The problem with this methodology is that characteristic peaks are smoothed and the averaged profile would therefore not represent the original profiles. The approach presented in this thesis is based on the determination of a representative profile using various characteristics. Six characteristics, such as the number of EFCs and the round-trip efficiency, are calculated for each profile. Subsequently, the distributions of the characteristics of all profiles and their medians are calculated. The deviation from the median of all profiles is then calculated for each profile and each characteristic. For this purpose, the root mean square percentage error is calculated. The profile with the smallest root mean square percentage error in all six characteristics is then selected as the representative profile. One advantage of this method is that a real profile is determined as a representative profile for the set of profiles, whereby characteristic peaks are retained. In addition, the method is straightforward to

understand, reproduce and expand. If, in contrast, a random profile were selected, it could be an outlier profile with regard to individual characteristics. The methodology is implemented in a storage profile analyzer tool and presented in detail in chapter 3.1.

Another form of profiles related to EVs are vehicle driving demand and charging profiles (see Figure 2.3 f)). These profiles include discharging and recuperation during journeys and charging sequences when the vehicle is connected to the electricity grid. Related to this, SoC profiles can also be determined for vehicles, as displayed in Figure 2.3 g)). Moreover, in chapter 4.1 to 4.3 of this thesis power and energy capability profiles are created. These profiles are based on the driving profiles of commercial combustion engine vehicles. With the help of vehicle characteristics and assumptions about consumption, for example, vehicle driving demand and charging profiles of EVs are simulated. These profiles are used to determine the amount of power and energy a vehicle could additionally charge and discharge for V2X provision in every time step while being idle. Figure 2.3 h)) shows such a simplified power capability profile. It indicates the possible additional chargeable and dischargeable power. If the vehicle is at the charging station and already charged to a minimum SoC, the vehicle can still charge and discharge a constant amount of power. If it is on the road or unplugged, the power capability is zero. When the vehicle returns, the chargeable power is lower because the vehicle is already being charged. However, charging could also be interrupted and the battery could be discharged instead. For this reason, more power than the maximum charging station power can be released for the grid during the charging process. As a result, the dischargeable power during the charging process is greater than during idle times without charging. As soon as a threshold setpoint of minimum required SoC is reached, the full charging and discharging power is available again. For the exact calculation of the power capability profile, the available capacity and the service time of the respective market are also taken into account, as the vehicle may also be energy-limited due to a very high or very low SoC. Similarly to the power capability profile, an energy capability profile can be formed, which indicates at what time how much energy can additionally be charged and discharged. These power and energy capability profiles are used to determine possible revenues of commercial EVs on the FCR market in chapter 4.1 and to compile vehicle pools optimally for various V2G applications in chapter 4.2.

2.4.2 Profile analysis, clustering and anonymization

Electrical load profiles of households and companies are of particular relevance for grid operators and electricity supply companies. They use aggregated load profiles to predict electricity consumption at various grid connection points. Load profiles can be evaluated in different ways. First, a simple division into base and peak load is possible. An extension to five parameters was published by Price in 2009, adding rise time, high load duration and fall time to base and peak load [172]. In addition to the analysis in the time domain, load profiles can also be analyzed in the frequency domain using discrete fourier transformation (DFT) [173]. The advantage of the analysis in the frequency domain is that a data reduction is possible so that the amount of data to be stored is reduced compared to the time domain [172]. A prerequisite for all analyses of load profiles is the prior recording of these, which can be done using smart meters [173].

If a larger amount of data on load profiles is available, the clustering of these profiles is of particular relevance. Clustering creates groups of similar profiles and new load profiles can be assigned to one of the groups. The clustering can be carried out directly on the basis of the temporal load profiles or indirectly on the basis of features that are calculated from the profiles [174]. Analogous to load profile analysis in the frequency domain, feature-based clustering can save memory compared to clustering

temporal load profiles [175]. If residential load profiles are clustered, four time ranges should be considered according to Haben et al.: Overnight, morning, daytime and evening [176]. Clustering of household load profiles is often performed using the k-means algorithm [177–179].

In addition to load profile analysis and clustering, the generation of synthetic load profiles is a focus of research. Two approaches exist for the generation of synthetic household load profiles: bottom-up and top-down [180]. In the first approach, the load profiles are formed on the basis of cumulative consumption and temporal use data of individual consumers and appliances [181, 182]. Electric vehicles and heat pumps can also be taken into account [183]. The top-down approach instead uses aggregate data for countries or regions and breaks it down to individual households [180]. Here, for example, seasonality and distribution of households are used [184]. Another form of top-down approaches uses generative adversarial networks [185]. In this approach by Pinceti et al. the network learns from real hourly resolved weekly load profiles to generate synthetic load profiles [185].

Load profiles of households and businesses are sensitive data that are not willingly shared or made publicly available. However, since research institutions aim to use data from smart meters, Efthymiou et al. have developed a method to anonymize smart meter data [186]. Anonymization of entire temporal sequences was addressed by Pensa et al. by hiding infrequent, potentially sensitive, subsequences [187]. With their method they achieved k-anonymization, so that an individual household could not be distinguished from at least k-1 other households. The k-anonymization was extended by Machanavajjhala et al. to include l-diversity, where for each sensitive attribute in a data set, there must be at least l other attributes in the data set [188]. In addition to this anonymization of datasets, work also exists in which load profiles were modified. For instance, if load profiles are discretized, the error in power loss evaluations depends on the amount of discretization [189]. In addition, load profiles can be normalized in various ways [190]. Besides normalization to the maximum, minimum and maximum can also be used together. Last, one approach to anonymization is permutation of values. Li et al. permuted pairs of values every 50 to 100 h to randomly change the profile [191].

Following up on the research, chapter 3.3 presents a new methodology to anonymize load profiles via random permutations of base and peak sequences. For this purpose, individual load profiles are automatically divided into base and peak sequences in a python-based tool and, depending on the desired level of anonymization, the sequences are subsequently permuted randomly. Afterwards, the effects of anonymization on the load of BSSs are determined in simulations. The advantages of the method developed are easy traceability and the fact that a single load profile is sufficient to generate one or more anonymized load profiles. The tool is published open-source and can be used by industry and research [192].

2.5 Vehicle-to-X (V2X)

After introducing stationary applications in chapter 2.2, showing the growth of mobile applications in chapter 2.3 and discussing load profiles in chapter 2.4, a key question is to what extent vehicles can provide formerly stationary applications during idle periods. Private individuals and companies buy vehicles for mobility and for transporting goods. This has the highest priority and the vehicle is expected to be available for transportation when needed. But private cars are parked on average 97% of the time in Germany without being used for mobility [43]. Even if charging processes, buffer times and desired constantly available minimum SoCs are factored in, there remains a considerable amount of time in which the vehicle could be used for V2X. Manufacturers of e-Cars have also discovered the

potential of V2X [193]. There is an increasing number of manufacturers who are implementing or have announced bidirectionality for their e-Cars [193]. Developers of charging stations are now also working on bidirectional and no longer just unidirectional charging stations [193].

In the following, the concept of V2X and the various forms of it are presented first (section 2.5.1). Section 2.5.2 then explains the opportunities and barriers of V2X. After that, section 2.5.3 examines the role of aggregators and how pools of EVs can be formed. Section 2.5.4 then presents the financial potential of V2X in balancing markets. Subsequently, section 2.5.5 presents pilot projects and implementations of V2X. Finally, section 2.5.6 introduces V2X beyond e-Cars with a focus on e-Buses, electric trucks (e-Trucks) and e-Boats. Figure 2.4 provides an overview of the sections in this chapter.

2.5.1 Forms of V2X

A preliminary form of V2X is smart, unidirectional charging. This form of controlled charging can already relieve the electricity grid and generate revenue, for example [45, 46]. Vehicles can be equipped bidirectionally with additional software and hardware. For instance, the charging station must be capable of bidirectional charging. In addition, the communication interface must be expanded, as defined in ISO standard 15118 for communication between the car and the charging station [198].

The simplest form of V2X is **Vehicle-to-Load (V2L)**. Here, energy from the vehicle is used to power a consumer load. These loads can be construction sites or campsites, for example [199]. This allows EVs to be used to provide electrical energy in places without a grid connection or renewable generators with storage capabilities [199]. In 2011, for instance, V2L was used as an emergency power supply in Japan after an earthquake [199].

The next level of V2X is **V2H** or **V2B**. In the former, the vehicle is used to supply the house with electrical energy [199]. In the latter, the supply is made to a building, which is, for instance, a company [200]. These forms of V2X are BTM applications because they are carried out behind the

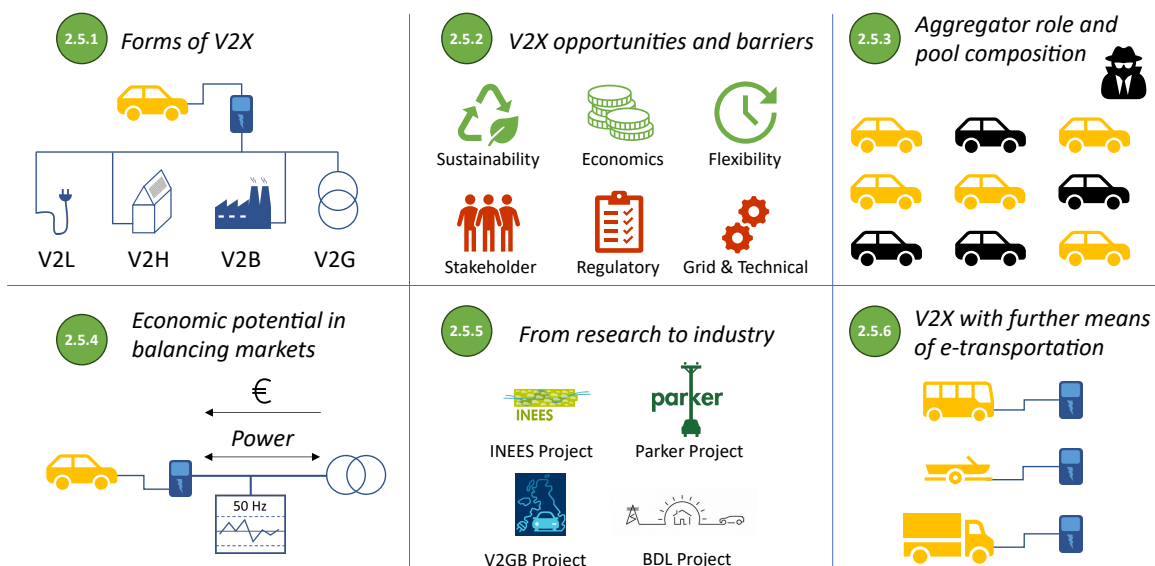


Figure 2.4: Overview of V2X sections. "From research to industry" section shows an excerpt of the projects with the logos from the final reports [194–197]. The green circles represent the section of the thesis in which the topic is addressed.

electric meter. In households, e-Cars can replace or supplement HSSs to serve as backup power or in SCI application. In addition, vehicles used for commuting could be charged with (surplus PV) electricity at the employer’s site and discharged in the evening at home to meet the household load. For businesses, residential or commercial EVs (e-Cars or e-Buses) could also be used as backup power. In addition, pools of EVs could also perform PS for the company, replacing or supplementing stationary commercial BSSs. If the vehicles are also at the company site in the evening or at night, for example in the case of commercial vehicles, these could also operate in SCI application by storing PV energy during the day and discharging it again in the evening and at night. V2H and V2B concepts are sometimes grouped together as vehicle-to-customer [47]. A special form of the BTM V2X applications is Vehicle-to-Vehicle (V2V) [201]. Here, one vehicle is discharged in order to charge another vehicle. This can make sense for commercial fleets or carsharing concepts if a vehicle is fully charged but is needed later than a vehicle that is not yet charged [201, 202].

The concept of using EVs during idle times for FTM applications is called **V2G** [201]. In V2G, the vehicles can be used for arbitrage trading on the intraday market to charge the vehicles at times of low prices and discharge them again at times of high prices. In addition, pools of vehicles can be used to provide balancing power to the electricity grid in the FCR application.

2.5.2 V2X opportunities and barriers

The V2X concepts presented bring opportunities, but barriers also exist to their implementation. First, all concepts represent a general improvement in the **sustainability** of vehicles. Instead of being used exclusively for mobility, the vehicle batteries can also be used during idle times. In chapters 3.2 and 4.2, we introduce the utilization ratio, which indicates the proportion of time a battery is used in stationary and mobile applications. We show in those works that the utilization ratio is increased by V2X provision. If the existing batteries in EVs are utilized more, the construction of new stationary BSSs can be reduced and thus sustainability improved.

Second, V2X concepts enable **business benefits** for vehicle owners and **economic benefits** for societies. Vehicle owners can sell their battery capacity to aggregators during idle periods. However, care must be taken to ensure that the aging costs of the battery due to V2X provision do not exceed the revenues [63, 203]. Possible revenues and profits from the provision of balancing services with EVs are discussed in detail in section 2.5.4. From a macroeconomic perspective, pools of EVs participating in the FCR market can reduce the cost of balancing power. In addition, the cost of grid expansion requirements can be reduced when vehicles meet peak loads by discharging or peak generation by charging [201].

Third, the vehicles introduce **flexibility** on the generation and consumption side. Through variable charging and discharging, they can support the expansion of renewable energy through V2H and V2G [199]. At the distribution grid level, this would allow more PV systems to be installed without causing voltage problems. Thus, V2X concepts contribute to the decarbonization of electricity supply.

Based on the advantages described above, the question arises as to why the currently available EVs are not yet V2X-capable. This has several reasons. First, there are **stakeholder barriers**. On the one hand, the ramp-up of electromobility has only been in full swing for a few years. Car manufacturers were focused on the development of EVs, so few resources were available for the ”add-on” V2X. On the other hand, established car manufacturers are new to the electricity sector. Before the electromobility, the transportation sector and the electric power sector were separate. This further complicates

the implementation of V2X on the car manufacturer side. However, many manufacturers have now recognized the potential of V2X and announced V2X capable vehicles [193].

But the implementation of V2X also means major changes for other stakeholders, which entails **grid barriers**. TSOs and distribution system operators (DSOs) always had to deal with large, centralized generators and a variety of consumers. Large-scale stationary BSSs are similar to existing pumped-storage power plants as energy storage facilities, and were therefore easier to integrate into the electricity grid from a regulatory perspective than many small BSSs. The development of smaller HSSs that could also provide grid services together as a pool required TSOs to expand their regulatory framework [204]. However, unlike HSSs, EVs are not always available and the grid connection point varies depending on the location of the vehicle. Accordingly, V2X-enabled EVs can sometimes be connected to bidirectional charging stations and sometimes to unidirectional charging stations. In addition, EVs can be connected to DC charging stations and to AC charging stations. In the former, the charging station converts the AC grid current into DC vehicle current when charging and vice versa when discharging. If a bidirectional EV is connected to the grid in this way, the necessary grid codes for grid connection can be implemented in the DC charging station [193]. However, if the vehicle is connected to AC charging stations, the AC/DC converter must be installed in the vehicle. Accordingly, the grid codes for the grid connection would have to be installed in the vehicle [193]. The vehicle's behavior would therefore have to vary depending on its location [193]. Furthermore, standards for the infrastructure and communication are required [199]. These are currently being created through adapted ISO standards [193]. Despite the mentioned difficulties, the European TSOs have recognized the potential of bidirectional vehicles and plan to adapt the market rules accordingly [101].

In addition to stakeholder and grid barriers, there are also **technical barriers**. Since the 1st generation of EVs dominate today's market and were often not developed with bidirectional charging capability, there has been little incentive for charging station developers to develop bidirectional charging stations. As a result, the market for bidirectional charging stations is still relatively small and prices are accordingly higher than those for unidirectional charging stations [205]. However, this is currently changing and more and more manufacturers are developing and producing bidirectional charging stations [193]. Another technical barrier in some countries like Germany and United Kingdom are missing smart meters [206]. These are needed to measure the charged and discharged energy at least quarter-hourly. This is especially relevant for V2G applications. To eliminate this problem, a new smart meter law has been enacted in Germany in May 2023 to accelerate the rollout [193, 207].

Lastly, there are **regulatory barriers** to the implementation of V2X. In general, taxes and levies are incurred for the consumption of electricity. The household electricity price in Germany in 2021 was around 0.322 €/kWh, of which only 0.079 €/kWh was for procurement and distribution [81]. At the same time, average wholesale electricity prices were below 0.07 €/kWh [81]. If a V2X-capable EV now pays the household electricity price including taxes and levies, the price spreads would have to be extremely wide to achieve a profit margin. The fact that the electricity would only be temporarily stored in the vehicles and then sold to end consumers, who in turn have to pay taxes and levies, leads to double taxation [193]. According to Hecht et al., one solution to this could be to reimburse the taxes and levies on the electricity fed back to the EV owner [193].

2.5.3 Aggregator role and pool composition

In order to use EVs for V2X provision, aggregators are required that bundle the capacities of the vehicles and decide on the charging and discharging processes [208, 209]. The need for aggregators arises from the structure of the electricity markets. If FCR is to be provided in Central Europe, a minimum capacity of 1 MW is required and the minimum volume on the EPEX intraday market is 100 kW [48, 105]. In addition to interfaces to the EVs, aggregators also need interfaces to the grid operator [208]. Independent of V2X, aggregators enable smart, cost-effective charging of the EV fleet [121, 210, 211]. In addition, algorithms have been developed on how aggregators can automatically bundle capacities, anticipate driving behavior, cover all charging needs and bid on the electricity markets [212, 213].

When selecting EVs for a pool or fleet to provide V2X, aggregators can use all vehicles of one company [214]. However, as early as 2011, Bessa et al. found that some EV types are better suited to various V2X services than others [215]. The authors stated that at that time, fuel cell vehicles were best suited for peak power sales and battery EVs for the regulation reserve market [215]. The authors also noted in 2011 that the ancillary service market could become saturated with high EV participation [215]. In 2014, Schuller et al. found that V2G could be particularly worthwhile for retirees with high charging power outlets [211]. The driving habits of this group of people make their vehicles particularly interesting for V2X aggregators.

Following on from the research results, chapter 4.2 answers the question of how pools of commercial e-Cars can be composed in an optimized manner. For this purpose, a new methodology on the basis of the energy and power capability profiles of the vehicles is developed. An optimization method is applied to determine which vehicle pool composition would generate the highest revenue per vehicle on the FCR, intraday and day-ahead markets. This optimization problem is non-linear, as the revenue is divided by the number of vehicles in the pool. If a vehicle is added to the pool, the revenue must be shared with another vehicle. In addition, the decision variables are integer, as a vehicle can only be completely part of the pool or not. For this nonlinear optimization with integer decision variables, genetic algorithms are a suitable approach used in this work [61, 216, 217]. This metaheuristic optimization algorithm is based on inheritance, mutation and recombination [216]. Genetic algorithms can solve the non-linear optimization problem with large solution space relatively efficiently and faster than other algorithms [217]. A disadvantage of genetic algorithms is that these metaheuristic approaches do not necessarily find the global optimum. The optimized pools composed in chapter 4.2 are then analyzed in chapter 4.3. Influencing factors such as economic sector and battery size are taken into account.

For the optimal pool composition, a utilization ratio is defined for the vehicles that describes the proportion of time the vehicles are used for mobility or V2G provision. In chapter 3.2, in which only unidirectional charging strategies are evaluated, this value is called temporal utilization ratio. The additionally introduced dual use ratio in chapter 4.2 also describes the proportion of the possible V2G time during which the EV is actually charged or discharged. In addition, the temporal V2G-ready ratio is defined in chapter 3.2. This ratio indicates what proportion of the total time a vehicle type can be used for V2G. In chapter 5, this parameter is called temporal V2X ready ratio, as not only V2G but also V2B is taken into account there.

2.5.4 Economic potential in balancing markets

The economic potential of V2X depends on many influencing factors. First of all, EV models, installed batteries and wallbox types are diverse. Which LIB is installed and how do the battery cells degrade due

to the additional load? Is the vehicle battery capacity 20 kWh or 100 kWh? Is the vehicle connected to an 11 kW charger at home or to a 200 kW fast charging station on the road and what are the conversion efficiencies? Secondly, the driving behavior of the vehicle owner varies. Is the vehicle used for commuting or only as a second car? Thirdly, revenue potential depends on the possible markets at the location of the respective vehicle. These vary depending on the country or region. Finally, all parameters are subject to development over time. Battery technologies, battery capacities, wallboxes (power and bidirectionality), driving behavior and market prices develop or vary over time. These points make it difficult to make fundamental statements about the economic potential of V2X. In the following, the results of some published case studies and simulations on possible revenues from the provision of balancing power by EVs are presented.

In 2005, Kempton and Tomić calculated potential annual revenues of \$ 4928 if frequency regulation was provided by a Toyota RAV4 in California in 2003 [218]. The revenue was offset by costs of \$ 2374 [218]. Here they assumed a NiMH battery and round trip efficiencies of 73 % [218]. In 2019, Thingvad et al. calculated possible annual revenues of 1395 € if Frequency Normal Operation Reserve was provided with Nissan e-NV200 (24 kWh) and Nissan LEAF (30 kWh) in Eastern Denmark [46]. In their work, the authors assumed V2G use between 4 p.m. and 7 a.m. with a possible charging and discharging power of 10 kW [46]. Bañol Arias et al. extended the work to include costs and calculated annual profits of between 100 € and 1100 € per EV [219]. Thingvad et al. carried out field tests and after five years of operation determined the battery ageing and the real revenue of EVs providing balancing power in Denmark [63]. Taking into account battery degradation and conversion losses and neglecting investment and maintenance costs, annual profits of 751 € per EV were found [63]. Doumen et al. determined the potential profit of EVs on the Dutch ancillary service market in 2019 [220]. In addition to revenue, they also took investment and operational costs into account and came to the conclusion that FCR provision with FCRs in the Netherlands was not worthwhile at that time, as the annual profit in the best-case scenario was around -410 € [220]. In their work on multi-use with EVs, Englberger et al. calculated 2224 € in annual cash flow when FCR provision is combined with SCI, PS and spot market trading [9]. In this study, e-Car profiles were simulated with the emobpy tool which correspond to the mobility behavior of private cars in Germany [50]. The prices for FCR and intraday trading were based on the year 2020 and the location Germany [9].

In chapter 4.1 of this thesis, the question of potential revenues of commercial EVs on the FCR market in Germany is answered. In addition, the influence of the increasing flexibilization of the FCR market from weekly to daily to 4-hour provision is examined. For this purpose, real driving data from commercial combustion vehicles in Germany is used, equivalent EV battery capacities are estimated using the vehicle size and the power and energy capability profiles of the EVs already presented in section 2.4.1 are formed. These profiles are used to estimate potential revenues on the FCR market. This resulted in potential revenues of 450 € to 750 € per vehicle in 2021. Following on from this, the profiles are used in chapter 4.2 to compile optimized vehicle pools. The chapter also introduces the power utilization rate. This rate describes what proportion of the possible EV pool power is actually used in FCR provision. Due to regulatory requirements and bid increments of 1 MW, not all of the power can be marketed for FCR. Chapter 4.3 then examines, among other things, how a reduction in increments and minimum bids affects revenue in the FCR market.

2.5.5 From research to industry

The potential of V2X was already recognized over 20 years ago [221]. In the last decade, in parallel with the growth of electromobility, a number of research and pilot projects were launched worldwide to test the V2X capability of EVs.

In California, a project called *Vehicle-to-grid demonstration project: Grid regulation ancillary service with a battery electric vehicle* already took place in the early 2000s [222]. In this project, an e-Car was expanded to include bidirectional charging capability in order to test the provision of balancing power. An aggregator function was then developed that act between the grid operator and the vehicle and informed the vehicle via the internet which power was to be charged and discharged. The results of the project were that the wireless data transmission times met the ISO conditions and the energy throughput during the provision of balancing power roughly corresponded to the load of daily driving. [222]

From 2012 to 2015, the *INEES* project took place in Germany, which investigated the intelligent grid connection of e-Cars for the provision of ancillary services [194, 223]. For the one-year fleet trial, 20 Volkswagen e-Ups were expanded to include bidirectional charging capability and tested for the provision of aFRR (then called secondary control reserve). The results of the project were that pools of EVs are generally technically capable of providing balancing power, but the load leads to increased battery degradation. [194, 223]

In the *Los Angeles Air Force Base Vehicle-to-Grid Demonstration* project, 29 combustion vehicles were replaced by bidirectional EVs by 2018 and tested for frequency regulation provision [224]. Over a period of 20 months, the EVs generated 255 MWh of up regulation and 118 MWh of down regulation. This corresponds to an average of around 15 kWh of additional discharged energy per day and vehicle and 6.5 kWh of additional charged energy per day and vehicle. The capacity loss of the vehicle batteries was between 5 % and 10 %, whereby the sole influence of V2G use could not be determined. However, since, according to the authors, the vehicles only consumed an average of 1.4 kWh per day for trips, a large proportion of the degradation can be attributed to the provision of V2G. [224]

The *Parker* project was carried out in Denmark from 2016 to 2018 [195, 225]. In this field test, FCR was successfully provided with various EVs models and DC V2G chargers. Potential revenues were also determined here, but these depend heavily on the influencing factors of FCR prices, V2G charger cost and efficiency, energy costs and battery ageing. As a result, the profit per car and year in the test was between -955 € and 2304 €. [195, 225]

Furthermore, the *V2GB - Vehicle to Grid Britain* project ran from 2018 to 2019 [196]. This project determined value and costs of V2G in the UK. One result was that by reducing the need for grid expansion due to peak demand reduction, £ 200 million can be saved between 2020 and 2030 compared to uncontrolled charging. [196]

Between 2019 and 2023, the German research project *BDL - Bidirectional Charging Management* investigated which use cases could be of interest for V2X [197]. For this purpose, 20 test vehicles were tested in the field for V2X provision. The project partners came to the conclusion that V2H, V2B and V2G will all be economically viable in the future, with the economic viability of V2H being the most robust in the evaluations. [197]

In addition to the aforementioned research projects, there have also been a number of industrial pilot projects in recent years. A wide variety of companies have already tested V2X [226, 227]. In June

2023, Renault announced that the Renault 5, which will be sold from 2024, will be V2G-capable [228]. Other manufacturers have also announced bidirectionality for their e-Cars, although some of these are limited to V2L [193].

2.5.6 V2X with further means of electric transportation

Due to the expected market size and the long idle times, V2X research is largely focused on e-Cars. However, the relatively large battery capacities and predictable driving style of e-Buses have also led to an increased investigation of V2X provision with e-Buses in recent years [47, 229, 230]. Already in 2014, Noel et al. compared the use of V2G-capable electric school buses with diesel-powered school buses [231]. The authors concluded that in each case of their sensitivity analyses the e-Bus would bring a net present benefit [231]. Part of the benefit was V2G revenue, which amounted to \$15,000 per year by participating in the US PJM frequency regulation market [231]. Verbrugge et al. also recommended including V2X features in e-Bus charging management strategies in their 2021 publication [230]. Manzoli et al. found in 2022 that it would be economical for e-Bus operators to provide V2G below 100 €/kWh battery replacement costs [232]. This could reduce operating costs by 38 % in 2030 [232]. A paper by Fan et al. analyzed in 2023 the V2G provision with e-Buses in Japan and concluded that the revenue from the provision is lower than the revenue from bus tickets and that arbitrage trading with e-Buses in Japan is more economical than FCR provision [233].

Alongside e-Buses, there is also research into the provision of V2X with e-Trucks [234, 235]. In 2012, De los Rios et al. investigated the reduction of operating costs of a fleet of delivery trucks, assuming that the trucks were V2G capable [234]. They came to the conclusion that the total cost of ownership could be reduced by 5 to 11 % through V2G [234]. Furthermore, Zhao et al. showed in 2016 that V2G provision with e-Trucks can not only reduce the total cost of ownership, but also greenhouse gas emissions [235].

Moreover, some research work exists on V2X provision with e-Boats and electric ships [236–238]. In 2019, Mahmud et al. published a method in which they used the energy from bidirectional e-Boats to cover the electrical demand and provide ancillary services on a remote island [236]. Two years later, Pintér et al. published a study on the energy storage potential of "boat-to-grid" at Lake Balaton in Hungary [237]. According to the authors, the e-Boats available there in 2021 had a total capacity of 4.8 MWh and therefore represent a potential that should be exploited using V2G [237]. Jozwiak et al. used the flexibility of e-Cars and e-Boats in their investigations of a marina in Denmark [238]. They also calculated possible cost savings through V2G with e-Cars and the flexibility of e-Boats.

Chapter 5 of this thesis aims to fill the research gap on the V2X use of e-Buses and e-Boats and the associated additional load on the LIBs. The temporal utilization ratio and the resulting V2X ready ratio are relevant for V2X use with various vehicles. In addition, the effects on battery-relevant parameters, the predictability of the driving behavior and the available capacity and power are important indicators. Chapter 5 examines those important indicators and shows the predictability of the EVs. Moreover, it analyzes how the V2X ready ratio varies over the course of the week. In addition, parameters relevant to LIBs with and without V2X provision are examined and the effects of V2X on the degradation behavior of e-Car LIBs are investigated using a degradation model.

3 Battery applications and load profile anonymization

Chapter 3 of this thesis summarizes three research publications on BSS applications and load profiles. First, section 3.1 presents an investigation of stationary BSSs in the three applications SCI, FCR and PS. It also presents a methodology for determining representative storage power profiles from a set of profiles. Then, in section 3.2, the three mobile BSS applications e-Car, e-Bus and e-Boat are examined and the impact on the batteries in these applications is investigated in addition to the energy consumption. Finally, section 3.3 presents a methodology that can be used to gradually anonymize electrical load profiles.

3.1 Investigation of stationary battery storage systems in various applications

This section presents the research paper entitled *Standard battery energy storage system profiles: Analysis of various applications for stationary energy storage systems using a holistic simulation framework* [1]. The paper examines three stationary applications for BSSs and determines representative storage load profiles. Representative standard load profiles, such as the H0 load profile and worldwide harmonized light vehicles test procedure (WLTP) load profiles, exist for private households in Germany and e-Car loads [166, 239]. Such representative load profiles were lacking for BSSs in stationary applications. This made it difficult to compare simulation results from different institutions if they are based on various assumptions or locations. If, for example, the performance of a new battery technology is to be assessed and compared with established technologies in stationary applications, distortions may occur due to variable load and generation profiles. This section presents a method for generating representative load profiles of stationary BSSs. Furthermore, storage and SoE profiles are also published as open-access data to enable their use in other works.

The work focuses on the three stationary applications SCI, PS and FCR. The applications are simulated using input profiles in the simulation tool SimSES. For the households in SCI applications 74 open-access household load profiles and one PV generation profile are used, for the PS application 36 industrial load profiles and for the FCR application five grid frequency profiles are used. The systems and energy management system strategies are designed according to regulatory requirements (FCR) and typical configurations (SCI and PS). This results in a number of storage load and SOE profiles, which are then analyzed in a *profile analyzer tool* developed within this work. The *profile analyzer tool* quantifies six key characteristics with relevance to layout, performance and ageing related behavior of the BSS for each profile, such as average SoC and number of EFCs. The median values of the six key characteristics are then determined for each set of profiles of an application and design. The profile that has the minimum root mean square percentage error from the median value in all six characteristics is then selected as the reference profile.

The research questions answered in this section are:

1. What are typical stationary applications of BSSs and how are LIBs utilized in these applications?
2. How can representative profiles be determined from a set of stationary BSS load profiles?

The results of this section show that stationary BSSs are stressed differently in the three applications. The annual EFCs range from 19 to 282 and the round-trip efficiency varies between 83 and 93%, also depending on the system design. Furthermore, mean cycle depths, length of resting periods and changes of sign vary in the three applications. In addition, a methodology for extracting representative storage load profiles is developed and published and the reference profiles determined are published open-access as part of the publication.

The results regarding the utilization of LIBs in stationary applications are then compared with the load in mobile applications in section 3.2. In addition, the load profiles determined in the stationary applications are used in chapter 5 to simulate the V2X provision of e-Cars, e-Buses and e-Boats. For this purpose, depending on the available pool size, a fraction of the power provided by the stationary BSS is provided by the vehicle during idle times.

Author contribution

Daniel Kucevic was one of two first authors tasked with coordinating and writing the paper and developing SimSES. Benedikt Tepe was the other first author, who programmed the *profile analyzer tool* and wrote contents within the data preparation, analysis and results. Both Daniel Kucevic and Benedikt Tepe contributed equally to this work. Stefan Englberger helped with programming and writing the peak-shaving algorithm. Anupam Parlikar helped with gathering data and the selection of the characteristics. Markus Mühlbauer was co-responsible for the dynamization of the input data and helped with the selection of the characteristics. Both Oliver Bohlen and Andreas Jossen contributed via fruitful scientific discussions. Holger Hesse reviewed the manuscript and was giving valuable input throughout the manuscript preparation. All authors discussed the data and commented on the results.

Standard battery energy storage system profiles: Analysis of various applications for stationary energy storage systems using a holistic simulation framework

Daniel Kucevic, Benedikt Tepe, Stefan Englberger, Anupam Parlikar, Markus Mühlbauer, Oliver Bohlen, Andreas Jossen and Holger Hesse

Journal of Energy Storage, Volume 28, 2020

Permanent weblink:

<https://doi.org/10.1016/j.est.2019.101077>

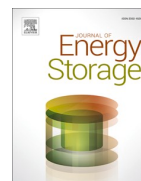


Reproduced under the terms of the Creative Commons Attribution 4.0 License (CC BY, <http://creativecommons.org/licenses/by/4.0/>), which permits unrestricted reuse of the work in any medium, provided the original work is properly cited.



Contents lists available at ScienceDirect

Journal of Energy Storage

journal homepage: www.elsevier.com/locate/est

Standard battery energy storage system profiles: Analysis of various applications for stationary energy storage systems using a holistic simulation framework

Daniel Kucevic^{a,1,*}, Benedikt Tepe^{1,a}, Stefan Englberger^a, Anupam Parlikar^a, Markus Mühlbauer^b, Oliver Bohlen^b, Andreas Jossen^a, Holger Hesse^a

^a Institute for Electrical Energy Storage Technology, Technical University of Munich (TUM), Arcisstr. 21, Munich 80333, Germany

^b Department for Electrical Engineering and Information Technology, Munich University of Applied Sciences (HM), Lothstr. 64, Munich 80335, Germany

ARTICLE INFO

Keywords:

Battery energy storage system
Lithium ion
Storage system design
Stationary application
Operation strategy
Standard profiles

ABSTRACT

Lithium-ion batteries are used for both stationary and mobile applications. While in the automotive industry standard profiles are used to compare the performance and efficiency of competing vehicles, a similar comparative metric has not been proposed for stationary battery energy storage systems. Because standard profiles are missing, the comparable evaluation of different applications with respect to efficiency, long-term behavior and profitability is very difficult or not possible at all. This work presents a method to create these standard profiles and the results are available as open data for download. Input profiles including frequency data, industry load profiles and household load profiles are transformed into storage profiles including storage power and state of charge using a holistic simulation framework. Various degrees of freedom for the energy management system as well as for the storage design are implemented and the results are post-processed with a profile analyzer tool in order to identify six key characteristics, these being: full-equivalent cycles, efficiency, depth of cycles, resting periods, number of changes of sign and energy throughput between changes of sign. All applications examined in this paper show unique characteristics which are essential for the design of the storage system. E.g., the numbers for annual full-equivalent cycles vary from 19 to 282 and the efficiency lies between 83% and 93%. With aid of this work in conjunction with the *open data* results, users can test and compare their own cell types, operation strategies and system topologies with those of the paper. Furthermore, the storage power profiles and state of charge data can be used as a reference for lifetime and profitability studies for stationary storage systems.

1. Introduction

A high share of renewable energies poses new challenges to the power grid. Due to decreasing costs of Lithium-Ion Battery (LIB), stationary Battery Energy Storage Systems (BESSs) are discussed as a viable building block in this context. In Germany, the installed storage power with batteries increased from 126 MW in 2015 to over 700 MW in 2018 [1]. Many use cases seem to be of interest for BESSs, as summarized in a report by Eyer and Corey [2]. In particular, the provision of Frequency Containment Reserve (FCR), Peak Shaving (PS) in the industry sector and Self-consumption Increase (SCI) in the private sector are seen as the most prominent applications for BESSs [3,4]. There seems to be

consensus, that these applications are the main drivers for the stationary battery storage market. However, if it comes to quantitative analyses of profitability, efficiency and aging of storage systems in a singular use case or even across applications, striking differences in numbers become apparent. In order to make single applications easier to compare, open-source available reference profiles for stationary BESS, similar to the widely used Worldwide Harmonized Light Vehicles Test Procedure (WLTP) for electric vehicles applications, are suggested herein and may help to assess the performance of BESSs.

1.1. Literature review

The state of the art of LIB based stationary BESSs is reviewed e.g. by

* Corresponding author.

E-mail address: daniel.kucevic@tum.de (D. Kucevic).

¹ These authors contributed equally to this work.

<https://doi.org/10.1016/j.est.2019.101077>

Received 19 August 2019; Received in revised form 8 October 2019; Accepted 13 November 2019

Available online 28 January 2020

2352-152X/© 2020 The Authors. Published by Elsevier Ltd. This is an open access article under the CC BY license (<http://creativecommons.org/licenses/by/4.0/>).

List of Abbreviation		IP	Input Profile
AC	Alternating Current	LFP	Lithium-Iron-Phosphate
BESS	Battery Energy Storage System	LIB	Lithium-Ion Battery
C	Carbon-Graphite	NMC	Nickel-Manganese-Cobalt-Oxide
DC	Direct Current	OCV	Open Circuit Voltage
DOC	Depth of Cycle	PE	Power Electronics
DOF	Degrees of Freedom	PER	Power to energy ratio
E-rate	Energy Rate	PS	Peak Shaving
ECM	Equivalent Circuit Model	PV	Photovoltaic
EMS	Energy Management System	SCI	Self-consumption Increase
FCR	Frequency Containment Reserve	SimSES	Simulation Tool for Stationary Energy Storage Systems
FEC	Full Equivalent Cycles	SP	Storage Profile
IDM	Intra-Day Market		

Diouf et al. [5] and Hesse et al. [3]. Both conclude that LIB based stationary BESSs have advantages in different stationary applications compared to alternative technologies. A more general overview of stationary storage systems, including other storage technologies, is given by Palizban and Kauhaniemi [6], Resch et al. [4] and Dunn et al. [7]. All authors highlight the high efficiency of LIB-based BESSs, but the numbers, due to different definitions, vary from less than 90% up to 94%. A systematic review of Energy Management System (EMS) for BESS was published by Weitzel and Glock [8]. The placement in distribution grids of stationary BESS is summarized in the review of Das et al. [9]. An example for optimized placement using simultaneous perturbation stochastic approximation method was published by

Carpinelli et al. [10].

Regarding the provision of FCR with BESS, a number of papers have been published in the past. Specifically for several techno-economic evaluations different approaches exist [11–15]. Munderlein et al. [16] analyzed a large scale 5 MW and 5 MWh BESS in the FCR market. Apart from the fact that the focus of the individual authors is different, it is noticeable that many different numbers exist. For example the authors in [16] determined 147 Full Equivalent Cycles (FEC) per year, while the numbers of FECs in [13] varies from 207 to 254 per year.

In the case of SCI, many publications with various objectives exist. The publications can be split into economic analyses [17–20] and sizing of the system [21–23]. All authors conclude that a BESS for SCI can be

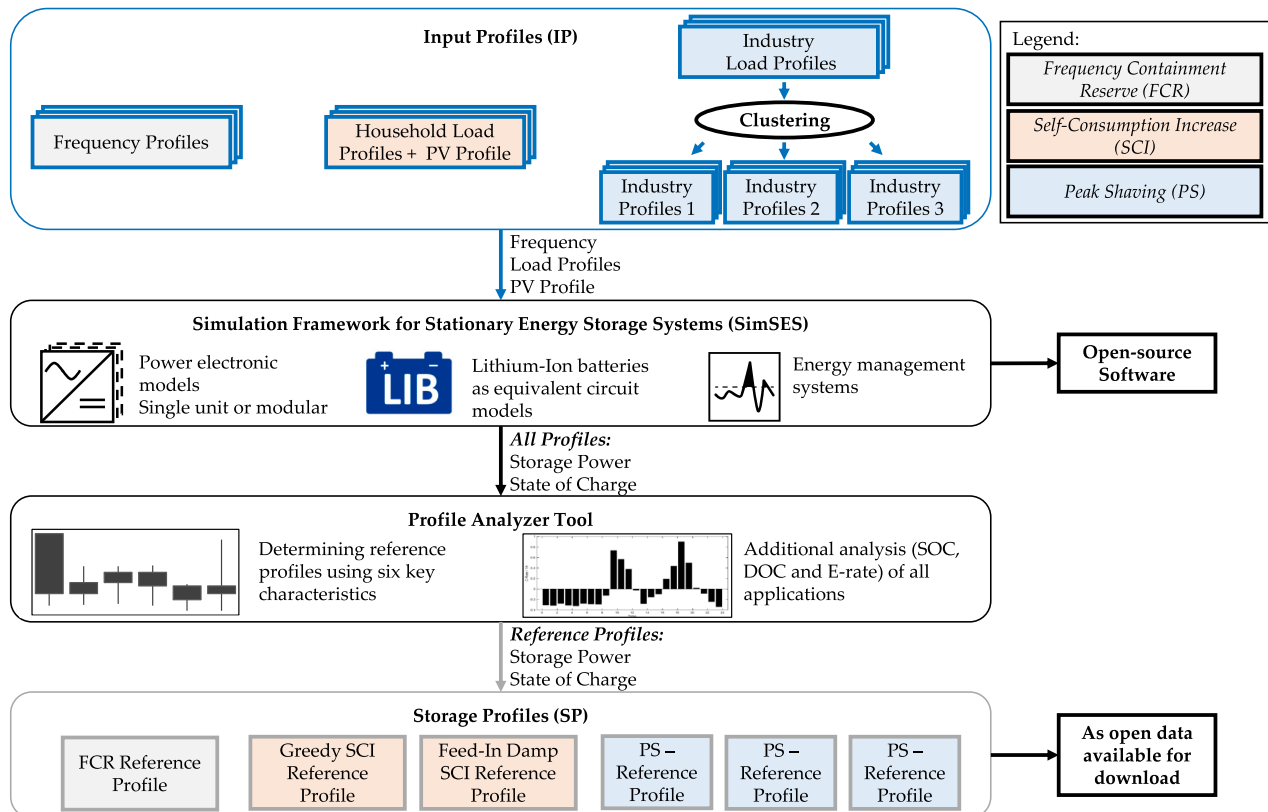


Fig. 1. Graphical overview of this work. The input profiles including frequency data, industry load profiles and household load profiles are transformed into storage profiles including storage power and state of charge using the simulation framework SimSES. The selection of suitable reference profiles is done with a profile analyzer tool developed as part of this publication.

economically viable, if the Photovoltaic (PV) unit and the storage capacity are dimensioned correctly. However, a wide variety of input data and parameters for the storage system (e.g. the efficiency for the LIB varies from 95% in [21] to 98% in [20]) are used in the publications, which makes comparability difficult.

For industry PS BESSs with LIB, fewer publications are available, in contrast to SCI BESSs. Martins et al. [24] present an approach for an optimal component sizing and the authors also performed an economic analysis. They showed in a case study that the number of FEC varies between 1 and 51 per year. Dagdougui et al. [25] show an EMS for a real world example. They optimized the size of a PS BESS for a university campus. It has been found that in this example the economically optimal storage capacity is 436 kWh. Telaretti and Dusonchet [26] conducted an economic analysis and compared the use of LIB in PS applications with three other electrochemical technologies: Lead-acid, flow based batteries and sodium-sulphur.

Although each author makes different assumptions and sets the focus differently, the results, some of which are very diverse, indicate that open data available standards for stationary BESS are desired.

1.2. Scope of this work

This work presents a method to create standard Storage Profile (SP) including the storage power and the SOC from Input Profile (IP) including frequency data, industry load profiles and household load profiles. The IPs are transformed into SPs by using the holistic simulation framework Simulation Tool for Stationary Energy Storage Systems (SimSES). Various Degrees of Freedom (DOF) for the EMS and the system configuration are implemented in SimSES and the results are post-processed with a newly developed profile analyzer tool in order to identify some key characteristics, such as efficiency, FEC or Depth of Cycle (DOC).

Fig. 1 shows the scope of this paper in detail. The simulation framework, as well as the results, including SPs and the SOCs, are made available as open-source. The results are available in one second resolution and may facilitate the comparison of the same applications among each other in the future. As an example, own system configurations or developed EMS can be compared with the numbers of this paper. Furthermore, the open-source available data can be used as a reference for lifetime and profitability studies for LIBs.

1.3. Paper structure

Section 2 gives an overview of the origin of the IPs and the pre-processing of the raw data sets. Section 3 describes the simulation tool SimSES with various DOFs and the developed EMS. In the remaining part of the paper, the SPs are analyzed (Section 4) and the choice of the reference profiles (Section 5) is described. Section 6 gives an outlook to future work and concludes this paper.

2. Profile data and preparation

In this chapter, the database of household load profiles, industry load profiles and frequency data is explained (Section 2.1). Herein, the data sources and time frames are described. The processing of this data is covered in Section 2.2. Subsequently, the normalization of the profiles is illustrated, which is required for comparison of data (Section 2.3). Finally, Section 2.4 covers the clustering of profiles.

2.1. Data basis

The creation of reference load and storage profiles demands a database that is sufficiently detailed to represent the specific type of profile. As described in Section 1, this paper considers three different applications of storage systems: SCI in the private sector, PS in the industry sector and the provision of FCR. These three applications require specific

Table 1

Storage applications, the data basis, the required data and the data resolution used in this work.

Application:	FCR	SCI	PS
Database	5 years of Frequency Data	74 yearly load profiles & one PV generation profile	36 yearly industry load profiles
Data resolution (raw data)	1 s	1 s	15 min
Data resolution (simulation)	1 s	1 s	1 s

data with specific resolution which is displayed in Table 1.

Firstly, high resolution frequency data is required to investigate the storage application of FCR [27]. This one second resolution data for the years 2013 until 2017, that can be measured at every socket within the synchronous grid of Continental Europe, is provided by the transmission system operator *50hertz Transmission GmbH* [27]. Exemplary data of the year 2017 is shown in Fig. A.12.

The analysis of the performance of SCI requires household load profiles and photovoltaic generation profiles. Therefore, 74 load profiles published by the *HTW Berlin* are used [28]. Moreover, one photovoltaic profile measured at *TU Munich* which was already published in several previous papers [17,19,29] was used. These profiles also have a resolution of one second. To perform PS with a storage system, industry load profiles are needed. Therefore, 36 annual industry profiles with a resolution of 15 min are gathered within the *EffSkalBatt* project² Frequency data, household load profiles and industry load profiles work as IPs for SimSES (see Fig. 1) which will be explained in Section 3.

2.2. Data processing

The gathered data of frequency, load and photovoltaic profiles is processed before using them within the simulations. The frequency data for performing FCR with a BESS contains some doubtful values (< 49 Hz or > 51 Hz). All such values were replaced by linear interpolation of frequencies before and after. As the raw industry load profiles used for PS have a resolution of 15 min, this data is transformed into profiles with a resolution of one second. For this reason, the following procedure is applied to create second-based profiles: First, the 15-min points are interpolated linearly to create points based on minutes. Then random numbers are build, which replace each interpolated value. Each random number lies within the coefficient of variation of 0.25 of the normal distribution with a mean of the interpolated value. Afterwards, the minute-based values are interpolated linearly again to reach a second-based load profile.

This procedure only estimates the high-resolution load profile. Possible load peaks that just appear for a few seconds are not taken into account. Those short peaks are crucial when regarding battery lifetime and safety [30,31]. Within the application of PS the presented procedure to reach second-based load profiles is sufficient, as the storage system only has to provide the required energy when peaks appear as long as the storage's power is sufficient. The required energy can also be extracted from the 15-min load profile. Moreover, the yearly industry load profiles are chopped to match a Monday to Sunday pattern.

2.3. Normalization

After the aforementioned data pre-processing, the industry profiles are normalized, which is necessary for a comparison of profiles. The

² EffSkalBatt Project: Efficient scalable system technology for stationary storage systems. Research project funded by the Federal Ministry for Economic Affairs and Energy (BMWi) with grant number 03ET6148 (<http://www.ees.ei.tum.de/en/research/effskalbatt/>).

industry profiles are normalized to their maximum value within the year. Thus, the maximal value of each profile is one and the minimal value is zero. This normalization method on each highest peak might differentiate profiles that are similar except for their highest peaks. If only those load profiles were compared, this method would not be appropriate. However, regarding the application of peak shaving, which concentrates on the highest peaks, those profiles are very different. With this method of normalization users can compare their own profiles with the published ones and add their profiles to the simulation. The raw data of household load profiles is already normalized to each maximal value.

2.4. Clustering

Prior to the creation of reference profiles from the pre-processed data, a clustering of the different groups of profiles is considered. This is due to the fact that, for example, the industry profiles do not all have homogeneous curves. Thus, similar profiles are clustered into groups. The clustering is performed using the simulation platform MATLAB® and the clustering algorithm k-means with euclidean distances as measure of dissimilarity [32]. The k-means algorithm was chosen, as it appears to be the most prominent one when comparing electric load profiles [33–35]. Other possible clustering methods would have been the hierarchical clustering or self-organizing maps, as published in [36] and [37].

When comparing the household load profiles to each other, they appear very homogeneous. The average value of each yearly household load varies between 0.6% and 4.4% of its yearly maximum value. In addition, the mean absolute deviations of the profiles' offsets lie between 0.8 and 3.6 percentage points. In contrast to that, the industry load profiles show bigger variations. The mean load of each profile lies between 30% and 75% of the profile's yearly maximum. Thus, the industry profiles' offsets are substantially higher than the households' ones due to their increased base load. The industry loads' mean absolute deviations vary between 0.8 and 23 percentage points.

As a consequence, the industry load profiles are clustered into three different groups while the household load profiles remain in one group. The number of three is chosen because three is the best compromise between differentiation and effort.

Cluster 1 and 3 have an average load of 70% to 80% during the day and a base load of 20 to 30% at night but are shifted by a few hours. During the weekend, Cluster 1 exhibits the typical nightly base load while the load of Cluster 3 only sees the base load on Saturdays. In comparison, Cluster 2 does not have a typical day vs. night load profile. During working days the load varies between 50% and 100% and on weekends between 35% and 70%.

3. Simulation framework for stationary energy storage systems

To generate battery profiles and SPs from the IPs in Section 2 the software SimSES was used. SimSES is a modular object-oriented simulation tool, which was initiated by Naumann and Truong [38] and is now being further developed by the authors. The software allows the flexible usage of components, such as the power electronic or battery cell, of a BESS. The software code is programmed in MATLAB®, but will be converted to Python in the future and made available completely open-source. The current open-source version, including the simulation scripts for this publication and a link to the code of SimSES can be found online³. In this chapter the structure of SimSES (Section 3.1), the developed operation strategies (Sections 3.2–3.4) as well as the components used (Section 3.5) will be described.

³ <http://www.ees.ei.tum.de/simses/>

3.1. Simulation structure

In SimSES the battery is implemented as a single-cell Equivalent Circuit Model (ECM). The terminal voltage U_T of each cell is calculated from the Open Circuit Voltage (OCV) and the voltage drop (overvoltage) ΔU across the series resistance R_i , due to the current I (Eq. 1). The OCV is a function of the SOC. The series resistance R_i is dependent on the current direction sign $\text{sgn}(I)$, the temperature T and the SOC.

$$U_T = U_{OCV} - \Delta U = U_{OCV} - I \cdot R_i(\text{SOC}, \text{sgn}(I), T) \quad (1)$$

The Power Electronics (PE) efficiency is modeled as a function which relies on the absolute output power $|P_{\text{Storage}}|$, the rated power P_{Rated} and the current direction $\text{sgn}(I)$ (Eq. 2). Fixed PE efficiency values or other functions, for example based on own investigations, can be modeled in SimSES as well. Beside the Direct Current (DC)/Alternating Current (AC) link, the PE can also include a transformer model.

$$\eta_{PE} = f(|P_{\text{Storage}}|, P_{\text{Rated}}, \text{sgn}(I)) \quad (2)$$

The core of SimSES is the EMS, which allows to simulate various tasks for a stationary BESS. As described in Section 1, the focus of this work is on the single-use applications FCR, SCI and PS.

3.2. Frequency containment reserve

The EMS for providing FCR in SimSES was developed according to the German regulatory framework [39,40]. The requested charging and discharging power $P_{\text{Storage,set}}$ is proportional to the frequency deviation Δf and is dependent on the prequalified power P_{PQ} , which has a minimum of 1 MW (Eq. 3). Below 49.8 Hz or above 50.2 Hz $P_{\text{Storage,set}}$ is set to $\pm P_{PQ}$.

$$\begin{aligned} P_{\text{Storage,set}}(t) &= P_{PQ} \frac{\Delta f(t)}{0.2 \text{ Hz}} & \text{for } |\Delta f| \leq 0.2 \text{ Hz} \\ P_{\text{Storage,set}}(t) &= P_{PQ} & \text{for } \Delta f > +0.2 \text{ Hz} \\ P_{\text{Storage,set}}(t) &= -P_{PQ} & \text{for } \Delta f < -0.2 \text{ Hz} \end{aligned} \quad (3)$$

If the SOC falls below a predefined lower limit (SOC_{low}) or it exceeds an upper limit (SOC_{high}) the BESS in these simulations charges or discharges by trading energy on the electricity market, in particular the Intra-Day Market (IDM) [14]. Due to the current legal interpretation (May 9, 2019) [41], a BESS in the FCR market has to ensure that at all times the full prequalified power P_{PQ} can be provided for 15 min as long as the frequency f is in normal progression. The normal progression means that the frequency deviation Δf is continuously less than 50 mHz or none of the following criteria is met:

- $|\Delta f| > 200 \text{ mHz}$
- $|\Delta f| > 100 \text{ mHz}$ for more than 5 min
- $|\Delta f| > 50 \text{ mHz}$ for more than 15 min

The SOC limits also depend on the prequalified power P_{PQ} and the storage capacity E_{BESS} , and are calculated according to Eq. 4.

$$\text{SOC}_{\text{high}} = \frac{E_{\text{BESS}} - 0.25 \text{ h} \cdot P_{PQ}}{E_{\text{BESS}}} \quad \text{SOC}_{\text{low}} = \frac{0.25 \text{ h} \cdot P_{PQ}}{E_{\text{BESS}}} \quad (4)$$

To reach these limits as infrequently as possible, the efficiency must be taken into account and therefore the SOC setpoint is above 50% (Eq. 5). The mean efficiency η_{mean} is calculated at the beginning of the simulations and is dependent on the efficiency of the battery and PE.

$$\text{SOC}_{\text{Offset}} = 0.5 \cdot \frac{(1 - \eta_{\text{mean}}^2)}{(1 + \eta_{\text{mean}}^2)} \quad \text{SOC}_{\text{Set}} = 50\% + \text{SOC}_{\text{Offset}} \quad (5)$$

Additionally to the SOC setpoint shift, the regulatory framework in Germany allows three different DOFs:

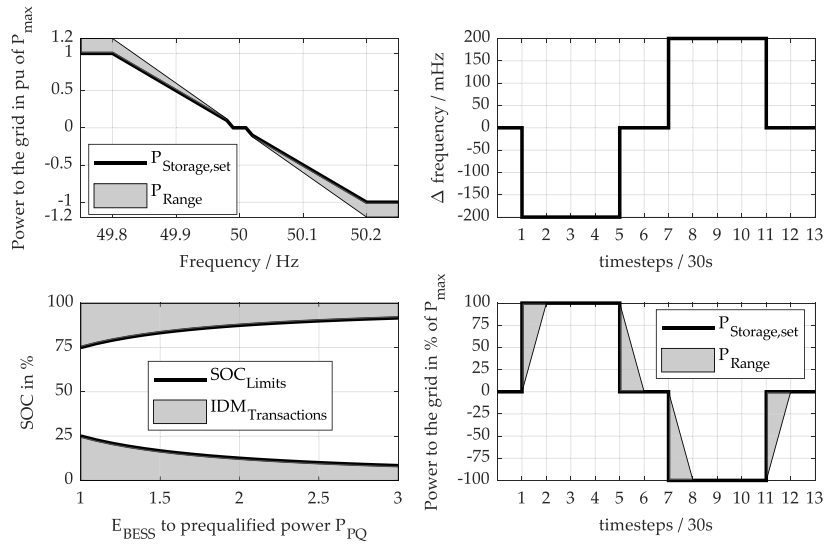


Fig. 2. Degrees of freedom and the SOC limits, depending on the prequalified power P_{PQ} . The top left subfigure shows the frequency dead band and the possible overfulfillment. The two subplots on the right show the slope and the bottom left subfigure shows the SOC limits.

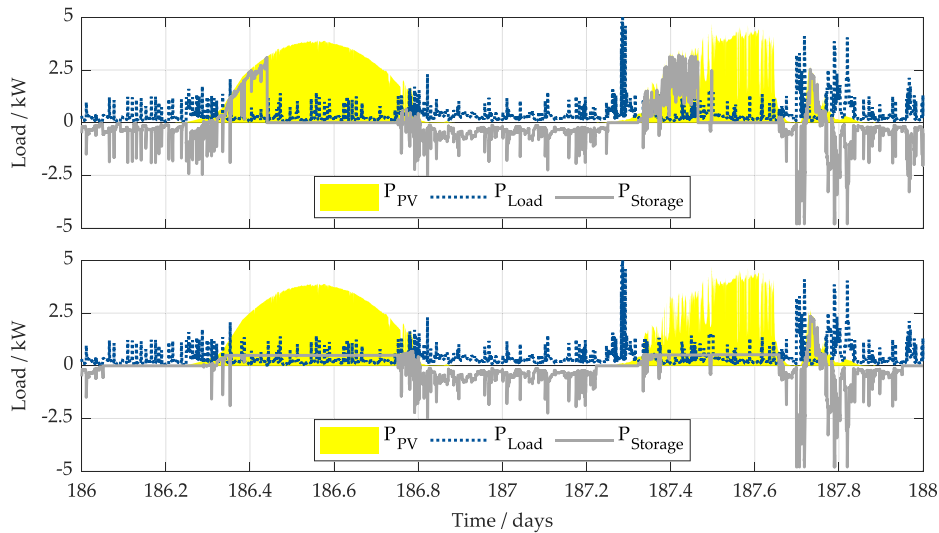


Fig. 3. Operation Strategies (top=*greedy*, bottom=*feed-in damping*) for the Residential Photovoltaic Battery Storage System. The shaded yellow area shows the generation of the PV power system, the blue line shows the load of the household and the gray line shows the storage power (positive=charging). (For interpretation of the references to color in this figure legend, the reader is referred to the web version of this article.)

- **Frequency dead band:** In the frequency range between 49.99 Hz and 50.01 Hz, the output power of the BESS can be set to 0 MW and must not follow the frequency derivation according to Eq. 3.
- **Overfulfillment:** It is allowed to overfulfill the requested power (Eq. 3) by 20 %.
- **Slope:** The requested FCR power (Eq. 3) must be provided within 30 s or earlier. Therefore, the slope of the provided FCR power can be adjusted within the time interval of 30 s allowing to control the charging or discharging rate.

In SimSES all DOF are only used, if the requested power either brings the SOC closer to optimum again or at least not further away. All degrees of freedom as well as the SOC limits, depending on the prequalified power P_{PQ} , are shown schematically in Fig. 2.

3.3. Residential photovoltaic battery storage system

In SimSES two different operation strategies for the SCI of BESS are implemented: *Greedy* and an extension of *feed-in damping* based on Zeh and Witzmann [29].

Greedy

The EMS for the greedy algorithm works with a simple comparison between the generation of the PV power system P_{PV} and the consumption by the household P_{load} at each timestep. Whenever a solar surplus occurs ($P_{PV} > P_{load}$), the BESS is charged and vice versa (Eq. 6). This conventional strategy is shown in Fig. 3 (top). These summer days show that the BESS is fully charged at around 9AM, which causes a rapid rise of the power fed into the grid. Another disadvantage of this strategy is the high charging power, which may lead to a faster decrease of the LIB capacity due to an increase of lithium plating as described in [30].

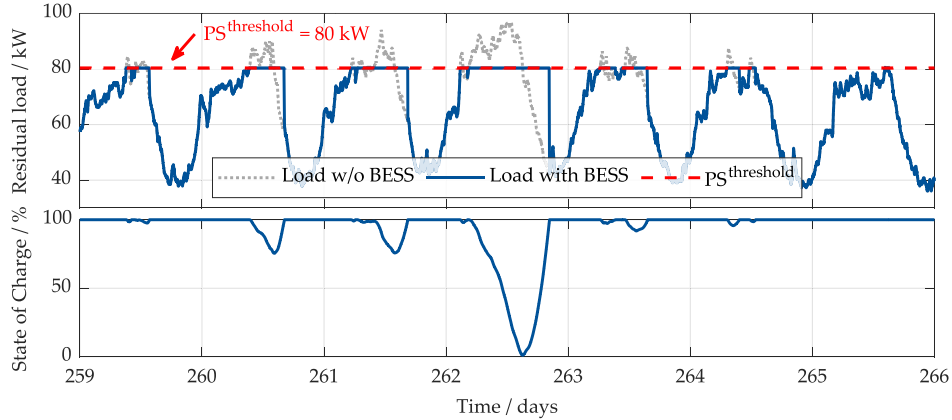


Fig. 4. Exemplary week of an industry load profile and its optimized PS threshold $PS^{threshold}$ following the PS operating strategy. The power above the threshold is provided by a stationary BESS. The solid blue line shows the industry load profile with the PS BESS. The associated SOC is illustrated at the subplot at the bottom. (For interpretation of the references to color in this figure legend, the reader is referred to the web version of this article.)

$$P_{Storage} = P_{PV} - P_{load} \quad (6)$$

Feed-in damping

In order to reduce the maximum power fed into the grid, a nearly constant BESS charging power $P_{Storage,Ch}$ during the whole daytime is calculated by the EMS. Reducing the maximum feed-in power allows for a higher self-consumption rate, if the maximum feed-in power is limited by the distribution grid operator as described in [19]. If a surplus ($P_{PV} > P_{load}$) occurs, the charging power $P_{Storage,Ch}$ is calculated by dividing the remaining battery capacity $E_{BESS,re}$ by the predicted remaining time t_{re} , until the load is higher than the PV generation, and the mean efficiency η_{mean} of the BESS (Eq. 7).

In this work, a perfect foresight for the duration of PV generation is assumed. If there is a higher consumption by the household than generation by the PV power system, the BESS is discharged. Fig. 3 (bottom) displays this operation strategy. In contrast to the *greedy* algorithm, the charging power is constant during the whole first day. The second day shows a more cloudy day. The remaining time t_{re} at this day is smaller than in day 1, so according to Eq. 7 the charging power $P_{Storage,Ch}$ is higher. In addition, the second day also shows that after the PV generation surpasses load again ($P_{PV} - P_{load} > 0$), the remaining time t_{re} is recalculated. In this case, the storage can be charged with the full power, due to the short remaining time t_{re} .

$$P_{Storage,Ch} = \frac{E_{BESS,re}}{t_{re} \cdot \eta_{mean}} \quad \text{for } P_{PV} > P_{load} \quad (7)$$

3.4. Peak shaving storage system

Motivated by a tariff system consisting of an energy and a power related component, the storage application PS has the goal to minimize the maximum power peak value within a defined accounting period. Particularly large electricity consumers (annual demand > 100 MWh (in Germany)) can reduce the peak power provided by the power grid, which directly results in reduced operating expenses in form of reduced grid charges [42].

In order to reduce the power at the point of common coupling, the excess demand has to be covered by another power providing unit, such as a BESS. The BESS is used to decouple the supply and demand over a specified time. To maximize the benefit of the application, it is important that the dimensioning of the storage system is the best possible match for the power demand curve. Similar to other publications [43–45], a two-step approach of a linear programming algorithm and SimSES is applied.

First, a pre-processing linear optimization algorithm is used to

Table 2

Parameters of the simulated Lithium-ion cells. Celltype 1 is a Lithium-ion battery with a Lithium-Iron-Phosphate (LFP) cathode and a Carbon-Graphite (C) anode. Celltype 2 is a Lithium-ion battery with a Nickel-Manganese-Cobalt (NMC) and a Carbon-Graphite (C) anode.

Parameter	Unit	Cell 1 [46]	Cell 2 [50]
Cell Identification	-	US26650FTC1	IHR18650A
Manufacturer	-	Murata	E-ONE Moli Energy Corp.
Chemistry	-	LFP:C	NMC:C
Capacity	mAh	2850	1950
Max. Charge Current	A	2.85	2
Max. Discharge Current	A	20	4
Nominal Voltage	V	3.2	3.7
Voltage Range	V	2 - 3.6	3 - 4.2

minimize the power value for the peak shaving threshold $PS^{threshold}$, while it complies with the necessary constraints, such as meeting the power demand, and satisfying the energy and power specifications of the BESS. Depending on the shape of the load profile, the resulting value of the power threshold varies. Secondly, the resulting peak shaving threshold is used as an input parameter for the operation strategy within SimSES. This operation strategy works as follows: as soon as the power at the point of common coupling (from the grid) is above the specified threshold, the additionally required power is provided by the BESS, as illustrated in Fig. 4. In addition, the BESS will recharge if the power value is below the previously determined optimal peak shaving threshold. This ensures that the charging of the storage system does not cause the exceedance of the threshold.

Through a close coordination of the two simulation tools in the chosen two-stage approach, both a near optimal PS threshold is found and simultaneously, the detailed technical specifications of the BESS are simulated via SimSES.

3.5. Simulation parameters

The battery cell used in all simulations was a LIB with a Lithium-Iron-Phosphate (LFP) cathode and a Carbon-Graphite(C) anode [46]. It is worth to mention, that other LIB types are also implemented in the simulation tool but the LFP:C cell is a promising battery chemistry for stationary applications, because of its characteristics such as high thermal stability, long cycle as well as calendar lifetime [3,47,48]. The parameterization of the ECM for the simulated LFP:C cell was carried out by Naumann [49].

To analyze the effects of cell selection, another cell with a Nickel-

Table 3

Summary of the parameters for the simulation of the three applications with SimSES.

Application:	FCR	SCI	PS
Battery	LFP:CNMC:C	LFP:C	LFP:C
Storage Capacity	1.6 MWh	5 kWh	100 kWh
Max. Power	1.6 MW	5 kW	40 kW
PE mode	modular single unit	single unit	single unit
PV Power	-	5 kWp	-
Operation Strategy	15 min criteria	greedy feed-in damp	simple
PER	0.7	-	-
IDM Power	0.48 MW	-	-
PS-Limit	-	-	variable 62 - 92%

Manganese-Cobalt-Oxide (NMC) cathode and a C anode [50] was also simulated in the FCR application. The characterization of this cell is based on the work of Schuster [51]. The self-discharge and the temperature dependency of the cell is neglected in this work. Table 2 summarizes the parameters of these battery cells.

The PE is implemented as a function, which shows a high efficiency above 10% of the rated power P_{Rated} (Eq. 8). Exemplary values used for a high efficiency PE are $k = 0.0345$; $p_0 = 0.0072$, according to Notton et al. [52]. Here η_{PE} is independent of the direction of the power flow and no hysteresis is implemented. The maximum efficiency is observed at $0.46 \cdot P_{\text{Rated}}$ with an efficiency $\eta_{\text{PE}} = 96.9\%$.

$$\eta_{\text{PE}} = \frac{\frac{|P_{\text{Storage}}|}{P_{\text{Rated}}}}{\frac{|P_{\text{Storage}}|}{P_{\text{Rated}}} + p_0 + k \cdot \left(\frac{|P_{\text{Storage}}|}{P_{\text{Rated}}}\right)^2} \quad (8)$$

Frequency Containment Reserve

As already shown by others [3,13,14], a BESS in the FCR market is mostly in part-load operation. In order to achieve a high part-load efficiency, we minimized the inverter losses by modularization of the PE-unit into three identical smaller units based on the work of Schimpe et al. [53]. At 80% power of the rated power of PE unit 1, PE unit 2 starts to work. At 80% power of the rated power of PE unit 1 and PE unit 2, PE unit 3 starts to work. There is no hysteresis included in the simulations, which means that the switch-off values are equal to the switch-on values. According to the modeled PE efficiency, the average efficiency of this PE combination is 96%. This PE combination, together with the simulated LIB ($\eta_{\text{LIB}} = 96\%$), results in an SOC shift, according to Eq. 5, of 54%.

In this work the BESS capacity E_{BESS} is set to 1.6 MWh with a maximum power of 1.6 MW. The prequalified power P_{PQ} is 1.12 MW, which results in a Power to Energy Ratio (PER) of 0.7. Thus, the available IDM power is 30% of the total BESS power. The losses of a transformer model for a potential integration to higher grid voltage levels, which would be necessary having a 1.6 MW / 1.6 MWh storage, are neglected.

Residential Photovoltaic Battery Energy Storage System

To ensure comparability, the simulations are carried out with a fixed annual household load $E_{\text{load,a}}$ of 5,000 kWh, which rounded corresponds to the mean of the IP. According to the work of Weniger et al. [21] and Hoppmann et al. [54], the PV system and the BESS can be operated economically in the ratio 1:1:1. An annual household load $E_{\text{load,a}}$ of 5,000 kWh leads to a PV peak power of 5 kWp and a BESS capacity E_{BESS} of 5 kWh.

Peak Shaving Storage System

For the PS application, 36 anonymized annual load profiles from commercial electricity consumers are utilized. In order to generate comprehensive standardized profiles, all normalized load curves are scaled to a peak power of 100 kW (see Section 2.3). The BESS is characterized by a nominal energy content of 100 kWh. We assume that

100% of the nominal storage energy and a rated power of 40 kW for the system's PE unit (consisting of a single inverter) can be used to operate the application.

Table 3 summarizes the parameter set for each simulation in SimSES. Other components, such as

- a transformer model for a potential integration to higher grid voltage levels,
- a cell-to-cell connection resistance,
- a battery management system,
- a thermal model for each cell as well as a thermal model for the whole storage system,
- an aging model of the battery cell as well as all other subcomponents,

were neglected in this paper, but can be modeled in principle in SimSES.

4. Storage profile analyzer tool

One goal of this work is finding reference SPs for the different storage applications. Therefore, groups of SPs were created using the software SimSES. In this chapter, a storage profile analyzer tool is presented which aims to extract the reference SP for each of the groups. The idea and the reasons for the analyzer tool are described in Section 4.1. Afterwards, the different characteristics are explained in Section 4.2. Finally, the determination of reference profiles from the characteristics is described in Section 4.3. Moreover, Appendix B provides some further analysis of the SPs including the distribution of the energy rate (E-rate). The E-rate at each timestep i is defined according to Eq. 9.

$$E_{\text{rate},i} = \frac{P_{\text{Storage},i}}{E_{\text{BESS}}} \quad (9)$$

4.1. Reasons for the storage profile analyzer tool

The extraction of a reference SP can be done in different kind of ways. Taking the mean SP by calculating the mean of all the SPs for the different applications is one option. This would lead to a smoothing of the profiles. Distinctive peaks would be neglected and the profiles would not be representative anymore. A more viable approach is the selection of one SP as reference SP for each application. Here, a median profile has to be found which represents the group of profiles. This selection is done using the storage profile analyzer tool. The tool takes the load of the storage and SOC data as input variables and outputs the characteristics described in the following subsection.

4.2. Extracted characteristics from profiles

To better analyze and compare the storage load profiles, six characteristics were defined which are distinctive for the profiles of the different applications. Those six characteristics aim to represent the differences within the storage applications.

1. Number of full equivalent cycles (FEC)

The total number of cycles FEC_{year} within the year is calculated by dividing the positive energy throughput $E_{\text{year}}^{\text{pos}}$ by the storage capacity E_{BESS} (Eq. 10). The FEC_{year} varies between the applications and affects the aging of the battery [30].

$$\text{FEC}_{\text{year}} = \frac{E_{\text{year}}^{\text{pos}}}{E_{\text{BESS}}} \quad (10)$$

2. Efficiency (η_{BESS})

The efficiency of the analyzed storage η_{BESS} is calculated by counting the yearly energy that is extracted from the storage system $E_{\text{year}}^{\text{neg}}$ divided by the energy that is stored in the storage system $E_{\text{year}}^{\text{pos}}$. The SOC at the beginning of the year and at the end of the year is taken into account as well (Eq. 11). This characteristic displays the losses in the storage system

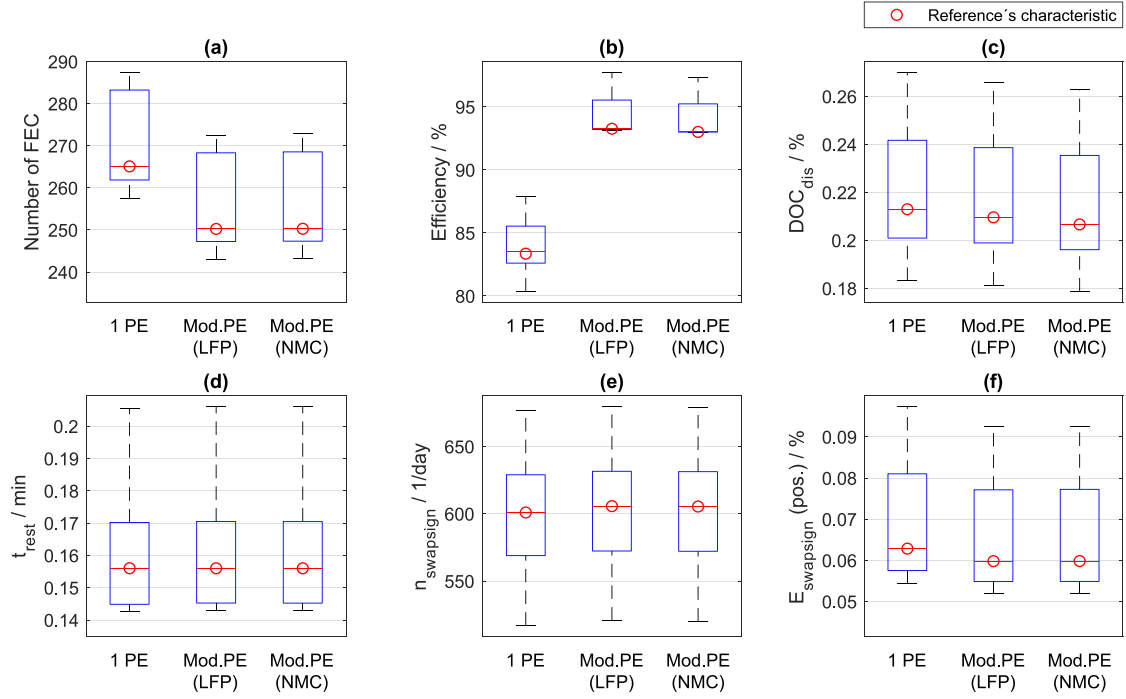


Fig. 5. Characteristics of a BESS providing FCR. The left box in each plot shows a BESS with one PE unit and a LFP:C cell. The center one in each plot shows a BESS with three modular PE units and a LFP:C cell and the right box in each plot shows a BESS with three modular PE units and a NMC:C cell.

while operating in the specific application. For the calculation of the efficiency the surrounding temperature and the thermal management are not taken into account.

$$\eta_{\text{BESS}} = \frac{|E_{\text{year}}^{\text{neg}}|}{E_{\text{year}}^{\text{pos}} - [\text{SOC}_{\text{end}} - \text{SOC}_{\text{start}}] \cdot E_{\text{BESS}}} \quad (11)$$

3. Cycle depth in discharge direction (DOC_{dis})

The average DOC in discharge direction is calculated by using the SOC data of the current profile. This characteristic describes how deep the battery is discharged before recharging it. A higher DOC may lead to a higher cyclic aging of the battery [55]. To enable a comparison between the applications (different capacities) the DOC is measured in percentage of the total battery capacity. In SimSES a half-cycle detector is implemented. The beginning of the half-cycle is a change from charging respectively resting to discharging. Analogously the end is at every change from discharging to charging or if the BESS reaches an SOC of 0%. Then the DOC is calculated by subtracting the SOC at the beginning and the SOC at the end of the half-cycle (see Eq. 12). Taking only the change from discharging to charging leads to a dependency of the DOC on the resolution. Many small changes of load might outweigh larger trends.

$$\text{DOC}_{\text{dis}} = \text{SOC}_{\text{cycle,start}} - \text{SOC}_{\text{cycle,end}} \quad (12)$$

4. Number of changes of sign (n_{swapsign})

Depending on the storage application, the SP might change from charging to discharging and vice versa very often or just a few times per day. Those changes of signs activate the power electronics. When analyzing experimental SPs the user of the storage profile analyzer tool would have to define a threshold value to prevent faults of noise when the SP is close to zero. As the simulated SPs do not show the noise, a threshold value is not necessary.

5. Length of resting periods (t_{rest})

As the BESS is not used continuously over time, the length of resting periods represent another characteristic. During those times, the BESS is neither charged nor discharged. Here, the average value of resting

period length in minutes is calculated. Depending on the application the length of those resting periods may vary significantly. This characteristic is chosen because auxiliary users can be turned off and other applications can be performed during long resting periods.

6. Energy between changes of sign (E_{swapsign})

Another chosen characteristic is the energy that is charged or discharged between changes of signs, respectively. The amount of the energy is normalized to the battery's capacity and thus comparable between the different applications with different capacities. Here charged and discharged energy are calculated separately.

4.3. Determination of reference profiles

The storage profile analyzer tool extracts the different characteristics from each of the profiles of the specific group of SPs. For each application the characteristics can then be displayed in boxplots to visualize the spread and show the median values.

To determine each reference profile the percentage error δ of each profile's characteristic to the median characteristic is calculated (Eq. 13). This is done by subtracting the median of the characteristic \tilde{K}_j from the profile's characteristic K_j , dividing the difference by the median of the characteristic and multiply the result with 100. Here, i is the number of the profile and j the number of the characteristic.

Afterwards, the root mean square percentage error (RMSPE) is identified for each profile (Eq. 14). This is done by taking the sum of the absolute percentage errors, dividing it by six (six characteristics), squaring it and extracting the root. This way all characteristics are weighted equally.

$$\delta_{i,j} = \frac{K_{i,j} - \tilde{K}_j}{\tilde{K}_j} \cdot 100 \quad (13)$$

$$\text{RMSPE}_i = \sqrt{\left(\frac{\sum_{j=1}^6 |\delta_{i,j}|}{6} \right)^2} \quad (14)$$

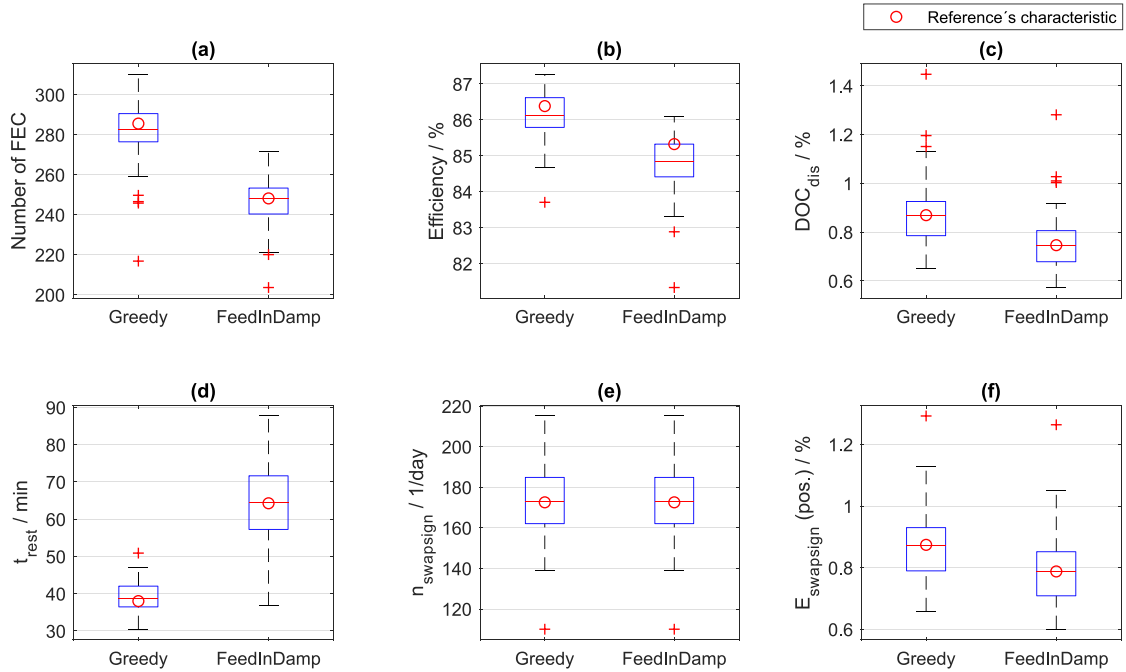


Fig. 6. Characteristics of an SCI performing BESS. The left box in each plot shows a SCI with *greedy* algorithm. The right box in each plot shows a SCI with the *feed-in damping* algorithm.

The reference profile is then chosen as the profile which has the minimum root mean squared percentage error. Thus, this profile represents the group of profiles, while maintaining its variations and peculiarities.

5. Results and discussion

The storage profile analyzer tool outputs characteristics and reference SPs which will be compared and discussed in this section. First, the characteristics of the different applications (FCR, SCI, PS) are displayed in Section 5.1. Here, a comparison is done within each application between power electronics and battery technology (FCR), operation strategies (SCI) and the three PS clusters. Afterwards, the characteristics of the reference SPs for different applications are compared to each other and thus differences in usage and load are explained (Section 5.2). Finally, exemplary days and weeks of the reference SP are shown and discussed (Section 5.3).

5.1. Characteristics of storage profiles of different applications

As described in Section 3, the simulated storage applications are FCR, SCI and PS. For each group of SPs performing one application, the different characteristics can be displayed in boxplots. These boxplots show the spread of the characteristics of a storage system performing the specific application. Each boxplot is created by using the characteristics of all the SPs. That means that for FCR five SPs, for SCI 74 SPs and for PS 36 SPs were used. Each profile contributes to each boxplot with one value. Those are the yearly number of FEC, the efficiency (η_{EES}) over the year, the average DOC in discharge direction, the average length of resting periods (t_{rest}), the average changes of sign per day ($n_{swapsign}$) and the average energy between changes of signs ($E_{swapsign}$). Each boxplot contains a red line which represents the median value. Moreover, the blue boxes display the 25th and the 75th percentiles, while the black whiskers correspond to a maximal absolute value of 2.7 times the standard deviation. The red crosses which are displayed above and underneath the boxplots show outlier outside of the box and whiskers. In

addition, the red dot in each boxplot shows the value of the reference profile's characteristic (see Section 4.3). The average distance between the median value and the reference value is 2%. The distributions of SOC, DOC in discharge direction and E-rate for all profiles and for the reference profiles of each application can be found in the appendix (Figs. B.21–B.28).

Fig. 5 displays the SPs characteristics of a BESS providing FCR. The PE units were varied as one differentiation while using the same battery technology (LFP:C). First of all, one PE unit was used (each left boxplot). Then a modular PE device was applied (each center boxplot). In addition to that, as a third boxplot, the LIB technology was varied as described in Section 3.5. Here also a modular PE device was used with a NMC:C LIB.

The first characteristic (Fig. 5 (a)) is the number of FEC within the year. Using only one PE unit leads to an increased number of FEC within the year compared to modular PE units. The high number of yearly cycles (> 240 FEC in all simulations), in combination with a small DOC (Fig. 5 (c)) requires a BESS, which has a high cycle stability in the middle SOC range (see also Appendix B.21–B.23).

The efficiency (Fig. 5 (b)) can be significantly increased when using modular PE units or at least having a PE with a high part-load efficiency. Furthermore, there are almost no long resting periods (Fig. 5 (d)) and the number of sign changes (Fig. 5 (e)) is higher compared to the other applications under test. Therefore, the PE must have a high control speed to meet these requirements. The positive energy of changes of sign (Fig. 5 (f)) is a little smaller when having modular PE compared to only one device. The variation of the cell shows hardly any influence - underlining, that choosing a suitable PE design is key for improving the system's efficiency. It is worth to mention here, that battery aging was not modeled.

Fig. 6 displays the SP characteristics of a SCI BESS. The order of the six boxplot-types is the same as described before. Only the ranges of the y-axes are different as a comparison within the SCI BESS is done at this point. Here, each diagram contains one boxplot for the *greedy* operation strategy and one for the *feed-in damping* strategy (see Section 3.3). The smoothing of the load at *feed-in damping* strategy leads to a smaller number of FEC (Fig. 6 (a)), a smaller DOC (Fig. 6 (c)), a higher length of resting periods (Fig. 6 (d)) and a smaller amount of charged energy

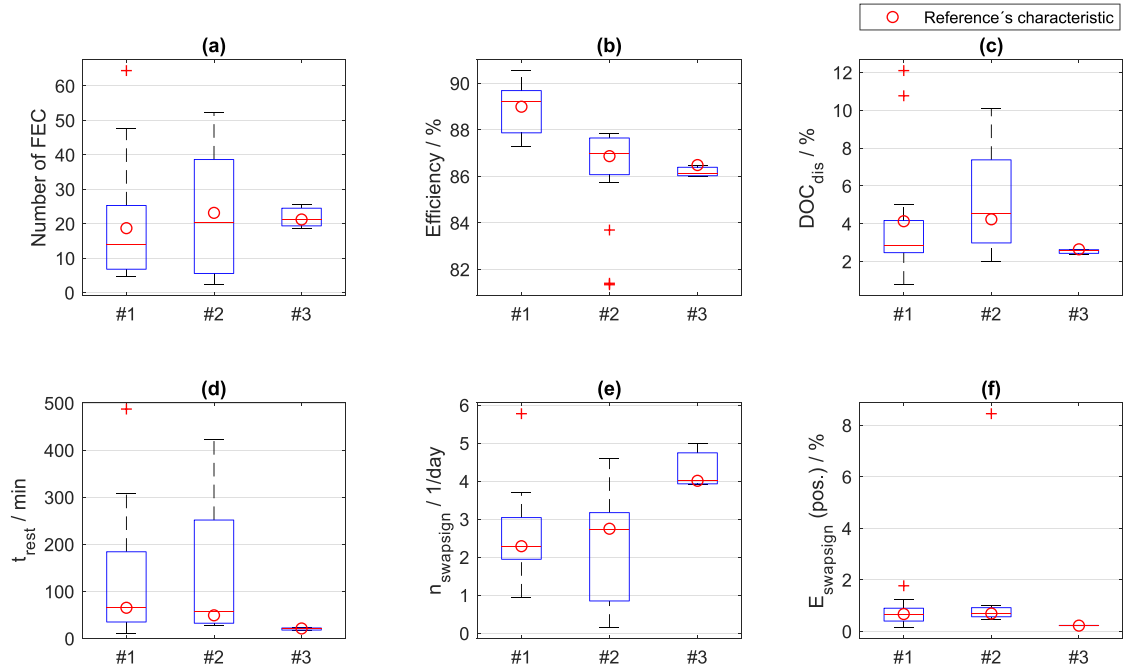


Fig. 7. Characteristics of a BESS in a PS application. The left box in each plot shows the characteristics for IP cluster 1. The box in the center for IP cluster 2 and the right one for IP cluster 3.

between sign changes (Fig. 6 (f)) compared to the *greedy* algorithm. The efficiency of the SCI BESS with *feed-in damping* algorithm is lower than with *greedy* algorithm (Fig. 6 (b)). This is due to the fact that the *feed-in damping* storage system is more often in the partial-load range where the PE has a lower efficiency.

While the lower efficiency is a disadvantage, the *feed-in damping* algorithm also leads to smaller Es-rate and lower rest times of high SOC compared to *greedy* algorithm (Appendix B.24 and B.25). Those two properties are advantages of the *feed-in damping* algorithm as longer periods of high SOC may lead to an increased calendar aging [56]. Home storage system manufacturers should take these findings into consideration and try to avoid simple rule based strategies (*greedy*). Moreover, both algorithms lead to the same number of changes of signs per day (Fig. 6 (e)), as only the time of changes vary.

The SP characteristics of a BESS in the PS application are displayed in Fig. 7. The order of the diagrams is the same but the range of y-axes is different. The three box plots in each diagram contain the SP characteristics of the three clusters of IP (see 2.4). In contrast to the other two applications (FCR and SCI) the spread of the characteristics within each group is higher. The DOC, for example, varies between 2% and 10% for cluster 2. Thus, the storage's load varies significantly depending on the industry IP. Only cluster 3 shows relatively consistent characteristics in all diagrams.

5.2. Comparison of characteristics of reference storage profiles

After the analysis of the characteristics of each application's SPs, a comparison between application SPs is done in this subsection. Therefore, the six characteristics of each reference profile are displayed in spider diagrams with the same ranges to enhance comparability (Fig. 8). For the application of FCR the reference profiles' characteristics of one PE unit and a modular PE device are displayed (top). The modular PE with an NMC:C cell is not displayed as its characteristics are almost similar to the LFP:C ones (see Fig. 5). For SCI the reference characteristics of the two algorithms are shown (middle) and the PS characteristics are displayed for the three clusters (bottom).

FCR leads to a relatively high number of cycles (> 240 FEC) and small average DOCs of 0.2%. Moreover, the average resting period length is small (< 10 s) and the average number of changes of sign is relatively high (600 per day). This is due to the fact, that the grid frequency fluctuates around 50 Hz and the storage system reacts quickly on frequency changes by charging or discharging the battery (see Fig. A.12). The efficiency of the storage system performing FCR with modular PE is relatively high (93%). Using only one PE device leads to a reduced efficiency of 83%. This is because of the low converter efficiency in part-load operation.

Operating the storage system for SCI leads to similar number of cycles within the year as the application of FCR. Compared to the modular PE FCR application, the efficiency is lower (approx. 85%). The average DOC is higher when performing SCI than when performing FCR (0.9% to 0.75%). The average length of resting periods is much higher when operating as a SCI BESS than when performing FCR (38 to 65 min). During winter nights, for example, the storage rests for several hours, which increases the average resting period length. Moreover, the changes of signs per day are much lower than the characteristic of FCR. 170 changes of signs per day on average still appear to be high for a SCI BESS. This is due to the fact, that during charging of the storage system by photovoltaic energy, a short increase of load or a decrease of generation (e.g. clouds) can lead to a change of sign.

Performing PS as an application leads to a much smaller number of cycles (FEC < 30) and changes of sign ($n_{swapsign} < 4$ per day) compared to FCR or SCI. In contrast to that, the average DOC is higher than the other applications reference characteristics (2% to 5%). The average length of resting periods is in the same range as the SCI characteristics (20 to 65 min). Thus, it is in resting mode for a longer period of time, it does not switch between charging and discharging very often and it is discharged relatively deep, when a discharge cycle is initiated. The storage's efficiency when performing PS is between 86% and 89%. The small number of FEC, in addition to the long average length of resting periods suggests potential benefits of application stacking (multi-use) for this application. However, this requires a sufficient power load forecast.

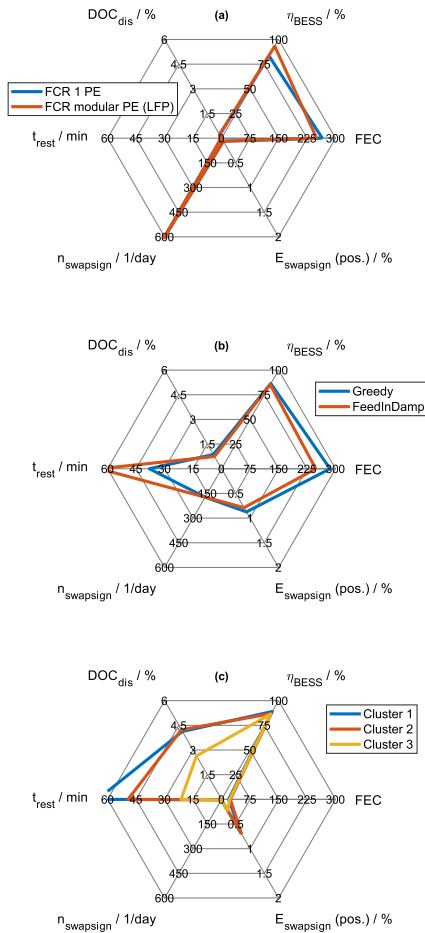


Fig. 8. Spider diagrams of the six characteristics of each reference profile (a: FCR, b: SCI and c: PS).

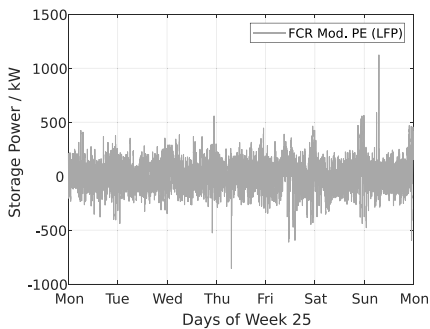


Fig. 9. Reference Storage Profile of a BESS providing FCR. Exemplary week in June.

5.3. Reference storage profiles of different applications

After the analysis of the SP characteristics and the comparison between the different storage applications, exemplary weeks of the reference profiles are shown in this Section. As described in Section 2, the FCR reference profile and the SCI reference profile exist for a whole year. The PS reference profile is for 51 weeks starting with a Monday. Appendix A shows all complete reference profiles. All reference SPs as

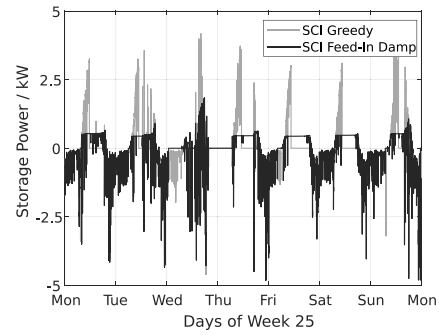


Fig. 10. Reference Storage Profile of a BESS performing SCI. Exemplary week in June.

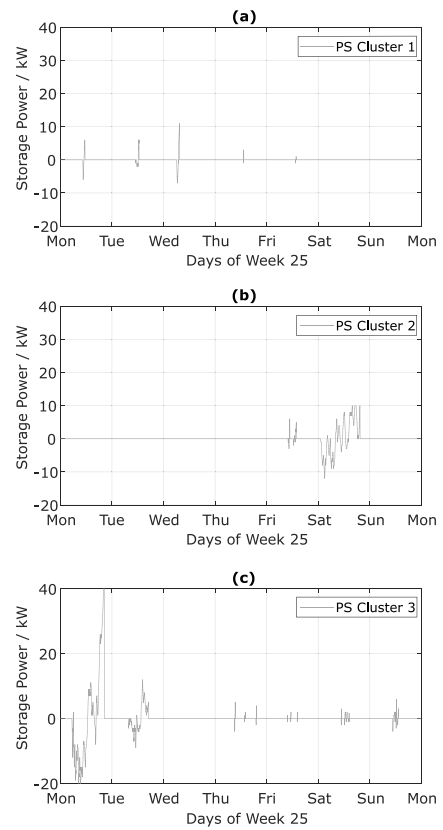


Fig. 11. Reference Storage Profile of a BESS in a PS application. Exemplary week in June. (a: Cluster 1, b: Cluster 2 and c: Cluster 3).

well as the SOC at each timestep are available online free of charge, and are hosted on the servers of TU Munich [57].

As an example, the 25th week of the reference profile of the FCR application with modular PE and LFP:C battery technology is displayed in Fig. 9. The diagram's y-axis shows that the maximum power in this week is around 1.1 MW. IP for this resulting reference profile was the second year frequency profile [27] (year 2014, see Section 2.1). The profile shows a high fluctuation, which results in small DOCs, a lot of changes of sign and very short resting periods (see Section 5.2). To enable a greater degree of clarity, the profiles of FCR with one PE module and with NMC:C cell (modular PE) are not displayed within the diagram. These two show a similar course with high fluctuation.

Fig. 10 depicts the 25th week of the reference profiles of the two SCI BESS with *greedy* and *feed-in damping* algorithm. Input profile for those two resulting reference profiles was the 28th household load profile from the 74 *HTW-Berlin* load profiles [28] (see Section 2.1). As this week falls in June, the storage system gets charged by the PV generation during the day. In the evening and during the night it gets discharged until the battery is empty (e.g. Thursday night). The differences in the two operating strategies were explained in Section 3.3. The *feed-in damping* profile shows the typical limitation of the energy feed into the grid, which leads to lower Es-rate for the BESS.

The reference profiles (exemplary week 25) of the three clusters of PS application are shown in Fig. 11 (a: Cluster 1, b: Cluster 2, c: Cluster 3). Here, the maximal storage power was chosen as 40 kW (see Section 3.5). As described in the previous section, the PS BESS has the fewest number of cycles and changes of signs per day. The reference SPs confirm these numbers. Moreover, the relatively long resting periods and the differences between the three clusters are visible as well. The PS threshold values for the three clusters are set to 66 kW, 83 kW and 80 kW according to the pre-processing optimization in Section 3.4.

6. Conclusion and outlook

In this paper we presented a method to create standard profiles for stationary battery energy storage systems, the results of which are available as *open data* for download. Input profiles including frequency data, industry load profiles and household load profiles are pre-processed using a normalization and clustering method. These input profiles are then transformed into storage profiles including the storage power and the state of charge using a holistic simulation framework (SimSES). This modular object-oriented tool was used to analyze three standard applications for stationary battery energy storage systems in detail and an energy management system was programmed for the different applications: (i) The energy management system for providing frequency containment reserve in SimSES was developed according to the German regulatory framework and various degrees of freedom; the efficiency was taken into account to minimize the intra-day market transactions. Moreover, a modular power electronics topology was used. (ii) In addition to a simple *greedy* algorithm, a *feed-in damping* algorithm has been implemented for a residential battery energy storage system, which charges the storage system at a low E-rate over the whole day. (iii) A two-step approach with a linear programming algorithm and SimSES was applied for an industrial peak shaving battery energy storage systems to minimize the maximum power peak value.

The results have been post-processed using a storage profile analyzer tool in order to figure out six key characteristics of the different applications. These characteristics are essential for the design of a stationary battery energy storage system. For example, for a battery energy storage system providing frequency containment reserve, the number of full equivalent cycles varies from 4 to 310 and the efficiency from 81% to 97%. Additional simulations done with SimSES for one year showed a degradation from 4% (frequency containment reserve) to 7% (peak shaving).

The *open data* available results, including storage power as well as state of charge for all reference storage profiles, with a resolution of one second can be used for comparison with other self-developed energy management systems. Furthermore other system topologies or self-developed power electronic models can be simulated with SimSES and the simulation-outcome can be assessed against the numbers presented in this paper. Scientists are encouraged to conduct aging studies or battery management system tests using the platform SimSES and data provided herein.

In order to compare both different cell chemistries as well as storage technologies, future work could focus in more detail on battery degradation. Future applications for stationary battery energy storage systems could be: buffer-storage system to reduce the peak power at (fast-) charging stations, uninterruptible power supply or island grids. As soon

as the first data sets are available, it might be worthwhile to analyze these use cases more precisely.

Authors Contribution

D.K. was the principle author tasked with coordinating and writing the paper and developing SimSES; B.T. programmed the profile analyzer tool and wrote contents within the data preparation, analysis and results; S.E. helped with programming and writing the peak-shaving algorithm; A.P. helped with gathering data and the selection of the characteristics. M.M. was co-responsible for the dynamization of the input data and helped with the selection of the characteristics. Both O.B. and A.J. contributed via fruitful scientific discussions. H.H. reviewed the manuscript and was giving valuable input throughout the manuscript preparation.

Declaration of Competing Interest

The authors declare that they have no known competing financial interests or personal relationships that could have appeared to influence the work reported in this paper.

Acknowledgments

This work was financially supported by the Federal Ministry for Economic Affairs and Energy within the open_BEA project (Grant No. 03ET4072) and the EffSkalBatt project (Grant No. 03ET6148). Both projects are cared by Project Management Juelich. The responsibility for this publication rests with the authors.

Appendix A. Input and reference profiles

Fig. A.12 shows the frequency data (IP) of the whole year 2017 (top) and of one exemplary day (185) of year 2017 (bottom). The Figs. A.13–A.20 show the complete reference profiles. The FCR reference profile and the SCI reference profile are for a whole year. The PS reference profile are for 51 weeks starting with a Monday. All reference

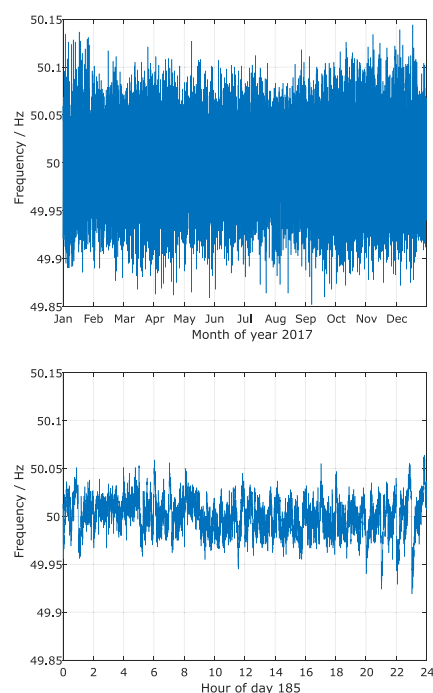


Fig. A.12. Sample sections of frequency data of the whole year 2017 (top) and of one exemplary day (185) of year 2017 (bottom).

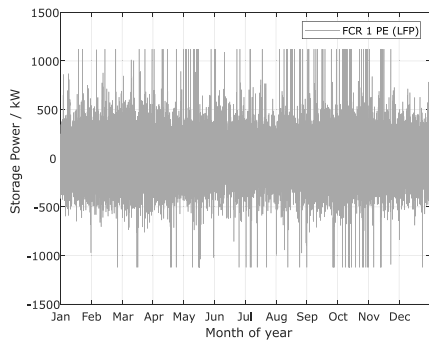


Fig. A.13. Yearly reference profile of a simulated BESS with one PE unit and a LFP:C cell providing FCR.

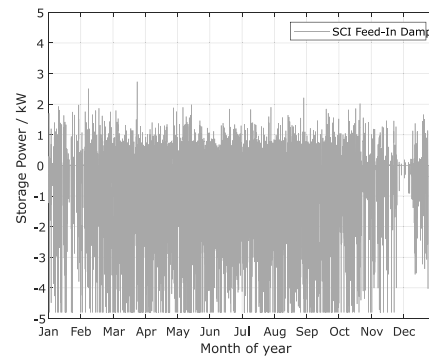


Fig. A.17. Yearly reference profile of a BESS for SCI with one PE unit and a LFP:C cell with the *feed-in damping* algorithm.

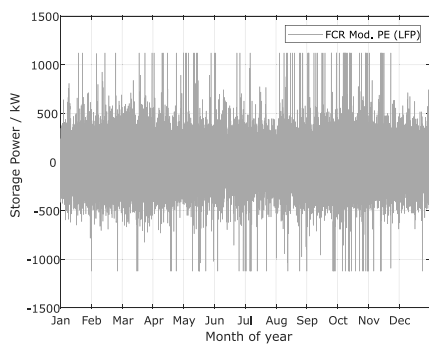


Fig. A.14. Yearly reference profile of a simulated BESS with three modular PE units and a LFP:C cell providing FCR.

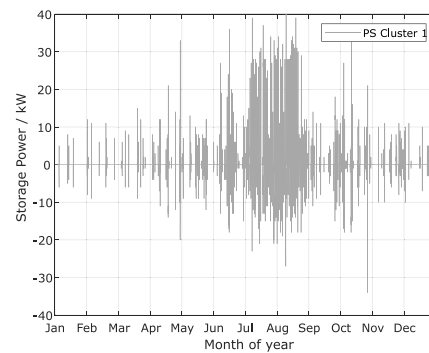


Fig. A.18. Yearly reference profile of a BESS in the application of PS with one PE unit and a LFP:C cell in cluster 1.

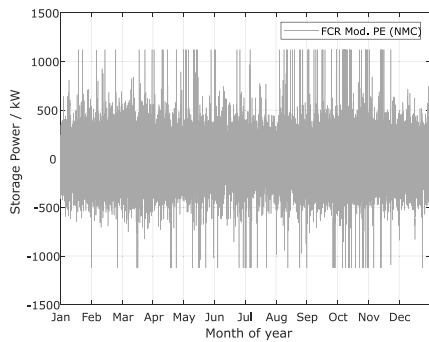


Fig. A.15. Yearly reference profile of a simulated BESS with three modular PE units and a NMC:C cell providing FCR.

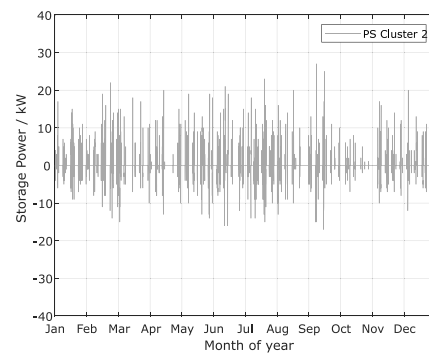


Fig. A.19. Yearly reference profile of a BESS in the application of PS with one PE unit and a LFP:C cell in cluster 2.

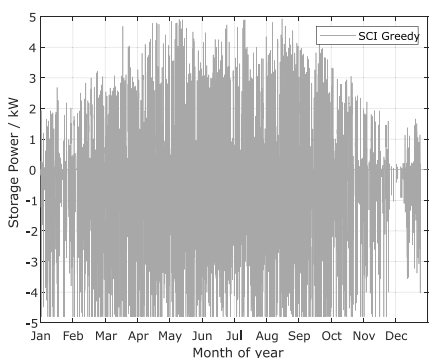


Fig. A.16. Yearly reference profile of a BESS for SCI with one PE unit and a LFP:C cell with the *greedy* algorithm.

SP as well as the SOC at each timestep can be downloaded in a MATLAB R2019a® data format (*mat*) or hierarchical data format (*hdf5*) from the servers of TU Munich [57].

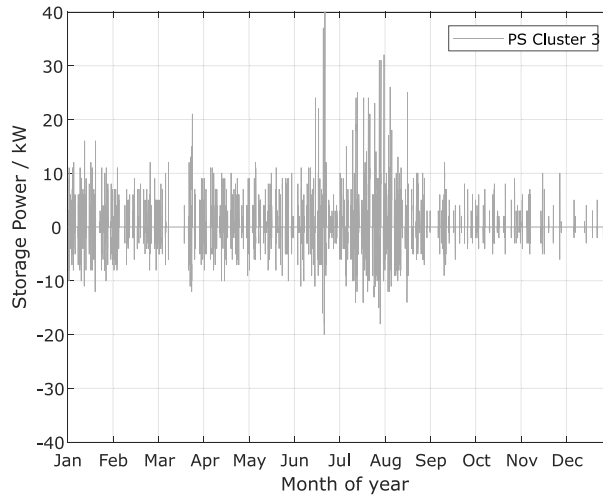


Fig. A.20. Yearly reference profile of a BESS in the application of PS with one PE unit and a LFP:C cell in cluster 3.

Appendix B. Further analysis with SimSES

B1. Frequency containment reserve

Figs. B.21, B.22 and B.23 shows additional analysis for the simulations of a BESS providing FCR. The left-hand plots (a, d) show the

distribution of the SOC, the middle one (b, e) show the distribution of the DOC and the right-hand plots (c, f) show the distribution of the E-rate. The three plots at the top (a-c) at each figure show the mean results of all 5 simulations. The three plots at the bottom (d-f) show at each figure the result for the reference profile. All plots have a logarithmic y-axis.

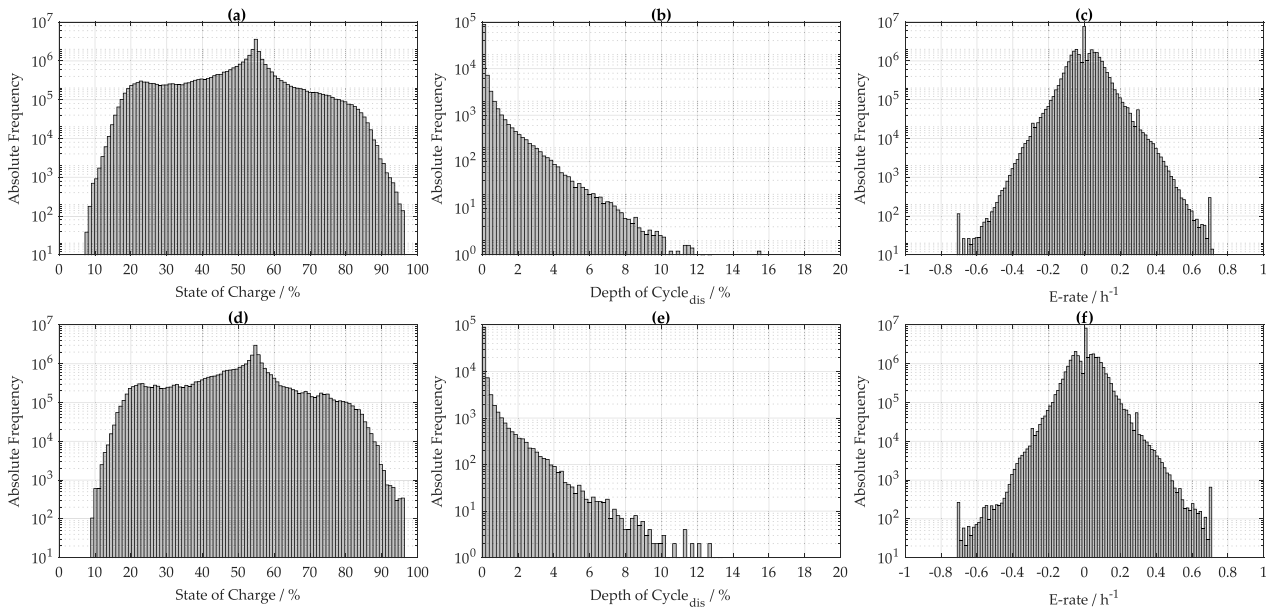


Fig. B.21. Additional analysis, SOC (a, d), DOC (b, e) and E-rate (c, f), of a simulated BESS with one PE unit and a LFP:C cell providing FCR. The three plots at the top (a-c) show the mean results of all 5 simulations. The three plots at the bottom (d-f) show the result for the reference profile.

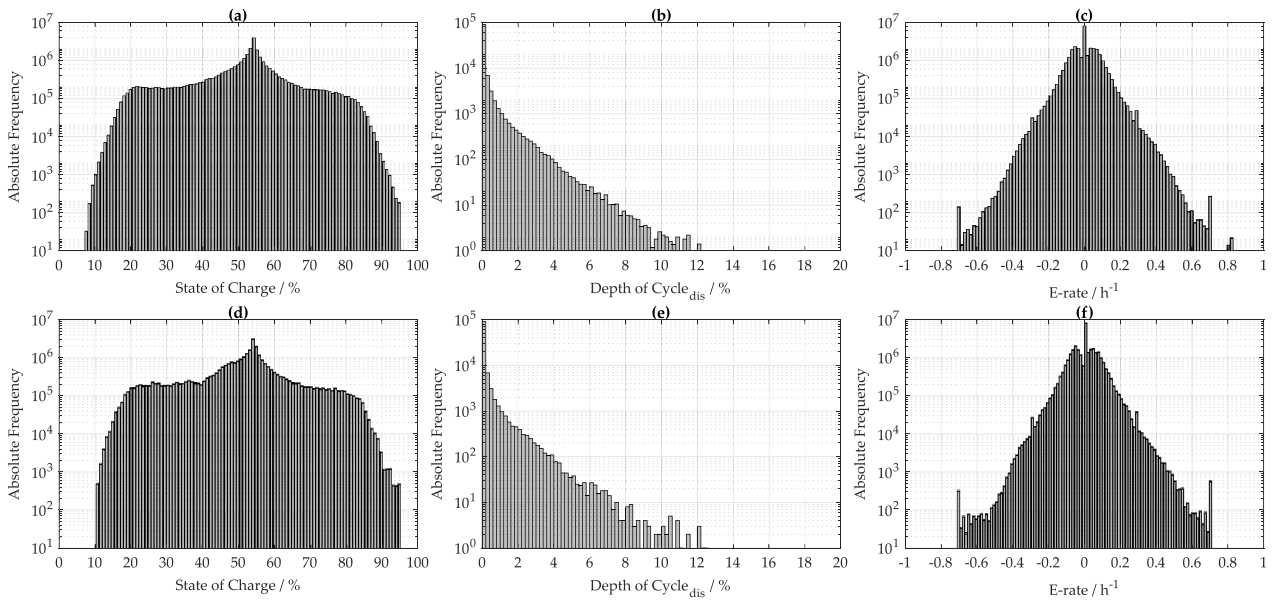


Fig. B.22. Additional analysis, SOC (a, d), DOC (b, e) and E-rate (c, f), of a simulated BESS with three modular PE units and a NMC:C cell providing FCR. The three plots at the top (a-c) show the mean results of all 5 simulations. The three plots at the bottom (d-f) show the result for the reference profile.

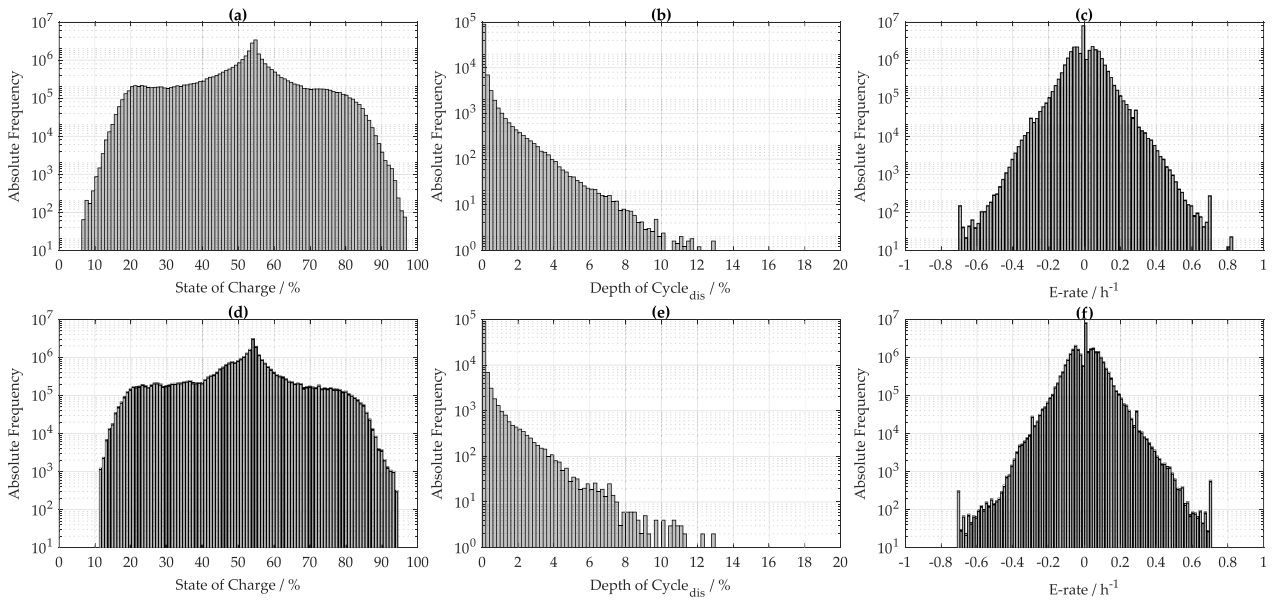


Fig. B.23. Additional analysis, SOC (a, d), DOC (b, e) and E-rate (c, f), of a simulated BESS with three modular PE units and a LFP:C cell providing FCR. The three plots at the top (a-c) show the mean results of all 5 simulations. The three plots at the bottom (d-f) show the result for the reference profile.

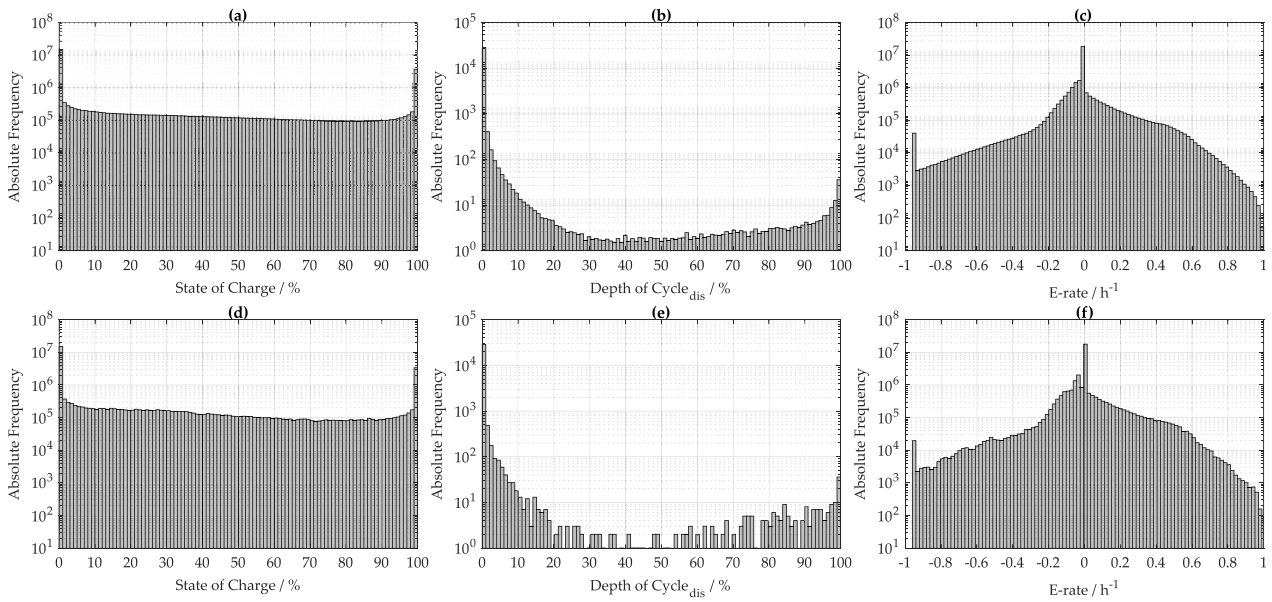


Fig. B.24. Additional analysis, SOC (a, d), DOC (b, e) and E-rate (c, f), of a SCI BESS with one PE unit and a LFP:C cell with the *greedy* algorithm. The three plots at the top (a-c) show the mean results of all 74 simulations. The three plots at the bottom (d-f) show the result for the reference profile.

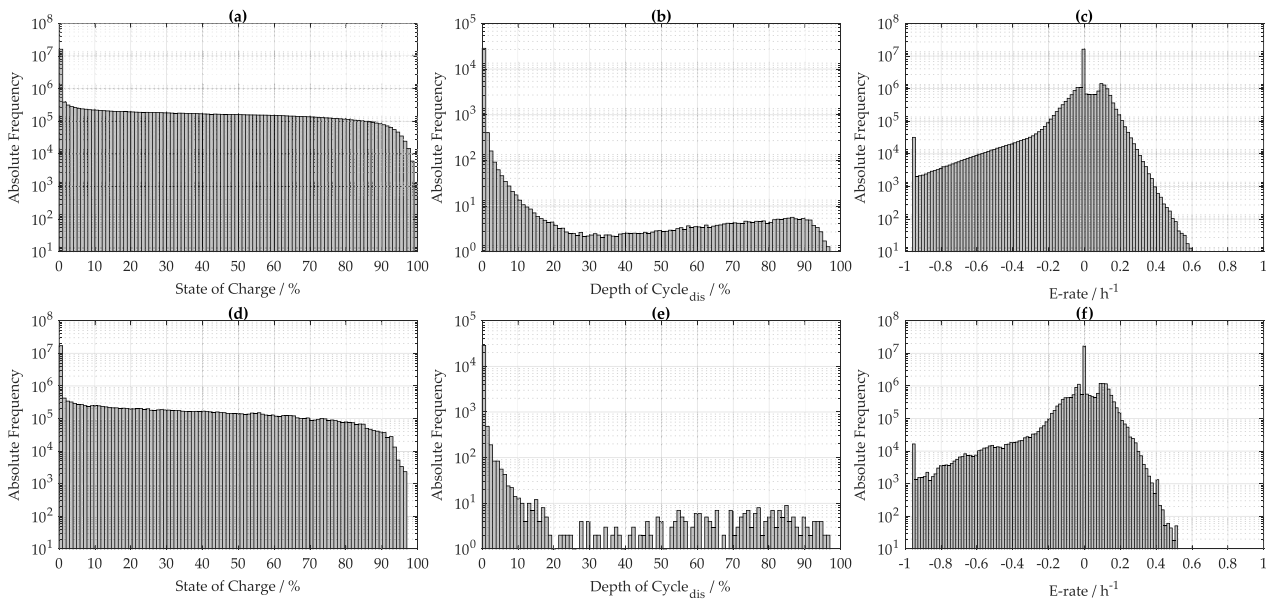


Fig. B.25. Additional analysis, SOC (a, d), DOC (b, e) and E-rate (c, f), of a SCI BESS with one PE unit and a LFP:C cell with the *feed-in damping* algorithm. The three plots at the top (a-c) show the mean results of all 74 simulations. The three plots at the bottom (d-f) show the result for the reference profile.

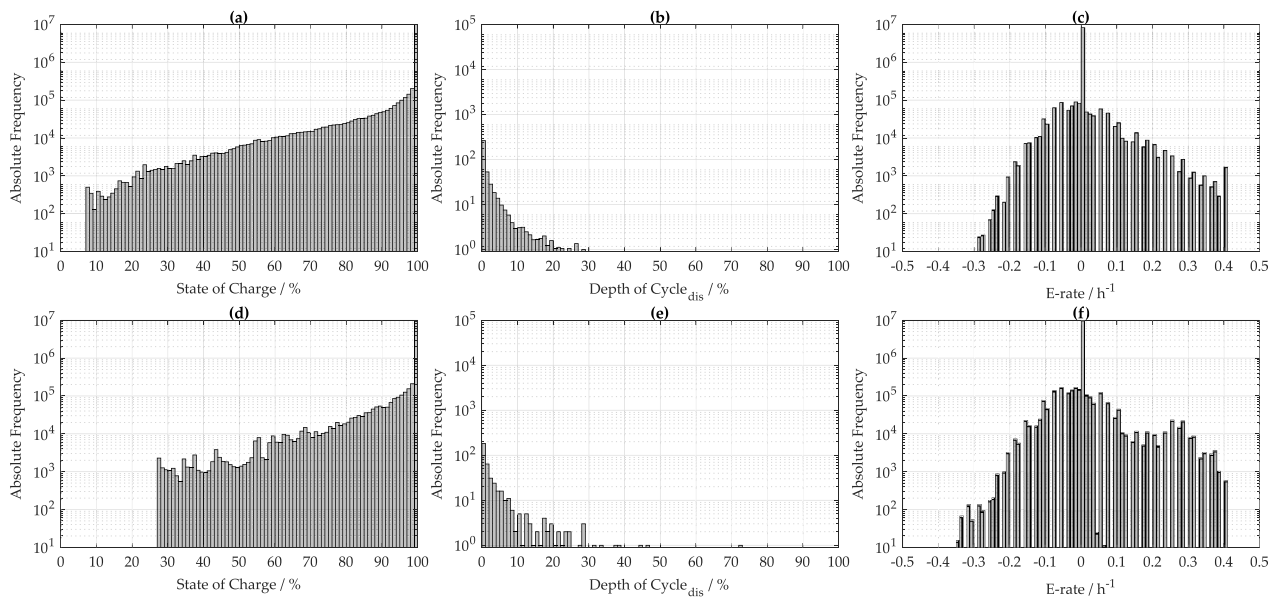


Fig. B.26. Additional analysis, SOC (a, d), DOC (b, e) and E-rate (c, f), of a BESS in the application of PS with one PE unit and a LFP:C cell in cluster 1. The three plots at the top (a-c) show the mean results of all simulations in cluster 1. The three plots at the bottom (d-f) show the result for the reference profile in cluster 1.

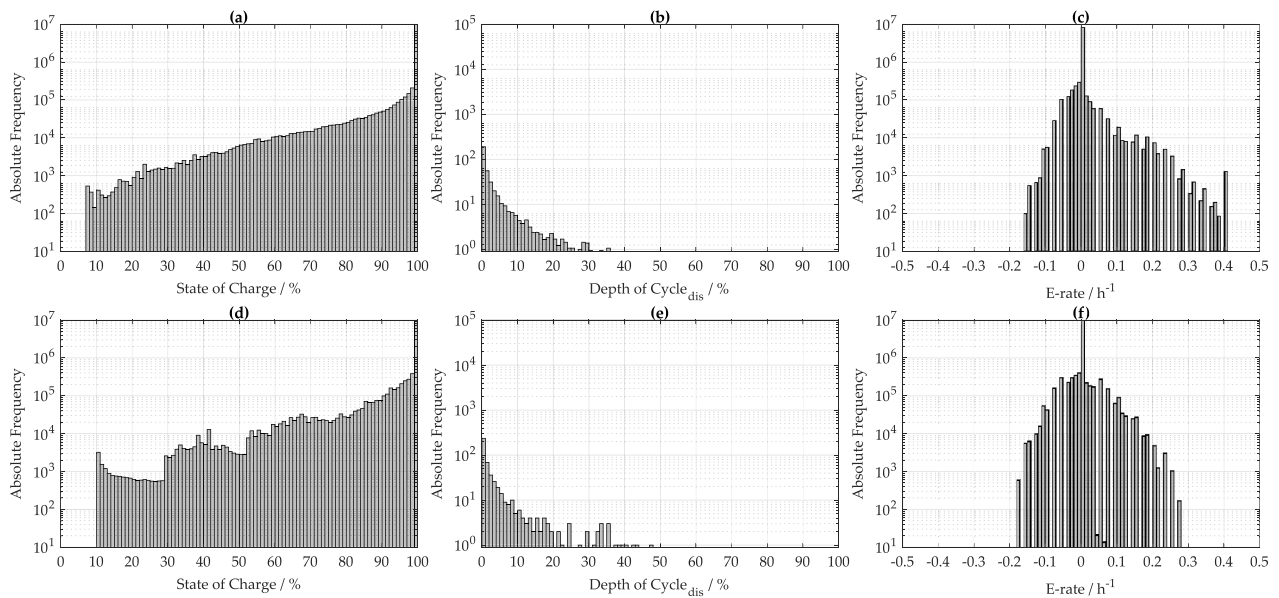


Fig. B.27. Additional analysis, SOC (a, d), DOC (b, e) and E-rate (c, f), of a BESS in the application of PS with one PE unit and a LFP:C cell in cluster 2. The three plots at the top (a-c) show the mean results of all simulations in cluster 2. The three plots at the bottom (d-f) show the result for the reference profile in cluster 2.

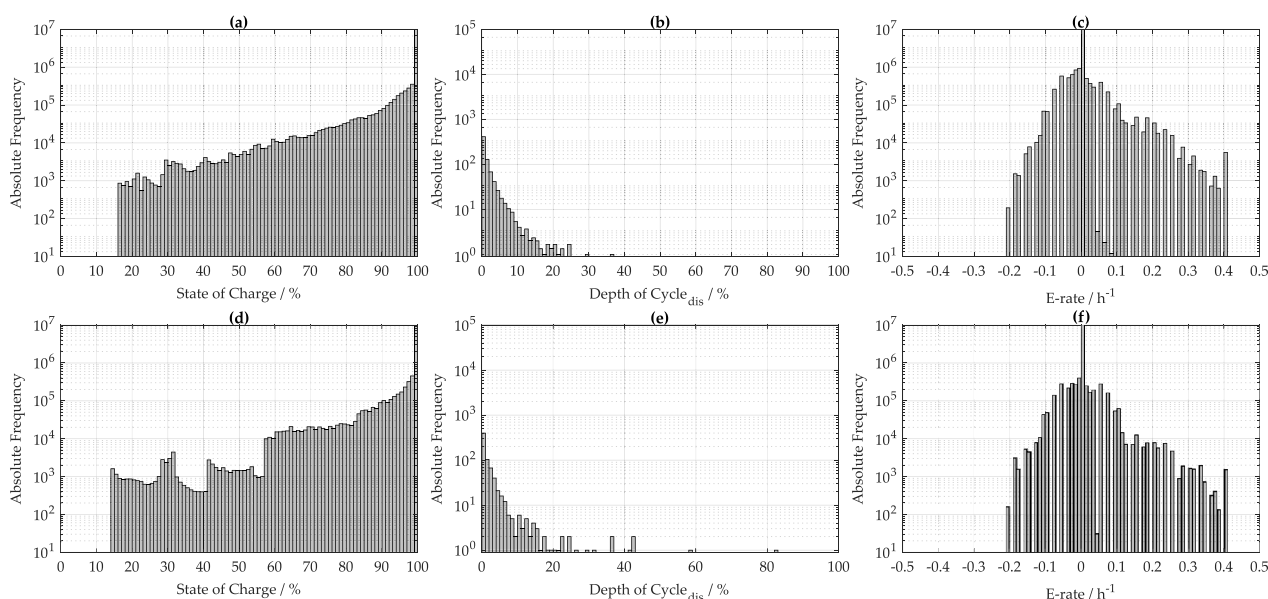


Fig. B.28. Additional analysis, SOC (a, d), DOC (b, e) and E-rate (c, f), of a BESS in the application of PS with one PE unit and a LFP-C cell in cluster 3. The three plots at the top (a-c) show the mean results of all simulations in cluster 3. The three plots at the bottom (d-f) show the result for the reference profile in cluster 3.

B2. Residential photovoltaic battery storage system

Figs. B.24 and B.25 shows additional analysis for the simulations of a SCI BESS. The left-hand plots (a, d) show the distribution of the SOC, the middle one (b, e) show the distribution of the DOC and the right-hand plots (c, f) show the distribution of the E-rate. The three plots at the top (a-c) at each figure show the mean results of all 74 simulations. The three plots at the bottom (d-f) show at each figure the result for the reference profile in the respective cluster. All plots have a logarithmic y-axis.

B3. Peak shaving storage system

Figs. B.26, B.27 and B.28 shows additional analysis for the simulations of a BESS in the application of PS. The left-hand plots show the distribution of the SOC, the middle one (b, e) show the distribution of the DOC and the right-hand plots (c, f) show the distribution of the E-rate. The three plots at the top (a-c) at each figure show the mean results of all simulations in the respective cluster. The three plots at the bottom (d-f) show at each figure the result for the reference profile in the respective cluster. All plots have a logarithmic y-axis.

Supplementary material

Supplementary material associated with this article can be found, in the online version, at doi:10.1016/j.est.2019.101077

References

- [1] TEAM CONSULT G.P.E. GmbH, Bedeutung der energiespeicherbranche für das energiesystem und die gesamtwirtschaft in deutschland (in german): pressekonferenz messe düsseldorf gmbh & bves bundesverband energiespeicher e. v. zur energy storage Europe 2018, 13.03.2018, https://www.bves.de/wp-content/uploads/2018/03/PK_ESE_Praesentation_2018.pdf.
- [2] J. Eyer, G. Corey, Energy Storage for the Electricity Grid: benefits and Market Potential Assessment Guide: a Study for the Doe Energy Storage Systems Program.
- [3] H. Hesse, M. Schimpe, D. Kucevic, A. Jossen, Lithium-ion battery storage for the grid—a review of stationary battery storage system design tailored for applications in modern power grids, *Energies* 10 (12) (2017) 2107, <https://doi.org/10.3390/en10122107>.
- [4] M. Resch, J. Bühler, M. Klausen, A. Sumper, Impact of operation strategies of large scale battery systems on distribution grid planning in germany, *Renew. Sustain. Energy Rev.* 74 (2017) 1042–1063, <https://doi.org/10.1016/j.rser.2017.02.075>.
- [5] B. Diouf, R. Pode, Potential of lithium-ion batteries in renewable energy, *Renew Energy* 76 (2015) 375–380, <https://doi.org/10.1016/j.renene.2014.11.058>.
- [6] O. Palizban, K. Kauhaniemi, Energy storage systems in modern grids—matrix of technologies and applications, *J. Energy Storage* 6 (2016) 248–259, <https://doi.org/10.1016/j.est.2016.02.001>.
- [7] B. Dunn, H. Kamath, J.-M. Tarascon, Electrical energy storage for the grid: a battery of choices, *Science* 334 (6058) (2011) 928–935, <https://doi.org/10.1126/science.1212741>.
- [8] T. Weitzel, C.H. Glock, Energy management for stationary electric energy storage systems: a systematic literature review, *Eur. J. Oper. Res.* (2017), <https://doi.org/10.1016/j.ejor.2017.06.052>.
- [9] C.K. Das, O. Bass, G. Kothapalli, T.S. Mahmoud, D. Habibi, Overview of energy storage systems in distribution networks: placement, sizing, operation, and power quality, *Renew. Sustain. Energy Rev.* 91 (2018) 1205–1230, <https://doi.org/10.1016/j.rser.2018.03.068>.
- [10] G. Carpinelli, F. Mottola, C. Noce, A. Russo, P. Varilone, A new hybrid approach using the simultaneous perturbation stochastic approximation method for the optimal allocation of electrical energy storage systems, *Energies* 11 (6) (2018) 1505, <https://doi.org/10.3390/en11061505>.
- [11] A. Oudalov, D. Chartouni, C. Ohler, Optimizing a battery energy storage system for primary frequency control, *IEEE Trans. Power Syst.* 22 (3) (2007) 1259–1266, <https://doi.org/10.1109/TPWRS.2007.901459>.
- [12] R. Hollinger, L.M. Diazgranados, F. Braam, T. Erge, G. Bopp, B. Engel, Distributed solar battery systems providing primary control reserve, *IET Renew. Power Gener.* 10 (1) (2016).
- [13] J. Fleer, P. Stenzel, Impact analysis of different operation strategies for battery energy storage systems providing primary control reserve, *J. Energy Storage* 8 (2016) 320–338, <https://doi.org/10.1016/j.est.2016.02.003>.
- [14] A. Zeh, M. Müller, M. Naumann, H. Hesse, A. Jossen, R. Witzmann, Fundamentals of using battery energy storage systems to provide primary control reserves in germany, *Batteries* 2 (3) (2016) 29, <https://doi.org/10.3390/batteries2030029>.
- [15] Y.J.A. Zhang, C. Zhao, W. Tang, S.H. Low, Profit-maximizing planning and control of battery energy storage systems for primary frequency control, *IEEE Trans Smart Grid* 9 (2) (2018) 712–723, <https://doi.org/10.1109/TSG.2016.2562672>.
- [16] J. Münderlein, M. Steinhoff, S. Zurmühlen, D.U. Sauer, Analysis and evaluation of operations strategies based on a large scale 5 mw and 5 mwh battery storage system, *J. Energy Storage* 24 (2019) 100778, <https://doi.org/10.1016/j.est.2019.100778>.
- [17] M. Naumann, R.C. Karl, C.N. Truong, A. Jossen, H.C. Hesse, Lithium-ion battery cost analysis in pv-household application. 9th International Renewable Energy Storage Conference, IRES 2015 73, 2015, pp. 37–47, <https://doi.org/10.1016/j.egypro.2015.07.555>.
- [18] F. Cucchiella, I. D'Adamo, M. Gastaldi, Photovoltaic energy systems with battery storage for residential areas: an economic analysis, *J. Clean. Prod.* 131 (2016) 460–474, <https://doi.org/10.1016/j.jclepro.2016.04.157>.
- [19] C.N. Truong, M. Naumann, R.C. Karl, M. Müller, A. Jossen, H.C. Hesse, Economics of residential photovoltaic battery systems in germany: the case of teslas powerwall, *Batteries* 2 (2) (2016) 14, <https://doi.org/10.3390/batteries2020014>.
- [20] H. Hesse, R. Martins, P. Musilek, M. Naumann, C. Truong, A. Jossen, Economic optimization of component sizing for residential battery storage systems, *Energies* 10 (7) (2017) 835, <https://doi.org/10.3390/en10070835>.

- [21] J. Weniger, T. Tjaden, V. Quaschnig, Sizing of residential pv battery systems. 9th International Renewable Energy Storage Conference, IRES 2015 46, 2014, pp. 78–87, <https://doi.org/10.1016/j.egypro.2014.01.160>.
- [22] R. Tang, B. Yildiz, P.H. Leong, A. Vassallo, J. Dore, Residential battery sizing model using net meter energy data clustering, *Appl. Energy* 251 (2019) 113324, <https://doi.org/10.1016/j.apenergy.2019.113324>.
- [23] F.M. Vieira, P.S. Moura, A.T. de Almeida, Energy storage system for self-consumption of photovoltaic energy in residential zero energy buildings, *Renew Energy* 103 (2017) 308–320, <https://doi.org/10.1016/j.renene.2016.11.048>.
- [24] R. Martins, H. Hesse, J. Jungbauer, T. Vorbuchner, P. Musilek, Optimal component sizing for peak shaving in battery energy storage system for industrial applications, *Energies* 11 (8) (2018) 2048, <https://doi.org/10.3390/en11082048>.
- [25] H. Dagdougui, N. Mary, A. Beraud-Sudreau, L. Dessaint, Power management strategy for sizing battery system for peak load limiting in a university campus. 2016 IEEE Smart Energy Grid Engineering (SEGE), IEEE, 21.08.2016 - 24.08.2016, pp. 308–312, <https://doi.org/10.1109/SEGE.2016.7589542>.
- [26] E. Telaretti, L. Dusonchet, Battery storage systems for peak load shaving applications: Part 2: economic feasibility and sensitivity analysis. 2016 IEEE 16th International Conference on Environment and Electrical Engineering (EEEIC), IEEE, 07.06.2016 - 10.06.2016, pp. 1–6, <https://doi.org/10.1109/EEEIC.2016.7555795>.
- [27] 50Hertz Transmission GmbH, Archiv netzfrequenz (in german): daten der entso-netzfrequenz, 2019, <https://www.50hertz.com/de/Transparenz/Kennzahlen/Regelenergie/ArchivRegelenergie/ArchivNetzfrequenz>.
- [28] T. Tjaden, J. Bergner, J. Weniger, V. Quaschnig, Repräsentative elektrische lastprofile für wohngebäude in deutschland auf 1-sekündiger datenbasis (in German), <https://pvspeicher.htw-berlin.de/daten/>.
- [29] A. Zeh, R. Witzmann, Operational strategies for battery storage systems in low-voltage distribution grids to limit the feed-in power of roof-mounted solar power systems, *Energy Procedia* 46 (2014) 114–123, <https://doi.org/10.1016/j.egypro.2014.01.164>.
- [30] P. Keil, A. Jossen, Charging protocols for lithium-ion batteries and their impact on cycle life—an experimental study with different 18650 high-power cells, *J. Energy Storage* 6 (2016) 125–141, <https://doi.org/10.1016/j.est.2016.02.005>.
- [31] G. Ning, B. Haran, B.N. Popov, Capacity fade study of lithium-ion batteries cycled at high discharge rates, *J. Power Source*. 117 (1–2) (2003) 160–169, [https://doi.org/10.1016/S0378-7753\(03\)00029-6](https://doi.org/10.1016/S0378-7753(03)00029-6).
- [32] B. Everitt, *Cluster analysis*, in: *Wiley series in probability and statistics*, Wiley, Chichester West Sussex U.K., 2011.
- [33] A. Al-Wakeel, J. Wu, K-Means based cluster analysis of residential smart meter measurements, 9th International Renewable Energy Storage Conference, IRES 2015 88 (2016) 754–760, <https://doi.org/10.1016/j.egypro.2016.06.066>.
- [34] G. Le Ray, P. Pinson, Online adaptive clustering algorithm for load profiling, *Sustain. Energy Grids Netw.* 17 (2019) 100181, <https://doi.org/10.1016/j.segan.2018.100181>.
- [35] G.J. Tsekouras, N.D. Hatzigiorgiou, E.N. Dialynas, Two-stage pattern recognition of load curves for classification of electricity customers, *IEEE Trans. Power Syst.* 22 (3) (2007) 1120–1128, <https://doi.org/10.1109/TPWRS.2007.901287>.
- [36] F. McLoughlin, A. Duffy, M. Conlon, A clustering approach to domestic electricity load profile characterisation using smart metering data, *Appl. Energy* 141 (2015) 190–199, <https://doi.org/10.1016/j.apenergy.2014.12.039>.
- [37] T. Räsänen, D. Voukantsis, H. Niska, K. Karatzas, M. Kolehmainen, Data-based method for creating electricity use load profiles using large amount of customer-specific hourly measured electricity use data, *Appl. Energy* 87 (11) (2010) 3538–3545, <https://doi.org/10.1016/j.apenergy.2010.05.015>.
- [38] M. Naumann, C.N. Truong, M. Schimpe, D. Kucevic, A. Jossen, H.C. Hesse, *Simses: Software for techno-economic simulation of stationary energy storage systems*. International ETG Congress 2017, in: *ETG-Fachbericht*, VDE Verlag, Berlin and Offenbach, 2017, pp. 442–447.
- [39] Deutsche Übertragungsnetzbetreiber, Eckpunkte und freiheitsgrade bei erbringung von primaerregelleistung (in German): Leitfaden für anbieter von primaerregelleistung, <https://www.regelleistung.net/ext/static/prequalification?lang=en>.
- [40] Deutsche Übertragungsnetzbetreiber, Anforderungen an die speicherkapazitaet bei batterien für die primaerregelleistung (in German), https://www.bves.de/wp-content/uploads/2015/08/2015_08_26_Anforderungen_Speicherkapazitaet_Batterien_PRL.pdf.
- [41] BVES, Beschränkung der ünb für speicher im regelenergiemarkt ist rechtswidrig (in German), 09.05., 2019, https://www.bves.de/uenb_rechtswidrige_blockade/.
- [42] German Federal Office of Justice, Stromnetzentgeltverordnung (in German): Stromnev, 2005-07-25, <https://www.gesetze-im-internet.de/stromnev/BJNR222500005.html>.
- [43] S. Englberger, H.C. Hesse, C.N. Truong, A. Jossen, Autonomous versus Coordinated Control of Residential Energy Storage Systems - Monitoring Profit, Battery Aging, and System Efficiency, in: D. Schulz (Ed.), *NEIS 2018*, VDE VERLAG GMBH, Berlin, 2019, pp. 1–7.
- [44] S. Englberger, H. Hesse, D. Kucevic, A. Jossen, A techno-economic analysis of vehicle-to-building: battery degradation and efficiency analysis in the context of coordinated electric vehicle charging, *Energies* 12 (5) (2019) 955, <https://doi.org/10.3390/en12050955>.
- [45] D. Kucevic, C.N. Truong, A. Jossen, H.C. Hesse, *Lithium-ion Battery Storage Design for Buffering Fast Charging Stations for Battery Electric Vehicles and Electric Buses*, in: D. Schulz (Ed.), *NEIS 2018*, VDE VERLAG GMBH, Berlin, 2019, pp. 1–6.
- [46] Murata, Data sheet of Sony fortelion us26650ftc1 battery cell, 2017.
- [47] A.-I. Stan, M. Swierczynski, D.-I. Stroe, R. Teodorescu, S.J. Andreasen, Lithium ion battery chemistries from renewable energy storage to automotive and back-up power applications — an overview. 2014 International Conference on Optimization of Electrical and Electronic Equipment (OPTIM), IEEE, 2014, pp. 713–720, <https://doi.org/10.1109/OPTIM.2014.6850936>.
- [48] M. Müller, L. Viernstein, C.N. Truong, A. Eiting, H.C. Hesse, R. Witzmann, A. Jossen, Evaluation of grid-level adaptability for stationary battery energy storage system applications in europe, *J. Energy Storage* 9 (2017) 1–11, <https://doi.org/10.1016/j.est.2016.11.005>.
- [49] M. Naumann, *Techno-economic evaluation of stationary battery energy storage systems with special consideration of aging*, Technical University of Munich, Munich, 2018. Phd thesis.
- [50] Molicel, Product data sheet model ihr-18650a.
- [51] S.F. Schuster, *Reuse of Automotive Lithium-Ion Batteries: An Assessment from the Cell Aging Perspective*, Universitätsbibliothek der TU München, München, 2016. Dissertation.
- [52] G. Notton, V. Lazarov, L. Stoyanov, Optimal sizing of a grid-connected pv system for various pv module technologies and inclinations, inverter efficiency characteristics and locations, *Renew Energy* 35 (2) (2010) 541–554, <https://doi.org/10.1016/j.renene.2009.07.013>.
- [53] M. Schimpe, M. Naumann, N. Truong, H.C. Hesse, S. Santhanagopalan, A. Saxon, A. Jossen, Energy efficiency evaluation of a stationary lithium-ion battery container storage system via electro-thermal modeling and detailed component analysis, *Appl. Energy* 210 (2018) 211–229, <https://doi.org/10.1016/j.apenergy.2017.10.129>.
- [54] J. Hoppmann, J. Volland, T.S. Schmidt, V.H. Hoffmann, The economic viability of battery storage for residential solar photovoltaic systems – a review and a simulation model, *Renew. Sustain. Energy Rev.* 39 (2014) 1101–1118, <https://doi.org/10.1016/j.rser.2014.07.068>.
- [55] S.F. Schuster, T. Bach, E. Fleder, J. Müller, M. Brand, G. Sextl, A. Jossen, Nonlinear aging characteristics of lithium-ion cells under different operational conditions, *J. Energy Storage* 1 (2015) 44–53, <https://doi.org/10.1016/j.est.2015.05.003>.
- [56] M. Naumann, M. Schimpe, P. Keil, H.C. Hesse, A. Jossen, Analysis and modeling of calendar aging of a commercial lifepo4/graphite cell, *J. Energy Storage* 17 (2018) 153–169, <https://doi.org/10.1016/j.est.2018.01.019>.
- [57] D. Kucevic, B. Tepe, S. Englberger, A. Parlikar, M. Muehlbauer, O. Bohlen, A. Jossen, H. Hesse, Standard battery energy storage system profiles: dataset, doi:10.14459/2019mp1510254.

3.2 Investigation of mobile battery storage systems in various applications

In this section, the research work entitled *Lithium-Ion Battery Utilization in various Modes of e-Transportation* is presented [4]. Following the analysis of stationary applications in the previous section, the mobile applications e-Car, e-Bus and e-Boat are evaluated in this section. While vehicle manufacturers know the requirements for LIBs in their applications, publicly available data on the impact on batteries in vehicles is scarce. However, the impact in various applications is essential for the further development of battery technologies, for the evaluation of battery aging and for the estimation of the V2X potential. For this reason, this section presents analyses and evaluations of the load on LIBs in e-Cars, e-Buses and e-Boat. As in the previous section, the load profiles are published as open data so that they can be used in further work in industry and research.

For the paper in this section, SimSES was extended from stationary applications to mobile applications. In addition to the vehicle power profile, which specifies the power that the vehicle should discharge and recuperate during trips, a binary profile is also required as an input profile. This binary profile specifies the time at which a vehicle is connected to the electricity grid and the time at which the vehicle is driving or parked but unplugged. The assumption here is that the vehicles are always plugged in when they are at home, in the depot or in the dock. The load profile is then followed during trips. During idle times, in contrast, different charging strategies are implemented. In addition to simple, uncontrolled charging after arrival to 100 %, charging with minimum power until departure and paused charging are also possible. In the latter case, the vehicle is first charged to a medium SOC, then paused and only fully charged shortly before departure. Various input profiles were collected to enable the simulation of the three vehicle types. For the e-Cars, the simulation tool *emobpy* was used, which simulates the driving behavior of private e-Cars in Germany. The tool was used to simulate 60 e-Cars over a period of one year. For the simulation of the e-Buses, we received data from Hamburger Hochbahn AG from 82 e-Buses over a period of up to 14 months. After filtering, 53 of these e-Bus data sets were considered in the evaluation. The e-Boats were simulated using six datasets from Torqeedo, with data spanning three to nine months. Subsequently, the data is used as input to SimSES for in depth battery performance analysis. First, the energy consumption of the e-Buses and e-Cars is evaluated, as data on distances traveled was transmitted for these two vehicle types. In addition, various battery-relevant parameters are determined for all vehicle types and compared with those of stationary applications from section 3.1. Finally, the influence of the charging strategies is investigated.

The research questions answered in this section are:

1. How can various transportation modes be reproducibly simulated to obtain battery usage and health indications?
2. How much energy do e-Cars and e-Buses consume in the exemplary datasets, and what is the influence of the ambient temperature on consumption?
3. What is the typical stress of mobile battery storage systems in various transportation modes regarding different parameters?
4. To what extent are battery-relevant parameters in mobile applications similar to stationary applications and could therefore similar cells be used in those applications?
5. What's the influence of charging strategies on the considered parameters?

The results of this work include energy consumption analyses of the buses. These show that the buses

consume between 1 and 1.5 kWh/km and are minimal at 20 °C ambient temperature. Moreover, the analyzed e-Buses perform 0.4 to 1 EFCs per day, while the analyzed e-Cars make less than 0.18 EFCs per day. The daily EFCs of the e-Boats range between 0.026 and 0.3. The comparison with stationary BSSs from section 3.1 shows that the applications SCI, FCR and e-Bus in particular are similar in terms of some parameters such as the EFCs. The collected and generated data is made available open-access in the same way as in section 3.1.

The mobile application data from this section is used in chapter 5 to simulate the V2X provision of the three vehicle types. In addition, the unidirectional, paused charging strategy is used as a basis and V2X charging strategies are developed. The idea of V2X is also elaborated in sections 4.1 to 4.3 with a focus on commercial e-Cars and V2G provision.

Author contribution

Benedikt Tepe was the principle author tasked with coordinating and writing the paper and developing the methodology for the mobile storage data. Sammy Jablonski contributed to the data analysis and focused on the electric bus energy consumption. Holger Hesse reviewed the manuscript and gave valuable input throughout the manuscript preparation. Andreas Jossen contributed via fruitful scientific discussions and reviewed the manuscript. All authors discussed the data and commented on the results.

Lithium-ion battery utilization in various modes of e-transportation

Benedikt Tepe, Sammy Jablonski, Holger Hesse and Andreas Jossen

eTransportation, Volume 18, 2023

Permanent weblink:

<https://doi.org/10.1016/j.etrans.2023.100274>



Reproduced under the terms of the Creative Commons Attribution 4.0 License (CC BY, <http://creativecommons.org/licenses/by/4.0/>), which permits unrestricted reuse of the work in any medium, provided the original work is properly cited.



Contents lists available at ScienceDirect

eTransportation

journal homepage: www.journals.elsevier.com/etransportation

Lithium-ion battery utilization in various modes of e-transportation

Benedikt Tepe^{a,*}, Sammy Jablonski^a, Holger Hesse^b, Andreas Jossen^a

^a Chair of Electrical Energy Storage Technology, Department of Energy and Process Engineering, School of Engineering and Design, Technical University of Munich (TUM), Germany

^b Kempten University of Applied Sciences, Department of Mechanical Engineering, Institute for Energy and Propulsion Technologies, Germany

ARTICLE INFO

Keywords:

Lithium-ion battery stress factors
Modes of transportation
Mobile applications
Electric cars
Electric buses
Electric boats

ABSTRACT

The electrification of the transportation sector leads to an increased deployment of lithium-ion batteries in vehicles. Today, traction batteries are installed, for example, in electric cars, electric buses, and electric boats. These use-cases place different demands on the battery. In this work, simulated data from 60 electric cars and field data from 82 electric buses and six electric boats from Germany are used to quantify a set of stress factors relevant to battery operation and life expectancy depending on the mode of transportation. For this purpose, the open-source tool *SimSES* designed initially to simulate battery operation in stationary applications is extended toward analyzing mobile applications. It now allows users to simulate electric vehicles while driving and charging. The analyses of the three means of transportation show that electric buses, for example, consume between 1 and 1.5 kWh/km and that consumption is lowest at ambient temperatures around 20 °C. Electric buses are confronted with 0.4–1 equivalent full cycle per day, whereas the analyzed set of car batteries experience less than 0.18 and electric boats between 0.026 and 0.3 equivalent full cycles per day. Other parameters analyzed include mean state-of-charges, mean charging rates, and mean trip cycle depths. Beyond these evaluations, the battery parameters of the transportation means are compared with those of three stationary applications. We reveal that stationary storage systems in home storage and balancing power applications generate similar numbers of equivalent full cycles as electric buses, which indicates that similar batteries could be used in these applications. Furthermore, we simulate the influence of different charging strategies and show their severe impact on battery degradation stress factors in e-transportation. To facilitate widespread and diverse usage, all profile and analysis data relevant to this work is provided as open data as part of this work.

1. Introduction

The market introduction of lithium-ion battery technology in the 1990s and its advancement since then is considered as enabler for the widespread electrification of the transportation sector [1]. Cars, buses, and boats are increasingly powered by electricity, replacing internal combustion engine-based propulsion systems [2–4]. Sales of electric cars (e-Cars) worldwide doubled to a total of 6.6 million from 2020 to 2021 [2]. In the same timeframe, sales of electric buses (e-Buses) increased by 40% worldwide, although the total number of buses remained constant [2]. For example, Hochbahn Hamburg, the operator of Hamburg's subways and buses, plans to electrify its entire bus fleet by 2030 [5]. The global market for electric boats (e-Boats) is also expected to double in volume from 2022 to 2028 [4]. These three modes of transportation vary in several aspects, such as average travel distance and frequency. In addition, vehicle usage also varies within a mode. For example, e-Buses

typically travel longer distances than e-Cars, and e-Cars themselves may be used for daily commuting or just for leisure activities. Accordingly, the load on the battery system and the time available for charging the vehicles differs.

The present work analyzes the battery system load of different e-transportation modes. For this purpose, field data were collected from industry partners for the e-Buses and e-Boats. For e-Car data, a simulation tool is used, which is based on mobility data and simulates driving behavior. The collected data is used to emulate trips and charging behavior of the mobile applications with the help of *SimSES*, an open-source simulation tool extended for this purpose [6,53]. In an energy consumption analysis, the consumption of the vehicles is compared, and, for the e-Buses, the influence of the outside temperature is also shown. Various battery parameters such as the average state of charge (SOC), are then derived and compared. In addition, the parameters of the mobile battery storage systems (BSSs) are compared with those of stationary BSSs in three applications. We also consider the influence of

* Corresponding author. Electrical Energy Storage Technology, Technical University of Munich (TUM), Arcisstr. 21, 80333, Munich, Germany.
E-mail address: benedikt.tepe@tum.de (B. Tepe).

<https://doi.org/10.1016/j.etrans.2023.100274>

Received 12 May 2023; Received in revised form 21 July 2023; Accepted 22 August 2023

Available online 23 August 2023

2590-1168/© 2023 The Authors. Published by Elsevier B.V. This is an open access article under the CC BY license (<http://creativecommons.org/licenses/by/4.0/>).

Nomenclature	
<i>Abbreviations</i>	
BSS	Battery storage system
e-Boat	Electric boat
e-Bus	Electric bus
e-Car	Electric car
EMS	Energy management system
EPA	Environmental Protection Agency
EV	Electric vehicle
eVTOL	Electric vertical take-off and landing
FCR	Frequency containment reserve
KPI	Key performance indicator
LMP	Lithium-metal-polymer battery
NEDC	New European Driving Cycle
NMC	Nickel-manganese-cobalt lithium-ion battery
PHEV	Plug-in hybrid electric vehicle
PV	Photovoltaic
PS	Peak-shaving
RQ	Research question
SCI	Self-consumption increase
V2G	Vehicle-to-grid
WLTC	Worldwide harmonized Light-duty vehicles Test Cycles
<i>Parameters and variables</i>	
$b(t)$	Binary value indicating connection to electricity grid
C-rate	Charge rate
$C_{act}(t)$	Currently charged electrical charge
$C_{total}(t)$	Currently total possible capacity
$C_{rate, abs}(t)$	Currently absolute C-rate
Consumption _{trip}	Energy Consumption of a trip
ΔSOE_{trip}	Change in SOE
Δd_{trip}	Change in distance
DOC	Depth of cycle
DOD	Depth of discharge
EBSS	Energy content of battery
E_{year}^{pos}	Charged energy in the year
EFC	Equivalent full cycles
$ I(t) $	Currently absolute current
n	Total number of time steps
$P(t)$	Current power
SOE	State of energy
SOC	State of charge
$SOC_{cycle, start}(t)$	State of charge at the beginning of a cycle
$SOC_{cycle, end}(t)$	State of charge at the end of a cycle
$u(t)$	Binary value of current temporal utilization
$\mu_{utilization}$	Temporal utilization ratio
μ_{V2G}	Temporal V2G-ready ratio
$v(t)$	Binary value of current V2G-ready ratio

the charging strategy by emulating the load profiles using three different charging strategies. Finally, part of this publication is an open-data repository including all BSS load profiles for each of the three modes of transportation.

In the following, we first describe the state of the art and existing literature before defining the research questions and presenting the scope of the work. In this work, the term e-Cars is used for cars instead of the often-used “electric vehicles” to distinguish between the electric vehicles of e-Cars, e-Buses, and e-Boats.

1.1. Summary of existing literature

In recent years, the electrification of cars, buses, and boats has been advancing [2–4]. Accordingly, research interest in these topics is also increasing. In the following, we summarize the literature on e-Cars, e-Buses, and e-Boats relevant to this paper. We then address vehicle charging strategies and the state of the art on relevant storage and battery KPIs.

E-Cars are a relevant topic, as they change not only the mobility sector but also the energy sector [2]. For this reason, research interest focuses on various issues of e-Cars, such as charging strategies, including fast charging and vehicle-to-grid (V2G), the influence on the distribution grid [7] and battery thermal management systems [8]. However, research also addresses the use of e-Cars and typical car loads. For example, an analysis of the user behavior and energy consumption of e-Cars was conducted by De Cauwer et al., in 2015 [9]. In their work, the authors analyzed GPS data from the EVA and Move platforms in Belgium and measured the energy consumption of a Nissan Leaf. For the e-Cars of their dataset, a range of 5000 to 6000 km per year was derived, which is less than the annual distances covered by internal combustion vehicles. They also showed that real energy consumption on the road might account for between 18 and 23 kWh/100 km – a value 30%–60% higher than the consumption measured by the New European Driving Cycle (NEDC). Similar trends were obtained by Hao et al., in 2020, who analyzed data from 197 e-Cars and determined energy consumption levels that were 7%–10% higher than those determined using NEDC

[10]. A study by Chen et al., in 2020 evaluated data sets of 8000 e-Cars and plug-in hybrid electric vehicles (PHEVs) in Shanghai over a week and concluded that the e-Cars travel less than the PHEVs, averaging 32.6 km per day (compared to 36.3 km per day for the PHEVs) which is nearly 12,000 km per year [11]. Moreover, Tansini et al. conducted their tests on three e-Cars and determined consumption between 15 and 29 kWh/100 km with an average consumption of about 20 kWh/100 km [12]. In 2016, Zou et al. analyzed the driving behavior of taxi fleets consisting of 34 electrically powered taxis in Beijing [13]. On average, the taxis drove almost 118 km daily and consumed 11 to 30 kWh/100 km. The authors also analyzed battery charging characteristics and determined that 59% of the charging processes began between 30 and 50% SOC, and 74% were charged to an SOC higher than 90%. Consequently, the cabs were discharged by 40–70% during the trips. In the same year, Weldon et al. published a study of e-Car use in Ireland in which they evaluated eight privately used and seven commercially used e-Cars [14]. In contrast to Zou et al., the Weldon et al. study showed a wider distribution of SOCs at the start of charging: 58.7% of charging events started at an SOC between 50 and 100% [14]. However, this study used 2010 Mitsubishi i-MiEVs, which have a range of only 130 km. In addition, Zou et al. analyzed cabs, while Weldon et al. studied private and other commercially used e-Cars. Zhang et al. determined in a study of 55 e-Cars in Beijing that energy consumption depends on the outdoor temperature and that consumption is lowest at 15–20 °C [15]. They also showed that in Beijing, energy consumption was up to 10.26% higher for identical trips in winter than in the other three seasons. The descriptions of the state of research regarding e-Cars relevant to this work show that in practice they consume between 11 and 30 kWh/100 km and often cover smaller annual distances than internal combustion vehicles. Our work also presents the consumption and distances of a dataset of e-Cars but goes beyond this by evaluating and presenting further battery-relevant parameters.

In the literature, there are also studies of mobility behavior based on surveys. One is the “Mobility in Germany” study [16,17]. Results of the 2017 study were, for example, that on average, 3.1 trips and 39 km per person and day were made [17]. In addition, an e-Car in Germany is

used for 45 min per day on average, which means that it is not used almost 97% of the time [16]. Furthermore, the authors published statistics and probability distributions on mobility behavior in addition to these overall results. This data is used by *emobpy*, an open-source Python tool that can simulate the mobility behavior of e-Cars [18]. Since this tool is used in our work, we describe the simulation procedure and its parameters in chapter 2.

E-Buses have also gained importance in recent years, so annual publications on this topic have increased more than tenfold from 2008 to 2020 [19]. According to a review by Manzolli et al., the main trends of this research are vehicle and battery technology, fleet and energy management, and sustainability [19]. In the following, we focus on the research relevant to this paper on the driving behavior of e-Buses and the impact on battery systems. In 2015, Rogge et al. evaluated 1588 trips made by diesel buses operated by Stadtwerke Münster in Germany [20]. They used a method developed by Sinhuber et al. to dimension potential battery systems for the electrification of the buses and to simulate energy consumption [21]. The simulated energy consumption, including auxiliaries, ranged from 2.26 to 2.69 kWh/km, with a mean value of 2.47 kWh/km [20]. Three years later, in 2018, Gallet et al. evaluated 4135 e-Buses in Singapore, which traveled on average 186 km per day [22]. The mean value of the energy consumption was 1.75 kWh/km, with articulated e-Buses consuming an average of 2.47 kWh/km, double-decker consuming 2.34 kWh/km, and single-decker e-Buses consuming 1.62 kWh/km. At 1.35 kWh/km, Gao et al. also obtained similar consumption values [23]. In 2017, they published a framework evaluating diesel buses from Knoxville (USA) and using their driving patterns to simulate e-Buses. An evaluation of 99 e-Buses from seven cities in China was published by Wang et al., in 2020 [24]. They determined optimal speeds of 11–18 km/h to maximize battery efficiency using a random forest algorithm.

Furthermore, there is research on e-Buses that deals with charging management and associated degradation of the batteries. In 2018, Du et al. published an optimized control strategy for hybrid e-Buses to minimize life cycle costs by reducing battery aging [25]. Zhang et al. developed an optimized service and charging strategy for a fleet of e-Buses considering battery degradation and nonlinear charging profiles, which helped extend battery life by 47.2–96.1% [26]. They also found that the initial SOC when leaving the depot should be as low as possible for reduced degradation. In 2022, Manzolli et al. developed an optimization model for charging a fleet of e-Buses, including vehicle-to-grid (V2G) and consideration of battery degradation [27]. If battery replacement costs fall below 100 €/kWh, providing V2G with the e-Buses in the example country Portugal could become economically attractive. Analogous to the presentations of e-Cars, our work also extends the state of research on e-Buses concerning various battery-relevant parameters.

E-Boats are less of a focus of research than e-Cars and e-Buses, according to our research. Research focuses on designing and modeling pure and hybrid e-Boats [28–30]. In 2012, Spagnolo et al. published a design for an electric catamaran powered by photovoltaic (PV) and batteries [28]. Kabir et al. published a similar system for small ferries in Bangladesh in 2016 [29]. A year before, Soleymani et al. published a design and energy management of a 14-m hybrid e-Boat [30].

Another topic relevant to this work is vehicle **charging strategies**. The most straightforward charging strategy is the direct recharging of the vehicle after arrival at the charging station. We call this type of charging uncontrolled charging, analogous to our previous work and literature [31,32]. This type of charging places the vehicles in high SOC ranges, which has been shown to lead to higher calendar degradation of the batteries [33,34]. Smart charging of vehicles, in contrast, can reduce not only vehicle battery aging but also lower charging costs and reduce the concurrency of charging [35,36]. In 2016, Lacey et al. defined a delayed charging strategy where the vehicle was kept at low SOC after arrival and charged just before departure to reduce calendar degradation by lowering the average SOC [32]. In addition, the authors

identified “less frequent charging” as another option to reduce calendar degradation by not charging after every trip. In 2017, Al-Karakchi et al. published a charging strategy with periodic pauses to reduce pressure and temperature [37]. This strategy reduced the capacity loss of exemplary LG 18650 cells by 2.5% after 350 cycles. Instead, Chen et al. let users choose between three charging strategies, in which users could obey or not obey grid scheduling depending on their risk preference [38]. Houbbadi et al. published a charging strategy for an e-Bus fleet in 2019, in which they optimized the charging behavior considering battery degradation [39]. The optimized strategy performed even better in capacity loss than a delayed strategy, which they called *postponed*, and far better than an uncontrolled charging strategy, which they called *greedy*. In addition to the unidirectional charging strategies presented, there are also bidirectional charging strategies in which vehicles participate in electricity markets using V2G [40,41].

Analysis of battery health and performance is crucial to developing cost-effective electric vehicles. Several **battery parameters** are well-suited for deriving stress factors and health indicators. As described, for example, the SOC influences the aging of the batteries [32,34]. Furthermore, depths-of-discharge (DODs) and temperature are relevant for battery aging [42,43]. Especially for cyclic aging, the charge rate (C-rate) is another relevant parameter, which is the current divided by the nominal capacitance [44]. The energy throughput or, in relation to the battery capacity, the number of equivalent full cycles (EFCs) also contributes to this type of aging [44]. The parameters mentioned are generally relevant for batteries in mobile and stationary applications [45]. As proposed in previous work, the utilization ratio of mobile storage systems allows quantifying the proportion of time a vehicle battery is used, either to provide mobility or for V2G provision [31].

Research has already addressed driving patterns and energy consumption of e-Cars and e-Buses. There is generally less research on e-Boats, and much of it relates to sizing and design. The research gap we have identified relates to the stress on the battery due to driving patterns in various modes of e-transportation. To the best of our knowledge, the impact of driving and charging behavior on parameters relevant to battery life and performance indication has been looked at with insufficient accuracy for e-Cars and e-Buses and not at all for e-Boats. This work aims to expand the publicly available knowledge about e-transportation. In addition, we found that no simulation tool exists that can be used to simulate different modes of e-transportation and quantify the stress on the battery system. Furthermore, vehicle usage profiles are scarce and rarely available as open data. We want to contribute to covering these research gaps in this paper and answer the following research questions (RQs):

- RQ 1) How can various transportation modes be reproducibly simulated to obtain battery usage and health indications (Section 3.2)?
- RQ2) How much energy do e-Cars and e-Buses consume in the exemplary datasets, and what is the influence of the ambient temperature on consumption (Section 4.1)?
- RQ 3) What is the typical stress of mobile battery storage systems in various transportation modes regarding different parameters (Section 4.2)?
- RQ 4) To what extent are battery-relevant parameters in mobile applications similar to stationary applications and could therefore similar cells be used in those applications (Section 4.3)?
- RQ 5) What’s the influence of charging strategies on the considered parameters (Section 4.4)?

1.2. Contribution and scope of this work

This work aims to analyze and compare various transportation means, which we also refer to as mobile storage applications, in the following. For this purpose, field data from e-Buses and e-Boats were collected, and data from e-Cars were simulated. The data is used to

emulate the three use cases in the simulation tool *SimSES* [6]. For this purpose, energy management systems (EMSs) were developed to track mobile storage systems' power or SOC profiles and simulate charging strategies at parking times. This extension of the prior published *SimSES* tool enables the simulation of mobile storage applications by others so that the storage behavior can be simulated and evaluated. Furthermore, we derive and analyze various storage parameters that allow comparison between the three transportation means. We also show the impact of different charging strategies on the parameters. To enable the use of the data of the three battery applications, e-Cars, e-Buses, and e-Boats, we provide the profiles as open data as part of this publication. With the help of these profiles, researchers and industrial partners can make their own simulations or evaluations of transportation means. Accordingly, the work provides the basis for further research in the field of e-transportation. Based on the work, battery technologies for the different means of transport can be compared and optimized for the respective application in the long term.

Fig. 1 shows an overview of the work. After a presentation of the data basis in chapter 2, the data processing and the simulation in *SimSES* is done in chapter 3. Chapter 4 presents the results of the work before chapter 5 gives a summary and an outlook.

2. Database

For the present work, data on various mobile storage applications were collected and processed. The specifications of the raw data sets are shown in Table 1. To achieve a large number of data sets from privately used EVs, the simulation tool *emobpy* from DIW Berlin is used [18]. This tool uses statistics on the driving behavior of private individuals in Germany and the standardized driving cycles WLTC (Worldwide

Table 1
Datasets of the different transportation means.

	e-Car	e-Bus	e-Boat
Number of datasets	60	82	6
Origin Available data	Simulated Power, distance	Measured SOC, milage, ambient temperature	Measured SOC, power
Length of datasets	One year	One day to 14 months	3–9 months
Time	2021	2021–2022	2021
Sampling rate	60 s	10 s	5 s
Data resolution	Power: values derived from trips' energy consumption distance: 1 km for trips	SOC: 0.01% to 0.5% mileage: 0.1 km temperature: 0.1 °C	SOC: 1% power: 10 W
Industry/ Research Partner	<i>emobpy</i> (DIW Berlin) [18]	Hochbahn Hamburg	Torqueedo

harmonized Light-duty vehicles Test Cycles) and EPA (Environmental Protection Agency) to simulate the use of e-Cars. For example, it can simulate effects on the electricity grid due to charging behavior. For the present work, *emobpy* was extended together with DIW Berlin so that the power demand during trips can now be tracked to the second. To determine different driving profiles and power requirements of the e-Cars, various trips were simulated in *emobpy*: First, the three driver types of commuters, non-commuters, and free-time drivers were selected. The driving behavior of each of these three driver types was simulated over one year in ten simulation runs to account for a wide range of driving profiles determined by probability distributions. A time resolution of 60 s was chosen to reduce the duration and memory requirements of the simulations. Germany's mean hourly resolved temperature was used as the ambient temperature in the simulations. In general, *emobpy* allows the selection of one of 39 European countries as simulated ambient temperature [18].

Then, in the second step, the power profiles for the e-Cars were simulated for the two vehicle models, Volkswagen ID.3 (2020) and Tesla Model 3 (2020), using the three simulated driver types. These models were selected because they were among Europe's top three best-selling e-Car models in 2021 [46]. The results are a total of 60 e-Car load profiles. In addition to the load profiles, binary profiles were extracted that indicate whether the vehicle is parked at home or on the road. These binary profiles are used in *SimSES* to map the charging behavior with different charging strategies. Table A1 in the appendix shows the characteristics of the vehicles used for the simulation of the three applications. The assumed charging power for the e-Cars is 11 kW. We describe the use of these parameters for the *SimSES* simulation in section 3.2.

For the mobile application of e-Buses, data was exchanged with Hochbahn Hamburg, which is converting its entire bus fleet to e-Buses by 2030 [5]. Hochbahn Hamburg provided the SOC profiles of 82 e-Buses over up to 14 months for this work. The mileage, speed, and outside temperature were also measured and transmitted with the SOC data. The SOC profiles have a sampling rate of 10 s once the e-Bus is switched on. If the e-Bus is switched off, the SOC is not recorded. Thus, the charging behavior is not tracked. The six e-Bus models available in the dataset are listed in Table A1. For example, there are nine e-Buses from the manufacturer Evobus with Nickel–Manganese–Cobalt (NMC) lithium-ion batteries and a useable capacity of 190 kWh each. The total number of e-Buses in the table is 52, as 30 e-Buses are filtered out by the data processing described in section 3.1. We apply 150 kW as the maximum charging power at the bus depot for e-Buses with NMC battery and 80 kW for e-Buses with Lithium-metal-polymer (LMP) battery, as these are the charging power values of Hochbahn Hamburg. As the maximum power that can be charged and discharged from the batteries,

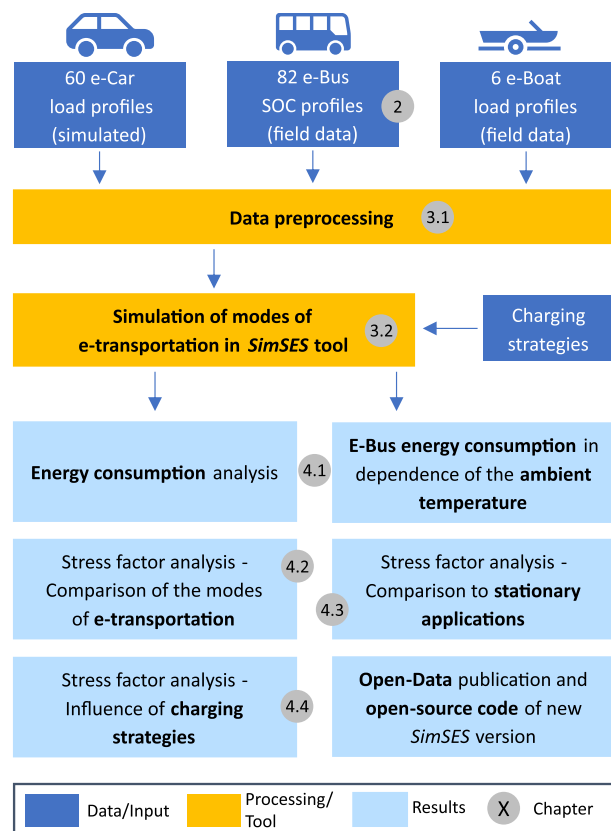


Fig. 1. Structure of the work and respective chapter number.

we apply 350 kW.

The third mobile application of batteries considered in this work is e-Boats. To analyze this application, we collaborated with Torqeedo, who develops and sells electric propulsion systems for e-Boats. Torqeedo provided data from six e-Boats over three to nine months (see Table A1). These six e-Boats represent a smaller database compared to the e-Cars and e-Buses. However, the datasets include ferries and private boats, so a range of exemplary electric boats can be represented. The data includes the SOC and the power balance with a resolution of 5 s. In contrast to the e-Cars and e-Buses, no information is available about the distances traveled. Table A1 also shows the battery capacity and power of the e-Boats. The capacities of the small e-Boats (1–2 t) are 30–40 kWh. In contrast, the large e-Boats (7.5–37 t) have capacities between 80 and 160 kWh. Regarding technical implementation, the 160-kWh e-Boats consist of four 40-kWh battery packs and the 80-kWh e-Boat consists of two 40-kWh battery packs. In the field, this allows variably connecting or disconnecting packs. We neglect this flexibility in this work and assume 160 kWh and 80 kWh battery packs for our simulations. The maximum powers are between 100 and 250 kW. Since the charging power of the e-Boats depends on the respective user and varies over time, we take the most frequently occurring charging power resulting from the load profiles as the standard charging powers. However, the most frequently occurring charging powers for Boat B and Boat C are 40 W and 630 W, respectively. For these two e-Boats, we specify 7 kW as the minimum power, so the most frequently occurring charging powers are 7.82 kW and 32.53 kW, respectively. These charging powers appear realistic for e-Boats with capacities of 80–120 kWh.

3. Methodology

This chapter focuses on the methodology of the work. First, section 3.1 deals with the preprocessing of the raw data. Then, section 3.2 explains the simulation of mobile storage applications in SimSES, including the charging strategies. Finally, section 3.3 describes relevant storage parameters used in the results to compare the mobile applications with each other and with stationary applications.

3.1. Preprocessing and analysis of raw data

As described in chapter 2, *emobpy* is extended to simulate the e-Cars so that the load during trips is also recorded and saved. The output of *emobpy* is 60 annual power profiles and binary profiles for the two vehicles and three driver types (compare Table 1 and Table A1). For the preprocessing, the software MATLAB was used. A first analysis of the

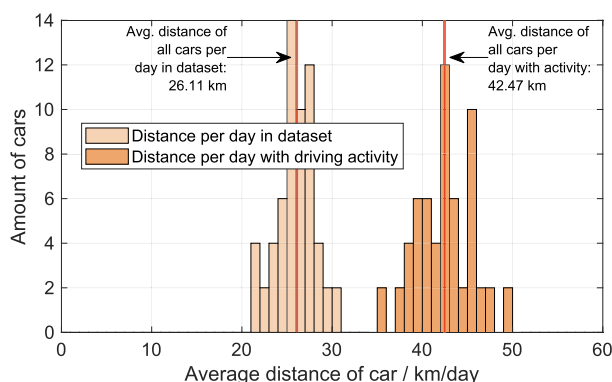


Fig. 2. E-Car dataset (60 e-Cars): Histograms of e-Car average trip distance in km per day normalized to total number of days (light orange) and normalized to only days with driving activity (orange), respectively. (For interpretation of the references to colour in this figure legend, the reader is referred to the Web version of this article.)

raw data is provided in Fig. 2, which shows two histograms of the average daily distances traveled by the e-Cars. In light orange, the annual distance driven by each e-Car is normalized to the total number of 365 days. In orange, the yearly distance is normalized to the number of days with driving activity. Overall, the simulated e-Cars travel 21–31 km per day on average. On a day with vehicle usage, the average distance is between 36 and 50 km. The distances traveled by the e-Cars in a year consequently range between 7700 and 11,100 km. Compared to the average mileage in Germany, which is 13,000 km, the private e-Cars simulated have relatively small mileages [47]. According to the developers of *emobpy*, one reason could be that the study *Mobility in Germany*, whose data the tool uses, only asks for distance categories of individual trips, e.g., “trip over 150 km”. Moreover, studies have shown that e-Cars often drive shorter distances than internal combustion vehicles. For example, De Cauwer et al. determined around 5500 km as the annual distance of two pure electric vehicle fleets in 2015 [9]. In their study from Ireland, Weldon et al. obtained 26–33 km per day (9490 to 12,045 km per year) [14]. Chen et al. found 32.63 km per day (11,900 km per year) for e-Cars in Shanghai [11]. Based on these study results, we accept the deviation from the mean value of the annual distance driven by e-Cars in Germany at this point.

The original e-Bus data is partitioned by day and is divided into individual CSV files for each e-Bus as a first step. Those files contain a timestamp and the SOC. In addition, a CSV is formed from timestamp and outdoor temperature, which allows an analysis of the influence of temperature on energy consumption in the further course of the present work (see section 4.1). Moreover, the following metadata is saved for each e-Bus: Bus number, bus manufacturer, battery type (NMC or LMP), useable battery capacity, average distance driven per day in kilometers, start time, and end time. Next, a data cleansing was performed in which requirements were defined that the individual e-Bus data records must fulfill to filter out small records and records with significant gaps (see

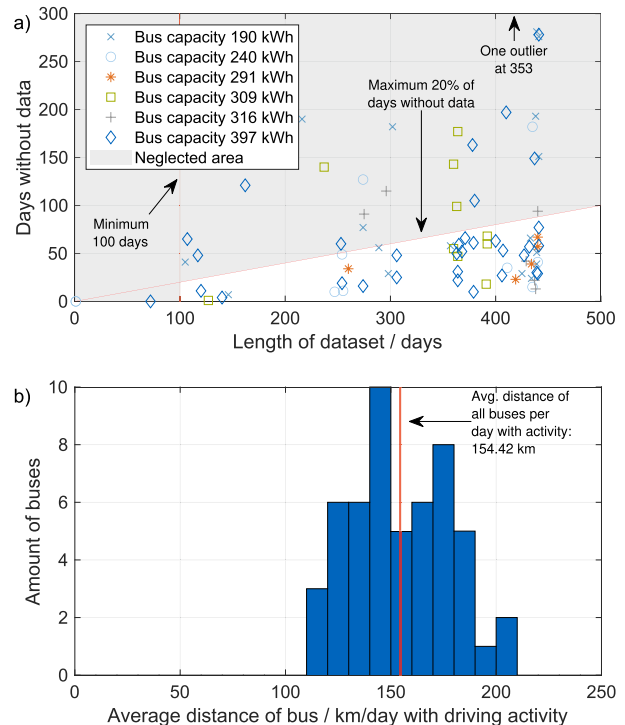


Fig. 3. E-Bus data analyzed - cleansing (a) and cleaned data analysis (b). (a) Scatter plot showing the days without data between the first and last day of a dataset over the total length of the dataset. (b) Histograms of the average driven distance in km per day for days with driving activity.

Fig. 3 a). Each e-Bus record must therefore contain at least 100 days of data. In addition, at most 20% of those days may be without recorded activity. On the one hand, days without activity may be due to the normal break days since fewer city e-Buses are used on weekends compared to workdays. On the other hand, the e-Buses may also be in the repair shop on these days. In addition, errors could also have occurred during data acquisition. For this reason, all e-Buses with more than 20% of inactivity are filtered out. This data cleansing leaves 52 e-Buses that meet the requirements. Fig. 3 b shows a histogram of the distances driven per day with driving activity, analogous to Fig. 2. The 52 filtered e-Buses travel between 113 and 207 km per day with recorded trips. If the e-Buses were used daily, this would correspond to an average of 56,210 km per year. Including the non-operating days, the e-Buses travel 94–189 km per day. This would correspond to 50,735 km per year.

To simulate mobile applications, *SimSES* requires a binary profile in addition to a power or SOC profile. This binary profile indicates whether the vehicle is connected to the grid at a certain point in time (1) or not (0). When the vehicle is connected, it can then be charged according to charging strategies, further explained in the following section. The raw data already includes information on whether the e-Car is currently not at home but on the road, at work, shopping, or at home. In this work, only at-home times are interpreted as possible charging times. Since the binary profile does not exist for the e-Buses and e-Boats, it is generated for each SOC respectively load profile separately, as explained in appendix section 6.2.

The six e-Boat datasets include three to nine months of data. The e-Boat types with battery capacity and power are shown in Table A1. Analogous to the e-Cars and e-Buses, the raw data of the e-Boats is evaluated in the following. Fig. 4 shows the distribution of recorded driving activity for all six e-Boat types. The white spots in between describe periods (days, weeks, or months) without recorded data. After consultation with Torqeedo, the gaps are not errors but show regular periods without activity. In contrast to the e-Car and e-Bus data, the e-Boat data does not include traveled distance measurements. The storage simulation tool *SimSES*, described in the following section, allows the simulation of the storage behavior in different temporal resolutions. If gaps occur in the data, *SimSES* interpolates between the last and the next data point. In the e-Boat simulations, this results in e-Boats being continuously discharged over several days and weeks when no data was available. To prevent this, power values of 0 W were inserted at the beginning and end of gaps with more than 1-h durations. This causes the simulated boat to stay idle in accordance with the original data.

3.2. Simulation of mobile applications in *SimSES*

The storage simulation tool *SimSES* has been developed at the Chair

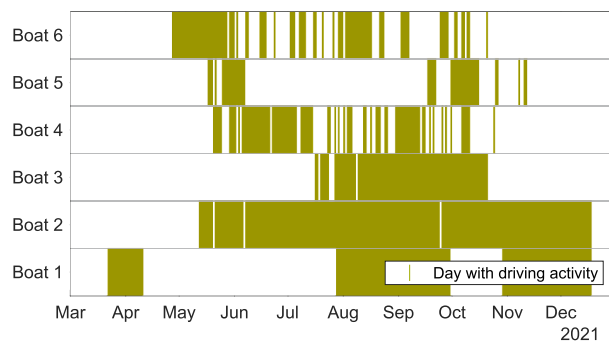


Fig. 4. E-Boats database - days with driving activity are green, and days without driving activity or no data are white. (For interpretation of the references to colour in this figure legend, the reader is referred to the Web version of this article.)

of Electrical Energy Storage Technology at the Technical University of Munich [6]. It enables the simulation of stationary energy storage systems in various applications. The time series simulation is complemented by a techno-economic analysis in which, e.g., efficiency and battery degradation are evaluated. *SimSES* can be used, for example, to simulate stationary home BSSs in self-consumption-increase (SCI) application and large-scale stationary BSSs in the frequency containment reserve (FCR) application. For the present work, *SimSES* is extended toward mobile BSSs. Mobile BSSs are, for example, e-Cars, e-Buses, and e-Boats that are temporarily used for mobility and are temporarily connected to the power grid. For this reason, *SimSES* first requires the binary profile to simulate the vehicles. Next, it requires the load or SOC profile during times when the vehicle is not connected to the grid. This is especially relevant since vehicles are not always connected when they are parked. For the simulation of mobile applications, *SimSES* follows the load profile during the on-the-road times. The resolution used in the simulations is the resolution of the original data shown in Table 1. If the vehicle is connected, charging occurs according to a specified charging strategy. This fundamental principle applies to all mobile applications considered in this work. However, since data on the e-Buses is only available as SOC values, an energy management system (EMS) based on SOC data (SOC-EMS) is developed in addition to a power-based EMS (Power-EMS). In this strategy, the storage system follows the SOC data when the binary value is zero and allows charging according to similar charging strategies as in the power-based EMS when the binary value is one. For this purpose, the EMS calculates the required battery power from the SOC value to reach the desired SOC in each timestep. This approach approximates the real battery power but depends on the resolution of the SOC and the sampling rate. Real power peaks are thus not captured on the one hand, and unrealistic power peaks can occur on the other hand due to short peaks in the SOC profile. The resolution of the e-Bus SOC models is given in Table A1 in the “other info” column. A difference between the Power-EMS and SOC-EMS is that the charging strategies in SOC-EMS charge to a target SOC at the time of departure. This is necessary because otherwise, more significant discrepancies between the SOC in *SimSES* and the original SOC could occur during the next trip, which *SimSES* compensates for with high-power charging or discharging. In the case of the Power-EMS, the battery is charged to 100% SOC until departure since the target SOC is unknown.

Three charging strategies have been implemented in the adapted version of *SimSES*, as depicted in Fig. 5: An uncontrolled charging strategy (a), a mean-power charging strategy (b), and a paused charging strategy (c). In uncontrolled charging, the vehicle is charged at maximum power up to 100% SOC (Power-EMS) or to the target SOC (SOC-EMS) immediately after connection to the electricity grid. In mean-power charging, perfect foresight determines when the vehicle will leave and charge accordingly with the power required to reach 100% SOC or the target SOC at departure time. In paused charging, the vehicle is charged to a minimum SOC immediately upon arrival (e.g., 60%), and subsequently, the charging process is paused. If the SOC at arrival is already above the specified minimum SOC, the current SOC is kept constant, as displayed in the night of January 26th in Fig. 5. During the pause, the EMS determines in perfect foresight when the vehicle will depart. Accordingly, the charging process continues at maximum power so that the vehicle reaches 100% SOC or the target SOC (SOC-EMS) at the time of departure. If 100% is set as the minimum SOC during the pause, this corresponds to the uncontrolled charging strategy. The other extreme is 0% minimum SOC during the pause. In this case, the vehicle would always hold the current SOC after arrival and only charge to 100% SOC or the target SOC shortly before departure. This work’s selection of charging strategies represents a sample of possible non-optimized charging strategies. In the field, aggregators of vehicles would develop optimized charging strategies. Examples of charging strategies with optimization algorithms would be minimizing electricity costs, minimizing distribution grid load, or minimizing battery degradation [32,33,35].

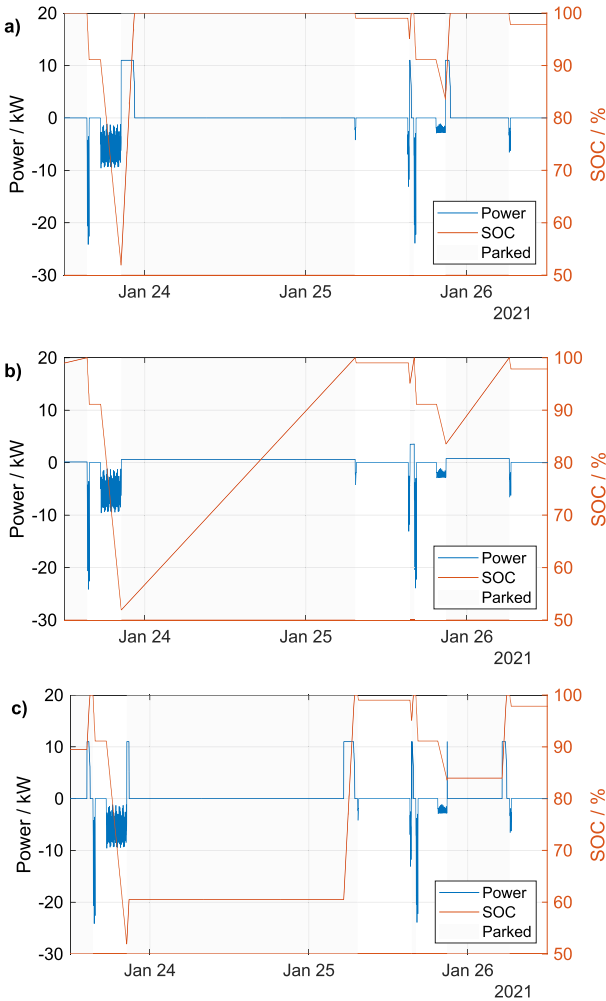


Fig. 5. Illustration of the three charging strategies for an exemplary time snapshot. a) Uncontrolled charging, b) mean-power charging, c) paused charging.

The Power-EMS has a unique feature: If the SOC drops below 2% during a long drive, a fast charge with 150 kW to 80% SOC is simulated. For this purpose, a fast-charging station is assumed to be available on these trips. The trip is postponed by the charging time and is continued after the charge. With the SOC-EMS, implementing fast charging is not required since the SOC profile would already have included the fast-charging process during a long trip. For the Power-EMS, the simulation of fast charging is necessary because, with small vehicle batteries, the desired driving distance might not be achieved with only home charging.

For the simulation of the mobile applications, the battery model of a lithium-ion NMC cell was used [42]. In addition, an inverter model by Notton et al. was applied [48]. The technical specifications of the battery cell are shown in Table A2 in the appendix.

3.3. Relevant mobile storage parameters

Storage systems can be characterized and evaluated in different applications with various parameters (see Section 1.1). In the following, we define the parameters used in this work.

The SOC of a storage system is defined as the fraction of the currently charged electrical charge ($C_{act}(t)$) to the total possible capacity ($C_{total}(t)$)

as displayed in equation (3.1). $C_{total}(t)$ is also time dependent since the total capacity of the battery reduces over time due to degradation effects. Over the entire duration of the simulation or the profile, there is a value for the SOC at every point in time. In our evaluations in section 4, we determine each vehicle's mean SOC for the different transportation modes. We also determine the SOC at the end of each trip, before the vehicle is connected to the electricity grid, i.e., the binary value becomes one. The SOC is relevant for lithium-ion batteries because both calendar and cyclic degradation depend on it [42–44]. High SOC values tend to lead to accelerated calendar aging [42,43], while cycling in high and low SOC ranges may lead to accelerated cyclic aging compared to a mid-range of 45–55% SOC [42]. In general, battery degradation depends on the individual cell type, but the SOC is often a relevant stress factor in battery degradation modeling [49]. For the e-Buses, the useable capacity is used as $C_{total}(t)$, as the tracked SOC data ranges from 0 to 100%. However, the tracked SOC could deviate from the real battery SOC if the bus manufacturer only releases a certain voltage range to be used.

The following parameter is the depth of cycles (DOCs), determined according to equation (3.2). For this purpose, it is calculated for each cycle how deep the battery was charged or discharged. The cycles can be determined in different ways. In *SimSES*, a half-cycle detector is implemented [6]. Another possibility would be, for example, the use of a rain flow counting algorithm [50]. Here, a distinction can also be made between the charging and discharging direction. The term depth of discharge (DOD) is often used in the discharging direction. Analogous to the mean SOC at the end of trips, we determine the mean DOD of the trips by subtracting the SOC at the beginning of each trip from the SOC at the end of the trip.

Another relevant parameter is the C-rate, which describes the current (I) at which the battery is charged or discharged in relation to its total capacity (C_{total}). The calculation of the C-rate is shown in equation (3.3). It can be calculated as an absolute value as in the equation or separately in charge and discharge direction. As described in section 2, the e-Bus data consists of SOC values. In *SimSES*, these SOC values are tracked during the trips, and the power is determined in each time step that must be charged or discharged to reach the target SOC. The current can then be used to determine the C-rate. We use the original power profiles for the e-Car and e-Boat data to determine the current directly from the power, not from a SOC profile. The cycles that the battery completes over a period of time are often referred to as equivalent full cycles (EFCs) or full equivalent cycles (FECs). Equation (3.4) describes the EFC calculation as implemented in *SimSES* [45]. For this purpose, the charged energy in the year (E_{year}^{pos}) is divided by the energy content of the battery (E_{BSS}).

Especially for mobile applications, another parameter is of relevance: The temporal utilization ratio $\mu_{utilization}$, the calculation of which is given in equation (3.5) and described in detail in [31]. This parameter represents the proportion of time a battery is charged or discharged in an application. For this purpose, the sum of the time steps at which the power $p(t)$ is not equal to zero is divided by the total number of time steps n . For vehicles, this ratio means the proportion of time the vehicle is discharged due to trips or charged. The rest of the time, the vehicle is not used and is either parked somewhere on the road or at the charging point without being charged. In Germany, for example, a study found that private cars are parked for more than 23 h per day on average, resulting in a utilization ratio of less than 5% [16]. For stationary BSSs, the temporal utilization ratio describes the proportion of time that the BSS is charged or discharged. The rest of the time, the BSS is connected but not in use.

The final parameter relevant to the transportation means is the temporal V2G-ready ratio μ_{V2G} . This parameter indicates the proportion of the time the vehicle is connected to the electricity grid but not being charged. The calculation of μ_{V2G} is shown in equation (3.6). Accordingly, the auxiliary variable $v(t)$ is one if the vehicle is neither charged nor discharged ($P(t) = 0$) and the binary value is one ($b(t) = 1$). For the e-

Bus, $b(t) = 1$ means that the e-Bus is in the depot, for the e-Car that it is at home, and for the e-Boat that it is at the dock. The variable μ_{V2G} is not simply one minus $\mu_{utilization}$, since the vehicles can also be on the road without being charged or discharged or without being connected to the electricity grid. With the help of μ_{V2G} , it is possible to estimate the temporal V2G potential of the vehicle. At this point, V2G is representative of all forms of power feedback from the vehicle, including vehicle-to-home (V2H), for example.

$$SOC(t) = \frac{C_{act}(t)}{C_{total}(t)} \quad (3.1)$$

$$DOC = SOC_{cycle,start} - SOC_{cycle,end} \quad (3.2)$$

$$C_{rate,abs}(t) = \frac{|I(t)|}{C_{total}(t)} \quad (3.3)$$

$$EFC = \frac{E_{year}^{pos}}{E_{BSS}} \quad (3.4)$$

$$\mu_{utilization} = \frac{\sum_{t=1}^n u(t)}{n} \quad (3.5)$$

$$\mu_{V2G} = \frac{\sum_{t=1}^n v(t)}{n} \quad (3.6)$$

$$\text{With: } u(t) = \begin{cases} 1, & P(t) > 0 \vee P(t) < 0 \\ 0, & P(t) = 0 \end{cases}$$

$$v(t) = \begin{cases} 1, & P(t) = 0 \wedge b(t) = 1 \\ 0, & \text{otherwise} \end{cases}$$

3.4. Procedure for determining e-bus energy consumption in dependence on the ambient temperature

The e-Bus data includes not only the SOC profiles but also data on the mileage and the ambient temperature of the e-Buses. In Section 4.1, the energy consumption of the e-Buses is determined as a function of ambient temperature. Therefore, a combination of raw data (mileage and ambient temperature) and simulation results (energy consumption) from *SimSES* is used. To obtain a complete dataset for the e-Bus mileage, forward filling is used since the mileage is not recorded at each time sample. The *SimSES* simulations are performed with a resolution of 10 s, which can be directly matched with the raw data samples. Thus, the entire dataset contains the ambient temperature, e-Bus mileage, battery SOCs, and states of energy (SOEs). Here, the SOE indicates the total amount of electrical energy in kWh contained in the battery. For further analysis, the data is split into individual trips. Trips are time intervals during which the e-Buses are not connected to the grid, and an increase in mileage is observed. To disregard times when the e-Buses are connected to the grid, we check the binary value for $b(t) = 0$. Additionally, we defined the following criteria for a valid trip:

- 2 h < trip duration < 24 h
- 20 km < trip distance < 300 km

Trips of less than 2 h and 20 km are neglected to ensure no service or test drives are considered. In regular operation, e-Buses are charged each night. Trips of more than 24 h are disregarded to disregard unusual operation. Finally, a bug in logging the mileage led to unreasonable jumps in the mileage counter. Overall, the analyzed e-Buses usually cover between 84 and 130 km in a complete shift of 8 h. Thus, an upper limit of 300 km is appropriate to filter out faulty mileage readings without neglecting valid trips. This procedure yields more than 22,000 trips for all 52 e-Buses.

During each trip, the e-Bus undergoes a change of SOE and mileage. The average energy consumption for each trip is computed as the fraction of change in SOE (ΔSOE) and distance driven (Δd):

$$Consumption_{trip} = \frac{\Delta SOE_{trip}}{\Delta d_{trip}} \quad (3.7)$$

Additionally, the mean ambient temperature of each trip is computed to allow for the analysis of ambient temperature-sensitive energy consumption behavior.

4. Results

This chapter presents the results of our work. Section 4.1 describes the results on the energy consumption of the individual mobile applications. In addition, we provide an in-depth analysis of the consumption of the e-Buses depending on the ambient temperature. Section 4.2 compares the effects of the applications on the batteries with each other using the parameters presented. Subsequently, we compare these with the parameters of stationary applications in section 4.3. Lastly, the influence of the charging strategies on the parameters is shown in section 4.4.

4.1. Energy consumption analysis of e-cars and e-buses

This section shows the energy consumption results of the three transportation modes. At this point, the energy consumption refers only to the DC side and neglects, for example, charging losses. Fig. 6 a) shows the total energy consumption of the e-Cars over the distance traveled. The simulations were performed with *emobpy* over one year, and the models chosen are the Tesla Model 3 and the Volkswagen ID.3 (see section 2). As described in section 3.1, the distances traveled range from 7700 to 11,100 km. The Tesla and the Volkswagen were simulated for each mobility behavior, resulting in each distance value occurring once in the diagram for each vehicle type. The energy consumed by the e-Cars was determined in *SimSES* and ranges from 1450 to 3200 kWh. The two lines in the graph indicate consumptions of 20 kWh/100 km and 30

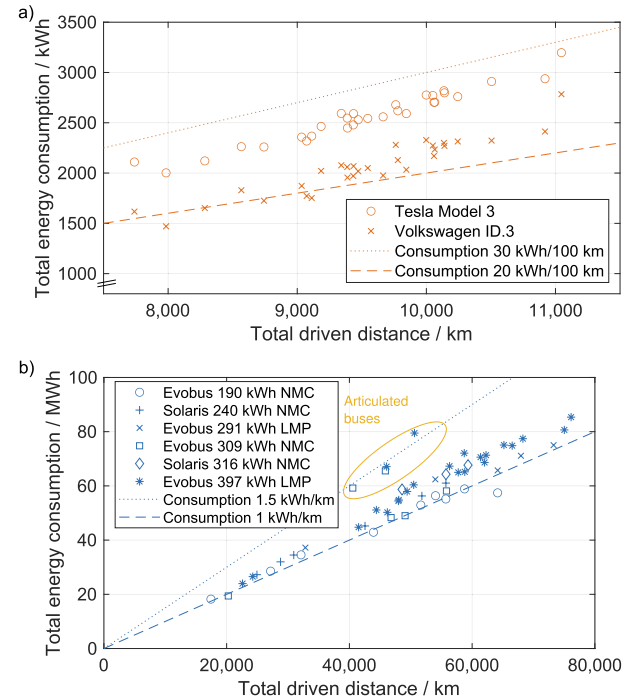


Fig. 6. a) Simulated e-Car energy consumption analysis separated by model. Tesla Model 3 avg. consumption: 26.78 kWh/100 km; Volkswagen ID.3 avg. consumption: 21.38 kWh/100 km. b) E-Buses energy consumption analysis separated by e-Bus types.

kWh/100 km. Per 100 km, the e-Cars' energy consumption is between 18 and 29 kWh. The Tesla Model 3 has a higher consumption than the Volkswagen ID.3, in line with previous results [18].

Fig. 6 b) shows the energy consumption of the e-Buses over the distances driven, broken down by the e-Bus types. In contrast to the e-Car data, the e-Buses were not all measured over the same period (see Fig. 3 a). This increases the differences in the distances traveled by the e-Buses. Consequently, the e-Buses have traveled between 17,400 and 76,200 km. Analogous to Fig. 6 a), the two lines show exemplary energy consumption rates of 1 and 1.5 kWh/km. The diagram indicates that most e-Buses show an average consumption of 1–1.2 kWh/km. Four e-Buses show increased consumption of 1.4–1.6 kWh/km. These e-Buses are articulated buses, which explains the increased consumption. Apart from that, we did not find significant differences in average consumption between the different e-Bus models. Compared to the literature, the studied e-Buses investigated in this work show relatively low energy consumption (see section 1.1). On the one hand, this may be because the studied e-Buses are from the construction years 2019–2021, while the cited papers were published between 2015 and 2018 and therefore show older bus models. On the other hand, our results show only DC-side consumption, while other articles include charging losses in some cases. Moreover, Rogge et al. used a simulation model, not field data from e-Buses, and came up with over 2.2 kWh/km energy consumption in 2015 [20]. In 2017, Gao et al. already determined consumptions of 1.35 kWh/km for real e-Buses [23]. Lastly, the outdoor temperature significantly impacts energy consumption, as shown in more detail below. This can result in different energy consumption rates for identical e-Buses in different countries.

Fig. 7 also illustrates the consumption of the e-Cars and e-Buses per kilometer as boxplots, classified according to the models. The Volkswagen ID.3 consumes, on average, between 0.184 and 0.25 kWh/km, while the Tesla Model 3 is between 0.25 and 0.29 kWh/km. The e-Buses consume, on average, between 0.89 and 1.58 kWh/km. E-Buses with smaller batteries tend to consume less energy than larger e-Buses, although the spread in the individual segments is relatively large in some cases. For example, the six 240-kWh e-Buses consume between 1.06 and 1.11 kWh/km, while the six 309-kWh e-Buses consume between 0.96 and 1.46 kWh/km. The two outliers in the 397-kWh e-Bus segment are two articulated e-Buses from Fig. 6 b). The two other outliers in Fig. 6 b) form the maximum in the 309-kWh e-Bus segment. Other reasons for differences in individual e-Bus consumption could be external influences, such as the outside temperature or route-characteristics, in addition to the general driving style. We, therefore, perform an analysis of consumption depending on the outdoor temperature in the following paragraphs.

As described in section 2, the e-Bus data contains values for the

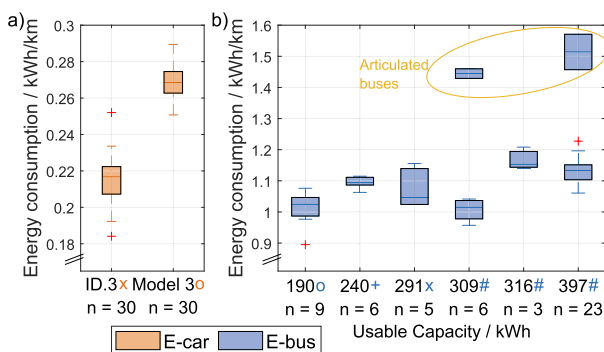


Fig. 7. Simulated e-Car (a) and field-data e-Bus (b) boxplots of the vehicle mean energy consumption per kilometer for the different models. The symbols next to the type correspond to the symbols in Fig. 6. The numbers below the types indicate the number of car or bus types in the data sets.

ambient temperatures of the e-Buses. Therefore, we analyze the trip energy consumptions of the 52 e-Buses described in Section 3.1 in dependence on the ambient temperature according to the methodology explained in Section 3.4. Each trip thus yields an average trip consumption and an average ambient temperature. All trips are weighted equally for the boxplots in Figs. 8 and 9.

Fig. 8 shows the energy consumption of all trips in dependence on the average trip ambient temperature from 10 to 30 °C. Generally, e-Buses show minimal consumption at 20–22 °C. The analysis of all e-Buses and their respective trips yields the lowest median consumption at 21 °C with a value of 0.98 kWh/km. Consumption increases for higher temperatures mainly due to air conditioning. The e-Buses show an increase to a median consumption of 1.16 kWh/km at an ambient temperature of 30 °C (+19%). For decreasing temperatures, electric heating shows an analogous increase in energy consumption. At 10 °C, a median consumption of 1.24 kWh/km (+27%) can be observed. Overall, the e-Bus energy consumption increase is almost symmetric regarding temperature variation from 10 to 30 °C. As a rule of thumb, energy consumption increases by 2–3% per 1 °C change in ambient temperature.

Fig. 9 shows the resulting consumption behaviors depending on the ambient temperature for the two specific types of e-Buses, Solaris 240 kWh and Evobus 309 kWh (excluding the two articulated buses of this type). The boxplots of the other four types are displayed in Appendix Fig. A2. The consumptions of the individual e-Bus categories reveal an almost identical behavior above 14 °C. At lower temperatures, the trends differ substantially. E-Buses of type Evobus 309 kWh show the expected behavior of increasingly higher consumption at lower ambient temperatures. The lowest median consumption of this type is found at 22 °C with 0.89 kWh/km. At –2 °C, the median consumption doubles to 1.77 kWh/km. E-Buses of type Solaris 240 kWh have a minimum consumption of 0.94 kWh/km at a temperature of 21 °C. The consumption climbs for decreasing temperatures to a maximum median value of 1.37 kWh/km at 8 °C, an increase of 46%. A sudden drop to a median consumption of 1 kWh/km is observable for temperatures below this threshold. The reason behind this divergence is the heating method. All E-Buses in this analysis contain a hybrid heating solution consisting of an electric heater and fossil fuel heating. The operation strategy of the latter differs between bus manufacturers. In this analysis, Solaris' 240 kWh e-Buses seem to switch to exclusive fossil fuel heating when the temperature drops below 8 °C. Such an operation strategy conserves battery to extend the driving range but has the disadvantage that these e-Buses remain dependent on fossil fuels.

4.2. Comparison of mobile applications

Following the analysis of e-Car and e-Bus consumption, this section compares the stress on the batteries in the three mobile storage applications. Fig. 10 (a) shows the distributions of the energy consumption of

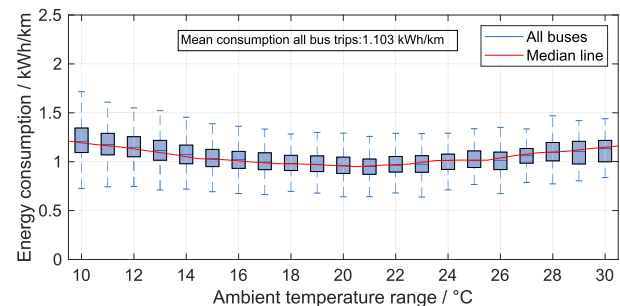


Fig. 8. Boxplot diagram of the energy consumption depending on the ambient temperature for all e-Buses of all categories. Outliers are removed to not distract from the general trend. The complete diagram with outliers is displayed in Appendix Fig. A1.

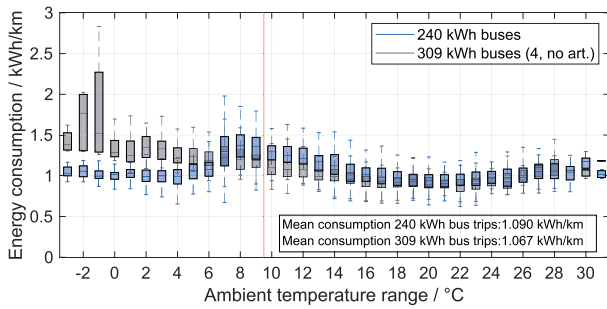


Fig. 9. Boxplots of the energy consumption of the e-buses “Solaris 240 kWh” and “Evobus 309 kWh” in dependence on the outside temperature. The red vertical line indicates the X-axis limit from Fig. 8. Outliers are removed to not distract from the general trend. The complete diagrams with outliers are shown in Appendix Fig. A2. (For interpretation of the references to colour in this figure legend, the reader is referred to the Web version of this article.)

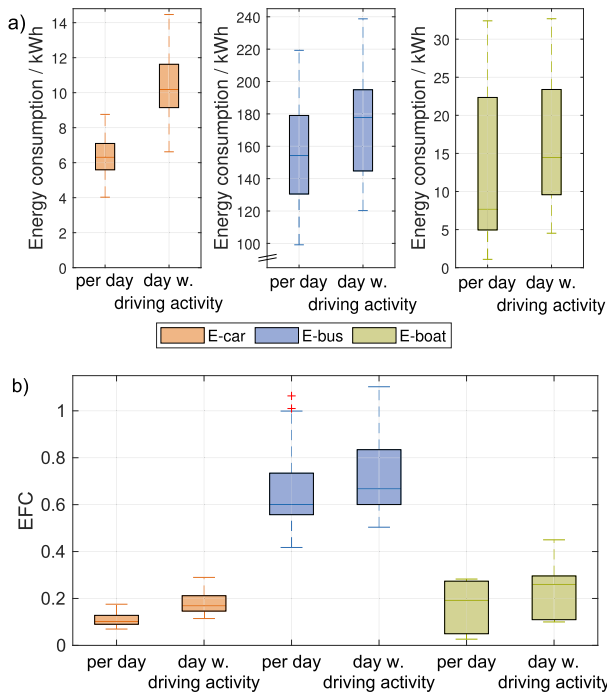


Fig. 10. Boxplots showing energy consumption (a) and equivalent full cycles (EFCs) (b) for all vehicle types analyzed. Data normalized per day and per day with driving activity.

the three means of transport as boxplots. The left boxplot indicates the average energy consumption of the vehicles per day over the respective dataset length. The boxplot on the right shows the average daily energy consumption on which driving activities occurred. The simulated e-Cars thus consume a median of 6.3 kWh per day. On days when the e-Cars are used, they consume a median of 10.1 kWh. In contrast, the e-Buses consume 99 to 220 kWh per day. Since the e-Buses drive more frequently than the e-Cars, the right boxplot of the e-Buses differs only slightly from the left boxplot. The energy consumption of the e-Boats shows the most significant spread. There are e-Boats that consume, on average, only 1 kWh per day and e-Boats that consume 32.5 kWh per day. One reason for this could be the significant differences in e-Boat sizes. For example, the lightest e-Boat weighs only 1 ton, and the heaviest is 37 tons (see Table A1). In addition, the e-Boats drive with different

frequencies. The e-Boat that needs only 1 kWh per day consumes 4.5 kWh on days with trips and thus forms the minimum in the right boxplot. In contrast, the e-Boat that consumes 32.5 kWh per day also travels almost daily, so the maximum of the right boxplot is 32.8 kWh.

Below, Fig. 10 (b) shows the EFCs of the three means of transport also as boxplots and once per day and once per day with driving activity. As the battery capacities of the three means of transport vary, the daily EFCs do not differ as much as the energy consumption in Fig. 10 (a). The simulated e-Cars make between 0.07 and 0.18 EFCs per day with a median of 0.102 EFCs. The median value corresponds to about 37 EFCs per year. If only the days on which trips occurred are considered, the EFCs increase by 50%–70% for the e-Cars. The e-Buses make more EFCs despite having larger battery capacities ranging from 190 to 397 kWh. The median here is 0.60 EFCs per day and 0.67 EFCs per day with driving activity. Since the e-Buses run on more days than the e-Cars, the EFCs per day of driving activity only increase by up to 23%. At the peak, there are even e-Buses that make a mean of 1.1 EFCs on the days they operate. Accordingly, if an e-Bus battery has a cycle life of, for example, 3000 EFCs, the e-Bus could be operated for 13.7 years at 0.6 EFCs per day. With 1.1 EFCs per day, the operation time would be 7.5 years. The e-Boats, in turn, make fewer EFCs than the e-Buses. On median, e-Boats make 0.19 EFCs per day and 0.26 EFCs per day with activity. Thus, on average, the batteries in the six e-Boats complete more equivalent full cycles than the batteries in the 60 simulated e-Cars but fewer than the 52 e-Buses. If the EFCs per day with driving activity are calculated for the e-Boats, they are only 0.8% higher for one e-Boat that drives almost every day than if the EFCs were calculated for all days. The other extreme is an e-Boat that only drives every fourth day, which results in 0.026 EFCs per day, then 0.1 EFCs per day with driving activity.

Next to energy consumption and EFCs, other parameters are of relevance for the three modes of transport. For this purpose, Fig. 11 presents further boxplots of the three mobile applications. The boxplots of the mean SOC of the means of transportation for the uncontrolled charging strategy are shown in Fig. 11 (a). The e-Cars show little spread; all have mean SOC of 97.6–98.8%. In contrast, the mean SOC of the e-Buses range from 72.8 to 88.7% SOC with a median of 81.2%. The median of the mean boot SOC is 91.9%. Overall, the analyzed e-Bus

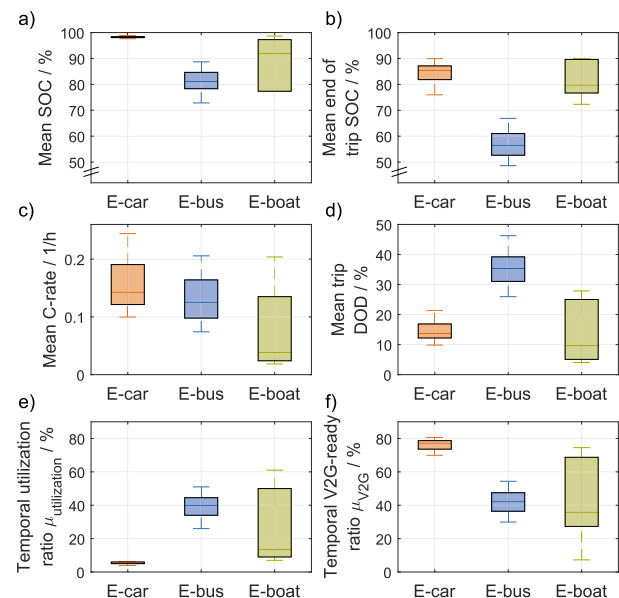


Fig. 11. E-Car (60, simulated), e-Bus (52, field data), and e-Boat (6, field data) boxplots of mean (a) and mean end of trip SOC (b), mean C-rate (c), mean trip DOD (d), temporal utilization ratio (e) and temporal V2G-ready-ratio (f). The bus SOC, C-rates, and DODs each refer to the useable capacity of the buses.

batteries are at the lowest average SOC due to frequent and long trips, e-Car batteries are at the highest average SOC, and e-Boat mean SOC varies the most. For the selection of battery cells for vehicles, this means that in the case of uncontrolled charging, vehicle batteries should have comparatively low calendar degradation in high SOC ranges. This is especially relevant for private e-Cars.

Fig. 11 (b) shows the mean end-of-trip SOC of the three transportation means. For this parameter, the SOC is measured at the end of each trip, and then all these SOC values are averaged for each vehicle. The e-Cars have mean end-of-trip SOC values of 76–90% with a median of approximately 85%. The e-Buses, in contrast, end their trips with a mean SOC of 48–67% and a median of 56.5%. Last, the e-Boats have similar mean end-of-trip SOC values as the e-Cars of 72–90% (median 79.7%).

Diagram (c) of Fig. 11 shows the boxplots of the mean absolute C-rate of the e-Cars, e-Buses, and e-Boats. The average C-rates, meaning the current at which the batteries are discharged and charged normalized to the battery capacity in Ah, are between 0.018 and 0.244 1/h for all means of transport. E-Cars have the highest average C-rates at 0.10 to 0.244 1/h compared to e-Cars and e-Boats. The mean C-rates of the e-Buses range from 0.07 to 0.21 1/h, and that of the e-Boats is below 0.21 1/h. Here, the six e-Boats can be separated into two groups according to their battery capacity: Group 1 is Boat 1–3 and has battery capacities of 80–160 kWh. Group 2 is e-Boat 4–6 with battery capacities of 30–40 kWh (see Table A1). Group 1 then has very low C-rates of 0.024–0.042 1/h with an average of 0.033 1/h. Group 2, in contrast, shows an average C-rate of 0.119 1/h. Since the charging strategy influences the mean C-rate, we discuss this impact in more detail in section 4.4.

Subfigure (d) of Fig. 11 shows the mean DODs of a trip for the three modes, respectively, analogous to the SOC in (b). The mean trip DODs of the e-Cars range from 9.8 to 21.4%, with a median of 13.7%. In contrast, the mean trip DODs of the e-Buses are with 26–46% and a median of 35.3% higher than those of the e-Cars. Per trip, the mean DODs of the e-Boats range from 4.2 to 27.9% (d). Accordingly, the dataset includes e-Boats that complete only short trips and other e-Boats that consume more than a quarter of the batteries' energy per trip on average.

Last, the bottom two plots of Fig. 11 show the temporal utilization ratio $\mu_{\text{utilization}}$ (g) and the temporal V2G-ready ratio μ_{V2G} (h), presented in section 3.3. The temporal utilization ratio indicates the proportion of the time the vehicle is charged or discharged. The e-Cars in Fig. 11 (g) are used for charging or discharging only 4–6% of the time. This is in line with the statistics for private e-Cars in Germany, according to which they are used for trips only 3–4% of the time [16]. If the time spent charging the e-Cars is added, the 4–6% for $\mu_{\text{utilization}}$ is obtained. The e-Buses investigated in this study are used much more frequently compared to private e-Cars, showing values of 26–51% for $\mu_{\text{utilization}}$. Consequently, the e-Buses are used a quarter to half of the time either for trips or for charging the batteries. The e-Boat datasets show the greatest variation for the temporal utilization ratio. Thus, some e-Boats are used only 7% of the time, and other e-Boats are used 62% of the time, which is more than the most used e-Buses. However, when analyzing the utilization ratio of the e-Boats, it should be considered that the e-Boat data is available for three to nine months, mainly between May and November (see Fig. 4). Thus, actual utilization ratios of some rarely used e-Boats could be even lower over a whole year.

The temporal V2G-ready ratio μ_{V2G} in Fig. 11 (h) represents the fraction of time a vehicle is parked at the depot/at home/at the dock and thus plugged but not charging. For example, the analyzed private vehicles are at home 70–80% of the time and are not charged. Accordingly, the e-Cars could be used for V2G provision during this time. Consistent with Fig. 11 (g), e-Buses have less potential for V2G deployment. They are in the depot 30–54% of the time without being charged. However, e-Buses drive more predictable than private e-Cars, which means that e-Buses could also be used for V2G one-third to one-half of the time. Generally, e-Boats that are regularly docked in harbors could be used for V2G deployment. The e-Boats analyzed in this work differ significantly in μ_{V2G} , analogous to Fig. 11 (g). Some e-Boats are at the dock only 7% of

the time without being charged. Other e-Boats, however, are idle up to 75% of the time. Consequently, the V2G potential of these means of transport depends strongly on the individual e-Boat.

Overall, the batteries in the means of transportation are stressed differently: E-Cars have relatively high mean SOC values with uncontrolled charging, are exposed to small DODs on average between charging events and undergo 0.1 to 0.2 cycles per day on average. For batteries in e-Cars, this means that calendar degradation is more relevant than cyclic degradation. Cells that exhibit accelerated calendar degradation at high SOC values appear less suitable for private e-Cars. In contrast, the average SOC of e-Buses is lower at around 80% when charging is uncontrolled. Furthermore, the e-Buses perform larger cycle depths between charging events and cope with 0.5–1 EFC daily. Accordingly, cyclic degradation appears more critical for the e-Buses than for the e-Cars studied in this work. Thus, cycle-stable battery cells should preferably be installed in e-Buses. The results for the e-Boats show the largest spreads, as there is a relatively large difference in driving patterns and usage among the six e-Boats. E-Boats should therefore be divided into subcategories when selecting battery cells. Generally, cycle depths between charging events are less than those of the e-Buses and may even be less than those of the e-Cars. The EFCs of the e-Boats are in the range of the e-Cars and, in some cases, below them. In view of the EFCs, mean SOC values, and C-rates, the use of typical e-Car batteries appears to make sense for most e-Boats. Regarding the temporal utilization ratio, especially private e-Cars are used rarely. This parameter is considerably higher for e-Buses. E-Boats also show a large spread here. The potential of vehicle utilization during idle times is demonstrated by the V2G-ready ratio: E-Cars and some of the e-Boats show the greatest potential, but the analyzed e-Buses are also parked in the depot for 30–54% of the time without being charged. Last, the estimated SOC values, C-rates, and DODs each refer to the useable capacity of the vehicles. By oversizing the battery and enabling specific voltage ranges, the actual battery SOC values might deviate from those shown, and the C-rates and trip DODs might decrease.

4.3. Comparison with stationary applications

Batteries are used in stationary applications in addition to the three mobile applications discussed in this work. For example, BSSs can be installed with PV systems to store PV surplus energy during the day and discharge the storage at night. This application leads to an increase in self-consumption (SCI). In addition, stationary BSSs can also be used to provide balancing power. In Central Europe, for example, there is a market for FCR in which BSSs can participate to balance frequency fluctuations in the grid. Another application of stationary BSSs is peak shaving (PS). In this application, which is often used at industrial sites, peak loads of the industrial customers are covered by the BSS, which reduces the power price of the electricity purchase. In a previous work, we evaluated the behavior of BSS in these three stationary applications concerning several battery parameters [45]. Fig. 12 compares three selected parameters of BSSs in mobile applications and values obtained for stationary applications. For the SCI boxplots, 74 simulated home storage profiles were evaluated for which the BSS was charged using the “greedy strategy,” as is further explained in [45]. The FCR application shows the results of five BSSs with an LFP battery cell and modular inverter. Last, the PS boxplots show the distribution of 36 BSSs in the PS application that were divided into three clusters [45]. In [45], we have already shown the EFCs and mean DODs. For this work, we evaluated the power profiles of the stationary BSSs in terms of mean SOC and temporal utilization ratio.

Fig. 12 a) shows the number of EFCs the batteries complete daily in the six applications. Stationary BSSs in SCI and FCR perform a similar number of EFCs, averaging 0.77 and 0.7, respectively, as e-Buses with an average of 0.66. In contrast, e-Cars and e-Boats make fewer EFCs per day, with averages of 0.11 and 0.17, respectively, and stationary BSSs in PS application make the fewest EFCs, with an average of 0.07. Fig. 12 b) represents the mean SOC of the batteries in the six applications. The

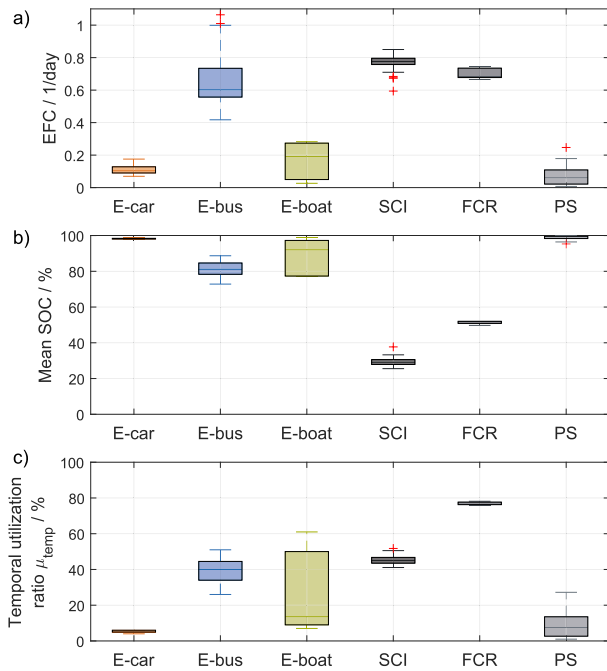


Fig. 12. Comparison of three parameters of mobile and stationary applications. SCI: self-consumption increase, FCR: frequency containment reserve, PS: peak-shaving.

mean SOC of BSSs in the PS application is in a similar range as the mean SOC of the private e-Cars when they are charged uncontrolled immediately upon arrival. We show the influence of charging strategies on the mean SOC in section 4.4. In contrast, the BSSs in the FCR application have mean SOC in the range of 49–53%. The mean SOC of BSSs in SCI are the lowest, ranging from 25 to 37%. Fig. 12 c) shows the temporal utilization ratio as displayed in Fig. 11 f) for the transportation means. The temporal utilization of the stationary BSSs varies considerably: While FCR-BSS are used about 75–80% of the time, the ratio for PS-BSSs is, on average, only 9%. The utilization ratio of the SCI-BSS is between 40 and 50%. The utilization ratios of the mobile applications are all below 62%, which is below or equal to the FCR and SCI-BSS temporal utilization ratios.

In total, the parameters of the mobile and stationary applications show that, for example, in terms of equivalent full cycles and utilization ratios, e-Buses and SCI place a similar load on the battery. The impact on batteries in stationary PS-BSSs are similar to the load that e-Car batteries see in terms of the three parameters: Low number of cycles, high mean SOC, and small usage times. Infrequently used e-Boat batteries experience similar loads as e-Cars and PS-BSS. As e-Buses, SCI BSS, and FCR BSS all post about a similar cycle load to a battery, those applications could aim for a similar type of cycle-stable battery. In contrast, e-Car, e-Boat, and PS BSS have low numbers of EFCs and could cope with a battery that does not provide high cycle stability. For the mean SOC, a similar interpretation is that calendar aging stability at high SOC values is relevant for e-Cars, e-Buses, e-Boats, and peak shaving, especially when the vehicles are charged uncontrolled. The temporal utilization ratio is of interest regarding V2G deployment. Thus, e-Cars could be combined with PS. However, a more detailed study is needed to determine whether e-Car use and PS demand coincide or at independent times of the day. The evaluation also suggests that discarded bus batteries designed for high cycles and medium utilization ratios could be used for SCI or FCR in second life. If, on the other hand, an increased number of cycles is already achieved in the first life of bus batteries, subsequent use in the PS application could make sense since this requires

fewer cycles. Discarded e-Car batteries, optimized for high energy and power density rather than high cycle life, could also be used in stationary PS applications in second life.

4.4. Influence of charging strategies

This section investigates the charging strategy’s impact on two parameters. For this purpose, the e-Cars, e-Buses, and e-Boats were simulated with the three charging strategies presented in section 3.2: uncontrolled charging, which was used for the results of the previous sections; charging with mean power; charging with a pause at 60% SOC. Fig. 13 shows the mean SOC (a) and mean C-rate (b) for the three strategies and the three modes of transportation. If the departure time is determined with the help of perfect foresight and charging is carried out with the mean power required, the mean SOC decreases because the vehicles are not parked for a long time at high SOC. This strategy reduces the median of all mean SOC by 3.4 (boats) to 8 (buses) percentage points. Above all, however, the mean C-rate is drastically reduced during charging. Thus, the C-rates of all vehicles are below 0.1 1/h. Especially the private e-Cars, with their long idle times between trips, show C-rates below 0.02 1/h with this strategy. In practice, this would correspond to charging rates of under 1.6 kW for the Tesla and under 1 kW for the Volkswagen. These low charging powers would lead to considerable efficiency losses in a wallbox designed for 11 kW [51], for example, which is why an economically optimal charging power probably lies between the mean power and the uncontrolled charging strategy power. The paused charging strategy, therefore, takes a different approach: After arrival, the vehicle is charged to a minimum SOC for spontaneous trips (60% in Fig. 13). The charging process is then paused and resumed shortly before the next journey. The effects of this strategy are shown in Fig. 13 on the right. Compared with the other two strategies, the paused charging strategy reduces mean SOC. Thus, the e-Cars have mean SOC around 90%, the e-Buses between 65 and 80%, and the e-Boats 76–97%. The generally still high SOC, despite the break at 60% SOC, are because trips often end at higher SOC (see Fig. 11 b). Note that active discharging down to 60% is not enforced in the simulations. The long idle time at high SOC increases the mean SOC despite applying the paused charging strategy. The mean charging rates of the vehicles in the paused strategy correspond to the rates of the uncontrolled strategy since charging is also performed at maximum charging power before and after the pause.

The break at 60% SOC is used as an example at this point to have

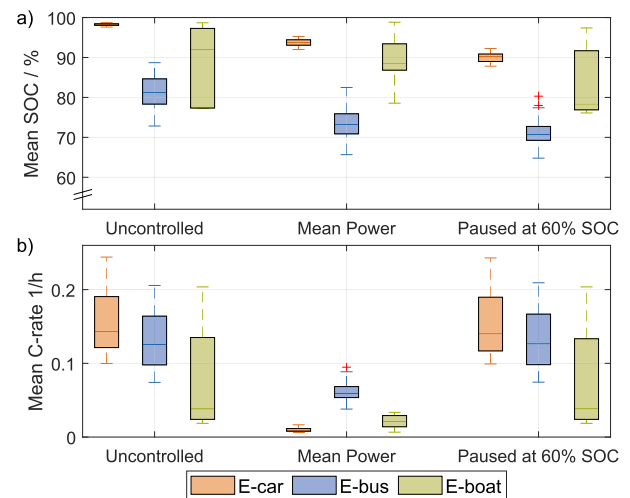


Fig. 13. Influence of charging strategies on mean SOC (a) and mean C-rate (b) for the three transportation means.

energy available for spontaneous departures. Generally, the setpoint value can vary between 0 and 100% SOC. A pause at 0% would mean that each vehicle is held at the arrival SOC and only charged shortly before departure. A delay at 100% SOC corresponds to the uncontrolled strategy. To show the impact of the pause SOC on the mean SOC, we have plotted the boxplots of all vehicle types for various pause thresholds in Fig. 14. If the pause SOC value is reduced from 100% progressively, the mean SOC decreases. However, the potential of further reducing the pause SOC eventually saturates in all three vehicle categories. In the case of e-Cars, for example, reducing the pause SOC from 80 to 60% results in only a one percentage point reduction in the median SOC. The negligible impact of the threshold on cars is because cars often end their trips at relatively high SOC (see Fig. 11 b) and subsequently hold the arrival SOC when the threshold SOC is below. As a result, the mean SOC remains high even at lower threshold SOC values. E-Boats and e-Buses, in contrast, saturate at lower pause SOC values. This is because their arrival SOC values are often lower than the arrival SOC values of the cars.

Overall, the evaluation shows the potential of charging strategies to reduce mean SOC and C-rate. For e-Cars, the results show that the mean SOC can be decreased by almost ten percentage points through paused charging. Due to the long idle times, this would certainly have a notable positive impact on calendar aging. The fact that the e-Cars often end their trips with a relatively high SOC means that a very low pause SOC does not significantly impact the mean SOC. Conversely, medium pause SOC values of 60% can also be selected without increasing the mean SOC significantly compared to a pause at 20%. For city e-Buses, the results imply that innovative charging strategies can reduce the mean SOC by over ten percentage points. E-Bus fleets often drive predictable routes. Furthermore, since trip DODs average below 50% (see Fig. 11), e-Buses could also be cycled in SOC ranges between 25 and 75%, thereby reducing calendar and cyclic aging of e-Bus batteries. The e-Boats can also reduce their mean SOC and C-rate depending on their driving style. Specifically, infrequently used e-Boats with small trip DODs could be cycled like the e-Buses by smart charging in medium SOC ranges. The same applies to frequent ferries as long as the route is foreseeable. Other charging strategies not simulated in this work could charge the vehicles to the SOC needed for the next day instead of 100%. This would further reduce the mean SOC but also require forecasting the required energy, which is more feasible for city buses than for private cars. In addition to these unidirectional strategies, bidirectional strategies could be developed to enable the deployment of V2G. Those strategies could build on the paused strategy, as the vehicle is charged to a minimum SOC for spontaneous trips and then paused until shortly before departure. During this pause, the vehicle could provide V2G services.

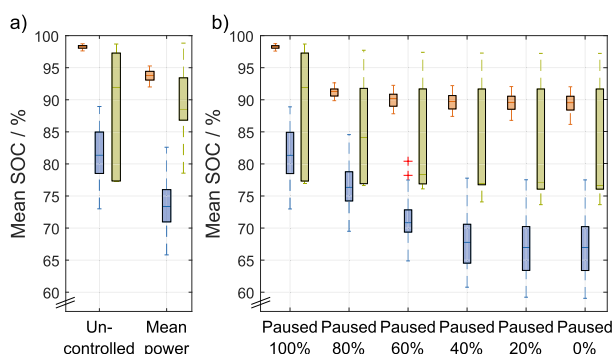


Fig. 14. Charging strategy sensitivity analysis: a) Mean vehicle SOC for the uncontrolled and the mean power charging strategy. b) Mean vehicle SOC for the paused charging strategy in dependence on the pause SOC. In the e-Bus simulations, a time resolution of 60s is chosen.

5. Conclusion and outlook

This work evaluated the impact of the operation of three electrified transportation modes on batteries using battery-relevant parameters. Simulated data from 60 e-Cars and field data from 82 e-Buses and six e-Boats were used. The data was pre-processed, analyzed, and filtered in the first step. Thus, 30 of the 82 e-Buses were filtered out due to insufficient data length or quality. For the analysis of the transportation modes, the simulation tool *SimSES* developed for stationary BSS was extended to mobile BSS by using vehicle availability as a binary value. The presentation of the *SimSES* extension in Section 3.2 answers RQ1, how various transportation modes can be simulated with an open-source storage simulation tool.

As the first part of the evaluation, we analyzed the energy consumption of the e-Cars and e-Buses. Here, we found that the simulated e-Cars consume between 0.18 and 0.29 kWh/km, while the consumption of the e-Buses is between 0.9 and 1.6 kWh/km (RQ 2). For the e-Buses, consumption increases with larger e-Bus batteries, probably due to the larger and heavier vehicles. However, the scatter within the e-Bus categories showed that other influencing factors could lead to higher or lower consumption. One of these influencing factors is the ambient temperature. If trips occurred around 20–22 °C, the e-Buses showed an average energy consumption of approximately 1 kWh/km. At higher and lower temperatures, consumption increased by about 2–3% per 1 °C symmetrically. At temperatures below 10 °C, the e-Bus models showed varying behavior. For e-Bus models with electric heating, consumption below 8 °C increased as the temperature dropped. For e-Bus models with additional conventional heating systems, consumption below 8 °C decreased again because the battery was not utilized for heating.

Next, we evaluated the stress on the vehicle batteries regarding various battery-relevant parameters (RQ 3). This analysis showed that e-Cars make between 0.07 and 0.18 EFCs per day, while e-Buses make 0.4 to more than 1 EFC per day. The six e-Boats analyzed make 0.026 to 0.28 EFCs per day. If only days with driving activity are considered, the EFCs increase by 50%–70% for e-Cars, up to 23% for e-Buses, and up to a factor of four for e-Boats. Regarding other parameters, the batteries in the means of transport are also differently stressed: Cars are often in high SOC ranges of 98% on average with uncontrolled charging and experience relatively small cycle depths of 10–22% during trips. E-Buses, in contrast, have mean SOC values of around 80% and experience larger mean trip cycle depths of up to 46%. The six e-Boats differ more in size and driving characteristics than the other two modes of transportation. The mean SOC values of the e-Boats range from 76 to 98.7%, and the trip cycle depths are between 4 and 28%. Accordingly, for the detailed characterization of specific e-Boats, they could be divided into subcategories, such as ferries and recreational boats. Furthermore, the analysis of the temporal utilization ratio and the temporal V2G-ready ratio showed that e-Cars are parked and idle for 70–80% of the time. During these times, e-Cars could provide V2G services. In contrast, the temporal V2G potential of e-Buses is lower at 30–54%. However, due to the predictability of departure times of city e-Buses, they could also provide V2G services well. E-Boats again showed more significant differences between recreational boats that are idle for extended periods and ferries that move a lot.

The comparison with stationary applications showed that the three parameters evaluated can have similarities with mobile applications (RQ 4). E-Buses and stationary home BSS (SCI) stress the batteries similarly concerning EFCs and utilization ratios, although the mean SOC values differ. Stationary BSSs in PS application and e-Cars result in equally low numbers of EFCs and low utilization ratios. In addition, the mean SOC values are similar in these two applications. Next, our sensitivity analysis of charging strategies showed that the mean SOC values of vehicles could be reduced by 8–13.8% points through smart charging strategies like paused charging at 60% SOC (RQ 5). In contrast, charging at the lowest possible power reduces the C-rate that vehicle batteries face to below 0.1 1/h for all vehicle types. These evaluations demonstrate the

potential of smart charging strategies to reduce battery aging stress factors.

Moreover, as part of this study, an open data repository is provided for both e-Bus and e-Boat data [52]. On the e-Bus side, we have uploaded the raw data and simulation results of the 52 used e-Buses. On the side of the e-Boats, the raw data and simulation results of the six e-Boats have been uploaded. Moreover, the e-Car results and the parameters determined are part of the open data repository. Others are encouraged to use the data in research and industry for their simulations and evaluations.

More in-depth analyses are possible building on our work. The six e-Boats represent only a small excerpt from the entire market of e-Boats. Due to the mix of ferries and private e-Boats, the results already show a range of the driving behavior of the e-Boats. Moreover, the e-Bus data and their consumption could be evaluated further, for example, based on speeds driven or weather conditions. If the vehicles were measured with a 1-s resolution, statements could also be made about the exact DOD, including recuperation, and not just about trip DODs. In addition, the work could be expanded to include other mobile applications. In this work, we have presented parameters that quantify the load on vehicle batteries. These parameters are partly stress factors that influence the degradation of batteries. Building on our work, aging models of specific battery cells could be used to quantify calendar and cyclic aging. Furthermore, the results can be used to explicitly optimize battery cells with respect to the load in the various transportation modes. In addition, all vehicle types have idle times in the depot or at home, during which the vehicles are not used. At these times, the vehicles could be used for V2G generation to utilize the resources used for battery production to the greatest extent possible. Finally, the evaluations can be used and extended to assess the second-life suitability of batteries from mobile applications for stationary applications.

CRedit authorship contribution statement

Benedikt Tepe: Conceptualization, Methodology, Software, Formal analysis, Investigation, Writing – original draft, Visualization. **Sammy Jablonski:** Conceptualization, Methodology, Writing – original draft,

Visualization. **Holger Hesse:** Conceptualization, Writing – review & editing, Supervision. **Andreas Jossen:** Resources, Writing – review & editing, Supervision.

Declaration of generative AI and AI-assisted technologies in the writing process

During the preparation of this work the authors used Grammarly and DeepL in order to improve the syntax and grammar of the text. After using these services, the authors reviewed and edited the content as needed and take full responsibility for the content of the publication.

Declaration of competing interest

The authors declare that they have no known competing financial interests or personal relationships that could have appeared to influence the work reported in this paper.

Data availability

In agreement with Hochbahn Hamburg and Torqeedo, we have published the data on which this publication is based, together with our simulation results, as open data [52]. The link in the reference leads to the media and publications repository of the Technical University of Munich. Moreover, the extended open-source version of *SimSES* can also be found in [52]. Recent versions of *SimSES* can be found in [53].

Acknowledgment

We thank Hamburger Hochbahn AG, Torqeedo, and DIW Berlin for their cooperation and data sharing, without which this work would not have been possible. This work was financially supported by the German Federal Ministry of Education and Research (BMBF) within the SimBAS project (Grant No. 03XP0338A), which is managed by Project Management Jülich. The responsibility for this publication rests with the authors.

Appendix

Raw data details

Table A1 shows detailed vehicle information about the three means of transportation

Preprocessing – Creation of binary profiles

Table A1

Vehicle information about the e-Cars, e-Buses, and e-Boats. The second column shows the number of records of the respective vehicle type after filtering. The last column gives additional information (e-Car: Driver type, e-Bus: SOC resolution, e-Boats: weight).

Data	#	Battery Capacity	Max. Battery Power	Charging Power	Vehicle info	Other info
Car A_F	10	45 kWh	93 kW	11 kW	VW ID.3	Driver type: Fulltime
Car A_P	10	45 kWh	93 kW	11 kW	VW ID.3	Parttime
Car A_L	10	45 kWh	93 kW	11 kW	VW ID.3	Leisure/Freetime
Car B_F	10	79.5 kWh	358 kW	11 kW	Tesla Model 3	Fulltime
Car B_P	10	79.5 kWh	358 kW	11 kW	Tesla Model 3	Parttime
Car B_L	10	79.5 kWh	358 kW	11 kW	Tesla Model 3	Leisure/Freetime
Bus A	9	190 kWh	350 kW	150 kW	Evobus NMC	SOC res. 0.5%
Bus B	6	240 kWh	350 kW	150 kW	Solaris NMC	0.4%
Bus C	5	291 kWh	350 kW	80 kW	Evobus LMP	0.5%
Bus D	6	309 kWh	350 kW	150 kW	Evobus NMC	0.5%
Bus E	3	316 kWh	350 kW	150 kW	Solaris NMC	0.01%
Bus F	23	397 kWh	350 kW	80 kW	Evobus LMP	0.5%
Boat 1	1	160 kWh	320 kW	8.93 kW	–	Weight: 7.5t
Boat 2	1	120 kWh	320 kW	7.82 kW	–	37t
Boat 3	1	80 kWh	160 kW	23.53 kW	–	18t
Boat 4	1	30 kWh	80 kW	8.73 kW	–	2t
Boat 5	1	40 kWh	80 kW	2.66 kW	–	1.5t
Boat 6	1	40 kWh	80 kW	5.58 kW	–	1t

For the creation of the e-Bus binary profiles, it is assumed that an e-Bus is connected to the grid if the SOC is greater than or equal to 99% or if the SOC increases, meaning the vehicle is charged (equation (6.1)). However, positive SOC deltas can also occur during journeys since the e-Bus can recuperate during braking while driving. In addition, there can be fluctuations in the SOC estimator so that the SOC increases slightly for a short time during trips. For this reason, we introduce as an additional condition that a contiguous depot time for charging the e-Bus must be at least 10 min long. Consequently, all binary values in the profile that are not part of a charging phase lasting at least 10 min are counted as journey times and set to zero. Finally, the binary profile is saved as CSV, together with the time stamp.

$$b(t) = \begin{cases} 1, SOC(t) \geq 99\% \vee \Delta SOC(t) > 0 \\ 0, otherwise \end{cases} \tag{6.1}$$

With: $\Delta SOC(t) = SOC(t) - SOC(t - 1)$.

In addition, analogous to the e-Buses, binary profiles of the e-Boats are created, which indicate whether the e-Boat is connected to the electricity grid. Since SOC and power data are available for the e-Boats, the binary profiles are formed according to equation (6.2). First, analogous to the e-Buses, the binary value is set to one when the SOC is at least 99%. Furthermore, the e-Boat is defined as connected to the electricity grid if the power is positive. As for the e-Buses, we further use the condition that a contiguous grid connection time must be at least 10 min long. This way, short periods during driving with positive power values are not counted as “connected to the grid”.

$$b(t) = \begin{cases} 1, SOC(t) \geq 99\% \vee P(t) > 0 \\ 0, otherwise \end{cases} \tag{6.2}$$

Lithium-ion battery specifications

Table A2
Lithium-ion battery cell specifications [42,54].

Manufacturer	Sanyo
Model	UR18650E
Capacity (minimum/typical)	2.05 Ah/2.15 Ah
Allowed voltage range	2.5 V–4.2 V
Proposed voltage range	3.0 V–4.1 V
Cathode active material	Li(NiMnCo)O ₂
Anode active material	Graphite
Electrolyte material	1 M LiPF ₆ in an EC/EMC (1:1) solvent mixture

Table A2 shows detailed vehicle information about the three means of transportation.

E-Bus energy consumption – temperature analysis

Fig. A1 depicts the boxplot diagram of the energy consumption of all buses depending on the ambient temperature, including outliers. In Fig. 8, the data is plotted without outliers. Moreover, Fig. A2 shows the energy consumption of all bus types separately depending on the ambient temperature.

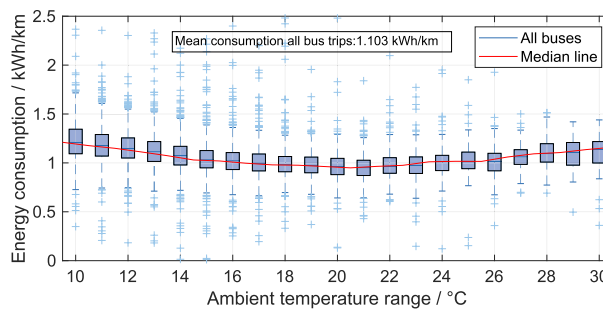


Fig. A1. Boxplot diagram of the energy consumption depending on the ambient temperature for all e-busses of all categories. Outliers are shown in blue to not distract from the general trend.

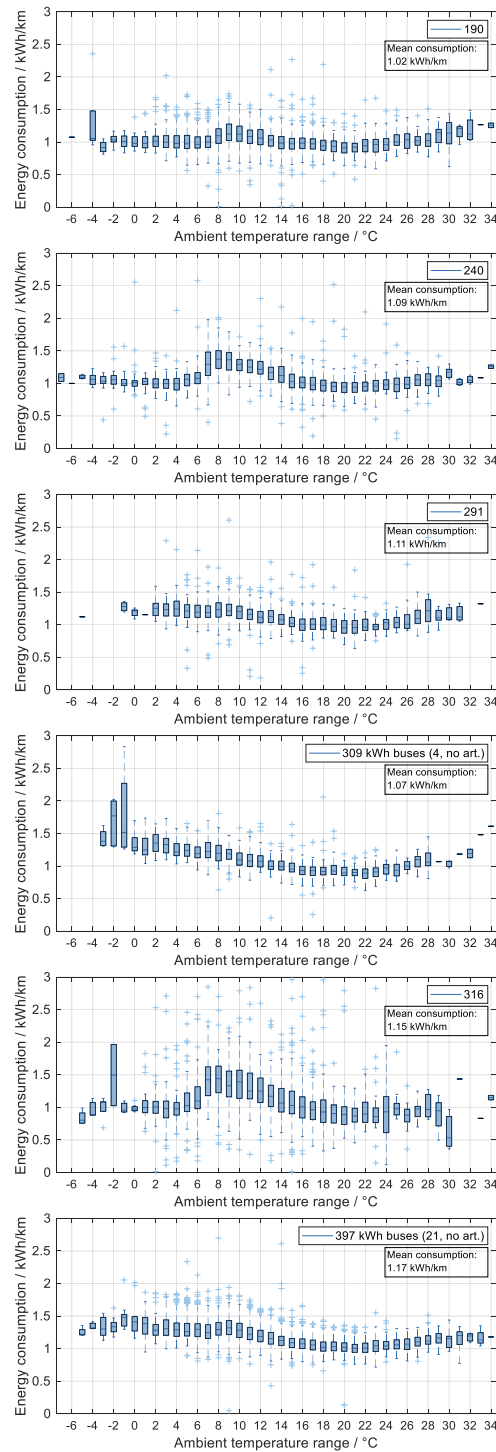


Fig. A2. Bus temperature analysis detailed boxplots of all types of e-Buses. The number in the legend indicates the e-Bus battery capacities. Two articulated buses in the 309-kWh category and two articulated buses in the 397-kWh category are excluded.

References

- [1] Li M, Lu J, Chen Z, Amine K. 30 Years of lithium-ion batteries. *Adv Mater* 2018;30(33):1800561. <https://doi.org/10.1002/adma.201800561>.
- [2] Bibra EM, Connelly E, Dhir S, Drtil M, Henriot P, Hwang I, et al. Global EV outlook 2022:securing supplies for an electric future. International Energy Agency (IEA); 2022.
- [3] Bloomberg New Energy Finance. *Electric buses in Cities: driving towards cleaner air and Lower CO2*. Bloomberg Finance LP; 2018.

- [4] Sameer J. Electric boat market size worth \$11.35 billion, globally, by 2028 at 13.7% CAGR: the insight partners. *GlobeNewswire* 2022. 8 November 2022; Available from: <https://www.globenewswire.com/en/news-release/2022/11/08/2551096/0/en/Electric-Boat-Market-Size-Worth-11-35-Billion-Globally-by-2028-at-13-7-CAGR-The-Insight-Partners.html>.
- [5] Randall C. Germany funds 472 new electric buses for Hamburg 2022, 1 April 2022; Available from: <https://www.electrive.com/2022/04/01/germany-funds-472-new-electric-buses-for-hamburg/>.
- [6] Möller M, Kucevic D, Collath N, Parlrikar A, Dotzauer P, Tepe B et al. SimSES: A holistic simulation framework for modeling and analyzing stationary energy storage systems. *J Energy Storage* 2022;49:103743. <https://doi.org/10.1016/j.est.2021.103743>.
- [7] Al-Ogaili AS, Tengku Hashim TJ, Rahmat NA, Ramasamy AK, Marsadek MB, Faisal M, et al. Review on scheduling, clustering, and forecasting strategies for controlling electric vehicle charging: challenges and recommendations. *IEEE Access* 2019;7:128353–71. <https://doi.org/10.1109/ACCESS.2019.2939595>.
- [8] Kim J, Oh J, Lee H. Review on battery thermal management system for electric vehicles. *Appl Therm Eng* 2019;149:192–212. <https://doi.org/10.1016/j.applthermaleng.2018.12.020>.
- [9] De Cauwer C, Maarten M, Heyvaert S, Coosemans T, van Mierlo J. Electric vehicle use and energy consumption based on realworld electric vehicle fleet trip and charge data and its impact on existing EV research models. *WEI* 2015;7(3):436–46. <https://doi.org/10.3390/wevj7030436>.
- [10] Hao X, Wang H, Lin Z, Ouyang M. Seasonal effects on electric vehicle energy consumption and driving range: a case study on personal, taxi, and ridesharing vehicles. *J Clean Prod* 2020;249:119403. <https://doi.org/10.1016/j.jclepro.2019.119403>.
- [11] Chen X, Li K, Zhang H, Yuan Q, Ye Q. Identifying and recognizing usage pattern of electric vehicles using GPS and on-board diagnostics data. In: Zhang G, editor. *International conference on transportation and development 2020*. Reston, VA: American Society of Civil Engineers; 2020. p. 85–97. <https://doi.org/10.1061/9780784483138.008>.
- [12] Tansini A, Di Piero G, Fontaras G, Gil-Sayas S, Komnos D, Curró D. Battery electric vehicles energy consumption breakdown from on-road trips. *SAE Int. J. Adv. & Curr. Prac. in Mobility* 2023;5(3):977–87. <https://doi.org/10.4271/2022-37-0009>.
- [13] Zou Y, Wei S, Sun F, Hu X, Shiao Y. Large-scale deployment of electric taxis in Beijing: A real-world analysis. *Energy* 2016;100:25–39. <https://doi.org/10.1016/j.energy.2016.01.062>.
- [14] Weldon P, Morrissey P, Brady J, O'Mahony M. An investigation into usage patterns of electric vehicles in Ireland. *Transport Res Transport Environ* 2016;43:207–25. <https://doi.org/10.1016/j.trd.2015.12.013>.
- [15] Zhang J, Wang Z, Liu P, Zhang Z. Energy consumption analysis and prediction of electric vehicles based on real-world driving data. *Appl Energy* 2020;275:115408. <https://doi.org/10.1016/j.apenergy.2020.115408>.
- [16] Nobis C, Kuhnimhof T. *Mobilität in Deutschland – MID. Ergebnisbericht.: Studie von infas, DLR, IVT und infas 360 im Auftrag des Bundesministers für Verkehr und digitale Infrastruktur (FE-Nr. 70.904/15)*. Bonn, Berlin. 2018.
- [17] Follmer R, Gruschwitz D. *Mobility in Germany – short report: Edition 4.0 of the study by infas, DLR, IVT and infas 360 on behalf of the Federal Ministry of transport and digital infrastructure (BMVI) (FE no. 70.904/15)*. Bonn, Berlin. 2019.
- [18] Gaete-Morales C, Kramer H, Schill W-P, Zerrahn A. An open tool for creating battery-electric vehicle time series from empirical data, emobpy. *Sci Data* 2021;8(1):152. <https://doi.org/10.1038/s41597-021-00932-9>.
- [19] Manzolli JA, Trovão JP, Antunes CH. A review of electric bus vehicles research topics – methods and trends. *Renew Sustain Energy Rev* 2022;159:112211. <https://doi.org/10.1016/j.rser.2022.112211>.
- [20] Rogge M, Wollny S, Sauer DU. Fast charging battery buses for the electrification of urban public transport—a feasibility study focusing on charging infrastructure and energy storage requirements. *Energies* 2015;8(5):4587–606. <https://doi.org/10.3390/en8054587>.
- [21] Sinhuber P, Rohlfis W, Sauer DU. Study on power and energy demand for sizing the energy storage systems for electrified local public transport buses. In: 2012 IEEE vehicle power and propulsion conference. IEEE; 2012. p. 315–20. <https://doi.org/10.1109/VPPC.2012.6422680>.
- [22] Gallet M, Massier T, Hamacher T. Estimation of the energy demand of electric buses based on real-world data for large-scale public transport networks. *Appl Energy* 2018;230:344–56. <https://doi.org/10.1016/j.apenergy.2018.08.086>.
- [23] Gao Z, Lin Z, LaClair TJ, Liu C, Li J-M, Birky AK, et al. Battery capacity and recharging needs for electric buses in city transit service. *Energy* 2017;122:588–600. <https://doi.org/10.1016/j.energy.2017.01.101>.
- [24] Wang S, Lu C, Liu C, Zhou Y, Bi J, Zhao X. Understanding the energy consumption of battery electric buses in urban public transport systems. *Sustainability* 2020;12(23):10007. <https://doi.org/10.3390/su122310007>.
- [25] Du J, Zhang X, Wang T, Song Z, Yang X, Wang H, et al. Battery degradation minimization oriented energy management strategy for plug-in hybrid electric bus with multi-energy storage system. *Energy* 2018;165:153–63. <https://doi.org/10.1016/j.energy.2018.09.084>.
- [26] Zhang L, Wang S, Qu X. Optimal electric bus fleet scheduling considering battery degradation and non-linear charging profile. *Transport Res E Logist Transport Rev* 2021;154:102445. <https://doi.org/10.1016/j.tre.2021.102445>.
- [27] Manzolli JA, Trovão JPF, Hengeler Antunes C. Electric bus coordinated charging strategy considering V2G and battery degradation. *Energy* 2022;254:124252. <https://doi.org/10.1016/j.energy.2022.124252>.
- [28] Spagnolo GS, Papalillo D, Martocchia A, Makary G. Solar-electric boat. *JTTs* 2012;2(2):144–9. <https://doi.org/10.4236/jtts.2012.22015>.
- [29] Kabir SL, Alam I, Khan MR, Hossain MS, Rahman KS, Amin N. Solar powered ferry boat for the rural area of Bangladesh. In: 2016 International conference on advances in electrical, electronic and systems engineering (ICAEEES). IEEE; 2016. p. 38–42. <https://doi.org/10.1109/ICAEEES.2016.7888005>.
- [30] Soleymani M, Yoosofi A, Kandi DM. Sizing and energy management of a medium hybrid electric boat. *J Mar Sci Technol* 2015;20(4):739–51. <https://doi.org/10.1007/s00773-015-0327-0>.
- [31] Tepe B, Figgenger J, Englberger S, Sauer DU, Jossen A, Hesse H. Optimal pool composition of commercial electric vehicles in V2G fleet operation of various electricity markets. *Appl Energy* 2022;308:118351. <https://doi.org/10.1016/j.apenergy.2021.118351>.
- [32] Lacey G, Putrus G, Bentley E. Smart EV charging schedules: supporting the grid and protecting battery life. *IET Electr Syst Transp* 2017;7(1):84–91. <https://doi.org/10.1049/iet-est.2016.0032>.
- [33] Rücker F, Bremer I, Sauer DU. Development and analysis of a charging algorithm for electric vehicle fleets extending battery lifetime. In: 2016 IEEE transportation electrification Conference, Asia-Pacific (ITEC Asia-Pacific); 2016. p. 29–33. <https://doi.org/10.1109/ITEC-AP.2016.7512917>.
- [34] Hu X, Xu Le, Lin X, Pecht M. Battery lifetime prognostics. *Joule* 2020;4(2):310–46. <https://doi.org/10.1016/j.joule.2019.11.018>.
- [35] Schuller A, Dietz B, Flath CM, Weinhardt C. Charging strategies for battery electric vehicles: economic benchmark and V2G potential. *IEEE Trans Power Syst* 2014;29(5):2014–22. <https://doi.org/10.1109/TPWRS.2014.2301024>.
- [36] Tuchnitz F, Ebell N, Schlund J, Pruckner M. Development and evaluation of a smart charging strategy for an electric vehicle fleet based on reinforcement learning. *Appl Energy* 2021;285:116382. <https://doi.org/10.1016/j.apenergy.2020.116382>.
- [37] Abdullah Al-Karakchi AA, Putrus G, Das R. Smart EV charging profiles to extend battery life. In: 2017 52nd International universities power engineering conference (UPEC). IEEE; 2017. p. 1–4. <https://doi.org/10.1109/UPEC.2017.8231961>.
- [38] Chen J, Huang X, Tian S, Cao Y, Huang B, Luo X, et al. Electric vehicle charging schedule considering user's charging selection from economics. *IET Gener, Transm Distrib* 2019;13(15):3388–96. <https://doi.org/10.1049/iet-gtd.2019.0154>.
- [39] Houbbadi A, Trigui R, Pelissier S, Redondo-Iglesias E, Bouton T. Optimal scheduling to manage an electric bus fleet overnight charging. *Energies* 2019;12(14):2727. <https://doi.org/10.3390/en12142727>.
- [40] Shaikat N, Khan B, Ali SM, Mehmood CA, Khan J, Farid U, et al. A survey on electric vehicle transportation within smart grid system. *Renew Sustain Energy Rev* 2018;81:1329–49. <https://doi.org/10.1016/j.rser.2017.05.092>.
- [41] Gschwendtner C, Sinsel SR, Stephan A. Vehicle-to-X (V2X) implementation: an overview of predominant trial configurations and technical, social and regulatory challenges. *Renew Sustain Energy Rev* 2021;145:110977. <https://doi.org/10.1016/j.rser.2021.110977>.
- [42] Schmalstieg J, Käbitz S, Ecker M, Sauer DU. A holistic aging model for Li(NiMnCo)O₂ based 18650 lithium-ion batteries. *J Power Sources* 2014;257:325–34. <https://doi.org/10.1016/j.jpowsour.2014.02.012>.
- [43] Naumann M, Schimpe M, Keil P, Hesse H, Jossen A. Analysis and modeling of calendar aging of a commercial LiFePO₄/graphite cell. *J Energy Storage* 2018;17:153–69. <https://doi.org/10.1016/j.est.2018.01.019>.
- [44] Naumann M, Spingler FB, Jossen A. Analysis and modeling of cycle aging of a commercial LiFePO₄/graphite cell. *J Power Sources* 2020;451:227666. <https://doi.org/10.1016/j.jpowsour.2019.227666>.
- [45] Kucevic D, Tepe B, Englberger S, Parlrikar A, Mühlbauer M, Bohlen O, et al. Standard battery energy storage system profiles: analysis of various applications for stationary energy storage systems using a holistic simulation framework. *J Energy Storage* 2020;28:101077. <https://doi.org/10.1016/j.est.2019.101077>.
- [46] Dataforce. Leading models of battery-electric passenger cars and light commercial vehicles by new registrations in the European Union in 2021. *Statista*. [July 18, 2023]; Available from: <https://www.statista.com/statistics/1301916/bev-leading-models-europe/>.
- [47] Kraftfahrt-Bundesamt. *Entwicklung der Fahrleistungen nach Fahrzeugarten (engl. German Federal Motor Transport Authority - development of mileage by vehicle type)*. [July 18, 2023]; Available from: https://www.kba.de/DE/Statistik/Kraftverkehr/VerkehrKilometer/vk_inlaenderfahrleistung/2021/verkehr_in_kilometer_kurzbericht.pdf.pdf?_blob=publicationFile&v=2.
- [48] Notton G, Lazarov V, Stoyanov L. Optimal sizing of a grid-connected PV system for various PV module technologies and inclinations, inverter efficiency characteristics and locations. *Renew Energy* 2010;35(2):541–54. <https://doi.org/10.1016/j.renene.2009.07.013>.
- [49] Collath N, Tepe B, Englberger S, Jossen A, Hesse H. Aging aware operation of lithium-ion battery energy storage systems: a review. *J Energy Storage* 2022;55:105634. <https://doi.org/10.1016/j.est.2022.105634>.
- [50] You S, Rasmussen CN. Generic modelling framework for economic analysis of battery systems. In: IET conference on renewable power generation (RPG 2011). IET; 2011. p. 122. <https://doi.org/10.1049/cp.2011.0147>.
- [51] Biron RA, Abdollahi Z, Hadidi R. Inverter's nonlinear efficiency and demand-side management challenges. *IEEE Power Energy Mag* 2021;8(1):49–54. <https://doi.org/10.1109/MPEL.2020.3047527>.
- [52] Tepe B, Jablonski S, Hesse H, Jossen A. Lithium-Ion Battery Utilization in various Modes of e-Transportation - Dataset. Available from: <https://mediatum.ub.tum.de/1709192>.
- [53] Chair of Electrical Energy Storage Technology, Technical University of Munich. *Simulation of stationary energy storage systems (SimSES)*. <https://gitlab.lrz.de/open-ees-ses/simses>.
- [54] Ecker M, Nieto N, Käbitz S, Schmalstieg J, Blanke H, Warnecke A, et al. Calendar and cycle life study of Li(NiMnCo)O₂-based 18650 lithium-ion batteries. *J Power Sources* 2014;248:839–51. <https://doi.org/10.1016/j.jpowsour.2013.09.143>.

3.3 Feature-conserving gradual anonymization of electrical load profiles

The paper entitled *Feature-conserving gradual anonymization of load profiles and the impact on battery storage systems* is presented in this section [3]. When working with load profiles, for example as input profiles for SimSES, the question of whether load profiles could be anonymized arose in discussions with industry partners. Original data that is as representative as possible is required by industry and research institutions in order to carry out realistic analyses and simulations. At the same time, data owners often have data protection concerns and prefer not to share data when in doubt. In addition, data is often protected by non-disclosure agreements. This is where this section of the thesis comes in. It presents a methodology that makes it possible to anonymize load profiles to varying levels in order to enable subsequent open access publication.

An open-source tool was developed for the work, which enables users to anonymize the load profiles via a graphical user interface. The approach of the methodology is to automatically divide load profiles into base and peak sequences. The user can then select the level to which the load profile should be anonymized. With simple anonymization in level 1, for example, the profile can be normalized to the maximum value. If the level of anonymization is increased to 2, a synthetic load profile is created based on features of the original profile. With stronger anonymization, the order of base sequences is additionally permuted randomly in level 3, the order of peak sequences is permuted randomly in level 4 or all sequences are permuted randomly in level 5. Two load profiles are used to demonstrate the functionality of the methodology. On the one hand, a second-based household load profile from RWTH Aachen University is used and, on the other, the load profile of a fast charging station, the data for which was provided by an industrial partner. The former corresponds to classic load profiles, while the latter corresponds to event-based load profiles. After anonymization at the various levels, the load profiles themselves are compared with each other. The tool can then be used to simulate stationary BSS applications in SimSES using the load profiles as input profiles. The household load profiles are simulated in the SCI application and the EV charging station load profiles in the PS application. Storage-relevant parameters are then compared and the effects of anonymization on the simulation results are evaluated.

The research questions answered in this section are:

1. How can load profiles be anonymized gradually and how could an open-source tool look like that allows anonymization and enables an easy and straightforward use in industry and research?
2. In which parameters do the anonymized load profiles differ from the original profiles and in which are they similar?
3. How much may an original load profile be modified to maintain parameters critical to a storage application?
4. How sensitive are the results from research question 3 to storage system design and adjustable parameters, such as the threshold between base and peak sequences?

The results of this section include the new methodology of anonymizing electrical load profiles at various levels. In addition, the analyses of the profiles show that time-invariant indicators are retained. However, the regularity is lost as a result of the anonymization, so that in time-dependent BSS applications, such as SCI, BSS-relevant parameters change to a greater extent. For example, EFCs are overestimated by up to 6% and self-sufficiency is underestimated by up to 9 percentage points.

The results showed that time-invariant indicators were preserved during anonymization. However, the random permutation of the order of the sequences meant that in time-dependent applications such as SCI, anonymization at higher levels led to a greater variation in battery-relevant parameters, for example, the SCR and the SSR.

Author contribution

Benedikt Tepe was the principle author tasked with coordinating and writing the paper and developing the load profile anonymization tool. David Haberschusz was responsible for the data acquisition and preparation. Jan Figgenger supported the coding and helped to visualize the results. Holger Hesse reviewed the manuscript and gave valuable input throughout the manuscript preparation. Dirk Uwe Sauer and Andreas Jossen contributed via fruitful scientific discussions and reviewed the manuscript. All authors discussed the data and commented on the results.

Feature-conserving gradual anonymization of load profiles and the impact on battery storage systems

Benedikt Tepe, David Haberschusz, Jan Figgener, Holger Hesse, Dirk Uwe Sauer and Andreas Jossen

Applied Energy, Volume 343, 2023

Permanent weblink:

<https://doi.org/10.1016/j.apenergy.2023.121191>

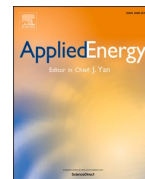


Reproduced under the terms of the Creative Commons Attribution 4.0 License (CC BY, <http://creativecommons.org/licenses/by/4.0/>), which permits unrestricted reuse of the work in any medium, provided the original work is properly cited.



Contents lists available at ScienceDirect

Applied Energy

journal homepage: www.elsevier.com/locate/apenergy

Feature-conserving gradual anonymization of load profiles and the impact on battery storage systems

Benedikt Tepe^{a,*}, David Haberschusz^{b,c,d}, Jan Figgenger^{b,c,d}, Holger Hesse^e, Dirk Uwe Sauer^{b,c,d}, Andreas Jossen^a

^a Technical University of Munich, TUM School of Engineering and Design, Department of Energy and Process Engineering, Chair of Electrical Energy Storage Technology, Germany

^b Institute for Power Electronics and Electrical Drives (ISEA), RWTH Aachen University, Germany

^c Institute for Power Generation and Storage Systems (PGS), E.ON ERC, RWTH Aachen University, Germany

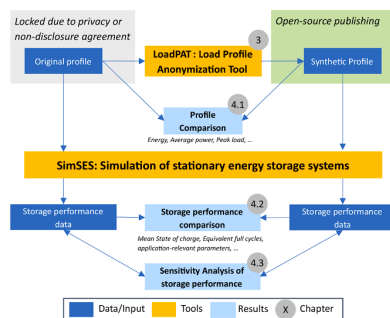
^d Juelich Aachen Research Alliance, JARA-Energy, Germany

^e Kempten University of Applied Sciences, Institute for Energy and Propulsion Technologies, Germany

HIGHLIGHTS

- Methodology for a feature-conserving gradual anonymization of load profiles.
- Application of the methodology to different load profiles and storage applications.
- Analysis of the effects on storage system operation using different KPIs.
- Demonstration of the open-source load profile anonymization tool LoadPAT.
- Methodology allows publishing load profiles similar to protected original profiles.

GRAPHICAL ABSTRACT



ARTICLE INFO

Keywords:

Open-source electric load profiles
Anonymization
Synthesizing
Household
EV charging station
Battery storage applications

ABSTRACT

Electric load profiles are highly relevant for battery storage research and industry as they determine system design and operation strategies. However, data obtained from electrical load measurements often cannot be shared or published due to privacy concerns. This paper presents a methodology to gradually anonymize load profiles while conforming to various degrees of anonymity. It segregates the original load profile into base and peak sequences and extracts features from each of the sequences. With the help of the features, a synthetic, anonymized load profile is created. Different levels of anonymization can be selected, which transform the original profile to the desired extent. A random permutation of the peak sequences or base sequences is used to achieve this transformation. Exemplary profiles from a household and an electric vehicle charging station are used to demonstrate the functionality of the anonymization. The indicators of the anonymized load profiles are compared with the original ones in both time and frequency domains, and the effects of load profile anonymization on the operation of battery storage systems in two scenarios are analyzed. While the anonymized load profiles retain the time-invariant indicators from the original profile, the permutation causes a loss of regularity

* Corresponding author at: Chair of Electrical Energy Storage Technology, Technical University of Munich (TUM), Arcisstr. 21, 80333 Munich, Germany.
E-mail address: benedikt.tepe@tum.de (B. Tepe).

<https://doi.org/10.1016/j.apenergy.2023.121191>

Received 28 October 2022; Received in revised form 24 February 2023; Accepted 21 April 2023

Available online 15 May 2023

0306-2619/© 2023 The Author(s). Published by Elsevier Ltd. This is an open access article under the CC BY license (<http://creativecommons.org/licenses/by/4.0/>).

in the load profiles. As a result, relevant indicators of battery storage systems subjected to these anonymized profiles deviate to a greater extent in time-dependent applications such as self-consumption increase. This is reflected in the overestimation of equivalent full cycles by up to 6% and underestimation of self-sufficiency by up to 9 percentage points. In time-independent applications such as peak shaving, however, the indicators can be well reproduced with deviations of up to 3% despite the lost regularity. In order to make the anonymization methodology usable for everyone, we present the open-source tool LoadPAT, in which users can anonymize their load profiles and choose their desired level of anonymization. This work is intended to further encourage the dissemination of open-source data.

Abbreviations

BSS	Battery storage system
BTM	Behind-the-meter
CDA	Conditional demand analysis
DFT	Discrete Fourier Transformation
EFC	Equivalent full cycles
EMS	Energy-management-strategy
EV	Electric vehicle
FTM	Front-of-the-meter
DOD	Depth of discharge
FCR	Frequency containment reserve
GUI	Graphical user interface
KPI	Key performance indicator
LoadPAT	Load profile anonymization tool
PS	Peak shaving
PV	Photovoltaic
RQ	Research question
SCI	Self-consumption-increase
SimSES	Simulation of stationary energy storage systems
SOC	State-of-charge

1. Introduction

We live in a time where individuals as well as companies and research institutions are constantly generating data. Between 2012 and 2020, the volume of digital data generated each year worldwide increased tenfold from 6.5 to 64.2 zettabytes [1]. Although not all of this data is stored, the data volume of storage capacity in 2021 also amounted to 7.9 zettabytes [2]. In the electricity sector, this development is being driven by the digitalization of grid monitoring and control and the increasing installation of smart meters [3,4]. At the same time, there is a trend towards openness of data, publications and code [5,6]. Research institutions, on the one hand, are interested in sharing collected and generated data and thus making it available to the community. Companies, on the other hand, often have privacy concerns about the possible sharing of data. This conflict gave rise to the present work. The goal is to develop a methodology for anonymizing electric load profiles. We present a load profile anonymization tool (LoadPAT), which can gradually anonymize load profiles, that may aid to a greater usage of sharing data through industry and facilitate an increase of resources available for applied research. In this work, we show the gradual anonymization in various levels that is possible using the tool and the impact on load profile key performance indicators (KPIs). In addition, simulations show the effects of the load profile anonymization on the behavior and load of battery storage systems (BSS) in different applications. With the help of LoadPAT, companies and research institutions can modify and thus anonymize load profiles according to their desired level before sharing with partners.

In the following, the existing literature on the topic of anonymization of load profiles is presented and the research gap is identified.

Subsequently, the research questions of this work are introduced before the scenario and the usage area of the tool are described.

1.1. Summary of existing literature

The topic of load profiles is relevant for research institutions and companies. The former need load profiles, for example, for simulations of the electricity grid or of BSSs. Companies such as distribution network operators make use of load profile data for estimating current and future consumption and for classifying customers [7]. Basically, in research on load profiles, a distinction can be made between load profile analyses including feature extraction and synthetic load profile generation. For the former, Table A1 in the Appendix shows existing literature, which will be described in more detail below.

1.1.1. Load profile analysis and feature extraction

In 2010, Price published methods for analyzing load profiles [8]. He defined five parameters for characterizing load shapes in the time domain: base load, peak load, rise time, high load duration and fall time. Li et al. built on Price's work in 2021 and published a load profile analysis in the time and frequency domains using Discrete Fourier Transformation (DFT) [9]. To do so, they used smart meter data from 188 buildings in Northern California with a time resolution of 15 min. The advantage of frequency domain analysis is that it captures the periodicity of the load profile as a baseline feature while allowing to reduce the amount of data to be stored [9]. DFT was also used by Campestrini et al. to evaluate SOC algorithms [10]. In this work, a number of driving profiles were analyzed to develop a representative synthetic profile in the frequency domain.

When clustering load profiles, a basic distinction can be made between direct clustering of time series profiles and indirect clustering via feature extraction [11]. In 2016, Haben et al. presented an analysis of smart meter data in which they identified the four key time periods overnight, morning, daytime, evening that should be considered for clustering residential load profiles [12]. In the same year, Al-Otaibi et al. published a feature extraction method to cluster daily load profiles based on these features [13]. In addition, clustering was performed after z-normalization, which considers the shape and disregards the magnitude of the profiles. The results showed that compared to using the whole daily load profiles (48 values), extracting features can reduce the dimensions significantly while the clustering is still successful. A similar procedure was used by Park et al. in 2019, who compared the direct clustering after z-normalization using the k-means algorithm with a Gaussian mixture model [14]. In this publication, the k-means algorithm produced better results with a shorter runtime. The same algorithm was used by Trotta 2020 to cluster one-hour annual load profiles of Danish households [15]. The result of this publication are four clusters describing the typical behavior of Danish households. Czétány et al. also used the k-means algorithm to cluster Hungarian households, as k-means was advantageous over a fuzzy k-means and an agglomerative hierarchical clustering [16]. In 2022, Elahe et al. published a new feature extraction technique for load profiles that can be used to identify households with plug-in hybrid vehicles [17]. For this purpose, they used different classifiers that utilize a set of extracted features from the load profile.

Table 1
Summary of literature on synthetic load profile generation and anonymization of load profiles.

Source	Date	Focus	Method	Sampling rate	Results
Aigner et al. [18]	1984	Creation with top-down approach	Conditional demand analysis	15 min	Breakdown of total household load to individual parts using the conditional demand analysis.
Bartels et al. [19]	1992	Creation with top-down approach	Conditional demand analysis	15 min	Publication of DELMOD which uses conditional demand analysis to create household load profiles for different days and seasons.
Pensa et al. [20]	2008	Anonymization of time series	k-anonymity	Arbitrary	Application of k-anonymity to records of sequences, which can be used for all types of records and profiles.
Widén et al. [21]	2010	Creation with bottom-up approach	Stochastic modeling	1 min	Activities of household members are simulated to create high resolution series. A validation with real data showed that the generated household load profiles are realistic.
Richardson et al. [22]	2010	Creation with bottom-up approach	Stochastic modeling	1 min	Creation of one-minute resolution household load profiles based on specific activities and patterns of active occupancy. Validation with field data in East Midlands, UK.
Efthymiou et al. [23]	2010	Anonymization of smart meter data	Escrow mechanism	1–5 min	Development of a method for anonymizing high frequent smart meter data using a third party escrow mechanism.
Ogasawara et al. [24]	2010	Normalization approach for time series	Normalization	Arbitrary	Presentation of ways to normalize all types of load profiles including dividing by maximum value, by using minimum and maximum value, and with adaptive neural networks.
Shouh et al. [25]	2013	Anonymization of time series	(k,P) - Anonymity	Arbitrary	Extension of k-anonymity by P-anonymity to (k, P)-anonymity. This can be used to preserve patterns effectively in addition to the standard k-anonymization.
Jambagi et al. [26]	2015	Creation with bottom-up and top-down approach	Activity based modeling	1 s	Development of a residential electricity demand model combining time use surveys with standard load profiles. A validation with measured data shows that the properties of the synthetic profiles are correct.
Müller et al. [27]	2020	Creation with bottom-up approach	Activity based modeling	1 min	Bottom-up approach model for electrical and thermal household load modelling regarding mobility behavior.
Han et al. [28]	2022	Creation with top-down approach	Decomposition and recombination	1 h	Generation of hourly household electrical load profiles using a statistical method of decomposition and recombination.

1.1.2. Synthetic load profile generation and anonymization

In addition to load profile analysis, clustering, and feature extraction, synthetic load profile generation and anonymization are most relevant to this work. Table 1 gives an overview of literature on synthetic load profile generation and anonymization. While some of the papers presented describe the generation and anonymization of general datasets and sequences, others deal explicitly with household load profiles. Basically, load profiles can be created using bottom-up and top-down methods [29]. The former use behavior and data from individual consumers to generate a load profile. The advantage of bottom-up methods is that user behavior can be aggregated, and thus general statements can be made. The disadvantage, however, is that user data must be available in sufficient quantity. For example, Widén et al. and Richardson et al. used household member activities to generate high-resolution load time series [21,22]. Müller et al. extended the idea of electric household behavior to thermal and mobility behavior [27]. Another bottom-up approach was presented by Li et al. in 2021, which can be used to generate synthetic load profiles for households, businesses, and industries based on the geographic location [30]. They use publicly available data and make three types of transformations: Temporal shifts, temporal permutations, and adding noise. Through these transformations, the authors perform a kind of anonymization without explicitly naming it anonymization. Top-down approaches do not use data from individual electrical appliances or persons, but aggregated data, such as national data, and break them down to individual households [29]. The advantage of these approaches is that no individual user data is required. The disadvantage is that it is not possible to draw conclusions about individual user behavior. As early as 1984, Aigner et al. published a study that made it possible to break down total household load to individual parts [18]. For this purpose, the authors used the conditional demand analysis (CDA) which uses various regression equations to account for factors such as desired temperature and size of the residence when creating load profiles [29]. The advantage of the methodology at that time was the significantly lower effort compared to direct measurements at the end user [18]. In 1992, Bartels et al. presented DELMOD, a model that also uses CDA to generate load profiles for different types of days for a given scenario [19]. This model

uses typical load profiles for different days and seasons and weather data that change the load profile. DELMOD has the advantage that detailed scenarios can be investigated and predictions can be made. In 2015, Jambagi et al. combined Richardson's approach (time use surveys) with a top-down approach of a standard load profile, making the aggregate results more realistic [26]. To generate hourly electrical load time series, Han et al. used statistical methods in 2022 [28]. In their top-down approach, they used three components of public data: seasonality, distribution of residuals and the trend. A different approach to the generation of synthetic load profiles was chosen by Pinceti et al [31]. They used generative adversarial networks to learn from hourly resolved real weekly load profiles and to generate synthetic load profiles. The disadvantage of this approach is that the training of the network takes a relatively long time. In contrast, the advantage is that the network can be used easily and quickly after training.

Regarding anonymization of load profiles, Efthymiou et al. have published a paper in which they present a method for anonymizing smart meter data [23]. For this purpose, they use an escrow service that aggregates data from different households. This method does not focus on the modification and adaptation of time series-based load profiles, but rather on the process of transmitting high-frequency data via a data aggregator. Focus on the anonymization of temporal sequences put, for example, Pensa et al., who use k-anonymization for this purpose. [20]. The k-anonymization can be applied to data sets and describes that the information of an individual cannot be distinguished from at least k-1 other individuals [32]. Pensa et al. applied this type of anonymization to datasets of sequences achieved k-anonymization of the data [20]. Shouh et al. extended the k-anonymization approach to another level, P-anonymization, which represents patterns within grouped time-series datasets [25]. This (k, P)-anonymization was shown in experiments to be resistant to linkage attacks while preserving pattern data. The concept of k-anonymization was extended by Machanavajjhala et al. to include l-diversity, which requires that for each sensitive attribute in data sets, at least l different attributes must occur [33]. A combination of k-anonymization and l-diversity consequently enables an anonymization that is more secure against attacks.

The presented variants of the anonymization of data sets have in

common that several load profiles must exist. However, the focus of the present work is on the anonymization of individual time series-based load profiles, which means that the presented variants are not applicable. For the modification of individual load profiles, Savov et al. published a paper in 2017 in which they analyzed the degree to which load profiles can be discretized [34]. The result was that the greater the discretization of the data, the greater the error in power loss evaluations in distribution grids. Ogasawara et al. presented ways to normalize load profiles in 2010 [24]. The normalization can be done by dividing by the maximum value, by using minimum and maximum of a profile and more complex by adaptive normalization with adaptive neural networks. The latter are a kind of sliding window techniques and have the advantage of creating individual data sequences from which statistical properties are determined for normalization. In their bottom-up approach, Li et al. used the aforementioned temporal permutation to change individual load profiles [30]. In their hourly load profiles, they permuted pairs of values every 50–100 h to add randomness.

Few open-source tools already exist for anonymization of data and creation of load profiles. The ARX tool, for example, is an anonymization tool for structured data sets [35]. With this tool, data can be adapted according to k -anonymization and l -diversity, among other methods. It also has a graphical user interface (GUI) that allows users to anonymize their data sets. However, multiple datasets are required for anonymization in this tool. Thus, it cannot be used for anonymizing individual load profiles. To generate synthetic load profiles, the aforementioned Pinceti et al. have published the LoadGAN tool [36]. This tool uses the methodology of generative adversarial networks and users can directly generate a desired number of load profiles in a desired resolution and length. The LPAT tool by Schaefer et al. splits load profiles into sub-load profiles, which are then used to dimension storage for a hybrid energy storage system [37]. The division into sub-profiles is done by DFT, low-pass filter and inverse DFT. As a result, a load profile is decomposed into several load profiles that have different frequencies and thus can be covered by different storage technologies. However, the goal here is not anonymization, but the determination of the storage requirements. Therefore, no permutation or normalization takes place.

1.1.3. Battery storage systems

Load profiles have a fundamental influence on the design and operation of BSS [38–40]. A collection of load profiles or a generation of anonymized load profiles is especially relevant for battery research, since simulations on storage applications depend strongly on the load profile of the household or company [38]. In general, stationary BSS are operated in various applications. These applications can be divided, for example, into in-front-of-the-meter (FTM) and behind-the-meter (BTM) applications [41]. The former are related to markets and the electricity grid, such as arbitrage trading and frequency containment reserve (FCR). The latter describe applications behind the meter on the consumer side, which can be peak shaving (PS) or self-consumption increase (SCI) of energy generated by photovoltaic (PV) systems. In addition to these singular applications, the applications can also be combined in multi-use scenarios, which can increase the profitability, but bring regulatory barriers with it [41]. Since the focus of this paper is on the use of the load profiles in the SCI application and the PS application these are considered in more detail below. At SCI, BSSs are installed to increase the consumption of self-generated energy and feed less energy into the grid. This can be done by private households or businesses. In Germany, for example, 430,000 home storage systems have been installed by the end of 2021 [42]. The household load profile has an impact on the design of home storage systems [40]. If a large part of the energy consumed is covered by PV during the day, the BSS can be designed smaller than if a large part is consumed in the evening or at night. BSS in PS application are used to cover peaks in the load profile [39]. This is mainly relevant for industrial customers, who must pay a fee per kW for the peak power in a year over a 15-minute period. Accordingly, the load profile is also relevant for the storage design in this

application.

Several KPIs are relevant for BSSs, which are being discussed in the following [38]. The parameters extracted at this point will be used in Section 4.2 to estimate the storage performance with the anonymized load profiles versus the original load profiles. The appendix Section 7.2 shows the equations of the different KPIs with a short description. In general, the degradation of BSSs is highly relevant in every application as it is decisive for the profitability. The degradation can be divided into cyclic and calendric ageing. On the one hand, cyclic degradation depends on the number of equivalent full cycles (EFCs), the depth of discharge (DOD), and the C-rate [43,44]. More EFCs, deeper DODs and larger C-rates lead to increased cyclic aging [44]. Calendar degradation, on the other hand, depends primarily on temperature and the state of charge (SOC) [45,46]. Particularly high, as well as particularly low temperatures and SOCs, usually lead to accelerated aging [44]. Two further parameters are of relevance especially for the SCI application: One is the self-consumption rate and the other is the degree of self-sufficiency [47,48]. The self-consumption rate describes the proportion of PV energy consumed locally and not fed into the grid. The degree of self-sufficiency specifies the independence from the electricity grid, thus the proportion of electricity consumption that can be covered by PV energy and battery discharge. The load profile of the household has a major impact on the two parameters [40]. For the PS application, another KPI is of particular importance: the fulfillment factor or performance criterion [49]. This factor describes at what proportion of the time a storage system was able to deliver the power requested by the energy management system. If a BSS operates in the PS application, failures and non-fulfillments of requested power can lead to enormous increases in power-related costs for the business. In addition, round-trip efficiency is described as a relevant parameter in the PS application [49].

The research gap we identified is manifold. On the one hand, many load profile analyses are limited to extracting features to cluster a set of profiles. On the other hand, bottom-up and top-down approaches exist to generate load profiles from, for example, user data. Various methods exist for anonymizing data, but these cannot be applied to individual load profiles because they require a larger data set. Existing open-source tools can either anonymize data (but not load profiles) or generate load profiles (but not anonymize existing ones). Often, the analyses, clustering methods and load profile generation methods are also limited to profiles with resolutions of 15 min [9,16], 30 min [13] or one hour [15,30,31]. In our point of view, what is missing is a methodology that can be used to gradually anonymize individual original load profiles with a high resolution of one to five minutes. In a publication by Beck et al, for example, 5 min was shown to be relevant for the sizing of the power of a storage system [50]. The presented methodology gives users the flexibility to decide to which degree the original load profile should be modified. Since modifying or anonymizing the load profile affects the design and operation of BSSs as described, we also investigate the impact of load profile anonymization on stationary BSSs in different applications. We will answer the following research questions (RQs) throughout the paper:

RQ1) How can load profiles be anonymized gradually and how could an open-source tool look like that allows anonymization and enables an easy and straightforward use in industry and research? (Section 3).

RQ2) In which parameters do the anonymized load profiles differ from the original profiles and in which are they similar? (Section 4.1).

RQ3) How much may an original load profile be modified to maintain parameters critical to a storage application? (Section 4.2).

RQ4) How sensitive are the results from RQ 3 to storage system design and adjustable parameters, such as the threshold between base and peak sequences? (Section 4.3).

1.2. Scope of this work

The goal of the present work is to develop a methodology through

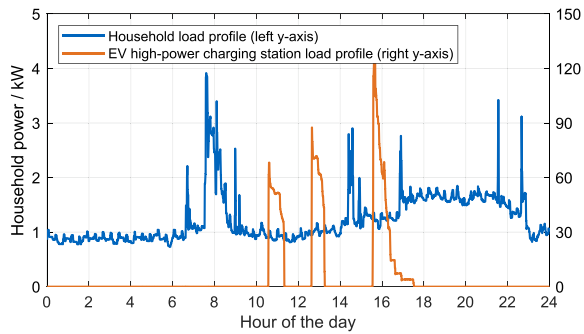


Fig. 1. Exemplary day of the household load profile (January 14th, 2021) and EV high-power charging station load profile (February 2nd, 2022).

Table 2
Database of load profiles of the different applications.

	Household load profile	Charging station load profile
Storage application	Home storage system	High Power EV Charger with buffer
Length of datasets	12 months	6 months
Time period	2021	Mid-January 2022 to Mid-July 2022
Resolution	1 min	1 min
Consumption	10.8 MWh	9.47 MWh
Peak Power	8.685 kW	248.1 kW
Industry/ Research Partner	ISEA RWTH	Industry Partner

which users from industry and research can modify load profiles that are protected by data privacy laws so that they can share them with partners. The extent to which the load profiles must be modified for this purpose is to be decided by the owner of the data. For this reason, our methodology is intended to be flexible and allow users to anonymize gradually. Our approach is to extract features from the original load profile and then to recreate it based on these features. For this purpose, we divide the load profile into base and peak sequences, whereby the threshold between the ranges can be freely adjusted. Subsequently, features such as the mean value and the length of the sequence are determined for each sequence. The anonymized synthetic load profile is then formed from these stored features. The degree of anonymization can then be varied via levels, which determine the variant of the permutations. For example, simple normalization is possible in level 1, while only peak sequences are permuted in level 3 and base and peak sequences are permuted in level 5. The flexibility for users derives from the choice of the threshold between base and peak sequences and the choice of the anonymization level. After generating the anonymized load profile, a storage system simulation model can be called and executed that simulates the original and the anonymized load profiles in different storage applications. In this way, we test the impact of anonymization on BSS operation. The BSS applications we analyze in this work are PS (where peak loads are covered by storage systems) and SCI of PV-generated energy for households using storage systems.

On the one hand, the developed methodology allows the anonymization of classical, continuous load profiles. On the other hand, it can also be used to anonymize load profiles that have idle sequences and peak sequences with high-power levels. In our analyses, such load profiles are from charging stations at which electric vehicles (EVs) charge or whose load is zero apart from standby consumption. Users can thus anonymize daily, weekly, or annual load profiles. In addition, the tool can be used to generate several similar synthetic load profiles from one original load profile. In this way, small data sets can be multiplied and used for data augmentation. Furthermore, storage operators can use the

tool to test a possible storage operation without having to give out or receive original load profiles. The contributions of this work are as follows:

- Methodology to gradually anonymize load profiles by permutation of base and peak sequences while retaining the parameters essential for battery storage use
- Analysis of effects of load profile anonymization on the parameters essential for battery storage utilization
- Demonstration of the open-source tool LoadPAT for providing research and industry the opportunity to share data and present results to public without conflicting with non-disclosure agreements

2. Database

For the present work, two types of load profiles were collected in exchange with an industrial partner and a research institution. These data can be classified in load profiles of a household and of an electric vehicle (EV) high-power charging station (see Fig. 1). The first is a typical load profile of a household, consisting of base load sequences and peak load sequences. The base load sequences result from appliances that always use electricity, such as refrigerators in private households. Peak load sequences are caused by more power demanding consumers used for a short time, such as kettles or electric stoves in private households. The EV high-power charging station load profile has a different pattern. It is composed of charging events and idle phases, in which the load is zero except for standby consumers. The charging stations for EVs provide high charging power during charging times but have very low power during resting periods without a connected EV.

The data used in this work and their parameters are shown in Table 2. The household load profile was measured by the ISEA of RWTH Aachen University within the WMEP home battery storage program [51]. It is used over a whole year with a resolution of 1 min. The EV high-power charging station load profile was provided by an industry partner. It also originates from a storage application as it was measured at a charging station with a buffer BSS. It has a length of 6 months with a resolution of 1 min. The annual energy consumption of the household is approximately equal to the half-year consumption of the charging station. However, the peak power of the household is only 8.7 kW, while the charging station load profile showed a peak power of 248.1 kW within the six months. The complete load profiles are shown in the appendix.

For this work, Python 3.8 was used with the Tkinter package to create LoadPAT and its GUIs [52]. Furthermore, MATLAB was used for data analysis and for the creation of the figures.

3. Methodology of the gradual anonymization

In this chapter, we describe the methodology of the feature-conserving load profile anonymization. First, the differences between the levels of anonymization are explained (Section 3.1). Subsequently, the features used for anonymization are described (Section 3.2). Afterwards, the computational process of the anonymization is described in Section 3.3. In Section 3.4, the interface to the BSS tool Simulation of stationary energy storage systems (SimSES) is described, and the storage parameters of the applications are defined. Finally, we describe how Monte Carlo simulations can be used to determine the influence of the level of anonymization and to measure the respective deviations from the original profile (Section 3.5). Beyond this presentation of the methodology, there is a presentation of the open-source tool including screenshots in the appendix (Section 7.4).

3.1. Levels of anonymization

The gradual anonymization methodology allows differentiation into different levels. Before the exact synthesis of load profiles is presented in

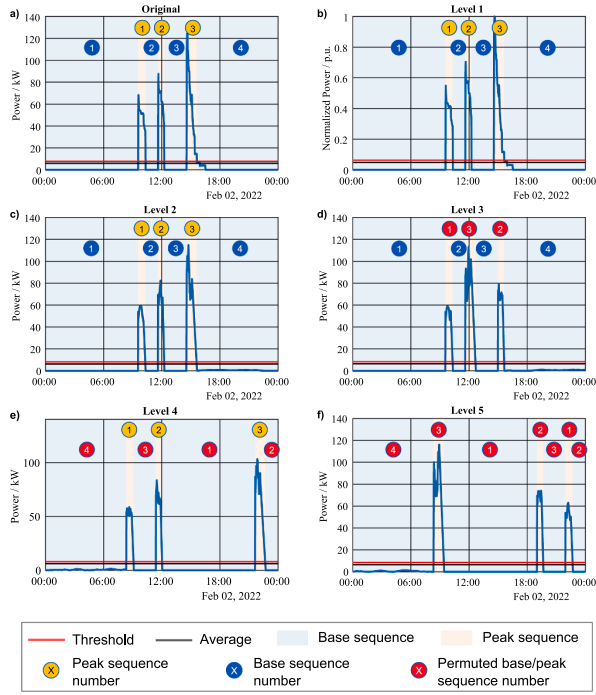


Fig. 2. Examples of daily anonymized load profiles depending on the level of anonymization.

Table 3
Difference between the levels of anonymization.

Number of Level	Description
Level 1	Copying of profile and normalization
Level 2	Feature extraction of sequences and profile creation based on features
Level 3	Level 2 + permutation of peak sequences
Level 4	Level 2 + permutation of base sequences
Level 5	Level 2 + permutation of peak sequences and permutation of base sequences

Table 4
Features extracted for the anonymization. Every feature is calculated for every base and peak sequence.

Peak Features	Base Features
Length/ timesteps of peak sequence without ramp-up and ramp-down (n)	Length/ timesteps of base sequence (n)
Maximum (P_{max})	Maximum (P_{max})
Minimum (P_{min})	Minimum (P_{min})
Mean of delta between two consecutive values (μ_{Δ})	Mean of delta between two consecutive values (μ_{Δ})
Standard deviation of delta between two values (σ_{Δ})	Standard deviation of delta between two values (σ_{Δ})
Probability of change of sign of the delta between two consecutive values ($P_{change\ of\ sign}$)	Probability of change of sign of the delta between two consecutive values ($P_{change\ of\ sign}$)
Mean of peak without ramp-up and ramp-down (μ)	Mean (μ)
Ramp-up length (n_{up})	
Ramp-down length (n_{down})	

the following sections, an example is used to explain the levels of anonymization. To illustrate the various levels of anonymization, Fig. 2 and Table 3 show the differences. The top left diagram (a) shows an

exemplary original load profile. This profile is an EV charging station load profile over the course of a day. At this point, a daily profile is chosen to explain the procedure of the anonymization. In the later course, the permutations are carried out over the half-year (EV charging station) or full-year profile (household). The original daily profile has three peak sequences and four base sequences.

In the anonymization level 1, the original profile is merely copied and can be normalized if desired (Fig. 2 b). This is to enable an exclusive normalization of load profiles. From level 2 onwards, features are determined for every peak and base sequence from the original profile and the profile is then reconstructed based on these features. In this level, the order of base sequences and peak sequences is maintained. Fig. 2 c shows an example of an anonymized load profile of level 2. This profile is remarkably similar to the original profile at first glance. However, at second glance, differences within the peaks become clear. These are due to the recreation of the profile using the features presented later. Thus, this level of anonymization can be applied by users of the method who want to modify or hide variations within base or peak sequences. The occurrence of peaks and base sequences in this level takes place at the same time as in the original profile. In level 3, sequences are exchanged for the first time (Fig. 2 d). The base or rest sequences are created identically to the original profile, while the peak sequences are randomly permuted (red colored circles). In the example, the maximum peak is now the second peak, whereas in the original profile it was the third one. Peak sequence 2 and 3 have swapped accordingly. It can also be seen that the peak shape differs. The random creation of the shape of the sequences will be explained in Section 3.3. The third level of anonymization can be applied when users want to hide the exact times at which conspicuous peaks occur. For example, times when industries use certain machines could be randomly shifted in the load profile. In level 4, instead of the sequence of peaks, the order of base sequences is randomly varied. In Fig. 2 e the maximum peak is again the third peak, for example. The very long base period (number 1) of over 9 h between midnight and 9:30 in the original profile is no longer present at the same place in this level. Instead, the profile starts with base sequence number four of about 8 h, which is at the end of the day in the original profile. Base sequence number one is now after the second peak. Anonymization in the fourth level changes the load profile more than in the levels before. The times at which characteristic peaks occur change due to the permutation of the base sequences, which means that the use of machines or larger household appliances can no longer be assigned to typical times in the load profile. Level 5 finally combines the variations of level 3 and level 4, randomly varying the order of base sequences and the order of peak sequences. As a result, it is now no longer possible to read the order of the peaks from the load profile. An example of this level is shown in Fig. 2 f. Users who select this level of anonymization change the load profile the most. Typical characteristics of the load profile still occur, but at completely randomized times. We will discuss the effects of the levels of anonymization in Section 0. The use of a daily load profile in this section serves to illustrate the levels. Within the results, the full profiles are used, resulting in a larger number of base and peak sequences. The permutations are always performed over the entire load profile present. For the EV charging profile this means over half a year and for the household load profile over one year. At this point, it should be noted that the division into the two types of sequences, base and peak, is only one possible way of analyzing the load profile that is commonly used. Alternatively, we could also divide the load profile into four types of sequences, as Haben et. al did with household load profiles [12].

3.2. Features extracted and used for the anonymization

To generate the anonymized load profiles according to levels 2 to 5, features of the base sequences and the peak sequences are calculated. These features are shown in Table 4. For each base sequence, the length of the sequence, the mean value, the standard deviation, and the

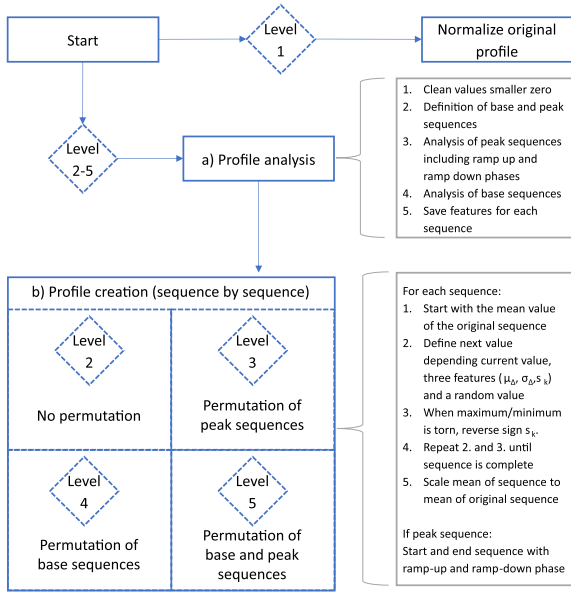


Fig. 3. Flow chart of the process of the anonymization.

maximum are saved. In addition, the mean delta between two values and the standard deviation of this delta are calculated. Moreover, the probability of a change in the sign of this delta is determined. For each peak sequence, basically the same values are determined. However, a distinction is made between ramp-up phase, peak without ramping and ramp-down phase. The mean value and the standard deviation are calculated for the peak without ramping. In addition, the length and the slope are determined for the ramp-up and ramp-down phases.

3.3. Computational process of the anonymization

This section describes the process of anonymization including the calculation of the individual values. Fig. 3 shows a flow chart of the process for clarification. If anonymization is to be performed in level 1 with normalization, the profile is normalized to its maximum value. If, in contrast, the desired level is between 2 and 5, the original load profile is analyzed (a) and a synthetic load profile is created (b).

In the profile analysis (a), the values of the original load profile are cleaned up by setting values smaller than zero to zero. Next, peak sequences are determined by checking at which points in time the load profile has values above the defined threshold. Conversely, base sequences are also determined in this way. If peak sequences are only one time step short, they are filtered out and count as part of the current base sequence. Afterwards, all peak sequences are analyzed one after the other. During this process, the features mentioned above are determined. The average value of the respective peak sequence is used as the threshold value for the end time of the ramp up. Likewise, for the start of the ramp down phase the time is used in which the load falls below the average value for the last time before the end of the sequence. With the help of the lengths, the start and end values of the ramp up and ramp down sequences, their slopes are then determined. After the peak sequences, the base sequences are analyzed, and the features shown in Table 4 are calculated. Finally, all values are saved for the subsequent creation of the synthetic load profile.

In the profile creation (b), the procedure depends on the selected level. According to the selected level, the order of the peak and base sequences is kept (level 2), the order of the peak sequences is randomly mixed (level 3), the order of the base sequences is randomly mixed (level 4) or both orders are randomly mixed (level 5). The synthetic profile is

then created sequence by sequence.

The procedure for generating the sequences is identical for peaks and base sequences. The general idea is to use the mean and standard deviation of the delta of the original sequence together with the probability that the delta changes its sign to generate synthetic values successively as displayed in equation (1). The average value μ of the sequence is selected as the start value of the synthetic profile P_1 . Starting from this, the next value is determined using the mean μ_Δ and standard deviation σ_Δ of the delta of the original sequence. For this purpose, the standard deviation is multiplied by the absolute of a random value from the standard normal distribution X . As shown in equation (2), the sign s_k used depends on the sign used in the last time step and the probability of a change of sign of the delta of the original profile p_{change} of $sign$. For example, if the probability were 100 %, the sign would be multiplied by -1 each time and thus the direction of the delta would be reversed in each timestep. Since a low probability of a change of sign could result in very low or very high power values, the values are limited by the maximum P_{max} and minimum P_{min} of the sequence displayed in equation (3). If one of the limits is torn, the sign s_k is reversed for the respective time step so that the range is maintained. If the other limit is exceeded due to the change of sign, the limit that was torn first is selected as the next value. This way, the synthetic sequence contains fewer sign changes than the original sequence, but this is accepted by the advantage of the more realistic power range. Restriction to the range between maximum and minimum power may cause the mean value of the synthetic sequence to differ significantly from the mean value of the original. This is the case when the maximum is far above, or the minimum is far below the mean value. An outlier upwards then leads to higher values, for example. To reduce this discrepancy between the original and synthetic mean values, the sequence is scaled to the mean value of the original sequence.

$$P_k = P_{k-1} + s_k \cdot (\mu_\Delta + \sigma_\Delta \cdot |X_k|) \quad (1)$$

$$s_k = s_{k-1} \cdot s_0 \quad (2)$$

$$P_{min} \leq P_k \leq P_{max} \quad (3)$$

With :
 $k = 2 \dots n$

$$P_1 = \mu$$

$$s_1 = 1$$

$$s_0 = \begin{cases} -1, & P_{change \ of \ sign} \\ +1, & 1 - P_{change \ of \ sign} \end{cases}$$

$$X_k \sim \mathcal{N}(0, 1)$$

n : Length of original sequence

In addition to the individual base and peak sequences, the synthetic profile also includes ramp-up and ramp-down phases before and after peak sequences. To take the ramp-up into account, the ramp-up is synthesized based on the last power value of the previous sequence and the mean value of the following sequence. From these two values and the known length of the ramp-up and ramp-down from the original profile, the slope is determined, and the values are appended to the profile. The slope of the original profile is not used here because the last value of the previous sequence fluctuates over each simulation and using the original slope and length may cause an overshoot or jump in the profile. In the ways described, the base sequences, ramp-up phases, peak sequences, and ramp-down phases are iteratively appended to each other to generate the synthetic profile. The order of the sequences depends on the selected level of anonymization, as described above.

Table 5
Storage parameters of the different applications used in the SimSES simulations.

	Home Storage System	High Power EV Charger with buffer
Profile description	Household load profile	Required load by charging EVs
Energy-management strategy (EMS)	SCI	Peak-Shaving
Battery capacity	8.8 kWh	140 kWh
Max. power of storage system	7 kW	250 kW
Photovoltaic (PV) – nominal power	9.3 kWp, Location: Munich	–
Peak-shaving-limit	–	32 kW

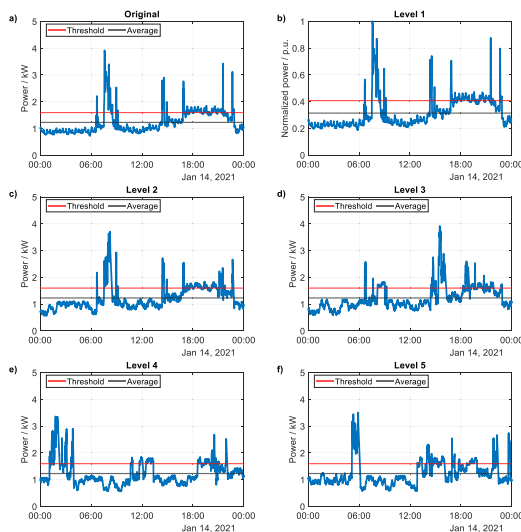


Fig. 4. Exemplary anonymized load profiles of a one-day household load profile.

3.4. SimSES interface and storage parameters

The storage system simulation tool SimSES is a python-based open-source tool that enables time-series-based simulation of storage systems [53]. In SimSES, a variety of parameters can be defined and varied. For example, users can select various energy-management-strategies (EMS) like PS or FCR or implement their own EMS [38]. Furthermore, various lithium-ion battery models with associated degradation models can be used. For a more detailed description of SimSES, please refer to [53].

In this work, SimSES is used to simulate BSSs in different applications using the original and the anonymized load profile. The applications are SCI for the residential load profile and PS for the EV charging station load profile. The standard sizing used in this work for the BSS in each application is shown in Table 5. In the SCI application the BSS is designed with 8.8 kWh and 7 kW, and the PV system has a power of 9.3 kWp, since this was the design of the original system surveyed by the ISEA of RWTH Aachen University. As the focus of this work is on the load profiles, the PV profile available in SimSES is used as the default PV profile. The PV generation profile was measured at the Professorship Power Transmission Systems of the Technical University of Munich in 2014. This profile corresponds to the location Munich and is scaled to the defined peak power of 9.3 kWp. The PV profile is open-source available as part of SimSES [53]. This peak power leads to a generated energy of the PV system of 8,373 kWh over the entire year. If the storage system is simulated with the described parameters and the original load profile over one year, 1,913 kWh are charged into the battery and 1,868

kWh are discharged from the battery.

In the PS application, the BSS is scaled to 140 kWh and 250 kW. The PS limit defined for the grid consumption is set to 32 kW in consultation with the industry partner whose load profile is being used. The designs are used for the simulations to show how the anonymization tool works and to quantify the impact on the BSS load. In Section 4.3, the influence of the design on the results is evaluated in more detail.

The battery model used in both storage applications simulations is a lithium-ion nickel-manganese-cobalt cell from Sanyo, whose parameters have been published by RWTH Aachen [45]. The DC/DC converter is modeled as lossless and the AC/DC converter is modeled following a publication by Notton et al [54].

3.5. Monte Carlo simulations

The generation of anonymized load profiles is based on random permutation of base and peak sequences in the different levels. This dependence on randomness leads to the fact that individual simulations can lead to special, non-representative results. Moreover, in the simulations, non-bijective mappings of load profile KPIs of the BSSs are created. Consequently, no inverse function can be formed to allow a correlation between storage behavior and load profile characteristics. Accordingly, 100 anonymized load profiles are generated for every level in Monte Carlo simulations. The results are ensembles in the solution space which are then evaluated statistically. In addition to the median of the typical KPIs, the scatter will also be shown in the results. In this way, we exclude the possibility that individual, very well-fitting results are displayed.

Overall, this chapter and the tool description in the appendix show how an open-source anonymization tool can be designed to allow gradual anonymization in different levels for easy and straightforward use in industry and research. LoadPAT is available open source, it has GUIs that make anonymization easy for users and it has setting options like level of anonymization and threshold between base and peak sequences.

4. Results

This chapter presents the results of the work. In Section 4.1, exemplary results of the anonymization are presented, and the load profiles are directly compared using various indicators. Subsequently, in Section 4.2 the simulation results of SimSES of the original and the anonymized load profiles are compared. For this purpose, relevant storage KPIs are compared for the different storage applications. Finally, Section 4.3 evaluates the influence of the threshold parameter between base and peak sequences, as well as the influence of BSS and PV design in sensitivity analyses.

4.1. Comparison of the original and the anonymized load profiles

In this section, exemplary results of LoadPAT simulation are presented. Subsequently, the results of the Monte Carlo simulations are compared with respect to the similarity of the load profiles. An example of the anonymization of the EV charging station load profile is already shown in Fig. 2, where a one-day load profile was anonymized to demonstrate the functionality of the tool. Fig. 4 shows a one-day original household load profile together with exemplary profiles of the different levels of anonymization. The diagrams show that, as with the EV charge point load profile, the profile changes more as the level of anonymization increases. Especially the permutation of the base and peak sequences is visible.

For the following results, the two systems are designed according to Table 5 and the load profiles from Table 2 are anonymized. Consequently, the annual load profile is used for the household and the six-month load profile for the EV charging station. Permutations therefore take place over the entire profile length and not just over one day. For

each level, 100 anonymizations are performed in Monte Carlo simulations and the storage is simulated with SimSES. The evaluations in this section refer to the direct comparison of the load profiles without SimSES.

Fig. 5 shows a comparison of four KPIs between the original and the anonymized profiles for the one-year household load profile. The KPIs are the mean (a), the standard deviation (b), the maximum value (c) and the energy (d). For each KPI, the results of the anonymization of the levels 2 to 5 are shown in boxplots. The boxes describe the inter quartile range from 25th to 75th percentile and the red line is the median. The black dashed vertical lines cover all values that are at most 1.5 times away from the maximum or minimum of the interquartile range. The red crosses show outliers that go beyond that. The horizontal dotted line represents the value of the original profile in each case.

Within the three KPIs of mean, standard deviation, and energy there is no major difference between the original load profile and the anonymized load profiles. Only the occurring maximum in the original load profile cannot be reproduced exactly (c). This KPI is underestimated by up to 20%. As described in Section 3.3 the values of the anonymized sequence fluctuate randomly around the average original sequence value and between the maximum and minimum of the original sequence. By generating the sequences in this way, the maximum of the original sequence is not reached in every anonymized sequence. This effect can also be seen in Fig. 4. In the original profile, the maximum value is 4 kW. In the anonymized load profiles of level 2, 4 and 5, however, the value of 4 kW is not reached. The outliers in Fig. 5 whose maximum is above the maximum of the original load profile exist because each sequence is scaled to the mean value of the original sequence after generation. This can cause the maximum of the original load profile to be exceeded in rare cases. In general, forcing the original maximum to be reached would be possible. For example, the synthetic profile could be scaled so that the maximum corresponds exactly to the maximum of the original load profile. However, this would severely overestimate the mean value and energy consumption. If instead only the maximum value of the synthetic profile is set to that of the original, an unrealistically short, large peak would result, which is also not representative of the original profile. For these reasons, an underestimation of the load peak is tolerated at this point. Furthermore, Fig. 5 shows that in all four KPIs, the differences between the levels of anonymization are not significant. This is because the permutation is not

considered within these four KPIs as they are all time independent.

Analogous evaluations are performed for the EV charging station load profile (appendix). The results are similar. Mean, standard deviation and energy are close to the original profile over all levels of anonymization. Furthermore, the maximum of the anonymized load profiles is again smaller than the original profile's maximum.

To determine the time-dependent similarity of the profiles to each other, a DFT of the original household load profile and of four exemplary profiles of the levels 2 to 5 was performed. This method has been used in the literature to cluster and classify load profiles based on periodic patterns [9,37]. The single-sided amplitude of the spectrum of the five profiles is shown in Fig. 6. The frequency range chosen is 0 mHz to 0.0275 mHz, since this corresponds to a period of 10 h to the length of the profile (12 months). The top graph represents the single-sided amplitude of the spectrum of the original profile. The gray shaded areas correspond to periods of about 12 h, 24 h, and 7 days. The original profile shows a pronounced amplitude especially for a period of 24 h and for a period of 12 h. This profile therefore seems to have a period or regularity over days and half days. The period over 24 h emerges because peaks occur with a regularity at approximately the same times of the day. The period over 12 h, whose amplitude is smaller, can be explained by morning and evening load peaks. The spectrum of the profile in level 2, generated using the features from the original load profile, also shows regularity over days and half days. From level 3, where the order of the peaks is randomly permuted, the amplitudes disappear almost completely. There is only a slight increase at the 24-hour period in the spectrum. In Level 4 and 5, in contrast, regularity is no longer recognizable. This is due to the random permutation of the order of the base sequences, whereby the occurrence of peak sequences is shifted in time.

Again, analogous to the industrial load profile, the frequency analysis was performed for the EV charge point profile. The results are shown in Appendix. The original EV charging station load profile shows a regularity over 24 h. In level 2 this regularity can be maintained, while the amplitude in level 3 is smaller but still existing. From level 4 upwards, the amplitude disappears completely.

Overall, the analysis of the load profiles shows that time independent KPIs are preserved despite anonymization. In contrast, the regularity of base and peak sequences is lost due to anonymization, especially from level 3 upwards.

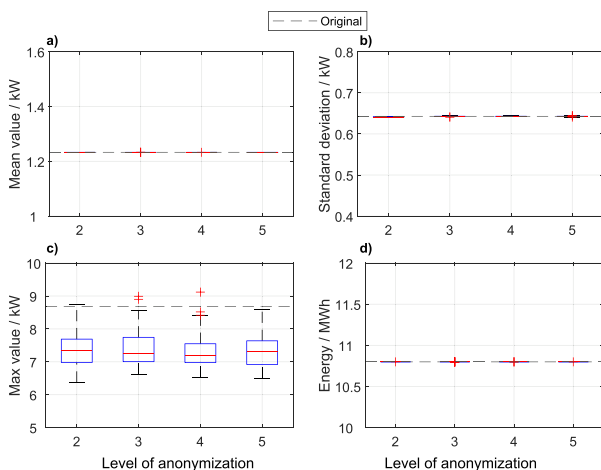


Fig. 5. Comparison of time independent KPIs of original and anonymized one-year household load profiles. 100 anonymized profiles were generated for each level of anonymization.

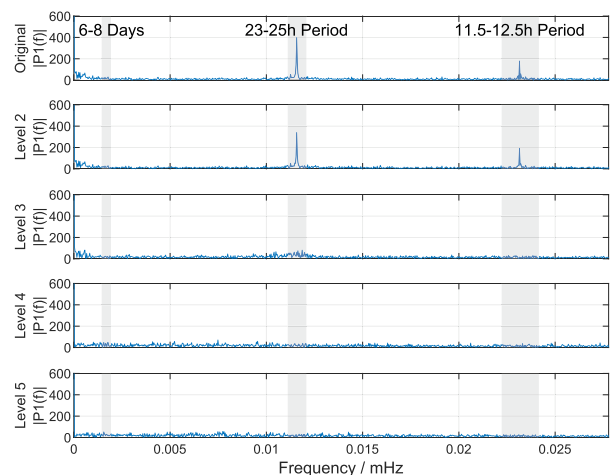


Fig. 6. Discrete Fourier transformation single-sided amplitude spectrum of one-year household load profile in the various levels. Resolution of data: 1 min.

4.2. Effects of the anonymization on relevant battery storage indicators

After the load profiles were directly compared in the previous section, the battery storage applications are now simulated in SimSES using the load profiles. For this purpose, SimSES is invoked as described in Section 3.4 and the operation is simulated once with the original load profile and 100 times with anonymized profiles in every level. Subsequently, various storage KPIs are compared, and it is checked to what extent the anonymization has influenced the behavior of the storage system.

Fig. 7 shows six storage KPIs for the annual household load profiles. The load profiles were used to simulate a BSS in SCI application as described in Section 3.4. The appendix shows the same KPIs with the absolute values of the six storage KPIs. The calculations of the KPIs are shown in the appendix Section 7.2. The deviation over the anonymization levels 2 to 5 compared to the result when using the original load profile. The KPIs shown are the mean SOC (a), the EFCs (b), the mean DOD (c), the mean C-rate (d), the self-consumption rate (e), and the self-sufficiency rate (f). Diagrams a), c), e) and f), on the one hand, show deviations in percentage points, since their original values are already in percent. Diagrams b) and d), on the other hand, show the deviation in percent since their original values are absolute. Above each diagram the absolute value of the KPI of the original load profile is given. Since the deviation from the original is considered at this point, the value of the original is drawn as a dashed line at zero in each case. As in the previous section, the values of the 100 anonymized load profiles are shown as boxplots for each level.

The figure shows that level 2 barely differs from the original in terms of the relevant storage KPIs. Mean SOC, EFCs, mean DOD and mean C-rate are close to the original load profile with small deviations within the 100 anonymizations. The self-consumption rate and the degree of self-sufficiency deviate from the original by only about 1% on average. From level 3 upwards, the deviations from the original are greater with up to 10 percentage points for the self-consumption rate. However, despite the permutations and the abandonment of regularity (see Section 4.1), greater anonymization beyond Level 3 does not lead to greater deviations in the KPIs relevant for BSS. Accordingly, anonymization in level 5 does not appear to be more critical than in level 3 with respect to the KPIs relevant for home storage systems. From level 3 upwards, the average SOC can still be reproduced well. In simulations of the degradation of the BSS with the anonymized load profiles, this would mean that the calendar degradation can be represented well. The mean C-rate deviates only slightly from the C-rate of the original profile, at about 5%.

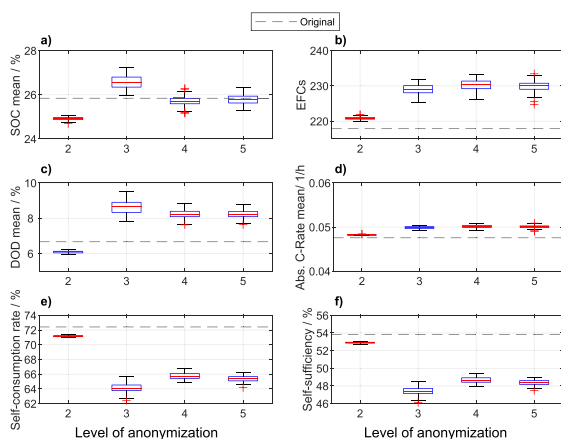


Fig. 7. Comparison of the deviation of BSS KPIs for the household load profile (1 year) in SCI application. a), c), e) and f) show the deviation in percentage points, b) and d) in percent. 100 anonymized profiles per level. PV: 9,3 kWp, E_{Bat} = 8,8 kWh, P_{Bat} = 7 kW.

The simulated BSSs make about 230 EFCs over the year from level 3 instead of 218 in the original. This corresponds to an overestimation of under 6%. Mean DOD is also overestimated by about 2 percentage points resulting in a value of 8 to 9% instead of the 6.7% in the original. The bottom two plots show that the self-consumption rate and self-sufficiency rate are underestimated from Level 3, with deviations of up to 9 percentage points.

In general, some of the results of the KPIs for the SCI case show a systematic overestimation (EFCs, DODs, C-rate) or underestimation (self-consumption rate and self-sufficiency rate) from level 3 to 5 compared to the original values. The original load profile has distinctive peaks especially during the day. The anonymized load profiles between level 3 and 5 have their distinctive peaks distributed over the 24 h. A fan chart over the course of the day with all values for the year once for the original load profile (a) and once for an exemplary load profile in level 3 (b) are shown in the appendix. This shows that the peaks from the daytime hours are distributed over the 24 h of the day due to the anonymization. The shift of the peak loads has an influence on the BSS KPIs. As a result, more energy is charged and discharged from the battery, so the BSS is fully discharged earlier at night and makes more EFCs overall. In addition, the BSS is discharged deeper during evening and night hours due to the load peaks which leads to an increase of mean DODs. The C-rate is slightly higher than the original since the BSS is charged more frequently during the day with high PV power because, for example, in level 3 higher day peaks are exchanged with lower peaks from the night and thus more power flows into the BSS. At level 4, the base sequences are permuted, which leads to even higher C-rates, since the higher base sequences from the daytime exchange with lower base sequences from the nighttime. Next, the self-consumption rate is lower, since less PV energy can be consumed immediately and, once the BSS is fully charged, a larger proportion of the PV energy is fed into the grid. In the evening and at night, more energy must be supplied from the grid, which decreases the degree of self-sufficiency. Since the effects mentioned occur in levels 3, 4 and 5, but do not increase in levels 4 and 5, the KPIs remain relatively constant at higher levels.

Fig. 8 shows BSS KPIs for the EV charging station load profile similar to Fig. 7 but over the period of six months instead of one year. Instead of self-consumption rate and degree of self-sufficiency, round-trip efficiency and fulfillment factor are displayed, as these are relevant for the PS application (see Section 1.1). The appendix again shows a diagram with the absolute values. The Y-axis scaling of the subfigures in Fig. 8 differs from the scaling in Fig. 7 to show the spread of the boxplots. Fig. 8

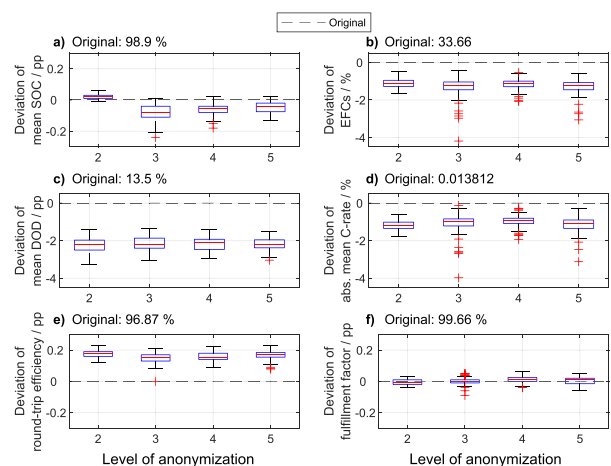


Fig. 8. Comparison of the deviation of BSS KPIs for the EV charging station load profile (6 months) in PS application. a), c), e) and f) show the deviation in percentage points, b) and d) in percent. 100 anonymized profiles. E_{Bat} = 140 kWh, P_{Bat} = 250 kW, Peak-Shaving with Threshold 32 kW.

shows that in all KPIs, the anonymized load profiles show only minor deviations from the value of the original load profile of up to 3% for the C-rate and 3 percentage points for the mean DOD. For example, the mean SOC deviates by only up to 0.3 percentage points. More importantly, the fulfillment factor corresponds to the original across all levels. In contrast to the SCI application, the deviation is constant over the four levels of anonymization. This is because the PS application does not depend on a time-varying PV generation. From level 3 onwards, the permutations cause a shift in the peaks, but this has no influence on the relevant BSS KPIs. This can also be seen from the fact that level 2, in which there are no permutations, deviates just as strongly in most KPIs as levels 3 to 5. The largest noticeable deviation across all six KPIs is mean DOD, which is underestimated by up to three percentage points, resulting in a mean of around 11.3% instead of 13.5%. To explain this underestimation, fan charts are included in the appendix showing the original load profile (a) and a level 3 anonymized load profile (b) over the course of the day. Similar to the fan charts of the household in, the diagrams show that there is a homogenization of the load peaks over the 24 h. This homogenization decreases the mean DOD of the BSS, since the BSS is discharged less frequently by several consecutive load peaks. Furthermore, the maximum of the peaks is smaller as described in Section 4.1, which leads to a decrease of the DOD. For the same reason, the average C-rate is smaller compared to using the original load profile.

Overall, our analyses reveal three results: First, load profiles for use in simulations of time-independent applications such as PS can also be anonymized up to level 5 and thus be strongly modified without changing KPIs relevant for BSS excessively. Smaller characteristic peculiarities in the sequences of the original load profile are consequently not relevant and can be replaced by mean values and random fluctuations. Second, load profiles in time-dependent applications such as SCI can easily be anonymized in level 2 without changing BSS KPIs drastically (approximately 1% in all KPIs). Vice versa, the anonymized profiles can well be used to design a BSS with suitable sizing and realistic estimation of battery degradation. From level 3, the deviations are larger by up to 9 percentage points, and users would have to decide for themselves whether the deviation is still within a reasonable range in order to realistically represent the original load profile through anonymization. Third, if it is decided to anonymize the load profile beyond level 2 in time-dependent applications, higher anonymization in level 4 or 5 does not lead to larger deviations in the relevant BSS KPIs compared to level 3. Accordingly, the load profiles can then be changed more strongly to achieve higher anonymization.

4.3. Sensitivity analysis of threshold and system design

In this section, we perform a sensitivity analysis of the SCI case with the household load profile to explain the impact of three sensitivity parameters on the results. The first sensitivity parameter is the threshold between base and peak sequences. This threshold describes the boundary between base and peak sequences as a multiple of the mean value of the load profile. It can be freely chosen by the users and is set to 130% in the base case, as this provides good separation between base and peak sequences. Basically, a shift in the threshold means that the division into base and peak sequences changes. If, on the one hand, the threshold is set very low, large power variations are all defined as peaks, which leads to larger fluctuations but lower maxima in the peak sequences of the anonymized load profile. If, on the other hand, it is set very high, the base sequences will have large fluctuations and the peak sequences become shorter but more pronounced.

Fig. 9 shows for the household load profile the six BSS KPIs for the original load profile and the medians of the four levels of anonymization over the varying threshold. The threshold is varied in a range from 90%

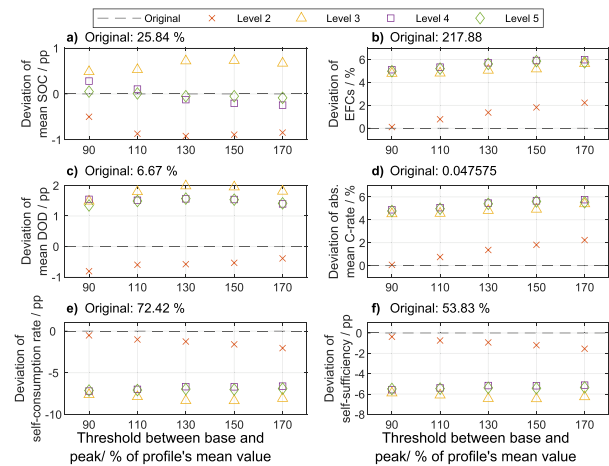


Fig. 9. Sensitivity analysis of the SCI use case with household load profiles: Threshold between base and peak sequences. Threshold defined as percentage of profile's mean value. The levels' values are the median values of 100 simulations. The subplots show the deviation of the results in the levels compared to the original in percentage (b, d) and percentage points (a, c, e, f).

to 170% in 20% steps. The diagram shows the deviations of the KPIs from the original value, which is set to 0 as in Fig. 7. The values of levels 2 to 5 correspond to the median value of 100 anonymizations. For a better understanding of the absolute values, a diagram showing the respective absolute KPIs is presented in Appendix. The number of EFCs increases over all levels slightly as the threshold rises (b). If the threshold is low, more shares of the profile are evaluated as peaks, so that the peak sequences have larger differences between their maximum and minimum. This leads to the fact that the maxima are reached less often and a larger part of the peak sequences can be covered by the PV energy. At a higher threshold the peak sequences become shorter, but more pronounced. These more pronounced peaks can no longer be covered directly by PV generation. Therefore, more peaks must be covered by the BSS, which increases the number of EFCs. Furthermore, the self-consumption rate (e) and self-sufficiency (f) decrease slightly in level 2 but remain relatively constant in levels 3 to 5. The decrease in level 2 comes from the larger fluctuations within the base sequences and the higher maxima in the peak sequences that occur at higher thresholds. This means that a slightly smaller proportion of the PV energy can be consumed directly. In the higher levels of anonymization, the permutations have already changed the load profiles in such a way that the influence of the threshold is lower than in level 2. Overall, Fig. 9 shows that level 2 deviates the least from the original across all thresholds, as expected. Over the varying threshold, however, the deviations within each level change only slightly. The influence of the choice of threshold is therefore small.

As a second parameter, the BSS capacity of the home storage system is varied. Fig. 10 shows the variation between 4.8 kWh and 12.8 kWh with a step size of 2 kWh in the same format as for the threshold variation. Again shows the absolute values, while Fig. 10 shows the deviation. In contrast to the variation of the threshold, this variation of capacity also changes the value of the original profile. Therefore, the original value is shown as a single line and not as a horizontal line. Since Fig. 10 shows the deviation from the original, the respective original value is again shown as 0.

Basically, shows that, for example, the EFCs decrease with increasing capacity, while the self-consumption rate and self-sufficiency increase. Here, the influence of the storage design on the six parameters exists as

expected. Analogous to the analysis of threshold sensitivity, level 2 again shows the smallest deviations from the original profile (Fig. 10). Furthermore, the deviation of levels 3 to 5 in terms of mean SOC (around +1 to -1.5 percentage points), mean DOD (around 2 percentage points), self-consumption rate (-9 to -5 percentage points) and degree of self-sufficiency (-7 to -4 percentage points) is approximately constant over the increase in BSS capacity. An increase in storage capacity, on the other hand, leads to greater deviations regarding EFCs (2 to 10 %) and mean C-rates (1 to 10%). These deviations are constant over the levels. As described in Section 4.2, the presented anonymization leads to more EFCs. If the BSS capacity is now increased, more energy can be discharged at night by peaks occurring only in the anonymized load profile. Thus, the deviations of EFCs increase with increasing BSS capacity. The same applies to the C-rate, which is higher on average because the BSS must more frequently cover the peak loads that cannot be covered by the PV system. Overall, this sensitivity analysis shows that anonymization is relatively robust with respect to the selected storage capacity.

Finally, Fig. 11 show the variation of the PV peak power between 5.3 kWp and 13.3 kWp in 2 kWp steps for the household load profile case. First, as with the BSS capacity variation, the influence of the size of the PV system on the KPIs can be seen: If the PV system is larger, the EFCs increase because more PV energy can be stored. Likewise, the mean C-rate increases, since the BSS is charged with a higher power due to the larger PV system. In addition, the self-consumption rate decreases and the self-sufficiency rate increases with increasing PV nominal power, as has already been confirmed using field data [51]. The results in Fig. 11 are similar to those in Fig. 10. The deviations across the enlarged PV system are relatively constant for mean SOC, mean DOD, self-consumption rate, and self-sufficiency. However, in contrast to the BSS evaluations, the deviations of the EFCs and mean C-rates are large for small nominal PV power of 5.3 kWp with up to 20% over the levels 3 to 5. If the PV system is small, the EFCs are therefore overestimated. The EFCs of the BSS in the original load profile are 137, while they are 163 when anonymized according to level 5 which is an overestimation of 19%. Basically, a smaller PV system can only insufficiently cover the load by the household (degree of self-sufficiency decreases). The permutation of the peak sequences and the possible shift to times without PV generation means that the BSS can be charged more during the day but is also discharged more at night. For this reason, EFCs increase especially when the nominal PV power is small.

Overall, this section answers the question of how sensitive the results

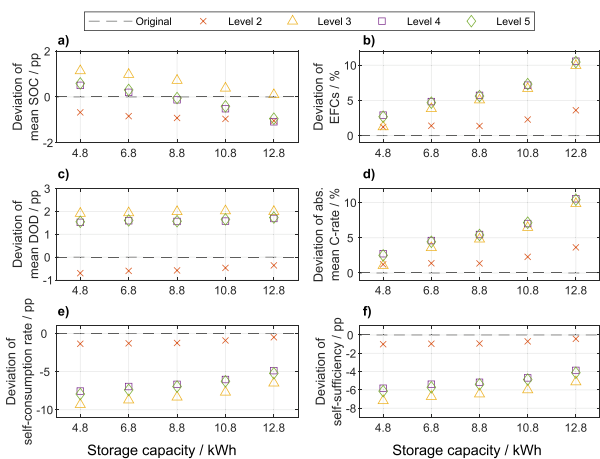


Fig. 10. Sensitivity analysis of the SCI use case with household load profiles: Storage capacity. The levels' values are the median values of 100 simulations. The subplots show the deviation of the results in the levels compared to the original in percentage (b, d) and percentage points (a, c, e, f).

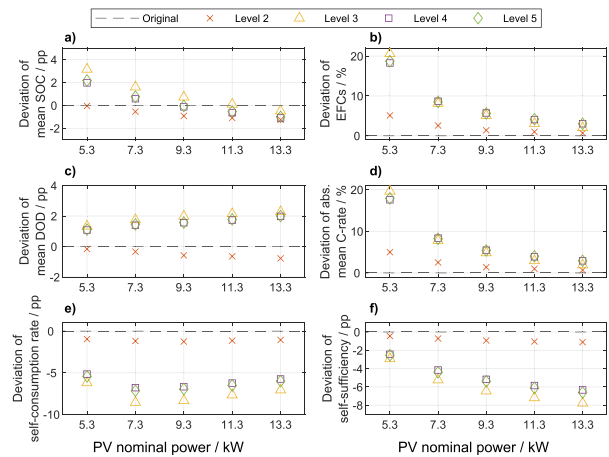


Fig. 11. Sensitivity analysis of the SCI use case with household load profiles: Nominal PV power. The levels' values are the median values of 100 simulations. The subplots show the deviation of the results in the levels compared to the original in percentage (b, d) and percentage points (a, c, e, f).

are to the threshold between base and peak sequences and the system design. The influence of the threshold is rated as low. The BSS KPIs change only slightly by varying the threshold and the deviations between original and the different levels of anonymization remain relatively constant. In principle, this also applies to the variation of the capacity of the BSS and the nominal power of the PV system. Only particularly large capacities of the BSS and small nominal PV power lead to stronger deviations between two KPIs of the anonymized load profiles and those of the original (EFCs and C-rate). A realistic dimensioning of the system design is therefore necessary.

5. Conclusion and outlook

This chapter summarizes the work in Section 5.1. Furthermore, in Section 5.2, we discuss the usability of the tool and the strengths and weaknesses of the methodology, and we give an outlook on how the presented work could be followed up.

5.1. Conclusion

In this work, a methodology of anonymization of load profiles is presented. For this purpose, the existing literature of load profile clustering and anonymization is presented first. Within this research we find that a methodology to gradually anonymize existing load profiles has not been published yet. Hence, we develop a methodology to fill this research gap. Our approach extracts features from the original load profile and separates the profile into base and peak sequences. A synthetic, anonymized load profile is then generated from the features of each sequence. The gradual anonymization is enabled by anonymizing in different levels. A simple normalization of the original load profile is possible in level 1. In Level 2, the features are extracted and used for profile generation along with random values of the standard normal distribution, which represent a type of noise. From level 3 on, peak or base sequences are permuted. In level 3, the peak sequences are permuted in a random way, which shifts peaks that are characteristic for the load profile in time. In level 4, the base sequences are permuted in a random manner. The order of the peaks is preserved, but they also shift in time due to the change in base sequences order. Finally, level 5 allows the combined permutation of base sequences and peak sequences. This results in more strongly modified load profiles. To make the presented methodology usable for the public, the open-source load profile anonymization tool LoadPAT was developed. LoadPAT is coded in Python

and can be used on any computer. This allows companies, research institutions and private individuals to keep the original data on their computers and to create and subsequently share the anonymized load profiles themselves. The methodology presented and LoadPAT answer our first research question, how load profiles can be anonymized gradually and how an open-source tool could look like that allows anonymization and enables an easy and straightforward use in industry and research (RQ 1).

Two load profiles were selected as use cases for testing the methodology within LoadPAT: A household load profile and an EV charging station load profile. For both use cases, 100 anonymized load profiles were created in Monte Carlo simulations across all possible levels. Subsequently, the anonymized load profiles were compared with the original load profile in each case. The results showed that the anonymized load profiles correspond to the original load profile in time-independent KPIs, such as the mean value or the standard deviation. However, a subsequent analysis of the amplitude of the DFT of the load profiles shows that the regularity of the load profiles is lost due to anonymization from level 3 upwards (RQ 2).

Afterwards, the original and anonymized load profiles are used as input profiles for the storage simulation tool SimSES and various storage applications are simulated. The household load profiles are used to simulate a SCI scenario. The EV charging station load profiles are used for a PS scenario. Our results show that anonymizing load profiles has only minor impact on KPIs relevant to BSS in time-independent storage applications such as PS. However, if time-dependent storage applications such as SCI (dependence on PV generation) are considered, anonymization from level 3 leads to larger variations in relevant KPIs. If, on the one hand, this variation is considered by users to be significant, anonymization should only be performed up to level 2. If, on the other hand, it is considered acceptable, anonymization can even be performed up to level 5, since the differences between the KPIs of level 3 and 5 are small (RQ 3).

Finally, we perform a sensitivity analysis in which we evaluate the influence of the threshold value between base and peak sequences and the influence of the system design (RQ4). This analysis indicates that although the choice of threshold leads to slightly different results, the deviations are relatively constant across the different levels of anonymization. The system design of storage capacity and PV system shows similar results. The KPIs relevant to BSS change with capacity and PV system size, as expected. The deviations across levels are also relatively constant here, except for particularly large capacities and particularly small PV systems.

5.2. Discussion and outlook

The presented methodology of LoadPAT allows the modification of load profiles so that characteristic times of peak and base phases are no longer identifiable. The methodology works for various types of load profiles such as the rather continuous household load profiles, but also the more event-based load profiles of EV charging stations. Moreover, the original load profile cannot be reconstructed from the anonymized load profiles, especially from level 3 onwards, due to the random permutations of a large number of peak or base sequences. In addition, the approach is easy to understand, does not require large data sets or processes with artificial intelligence involved. LoadPAT is easy to use because of the GUI including graphical representation of the load profiles. Users can select the threshold between base and peak sequences and the level of anonymization, and if needed, normalize the load profile to the maximum value. They can even simulate the created load profile in the tool in different storage applications. A weakness of the methodology is that characteristic peaks (e.g. typical machines of a company)

are shifted in time but can still be recognizable even at the highest level of anonymization. Here, the tool could be extended in the future to explicitly blur selected peaks. Furthermore, in the present version of the tool the resolution of the load profiles cannot be changed, and profiles cannot be shortened or extended. In addition, the permutations from level 3 are always performed over the entire length of the profile. A selectable period for the permutations, for example over weeks, could maintain seasonal fluctuations within the load profile. Another approach would be to extract a daily load profile from a monthly original load profile that is as representative as possible but anonymized. Similarly, a methodology could be developed to extract an anonymized, representative load profile from a set of load profiles. An approach that has already been published several times is the clustering of load profiles to summarize similar load profiles [14–16]. The LoadPAT methodology could be used to aggregate larger data sets of anonymized load profiles that would not be allowed to be shared without anonymization. Here, users could be allowed to upload their anonymized load profiles to a publicly available platform. This database could be made freely available to users from industry and research and thus contribute to the standardization of load profiles. In addition, the methodology could also be further developed and adapted so that real-time smart meter data can be anonymized with the goal of masking resident attendance times. Finally, the methodology could be extended to storage profiles that are not only positive but change sign through charging and discharging.

Data availability

The Load Profile Anonymization Tool (LoadPAT) presented in this paper can be downloaded as an open-source Python version from Gitlab [55]. The household load profile will be part of a future publication and the EV charging station load profile is subject to a non-disclosure agreement.

CRedit authorship contribution statement

Benedikt Tepe: Conceptualization, Methodology, Software, Formal analysis, Investigation, Writing – original draft, Visualization. **David Haberschusz:** Conceptualization, Methodology, Writing – original draft, Visualization. **Jan Figgner:** Conceptualization, Methodology, Writing – original draft, Visualization. **Holger Hesse:** Conceptualization, Writing – review & editing, Supervision. **Dirk Uwe Sauer:** Resources, Writing – review & editing, Supervision. **Andreas Jossen:** Resources, Writing – review & editing, Supervision.

Declaration of Competing Interest

The authors declare that they have no known competing financial interests or personal relationships that could have appeared to influence the work reported in this paper.

Acknowledgement

This work was financially supported by the German Federal Ministry of Education and Research (BMBF) within the SimBAS project (Grant No. 03XP0338A), which is managed by Project Management Jülich. The household profiles were measured in the research projects “WMEP PV-Speicher” (funding number 0325666), and “WMEP PV-Speicher 2.0 (KfW 275)” (funding number 03ET6117)”, both funded by the German Federal Ministry for Economic Affairs and Climate Action (BMWK). The responsibility for this publication rests with the authors.

Appendix

Existing literature on analysis and clustering of load profiles

Table A1

Equations of the storage KPIs

The KPIs used in this work for the behavior of the BSS are presented below. First, the mean SOC results from all SOC values of the storage profile (Equation (4)). We calculate the number of equivalent full cycles (EFCs) analogous to [38] after equation (5) using the energy charged into the storage system over the entire profile divided by the energy of the storage system. The mean DOD is also calculated analogously to [38] from the SOC at the start of the cycle minus the SOC at the end of the cycle (equation (6)). According to equation (7), the mean absolute C-rate is calculated using the absolute mean value of the current in ampere divided by the battery capacity in ampere-hours. The two KPIs relevant to self-consumption increase, the self-consumption rate and the degree of self-sufficiency, are derived from equation (8) and (9), respectively. The self-consumption rate, on the one hand, describes what proportion of the energy generated by the PV was consumed by the household or industry consumer. For example, if no energy is fed into the grid, the self-consumption rate is 100%; if half of the PV energy is fed into the grid, the self-consumption rate is 50%. The degree of self-sufficiency, on the other hand, describes the independence from the grid and therefore depends on the total consumption and the grid supply. If no energy is drawn from the grid, the degree of self-sufficiency is 100%, if half of the required energy is drawn from the grid, the degree of self-sufficiency is 50%. The round-trip efficiency is the energy discharged from the storage divided by the energy charged into the storage (equation (10)) [38].

The charged energy is corrected in the formula to account for the SOC offset between the beginning and end of the simulated period. The fulfillment factor, which is the percentage of time that the system was able to fulfill the requested service, is calculated using equation (11) [49]. Here, P^* stands for the realized power and P_{sys} for the power requested by the system.

$$SOC_{mean} = \frac{\sum_{t=1}^n SOC(t)}{n} \tag{4}$$

$$EFCs = \frac{E_{total\ profile}^{pos}}{E_{BSS}} \tag{5}$$

$$DOD_{mean} = \frac{\sum_{k=1}^m SOC_{cycle\ k, start} - SOC_{cycle\ k, end}}{m} \tag{6}$$

$$C - rate_{abs, mean} = \frac{|\bar{I}|}{C_{Battery}} \tag{7}$$

$$Self\ consumption\ rate = 1 - \frac{E_{grid\ feed\ in}}{E_{PV\ Generation}} \tag{8}$$

$$Self\ sufficiency = 1 - \frac{E_{grid\ supply}}{E_{load\ total}} \tag{9}$$

$$\eta_{BSS} = \frac{|E_{total\ profile}^{neg}|}{|E_{total\ profile}^{pos}| - [SOC_{end} - SOC_{start}] \bullet E_{BSS}} \tag{10}$$

$$Fulfillment\ factor = 1 - \frac{\int (|P^*(t) - P_{sys}(t)|) dt}{\int (|P_{sys}(t)|) dt} \tag{11}$$

With :

n : Length of load profile

Table A1
Summary of literature on load profile analysis and feature extraction.

Source	Date	Focus	Results
Price [8]	2010	Load analysis	Definition of five parameters to characterize load shapes in time-domain: Base load, peak load, rise time, high-load duration, fall time.
Haben et al. [12]	2016	Load analysis & clustering	Analysis of customer smart meter data including seven attributes that describe relative seasonal and intraweekly power and standard deviation. Those attributes of each profile are used in a finite mixture-based clustering.
Al-Otaibi et al. [13]	2016	Feature extraction for clustering	Calculation of specific maxima and minima in time range as features together with normalization and scaling leads to sufficient clustering results with much fewer features compared to 48 half-hour values of a daily load profile.
Wang et al. [11]	2019	Load analysis, forecasting & management	Review on smart meter data analytics: Load profiling can be done directly using the time-series and indirectly using suitable features extracted from the profile.
Park et al. [14]	2019	Clustering	Direct clustering of building load profiles extracting three fundamental profiles that 94% of 1,832,807 daily load profiles of 3,829 buildings can be assigned to
Trotta [15]	2020	Clustering (k-means)	Four clusters of Danish household load profiles are identified including seasonal fluctuations.
Li et al. [9]	2021	Load analysis	Combination of time-domain (based on the work of Price [2]) and frequency-domain load profile analysis of commercial office buildings. Time-domain analysis based on six key parameters of the load profiles.
Czétány et al. [16]	2021	Clustering	Three clusters of Hungarian household load profiles on daily and on yearly basis are identified. The K-means algorithm is favorable against fuzzy k-means and agglomerative hierarchical clustering.
Elahe et al. [17]	2022	Feature extraction	Identification of households with plug-in electric vehicles using a new feature extraction technique.

m : number of cycles

Illustration of the two original load profiles

The Figs. A1 and A2 describe the annual household load profile and the 6 months electric vehicle charging station load profile described in Section 2.

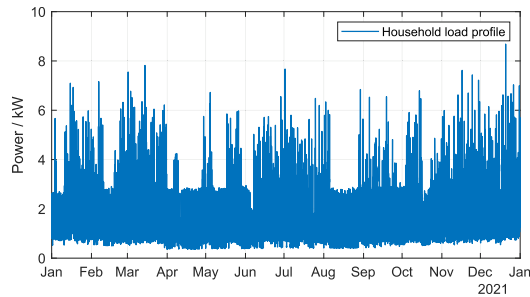


Fig. A1. Annual household load profile for 2021.

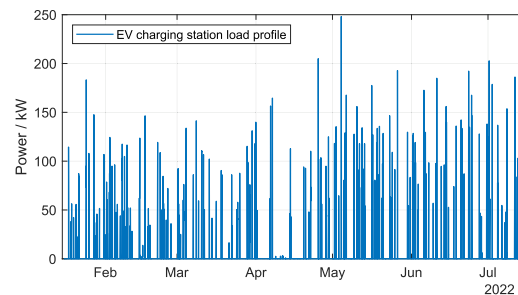


Fig. A2. 6 months electric vehicle charging station load profile from Mid-January 2022 until Mid-July 2022.

Description of LoadPAT

In this chapter we describe the open-source load profile anonymization tool LoadPAT. The basic idea of LoadPAT is to characterize a load profile and generate an anonymous, synthetic load profile based on various features. The similarity between the synthetic load profile and the original load profile can be distinguished by the user based on five anonymization levels. A screenshot of the GUI is shown in Fig. A3. On the left side, the levels of anonymization are explained. On the right side, the anonymization can be performed step by step. In step 1, the users browse to a CSV of the original load profile. Afterwards, the original profile is already plotted.

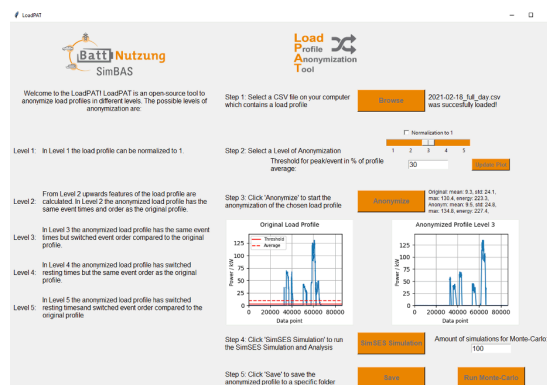


Fig. A3. Graphical User Interface of LoadPAT.

In step 2, users then select the level of anonymization. Here they can also click in a tick box on “Normalization to 1” to normalize the load profile to the maximum value. In addition, the threshold between base and peak sequences can be set in this step. This threshold is to be specified as a percentage value of the average value of the original profile. If, for example, 100% is selected, the threshold value corresponds to the mean value. In our simulations we choose as threshold 130%, as this provides good separation between base and peak sequences. To support the selection of the threshold value, the plot of the original profile shows once the average value of the profile dashed and once the threshold value. By clicking on “Update Plot”, users can update the original plot after changing the threshold value.

In step 3, the actual anonymization takes place. By clicking on the “Anonymize” button, the anonymization is performed. The methodology of the anonymization is explained in detail in Section 3.3. The anonymized profile then appears next to the original load profile, and the users can compare the profiles visually. Moreover, some key metrics like mean values, standard deviation and maximal values are displayed next to the “Anonymize” button. If users are not satisfied with the generated anonymous profile, they can generate a new profile by clicking the button again.

In step 4, users can simulate the original profile and the anonymized profile in a battery storage application via the storage simulation tool SimSES. Finally, in step 5, users can save their anonymized profile. To analyze the operation of LoadPAT, it is furthermore possible to run many anonymizations in Monte Carlo simulations followed by storage system simulations across all levels in succession.

In this work, SimSES is invoked by LoadPAT and a BSS is simulated in different applications using the original and the anonymized load profile. The GUI for using SimSES within LoadPAT, which appears when clicking the “SimSES Simulation” button in the main window of the GUI, is shown in Fig. A4. On the left side, users can set parameters. First, this is the storage capacity in kWh and the maximum power of the storage in kW, which is limited by the power electronics. In addition, the start SOC and the resolution of the time series simulation must be defined. Furthermore, a lithium-ion cell and the EMS can be selected via drop-down menus. Depending on the EMS, the size of the PV system (SCI) or the limit for PS must then be defined. Afterwards, the storage behavior can be simulated with the original load profile and with the anonymized load profile. By clicking the “Show Results” button after the simulations are completed, the results of the storage simulation are displayed on the right side. In the upper part, the key KPIs determined by SimSES for the original profile and the anonymized profile are displayed as a table together with the percentage deviation. Below this, histograms for the KPIs SOC, C-rate, DOD and temperatures are plotted, allowing users to compare these four KPIs graphically. Finally, users can save the results from SimSES by clicking on the corresponding button. If users are satisfied with the results, they can then save the anonymized profile in the main window of LoadPAT. As of this publication, users have access to three battery models, two NMC-based lithium-ion batteries (SanyoNMC and MolicelNMC) and one iron-phosphate lithium ion battery (SonyLFP), whose data have been published in various publications [43,45,46,56]. As EMS, users can choose between two strategies: A strategy of SCI of PV energy (ResidentialPvGreedy) and a PS strategy (SimplePeakShaving).

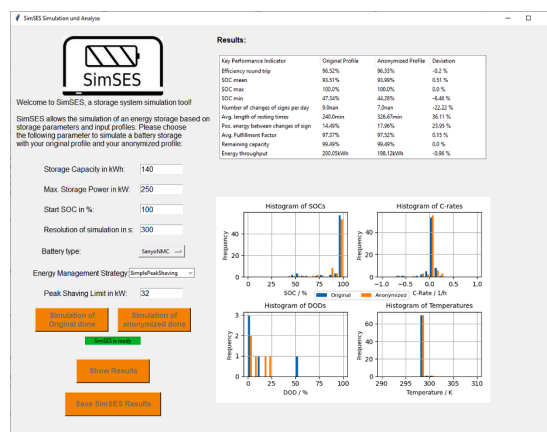


Fig. A4. Graphical User Interface of SimSES in LoadPAT.

Results of the comparison of the original and the anonymized load profile for the EV charging station load profile

Fig. A5 shows the comparison of load profiles for the EV charging station load profile. Fig. A6 shows the single-sided amplitude spectrum of the original profile and 5 exemplary anonymized load profiles for the EV charging station.

SimSES KPI comparison: Plots of absolute values

Figs. A7 and A8 show the comparison of the BSS KPIs for the household load profile anonymization and the EV charging station load profile anonymization in absolute values.

Fan chart of the original household load profile and an exemplary load profile anonymized in level 3

The Figs. A9 and A10 show fan charts of the original load profiles and one exemplary anonymized load profile from level 3 over the course of the day as mentioned in Section 4.2.

Results of the sensitivity analyses of Section 4.3

The Figs. A11–A13 show the absolute values of the BSS KPIs of the sensitivity analysis. In Section 4.3 Figure Fig. 9, Fig. 10 and Fig. 11 the deviations from the original values are displayed.

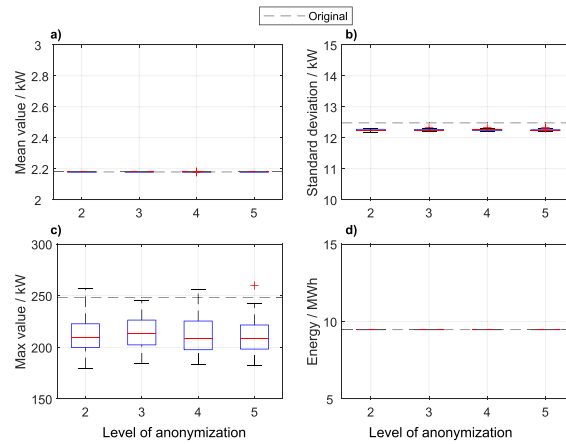


Fig. A5. Comparison of load profiles. EV charging station load profile (6 months). 100 anonymized profiles per original profile.

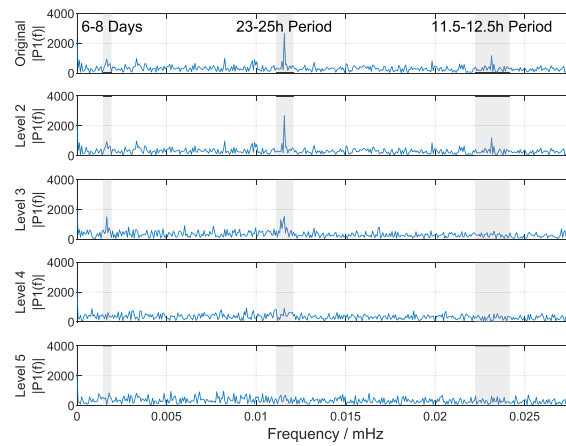


Fig. A6. Discrete Fourier Transformation single-sided amplitude spectrum of 6-months EV charging station profile in the different levels. Time resolution of profile: 1 min.

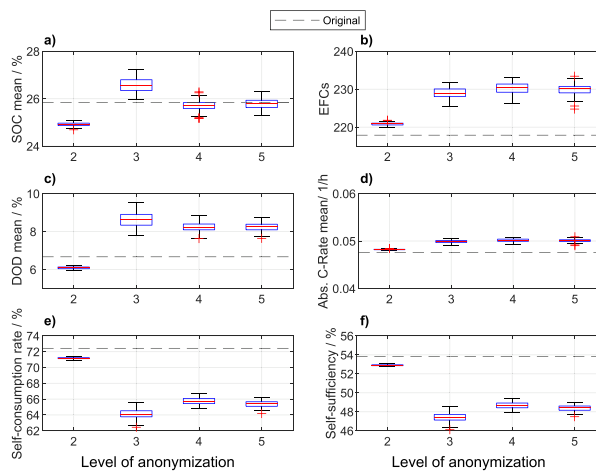


Fig. A7. Comparison of the BSS KPIs for the household load profile (1 year) in SCI application. 100 anonymized profiles per level. PV: 9,3 kWp, E_{Bat} = 8,8 kWh, P_{Bat} = 7 kW.

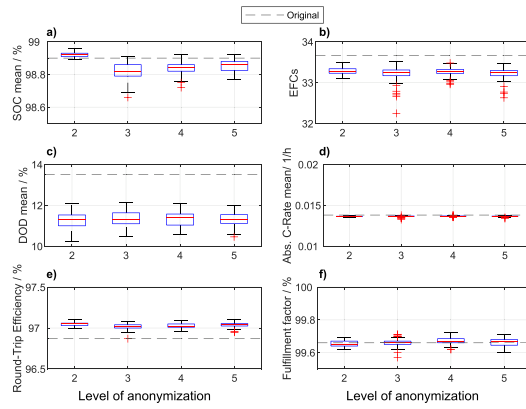


Fig. A8. EV charging station load profile (6 months). Comparison of SimSES characteristics. 100 anonymized profiles. $E_{Bat} = 140$ kWh, $P_{Bat} = 250$ kW, Peak-Shaving with Threshold 32 kW.

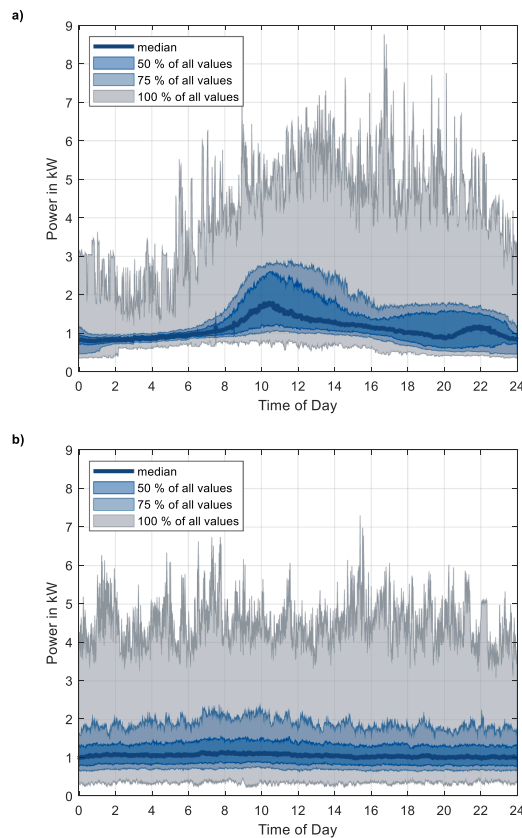


Fig. A9. Fan chart of the household load profiles over the course of the day. 365 values per minute (data for 1 year). The top diagram (a) shows the plot for the original load profile, the bottom diagram (b) the plot for an exemplary level 3 anonymized load profile.

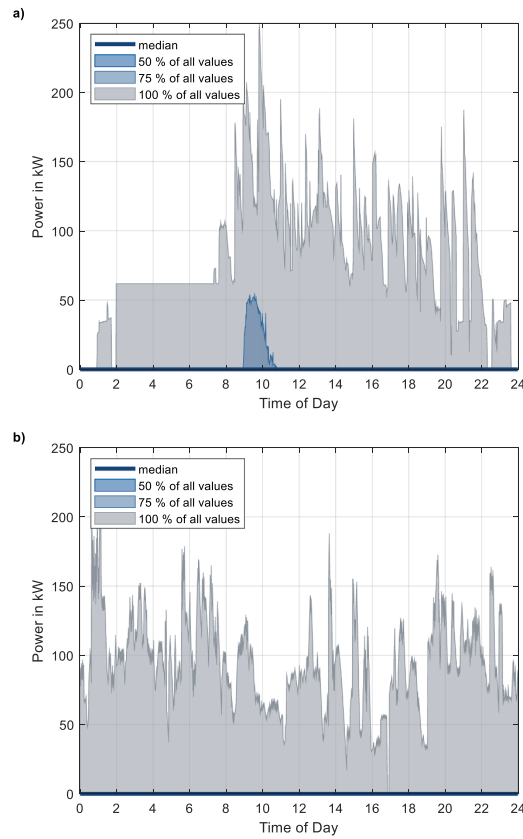


Fig. A10. Fan chart of the EV charging station load profiles over the course of the day. 181 values per minute (data for 6 months). The top diagram (a) shows the plot for the original load profile, the bottom diagram (b) the plot for an exemplary level 3 anonymized load profile.

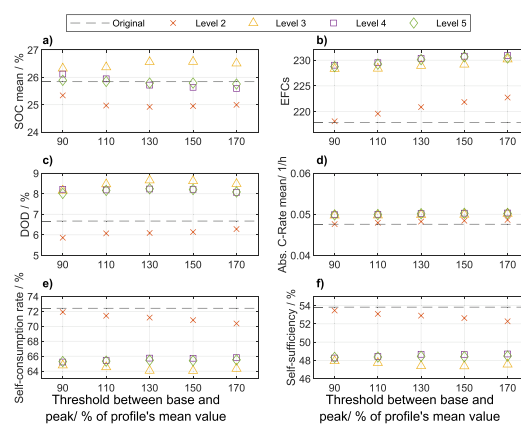


Fig. A11. Sensitivity analysis of the SCI use case with household load profiles: Threshold between base and peak sequences. Threshold defined as percentage of profile's mean value. The levels' values are the median values of 100 simulations. The subplots show the absolute values of the results in the levels.

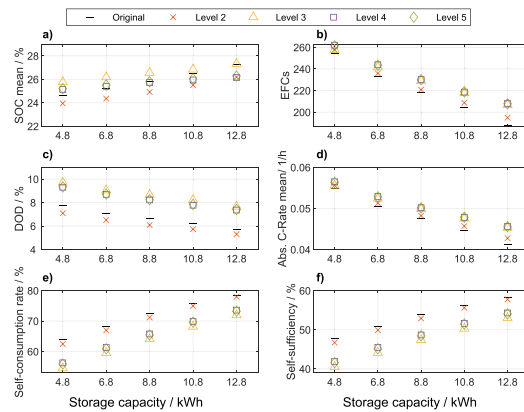


Fig. A12. Sensitivity analysis of the SCI use case with household load profiles: Storage capacity. The levels' values are the median values of 100 simulations. The subplots show the absolute values of the results in the levels.

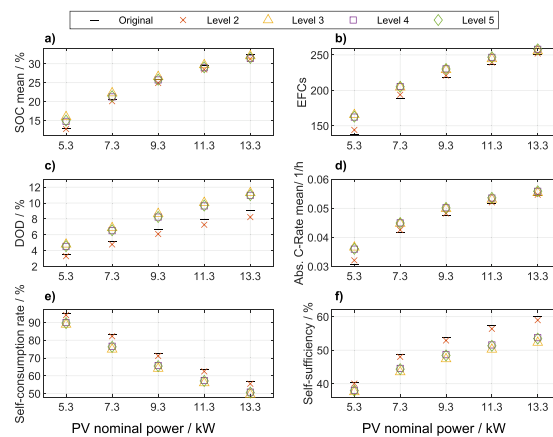


Fig. A13. Sensitivity analysis of the SCI use case with household load profiles: Nominal PV power. The levels' values are the median values of 100 simulations. The subplots show the absolute values of the results in the levels.

References

- [1] Reinsel D, Rydning J, Gantz JF. Worldwide global datasphere forecast, 2021-2025: The world keeps creating more data—now, what do we do with it all. IDC Corporate USA 2021.
- [2] Rydning J, Reinsel D. Worldwide Global StorageSphere Forecast, 2021–2025: To Save or Not to Save Data. IDC Corporate USA: That Is the Question; 2021.
- [3] Baidya S, Potdar V, Pratim Ray P, Nandi C. Reviewing the opportunities, challenges, and future directions for the digitalization of energy. *Energy Res Soc Sci* 2021;81:102243. <https://doi.org/10.1016/j.erss.2021.102243>.
- [4] Sovacool BK, Hook A, Sareen S, Geels FW. Global sustainability, innovation and governance dynamics of national smart electricity meter transitions. *Glob Environ Chang* 2021;68:102272. <https://doi.org/10.1016/j.gloenvcha.2021.102272>.
- [5] Robinson-Garcia N, Costas R, van Leeuwen TN. Open Access uptake by universities worldwide. *PeerJ* 2020. <https://doi.org/10.7717/peerj.9410>.
- [6] European Commission - Directorate-General for Research and Innovation. Trends for open access to publications. [October 27, 2022]; Available from: https://research-and-innovation.ec.europa.eu/strategy/strategy-2020-2024/our-digital-future/open-science/open-science-monitor/trends-open-access-publications_en.
- [7] Proedrou E. A comprehensive review of residential electricity load profile models. *IEEE Access* 2021;12:114–33. <https://doi.org/10.1109/ACCESS.2021.3050074>.
- [8] Price P. Methods for Analyzing Electric Load Shape and its Variability. California Energy Commission: Lawrence Berkeley National Laboratory; 2010.
- [9] Li H, Wang Z, Hong T, Parker A, Neukomm M. Characterizing patterns and variability of building electric load profiles in time and frequency domains. *Appl Energy* 2021;291. <https://doi.org/10.1016/j.apenergy.2021.116721>.
- [10] Campestri C, Horsche MF, Zilberman I, Heil T, Zimmermann T, Jossen A. Validation and benchmark methods for battery management system functionalities: state of charge estimation algorithms. *J Storage Mater* 2016;38–51. <https://doi.org/10.1016/j.est.2016.05.007>.
- [11] Wang Y, Chen Q, Hong T, Kang C. Review of smart meter data analytics: applications, methodologies, and challenges. *IEEE Trans Smart Grid* 2019;10(3): 3125–48. <https://doi.org/10.1109/TSG.2018.2818167>.
- [12] Haben S, Singleton C, Grindrod P. Analysis and clustering of residential customers energy behavioral demand using smart meter data. *IEEE Trans Smart Grid* 2016;7(1):136–44. <https://doi.org/10.1109/TSG.2015.2409786>.
- [13] Al-Otaibi R, Jin N, Wilcox T, Flach P. Feature construction and calibration for clustering daily load curves from smart-meter data. *IEEE Trans Ind Inf* 2016;12(2): 645–54. <https://doi.org/10.1109/TII.2016.2528819>.
- [14] Park JY, Yang X, Miller C, Arjunan P, Nagy Z. Apples or oranges? Identification of fundamental load shape profiles for benchmarking buildings using a large and diverse dataset. *Appl Energy* 2019;236:1280–95. <https://doi.org/10.1016/j.apenergy.2018.12.025>.
- [15] Trotta G. An empirical analysis of domestic electricity load profiles: Who consumes how much and when? *Appl Energy* 2020;275:115399. <https://doi.org/10.1016/j.apenergy.2020.115399>.
- [16] Czétányi L, Vámos V, Horváth M, Szalay Z, Mota-Babiloni A, Deme-Bélafi Z, et al. Development of electricity consumption profiles of residential buildings based on smart meter data clustering. *Energy Buildings* 2021;252:111376.
- [17] Elahe MF, Jin M, Zeng P. Knowledge-based systematic feature extraction for identifying households with plug-in electric vehicles. *IEEE Trans Smart Grid* 2022; 13(3):2259–68. <https://doi.org/10.1109/TSG.2022.3146556>.
- [18] Aigner DJ, Sorooshian C, Kerwin P. Conditional demand analysis for estimating residential end-use load profiles. *EJ* 1984;5(3). <https://doi.org/10.5547/ISSN0195-6574-EJ-Vol5-No3-6>.
- [19] Bartels R, Fiebig DG, Garben M, Lumsdaine R. An end-use electricity load simulation model. *Util Policy* 1992;2(1):71–82. [https://doi.org/10.1016/0957-1787\(92\)90055-N](https://doi.org/10.1016/0957-1787(92)90055-N).
- [20] Pensa RG, Monreale A, Pinelli F, Pedreschi D. Pattern-preserving k-anonymization of sequences and its application to mobility data mining. In: *International*

- Workshop on Privacy in Location-Based Applications PILBA'08. CEUR-WS.org; 2008. p. 44–60.
- [21] Widén J, Wäckelgård E. A high-resolution stochastic model of domestic activity patterns and electricity demand. *Appl Energy* 2010;87(6):1880–92. <https://doi.org/10.1016/j.apenergy.2009.11.006>.
- [22] Richardson I, Thomson M, Infield D, Clifford C. Domestic electricity use: a high-resolution energy demand model. *Energy Build* 2010;42(10):1878–87. <https://doi.org/10.1016/j.enbuild.2010.05.023>.
- [23] Efthymiou C, Kalogridis G. Smart Grid Privacy via Anonymization of Smart Metering Data. In: In: 2010 First IEEE International Conference on Smart Grid Communications. IEEE; 2010. p. 238–43.
- [24] Ogasawara E, Martinez LC, de Oliveira D, Zimbrão G, Pap GL, Mattoso M. Adaptive Normalization: A novel data normalization approach for non-stationary time series. In: The 2010 International Joint Conference on Neural Networks (IJCNN). IEEE; 2010. p. 1–8.
- [25] Shou L, Shang X, Chen K, Chen G, Zhang C. Supporting pattern-preserving anonymization for time-series data. *IEEE Trans Knowl Data Eng* 2013;25(4):877–92. <https://doi.org/10.1109/TKDE.2011.249>.
- [26] Jambagi A, Kramer M, Cheng V. Residential electricity demand modelling: Activity based modelling for a model with high time and spatial resolution. In: 2015 3rd International Renewable and Sustainable Energy Conference (IRSEC). IEEE; 2015. p. 1–6.
- [27] Müller M, Biedenbach F, Reinhard J. Development of an integrated simulation model for load and mobility profiles of private households. *Energies* 2020;13(15):3843. <https://doi.org/10.3390/en13153843>.
- [28] Han M, Johari F, Huang P, Zhang X. Generating hourly electricity demand data for large-scale single-family buildings by a decomposition-recombination method. *Energy Built Environ* 2022. <https://doi.org/10.1016/j.enbenv.2022.02.011>.
- [29] Grandjean A, Adnot J, Binet G. A review and an analysis of the residential electric load curve models. *Renew Sustain Energy Rev* 2012;16(9):6539–65. <https://doi.org/10.1016/j.rser.2012.08.013>.
- [30] Li H, Yeo JH, Bornsheuer AL, Overbye TJ. The creation and validation of load time series for synthetic electric power systems. *IEEE Trans Power Syst* 2021;36(2):961–9. <https://doi.org/10.1109/TPWRS.2020.3018936>.
- [31] Pinceti A, Sankar L, Kosut O. Synthetic Time-Series Load Data via Conditional Generative Adversarial Networks. In: 2021 IEEE Power & Energy Society General Meeting (PESGM). IEEE; 2021. p. 1–5.
- [32] Sweeney L. k-anonymity: A model for protecting privacy. *Int. J. Unc. Fuzz. Knowl. Based Syst.* 2002;10(05):557–70. <https://doi.org/10.1142/S0218488502001648>.
- [33] Machanavajjhala A, Kifer D, Gehrke J, Venkatasubramanian M. L-diversity: privacy beyond k-anonymity. *ACM Trans Knowl Discov Data* 2007;1(1):3. <https://doi.org/10.1145/1217299.1217302>.
- [34] Savov K-K, Stoyanov P, Stanev R, Stoilov D. Analysis of errors in distribution networks power losses calculations with relation to the time discretization intervals. In: In: 2017 15th International Conference on Electrical Machines, Drives and Power Systems (ELMA). IEEE; 2017. p. 42–6.
- [35] Prasser F, Kohlmayer F. Putting Statistical Disclosure Control into Practice: The ARX Data Anonymization Tool. In: Gkoulalas-Divanis A, Loukides G, editors. *Medical Data Privacy Handbook*. Cham: Springer International Publishing; 2015. p. 111–48.
- [36] Pinceti A, Sankar L, Kosut O. Generation of Synthetic Multi-Resolution Time Series Load Data; 2021.
- [37] Schaefer EW, Hoogsteen G, Hurink JL, van Leeuwen RP. Sizing of hybrid energy storage through analysis of load profile characteristics: a household case study. *J Storage Mater* 2022;52:104768. <https://doi.org/10.1016/j.est.2022.104768>.
- [38] Kucevic D, Tepe B, Englberger S, Parlikar A, Mühlbauer M, Bohlen O, et al. Standard battery energy storage system profiles: Analysis of various applications for stationary energy storage systems using a holistic simulation framework. *J Storage Mater* 2020;28. <https://doi.org/10.1016/j.est.2019.101077>.
- [39] Martins R, Hesse H, Jungbauer J, Vorbuchner T, Musilek P. Optimal component sizing for peak shaving in battery energy storage system for industrial applications. *Energies* 2018;11(8):2048. <https://doi.org/10.3390/en11082048>.
- [40] Linssen J, Stenzel P, Fleer J. Techno-economic analysis of photovoltaic battery systems and the influence of different consumer load profiles. *Appl Energy* 2017;185:2019–25. <https://doi.org/10.1016/j.apenergy.2015.11.088>.
- [41] Englberger S, Jossen A, Hesse H. Unlocking the potential of battery storage with the dynamic stacking of multiple applications. *Cell Rep Phys Sci* 2020;1(11):100238. <https://doi.org/10.1016/j.xcrp.2020.100238>.
- [42] Figgenger J, Hecht C, Haberschusz D, Bors J, Spreuer KG, Kairies K-P et al. The development of battery storage systems in Germany: A market review (status 2022). arXiv; 2022.
- [43] Naumann M, Spingler FB, Jossen A. Analysis and modeling of cycle aging of a commercial LiFePO₄/graphite cell. *J Power Sources* 2020;451:227666. <https://doi.org/10.1016/j.jpowsour.2019.227666>.
- [44] Collath N, Tepe B, Englberger S, Jossen A, Hesse H. Aging aware operation of lithium-ion battery energy storage systems: a review. *J Storage Mater* 2022;55:105634. <https://doi.org/10.1016/j.est.2022.105634>.
- [45] Schmalstieg J, Käbitz S, Ecker M, Sauer DU. A holistic aging model for Li(NiMnCo)O₂ based 18650 lithium-ion batteries. *J Power Sources* 2014;257:325–34. <https://doi.org/10.1016/j.jpowsour.2014.02.012>.
- [46] Naumann M, Schimpe M, Keil P, Hesse H, Jossen A. Analysis and modeling of calendar aging of a commercial LiFePO₄/graphite cell. *J Storage Mater* 2018;17:153–69. <https://doi.org/10.1016/j.est.2018.01.019>.
- [47] Moshövel J, Kairies K-P, Magnor D, Leuthold M, Bost M, Gährs S, et al. Analysis of the maximal possible grid relief from PV-peak-power impacts by using storage systems for increased self-consumption. *Appl Energy* 2015;137:567–75.
- [48] Truong C, Naumann M, Karl R, Müller M, Jossen A, Hesse H. Economics of residential photovoltaic battery systems in Germany: the case of Tesla's powerwall. *Batteries* 2016;2(2):14. <https://doi.org/10.3390/batteries2020014>.
- [49] Mühlbauer M, Bohlen O, Danzer MA. Analysis of power flow control strategies in heterogeneous battery energy storage systems. *J Storage Mater* 2020;30:101415. <https://doi.org/10.1016/j.est.2020.101415>.
- [50] Beck T, Kondziella H, Huard G, Bruckner T. Assessing the influence of the temporal resolution of electrical load and PV generation profiles on self-consumption and sizing of PV-battery systems. *Appl Energy* 2016;173:331–42. <https://doi.org/10.1016/j.apenergy.2016.04.050>.
- [51] Figgenger J, Haberschusz D, Kairies K-P, Wessels O, Tepe B, Sauer DU. Wissenschaftliches Mess- und Evaluierungsprogramm Solarstromspeicher 2.0: Jahresbericht 2018 2018. <https://doi.org/10.13140/RG.2.2.30057.19047>.
- [52] Python Software Foundation. tkinter — Python interface to Tcl/Tk. [October 27, 2022]; Available from: <https://docs.python.org/3/library/tkinter.html>.
- [53] Möller M, Kucevic D, Collath N, Parlikar A, Dotzauer P, Tepe B, et al. SimSES: A holistic simulation framework for modeling and analyzing stationary energy storage systems. *J Storage Mater* 2022;49. <https://doi.org/10.1016/j.est.2021.103743>.
- [54] Notton G, Lazarov V, Stoyanov L. Optimal sizing of a grid-connected PV system for various PV module technologies and inclinations, inverter efficiency characteristics and locations. *Renew Energy* 2010;35(2):541–54. <https://doi.org/10.1016/j.renene.2009.07.013>. <https://gitlab.lrz.de/open-ees-ses/loadpat>.
- [55] Tepe B. LoadPAT: Load Profile Anonymization Tool. TUM Chair of Electrical Energy Storage Technology; 2022.
- [56] Schuster SF, Bach T, Fleder E, Müller J, Brand M, SEXTL G, et al. Nonlinear aging characteristics of lithium-ion cells under different operational conditions. *J Storage Mater* 2015;1:44–53.

4 Vehicle-to-Grid provision with electric vehicle pools

Chapter 4 deals with the V2G provision with pools of commercial EVs. The three sections of the chapter each represent a research paper. Section 4.1 explains the basics of the work and generates the power and energy capability profile of the commercial vehicles. In addition, evaluations are made of the economic potential of FCR provision with vehicles. Section 4.2 builds on the results of section 4.1. A methodology is presented that can be used to optimize the composition of vehicle pools. Moreover, potential revenues in various markets are determined according to random and optimized pool composition. Section 4.3 then presents an analysis of the optimized pools from section 4.2. These are examined in terms of vehicle battery size and economic sectors of the vehicles involved.

4.1 Provision of frequency containment reserve using pools of electric vehicles

This section shows the results of the research paper entitled *The Influence of Frequency Containment Reserve Flexibilization on the Economics of Electric Vehicle Fleet Operation* [11]. The paper examines the provision of FCR by means of commercial e-Cars with regard to the increasing flexibilization of the FCR market. While FCR in Central Europe had to be provided over an entire week until mid-2019, time sectioning was reduced to 24 hours until mid-2020 and since then 4-hour time sections are tradable. At the same time, the minimal bid sizes have remained constant at 1 MW minimum offer and increment. These minimum bids prevent individual EVs from participating in the FCR market, but the increasing flexibility in terms of time makes FCR provision attractive for pools of EVs during idle times.

This work is based on a data set of over 460 commercial internal combustion vehicles from 14 economic sectors. These vehicles were equipped with GPS sensors and measured over different periods of time in order to record when the vehicles are at the company location and when they are on the road. In a mobility simulator, the driving profiles are then combined with e-Car measurements, for example from charging curves, and assumptions about battery capacity and energy consumption. Here, the driving behavior is broken down into weekly probability distributions for, for example, trip start, trip duration and trip distance. The output of the mobility simulator are energy and power capability profiles that indicate what energy and power a vehicle can charge and discharge at any given time. These profiles are then used to determine the potential FCR power of the commercial vehicles in the pool for the various FCR service periods and prices and how much potential revenue would have been generated.

The research questions answered in this section are:

1. How much FCR power can commercial EV fleets offer over different time periods?
2. What power uncertainty can be expected during different time slots due to mobility?
3. What would be the effect of further reductions in FCR service periods on the economics of EV fleets?

4. How much money can EVs expect to earn through FCR?

A key finding of this section is that the shortening of the service periods of the Central European FCR market has increased the economic attractiveness of participation with EVs. At the same time, a further shortening of the periods would not bring much added value, as the idle times are often longer than the current service periods of 4 hours. Possible revenues of commercial EVs in the 4h service periods in Germany are between 450 € and 750 € per vehicle and year for the considered time period of July 2020 to March 2022. This revenue does not represent the profit, as costs for battery ageing, losses, bidirectional charging stations and fleet management would have to be taken into account when calculating the profit. The calculated revenue is of a similar magnitude to previous publications (see section 2.5.4). However, comparability is always difficult due to various time periods, markets and driving profiles. Thingvad et al., for example, calculated €751 € as the profit for the provision of balancing services in Denmark [63]. However, this already included ageing costs and conversion losses.

The power and energy capability profiles generated in this section for the commercial e-Cars are used in section 4.2 to create optimized pool compositions for various markets. For this purpose, genetic algorithms are used to determine the revenue per vehicle in various pool compositions and pools with maximum revenue per vehicle are determined. In section 4.3, the optimized pools are then analyzed in terms of battery size and commercial sector.

Author contribution

Jan Figgenger was the principle author tasked with coordinating and writing the paper and developing the methodology. Benedikt Tepe collected large portions of the driving data, evaluated it, and assisted in the development of the methodology and results. Fabian Rücker und Ilka Schoeneberger completed the EV measurements and processed the data. Christopher Hecht mainly assisted with the methodology and preparation of the results. Andreas Jossen and Dirk Uwe Sauer contributed via fruitful scientific discussions and reviewed the manuscript. All authors discussed the data and commented on the results.

The influence of frequency containment reserve flexibilization on the economics of electric vehicle fleet operation

Jan Figgenger, Benedikt Tepe, Fabian Rücker, Ilka Schoeneberger, Christopher Hecht, Andreas Jossen and Dirk Uwe Sauer

Journal of Energy Storage, Volume 53, 2022

Permanent weblink:

<https://doi.org/10.1016/j.est.2022.105138>

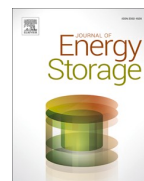


Reproduced under the terms of the Creative Commons Attribution NonCommercial-NoDerivatives 4.0 License (CC BY-NC-ND, <https://creativecommons.org/licenses/by-nc-nd/4.0/>), which permits non-commercial reuse of the work in any medium, provided the original work is properly cited.



Contents lists available at ScienceDirect

Journal of Energy Storage

journal homepage: www.elsevier.com/locate/est

Research Papers

The influence of frequency containment reserve flexibilization on the economics of electric vehicle fleet operation

Jan Figgenger^{a,b,c,*}, Benedikt Tepe^d, Fabian Rücker^{a,b,c}, Ilka Schoeneberger^{a,b,c}, Christopher Hecht^{a,b,c}, Andreas Jossen^d, Dirk Uwe Sauer^{a,b,c,e}^a Institute for Power Electronics and Electrical Drives (ISEA), RWTH Aachen University, Aachen, Germany^b Institute for Power Generation and Storage Systems (PGS), E.ON ERC, RWTH Aachen University, Aachen, Germany^c Juelich Aachen Research Alliance, JARA-Energy, Jülich, Germany^d Institute for Electrical Energy Storage Technology, TU Munich, Munich, Germany^e Forschungszentrum Jülich GmbH, Institute of Energy and Climate Research Helmholtz-Institute Münster: Ionics in Energy Storage (IEK-12), Jülich, Germany

ARTICLE INFO

Keywords:

Electric vehicle
Flexibilization
Frequency containment reserve (FCR)
Pooling
Virtual power plant
Vehicle-to-grid (V2G)

ABSTRACT

In recent years, the spot and ancillary service markets have become a relevant source of revenue for stationary battery storage systems. During this period, many markets have become increasingly flexible with shorter service periods and lower minimum power requirements. This flexibility makes the markets attractive for pools of electric vehicles (EVs), providing the opportunity to earn additional revenue. In this paper, multi-year measurement data from 22 commercial EVs are used to develop a simulation model to calculate the available power of an EV pool. In addition, the driving logbooks of >460 vehicles from commercial fleets of 14 different economic sectors are analyzed. Based on our simulations, we discuss the influence of shorter service periods on available pool power and power uncertainty. The key findings are that, especially at times with a high pool power, the uncertainty is low. This leads to the conclusion that commercial fleets offer a highly reliable power profile during known idle times depending on the economic sector. All investigated 14 sectors show high and reliable power availability at night and most show this availability also during weekends while others show a regular driving pattern seven days a week. These results are applicable to any energy market. To have a concrete use case, the impact of frequency containment reserve (FCR) flexibilization on the economics of an EV pool is analyzed using the German FCR market design from 2008 to 2022. It is shown that, depending on the fleet, especially the two recent changes in service periods from one week to one day and from one day to 4 h generate the largest increase in available pool power. Further future reductions in FCR service periods will only produce minor benefits, as idle times are often already longer than service periods. According to our analysis, revenues of about 450 €/a to 750 €/a could have been achieved per EV in the German FCR market between mid-2020 and the first quarter of 2022.

1. Introduction

This section presents the thematic overview, a summary of existing literature on vehicle-to-grid (V2G) concepts with focus on the provision of frequency containment reserve (FCR) through electric vehicles (EVs) and highlights the scientific contribution of this paper. Fig. 1 provides a graphical overview of the paper. First, two databases (EV measurements and driving data) and EV master data are used for the development of a simulation model. The results of the simulation model are power

capability profiles, which are the bidirectional power potential of different EV pools. The profiles are used together with historical FCR price data within a calculator to estimate FCR revenues for different market designs. We show that commercial fleets are generally capable of offering V2G services with a predictable uncertainty depending on day and time. Possible future flexibilization in form of shorter service periods will have only little impact on the available power compared to the current service periods of 4 h.

* Corresponding author at: Institute for Power Electronics and Electrical Drives (ISEA), Jaegerstrasse 17/19, D-52066 Aachen, Germany.
E-mail address: jan.figgenger@isea.rwth-aachen.de (J. Figgenger).

<https://doi.org/10.1016/j.est.2022.105138>

Received 29 December 2021; Received in revised form 10 May 2022; Accepted 14 June 2022

Available online 19 July 2022

2352-152X/© 2022 The Authors. Published by Elsevier Ltd. This is an open access article under the CC BY-NC-ND license (<http://creativecommons.org/licenses/by-nc-nd/4.0/>).

1.1. Motivation and contribution

The increasing integration of volatile renewable energy generation and flexible energy storage has led to an increasing flexibilization of spot and grid service markets in recent years. The term flexibilization refers on the one hand to the reduction of service periods for the respective market and on the other hand to the introduction of the required minimum power bids to participate in the market. Battery storage systems (BSSs), in particular stationary large-scale BSSs, already have a significant share of the global market for FCR. From this market, they continue to displace conventional market participants such as large power plants. In Germany, the share of stationary large-scale BSSs in the FCR market was about two thirds in 2021 [1–3]. However, these BSSs have the problem that they are refinanced exclusively from FCR revenue. The ensuing price competition in order to win a contract in the bidding process has led to a 50 % decrease in FCR prices from 2015 to 2020 and made the market increasingly unattractive as the main application for these large-scale BSSs [1]. For this reason, so-called multi-use concepts for BSSs are a promising way of generating revenue from various applications [4]. Decentralized BSSs can participate in virtual power plants at times when they do not fulfill their primary use. Such a pool can consist of BSSs of all types and includes stationary as well as mobile BSSs in the form of EVs. EVs, in particular, have a great potential of free battery capacities that are not used for mobility due to idle times of >95 % [5,6]. Especially commercially operated EVs often have short and regular (and thus plannable) distances and driving patterns that allow the provision of grid services [7]. Therefore, the increasing flexibility of the FCR market (decrease of minimum power bid from 5 MW to 1 MW and shortening of service periods from one month to 4 h in recent years) makes this market attractive for the fluctuating power of EVs in multi-use concepts. This paper analyses the influence of FCR flexibilization on the profitability of commercially operated EVs in the use case of the German market design, which should be representative for a large region of Central Europe, since the FCR market of Germany, Belgium, the Netherlands, France, Switzerland, and Austria is coupled and the price varies only slightly between the countries [8]. Even though there is a variety of scientific publications on FCR and EVs, none of the literature focuses on the recent and possible future FCR flexibilization and its impact on the economics of EV fleets potential in this market. While other publications focus mainly on optimized operation strategies and multi-use in a fixed market design, this paper analyzes the influence that the market changes themselves have on the economics of an EV fleet. Further, it quantifies the power uncertainty that different economic sectors have, which can be used by aggregators for all energy markets. This analysis has so far not been examined (see Section 1.2). We

contribute with our paper to fill this gap. The key research questions answered are:

1. How much FCR power can commercial EV fleets offer over different time periods? (Section 3.1)
2. What power uncertainty can be expected during different time slots due to mobility (Section 3.1)?
3. What would be the effect of further reductions in FCR service periods on the economics of EV fleets (Section 3.2)?
4. How much money can EVs expect to earn through FCR? (Section 3.3)

1.2. Literature review and differentiation

There are many publications on the provision of frequency regulation by stationary BSSs or EVs, each with a different focus and data. We divide our literature research into the areas (1) provision of FCR using BSSs and combination of applications (see Table 1), (2) simulation and optimization of frequency regulation using EVs (see Table 2), (3) demonstrations, experiments, and field tests of frequency regulation using EVs (see both Appendix, Tables 9 and 10), and (4) generation of revenues using fleets of EVs for the provision of frequency regulation. We classify the sources according to Table 1 into respective focal points, which we discuss individually in the following.

- (1) The provision of FCR with large-scale BSSs has been investigated and shown to be possibly profitable, depending on the energy-to-power ratio (EPR) and specific market conditions [9–11]. Especially the so-called “30-min” criterion when providing FCR with batteries in the German regulatory market had been determined as a crucial burden for providers [10,11]. This criterion required that the maximum offered bidirectional FCR power must be able to be provided for at least 30 min at any time within the respective service period. In 2019, the German federal network agency (FNA) obliged the transmission system operators (TSOs) to apply the 15-min criterion instead of the 30-min criterion for BSSs making the market more attractive to batteries due to smaller EPRs (see Section 2.6) [12]. Multi-use, the combination of different storage applications, has been studied for years [4,13–16]. The main results of these studies are that the combination of different storage products increases the economic attractiveness, but that there are regulatory hurdles to overcome [13–15]. In this context, Englberger et al. published an open-source tool simulating multi-use including an economical and a technical analysis [16]. However, all mentioned publications

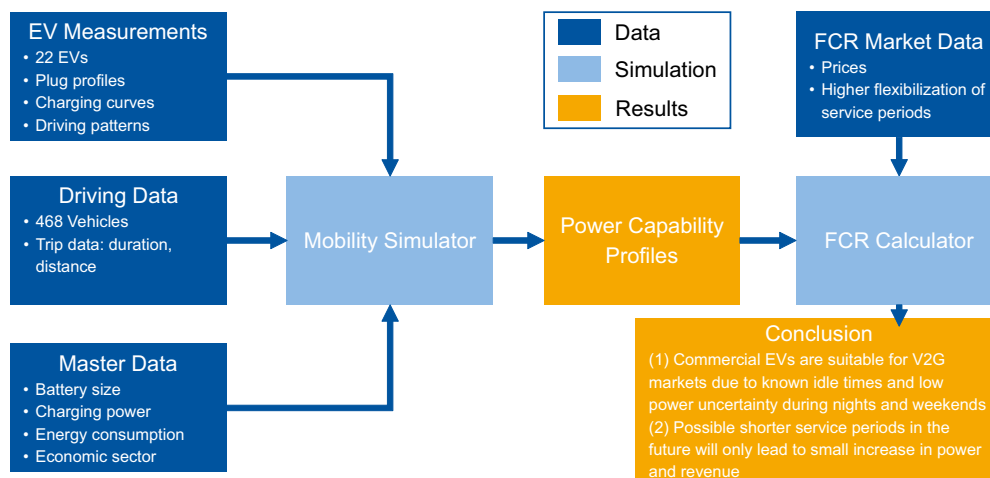


Fig. 1. Graphical abstract.

Table 1

Summary of selected literature of the provision of FCR using BSSs and multi-use.

	Source	Date	Focus	Results
FCR	Fleer et al. [9]	2016	Economics of the provision of FCR using BSS based on two case studies considering FCR prices and battery aging	<ul style="list-style-type: none"> - BSS only profitable with a power-to-energy ratio of 1:1, not with 1:2 - Decreasing battery prices will increase possible profit but could lead to lower achievable revenues due to market saturation
FCR	Zeh et al. [10]	2016	An optimal control algorithm for the operation of FCR with BSS is developed for the market conditions of 2015	<ul style="list-style-type: none"> - FCR Market conditions for BSS of August 2015 (30-min-criterion) lead to unprofitable operation
FCR	Thien et al. [11]	2017	Operation strategy for an installed 5-MW-BSS providing FCR is developed and influencing parameters are analyzed	<ul style="list-style-type: none"> - Benefits could be enhanced having better market conditions such as 15-min instead of 30-min-criterion
Multi-use	Fitzgerald et al. [13]	2015	Evaluation of different services BSS can provide in the US market including a meta-study and analysis of barriers	<ul style="list-style-type: none"> - Combination of applications increase the economic value - Despite technical readiness, regulatory hurdles exist that prevent an economically profitable use of BSS
Multi-use	Stephan et al. [14]	2016	Analysis of investment attractiveness of different single applications of BSS and their combination by developing a techno-economic model	<ul style="list-style-type: none"> - Combination of applications improves the investment attractiveness - Market barriers often prevent the combination of applications
Multi-use	Braeuer et al. [15]	2019	Evaluation of economics of BSS installed in German small and medium sized enterprises when combining applications of peak-shaving, FCR and arbitrage	<ul style="list-style-type: none"> - Individual applications are not profitable, but combination of applications are - Influence of arbitrage application is small
Multi-use	Englberger et al. [16]	2020	Simulation of energy storage systems serving multiple applications including an analysis of technical and economical parameters	<ul style="list-style-type: none"> - Application stacking more economical than single use - Publication of open-source tool which combines BSS applications

Table 2

Summary of literature about simulation and optimization of the provision of frequency regulation using EV fleets.

Source	Date	Focus	Results
Tomić et al. [19]	2007	Analysis of two fleets of utility EV providing power for regulation services in the US.	<ul style="list-style-type: none"> - V2G enables potential revenue streams for EV owner in most ancillary service markets
Han et al. [23]	2010	Proposition of an aggregator pooling EV to provide frequency regulation	<ul style="list-style-type: none"> - Development of an optimal control strategy for EV fleet considering battery energy capacity and desired final SOC for driving purpose
Sortomme et al. [20]	2012	Development of a V2G algorithm for the scheduling of the provision of the ancillary services load regulation and spinning reserves in US markets	<ul style="list-style-type: none"> - Algorithm combines several ancillary services - Simulations show that even though there are challenges, providing ancillary services can provide benefit for the owner, the aggregator and the grid.
Bessa et al. [24]	2012	Optimized bidding of EV fleet in day-ahead and secondary reserve Iberian market.	<ul style="list-style-type: none"> - Using an aggregator to optimize the bidding of energy decreases charging costs - Variables like the electricity price and the maximum available power in each time interval need to be forecasted
Codani [25]	2015	Simulation of participation of 200,000 EV in FCR market in France	<ul style="list-style-type: none"> - Potential revenue higher with bidirectional charging compared to unidirectional charging - A high number of EV might saturate FCR market
Hoogvliet et al. [21]	2017	Economic analysis of the potential revenue EV owners can raise when providing regulating power in the Netherlands	<ul style="list-style-type: none"> - Depending on EV type and driving pattern an EV owner can raise 120 € to 750 € per year when providing regulating and reserve power - Provision will lead to higher battery energy throughputs (11 % to 55 %)
David et al. [22]	2017	Economic analysis of the provision of frequency regulation using EV considering battery degradation and driving requirements	<ul style="list-style-type: none"> - EV with highest battery capacity lead to the greatest economic benefit, as the cyclic degradation is lowest - Major constraint is the power capability of the EV and the chargers - Incentives should be developed to convince EV owners to provide frequency regulation

focus on stationary applications and do not evaluate the flexibilization of the FCR market, on which this paper focuses.

- (2) The concept of Vehicle-to-Grid (V2G) was first introduced by Kempton et al. [17,18]. Since then, the concept has been studied extensively. Table 2 provides publications, in which the provision of FCR with EVs has been simulated and optimized. The provision of different frequency regulation products by EVs offers economic potential for the owner and the aggregator [19–22]. Furthermore, the grid can benefit from it [20]. Moreover, control algorithms for aggregators have been developed and bidding strategies optimized [23,24]. V2G can be carried out using unidirectional and bidirectional chargers. Despite their momentarily higher purchase costs, bidirectional chargers offer higher economic potential [25]. In addition, simulations show that the energy throughput is increased by the provision of frequency regulation, which might lead to increased battery degradation [21,22]. However, none of the mentioned publications evaluate the impact of recent and possible future FCR flexibilization as this

paper does. Further, the power uncertainty was not quantified before.

The concept of **second-life use** means that after years of use for mobility, vehicle batteries are removed from EVs and integrated into other applications like stationary BSSs in order to provide grid services or trade energy [26–28]. However, batteries contained in EVs can also be used to provide these V2G services within their first life, if they are temporarily not required for their primary use, namely mobility. We therefore call this concept “**dual use**”.

- (3) Several demonstration projects have been and are being carried out to investigate the provision of frequency regulation with EVs. Appendix, Table 9, gives a selection of such projects, while Appendix, Table 10, lists scientific publications done within these projects. In 2002, the first project on frequency regulation supply with EVs was implemented in California [29,30]. It showed that EVs are capable of providing frequency regulation to the grid. The German INEES project ran from 2012 to 2015 and analyzed the

provision of secondary control reserve with an EV fleet of 20 V2G-compatible vehicles [31,32]. The provision proved to be technically possible, but not profitable under the conditions prevailing at the time [31]. In addition, the impact on the distribution grid in terms of power quality and manageability was not assessed as negative [32]. Another demonstration project ran from 2013 to 2018 in California, within which 29 bidirectional EVs provided frequency regulation [33,34]. Among other things, optimization models were used to minimize operating costs and maximize revenue from ancillary services [34]. The so-called “Parker” project, within which many scientific findings were published, ran from 2016 to 2019 in Denmark [35–41]. The scientists showed that FCR supply is possible with unidirectional charging stations, but is economically much more attractive with bidirectional charging stations [36,37,40]. Furthermore, it was found that the response times and accuracies of the charge controllers are sufficient to provide control power [37,38]. Nevertheless, communication delays and measurement errors turned out to be practical obstacles [39]. Factors influencing the economic benefit of providing control power are the availability of vehicles, the charging efficiency and the operation strategy used [39–41]. In addition, an industrial project ran between 2018 and 2019 in which the provision of frequency regulation with a prequalified EV was successfully tested in Germany [42]. Another project, monitored by the German research institution FFE (Forschungsstelle für Energiewirtschaft e.V.), started in 2019 and analyses use-cases of EVs in different electricity markets [43]. To analyze the interaction between EVs, charging infrastructure and the grid, 50 EVs will be tested in the field [43,44]. The interconnection of EVs to a virtual power plant providing frequency regulation will be investigated in another industrial project until 2021 [45,46]. However, these projects focused on the demonstrations of V2G applications and did not focus on the market side as this paper does.

- (4) Different publications have taken a look at the possible revenues that pools of EVs can generate when providing FCR. As early as 2005, Kempton and Tomic estimated the possible annual revenues for the provision of frequency regulation using a Toyota RAV4 to reach \$ 4928 [5]. In 2019, Thingvad et al. analyzed the economic value of EV reserve provision in Northern Europe [40]. Assuming a power availability of 10 kW, the possible annual revenues resulted to 1395 €. One year later, Bañol Arias et al. published an analysis of the economic benefits for EV owners when participating in primary frequency regulation markets [41]. Their resulting profits (costs were subtracted from revenues) ranged between 100 € and 1100 € per EV and year. In 2021, Thingvad et al. published another paper about the provision of frequency regulation with EVs [47]. In this work, they published battery degradation data about EVs which had provided primary frequency regulation over a period of five years. Moreover, they calculated the revenues the EVs had generated. Including battery degradation costs and conversion losses and neglecting investment and maintenance costs, Thingvad et al. estimated a yearly profit of 751 €. Later in 2021, in Tepe et al. we published a work combining pools of EVs in an optimal manner [48]. In doing so, we estimated a yearly revenue per EV of 378 € in the German FCR market in 2020. However, none publication focused either on the influence of flexibilization nor power uncertainty of EV pools.

The most important project (without focus on FCR) for this paper, “GO-ELK”, was conducted by the Institute for Power Generation and Storage Systems at RWTH Aachen University [49]. Within this project, 22 commercially operated EVs were equipped with data loggers to measure quantities such as battery voltage and battery currents during charge and trips. The logged data build the basis of many of the results shown in this paper.

2. Methodology

This section describes the paper's methodology. It presents the used data, the developed driving profile generator, the modelling approach, and the market for FCR in Germany.

2.1. Data collection

This paper uses two databases containing the driving data of commercial vehicles. Table 3 compares the most important data of both databases and gives further information on calculations and assumptions.

2.1.1. Database “Measurements”

The first database, “Measurements”, was created by the Institute of Power Generation and Storage Systems (PGS) at RWTH University. The high-resolution data ($T = 1$ s) of commercially operated electric vehicles were measured between 2013 and 2016 within the project “Commercially operated electric vehicle fleets (GO-ELK)” [49]. In the project, four fleets of EVs were deployed in different sectors over a period of 30 months [49]. During their use, vehicle data (driving, charging and battery data) of the total of 22 EVs were recorded by data loggers in the vehicles and the charging stations. For a detailed description of data collection and adjustment, please refer to [49–52]. The values include battery voltage, battery current, start and end of a trip, distance travelled, consumption, and the location at the end of the trip. Further, the measurements were used to create charging curves as an input for the model (see Section 2.4).

2.1.2. Database “Logbooks”




The second database, “Logbooks”, was included within the project REM 2030 (regional eco mobility). The project was supervised among others by the Fraunhofer Institute for Systems and Innovation Research ISI and various institutes of the Karlsruhe Institute of Technology (KIT) and covered different topics of future urban mobility [53]. The goals were new innovative traffic concepts of individual mobility in order to avoid local emissions [53]. Within this project, Fraunhofer ISI collected travel data of commercial vehicles, which can be used free of charge for non-commercial purposes. The database contains over 91,000 journeys of 630 vehicles of different trades. We filtered the database so that only vehicles with a minimum number of one trip and a minimum logging duration of one week were considered. The vehicles are classified according to their economic sector (NACE criteria) [54]. The KIT classified the vehicles used from database “Logbook” into 15 economic sectors. Within the economic sector, there are further definitions of vehicle classes. The values include start and end of a trip, the distance travelled, and the location at the end of the trip.

The database “Logbooks” contains only vehicles with internal combustion engines. In order to model these as fully electric vehicles, the unrecorded consumption and the plug and unplug behavior must be estimated.

To estimate the consumption, the values shown in Appendix, Table 8, are used. These result from various studies, test results and manufacturer data sheets of EVs that are in the same vehicle class as the internal combustion engine vehicles. The average consumptions of the listed EVs range from 18 kWh/100 km and 27 kWh/100 km depending on the vehicle class [55]. To determine the consumption of the EVs in kWh per 100 km of a trip, the consumption is distributed normally around the average consumption of the vehicle class (expected value: average consumption of all EVs in Appendix, Table 8, and variance: 1 kWh / 100 km). This way, the effect of the temperature on the consumption is also statistically taken into account.

To estimate the plug and unplug behavior, the information on the location is used, which is given as the distance to the company site. Whenever the distance symbolizes that the car is parked at the company site, it is assumed to be plugged. Therefore, the assumption is made that every EV has an available charging point.

Table 3
Available data in the two databases used in this paper.

	Category	Database “Measurements” (22 cars)	Database “Logbooks” (468 of 630 cars)
Vehicle Data 	Product	see Appendix, Table 7 (e.g. Smart ED, Renault Zoe)	see Appendix, Table 8
	Vehicle class	small to medium	see Appendix, Table 8
	Type of vehicle drive	electrical drive	combustion drive
	Industry / trade	see Appendix, Table 7 (e.g. healthcare and energy provider)	see Appendix, Table 8
	Environment	urban and rural	urban and rural
Trip Data 	Start of trip	timestamp	timestamp
	End of trip	timestamp	timestamp
	Trip consumption in kWh	~15 to 25 kWh/100 km	18 to 27 kWh/100 km (see Appendix, Table 8)
	Trip distance	measured in km	measured in km
	Distance to company at trip end	taken from charge events	measured with GPS
Battery Data 	Max. charge power in kW	3.7 kW to 22 kW (AC)	according to “Measurements”
	Battery energy in kWh	16 kWh to 24 kWh	19.1 kWh to 80.7 kWh (see Table 8)
	Charging curve	measured in laboratory	according to “Measurements”
	Start of charging	measured timestamp	according to “Measurements”
	End of charging	measured timestamp	according to “Measurements”
Charging Station Data	Charge power	1.8 kW (single phase AC) to 11 kW (three phase AC)	according to “Measurements”

2.1.3. Combination of the two databases

For the combination of the datasets, the different data formats were unified and merged. For unification, driving profiles were created as both datasets contain start and end of a trip, distance travelled, and consumption (see Sections 2.2 and 2.3). These driving profiles are the input for the model described in Section 2.4. To merge the databases, the EVs from database “Measurements” were divided into the respective economic sectors and supplement the large KIT data set according to Appendix, Table 8. With 94 vehicles, the manufacturing sector has the largest number of vehicles, especially of the vehicle class “medium” (see Appendix, Fig. 23 (left)). This is followed by public administration (71 vehicles) and healthcare service (58 vehicles), in which mainly small vehicles are used. Some clusters follow with 30–40 vehicles and there are also four clusters with <10 vehicles each. This should be considered when looking at the results, as the power capability profiles in these cases are only based on small sample sizes. The average duration of data recording for most clusters is about 20 days (see Appendix, Fig. 23 (right)). The analyses of our database “Measurements” (data recording periods of more than one year) show that these relatively short durations are already sufficient to reliably map daily operations in the examined sectors.

2.2. Statistical analysis

In the following, we present a short statistical evaluation of the data

used. For better comprehensibility, we present the healthcare service as an example from database “Measurements”. This fleet shows the same driving pattern for the whole week, which makes the daily analysis done very representative. Further analyses on database “Logbook” indicate in general similar results as the evaluation done for the “Measurement” database. All vehicles of the two databases were evaluated analogously to the evaluations presented in this section. However, as this paper does not represent a mobility study, no further evaluations are made at this point and reference is made to mobility studies such as [56–59].

Fig. 2 shows the three events “plug & charge”, “end of charge”, and “unplug” of the Smart ED of a healthcare service. The health-care service runs in two shifts a day: 50 % of all unplug events are at around 7 a.m., which is the start of the first shift. It ends at around noon and the cars are plugged and charged. The second shift runs from around 2 p.m. to 9 p.m., which is again indicated by the “plug and charge events”.

The average distance (see Fig. 3) between two charging operations is about 40 km, although the maximum possible distance range of the vehicle is around 100 km. Further, the average duration between unplug and plug is about 8 h (see Fig. 4). All travel durations above about 8 h can be assigned to shifts after which no charging process is initiated. This is the case for about 30 % of all trips. The regular charging with 11 kW charging stations at the end of the shifts leads usually to a fully charged vehicle a short time after returning. While the average SOC after return is around 60 %, this value is often 100 % or near to 100 % when

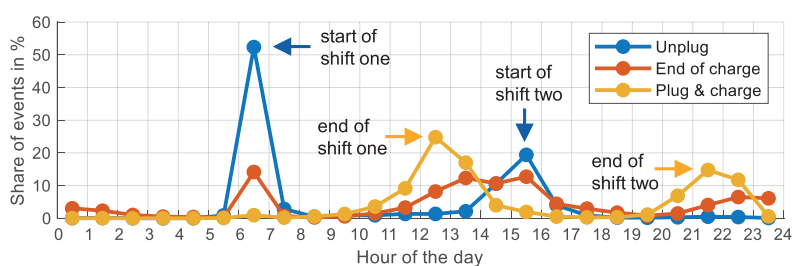


Fig. 2. Trip events of EVs in healthcare service (908 measured trips from database “Measurements”).

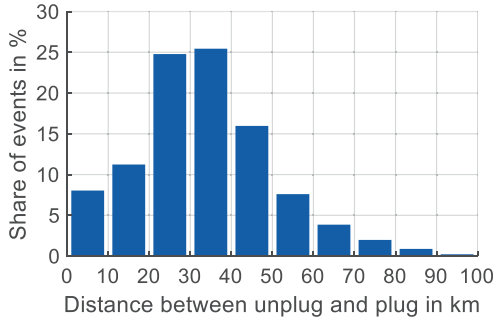


Fig. 3. Distance between unplug and plug (908 measured trips of EVs in healthcare service from database “Measurements”).

the vehicle starts a trip (see Fig. 5). The unplug events where the EV is not fully charged in the morning are mainly due to software issues with the internal SOC estimation showing values slightly below 100 % although the EV does not charge any more. The small amounts of needed energy underline the potential of free capacity ranges shown in recent literature (see Section 1.2). Due to the relatively short distances, the vehicle consumes on average only 40 % to 50 % of the battery energy capacity (see Fig. 6). The measurements also contain different consumptions as a function of the temperature as the EVs were measured over two years and thus within different seasons (a low temperature leads to high consumptions and vice versa).

2.3. Driving profiles

The statistical analysis is now used to generate driving profiles such as the probability of a trip start or day and time dependent distributions of distances, durations, and energy consumptions. The data is presented for a Smart ED that was part of the healthcare service fleet in the statistical analyses shown in Section 2.2.

The trip-start probability w_{start} of a plugged vehicle is calculated as a function of day and time. To get the trip-start probability, the number of unplug events are divided by the total number of days, when the car was connected to the charging station (see Eq. (1) and nomenclature in Appendix, Table 6).

$$w_{start}(t) = \frac{\sum_{n=1}^N trip_{start,n}(t)}{N} \quad (1)$$

$$with \ trip_{start,n}(t) = \begin{cases} 1, & \text{if trip started on day } n \text{ at time } t \\ 0, & \text{otherwise} \end{cases}$$

with N = number of days, where EV was plugged

The trip-start probabilities are exemplarily shown in Fig. 7. The probability for starting a trip is over 60 % for the first shift and is most likely between 6 a.m. and 7 a.m. During the second shift, with cumulated probability values of approx. 40 %, the number of unplugs is slightly lower. Outside the shifts, the probability of plugging out from the charging station with values below 10 % is relatively low. Further, the trip distances (Fig. 8), durations (Fig. 9), and normalized consumptions are sorted by day and time to ensure a realistic driving behavior of the analyzed vehicles. The figures show the probabilities and distribution clustered for 1 h for clearer presentation. The resolution used for simulations is 15 min and thus higher (see Section 2).

The value distributions presented, such as distance, duration, and consumption, are also evaluated as a function of time, resulting in

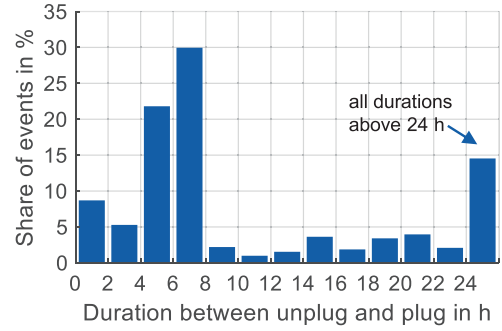


Fig. 4. Duration between unplug and plug (908 measured trips of EVs in healthcare service from database “Measurements”).

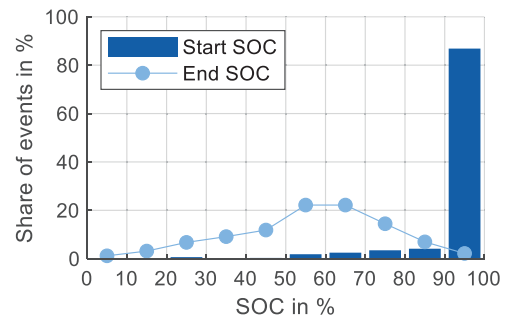


Fig. 5. SOC at unplug and plug (908 measured trips of EVs in healthcare service from database “Measurements”).

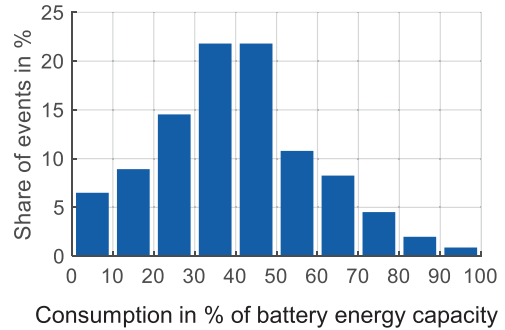


Fig. 6. Consumption between unplug and plug (908 measured trips of EVs in healthcare service from database “Measurements”).

separate distributions for each point in time. The distances driven and the durations between plug and unplug are subject to temporal fluctuations. Both, the longest distances and durations are the start of each trip of the two shifts in the healthcare service. Especially if the EV is not plugged after the end of the first shift, the distances and durations get longer as their values also cover the second shift and vice versa.

2.4. Modelling

The generated profiles are the input for an implemented mobility model. The model simulates the driving behavior and the grid

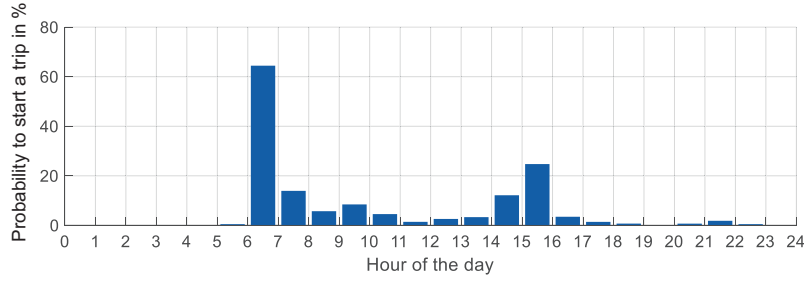


Fig. 7. Trip-start probability (Smart ED, healthcare service).

connection of EVs via the charging station. Fig. 10 presents the general structure of the simulation:

- If a vehicle begins a trip due to the calculated probability, it gets random but correlated values of the day and time-dependent distributions of distance, duration, and the normalized consumption per kilometer. The new EV data are updated with the given trip values and the car is plugged to the charging station after the given trip duration.
- If a vehicle does not begin a trip, it charges in case the state-of-energy (SOE) is lower than the required energy for the mobility. This is explained in more detail in the following Section 2.5.

The charging process of the vehicle is simulated with real charging curves measured in our laboratory at PGS RWTH Aachen University. Fig. 11 (left) depicts an 11 kW constant-power charge. The AC power on the grid side is larger than the DC power on the EV battery side, which shows the power losses due to the power converter. The efficiencies are around 93 % for the constant power phase and decrease during the power decline. Battery current and voltage are shown in Fig. 11 (right). The current values range in the case of this charge (11 kW) from 2 A to approximately 30 A at battery voltages of around 320 V to 390 V. During the constant power phase, current decreases while voltage increases with higher SOE. It is important to consider that at around 90 % SOE the constant-power charge turns into a constant-voltage phase resulting in a strong decline of current and power. When offering ancillary services, EVs with - in this case - SOEs above 90 % are therefore not chosen to participate in the pool because of their strong decline in power. That is why a charging SOE limit of the EV is implemented in the simulation. This limit is set dynamically and ensures that all logged trips could have been done, individually for each EV. The charging limit is mostly around 80 % of the SOE and is further explained in Section 2.5.

For the simulation, it is assumed that the EVs are solely charged at the company site and that all EVs have an available bidirectional charging point.

2.5. Virtual sectioning of the battery

The primary use of an EV is mobility. However, several studies as well as our presented data have shown that the average trip distance is quite low resulting in a low average energy needed for most trips. Thus, there are free energy capacities during most times that can be used for dual-use concepts in order to increase the economics of operation. Within these concepts, the primary use should not be limited by the secondary use. For dual use, the battery must be virtually divided into the energy range for primary use (mobility energy $E_{mobility}$) and the energy range for secondary use (marketable energy E_{market}), as shown in Fig. 12. The mobility energy must be ensured at any time in order to undertake the regular trips of the vehicle. It consists of a reserved minimum energy for spontaneous trips at any time and a trip energy within certain time windows, when the vehicles are general, is the difference of the total battery energy E_{Bat} and the current mobility energy as shown in Eq. (2). It is a derived quantity that describes how much of

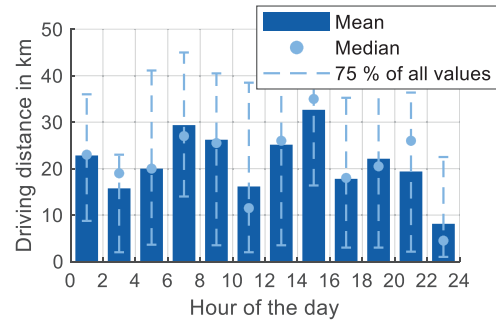


Fig. 8. Distance distributions as a function of the departure time (Smart ED, healthcare service).

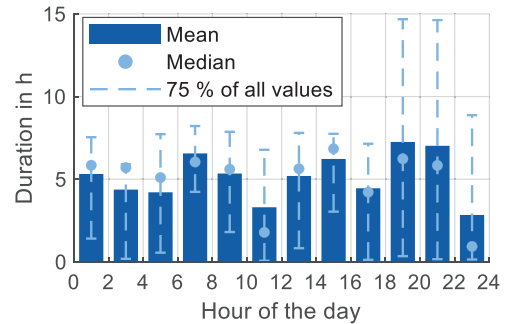


Fig. 9. Duration distributions as a function of the departure time (Smart ED, healthcare service).

the battery's rated energy capacity a user would allow to use for a secondary use such as FCR.

$$E_{market}(t) = E_{Bat} - E_{mobility}(t) \quad (2)$$

Based on the state of energy (SOE), the marketable energy can be divided into the charge energy E_{charge} and the discharge energy $E_{discharge}$ as shown in Eqs. (3)–(5) and in Fig. 12 (left).

$$E_{market}(t) = E_{charge}(t) + E_{discharge}(t) \quad (3)$$

$$E_{charge}(t) = E_{Bat} - SOE(t) \quad \forall SOE(t) > E_{mobility}(t) \quad (4)$$

$$E_{discharge}(t) = SOE(t) - E_{mobility}(t) \quad \forall SOE(t) > E_{mobility}(t) \quad (5)$$

In order to calculate the FCR power an EV can provide, some basic calculations are necessary that are described in the following. Generally, the FCR power can either be restricted by:

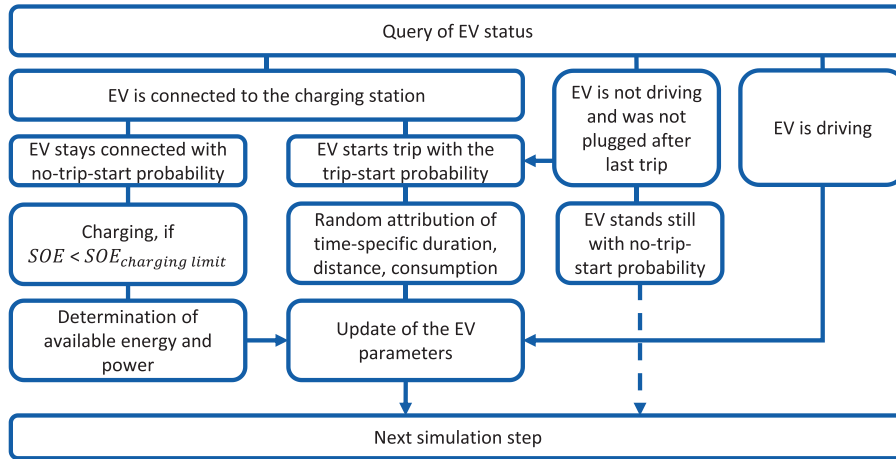


Fig. 10. Simulation flow of the implemented mobility model.

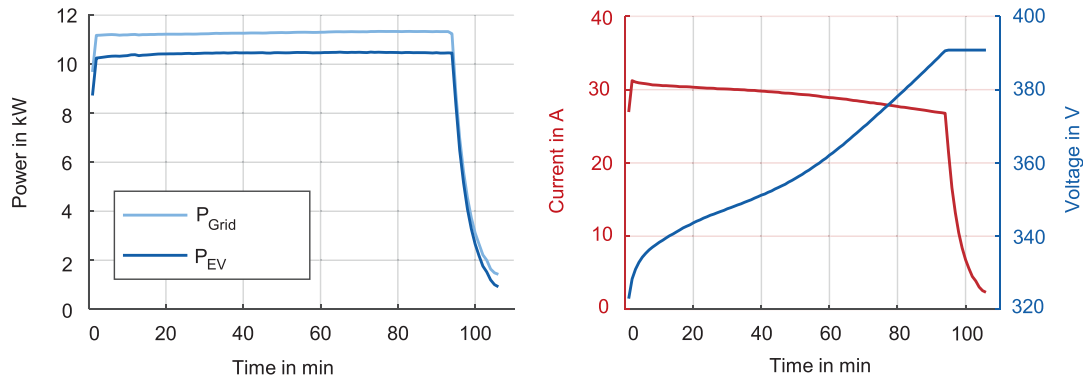


Fig. 11. Measured grid and battery power (left) and battery current and voltage (right) of a Smart ED during charge at 11 kW AC power.

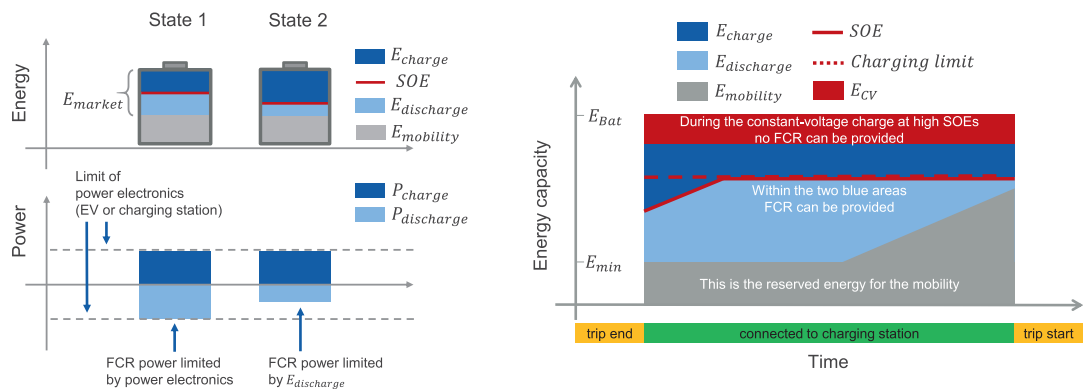


Fig. 12. Virtual division of the battery energy capacity and calculation of available power. Left: static. Right: time-dependent in the case of EVs. Inspired by [31].

1. the rated power P_{EV} of the battery converter of the EV,
2. the rated power P_{CS} of the charging station, or
3. the charge or discharge energy in combination with the time of power supply.

Eqs. (6) and (7) consider all three cases for calculating the available charge power P_{charge} and discharge power $P_{discharge}$ taking the service period ΔT_{supply} of the required 15 min full FCR power into account.

$$P_{charge}(t) = \min\left\{\frac{E_{charge}(t)}{\Delta T_{supply}}; P_{EV}; P_{CS}\right\} \quad (6)$$

$$P_{discharge}(t) = \min\left\{\frac{E_{discharge}(t)}{\Delta T_{supply}}; P_{EV}; P_{CS}\right\} \quad (7)$$

Example. Assumptions for calculating the charge power:

- $E_{Bat} = 50 \text{ kWh}$ (before constant voltage phase starts).
- $E_{mobility} = 15 \text{ kWh}$ (30 % of E_{Bat}); SOE = 30 kWh.
- $P_{EV} = 11 \text{ kW}$; $P_{CS} = 22 \text{ kW}$, $\Delta T_{supply} = 15 \text{ min} = 0.25 \text{ h}$.
- Calculation:
- $E_{charge} = 50 \text{ kWh} - 30 \text{ kWh} = 20 \text{ kWh}$

$$P_{charge} = \min\left\{\frac{20 \text{ kWh}}{0.25 \text{ h}}; 11 \text{ kW}; 22 \text{ kW}\right\}$$

$$= \min\{80 \text{ kW}; 11 \text{ kW}; 22 \text{ kW}\}$$

$$= 11 \text{ kW (power limited by EV in this case)}$$

For our simulation, we assume a bidirectional charging station. Although most of the current charging stations at the time this paper is submitted are unidirectional, broad literature expects EVs to play an important role in ancillary services of the future and bidirectional charging stations will probably emerge for V2G and vehicle-to-home (V2H) applications (see Section 1.2). However, many car manufacturers still do not provide any internal vehicle information such as the SOE to the charging station and prohibit the charge control as they use older Open Charge Point Protocols (OCPP version 1.5 or 1.6). Nevertheless, protocols like OCPP version 2.0 with the corresponding ISO 15118 protocol as well as the CHAdeMO protocol send information and allow charge and discharge control.

The required energy for mobility changes with the time of day and the day of the week depending on the use profile of the EV (see Fig. 12). In order to take the individual use profile of the EVs into account, the minimum energy required is calculated on the basis of historical journey data. In addition, a spontaneous mobility buffer of at least 30 % of the battery energy is implemented. This value is specified by users in a field test as the desired minimum for spontaneous trips [31]. Whenever the SOE is above the mobility energy, the vehicle can provide grid services as long as the SOE is not within the E_{CV} , where the constant-voltage charging phase takes place (see Fig. 11). In order to provide flexibility in charging and discharging the EV, an additional individual charge limit of about 80 % SOE is introduced (see Fig. 12 (right)). This upper limit is chosen as high enough that sufficient energy for all historical journeys is available. The individual charging limit ensures that the single EV is not yet in the constant-voltage phase of the charging process. If the energy for a trip exceeds the 80 %, the charging limit is not applied and the EV is charged to 100 % and cannot participate in FCR during this

Table 4
Frequency containment reserve market before July 2019, after July 2019 and after July 2020 [64,65].

	Before July 2019	July 2019 – July 2020	Since July 2020
Direction	Positive and negative power together		
Minimal bid	1 MW		
Minimal increment	1 MW		
Reaction time	30 s		
Provision time	15 min		
Remuneration	Pay-as-bid for power	Market-clearing-price for power	
Time sectioning	1 week	24 h	4 h
Tendering	Tuesdays, 3 pm	D-2, 3 pm,	D-1, 8 am
Demand Germany	551 MW - 620 MW	620 MW	573 MW

time.

2.6. Frequency containment reserve

This section presents the German FCR market design, its requirements for BSSs and the development of FCR prices.

2.6.1. The German FCR market

The frequency regulation is divided into frequency containment reserve (FCR, former primary control reserve), automatic frequency restoration reserve (aFRR, former secondary control reserve), and manual frequency restoration reserve (mFRR, former tertiary control reserve). The three types of frequency regulation have different activation times and replace each other consecutively as shown in Fig. 13. Within 30 s after a frequency deviation of >10 mHz, FCR units in Continental Europe Synchronous Area have to provide FCR automatically [60,61]. This way the frequency drop (respectively rise) is supposed to be stopped. Providers of FCR must offer both positive and negative FCR power for the same service period. It is important to notice that other regions such as the Nordic Balancing Markets [62] or the UK [63] also have faster frequency regulation markets.

The regulatory requirements for FCR varied during the last years as shown in Table 4. Appendix, Table 11, provides the decisions taken on FCR by the German Federal Network Agency (FNA) and the TSOs. Until mid-2011, FCR was tendered on a monthly basis in a pay-as-bid auction, which means that the supplier of FCR had to provide the service for one month continuously and the paid prices were the individual prices that providers bid in the auction [65,66]. From mid-2011 until July 2019, FCR was tendered weekly in a pay-as-bid auction [64,65] and the minimum bid size was decreased from 5 MW to 1 MW [65].

In July 2019, the service period was shortened to one day [65] and the pricing was modified to a market-clearing-price procedure for the offered power [64]. This means that every provider of FCR earns the price of the highest offer that is accepted for the respective bidding period. As a last modification, in July 2020, the service period was made even more flexible to six daily slots of 4 h each [64]. The EU had demanded this higher flexibility and short-term nature of FCR tenders [67].

2.6.2. Requirements on BSS and virtual power plants when participating in the FCR market

BSS are technically able to provide frequency regulation due to their fast reaction times and high cycle stability, which is required when, for example, offering FCR [10,68,69]. In 2015, the German TSOs had decided on a 30-min-criterion for BSS, when providing FCR [70]. As the storages had to provide the positive and negative power simultaneously over the period of one week, the TSOs wanted the BSSs (or pools of BSSs) to be able to provide the awarded power for at least 30 min (instead of the usual 15 min) [70]. Only when BSSs were added to an existing pool to increase its flexibility, 15 min were sufficient [70]. In 2019, the

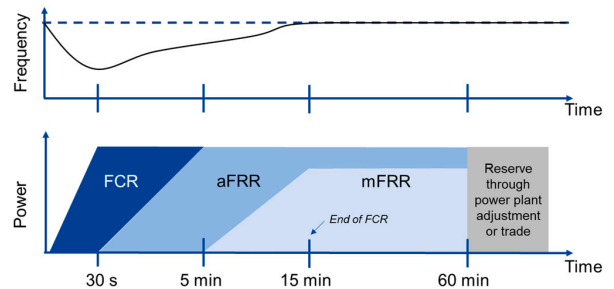


Fig. 13. Division of frequency regulation with exemplary frequency curve (top) and power type responsibilities (bottom) based on [60]. Figure shows only a frequency drop, although FCR is bidirectional.

German FNA rejected this request of the TSOs as it would have discriminated the BSSs operators [12]. In addition to this minimum required amount of energy, an FCR provider must also maintain an additional quarter of its prequalified power as a buffer [71]. This is to ensure that storage management activities can be provided at the same time as FCR provision. For example, a pool of EVs that wants to provide 3 MW of FCR power must have at least $(3 \text{ MW} \cdot 1.25 =) 3.75 \text{ MW}$ available. For a pool, the TSOs set a minimum size of 25 kW for the smallest plants and 2 MW for the pool [72]. A system may only participate in one pool at a time [72].

2.6.3. Development of the prices for FCR

Fig. 14 (left) shows the development of the FCR prices from 2008 to 2022. It contains all special features of the market history: the different service periods are marked by different colors. In addition, the range of values of 100 % of all prices shows that the monthly and weekly service periods still had a pay-as-bid price in contrast to the market-clearing price of the daily and four-hourly service periods. The FCR prices show volatility over the shown time period. Nevertheless, a clear trend towards falling prices can be seen from 2015 to the beginning of 2021. While prices in 2015 still averaged around 3600 €/MW/week (peaks above 6000 €/MW/week), by the beginning of 2021 they had fallen to <1500 €/MW/week. This was mainly due to the strong competition in the FCR market caused by the increasing number of large-scale BSSs [2]. However, from mid-2021 prices increased sharply to values in the range of 2000 €/MW/week to 4000 €/MW/week and spiked by the end of 2021 with prices of over 9000 €/MW/week. In 2022 the prices ranged from 2000 €/MW/week to 6000 €/MW/week. Therefore, the FCR prices followed the price development of all other energy markets. Further price developments stay unclear due to unpredictable situations like political tensions around Russian gas supply and the war in Ukraine.

Fig. 14 (right) shows the price ranges for different time spans of the four market designs. The prices for the monthly tendering were significantly higher than for other periods with a mean price of 3486 €/MW/week. While the prices averaged around 2585 €/MW/week during weekly service periods, the mean price during daily service periods was around 1281

€/MW/week and during the service period of 4 h 2531 €/MW/week.

3. Results

In this section the results are presented and discussed. First, the influence of flexibilization on the available power of an EV pool is examined. Subsequently, these results are used to calculate the revenue using the example of German FCR prices. These prices are representative for many countries in Central Europe.

3.1. Available power and uncertainty

As the EVs are on trips for several parts of the day, the available pool power fluctuates. Fig. 15 shows the distributions of the minimum bidirectional pool power of two exemplary clusters ((1) healthcare service care and (2) energy supply) for the current FCR market design of a service period of 4 h. In the following, the minimum bidirectional pool power is called “power capability profile”. The distribution shows all days of the year over a period of one week. While the median is represented by the thick line, the differently colored areas show the respective ranges of 50 %, 75 %, and 100 % of all values.

The two clusters are chosen as they are quite representative for the others. While the cluster energy supply shows a pattern that is different for the days Mon-Fri and Sat-Sun, the cluster healthcare service shows nearly the same pattern seven days a week although the power is higher at the weekend. The median power of the energy supply cluster ranges from around 40 % of the pool power during day to around 90 % during night and the weekend. The median power of the healthcare service cluster ranges from about 25 % during day to 80 % at night.

The power uncertainty is defined as the difference of the maximum and the minimum power within a certain time period. The two profiles both show a higher uncertainty during day than during night. Further, the energy supply cluster has only very small uncertainty values of a few percentage points during the weekends.

Fig. 16 shows the median power and the uncertainty for all 14 clusters. The following insights can be drawn from the analysis:

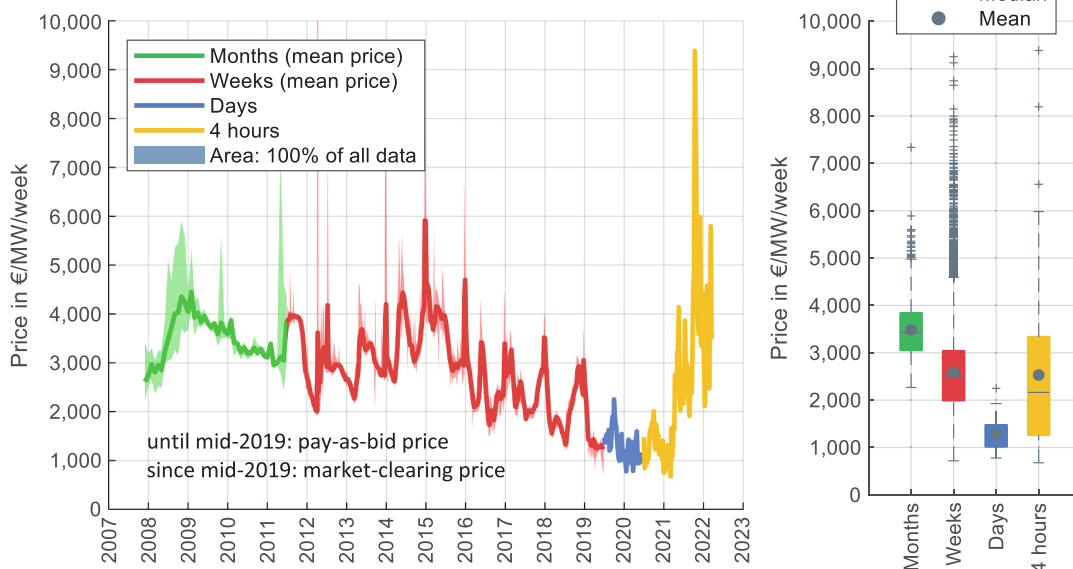


Fig. 14. Left: FCR price development per week until March 2022. Analyzed data from [8]. The prices of the periods of one month, one day and 4 h are scaled to a weekly price for comparability. Therefore, the monthly prices are divided by four, and the daily and four-hourly prices are summed up within the respective week. Right: FCR price ranges for each market design. Analyzed data from [8].

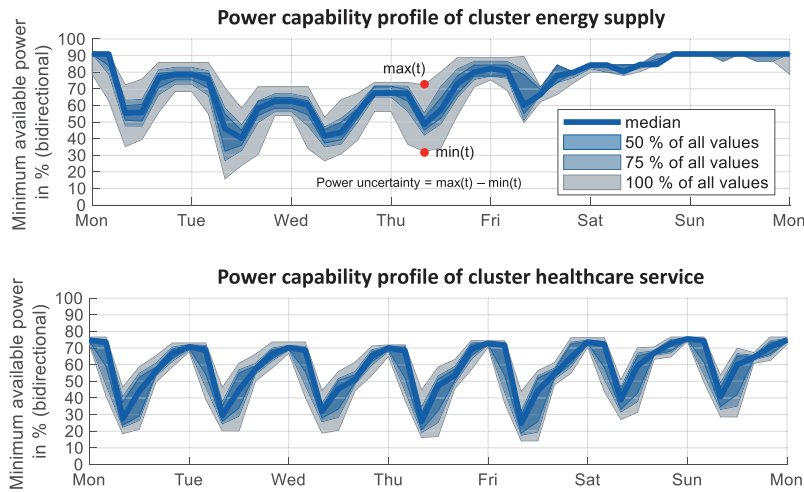


Fig. 15. Power capability profiles of the two clusters energy supply (top) and healthcare service (bottom) for all weekdays in the current FCR market design (service period of 4 h).

- Most clusters show either a clear difference between the days Mon-Fri and Sat-Sun (like the energy supply cluster, referred to as profile type A), or a similar pattern seven days a week (like the healthcare service cluster, referred to as profile type B).
- The median power is with values of around 70 %–80 % of the pool power higher during night than during day (around 40 %–50 %) for both A and B. Further, for the A profiles, the weekends show the highest median powers during the weekend with values around 90 %.
- The uncertainties and the median power have a negative correlation: Especially during the day, there are increased uncertainties around 40 % (up to 80 %). However, during night and weekends, the uncertainties are rather small with values often below 20 % as some vehicles are seldom or not driven at all during these times.
- The profiles already show that EVs are particularly suitable for short periods of ancillary services, as the availability of power varies greatly with the time.

3.2. The influence of FCR flexibilization on available power

Based on the time series of the power capability profiles, the influence of FCR flexibilization can be further investigated. The minimum power within a service period represents the available FCR power. Fig. 17 illustrates the impact of different service periods using the healthcare service power capability profile for an exemplary week. While the absolute minimum of the week determines the FCR power to be marketed in the case of a service period of one week, shorter service periods allow the fleet to be used even at times when many vehicles are connected to the charging stations and can provide power. The power minimum of the weekly service period is <20 % of the pool power. Since the EVs in this case drive about the same seven days a week, the flexibilization from weekly to daily service periods provides on five days (Mon-Fri) only a slight increase in the daily minimum to about 25 % of power. On weekends, slightly fewer trips by the pool EVs provide a minimum above 30 %. The FCR power at the service period of 4 h can follow the volatile profile much better and even corresponds to the

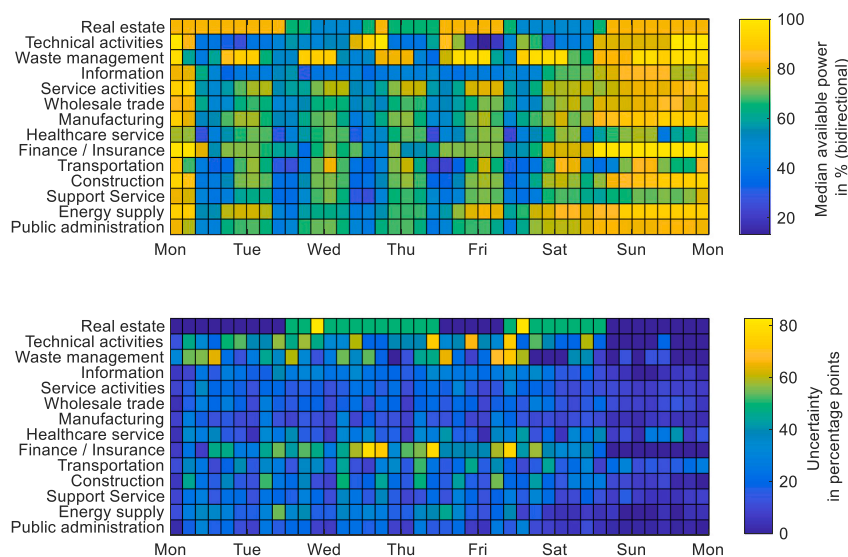


Fig. 16. Median available pool power (top) and uncertainty (bottom) of the EV operating in the chosen sectors.

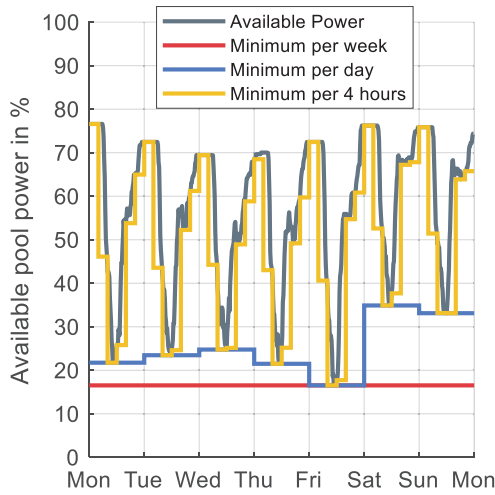


Fig. 17. Available pool power for different service periods for healthcare service cluster.

available pool power of 70 % to 80 % at night. At these times, the available power does not correspond to 100 %, since the vehicles are often not plugged overnight.

Fig. 18 aggregates these evaluations for a whole year and shows the ranges of available power within the year. The influence of the service period on the available power is shown exemplarily for the two clusters discussed before. In total, there are four “real” service periods of the historical and current FCR market designs (1 month, 1 week, 1 day, 4 h) and two fictitious shorter service periods of 1 h and 15 min respectively. The two performance periods of one month and one week are very similar and the available power values are close to the absolute minimum. This is because such long periods often result in a situation where many vehicles are on the road at some point. For this reason, the respective clusters can only offer little power to be able to guarantee service even under worst-case conditions. In such cases, a pool would have to be significantly oversized.

The change from weekly to daily service periods leads for the cluster energy supply already to significantly more time slices at which high

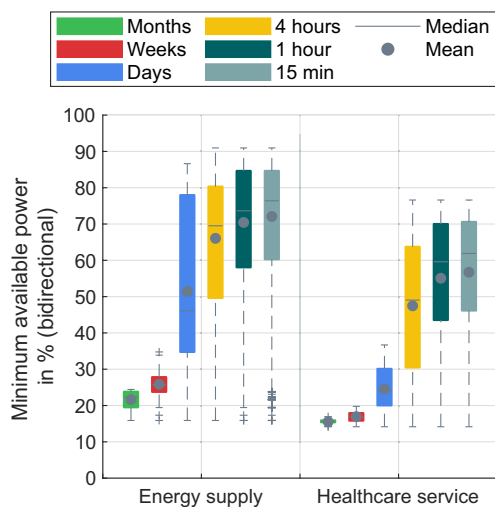


Fig. 18. Available pool power of the EV operating in the chosen sectors over one year.

powers can be offered. These are especially the weekends, where the cars do not drive that often. However, this change has significantly less effect on the available power of the healthcare service. This is because it operates nearly the same seven days a week and a service period of one day does therefore not bring much improvement. Nevertheless, if the service period is further reduced to 4 h, the power that can be offered by the healthcare service cluster also increases significantly. This increase is particularly due to the night when most of the EVs are connected to a charging station. Since the idle times are usually longer than 4 h, the further flexibilization through the 1-h and 15-min delivery periods will only result in slight increases in the available power for both clusters. The increase in power thus shows a decreasing sensitivity to the shortening of the performance period.

Fig. 19 shows the discussed flexibilization in form of shorter service periods for all 14 clusters. It becomes obvious for all clusters that it is either the change in service periods from weeks to days, the change from days to 4 h, or a combination of both which brings the highest increase in mean power. Depending on the profile, the increase in mean power at these two levels of flexibilization ranges from around 10 percentage points to 35 percentage points. The further shortening of the service time, on the other hand, has only a minor influence on the mean power to be offered. While the change from 4 h to 1 h still leads to an average increase of 4.6 percentage points, this value is only 1.4 percentage points for the change from 1 h to 15 min.

This means for the future that the revenue will mainly depend on the evolution of the FCR price, as further flexibilization of the market will only have a minor impact on the power that can be offered.

3.3. Achievable revenue

This section examines the development of the theoretical revenue of a 1000 EV pool with a charging power of 11 kW per EV.

Fig. 20 shows an example of the power capability profile for the healthcare service and the FCR price for a day in 2020 with a service period of 4 h. The following steps are taken to calculate the revenues. It becomes obvious that the FCR potential of the pool is limited both by the required buffer power (step 2) and the increment condition (step 3).

1. Determination of the minimum power in the respective service period.
2. Division of the minimum power by factor 1.25 in order to ensure the required 25 % power buffer.

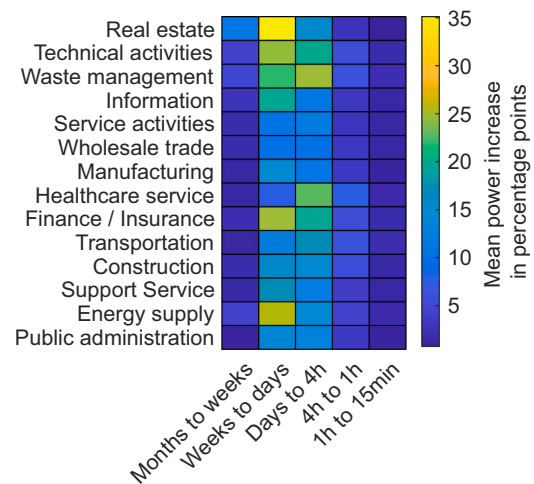


Fig. 19. The influence of flexibilization in form of shorter service periods on the mean power increase.

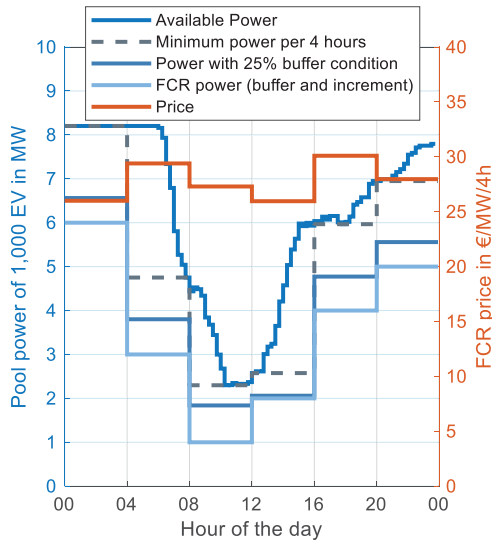


Fig. 20. Available pool power (with buffer and increment condition) and FCR price over one day (cluster: healthcare service).

3. Rounding down the power rest to an integer multiple of 1 MW to correspond to the minimum power of 1 MW and the increment of 1 MW in the current market design.
4. Multiplying the time-dependent FCR power by the time-dependent FCR price to determine revenues.
5. Summation of the revenues for the entire period and normalization to one week.

This procedure is performed for the whole time series of the annual simulations (in the case of the service period of 4 h the simulation is half a year) of all clusters for the three selected service periods of one week, one day and 4 h with historical prices.

Fig. 21 shows the results of the revenue per pool for the last service periods. The plot shows the achievable revenue per EV and year for all clusters based on an annual simulation of a 1000 EV pool for each cluster. Each box plot contains the 14 clusters for the different service periods. It can be seen that the revenues increase on average. The average revenue per EV increases from 263 €/a with weekly service periods, over 232 €/a (daily service period) up to 640 €/a with four-hourly service periods. Furthermore, the overall influence of flexibilization and falling prices clearly depends on the individual service profile as can be examined even more clearly in Fig. 22:

- The change from weekly to daily service periods was accompanied by increasing flexibility and falling FCR prices. For the majority of the clusters the increased flexibility did not overcompensate the falling prices with mean revenue decreases of 31 €/a and maximum decreases of around 180 €/a per EV. However, there are also some clusters for which the flexibilization dominated and their pool revenue increased by up to 136 €/a.
- The change from daily to four-hourly service periods was accompanied by increasing flexibility and increasing FCR prices. Both developments lead to an increase in revenues from 340 €/a to 500 €/a (mean: 408 €/a) per EV. In this case, volatile profiles that differ from day to day could benefit both from offering higher FCR power as well as from increasing prices.
- The overall change from weekly to four-hourly service periods was accompanied by increasing flexibility and nearly a constant mean

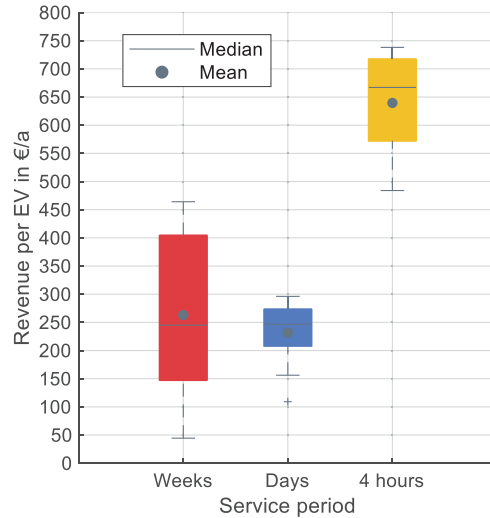


Fig. 21. Mean yearly revenue per EV based on simulation of 1000 EVs over the whole time of service period. Each box plot contains the mean of the 14 clusters.

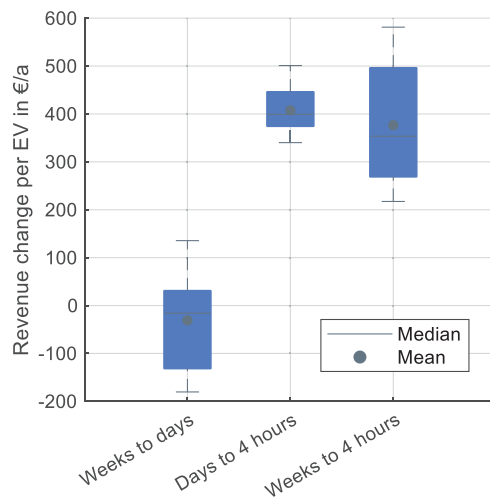


Fig. 22. Change in weekly revenues per EV based on simulation of 1000 EV pool over the whole time of service period. Each box plot contains the 14 clusters.

FCR. The flexibility overcompensates for the falling prices significantly with mean revenue increases per EV of around 380 €/a. Especially the revenue for pool profiles that have a volatile profile within a day such as the healthcare service cluster increased by up to 581 €/a per EV. These profiles can now use, for example, the night hours during which idle times are longer than the service periods of 4 h (see Fig. 17).

A detailed overview of the single sectors is given in Appendix, Fig. 24. We have also published an analysis that looks in more detail at the potential of each economic sector and vehicle size [73].

4. Discussion

In this paper, we estimated the revenue potential of EV fleets using historic market prices, mobility profiles of different fleets, and EV characteristics such as the battery size, charging power, and consumption. However, a few points need to be considered for further classification of the results. These relate to techno-economic points and aspects of the charging strategies.

4.1. Techno-economic aspects

In our study, we focused on achievable revenues. These revenues are necessarily offset by associated costs. The costs are mainly composed of hardware and transaction.

For the provision of FCR, a bidirectional charger for the EV is needed. Although, as of the beginning of 2022, most EVs are not used for bidirectional activities yet, but this situation could change quickly. Volkswagen, for example, announced that their EVs will have bidirectional features from 2022 onwards [74]. First bidirectional products for private car owners supporting both standards (CHAdeMO or ISO 15118) already exist [75] (around 6000 € per 7,4 kW wallbox [76]) and they will most likely become cheaper with a growing market.

Besides hardware, there are also operational expenditures such as metering costs, costs for pool management by an aggregator, and battery degradation due to increased battery cycling through FCR (around 250 equivalent full cycles per year for large-scale BSSs [1,69]). The battery degradation costs of two field projects are estimated to be 50 €/a – 100 €/a in [31] and 86 €/a in [47]. Further, the degradation is mainly influenced by calendar aging and not by cycle aging through V2G [47]. The only known source to the authors dealing with operational costs for EV dual use is the INEES project [31], in which the provision of aFRR through EVs was analyzed. The cost estimation for metering, communication, and battery degradation summed up to 700 € to 750 € per year for 2016 and is projected to be 110 € to 350 € per year for a future scenario with bidirectional EV and charging stations. Comparing the possible revenue with the operational costs as of 2022, the profit could probably be around a couple of 100 € per year. This estimate fits well to reported real-world income of 21 € per month (252 €/a) in 2019 for the most earning private EV providing balancing power in the Netherlands for the company Jedlix BV [77]. All in all, the profits can possibly be in low positive ranges, if capital expenditures are neglected. However, this best-case scenario implies that the aggregator is always awarded a contract in the FCR tendering, which is rather unlikely with the growing number of batteries in the market, especially in the future. Besides these costs, high penalties and exclusion of the FCR market could occur, if FCR power cannot be provided in case an unforeseen high number of EVs is on the road. Aggregators should therefore have either absolutely planable vehicle fleets such as busses or more reliable assets such as stationary BSSs or other power plants in their portfolio.

4.2. Charging strategies and “degrees of freedom”

We assumed that the EVs are plugged whenever they are at the company site and that every EV has an available bidirectional charging station. In case people do not plug the EVs regularly, the power profile would be lower. Further, if not every EV has its own charging station, the power profiles would be lower for two reasons: (1) fewer EVs could provide FCR simultaneously as not all are connected and (2) more time of the charging station would be occupied for charging the energy for the mobility as several EVs have to be charged after a shift.

In our estimation we assumed that the pool operator does not plan an optimal charge management of each individual EV. Therefore, the estimated revenue is the potential for a fleet with an undisturbed

charging profile. The active charging management of the EVs by the pool operator offers the possibility to increase the power available for FCR provision which in turn would increase the revenue. In [11] such a real-world operating strategy of FCR provision for a large-scale BSS is presented and discussed for the historic market design with the 30-min criterion. With an active charging management of each individual EV a pool operator could keep the fleet in a valid operating range to fulfill the 15-min criterion more often and to increase the pool's FCR power. Charge management often requires energy trading, e.g., from the continuous intraday market. One study [78] describing large-scale BSS operation in FCR market shows results where expenses for intraday recharge, trading services, and connection to trader sum up to about 15 % of income when operating 4 MW/4 MWh storage capacity.

Another way of charge management is the use of the “degrees of freedom” in the provision of FCR [79]. The ENTSO-E Handbook requests a minimum accuracy of the frequency measurement of 10 mHz. Therefore, FCR does not have to be provided if the deviation of the frequency is within 10 mHz from the nominal frequency of 50 Hz. However, FCR can be provided within this so called deadband. With the use of an accurate frequency measurement the charge management could opt to charge EVs with FCR in the deadband which reduces the costs of EV charging for users and can be regarded as additional revenue. Furthermore, due to power measurement accuracy limitations, an overfulfillment of provided FCR power of up to 20 % is permitted. Also, this degree of freedom could be used to maximize the energy gained for EVs during the provision of FCR and be seen as additional revenue. The last degree of freedom that can be taken advantage of by a pool operator is the specified ramp rate due to regulations. In the case of FCR, a total activation of the required power has to be activated within 30 s. A highly flexible unit, such as the battery of an EV, can react instantaneously in order to maximize energy when FCR is used to charge the EV. As an example for the impact of the degrees of freedom, one study [11] found that for a provision of 4 MW in the year 2014 with a large stationary storage system in Germany the energy gain due to the use of the degrees of freedom was 139 MWh. This rather complex topic for a real-world operating management for the provision of FCR with an EV fleet is a worthy research topic for the future.

5. Conclusion and outlook

This section draws a conclusion of the presented analyses and gives a brief outlook on market developments and future works.

5.1. Conclusion

Traditional grid services are undergoing a change of auction design towards flexibilization. A few years ago, the market for frequency containment reserve (FCR) to stabilize the grid frequency in Germany was provided exclusively by conventional power plants over service periods of up to one month. At present time, many large-scale battery storage systems as well as some battery pools are participating in the same market with service periods of less than one day. The market for FCR was a promising source of income for battery storage over the last years. After prices had fallen significantly in the face of the sharp increase in competition from battery storage systems, the prices increased sharply from 2021 onwards due to the political tensions with respect to gas imports and the war in Ukraine. This paper investigated the influence of FCR market flexibilization and FCR price development on the economics of EV fleet operation.

The service periods were shortened from one week over days to 4 h in accordance with the flexibility levels already achieved in the years until mid-2020. First, the average FCR price fell over years from 2585 €/MW/week during weekly service periods to an average price during daily

service periods of 1281 €/MW/week. Then, the price increased to an average price of 2531 €/MW/week during the service period of 4 h.

Regarding the available power, the flexibilization from either one week to one day or the flexibilization from one day to 4 h cause the highest increase in mean available power. A power increase of up to 35 % resulting from the flexibilization of service periods from one week to one day can especially be seen for profiles that have regular driving profiles during the days Mon-Fri and little activity on the days Sat-Sun. However, for EV fleets that have the same driving pattern seven days a week, the further FCR flexibilization to service periods of 4 h is needed to significantly increase available power. This power can especially be provided during the idle times at night. Further, the times of high power show also only small values of power uncertainty. This makes commercial fleets especially interesting for V2G services as the idle times are known.

Future possible flexibilization in form of shorter service periods like one hour and less will only have a small impact on an increase in available power as the idle times are often already significantly longer than the current service period of 4 h. Therefore, future income will largely depend on the uncertain development of FCR prices.

While the potential revenue was on average below 250 €/EV/a during the daily service periods, the mean revenue increased to around 650 €/EV/a for the service periods of 4 h from mid-2020 to March 2022. However, in all analyzed scenarios, the revenues are relatively low, and it remains questionable if they can overcompensate for the costs for metering, battery degradation, and pool management.

5.2. Outlook

In the future, we expect the flexibility of the spot and ancillary service markets to increase further. In parallel with a rapidly increasing number of EVs, there will be a huge potential of mobile BSS in the energy system for the near future. From an economic point of view, it is advantageous to use EVs during their idle times for grid service instead of leaving this potential unused. With respect to these developments, it is questionable which flexibility markets will remain and in what form and whether there will be new markets. The analyzed FCR market, for instance, has a volume of below 600 MW. The regulatory agencies could

decide to demand from EVs that they should have a frequency-dependent charging power profile. Such a law would effectively eliminate the FCR market as it is today. Such regulations are already part of the German renewable energy law (EEG), for example, which limits the feed-in power of photovoltaic systems. Furthermore, competition for aggregators will increase significantly. If there is enough battery capacity in the energy system, efficient pool management is essential.

CRedit authorship contribution statement

Jan Figgener: Conceptualization, Methodology, Software, Formal analysis, Investigation, Data Curation, Writing – Original Draft, Visualization. **Benedikt Tepe:** Conceptualization, Methodology, Software, Formal analysis, Investigation, Data Curation, Writing – Original Draft, Visualization. **Fabian Rücker:** Conceptualization, Methodology, Data Curation, Writing - Review & Editing. **Ilka Schoeneberger:** Conceptualization, Methodology, Data Curation, Writing - Review & Editing. **Christopher Hecht:** Methodology, Writing - Review & Editing. **Andreas Jossen:** Resources, Writing - Review & Editing, Supervision. **Dirk Uwe Sauer:** Conceptualization, Methodology, Resources, Writing - Review & Editing, Supervision.

Declaration of competing interest

The authors declare that they have no known competing financial interests or personal relationships that could have appeared to influence the work reported in this paper.

Acknowledgement

This work was partly done based on work within the research project “GO-ELK” (funding number 16SBS001C) funded by the German Federal Ministry for Digital and Transport (BMDV) and partly done within the research project “ALigN” (funding number 01M218006G) funded by the German Federal Ministry for Economic Affairs and Climate Action (BMWK). The authors of this publication are solely responsible for its content.

Appendix A

A.1. Abbreviations and nomenclature

Table 5
Abbreviations sorted alphabetically.

AS	Ancillary services
BSS	Battery storage system
EEG	German renewable energy law
ENTSO-E	European Network of Transmission System Operators for Electricity
EPR	Energy-to-power ratio
EV	Electric vehicle
FCR	Frequency containment reserve
FNA	(German) Federal Network Agency
NACE	European Classification of Economic Activities
OCPP	Open Charge Point Protocol
PGS	Institute for Power Generation and Storage Systems
RWTH Aachen University	Rheinisch-Westfälische Technische Hochschule Aachen
SOC	State-of-charge
SOE	State-of-energy
TSO	Transmission System Operator
V2G	vehicle-to-grid
V2H	vehicle-to-home

Table 6
Nomenclature.

w_{start}	trip start probability
P_{EV}	Rated power of the battery converter
P_{CS}	Rated power of the charging station
P_{charge}	Charge power for FCR
$P_{discharge}$	Discharge power for FCR
E_{Bat}	Battery energy capacity
E_{market}	Marketable energy
$E_{mobility}$	Reserved energy for mobility
E_{charge}	Charge energy for FCR
$E_{discharge}$	Discharge energy for FCR
ΔT_{supply}	Duration of FCR service period

A.2. Additional information on used databases

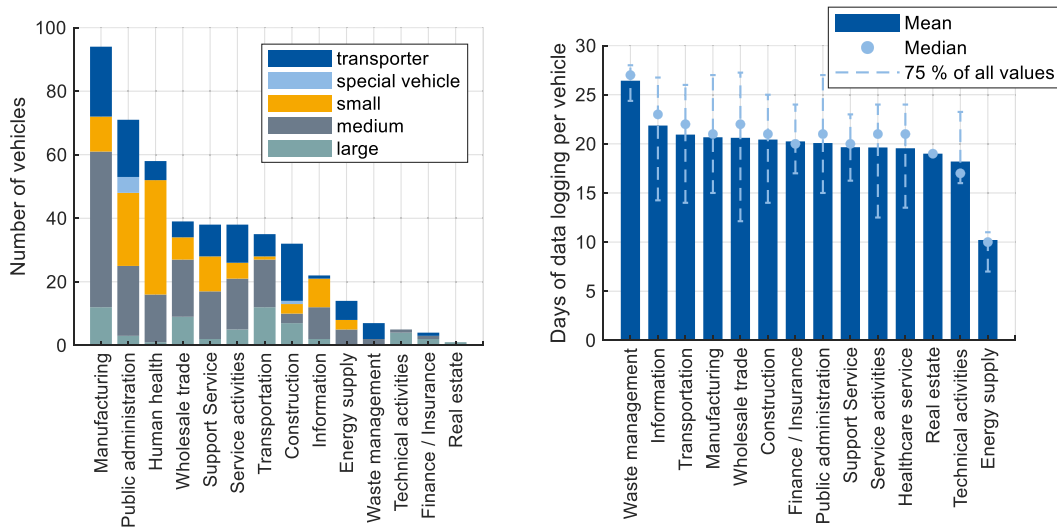


Fig. 23. Vehicles clustered according to economic sector (left) and mean duration of data logging (right) from database “Logbook”.

Table 7

EVs from database “Measurements” used in the project GO-ELK [49]. Some EVs were switched between the different trades, which is why the number of EVs is greater than the measured 22 EVs.

Healthcare service	Energy supply	Transportation	Public administration
Smart E.D. (17,6 kWh)	Nissan e-NV200 (24 kWh)	Nissan Leaf (24 kWh)	Kangoo ZE (22 kWh)
Smart E.D. (17,6 kWh)	Nissan Leaf (24 kWh)	Opel Ampera (16,5 kWh)	Peugeot iOn (16 kWh)
Smart E.D. (17,6 kWh)	Nissan Leaf (24 kWh)	BMW i3 (21,6 kWh)	Peugeot iOn (16 kWh)
Mitsubishi i-MiEV (16 kWh)	Smart E.D. (17,6 kWh)	Smart E.D. (17,6 kWh)	
VW e-up! (18,7 kWh)	Kangoo ZE (22 kWh)	Smart E.D. (17,6 kWh)	
Opel Ampera (16,5 kWh)	Nissan Leaf (24 kWh)	Smart E.D. (17,6 kWh)	
Nissan Leaf (24 kWh)		Smart E.D. (17,6 kWh)	
		Nissan Leaf (24 kWh)	

Table 8

Electric vehicle data used to assume battery capacity and energy consumption for database "Logbook". Calculation based on data from ADAC [55].

Vehicle size	Differentiation in REM2030 according to cubic centimeters (cc)	Assumed differentiation E-vehicles	Brand & model	Battery Capacity kWh	Consumption kWh/100 km	ADAC Real Consumption kWh/100 km	Factor between nominal and real consumption	Vehicle weight kg	Torque Nm
Small	Displacement <1400 cc	Torque <220 Nm & Weight 1400 kg to 2000 kg	Citroën C-Zero	14.5	12.6	–	–	1440	196
			Citroën E-Mehari	30	20	–	–	1838	166
			Peugeot iOn	14.5	12.6	16.94	1.34	1450	180
			Renault Zoe (22 kWh) Life	22	13,3	21.4	1.61	1943	220
			Smart Fortwo coupé electric drive	17,6	15,1	19.2	1.27	1150	130
			Average	19.10	14.52	18.89	1.39	1545	179
			Assumed	19.1	–	18.9	–	–	–
			BMW i3 (94 Ah)	33.2	13.1	17.4	1.33	1620	250
			Ford Focus Electric	33.5	15.4	22.4	1.45	2085	250
			Hyundai Ioniq Elektro	28	11.5	14.7	1.28	1880	295
Medium	Displacement 1400 cc to 2000 cc	Torque 220 Nm to 380 Nm & Weight 1600 kg to 2200 kg	KIA Soul EV	30	14.7	19.4	1.32	1960	285
			Mercedes-Benz B 250 e	28	16.6	20.2	1.22	2170	340
			Nissan Leaf	24	15	20.39	1.36	1965	280
			Opel Ampera-E	60	14.5	19.7	1.36	2056	360
			VW eGolf	24.2	12.7	18.2	1.43	1960	270
			Volvo C30 Electric	22.7	15	28.3	1.89	1995	220
			Average	31.36	14.35	20.08	1.40	1966	283
			Assumed	31.4	–	20.1	–	–	–
			Audi e-tron 55 quattro	95	23	–	–	2565	664
			BMW Concept ix3 (2020)	70	17.5 (calc)	–	–	–	561
			Hyundai Kona Elektro	39.2	14.3	–	–	1760	395
			Jaguar I-Pace	90	21.2	27.6	1.32	2208	696
			Tesla Model S P90D	90	17.8	24	1.35	2670	967
Large	Displacement 1400 cc to 2000 cc	Torque 220 Nm to 380 Nm & Weight 1600 kg to 2200 kg	Tesla Model X	100	20.8	24	1.15	2534	660
			Average	80.7	19.31	24	1.27	–	680
			Assumed	80.7	–	27 ^a	–	–	–
			Citroen Berlingo Electric L2	22.5	17.7 (NEFZ)	–	–	1644	200
			Iveco Daily Electric	28.2	–	–	–	2500	300
			Nissan e-NV200	24	16.5	22.8	1.38	1.640	254
			Peugeot Partner Electric	22.5	17.7	–	–	1664	152
			Renault Kangoo Z.E.	22	15.5	23.5	1.52	1520	226
			Streetscooter Work L Box	40	19.2 (NEFZ)	–	–	1640	200
			VW eCrafter	35.8	21.54	–	–	2522	290
Transporter	Displacement >1400 cc Weight < 3500 kg	Weight 1644 kg to 2600 kg & mostly 2–3 seats with a lot of storage size	Average	27.86	18.02	23.15	1.45	2158	232
			Assumed	27.9	–	25.2 ^a	–	–	–

^a As only few vehicles were tested by the ADAC, the real electricity consumption for large vehicles and transporter is calculated using the factor 1.4 (see small and medium average factor) and multiply it with the average nominal consumption.

A.3. Literature for further research

Table 9

Summary of projects working on the provision of ancillary services using EV fleets.

Source	Date	Name	Partner	Focus & results
[29]	2002	“Vehicle-to-Grid Demonstration Project: Grid Regulation Ancillary Service with a Battery Electric Vehicle” (V2GDP)	AC Propulsion, California Air Resources Board, California Environmental Protection Agency,	<ul style="list-style-type: none"> - Evaluation of the feasibility of the provision of grid regulation using EV - EV are able to provide grid regulation and the ISO system requirements regarding data transmission times could be fulfilled - Energy throughput when providing regulation power is equivalent to that resulting from daily driving
[31]	2012–2015	“Intelligente Netzanbindung von Elektrofahrzeugen zur Erbringung von Systemdienstleistungen – INEES”(Intelligent grid integration of EV to provide system services)	Fraunhofer IWES, LichtBlick SE, SMA Solar Technology AG, Volkswagen AG	<ul style="list-style-type: none"> - Field tests of the provision of secondary control reserve using a fleet of 20 V2G-capable EV - Provision is technically possible, but under current costs and revenue not profitable
[33]	2013–2018	Los Angeles Air Force Base Vehicle to Grid Demonstration (LAAFB)	Lawrence Berkeley National Laboratory (LBNL), Kisensum LLC	<ul style="list-style-type: none"> - Demonstration of a fleet of 29 bidirectional EV providing frequency regulation to generate revenue - Charging stations and EV should have a capacity/power ratio of at least two to participate in a fleet offering frequency regulation
[35]	2016–2019	The Parker Project (Parker)	DTU, Nuvve, Nissan, Inerso, Enel X, Groupe PSA, Mitsubishi Corporation, Mitsubishi Motors Corporation, Frederiksberg Forsyning	<ul style="list-style-type: none"> - Demonstration project to analyze the integration of V2G-capable EV into the electricity grid - Results show that EV are able to provide ancillary services - Recommendations are the planning of electrification of transportation, continuous research, “test zones and pilots on new market designs” and an international collaboration
[42]	2018–2019	Industrial Pilot Project	The Mobility House, ENERVIE, Amprion, Nissan	<ul style="list-style-type: none"> - Demonstration of the provision of FCR using one EV that got prequalified from the German TSO
[43]	2019–2021	“Bidirectional Charging Management – Field Trial and Measurement Concept for Assessment of Novel Charging Strategies”	BMW, FfE e.V., FfE GmbH, Kostal Industrie Elektrik GmbH, TenneT TSO GmbH, Bayernwerk Netz GmbH, Karlsruhe Institute of Technology (KIT), University Passau	<ul style="list-style-type: none"> - Analysis of the interaction between EV, charging infrastructure and the power grid - Identification and demonstration (using 50 EV) of use-cases of V2G in different markets.
[45,46]	2019–2021	Industrial Pilot Project	Tennet, Next Kraftwerke, Jedlix	<ul style="list-style-type: none"> - Field test of EV providing frequency regulation in a virtual power plant - Customers of Jedlix charging their EV receive financial benefit when providing secondary control reserve

Table 10

Summary of literature about demonstrations, experiments and field tests of the provision of frequency regulation using EV fleets.

Source	Date	Project	Focus	Results
Brooks, Gage [30]	2001	V2GDP	Analysis of ancillary services EV, hybrid vehicles and fuel-cell vehicles may provide by showing test results	<ul style="list-style-type: none"> - Field tests show that the EV is capable of providing power and thus benefit to the grid - EV might be able to achieve lower net ownership costs in comparison to conventional vehicles by providing grid services
Marinelli et al. [36]	2016	Parker	Centralized approach to provide FCR with EV using unidirectional charging and experimental validation of the approach	<ul style="list-style-type: none"> - Provision of FCR with EV by only using unidirectional charging is viable with fast response time
Thingvad et al. [37]	2016	Parker	Economic comparison of EV fleet providing Frequency Normal-operation Reserve (FNR) through unidirectional vs. bidirectional (V2G) charging in Eastern Denmark	<ul style="list-style-type: none"> - Bidirectional FNR is more lucrative (factor of 6.6–13.3) and viable than unidirectional as it can be applied longer and independently of the driven distance - Experiments show that EV are able to perform unidirectional FNR and bidirectional FNR with delay times of 1 respectively 5 s
DeForest et al. [34]	2017	LAAFB	EV fleet participating in California Independent System Operator (CASIO) frequency regulation market	<ul style="list-style-type: none"> - Development of a Day-Ahead optimization model applied to the Los Angeles Air Force Base EV fleet minimizing operation cost and maximizing revenue from ancillary service
Degner et al. [32]	2017	INEES	Analysis of the effects of EV secondary control reserve provision on the distribution grid using simulations and field tests	<ul style="list-style-type: none"> - Power quality of the distribution grid is not negatively influenced by the EV provision - The EV impact on the distribution grid can be anticipated and managed well
Hashemi et al. [38]	2018	Parker	Presentation of results from three different EV (Nissan Leaf, Peugeot iOn and Mitsubishi Outlander) providing FCR-N (frequency-controlled normal operation reserve) in Nord Pool energy market	<ul style="list-style-type: none"> - All three EV were able to respond within five seconds and with an accuracy of around 98 % - The depth-of-discharges (DoDs) were always smaller than 40 %

(continued on next page)

Table 10 (continued)

Source	Date	Project	Focus	Results
Bañol Arias et al. [39]	2018	Parker	Analysis of an EV fleet participating in Danish FNR market and determination of issues appearing in the field	- EV fleet is able to support the grid, e.g. in FNR market, but availability of the EV is crucial - Practical issues are “communication delays, measurement errors and physical equipment constraints” [39]
Thingvad et al. [40]	2019	Parker	Economic analysis of EV performing FNR in the Nordic countries considering requirements and losses	- The value of bidirectional FNR is much higher than providing unidirectional FNR - Suggestion: Aggregator should pay for the EV’s driving energy consumption to remunerate owners - Losses due to charger’s efficiency results in reduced revenue by 22 %
Bañol Arias et al. [41]	2020	Parker	Economic assessment of EV participating in FCR-N in the Nord Pool market from the owner’s perspective applying three operation strategies: complete pause, over-fulfillment, preferred operating point	- EV owners can achieve profits from the provision of FCR—N, mostly when choosing a smart operation strategy - Preferred operating point strategy resulted in highest profits (up to 1100€ per EV per year when bidding 10 kW) as it minimized the battery degradation and the unavailability times

Table 11

Summary of selected literature of German rules and regulations on the frequency containment reserve (FCR) market.

Source	Date	Content related to the provision of FCR using battery energy storage systems
VDN [80]	2007	TransmissionCode 2007: Network and system rules of the German transmission system operators In Appendix D: Documents for prequalification for the Provision of primary control power to TSO - Degrees of freedom, rules and requirements that must be met by a provider of FCR
FNA [65]	2011	German federal network agency (FNA) changes FCR bidding time from monthly to weekly
German TSO [79]	2014	Key points and degrees of freedom for the provision of FCR using BSS as an example
German TSO [70]	2015	Storage capacity requirements for the provision of FCR using batteries (e.g. 30-min-criterion)
FNA [64]	2018	German federal network agency (FNA) changes FCR bidding time from weekly to daily starting in July 2019 and from daily to 6 daily sections of 4 h starting in July 2020.
FNA [12]	2019	Decision of the German federal network agency (FNA) to stop the TSO from requiring the 30-min-criterion when providing FCR with BSS. From now on 15-min-criterion for all providers including BSS.
German TSOs [72]	2019	Minimal requirements on the IT when providing control reserve. When pooling small systems (< 25 kW per system, maximum pool size 2 MW) the connection between the systems can from now on be made via the internet.

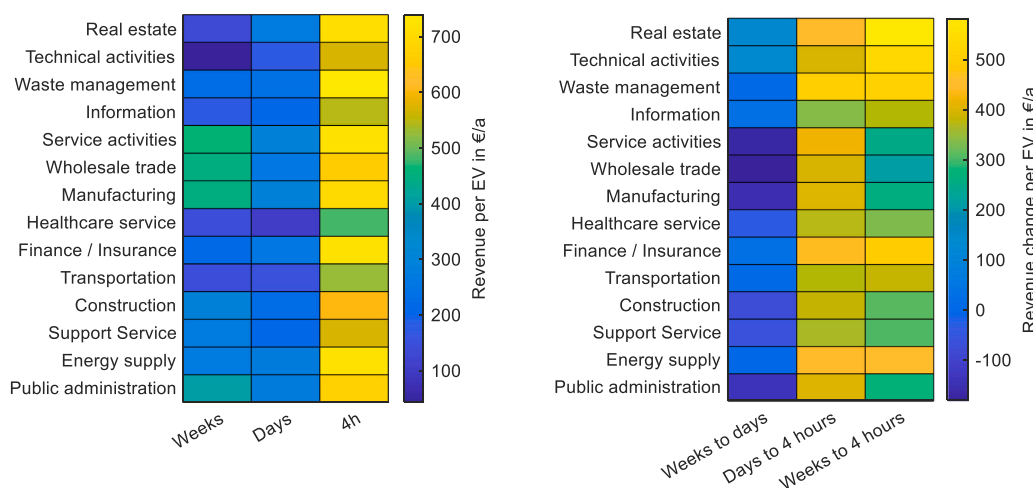


Fig. 24. Mean annual revenue (left) and revenue change (right) of the economic sectors.

References

[1] J. Figgner, P. Stenzel, K.-P. Kairies, J. Linßen, D. Haberschus, O. Wessels, et al., The development of stationary battery storage systems in Germany – status 2020, *J. Energy Storage* 33 (2021), 101982, <https://doi.org/10.1016/j.est.2020.101982>.
 [2] J. Figgner, P. Stenzel, K.-P. Kairies, J. Linßen, D. Haberschus, O. Wessels, et al., The development of stationary battery storage systems in Germany – A market review, *J. Energy Storage* 29 (2020), 101153, <https://doi.org/10.1016/j.est.2019.101153>.
 [3] J. Figgner, C. Hecht, D. Haberschus, J. Bors, K.G. Spreuer, K.-P. Kairies, et al., The development of battery storage systems in Germany – A market review (status 2022), 2022, <https://doi.org/10.48550/arXiv.2203.06762>.
 [4] S. Englberger, A. Jossen, H. Hesse, Unlocking the potential of battery storage with the dynamic stacking of multiple applications, *Cell Rep.Phys.Sci.* 1 (11) (2020), 100238, <https://doi.org/10.1016/j.xcrp.2020.100238>.

- [5] W. Kempton, J. Tomić, Vehicle-to-grid power fundamentals: calculating capacity and net revenue, *J. Power Sources* 144 (1) (2005) 268–279, <https://doi.org/10.1016/j.jpowsour.2004.12.025>.
- [6] C. Nobis, T. Kuhnimhof, *Mobilität in Deutschland MiD:Ergebnisbericht*, 2018.
- [7] C. Gschwendtner, S.R. Sinsel, A. Stephan, Vehicle-to-X (V2X) implementation: an overview of predominate trial configurations and technical, social and regulatory challenges, *Renew. Sustain. Energy Rev.* 145 (2021), 110977, <https://doi.org/10.1016/j.rser.2021.110977>.
- [8] German Transmission Grid Operators: 50 Hertz, Amprion, Tennet, TransnetBW. REGELLEISTUNG.NET: Internetplattform zur Vergabe von Regelleistung, Available from, <https://www.regelleistung.net>, May 05, 2020.
- [9] J. Fleer, S. Zurmühlen, J. Badedá, P. Stenzel, J.-F. Hake, D.U. Sauer, Model-based economic assessment of stationary battery systems providing primary control reserve, *Energy Procedia* 99 (2016) 11–24, <https://doi.org/10.1016/j.egypro.2016.10.093>.
- [10] A. Zeh, M. Müller, M. Naumann, H. Hesse, A. Jossen, R. Witzmann, Fundamentals of using battery energy storage systems to provide primary control reserves in Germany, *Batteries* 2 (3) (2016) 29, <https://doi.org/10.3390/batteries2030029>.
- [11] T. Thien, D. Schweer, D. Vom Stein, A. Moser, D.U. Sauer, Real-world operating strategy and sensitivity analysis of frequency containment reserve provision with battery energy storage systems in the German market, *J. Energy Storage* 13 (2017) 143–163, <https://doi.org/10.1016/j.est.2017.06.012>.
- [12] Bundesnetzagentur für Elektrizität, Gas, Telekommunikation und Eisenbahnen. Beschluss BK6-17-234, 2019.
- [13] Mandel Fitzgerald, et al., *The Economics of Battery Energy*, 2015.
- [14] A. Stephan, B. Battke, M.D. Beuse, J.H. Clausdeinken, T.S. Schmidt, Limiting the public cost of stationary battery deployment by combining applications, *Nat. Energy* 1 (7) (2016) 334, <https://doi.org/10.1038/nenergy.2016.79>.
- [15] F. Brauer, J. Rominger, R. McKenna, W. Fichtner, Battery storage systems: an economic model-based analysis of parallel revenue streams and general implications for industry, *Appl. Energy* 239 (2019) 1424–1440, <https://doi.org/10.1016/j.apenergy.2019.01.050>.
- [16] S. Englberger, H. Hesse, N. Hanselmann, A. Jossen, SimSES Multi-Use: a simulation tool for multiple storage system applications, in: 2019 16th International Conference on the European Energy Market (EEM), IEEE, 2019, pp. 1–5.
- [17] W. Kempton, S.E. Letendre, Electric vehicles as a new power source for electric utilities, *Transp. Res. Part D: Transp. Environ.* 2 (1997).
- [18] W. Kempton, J. Tomić, S. Letendre, A. Brooks, T. Lipman, Vehicle-to-grid power: battery, hybrid, and fuel cell vehicles as resources for distributed electric power in California, 2001.
- [19] J. Tomić, W. Kempton, Using fleets of electric-drive vehicles for grid support, *J. Power Sources* 168 (2) (2007) 459–468, <https://doi.org/10.1016/j.jpowsour.2007.03.010>.
- [20] E. Sortomme, M.A. El-Sharkawi, Optimal scheduling of vehicle-to-grid energy and ancillary services, *IEEE Trans. Smart Grid* 3 (1) (2012) 351–359, <https://doi.org/10.1109/TSG.2011.2164099>.
- [21] T.W. Hoogvliet, G. Litjens, W. van Sark, Provision of regulating- and reserve power by electric vehicle owners in the Dutch market, *Appl. Energy* 190 (2017) 1008–1019, <https://doi.org/10.1016/j.apenergy.2017.01.006>.
- [22] A.O. David, I. Al-Anbagi, EVs for frequency regulation: cost benefit analysis in a smart grid environment, *IET Electr. Syst. Transp.* 7 (4) (2017) 310–317, <https://doi.org/10.1049/iet-est.2017.0007>.
- [23] S. Han, S. Han, K. Sezaki, Development of an optimal vehicle-to-grid aggregator for frequency regulation, *IEEE Trans. Smart Grid* 1 (1) (2010) 65–72, <https://doi.org/10.1109/TSG.2010.2045163>.
- [24] R.J. Bessa, M.A. Matos, F.J. Soares, J.A.P. Lopes, Optimized bidding of an EV aggregation agent in the electricity market, *IEEE Trans. Smart Grid* 3 (1) (2011) 443–452, <https://doi.org/10.1109/TSG.2011.2159632>.
- [25] P. Codani, M. Petit, Y. Perez, Participation of an electric vehicle fleet to primary frequency control in France, *IJHEV* 7 (3) (2015) 233, <https://doi.org/10.1504/IJHEV.2015.071639>.
- [26] J. Neubauer, A. Pesaran, The ability of battery second use strategies to impact plug-in electric vehicle prices and serve utility energy storage applications, *J. Power Sources* 196 (23) (2011) 10351–10358, <https://doi.org/10.1016/j.jpowsour.2011.06.053>.
- [27] C. Heymans, S.B. Walker, S.B. Young, M. Fowler, Economic analysis of second use electric vehicle batteries for residential energy storage and load-levelling, *Energy Policy* 71 (2014) 22–30, <https://doi.org/10.1016/j.enpol.2014.04.016>.
- [28] S.J. Tong, A. Same, M.A. Kootstra, J.W. Park, Off-grid photovoltaic vehicle charge using second life lithium batteries: an experimental and numerical investigation, *Appl. Energy* 104 (2013) 740–750, <https://doi.org/10.1016/j.apenergy.2012.11.046>.
- [29] A.N. Brooks, Vehicle-to-grid Demonstration Project: Grid Regulation Ancillary Service With a Battery Electric Vehicle, California Environmental Protection Agency, Air Resources Board, Research, 2002.
- [30] A Brooks T Gage AC Propulsion. Integration of electric drive vehicles with the electric power grid—a new value stream. In: 18th International Electric Vehicle Symposium and Exhibition, Berlin, Germany. Citeseer, p. 20–24.
- [31] G. Arnold, R. Brandl, T. Degner, N. Gerhardt, M. Landau, D. Nestle, et al., *Intelligente Netzanbindung von Elektrofahrzeugen zur Erbringung von Systemdienstleistungen - INEES: Abschlussbericht*, 2015.
- [32] T Degner G Arnold R Brandl J Dollichon A Scheidler Grid Impact of Electric Vehicles with Secondary Control Reserve Capability. In: Proceeding of the 1st E-Mobility Power System Integration Symposium.
- [33] D. Black, J.S. MacDonald, N. DeForest, C. Gehbauer, *Los Angeles Air Force Base Vehicle-to-grid Demonstration: Final Project Report*, 2017.
- [34] N. DeForest, J.S. MacDonald, D.R. Black, Day ahead optimization of an electric vehicle fleet providing ancillary services in the Los Angeles Air Force Base vehicle-to-grid demonstration, *Appl. Energy* 210 (2018) 987–1001, <https://doi.org/10.1016/j.apenergy.2017.07.069>.
- [35] P.B. Andersen, S.H. Toghroljerdi, T. Meier Sørensen, B.E. Christensen, J.C. Morell Lodberg Høj, A. Zecchino, *The Parker Project: Final Report*, 2019.
- [36] M. Marinelli, S. Martinenas, K. Knezović, P.B. Andersen, Validating a centralized approach to primary frequency control with series-produced electric vehicles, *J. Energy Storage* 7 (2016) 63–73, <https://doi.org/10.1016/j.est.2016.05.008>.
- [37] A. Thingvad, S. Martinenas, P.B. Andersen, M. Marinelli, O.J. Olesen, B. E. Christensen, Economic comparison of electric vehicles performing unidirectional and bidirectional frequency control in Denmark with practical validation, in: 2016 51st International Universities Power Engineering Conference (UPEC), IEEE, 2016, pp. 1–6.
- [38] S. Hashemi, N.B. Arias, P. Bach Andersen, B. Christensen, C. Traholt, Frequency regulation provision using cross-brand bidirectional V2G-enabled electric vehicles, in: 2018 IEEE International Conference on Smart Energy Grid Engineering (SEGE), IEEE, 2018, pp. 249–254.
- [39] N. Bañol Arias, S. Hashemi, P.B. Andersen, C. Traholt, R. Romero, V2G enabled EVs providing frequency containment reserves: field results, in: 2018 IEEE International Conference on Industrial Technology (ICIT), IEEE, 2018, pp. 1814–1819.
- [40] A. Thingvad, C. Ziras, M. Marinelli, Economic value of electric vehicle reserve provision in the Nordic countries under driving requirements and charger losses, *J. Energy Storage* 21 (2019) 826–834, <https://doi.org/10.1016/j.est.2018.12.018>.
- [41] N. Bañol Arias, S. Hashemi, P.B. Andersen, C. Traholt, R. Romero, Assessment of economic benefits for EV owners participating in the primary frequency regulation markets, *Int. J. Electr. Power Energy Syst.* 120 (2020), 105985, <https://doi.org/10.1016/j.ijepes.2020.105985>.
- [42] C. Randall, Nissan V2G project in Germany shows results, Available from, <https://www.electrivedrive.com/2019/01/29/v2g-project-in-germany-shows-results/>, April 21, 2020.
- [43] M. Hinterstocker, M. Müller, T. Kern, A. Ostermann, P. Dossow, C. Pelling, et al., Bidirectional Charging Management - Field Trial And Measurement Concept for Assessment of Novel Charging Strategies, 2019. Dublin.
- [44] T. Kern, P. Dossow, S. von Roon, Integrating bidirectionally chargeable electric vehicles into the electricity markets, *Energies* 13 (21) (2020) 5812, <https://doi.org/10.3390/en13215812>.
- [45] C. Schaudwet, E-Autos als Netzpuffer: Next Kraftwerke kooperiert mit Tennet und Jedlix, Available from, <https://bizz-energy.com/e-autos-als-netzpuffer-next-kraftwerke-kooperiert-mit-jedlix>, April 21, 2020.
- [46] J. Aengenvoort, Next Kraftwerke and Jedlix launch initiative to use electric car batteries for grid stability, Available from, <https://www.next-kraftwerke.com/news/next-kraftwerke-jedlix-launch-initiative-to-use-electric-car-batteries-for-grid-stability>, April 21, 2020.
- [47] A. Thingvad, L. Calearo, P.B. Andersen, M. Marinelli, Empirical capacity measurements of electric vehicles subject to battery degradation from V2G services, *IEEE Trans. Veh. Technol.* 1 (2021), <https://doi.org/10.1109/TVT.2021.3093161>.
- [48] B. Tepe, J. Figgener, S. Englberger, D.U. Sauer, A. Jossen, H. Hesse, Optimal pool composition of commercial electric vehicles in V2G fleet operation of various electricity markets, *Appl. Energy* 308 (2022), 118351, <https://doi.org/10.1016/j.apenergy.2021.118351>.
- [49] Uniper Technologies GmbH, Hochschule Ruhr West, Institute for Power Generation and Storage Systems at RWTH Aachen University. Gewerblich operierende Elektro-Kleinflotten (GO-ELK) Abschlussbericht GO ELK: Berichtszeitraum: 01.2013-06.2016. Uniper Technologies GmbH, 2016.
- [50] I Bremer F Ruecker DU Sauer. Investigation of li-ion battery state of health detection in electric vehicles - a comparison of simulation results and field measurement. In: 2016 IEEE Transportation Electrification Conference and Expo, Asia-Pacific (ITEC Asia-Pacific), p. 18–23.
- [51] F. Rücker, I. Bremer, S. Linden, J. Badedá, D.U. Sauer, Development and evaluation of a battery lifetime extending charging algorithm for an electric vehicle fleet, *Energy Procedia* 99 (2016) 285–291, <https://doi.org/10.1016/j.egypro.2016.10.118>.
- [52] F. Rücker J Bremer DU Sauer. Development and analysis of a charging algorithm for electric vehicle fleets extending battery lifetime: 2016 IEEE Transportation Electrification Conference and Expo, Asia-Pacific (ITEC Asia-Pacific) June 1-4, 2016, BEXCO, Busan, Korea. Piscataway, NJ: IEEE.
- [53] M Wietschel. Das Innovationscluster Regional Eco Mobility (REM 2030): Systemkonzepte für die urbane Mobilität von morgen. Karlsruhe.
- [54] Eurostat, *NACE Rev. 2: Statistical Classification of Economic Activities in the European Community*, 2nd ed., Office for Official Publications of the European Communities, Luxembourg, 2008.
- [55] Allgemeiner Deutscher Automobil-Club e.V. ADAC-Autotest, 2020.
- [56] Claudia Nobis und Tobias Kuhnimhof. Mobilität in Deutschland – MiD. Ergebnisbericht: Studie von infas, DLR, IVT und infas 360 im Auftrag des Bundesministers für Verkehr und digitale Infrastruktur. Bonn, Berlin.
- [57] I. Frenzel, J. Jarass, S. Trommer, B. Lenz, *Erstnutzer von Elektrofahrzeugen in Deutschland: Nutzerprofile, Anschaffung, Fahrzeugnutzung*. Berlin, 2015.
- [58] C. Eisenmann, B. Chlund, T. Hilgert, S. von Behren, P. Vortisch, *Deutsches Mobilitätspanel (MOP) – Wissenschaftliche Begleitung und Auswertungen Bericht 2016/2017: Alltagsmobilität und Fahrleistung*. Karlsruhe, 2018.
- [59] infas institut für angewandte sozialwissenschaft gmbh, *Deutsches Zentrum für Luft- und Raumfahrt e.V. Mobilität in Deutschland 2008: Tabellenband*. Bonn und Berlin; 2010.

- [60] Consentec GmbH, Description of Load-frequency Control Concept And Market for Control Reserves: Study Commissioned by the German TSOs (Ordered by 50Hertz Transmission GmbH), 2014.
- [61] F. Müsgens, A. Ockenfels, M. Peek, Economics and design of balancing power markets in Germany, *Int. J. Electr. Power Energy Syst.* 55 (2014) 392–401, <https://doi.org/10.1016/j.ijepes.2013.09.020>.
- [62] A. Khodadadi, L. Herre, P. Shinde, R. Eriksson, L. Soder, M. Amelin, Nordic balancing markets: overview of market rules, in: 2020 17th International Conference on the European Energy Market (EEM), IEEE, 2020, pp. 1–6.
- [63] National Grid ESO, Dynamic Containment: Technical Requirements, 2021.
- [64] Bundesnetzagentur für Elektrizität, Gas, Telekommunikation und Eisenbahnen. Beschluss BK6-18-006, 2018.
- [65] Bundesnetzagentur für Elektrizität, Gas, Telekommunikation und Eisenbahnen. Beschluss BK6-10-097, 2011.
- [66] F. Müsgens, A. Ockenfels, M. Peek, Balancing power markets in Germany: timing matters, *Z. Energiewirtschaft* 36 (1) (2012) 1–7, <https://doi.org/10.1007/s12398-011-0068-7>.
- [67] European Commission, Commission Regulation (EU) 2017/2195 of 23 November 2017 Establishing a Guideline on Electricity Balancing, 2017.
- [68] H. Hesse, M. Schimpe, D. Kucevic, A. Jossen, Lithium-ion battery storage for the grid—a review of stationary battery storage system design tailored for applications in modern power grids, *Energies* 10 (12) (2017) 2107, <https://doi.org/10.3390/en10122107>.
- [69] D. Kucevic, B. Tepe, S. Englberger, A. Parlikar, M. Mühlbauer, O. Bohlen, et al., Standard battery energy storage system profiles: analysis of various applications for stationary energy storage systems using a holistic simulation framework, *J. Energy Storage* 28 (2020), 101077, <https://doi.org/10.1016/j.est.2019.101077>.
- [70] Deutsche Übertragungsnetzbetreiber. Anforderungen an die Speicherkapazität bei Batterien für die Primärregelleistung, 2015.
- [71] German Transmission Grid Operators: 50 Hertz, Amprion, Tennet, TransnetBW. Präqualifikationsverfahren für Regelreserveanbieter (FCR, aFRR, mFRR) in Deutschland ("PQ-Bedingungen"), 2020.
- [72] Deutsche Übertragungsnetzbetreiber, Mindestanforderungen an die Informationstechnik des Reservenanbieters zur Erbringung von Regelreserve, 2019.
- [73] B. Tepe, J. Figgener, S. Englberger, A. Jossen, D. Uwe Sauer, H. Hesse, Analysis of optimally composed EV pools for the aggregated provision of frequency containment reserve and energy arbitrage trading, in: 5th E-mobility Power System Integration Symposium (EMOB 2021), Institution of Engineering and Technology, 2021, pp. 175–180.
- [74] A.G. Volkswagen, Power Day: Volkswagen presents technology roadmap for batteries and charging up to 2030, Available from, <https://www.volkswagenag.com/en/news/2021/03/power-day-volkswagen-presents-technology-roadmap-for-batteries.html>.
- [75] Wallbox UK Ltd, Quasar bidirectional charging station, Available from, http://www.wallbox.com/en_uk/quasar-dc-charger.
- [76] Besserladen.de, Wallbox Quasar, Available from, <https://besserladen.de/produkt/wallbox-quasar-bidirektionale-ladestation/>.
- [77] B.V. Jedlix, Generate earnings based on when you charge your EV, Available from, <https://www.jedlix.com/en/blog/generate-revenues-with-the-charging-moment-of-your-ev/>.
- [78] J. Münderlein, M. Steinhoff, S. Zurmühlen, D.U. Sauer, Analysis and evaluation of operations strategies based on a large scale 5 MW and 5 MWh battery storage system, *J. Energy Storage* 24 (2019), 100778, <https://doi.org/10.1016/j.est.2019.100778>.
- [79] German Transmission Grid Operators: 50 Hertz, Amprion, Tennet, TransnetBW. Eckpunkte und Freiheitsgrade bei Erbringung von Primärregelleistung, 2014.
- [80] Verband der Netzbetreiber – VDN, e.V. Transmission Code 2007, 2007. Berlin.

4.2 Optimal pool composition of electric vehicles in various vehicle-to-grid applications

This section presents the research paper entitled *Optimal pool composition of commercial electric vehicles in V2G fleet operation of various electricity markets* [2]. For the provision of balancing power or for arbitrage trading on the electricity markets, EVs must be combined in pools. This is because the power required on these markets often cannot be provided by individual vehicles alone. Aggregators who are considering potential EVs for their pool have various options. They can approach large companies, such as the postal service, and include all of the company's EVs in the pool. The fleets of large companies may already be large enough to provide FCR, for example. In addition, there are many smaller companies that only own a few EVs. Aggregators could now blindly add the EVs of any small company to the pool and equip them with bidirectional charging stations. However, it can happen that the vehicles are on the road a lot and can only rarely support the pool. This is where this section comes in: If they know the driving behavior of commercial vehicles, can aggregators compile their pools in a smart way and only include those vehicles in the pool and equip them with a bidirectional charging station that represent significant added value for the pool?

This section is based on the power and energy capability profiles of 468 commercial EVs from various economic sectors from section 4.1. The aim of the optimization in this section is to identify pool compositions that maximize the revenue per participating vehicle in different markets. Since this is a non-linear optimization problem with discrete decision variables, genetic algorithms are used to maximize the revenues per vehicle in the FCR, intraday arbitrage and day-ahead arbitrage markets. Accordingly, only vehicles are included in the pool that increase the potential revenue to such an extent that the revenue per vehicle increases. The achievable revenue with an optimized profile combination is then compared with randomly compiled vehicle pools. Furthermore, the influence of V2G provision on battery degradation is examined in the SimSES simulation tool using one specific driving profile. For this purpose, the daily driving behavior of one commercial EV is repeated over several years to estimate the degradation.

The research questions answered in this section are:

1. Can aggregators of EV pools gain a competitive advantage through smart selection of vehicles?
2. How large are potential revenues in various electricity markets for random and for optimized pools?
3. Which markets are more interesting: balancing power or arbitrage?
4. What is the influence of dual use on battery degradation?
5. Could potential revenues from V2G participation cover the cost of additional degradation?

The results of the work show that aggregators can gain competitive advantages through smart pool composition. In detail, the revenue per vehicle can be increased by up to seven times through optimized pool composition compared to random pools. Randomly composed EV pools would have generated an average of just under 220 € per EV and year. For the calculation, the average price between July 2020 and December 2020 is calculated for each 4-hour time slice of the week. The annual revenue is then estimated from the weekly revenue. The reduction in annual revenues compared to the previous section is due to the fact that different time periods are considered. From July 2020 to December 2020, the time period considered in this section, FCR prices were significantly lower than between January 2021 and March 2022. In the previous section the FCR prices of the time period between

July 2020 and March 2022 were used. This larger data set in the previous section is due to delays in the publication process and the reviewers' requirements to use the latest FCR prices. The large differences again show the difficulty of comparing results of the economic V2X potential from different publications. Nevertheless, it is possible to make a comparison within a work, for example between randomly composed and optimized pools. The optimized pools in this work would have generated 378 € per vehicle and year, which corresponds to an increase of 72 % compared to the randomly composed pools. Another result of this section is that the FCR market would have been more attractive in 2020 than arbitrage trading on the intraday or day-ahead market. An exemplary simulation and subsequent ageing analysis shows that the V2G revenue can cover the battery ageing costs. Whether the revenue from V2G can cover the total costs depends on the specific costs for metering units, bidirectional charging points and aggregators.

The optimized vehicle pools created in this section are evaluated in section 4.3 with regard to their battery capacity and their economic sector. In addition, section 4.3 examines what further flexibilization of the FCR market in terms of minimum bid size and increment would mean for the optimal pool composition and potential revenues. Moreover, the influence of V2X provision on battery degradation is examined in chapter 5 on a larger scale and not just on the basis of one vehicle.

Author contribution

Benedikt Tepe was the principle author tasked with coordinating and writing the paper and developing the methodology of the optimization. Jan Figgenger developed the arbitrage trading algorithm and focused on data acquisition. Stefan Englberger supported in the development of the optimization algorithms. Dirk Uwe Sauer and Andreas Jossen contributed via fruitful scientific discussions and reviewed the manuscript. Holger Hesse reviewed the manuscript and gave valuable input throughout the manuscript preparation. All authors discussed the data and commented on the results.

Optimal pool composition of commercial electric vehicles in V2G fleet operation of various electricity markets

Benedikt Tepe, Jan Figgenger, Stefan Englberger, Dirk Uwe Sauer, Andreas Jossen and Holger Hesse

Applied Energy, Volume 308, 2022

Permanent weblink:

<https://doi.org/10.1016/j.apenergy.2021.118351>

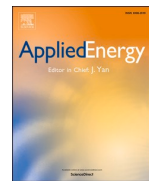


Reproduced under the terms of the Creative Commons Attribution 4.0 License (CC BY, <http://creativecommons.org/licenses/by/4.0/>), which permits unrestricted reuse of the work in any medium, provided the original work is properly cited.



Contents lists available at ScienceDirect

Applied Energy

journal homepage: www.elsevier.com/locate/apenergy

Optimal pool composition of commercial electric vehicles in V2G fleet operation of various electricity markets

Benedikt Tepe^{a,*}, Jan Figgner^{b,c,d}, Stefan Englberger^a, Dirk Uwe Sauer^{b,c,d}, Andreas Jossen^a, Holger Hesse^a

^a Institute for Electrical Energy Storage Technology, Technical University of Munich (TUM), Germany

^b Institute for Power Electronics and Electrical Drives (ISEA), RWTH Aachen University, Germany

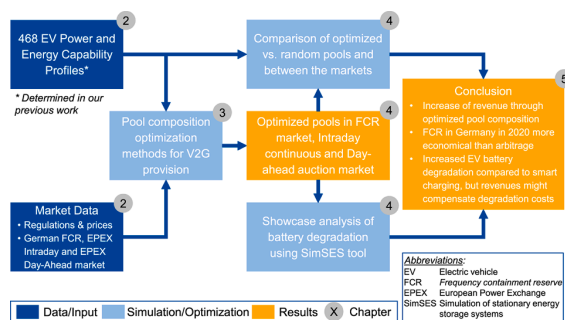
^c Institute for Power Generation and Storage Systems (PGS), E.ON ERC, RWTH Aachen University, Germany

^d Juelich Aachen Research Alliance, JARA-Energy, Germany

HIGHLIGHTS

- Methodology to optimize commercial EV pool composition for V2G services.
- Simulation of EV pooling to provide balancing power (FCR) and arbitrage trading.
- Optimized pool composition enables an increase in revenue per EV of up to 7-fold.
- Showcase analysis of battery-specific costs arising from degradation in V2G.

GRAPHICAL ABSTRACT



ARTICLE INFO

Keywords:

Electric vehicles (EVs)
 Vehicle-to-grid (V2G)
 Optimized profile combination
 Vehicle fleet
 Dual use
 Grid services
 Frequency containment reserve (FCR)
 Intraday market
 Day-ahead market

ABSTRACT

The market ramp-up of electromobility is shifting vehicle-to-grid (V2G) issues into the focus of research and industry. Electric vehicles (EVs) have the potential to support the trend towards renewable energies in their role as storage units during idle times. To participate in balancing power and energy markets, EVs are pooled via aggregators. Instead of a random composition, aggregators can smartly compose their pools and add only those vehicles that actually contribute to the pool's performance, gaining advantages over competitors. The optimization methods presented in this paper form optimized pool combinations based on the power and energy capability profiles of commercial EVs. Genetic algorithms are used to determine the revenues of the possible pools per participating EV. The use cases analyzed are the provision of balancing power on the frequency containment reserve (FCR) market of Central Europe and energy arbitrage trading on the European power exchange intraday continuous and day-ahead auction spot markets. The results show that through smart pool composition, an aggregator can increase revenue per vehicle by up to seven-fold across the markets compared to randomly assembled pools. In the Central European market, for example, the potential V2G revenues on the FCR market (380 €) exceeded those of arbitrage trading (28 € – 203 €) in 2020. In a simulation, we show the

* Corresponding author at: Institute for Electrical Energy Storage Technology, Technical University of Munich (TUM), Arcisstr. 21, 80333 Munich, Germany.
 E-mail address: benedikt.tepe@tum.de (B. Tepe).

<https://doi.org/10.1016/j.apenergy.2021.118351>

Received 9 July 2021; Received in revised form 12 November 2021; Accepted 5 December 2021

Available online 17 December 2021

0306-2619/© 2021 The Authors. Published by Elsevier Ltd. This is an open access article under the CC BY license (<http://creativecommons.org/licenses/by/4.0/>).

increased degradation of the vehicle battery in V2G operation compared to sole use for mobility with a smart charging strategy. However, the additional revenue can make V2G financially worthwhile, depending on costs for measuring equipment, bidirectional charging stations, and aggregator costs.

Abbreviations	
BSS	Battery storage system
BTM	Behind-the-meter
CESA	Continental European Synchronous Area
EEX	European Energy Exchange
EFC	Equivalent full cycles
ENTSO-E	European Network of Transmission System Operators for Electricity
EOL	End of life
EPEX	European Power Exchange
ERCOT	Electric Reliability Council of Texas
EV	Electric vehicle
FCR	Frequency containment reserve
FTM	Front-of-the-meter
GA	Genetic algorithm
NACE	European Classification of Economic Activities
NMC	Nickel-Manganese-Cobalt
PGS	Institute for Power Generation and Storage Systems
RQ	Research question
RWTH Aachen University	Rheinisch-Westfälische Technische Hochschule Aachen
SimSES	Simulation of stationary energy storage systems
SOC	State-of-charge
SOE	State-of-energy
TSO	Transmission system operator
V2G	Vehicle-to-grid
WPC	Wasted power capability

1. Introduction

The ongoing shift from conventional, centralized energy producers to renewable, decentralized energy producers in Germany has become known worldwide as the “Energiewende” [1,2]. An ambitious goal now being pursued globally is the transformation of transportation from internal combustion engines to electrically powered vehicles. Worldwide, 10 million EVs were already in use at the end of 2020 [3]. The German government, for example, plans to have 7 to 10 million electric vehicles (EV) on German roads by 2030 [4]. The vehicles’ storage capacities offer an exceptionally large potential: 7 million EVs with an average assumed energy capacity of 50 kWh have a total capacity of 350 GWh. If each EV were connected to the grid with an average power of 11 kW, the maximal total available power would be 77 GW, which corresponds approximately to the maximum electricity demand in Germany in 2019 [5]. Thus, on the one hand, if all EVs charged simultaneously at the time of the peak load, the peak load could double. On the other hand, the EVs could provide power to cover the entire load in Germany for a short time. Since, for example, German private vehicles are parked 97 % of the time, the additional use of vehicles to provide power for the electricity grid in the form of V2G is a promising approach [6]. This additional use of EV batteries can provide economic benefits to the owner through lower total costs of ownership [7]. Furthermore, from a national economic perspective, a higher utilization rate results in a more efficient use of resources. In this context, the use of EVs via V2G could reduce the

number of required stationary storage systems [8].

Alongside the concept of second life, or second use, there is another, more recent concept: dual use [9,10]. In dual use, the vehicle is used alternately for mobility and for V2G applications over periods of minutes, hours, and days. The priority here is mobility for the vehicle owner. Only free capacities are used in dual use to serve other applications by means of V2G. The power that an EV can charge and discharge is usually not sufficient to participate in balancing power markets and spot markets. For this reason, aggregators, which bundle the capacities of individual EVs in pools, emerge [11,12]. These so-called virtual power plants can then participate together in those markets [13].

In order to gain competitive advantages, aggregators could assemble their pools as efficiently as possible and not accept vehicles randomly. The optimization methods presented in this paper can help them to assemble their pools in the most efficient way. Knowing the driving profiles of the possible participants, aggregators can use the optimization methods as a basis for assembling their pools in such a way that each participating vehicle actually contributes. Without knowledge of the profiles, aggregators should measure or estimate the EV by known vehicles with similar characteristics before including it in the pool. In this way, the economic attractiveness of potentially adding an EV can be estimated.

Fig. 1 gives an overview of the present work. We used driving data of 468 EVs to determine power and energy capability profiles, that were presented in detail in a previous paper [10]. In this work, we use the profiles together with market data in the optimization methods. The markets considered here are the frequency containment reserve (FCR) market in central Europe, as well as the EPEX day-ahead auction and intraday continuous market. In the optimization, the revenue per participating vehicle of the pool is maximized. Consequently, only vehicles that make an essential contribution to the marketable pool power are included in the pool.

In the following, we first summarize existing literature on V2G and EV fleet operation. Afterwards, we describe the scenario considered in this work.

1.1. Summary of existing literature

Since the turn of the century, the research field of electric vehicles and, in particular, the V2G sub-area has attracted much interest [14,15]. Thereby, it was shown that the use of EVs in electricity markets is

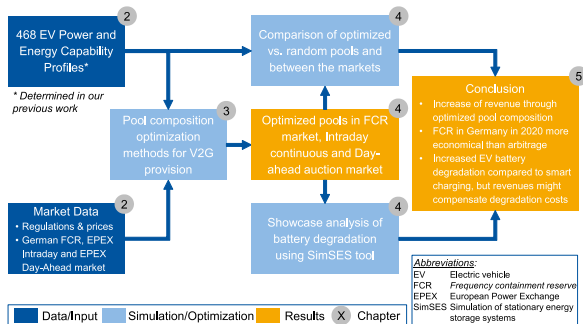


Fig. 1. Graphical overview of this work.

Table 1Summary of literature about **simulation and optimization** of trading on spot markets with EV fleets.

Source	Date	Focus	Results
Bessa [34]	2011	Optimization of an aggregated EV fleet trading in the Iberian day-ahead market and providing secondary reserve in the Iberian ancillary services market.	<ul style="list-style-type: none"> - Optimized bidding reduces charging costs compared to naïve charging. - The additional provision of positive and negative secondary reserve is economically even more worthwhile.
Schuller [35]	2014	Simulation and economic comparison of smart V2G vs. smart unidirectional vs. as-fast-as-possible charging considering degradation.	<ul style="list-style-type: none"> - Smart charging strategies decrease charging costs by a minimum of 32 % (employees' driving profile) to 51 % (retirees' driving profile) in the considered scenario compared to charging the EV as fast as possible. - Adding V2G capability leads to reduced costs of 39 % to 45 % (employees driving profile). - V2G can be beneficial, but regulatory incentives are required.
Kiaee [36]	2015	Calculation of possible savings by clever charging of EV including V2G.	<ul style="list-style-type: none"> - Allowing V2G and using a smart control strategy reduces charging costs by 13.6 % compared to using only unidirectional charging.
Sánchez-Martín [37]	2015	Development of a stochastic programming model to optimize charging process of EV from day-ahead and intraday market and provision of regulating reserves.	<ul style="list-style-type: none"> - Energy costs for charging EVs can be reduced by 1 % to 15 % depending on price spreads and other characteristics analyzed in case studies.
Shang [38]	2016	Creation of a stochastic optimization model to investigate the profitability of electricity arbitrage with PHEV.	<ul style="list-style-type: none"> - Owners of PHEVs cannot generate additional revenue through arbitrage when considering battery degradation even when assuming optimistic future costs. - Reducing the costs of battery degradation or combination arbitrage with various applications could make arbitrage trading profitable.
Guo [26]	2017	Development of a bidding strategy for an aggregator of EVs to participate in the day-ahead market.	<ul style="list-style-type: none"> - Developed bidding strategies improve handling of risks in day-ahead markets. - V2G only worthwhile if costs for discharging and distribution tariff are reduced.
Giordano [27]	2020	Optimization of day-ahead charging of an EV pool developing completely automated aggregator.	<ul style="list-style-type: none"> - Aggregator costs can be reduced by up to 57 % when applying V2G energy arbitrage in the Italian day-ahead market compared to no V2G without restricting EV users.
Zheng [39]	2020	Optimal bidding strategy in the day-ahead market is developed.	<ul style="list-style-type: none"> - Stochastic optimization model maximizes aggregator's revenues involving multiple agent modes.

basically possible, but that there are still regulatory restrictions [16,17]. These lead to economic uncertainty regarding possible business cases [14,15]. In addition, increased battery degradation and lack of aggregation concepts were identified as technical barriers to the widespread implementation of V2G in 2017 [14,18]. Here, the increase in degradation depends largely on the energy throughput and is sensitive to the charging strategy, as Bishop et al. discovered in 2013 [19]. Petit et al. showed an increase in degradation in 2016 for LFP and NCA based lithium ion batteries [20].

There are also social obstacles: From the perspective of EV owners, a guaranteed minimum range and their range anxiety are the greatest influencing factors on the willingness to participate in V2G [21,22]. Nevertheless, V2G offers great potential: In recent years, much progress has been made in battery research and battery costs have been gradually reduced [16,23]. In addition, V2G has been tested in many field tests [24,25]. Moreover new aggregator concepts have been developed [26,27]. Therefore, the authors expect V2G to become relevant to a considerable extent in the future.

For the provision of V2G, various electricity and power markets are of interest [16,28]. The focus of this work lies in the FCR market and the participation in European Power Exchange (EPEX) spot markets for arbitrage trading. Other methods sufficiently considered in research are for example the optimized charging of EVs [29,30].

The provision of balancing power using EVs was shown to be feasible in various field tests [24,25]. Moreover, optimization algorithms have been developed to improve performance [31], and economic analyses have been carried out to estimate possible revenue [32,33]. We published an in-depth review of the literature on performing frequency regulation with EVs in our previous work [10].

Two other markets in which pools of EVs can participate are part of the EPEX spot market. The markets analyzed in this paper are the day-ahead auction market and the intraday continuous market used for energy arbitrage. Algorithms that maximize energy arbitrage revenues using stationary battery storage systems (BSSs) have already been developed [40,41]. Others do not only include BSS, but also wind and photovoltaic into virtual power plants optimizing profits from arbitrage trading [42]. According to a study, the profitability of arbitrage trading

depends more on technical parameters such as efficiency and self-discharge than on price volatility [43]. Furthermore, the consideration of battery degradation has a major impact on profitability [41]. One study has shown that it can reduce revenues by 12–46% [44]. Another publication analyzing the US American ERCOT market showed that increasing calendar life of lithium-ion BSS provides greater benefits than increasing cycle life while energy arbitrage trading [45].

The pooling of EVs by means of an aggregator also offers the possibility of participating in arbitrage trading [11]. Table 1 gives an extract of publications on simulation and optimization of trading on spot markets with EV fleets sorted by publication year. Several research works showed that optimized bidding in the spot markets reduces charging costs for an EV fleet [35,36]. Shang et al. investigated the profitability of arbitrage using plug-in hybrid vehicles and showed that it is not economical considering battery degradation [38]. Giordano et al. showed that using V2G aggregator costs of day-ahead market charging of EV fleets could be reduced without restricting EV owners [27]. Zhou et al. developed scheduling models for EV charging regarding dynamic electricity prices and inconvenience for the EV owners [46].

When using EVs to provide balancing power or arbitrage trading, the uncertainty of vehicle availability should be considered. Therefore, Tuhnitz et al. modeled smart charging strategies by applying reinforcement learning to EV fleets relieving grid congestion [47]. The comparison with optimization-based strategies showed that their strategy could better handle uncertainties such as spontaneous trips. The individual driving behavior of EV owners in the pool determines the total available capacity and power [48]. For example, Han et al. estimated the achievable power capacity of EVs using probability density functions in 2011 [49]. Fluhr et al. developed a stochastic model to estimate the availability of EVs for the provision of grid balancing services [50]. They concluded that at least 90 % of all EVs are parked (anywhere) at all times and more than one quarter is parked at home.

Aside from the optimized bidding strategies and the field tests for providing FCR and arbitrage with EVs, the power capability profiles of individual vehicles have received little to no attention in research. These power capability profiles indicate how much power a vehicle can currently charge or discharge in addition to its primary use, which is

Table 2
Fleet categories and scenario considered in this work (commercial, <50 EVs).

Category	Description	Fleet Size	Example
Private	Cars in private ownership	typically 1-2	Private households
Private + Commercial	Cars used for private and commercial mobility	variable	Employees in field service
Commercial	Company cars	< 50 EV > 50 EV	Small and Medium-sized companies Postal services

Table 3
Market characteristics of the markets considered in this work.

	Frequency containment reserve (FCR) [57]	Intraday continuous market [60]	Day-ahead auction market [60]
Market Direction	ancillary service bidirectional obligatory	energy unidirectional & bidirectional possible (buy or sell)	energy unidirectional & bidirectional possible (buy or sell)
Provision time	15 min (to be activated in < 30 s)	minimum 15 min	minimum 1 h
Time sectioning	4 h	15 min	1 h
Minimal bid	1 MW (Demand in Germany in 2020: 573 MW)	0.1 MW (0.025 MWh)	0.1 MW (0.1 MWh)
Minimal increment	1 MW	0.1 MW	0.1 MW
Remuneration	market-clearing price (power)	pay-as-bid price (energy)	market-clearing price (energy)
Typical price range in 2020	~ 30 €/MW/4h	~ 10–60 €/MWh	~ 20–50 €/MWh
Tendering	8 a.m. (D-1)	from 3p.m.(D-1) up to 5 min before power provision	12 a.m. (D-1)

mobility or its charging [10]. Although driving profiles have received strong attention in the literature and have been analyzed, for example, in [35,51], the clever composition of pools of EVs has not yet been considered in depth. To the best of our knowledge, the targeted inclusion or rejection of vehicles to compose the most efficient vehicle pools for different markets has not been explored in more detail. With our work of optimized pool composition based on capability profiles, we aim to address this research gap. The methods presented can help aggregators to increase their profitability and gain competitive advantages. We consider the FCR market and arbitrage trading on the EPEX Spot markets intraday continuous and day-ahead auction. In detail, we would like to answer the following research questions (RQs) in the course of the paper:

- RQ1) Can aggregators of EV pools gain a competitive advantage through smart selection of vehicles? (Section 4.1)
- RQ2) How large are potential revenues in various electricity markets for random and for optimized pools? (Section 4.1)
- RQ3) Which markets are more interesting: balancing power or arbitrage? (Section 4.1)
- RQ4) What is the influence of dual use on battery degradation? (Section 4.2)
- RQ5) Could potential revenues from V2G participation cover the cost of additional degradation? (Section 4.2)

1.2. Scenario

Fleets of vehicles generally exist in different sizes. In this work, we distinguish between the categories (1) private households and (2)

industries (see Table 2). Private households usually own one or two vehicles, rarely a few more. The size of fleets with vehicles that are used in combination for private and commercial purposes can vary significantly. Commercially used vehicles of small and medium-sized companies form fleets of typically up to 50 vehicles¹. In contrast, fleets of large companies or companies that operate in the transport or postal sector consist of up to several hundred vehicles. These large fleets can participate independently in power and energy markets because they meet minimum bid sizes. The vehicles considered in this work for dual use are fleets of small and medium-sized companies. For these fleets, a separate participation in electricity markets is only conditionally worthwhile. A smart charging of EVs by trading on the intraday continuous market would be possible, for example. In contrast, arbitrage trading or the provision of balancing power is only possible with larger or combined fleets. Thus, in this work, we combine EVs of these small and medium-sized companies into larger pools of up to 468 EVs.

The optimization methods presented in this work form pools of vehicles based on the power capability profiles of EVs of small and medium-sized companies. The objective is to maximize the revenue per participating vehicle. Thus, the highest possible revenue with the lowest number of vehicles is searched for. Aggregators who are able to forecast the driving profiles of their potential vehicles can use the algorithms presented in this work. Alternatively, aggregators could measure EVs over a period of, for example, two weeks before deciding to include them in the pool. This way, they can only include those vehicles in their pool and equip them with bidirectional charging stations that add value to their pool. Consequently, they would only offer participation in the virtual power plant to these vehicles and would therefore only reward these EVs financially. In contrast, aggregators could blindly assemble their pools. For this reason, we will compare the optimized pools with randomly assembled pools of the same number of vehicles. In principle, total aggregator revenues increase as the number of EVs in the pool increases. Thus, in a large market of possible EVs in the future, aggregators would not limit themselves to the maximum number of 468 EVs used in this work. However, the methodology is also applicable to more EVs leading to higher efficiencies compared to random pool compositions.

Another potential use of the algorithm is the retrofitting of only a few vehicles of large fleets from combustion engines to electric drives. These vehicles to be retrofitted could be selected according to their potential to participate in electricity markets considering their driving profiles.

In this paper, we assume that EVs will be mostly V2G capable in the future. Some car manufacturers, such as Nissan, already sell V2G-capable vehicles [15]. Furthermore, BMW and Renault, for example, are testing V2G in research projects [52,53]. Volkswagen has also announced plans to introduce bidirectional charging for its vehicles [54]. Other stakeholders include transmission system operators that have already recognized the potential of V2G flexibilities and grid support and are planning to adapt market rules accordingly [55].

Furthermore, we first maximize the potential revenues EVs can generate in the various markets. However, the additional degradation costs of the vehicle battery can be significant depending on the control algorithms [18,56]. Degradation of EV batteries has shown to be the greatest concern of EV owners when participating in V2G [21]. Thus, we investigate the additional degradation of the vehicle batteries in dual use using an exemplary driving profile in Section 4.2. In this work, costs for equipping the participating vehicles with smart metering devices and bidirectional charging stations are neglected, since these costs are incurred per vehicle and therefore reduce the revenues per vehicle of optimized pools as well as the random pools equally. After the presentation of the scenario, the following chapter deals with the basic data of the work.

¹ The limit of 50 vehicles is not fixed, but only represents the order of magnitude and separates the categories.

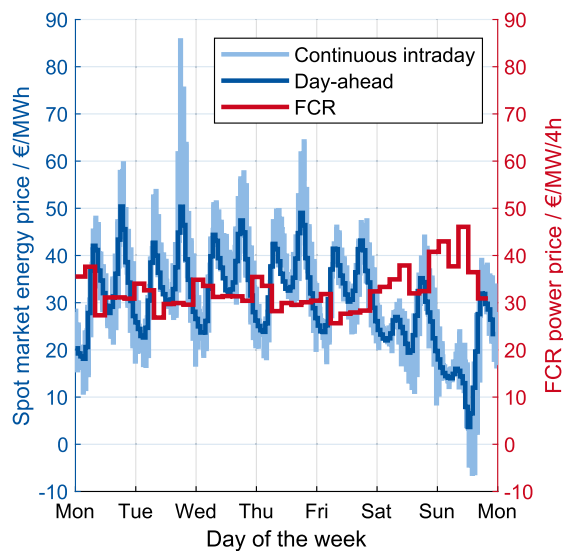


Fig. 2. Average weekly prices in 2020 for a) EPEX intraday continuous (weighted average pay-as-bid price), b) EPEX day-ahead auction (market-clearing price) and c) frequency containment reserve (FCR) provision in Germany (market-clearing price).

2. Database

This chapter describes the database of the present work. For this purpose, Section 2.1 explains the rules of the electricity markets under consideration. In addition, we present and analyze the price data of the markets. Section 2.2 presents the EV data. There, we describe the basis of the driving data and how profiles for the optimal pool composition are obtained from these data.

2.1. Electricity market rules and price data

This chapter presents the three markets identified in the literature research as potential areas of application for EVs. These include the FCR market as an ancillary service market and the two spot markets of (a) the intraday continuous market and (b) the day-ahead auction market. Table 3 provides an overview of the most important market characteristics and Fig. 2 depicts the weekly average prices for all markets. The respective subsections refer to both the characteristics and the price developments. Since this paper does not include bidding strategies, exclusively average prices are discussed.

2.2. Frequency containment reserve market (FCR)

FCR is the fastest of the three frequency regulation types in the Continental European Synchronous Area (CESA). Within the CESA, a total of 3,000 MW of FCR power is reserved, which is distributed among the member states according to generation capacity [57]. In 2020, Germany required 573 MW, which is tendered via the portal of the four transmission system operators (TSOs) as an anonymous tender auction and tendered according to a market-clearing power price [57]. The tendered power must be held in reserve as bidirectional power of an integer multiple of 1 MW for a time section of four hours at a time [57]. However, in accordance with the requirements of the TSOs, the permanent provision of power must only take place for 15 min in a specific call, whereby it must be possible to provide the full power after 30 s [57]. In addition, for limited energy storage such as batteries, a minimum power buffer of 25% of the FCR power must always be maintained [57]. Detailed market and price analyses can be found in [58] and [59]. The average prices were around 30 €/MWh/4h in 2020 and Sat-Sun had

higher prices than weekdays Mon-Fri (see Fig. 2).

2.3. Intraday continuous market

In the intraday continuous market, energy is traded on a quarter-hourly basis in various block sizes of minimum 15 min [60]. Supply and demand are matched in a pay-as-bid process, resulting in a variety of prices for each quarter hour. The smallest tradable unit of power is 0.1 MW [60], which means that a minimum of 25 kWh can be provided in a quarter hour. The average price shows high volatility; in 2020 average prices of over 80 €/MWh but also negative prices occurred (see Fig. 2). In general, prices ranged predominantly between 10 €/MWh and 60 €/MWh. Further information on the intraday continuous market can be found in [61].

2.4. Day-ahead auction market

On the day-ahead market, participants trade energy hourly in various block sizes of at least one hour for the following day. Unlike the intraday continuous market, supply and demand are matched together in a market-clearing price. The traded power over the traded provision time corresponds to the integer multiple of 0.1 MW [60]. From this value, it follows that the traded energy corresponds to an integer multiple of 0.1 MWh due to the minimum block size of one hour. The hourly-changing price shows less volatility than the intraday curve and was around 20 €/MWh and 50 €/MWh in 2020 (see Fig. 2). Further price information can be found in [61], which also describes the impact of the Covid-19 pandemic.

2.5. Vehicle data and capability profiles

The optimized pool composition requires profiles that describe how much power and energy a vehicle can charge or discharge at any given time. We call these profiles power capability profiles and energy capability profiles, respectively. In a previous paper, we described in detail how the power and capability profiles are determined from vehicle and driving data [10]. In this section, the most important points are briefly discussed. In addition, we explain the formation of intraday and day-ahead profiles.

The basis of this work is two databases: One being measured data from the Institute of Power Generation and Storage Systems (PGS) at RWTH Aachen University in the project “Commercially operated electric vehicle fleets (GO-ELK)” [62]. In this project, data loggers measured 22 EVs. A database from the REM 2030 (regional eco mobility) project was also used [63,64].

Using the vehicle data, we first carried out a statistical evaluation. For this purpose, probabilities for start, duration, and distance were determined over the course of the day and week. Using the statistical data of the vehicles, driving profiles were created in the second step. Afterwards, a simulation model to simulate driving profiles from the probability data was developed. As in our first work, a minimum of 30% of the capacity is reserved for spontaneous mobility. For the charging process, we used measured charging curves from the PGS at RWTH Aachen University [10].

Weekly driving profiles were simulated for each vehicle. To determine the power and energy capability profiles during parking times, we divided the respective vehicle battery virtually into energy for mobility (primary use) and freely available energy for dual use. This freely available energy over time results in the energy capability profile. The power capability profile indicates the power that a vehicle can charge and discharge at any given time when it is parked at the company site. This power depends on a) the power electronics of the EV, b) the power electronics of the charging station, and c) the available energy and the provision time over which the power must be delivered (depending on the market). Accordingly, the capability profiles for the different markets vary. At the FCR market the provision time is 15 min. The power

must therefore be provided over 15 min. The same applies to the intraday market. In the day-ahead market, in contrast, time slices are marked by the hour. This results in different capability profiles for the different markets.

Similar to our previous work, we formed profiles of 468 vehicles from the REM 2030 database. These 468 vehicles meet the following three criteria: a) the vehicle was measured over at least one week, b) the vehicle must make at least one trip, and c) the vehicle must be at the company site at least once. In our previous work, we clustered the power capability profiles according to the economic sectors. In this work, we do not cluster the profiles but use each profile separately.

In the two optimization methods presented in the next chapter, we use both the energy and power capability profiles. For the optimization of the pool composition in the FCR market, the power capability profiles of each vehicle over one week are used. For optimization in the spot markets, the energy and power capability profiles are both used. In the intraday continuous market optimization, 15-minute continuous trading and in the day-ahead auction market, 1-hour auction trading were considered. Due to the different provision times, the power capability profiles for the two markets vary, while the energy capability profiles are the same (see Section 0). In this work, we use weekly profiles because commercial vehicle profiles are relatively constant over a period of months and years.

3. Methodology

In this chapter, we present the methodology of building optimal pool compositions. Section 3.1 deals with the optimization method for balancing power markets, in our case the FCR market. Afterwards, in Section 3.2 we present the optimization method for arbitrage trading using energy and power capability profiles. In both sections, we provide examples using three EVs to show the functionality of the optimization methods.

3.1. Optimized combination of power capability profiles in balancing power markets

For optimization in balancing power markets, we use the weekly power capability profiles of the EVs introduced in Section 2.2. The goal of optimization is to maximize the revenues per EV contained in the pool. The optimizer consequently finds the optimal number of vehicles. Thereby, potential costs of the aggregation are ignored. Section 3.1.1 explains the optimization problem for the FCR market. In Section 3.1.2, we discuss the results of optimization. Afterwards, in Section 3.1.3, we present a linear optimization method with an assumed fixed number of EVs.

3.1.1. Optimization problem in balancing power markets

The optimization problem of adding EVs to a pool to maximize the revenue per EV contained in the pool is nonlinear with discrete decision variables. An EV x can be part of the pool (1) or not (0). Eq. (1) shows the optimization problem of finding the maximum FCR revenues per EV in the pool (Rev_{FCR}). The revenue depends on the decision variable \vec{x} , the price of FCR provision during each service period of a week (\vec{price}_{FCR}) and the EV power capability profiles consisting of the maximal possible charging (P_{ch}) and discharging power (P_{dis}). As weekly price curves, we use the average prices of each of the weekly 42 four-hour service periods of the second half of 2020 (see Section 2.1.1). The objective function Rev_{FCR} is calculated using Eq. (2). The decision variable \vec{x} is a column vector that can contain the values 1 (in the pool) and 0 (not in the pool). The matrices P_{ch} and P_{dis} contain the EV power capability profiles in charge and discharge directions.

In the following, the individual parts of the objective function are described:

- 1) $\vec{a} = \min(P_{ch} \bullet \vec{x}, P_{dis} \bullet \vec{x})$ calculates the minimum of the charging and discharging power capability of the composed pool at any time depending on the decision variable \vec{x} . This is done because FCR must be provided simultaneously in both directions (Section 2.1.1). Thus, the minimum possible charging and discharging power determines the power that can be offered on the FCR market. \vec{a} is then an m -dimension vector with the number of timesteps (m).
- 2) $b = \lfloor \min(a_{(i-1) \bullet 16+1, \dots, i \bullet 16}) / 1.25 \rfloor$ takes the minimum value of the pool power in the specific service period i since only the minimal appearing power can be offered during the timeslot. A week has 42 4-hour service periods and each of these service periods contains 16 values corresponding to quarter hours. Furthermore, the value is divided by 1.25, since an additional 25% of the prequalified power must be kept available for storage management activities when offering FCR (see Section 2.1.1). Accordingly, only 80% of the minimum power can be used for FCR. Afterwards, the value is rounded down to multiples of 1 MW, since only multiples of 1 MW can be traded on the FCR market. If participating in the FCR market through aggregators, smaller units of power could also be marketed, but this is not assumed at this point.
- 3) The pool minimum of each time slot is then multiplied by the mean FCR price of the service period, and the resulting revenues are summed up for the weekly 42 service periods of four hours each.
- 4) This sum is then divided by the number of vehicles and multiplied by 52 weeks per year to estimate the revenue per year and vehicle.

$$\max Rev_{FCR} \left(\vec{x}, \vec{price}_{FCR}, P_{ch}, P_{dis} \right) \quad (1)$$

$$Rev_{FCR} = 52 \cdot \frac{\sum_{i=1}^{42} Price_{FCR}^i \bullet \left[\min \left(\left[\min(P_{ch} \bullet \vec{x}, P_{dis} \bullet \vec{x}) \right]_{(i-1) \bullet 16+1, \dots, i \bullet 16} \right) / 1.25 \right]}{\sum_{j=1}^n x_j} \quad (2)$$

With:

$$\vec{x} = \begin{bmatrix} x_1 \\ x_2 \\ \vdots \\ x_n \end{bmatrix} \quad x_j \in \{0; 1\} \quad j = 1 \dots n$$

n : Number of Profiles

$$P_{ch} = \begin{bmatrix} P_{ch_1}^1 & P_{ch_2}^1 & \dots & P_{ch_n}^1 \\ P_{ch_1}^2 & P_{ch_2}^2 & \dots & P_{ch_n}^2 \\ \vdots & \vdots & \ddots & \vdots \\ P_{ch_1}^m & P_{ch_2}^m & \dots & P_{ch_n}^m \end{bmatrix}$$

$$P_{dis} = \begin{bmatrix} P_{dis_1}^1 & P_{dis_2}^1 & \dots & P_{dis_n}^1 \\ P_{dis_1}^2 & P_{dis_2}^2 & \dots & P_{dis_n}^2 \\ \vdots & \vdots & \ddots & \vdots \\ P_{dis_1}^m & P_{dis_2}^m & \dots & P_{dis_n}^m \end{bmatrix}$$

m : Number of Timesteps

$$\vec{price}_{FCR} = \begin{bmatrix} price_{FCR}^1 \\ price_{FCR}^2 \\ \vdots \\ price_{FCR}^{42} \end{bmatrix}$$

To solve the described optimization problem, MATLAB's genetic

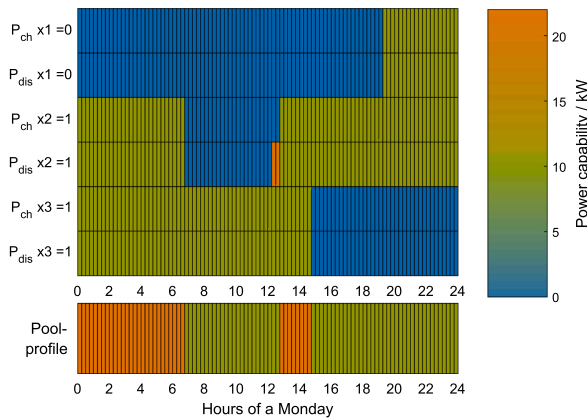


Fig. 3. Three power capability profiles (each in positive and negative directions) and their optimized pool profile for frequency containment reserve (FCR) provision.

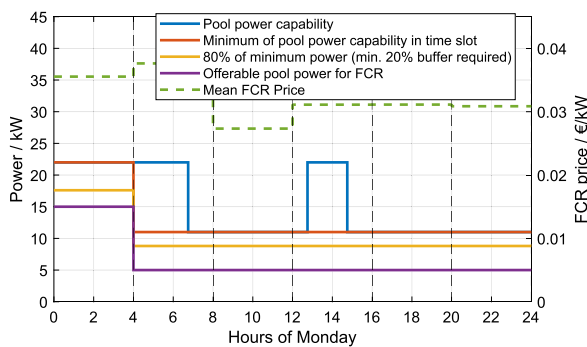


Fig. 4. Course of the pool's power capability profile, the minimum of the pool power capability in every service period and the offerable pool power for FCR for the pool of Fig. 3. Mean FCR price for the six time slots of Mondays between July 1st and December 31st 2020 from [57]. Minimum and increment: 5 kW; Revenue/EV/year: 241.5 €.

algorithm (GA) toolbox is applied [65,66]. Genetic algorithms are metaheuristic algorithms that use experience from nature to determine a feasible and well-suited solution by means of inheritance and crossing. Each new generation represents a further possible solution to the optimization problem. The optimization problems to be solved by genetic algorithms often have several local optima. For this reason, the algorithms use mutations during inheritance, so that the chance of finding a global maximum increases. Restarts at different positions also contribute to this goal. Due to their metaheuristics, genetic algorithms do not necessarily find the global optimum [66]. In 1996, genetic algorithms were already proposed in publications for metaheuristic optimization in different applications [67]. Since then, they have been further developed and are used, for example, for the optimization of hybrid generation systems consisting of photovoltaic, wind and storage systems [68,69].

The optimization problems presented in this paper are nonlinear. Adding or removing one vehicle can either increase or decrease the revenue per vehicle. MATLAB's GA can approximately solve this nonlinear optimization problem with discrete decision variables [65]. Since each of the 468 vehicles used has two possibilities (0 or 1), there are $2^{468} \approx 7.6 \cdot 10^{140}$ possible pool compositions. This number of combinations can no longer be checked manually. For this reason, in the next section the optimization is performed in a simplified way as an example with three power capability profiles for one day.

3.1.2. Results of optimization using three profiles

In this section, exemplary power capability profiles of three EVs are used (x1, x2, x3) and the pool's revenue per EV is maximized using the presented algorithm. As a condition, it was demanded here that at least 5 kW must be provided. Furthermore, increments of 5 kW are possible. For the provision of FCR, this condition will be set to 1000 kW with increments of 1000 kW. In addition, only one day is considered (Monday) at this point. The mean FCR prices for the six service periods of Mondays are used in this exemplary optimization.

In Fig. 3, the absolute values of three exemplary power capability profiles x1, x2 and x3 are depicted in positive and negative directions. EV x1 can provide 11 kW in positive and negative directions from approximately 7p.m. until midnight. EV x2 can provide 11 kW the whole day except for a time section between 6:45 a.m. and 12:45p.m. Moreover, EV x2 could provide positive power of 22 kW between 12:15p.m. and 12:45p.m. by stopping the charging process and discharging its battery instead. During those 30 min, the EV cannot provide negative power since the EV is already charging with its maximum power of 11 kW. EV x3 can provide positive and negative power of 11 kW from midnight to 2:45p.m.

The optimizer chooses the profiles x2 and x3 to be in the pool. Using those two maximizes the revenue per EV. Adding profile x1 to the pool would increase the available pool power in the service period from 8p.m. to midnight. However, the additional pool revenue would not be high enough to increase the revenue per EV, since the pool revenues had to be divided among three EV owners. For this reason, EV x1 is not used in the pool. Furthermore, the resulting pool profile shows that only the minimum amount of positive and negative power is used. Since EV x2 can provide 22 kW of positive power between 12:15p.m. and 12:45p.m., the pool would be able to offer 33 kW of positive power. However, since the negative pool power is 11 kW, the possible FCR pool power is 11 kW during those 30 min.

Fig. 4 shows the available pool power capability during Monday (blue line) and the minimum pool power in each 4-hour service period (red line). Due to the buffer of at least one fourth of the FCR power, another 20% is subtracted from this minimum (yellow line). Moreover, the figure contains the offerable pool power when providing balancing power with the described condition of a minimum and an increment of 5 kW (purple line). The pool can provide 15 kW during the first time slot and 5 kW during all others. Using the FCR prices displayed in Fig. 4 the yearly revenue per EV can be estimated. Since we made simplifications in this example, the annual revenues are not realistic in practice.

To demonstrate that the optimization method work correctly, the revenues per vehicle and year were calculated manually for all combinations of the three profiles (see Appendix Fig. A1). The diagram shows that the combination of profiles x2 and x3 leads to the highest revenue per EV.

3.1.3. Linear optimization with fixed number of vehicles

Another approach than finding the optimal number of EVs would be to specify an exact number of vehicles to be selected optimally. The genetic algorithm could receive a fixed number in a constraint. However, the metaheuristic optimization of the FCR market showed that the algorithm cannot guarantee to find the global optimum and might become stuck in a local optimum. For this reason, we created a linear optimization algorithm that uses a fixed number of vehicles as a constraint. We specified to this optimizer that it should select the best 100 EVs out of all possible EVs, for example, and maximize the revenue per vehicle.

The mixed-integer linear problem has two integer decision variables. First, the offered power that is provided from the EV pool (\vec{P}^{FCR}). Second, a binary variable (\vec{x}) that determines if a specific power capability profile is selected in the optimized vehicle pool. Depending on the defined input parameter of the number of vehicles in the optimized pool (N), the decision variables are optimized in the objective function (3)

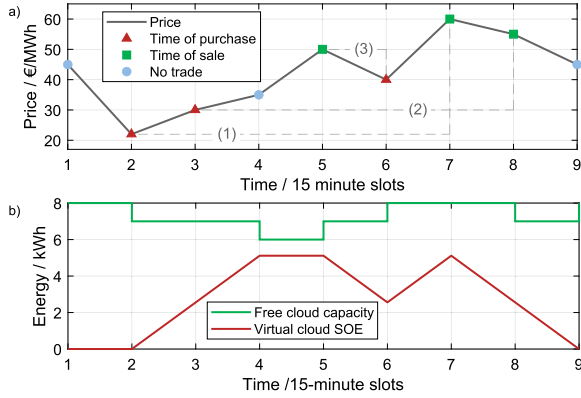


Fig. 5. Working principle of the arbitrage algorithm. a) Exemplary price curve and trading activity. b) Free cloud capacity and virtual cloud SOE curve.

and two constraints.

$$\max \sum_{i=1}^{42} P_i^{FCR} \bullet price_i^{FCR} \quad (3)$$

$$\vec{P}^{FCR} = \begin{bmatrix} P_1^{FCR} \\ P_2^{FCR} \\ \vdots \\ P_{42}^{FCR} \end{bmatrix}$$

The first constraint (4), determines that FCR power is provided in the respective 1 MW increments and that the reserve power of 25% is added when participating in the market. Since the FCR is a symmetrical product that must be provided in both positive and negative directions, the lesser of the charging and discharging power indicates the power offered.

Eq. (5) guarantees that the sum of activated EVs in the optimized vehicle fleet corresponds exactly to the defined input parameter. The sum over all participating EVs (Eq. (5)) corresponds to the denominator in the genetic algorithm (Eq. (2)). In the genetic algorithm, we divided by the sum to optimize the revenue per vehicle over all possible quantities.

$$\vec{P}^{FCR} \bullet 1MW \bullet 1.25 \leq \sum \vec{x} \bullet \min(P_{ch}, P_{dis}) \quad (4)$$

$$\sum_{j=1}^n x_j = N \quad (5)$$

The optimizers presented in this section are applied to the 468 power capability profiles in the FCR market and the results are presented in Section 4.1.

3.2. Optimization of the combination of power and energy capability profiles for arbitrage in spot markets

In this section, the optimizer for arbitrage trading on the intraday continuous and day-ahead auction market is presented. As before, we maximize the revenue per participating EV. Section 3.2.1 shows the optimization problem and explains the algorithm. Afterwards, Section 3.2.2 shows an example of arbitrage trading using three vehicles.

3.2.1. Optimization problem for arbitrage in spot markets

Arbitrage trading differs from smart charging, which is often used in the literature. In smart charging, purchases on the spot market are optimized for charging vehicles at times of low electricity costs. The arbitrage trading presented here, in contrast, is based on a free cloud

capacity. This free cloud capacity is the sum of the free capacities of all vehicles in the pool. Moreover, we calculate a virtual cloud SOE, which represents the virtual state of energy of the pool. By using only the free capacities, the primary use of the EVs is not limited. In the following, the optimization process and the algorithm for the calculation of arbitrage revenue are explained.

In principle, this optimization maximizes the revenue per participating EV. For this purpose, we use another genetic optimization algorithm that varies the composition of the pool, calls the arbitrage algorithm, and receives the revenues per participating EV. Here, taxes and fees payable by households when purchasing electricity are excluded, similar to [70]. At the beginning, we define three characteristic values: The minimum price spread in €/MWh, the one-way efficiency of charging and discharging respectively, and the minimum bid size to trade on the intraday continuous or day-ahead auction market. The minimum price spread is set at 10 €/MWh, since this significantly reduces the number of cycles that the batteries make, while barely reducing revenues [70]. As one-way efficiency, we assume 93 % in both directions based on measurements [10]. In addition, 100 kW is used as the minimum offer size and increment analogous to the EPEX Spot markets. For hourly day-ahead auction trading, this means trading in 100 kWh increments. For 15-minute intraday continuous trading, 25 kWh increments are traded. A trade will not be executed below the minimum price spread and the minimum bid size.

The arbitrage algorithm then receives the following input data:

- The three characteristic values defined beforehand (minimum price spread, efficiency, minimum bid size).
- Average 15-minute-prices of the EPEX intraday continuous market from 2020 or the 1-hour-prices of the EPEX day-ahead auction market from 2020, respectively.
- Aggregated free cloud capacity of the current composite pool in kWh for every time slot of 15 min or 1 hour, respectively.
- Power capability profile of each participating EV including distinction between grid-sided and battery-sided power weighted with the efficiency.

Since bidding strategies are not a focus of this paper, average prices for the two markets under consideration are used. The algorithm thus calculates the possible revenues on this basis and does not try to beat these average prices through bidding procedures. In general, the algorithm identifies purchase times of low prices and assigns them to high price sale times. An exemplary price development and the SOE curve resulting from arbitrage trading are shown in Fig. 5. First, the price minimum of the period under consideration is determined and is marked as the first time of purchase (Time 2). Afterwards, a possible time of sale is iteratively searched for starting with the time of highest price (Time 7). The trade is executed when:

- the virtual cloud SOE remains between zero and the maximum free cloud capacity,
- the trade exceeds the minimum price spread and the minimum offer.

If these conditions cannot be met, this potential sale time is temporarily excluded and the time of the next highest price is tested as a sale time. This method is executed iteratively until a suitable sale time has been determined. The purchase and sale times are blocked for further iterations and the temporarily excluded purchase times are released again.

A purchase at time 2 and a sale at time 7 is possible, so that combination (1) from Fig. 5 can be executed. The combination is marked by the dashed line. Next, time 8 is selected as time of sale and time 3 as time of purchase. This combination also does not violate any conditions and is therefore executed as combination (2). Subsequently, time 5 is identified as the next time of sale. The next lowest purchase price is at time 4, but since this trading would exceed the maximum virtual capacity, this time

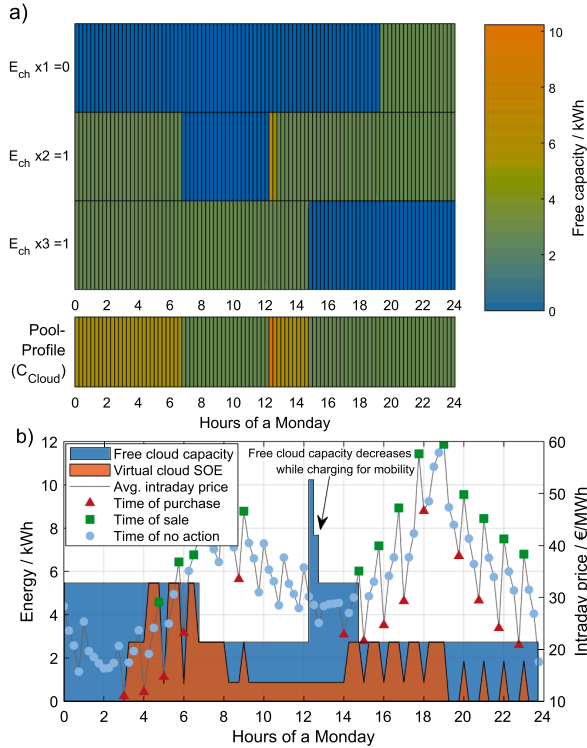


Fig. 6. a) Negative energy capabilities of three EVs in 15-minute resolution over a Monday and pool profile (free cloud capacity) in 15-minute resolution. b): Free cloud capacity and virtual cloud state-of-energy (SOE) with average intraday continuous price curve and marked prices of purchase and sale.

of purchase cannot be realized. Instead, since the virtual battery already contains energy before the sale, times of purchase after the time of sale are also permitted. Within this search, time 6 is identified as the time of purchase and time 5 is set as the time of sale (see combination (3)). A sale time that lies before its assigned purchase time retroactively changes the physical assignment of purchase and sale times, but this has no effect on the accounting. The resulting revenue is then calculated according to Eq. (6), considering the losses that occur during charging and discharging.

$$Rev_{Arbitrage} = \sum_{n=1}^{\#trades} (Price_{sale_n} - Price_{purchase_n}) \cdot P_n \cdot \Delta T \cdot \eta_{round-trip} \quad (6)$$

The optimizer then receives the resulting revenues of the current pool composition. Then, the algorithm is started with a different pool composition and its revenues are calculated. As in FCR optimization, this genetic optimization uses inheritance and mutation to change the pool composition in order to determine the optimal pool composition (see Section 3.1).

3.2.2. Results of optimization using three profiles

Similar to the FCR optimization, the spot market optimization is now presented with three exemplary profiles (x1, x2, and x3). In this example, the intraday continuous market with its 15-minutes resolution is used. The explanations are also valid for the day-ahead auction market with its 1-hour resolution. Furthermore, in this example we only consider Monday instead of the whole week, analogous to the FCR example. In addition, only this example defines 1 kWh as the minimum bid size, since the three vehicles cannot reach a bid size of 25 kWh required by the EPEX. However, the efficiency and the price spread are assumed to be 93 % and 10 €/MWh respectively, as described above.

Fig. 6 a) shows the negative energy capability profiles (energy that can be charged) of the exemplary vehicles x1, x2 and x3 in 15-minute resolution during Monday. EV x1 is on the road until 7 p.m. and can store 2.7 kWh after arrival. EV x2 is on the road between approx. 7 a.m. and 12:30 p.m. and can also store 2.7 kWh during the parking time. In addition, it can store up to 7.5 kWh for a short time after arrival at 12:30 p.m., since the vehicle battery then has a lower SOE due to the journey just completed. Vehicle x3 is connected until 2 p.m. and can store 2.7 kWh of energy at any time. The optimizer selects EV x2 and x3 for the pool so that the free cloud capacity shown corresponds to the sum of the free capacities of EV x2 and EV x3.

In Fig. 6 (b), the free cloud capacity and the virtual cloud SOE are shown. Moreover, the average Monday intraday continuous price curve is displayed (right y-axis). Purchase times are marked with a red triangle and sale times with a green square. The arbitrage algorithm determines 14 trades on Monday with the pool consisting of EV x2 and EV x3. At the times of purchase, most often 2.75 kWh are purchased on the grid side, of which 2.56 kWh are stored due to efficiency. At the times of sale, 2.38 kWh are then delivered to the grid. The revenue is finally calculated according to Eq. (6) over one year at 86.2 €. The results of the manual calculation of the intraday continuous revenue of the various combinations of x1, x2 and x3 are shown in Fig. A2. Analogous to the FCR optimization, the optimizer found the combination with the highest revenue per participating EV.

4. Results

This chapter shows the results of the optimization of the various pool compositions. Section 4.1 analyzes the weekly profiles of the optimized pools. In addition, the revenues of the optimized pools are compared with the revenues of randomly assembled pools of the same number of vehicles. Section 4.2 examines the additional degradation of EV batteries in dual use. Here, an example is used to simulate battery degradation during uncontrolled charging, primary use-oriented charging and dual use-oriented charging.

4.1. Comparison between optimized and random pools

First, the optimized pools are compared to randomly assembled EV pools. For this purpose, the optimization problems presented in chapter 3 are solved. The results are optimized pool compositions that provide maximum revenue per participating EV. In the following, the results for the provision of FCR and arbitrage trading on the intraday continuous and day-ahead auction market are presented. This is followed by an economic comparison of all markets.

4.1.1. FCR market comparison

First, the results of the optimization of pool composition in the FCR market are explained. Fig. 7 shows the accumulated weekly pool profile of one random EV pool (a) and the optimized pool (b) when providing FCR. The corresponding assumptions and the results of the optimization are presented numerically in Table 4. The achievable prices are derived from the mean values of the 42 weekly 4 h-slots of the months July to December in the year 2020. In addition, as usual in the FCR market, 1 MW was assumed as the offerable minimum power increment. The power capability profiles introduced in Section 2.2 were used for the FCR optimization.

If the annual revenue per vehicle is maximized, the optimization method selects 243 EVs, resulting in a total revenue of about 92,000€. Per participating EV, 378 € can be generated yearly. If FCR were provided 10,000 times using a random pool of 243 EVs, the total yearly revenue would on average be 53,400 €, which results in 220 € per vehicle. In this case, the standard deviation of revenue per vehicle is 9.5 €.

The power values displayed in Fig. 7 show the minimum power capability in both directions at any time, since positive and negative FCR

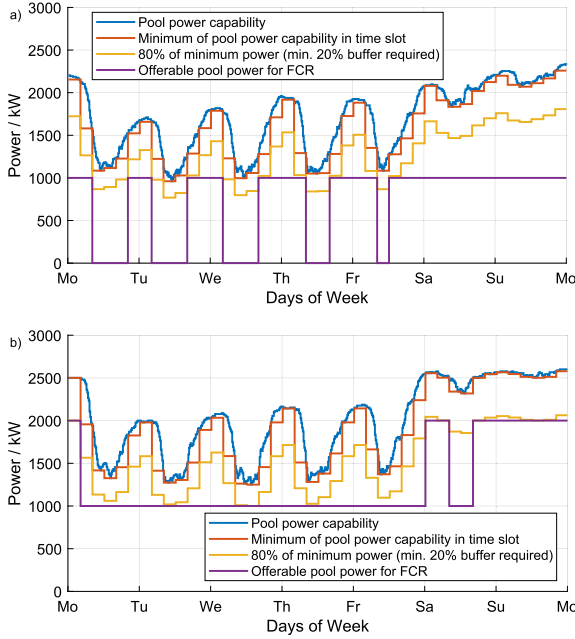


Fig. 7. Weekly pool profiles of one random pool of 243 EVs (a) and the optimized pool of 243 EVs (b) when providing frequency containment reserve (FCR). Since at least an additional 25% of the offered FCR power must be provided as buffer, 20% of the minimum pool power capability is blocked (see Section 2.1.1).

Table 4
Assumptions and results of FCR pool optimization.

Parameter	Value/ Data	
FCR prices	Average prices of 4 h-slots between July and September 2020	
Minimum bid and increment	1000 kW	
Parameter	Optimized pool	Mean of 10,000 random pools
Number of EVs		243
Power utilization rate (τ_{PUR})	62.2 %	39.3 %
Annual Pool Revenue	91,854 €	53,367 €
Annual Revenue per EV	378 €	220 €

must be supplied simultaneously (see 2.1.1). The randomly assembled pool can offer a maximum of 1 MW. Particularly during daytimes on weekdays the power that can be offered drops below 1 MW due to the required buffer of 25% of the offered power. If the composition of the pool is optimized, the pool can provide 1–2 MW to the FCR market. The pool can use its available power more efficiently, generating higher revenues per EV. During the weekdays, the pool offers 1 MW, although the pool could often offer 1.5 MW at night. On weekends, the optimized pool can offer 2 MW apart from Saturday noon. Comparing the random pool's available power and the optimized pool's power, it can be seen that the optimizer only includes the minimum required number of EVs in the pool to provide the 1 MW or 2 MW, respectively.

A parameter introduced at this point is the power utilization rate (τ_{PUR}). This value describes quantitatively how much of the possible usable power is actually used for FCR provision. For this purpose, the difference between the available power (power capability) and the offerable FCR power is calculated and scaled to the power capability (Eq. (7)). The average value is then calculated over the 672 15-minute time periods of the week and subtracted from one. Graphically, the parameter represents the mean percentage gap between the blue and purple curves from Fig. 7. At a value of one, the curves lie on top of each other, and the

entire power is used. At a value of zero, none of the possible power is used. Due to the required buffer of 25% of the FCR power (i.e., min. 20% of the power capability), the maximum achievable τ_{PUR} is 80%.

$$\tau_{PUR} = 1 - \frac{1}{672} \sum_{t=1}^{672} \frac{\text{power capability}(t) - \text{FCR power}(t)}{\text{power capability}(t)} \quad (7)$$

The values of τ_{PUR} for pool compositions of 10,000 random pools and the optimized pool are displayed in Table 4. While the random pools on average reach a τ_{PUR} of 39%, the optimized pool improves the τ_{PUR} to 62%. Consequently, the optimal pool makes better use of its potential and increases its efficiency (see Fig. 7). Thus, the usage of the V2G potential in the FCR case is increased though the optimized pool combination by almost 60%.

Since the optimizer determined the optimal number of vehicles at 243 EVs and we compared the result with a random pool of 243 EVs, in the following, the pool is composed of a fixed number of EVs. For this purpose, the linear optimization method presented in Section 3.1.3 is used. We chose a fixed number of 50 to 450 vehicles with equidistant distances of 50 vehicles to cover the spectrum between very few EVs and the maximum number of 468 possible EVs. After the optimization, 10,000 random pools with the respective fixed number were composed and the revenue per EV was determined. The results of the optimization with a variable number of EVs (orange dot), the optimization with a fixed number of EVs (blue dot) and random pools (boxplots) are depicted in Fig. 8. It turns out that an amount of 50 or 100 EVs is not sufficient to provide FCR power. From 115 EVs on, FCR can be offered in the optimal case. Random EV pools can increase their revenue per vehicle as the number of vehicles increases. This is because they can better serve the increments of 1 MW when increasing their number. Due to these increments, the revenue per vehicle is also not linear but drops briefly between 150 and 250 vehicles for the optimized pools, for example. Revenue per vehicle also appears to converge as the number increases, changing little between 350 and 450 vehicles. However, this is because 468 vehicles were considered in this analysis. If, for example, 1,000 different EVs were considered, revenues would probably not converge between 350 and 450. The optimizer achieves an increase in revenue per EV in each case. However, its advantage decreases as the number of EVs increases. Again, the small advantage of the optimizer at 450 vehicles exists because we considered 468 vehicles in total.

As shown with the genetic algorithm, the optimizer found the optimal number of EVs to maximize revenue per EV at 243 vehicles. Especially at a fixed 150 EVs, the advantage of the optimizer becomes apparent: While the random pools reach an average of 109 €/EV and a maximum of 160 €/EV, the optimizer can generate 370 €/EV. The increase in revenue corresponds to a factor of 2.3 compared to the best random case and 3.4 compared to the average of the random pools.

4.1.2. Intraday continuous market comparison

In addition to providing balancing power, EV energy can also be traded on the spot market. The optimization of arbitrage trading on the intraday continuous market that was used here was explained in Section 3.2. Executing this optimization results in an optimized pool of 48 vehicles, whose free cloud capacity and virtual cloud SOE are shown in Fig. 9 (a). By using the widest possible price spreads, areas are created where the free capacity of the vehicle batteries is not used, such as Saturday and Sunday mornings. Diagram b) of Fig. 9 shows the weekly mean weighted average price curve of the 15-minute intraday continuous prices. In addition, buy and sell times are color-coded. Thereby the algorithm uses the spread limit of 10 €/MWh shown in Table 5. Possible transactions below this threshold are not executed. Furthermore, Table 5 numerically shows the assumptions and results of intraday optimization. If the revenues per participating EV are optimized in the intraday continuous market, the optimization method selects 48 of the 468 possible EVs. These generate annual profits of 9,748 €, which corresponds to 203 € per participating EV. If the aggregator adds 48 random

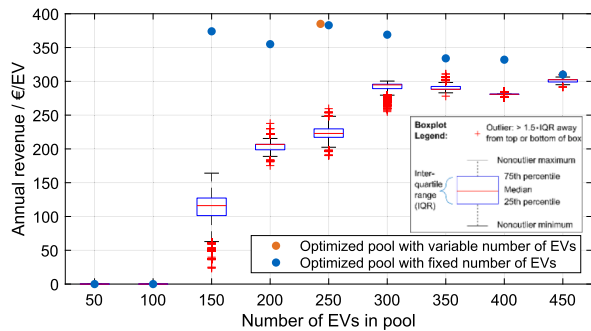


Fig. 8. FCR optimization: Annual revenue per EV when a fixed number of EVs are specified (boxplot: 10,000 random pools, dots: optimized pools).

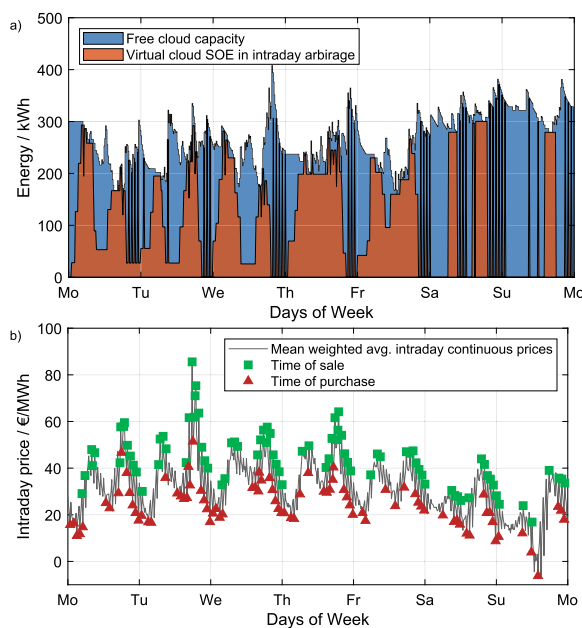


Fig. 9. Intraday continuous optimization: Free cloud capacity and virtual cloud SOE of the pool (a) and times of sale and purchase including intraday continuous prices (b).

vehicles to the pool, the total annual revenue would be 3,649 € on average, which corresponds to 76 € per participating EV (standard deviation of 8.1 €/EV).

Analogous to the FCR case, optimization including finding the optimal number was followed by optimization for a fixed number of EVs. In contrast to the FCR case, the number was given to the genetic algorithm as a constraint instead of developing a linear optimizer due to the complexity of the function. The results of the optimized (points) and the random pools (boxplots) are depicted in the same way as in the FCR case in Fig. 10.

The intraday case shows that as few as 50 vehicles can already provide arbitrage trading. Furthermore, the revenues per EV are relatively constant for random pools over all analyzed vehicle numbers between 48 € and 103 €. The optimal number of 48 EVs achieves revenues of 203 € per vehicle (orange dot). With an increasing number of vehicles, the advantage of the optimizer decreases again. For example, with 150 vehicles, the optimizer achieves annual revenues of 118 € per EV, while the random pools can only generate 77 € on average.

Table 5 Assumptions and results of intraday continuous arbitrage pool optimization.

Parameter	Value/ Data	
Intraday continuous prices	Weighted average prices of 15-minute slots on weekly basis of the year 2020	
Minimum bid and increment	0.1 MW	
Assumed efficiency	93 % one-way (86.49 % round-trip)	
Spread limit	10 €/MWh	
Parameter	Optimized pool	Mean of 10,000 random pools
Number of EVs		48
Energy bought and sold	784 MWh/678 MWh	283 MWh/244 MWh
Avg. Price of Energy bought and sold	21.77 €/MWh/39.55 €/MWh	21.92 €/MWh/40.28 €/MWh
Annual Pool Revenue	9,748 €	3,649 €
Annual Revenues per EV	203.1 €	75.9 €

4.1.3. Day-ahead auction market comparison

Arbitrage trading can also take place on the day-ahead auction market. If optimization is executed for the day-ahead market, the optimization method selects 61 EVs that maximize the revenue per EV. The resulting free cloud capacity is shown over the course of the week together with the virtual cloud SOE in Fig. 11 (a). The lower diagram shows the weekly course of the average day-ahead auction prices together with color-coded buy and sell times. Table 6 shows the numerical assumptions and results. In general, the assumptions in the day-ahead optimization were the same as in the intraday optimization. Instead of the quarter-hourly intraday continuous prices, the hourly day-ahead auction prices were assumed as the average weekly price curve. In the day-ahead arbitrage optimization, the profiles introduced in Section 2.2 were used.

In the day-ahead auction market, annual revenues for the 10,000 random pools of 61 EVs amount on average to 11 €, which is about 0.17 € per EV. The very low average revenues are because a random pool of 61 EVs often cannot do any arbitrage trading at all on the day-ahead market due to the delivery time of 1 h. Out of the 10,000 random pools, 9,413 could not generate any arbitrage revenue on the day-ahead market. The average revenue of the pools that could generate any revenue at all was 3.50 €/EV.

The selected 61 EVs of the optimizer reach around 1,700 €, which is about 28 € per EV. Due to the longer provision time of the day-ahead auction market, the arbitrage algorithm can trade far less in this market compared to the intraday continuous market and exploit fewer price spreads (Fig. 11).

Analogous to the intraday case, we analyze fixed numbers of vehicles in the following. The results of the optimization with a fixed number are depicted in Fig. 12. In contrast to the intraday continuous market, 50 EVs are not sufficient for arbitrage trading on the day-ahead market due to the longer delivery time. However, the optimal number of EVs selected from the pool is 61 as the orange dot in Fig. 12 shows. As the number increases, the revenue per vehicle converges to about 13 € per vehicle. The optimizer again has the greatest advantage with small pools. Here it can select the best EVs and, for example, reaches 20 € per EV with 150A vehicles. In contrast, 10,000 random pools of 150 vehicles generate on average only 11.74 € per vehicle. Consequently, the advantage of the optimizer over random pool compositions is again evident in this case.

4.1.4. Comparison between the markets

Following individual considerations of the optimized pools of the three markets, the potential revenues between the markets are now compared. The increase in annual revenue per EV through optimization in the three markets is shown in Fig. 13. The revenue from participation in the FCR market can be increased by 72 % from 220 € to 378 € through optimized pool composition. The earnings from intraday continuous arbitrage trading can be increased by 167 % from 76 € to 203 €. On the

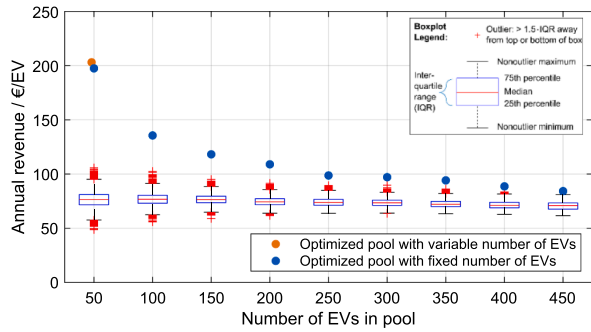


Fig. 10. Intraday continuous optimization: Annual revenue per EV when a fixed number of EVs is specified (boxplot: 10,000 random pools, blue dot: optimized pool). (For interpretation of the references to color in this figure legend, the reader is referred to the web version of this article.)

day-ahead market, optimization of the pool can yield 28 € per EV instead of an average of 3.5 € when only considering random pools of 61 EVs that actually generate any revenue. This is an increase in revenue by almost 7-fold.

A comparison of the possible markets shows that participation in the FCR market could generate significantly higher revenues than arbitrage trading in 2020. Without optimization, it is most economical in all cases to include as many EVs as possible in the pool, since revenue per EV increases as the number of vehicles increases with random pool composition (see Fig. 8, Fig. 10 and Fig. 12). With optimization, the revenue on the FCR market is 1.9 (vs. intraday) and 13.5 times (vs. day-ahead) higher than the income that can be generated by arbitrage trading.

With respect to pool sizes, however, it is important to note that small vehicle pools of <100 EVs do not meet the 1 MW minimum for FCR (see Fig. 8). Pools of this size that have already been assembled could

consequently provide arbitrage trading, whereby the intraday continuous market is more flexible and promises higher revenues compared to the day-ahead auction market.

Overall, these analyses demonstrate that the optimal pool composition using the capability profiles can substantially increase the revenues an aggregator can generate in the markets. Thus, the optimized profile combination is relevant for an aggregator to achieve competitive advantages.

4.2. What is the influence of dual use on battery degradation?

For an estimation of battery degradation costs, the degradation of a vehicle battery in “normal” operation and in dual use operation is compared in the following. The log data of vehicles used in this work, from which the power capability profiles were determined, do not include power profiles for the trips (see Section 2.2). Thus, the estimation of the charged and discharged power during a trip is based on the data measured by Bremer et al. [71]. This vehicle is part of a geriatric care fleet that runs two shifts daily (approximately 6 a.m. to 2p.m. and 3p.m. to 10:30p.m.). The vehicle model is a Smart fortwo electric drive with an energy capacity of 18 kWh [71]. For the following analysis, we assumed the vehicle with this driving profile would have been part of each pool. To do this, five daily power profiles and corresponding state-of-charge (SOC) profiles were formed (Fig. 14 and Appendix Figs. A3-A7), representing the following five cases:

- Uncontrolled charging (UC)
- Primary use-oriented charging (PUC)
- Dual use-oriented charging for FCR provision (DUC-FCR)
- Dual use-oriented charging for intraday continuous arbitrage (DUC-ID)
- Dual use-oriented charging for day-ahead auction arbitrage (DUC-DA)

With UC, the EV battery is immediately recharged to a SOC of 100 % upon arrival at the company site, i.e., at the end of the shifts (Fig. A3). Between shifts, the SOC is kept constant at 100 %. The PUC strategy, however, charges only enough to fulfill the mobility needs (Fig. A4). For this purpose, we defined a reserved capacity for the mobility as a function of time. The reserved capacity defines the minimum SOC at any time during the day. Since shifts occur between 6 a.m. and 10:30p.m., a minimum SOC of 60 % was defined for these times. Outside of these times, the minimum SOC is 30 %. This way, there is enough energy in the vehicle battery for spontaneous trips and the required energy is available for typical shifts. This type of charging corresponds to a smart charging strategy, since high SOC over longer periods of time lead to accelerated degradation of the battery [20,72,73].

In the three dual use strategies, the EV provides FCR (DUC-FCR) or trades on the intraday continuous (DUC-ID) or day-ahead auction market (DUC-DA). A default SOC of 68% was chosen to form the respective SOC curves (Figs. A5-A7). This SOC allows cycling for the second use during parking times without restricting mobility. For the simulation of FCR provision when the EV is parked at the company’s site, a standard battery energy storage load profile in FCR operation was used (Fig. A5) [74]. For the simulation of intraday continuous and day-ahead trading, Wednesday trading from Section 4.1 was used and scaled to one vehicle, i.e., divided by the number of vehicles in the optimized pool (Figs. A6-A7).

Since the vehicle under consideration is used as a geriatric care EV, it is assumed for this estimation of EV battery degradation that the SOC profiles are repeated 365 times per year and over several years. In reality, the driving profile and FCR generation or electricity trading will vary over the days and years. These profiles are then simulated with the

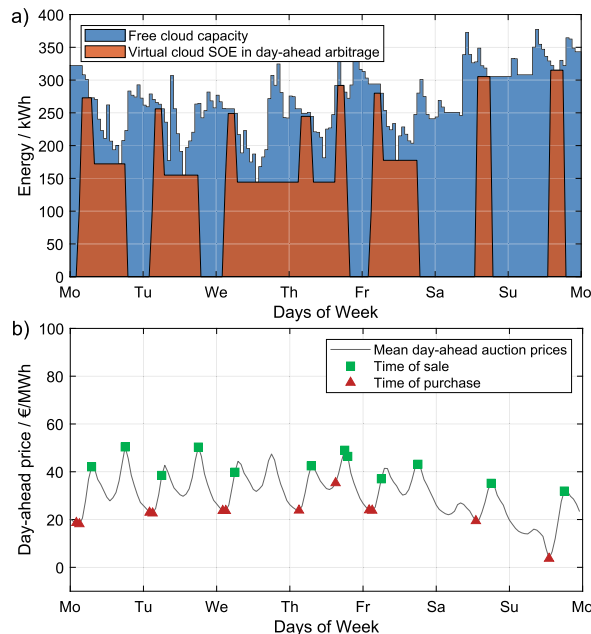


Fig. 11. Day-ahead optimization: Free cloud capacity and virtual cloud SOE of the pool (a) and times of sale and purchase including day-ahead auction prices (b).

Table 6
Assumptions and results of day-ahead auction arbitrage pool optimization.

Parameter	Value/ Data	
Day-ahead auction prices	Average hourly day-ahead auction prices of the year 2020	
Minimum bid	0.1 MW	
Assumed efficiency	93 % one-way (86.49 % round-trip)	
Spread limit	10 €/MWh	
Parameter	Optimized pool	Mean of 10,000 random pools
Number of EVs		61
Energy bought and sold	108 MWh	0.57 MWh
	93 MWh	0.49 MWh
Avg. Price of Energy bought and sold	19.77 €/MWh	11.70 €/MWh
	41.13 €/MWh	35.03 €/MWh
Annual Pool Revenue	1,702 €	10.66 €
Annual Revenues per EV	27.91 €	0.17 €

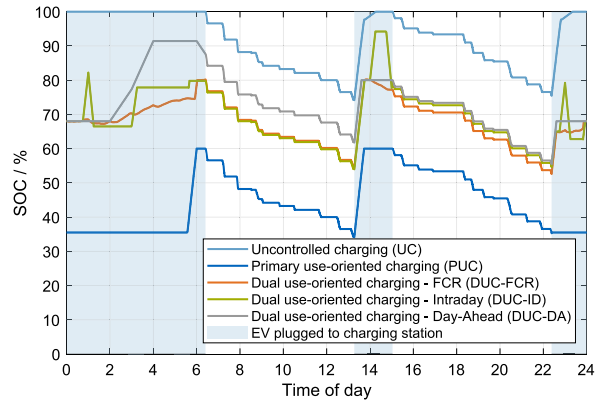


Fig. 14. Daily SOC-Profiles of the five considered cases.

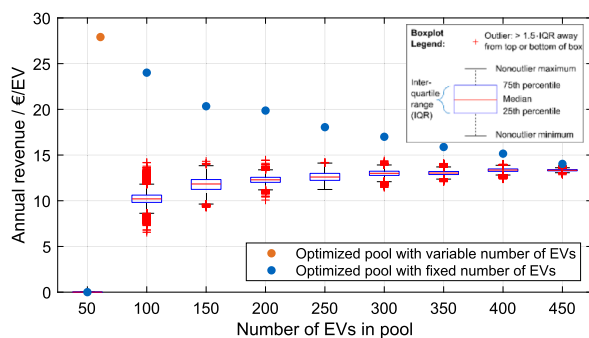


Fig. 12. Day-ahead optimization: Annual revenue per EV when a fixed number of EVs is specified (boxplot: 10,000 random pools, dots: optimized pools).

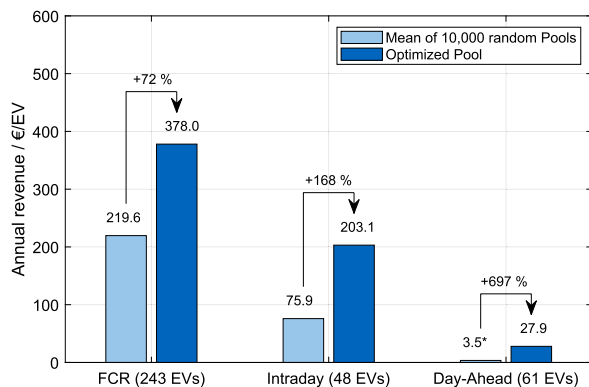


Fig. 13. Comparison of revenues in the three markets between the 10,000 random pools and the optimized pool (* Mean for random day-ahead pools of 61 EVs that could generate any revenue; 94% of the 10,000 pools could not generate any revenue).

storage simulation tool SimSES² (Simulation of stationary energy storage systems) to determine the degradation [75,76]. Here, a 1-minute resolution was chosen to allow an optimum between accuracy and computational time. In the simulation, parameters such as the capacity of 18 kWh are defined and the specified SOC curve is traced. For this purpose, a lithium-ion battery technology NMC (Nickel-Manganese-

Cobalt) was assumed to be the vehicle battery. The battery and degradation model of this cell type are based on a publication from Schmalstieg et al. [72]. The assumed fixed ambient temperature was 15 °C. Since vehicles might be parked in garages, this value is above the average temperature of 10.6 °C in Germany in 2020 [77]. A remaining capacity of 80% was selected as the end of life (EOL) of the battery in the simulations, analogous to the literature [72].

The results of the five simulations are shown in Table 7 and Fig. 15 (a). The case of uncontrolled charging (UC) leads to an average SOC of over 90% and a battery lifetime of about 7.7 years. In contrast, for the PUC case with an average SOC of 44.4%, the vehicle battery reaches its end of life after 12.8 years. This shows the advantage of a smart charging strategy, which in this simulation and with this profile leads to an increase in lifetime of 66%. The dual use with the EV leads to a mean SOC between 67% and 74% and a lifetime between 7.4 and 11.8 years, depending on the case. In this example, dual use in FCR and day-ahead case is better than uncontrolled charging (UC) in terms of battery aging, but worse than smart charging (PUC). Only intraday continuous arbitrage trading leads to a slightly lower lifetime than UC. The average annual equivalent full cycles (EFC) that the vehicle battery experiences without dual use are already relatively large at 160 due to the use of the vehicle in two shifts. With dual use, the annual EFCs increase up to 317 for intraday continuous arbitrage. In contrast, the EFCs for FCR provision and day-ahead trading are only slightly higher than the EFCs without dual use. This is because the exemplary supply or exemplary trading is very much in the EV's favor. In Fig. 14, it can be seen that the provision of FCR between 2 a.m. and 6 a.m. results in less need to charge the vehicle. The same applies to day-ahead trading between 2 a.m. and 4 a.m. By assuming that this day is repeated 365 times per year for several years, this results in only slightly more battery degradation of DUC-FCR and DUC-DA compared to PUC.

Table 7 additionally shows a utilization ratio. This ratio indicates the proportion of time the EV is on the road (not at company site) or in V2G provision. The value therefore indicates how often the vehicle battery is used. Dual use increases this utilization ratio: For example, almost 70% for intraday trading and 100% for FCR provision, since the vehicle provides FCR or is recharged as soon as it is parked at the company site. In addition, the dual use ratio shows the proportion of time the EV is parked at the company location that is used for FCR provision or trading.

After the example aging simulation, the costs for the battery are now compared with the possible revenues in the three markets considered (Fig. 15 (b)). According to a study, the average lithium-ion battery pack prices in 2020 were 137 \$/kWh, which is roughly equivalent to 114 €/kWh [78]. A vehicle battery pack with a capacity of 18 kWh therefore cost 2,052 € in 2020. If these costs are evenly distributed over the number of lifetime years, the battery costs without dual use range between 160 € (PUC) and 276 € (UC) for the example year 2020. The

² <http://www.simses.org>, open-source version 1.0.4

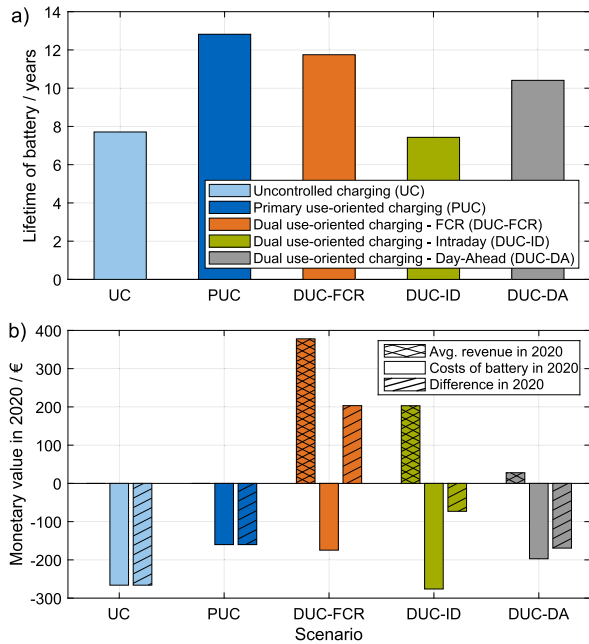


Fig. 15. Comparison of lifetime (a) and costs of battery and avg. revenues (b) for the five cases.

battery costs in dual use range between 175 € (DUC-FCR) and 276 € (DUC-ID). In Fig. 15 (b), the costs are plotted negatively. The average revenues per EV of the optimized pools in 2020 for the dual use cases are shown as positive values. Here, it can be seen that the revenues exceed the battery costs in the case of FCR supply. For intraday and day-ahead arbitrage, the battery costs are higher than the potential revenues. In the UC and PUC cases, no revenue is generated.

The comparison of the cases shows that, in regard to battery costs and revenues, all cases are better than the UC case. In the DUC-DA case, the difference between revenues and battery costs is slightly less than the difference in the PUC case due to low revenues in the day-ahead auction market. Smart charging according to PUC therefore seems to be more profitable than arbitrage trading on the day-ahead auction market. However, for intraday trading and especially for FCR provision, the difference is above that of the PUC case. Here, dual use is economically more attractive than smart charging according to PUC, since additional costs of the dual use cases, metering point operation, bidirectional charging stations, and possible aggregator costs should be considered. This means that for the FCR case, for example, these additional costs must not exceed 203 € per EV to generate a profit in 2020. These costs should not exceed 363 € to make the DUC-FCR case worthwhile compared to the PUC case.

It should be kept in mind that in this analysis we assumed that the revenues of the DUC Cases are equally distributed among all vehicles,

Table 7 Results of the five simulated cases for analysis of battery degradation with and without dual use operation.

Case	Lifetime in years	Mean SOC	EFC Total	Avg. EFC per year	Utilization ratio	Dual use ratio
UC	7.71 a	91.6 %	1,261	164	59.2 %	0 %
PUC	12.82 a	44.4 %	2,117	165	59.2 %	0 %
DUC-FCR	11.75 a	67.7 %	2,188	186	100 %	100 %
DUC-ID	7.43 a	69.4 %	2,358	317	69.9 %	26.3 %
DUC-DA	10.41 a	73.4 %	1,825	175	71.6 %	30.3 %

even though the EV under consideration is on the road 59% of the time. The aggregator could also distribute its revenue based on provisioning and therefore the simulated EV would likely generate less revenue. In addition, battery costs were assumed that do not necessarily correspond to the final customer prices due to, e.g., taxes. However, it can also be assumed that battery costs will continue to decrease in the future, so that a repurchase could possibly be below the assumed 2,052 €. On the other hand, FCR revenues could also decline further in the future due to market saturation. Moreover, the aging model used in this analysis is from the year 2014 and new battery cells are likely to degrade slower. This could make the DUC cases even more attractive. Finally, this analysis used a vehicle that is frequently on the road a lot with its battery already frequently cycled in primary use. This results in little time for dual use. An analysis with, for example, private vehicles that are idle 95% of the time could lead to different results.

5. Conclusion and outlook

This section summarizes the main findings of the paper and discusses the results. Moreover, it provides an outlook on further developments and emerging research questions.

5.1. Conclusion

In this work, we show that aggregators of EVs for V2G use can gain competitive advantages through optimized vehicle selection. Therefore, optimization methods are developed that determine which combinations of vehicles would be economically favored based on the power capability profiles of the vehicles. The power capability profiles used are determined from driving data of 468 commercial vehicles and explicitly presented in a previous publication [10]. As potential markets, FCR provision in Central Europe as well as arbitrage trading on the EPEX intraday continuous and day-ahead auction markets are analyzed.

The possible yearly revenues in the three markets vary from only 5–30 € per EV (day-ahead) to 220–380 € per EV (FCR), which answers research question 2 (RQ2). In all three markets, optimal pool composition can increase revenue per participating EV compared to random pools of the same number of vehicles. In the FCR market, revenue per vehicle can be increased by 72% with the optimal number of vehicles when using optimization compared to the mean of random pools. If, for example, 150 EVs are used to provide FCR, revenue can be doubled to tripled compared to a random pool selection. For arbitrage trading in the intraday continuous market, optimization achieves a 160% increase in revenue. In the day-ahead auction market, the increase in revenue is even larger with an almost 7-fold increase compared to random pools of the same number that could generate revenue. If, for example, 150 vehicles are optimized in intraday or day-ahead trading, revenues increase by 66% or 79%, respectively, compared to the average of random pools of the same size. In total, we show that aggregators of EV pools gain a competitive advantage through smart selection of vehicles (RQ1). This higher efficiency can bring a relevant market advantage for aggregators, since costs are incurred per connected vehicle (bidirectional charging station, metering equipment). Especially with a high penetration of EVs in the future and thus a large number of possible EVs for V2G, we expect that intelligent pool aggregation will be crucial for profitability. As the number of potential vehicles increases beyond the 468 EVs considered, the optimal number of EVs in the pool will also increase.

A direct comparison between the markets reveals that in 2020 the FCR provision is the most profitable application (RQ3). Here, revenues greater by a factor of 1.9 (vs. intraday) and 13.5 (vs. day-ahead) could have been achieved. However, it is worth mentioning that for smaller pools of EVs (<100) intraday and day-ahead markets are favorable as long as no taxes and fees have to be paid, since the FCR market requires a minimal provision of 1 MW. Alternatively, pools could merge to achieve the minimum power to provide FCR. In the arbitrage markets, seven times the revenue can be generated on the intraday continuous market

compared to the day-ahead auction market. In addition, the intraday market with its 15 min provision time is more flexible than the day-ahead auction market with 1 h each.

While the optimization itself is limited to a revenue analysis, we also conducted a degradation study revealing additional costs from battery degradation. Here, an example driving profile and a provision of the three dual uses is simulated to account for additional battery degradation. Interestingly, dual use showed reduced degradation compared to uncontrolled charging in the FCR and the day-ahead case, which is attributed to the lower average SOC. For the intraday case, the lifetime is slightly reduced compared to uncontrolled charging. A primary use-oriented smart charging shows the least degradation (RQ4). Afterwards, the revenues on the markets are compared with the costs of degradation. The revenues clearly surpass the aging costs, in particular for the FCR and intraday cases. The day-ahead case is slightly worse than the smart charging case (RQ5).

5.2. Discussion

In the following section, we frame and discuss the results. First, it is important to explain that in the results presented, we maximize revenues (not profit) based on the power capability profiles (for FCR) or free cloud energy capacity and available power (for intraday and day-ahead) and average prices. Possible costs of the aggregator (e.g., fixed costs or costs for bidirectional charging stations) or due to the additional degradation of the batteries were neglected in the first analysis (Section 4.1). However, the exemplary simulation of vehicle battery degradation showed that market revenues could compensate for the additional degradation costs. In this example, we used one daily profile of a vehicle that is on the road for 60% of the time and already makes 165 equivalent full cycles per year even without V2G. To be able to depict degradation of vehicle batteries in particular more accurately, we will develop time series simulations in future publications that can simulate the retrieval and provision in more detail. In this work, however, the focus is on the optimization of EV pools. Regarding the fixed costs of aggregators, if our methodology is used, they could add their own costs to be covered by all participating EVs, which would create larger EV pools.

In terms of the markets under consideration, there are also a few points to note. On the one hand, the FCR provision neglects a possible necessary additional purchase on the spot markets. On the other hand, possible degrees of freedom in the provision of FCR are not considered, which might increase revenues. Furthermore, the arbitrage algorithm is rudimentary without a smart charging strategy. Incoming EVs are not discharged when the SOC is still high in order to have a larger free pool capacity. Instead, only the free cloud capacity that is available after primary use is utilized. This does not limit the EV owners in their mobility, but does lead to lower achievable revenues. Furthermore, lower purchase prices and higher sell prices than the mean prices could be obtained in the spot market by smart trading [70]. In addition, analogous to [70], it is assumed that no taxes and fees are incurred on the purchase of energy in spot market trading. Adding these taxes, which private households usually must pay, would make the arbitrage case unprofitable. In addition, differentiation between behind-the-meter (BTM) and in front-of-the-meter (FTM) must be taken into account in multi-use concepts [79]. This also applies to vehicles that charge energy through, e.g., FCR (FTM) and then use this energy for mobility (BTM). We address this issue in another recently published [80].

To solve the optimization problem, we used a genetic algorithm as described. This metaheuristic optimization does not necessarily find the global optimum, but, as shown in the results, a very good solution. Should aggregators use the method with a very high number of profiles,

the runtime of the genetic algorithm will increase significantly. The runtime for the 468 profiles on one workstation was just under 2 h. Alternatively, the linear optimization presented in Section 3.1.3 can be performed iteratively for all possible numbers of EVs, which finds the global optimum, but leads to an even longer runtime.

Regarding the revenues that can be generated in the various markets in the medium to long term, it should be considered that potential revenues in the FCR market could continue to fall due to increasing market saturation. In contrast, price spreads on spot markets could continue to increase due to a further increase in renewable generators with fluctuating electricity generation. Consequently, the achievable revenues could converge and arbitrage on the spot markets could become economically more interesting. However, we conclude from the results presented that optimizing vehicle pools from an aggregator's perspective can be extremely economically rewarding in other markets as well.

5.3. Outlook

In this work, we presented the benefit of an optimal pool composition by means of optimization methods. In this section, possible further developments and emerging research topics are stated:

The *database* of the present work is formed by 468 commercial vehicles. An application of the methodology to private vehicles could also be interesting for aggregators. For implementation, however, these would have to be encouraged to participate through clever business models [15]. In addition, we expect that the potential of optimized pool composition will be even greater in practice with a larger database, if the aggregator can select vehicles specifically across the entire market. In addition, aggregators could also add stationary energy storage systems or renewable energy systems to their pools to exploit other flexibilities.

The *markets* analyzed in this paper are the FCR market in Germany and the EPEX Spot market. Beyond these markets, further balancing power markets such as automatic frequency restoration reserve (aFRR) could be analyzed. This market allows the provision of positive or negative power separately, which could allow EVs to be charged at low cost when negative control power is provided. However, the FTM-BTM issue would have to be considered and taxes and fees might have to be paid in arrears [80]. In addition, minimum bid sizes of, for example, 1 MW in the FCR market impose regulatory barriers for new players in the V2G field [81]. However, these barriers, especially for pools of EVs, have been recognized by the TSOs and could be reduced in the future [55]. We will analyze the impact of reduced minimum offer sizes on the FCR market in another future paper on the topic. Other interesting markets for V2G capable vehicles may be emerging flexibility markets in distribution grids. Furthermore, the methodology of the optimization methods could be applied to further international markets.

Regarding the *strategy* of the aggregator, spot markets are only used for arbitrage trading in this work. The vehicles are not discharged in a targeted manner, but only free capacities were used. A further development would be smart charging strategies. Those could first discharge the EVs after arrival and then charge them at night at low cost. However, power capability profiles are not sufficient for this and are to be further developed in the future based on time series simulations. These time series simulations could also be used to simulate and optimize the retrieval of EVs in a pool. For example, the degradation of the batteries could be considered. From the aggregator's point of view, a dynamic pool formation in which the vehicles are not assigned to a fixed market but switch variably between the markets could also be interesting. This could also be a response to expected market saturation effects at FCR [10,82].

Moreover, *business models* need to be developed that allow EVs to be applied in dual use. Here, for example, the aggregator could own the vehicle battery and lease it to the owner of the vehicle [83]. In addition, an aggregator could offer the vehicle owner discounted charging when participating in the pool compared to normal charging. Billing concepts could also be developed in which vehicles that contribute more to the pool power could generate higher revenues. Moreover, original equipment manufacturers could act as aggregators themselves, engaging vehicle buyers as long-term, permanent customers rather than just selling the vehicle [15]. For them in particular, the dual use of the vehicle battery in island grid operation during power outages could become a selling point.

Overall, the concept of dual use, meaning the switch of usage of EVs between mobility and V2G in idle times, offers a lot of potential for research and development and a potentially very large and lucrative market in the future.

CRedit authorship contribution statement

Benedikt Tepe: Conceptualization, Methodology, Software, Formal analysis, Investigation, Writing – original draft, Visualization. **Jan Figgener:** Conceptualization, Methodology, Software, Formal analysis, Investigation, Writing – original draft, Visualization. **Stefan Englberger:** Methodology, Software. **Dirk Uwe Sauer:** Resources, Writing – review & editing, Supervision. **Andreas Jossen:** Resources, Writing – review & editing, Supervision. **Holger Hesse:** Conceptualization, Writing – review & editing, Supervision.

Declaration of Competing Interest

The authors declare that they have no known competing financial interests or personal relationships that could have appeared to influence the work reported in this paper.

Acknowledgement

This work was financially supported by the German Federal Ministry for Economic Affairs and Energy within the open BEA project (Grant No. 03ET4072) and the German Federal Ministry of Education and Research within the SimBAS project (Grant No. 03XP0338A) as part of the Competence Cluster Battery Utilisation Concepts (BattNutzung), which are both managed by Project Management Jülich. The responsibility for this publication rests with the authors.

Appendix

A.1. Results of manually calculated optimization problems

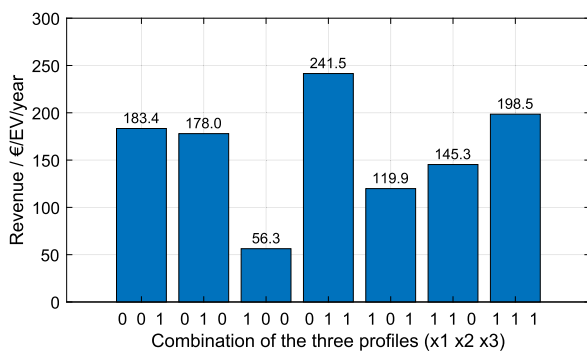


Fig. A1. Manual calculation of revenue per EV (FCR) and year for all combinations of the three EV profiles in Fig. 3.

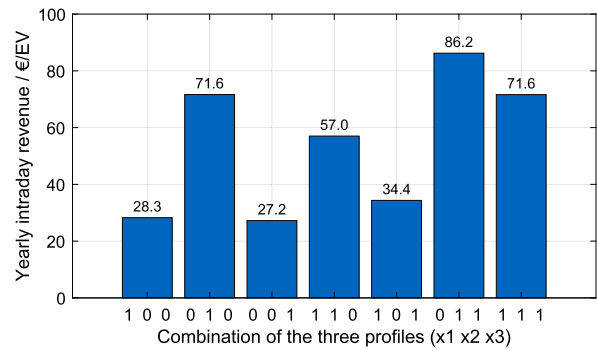


Fig. A2. Manual calculation of revenue (intraday continuous) per EV and year for all combinations of the three EVs in Fig. 6.

A.2. Profiles of degradation analysis

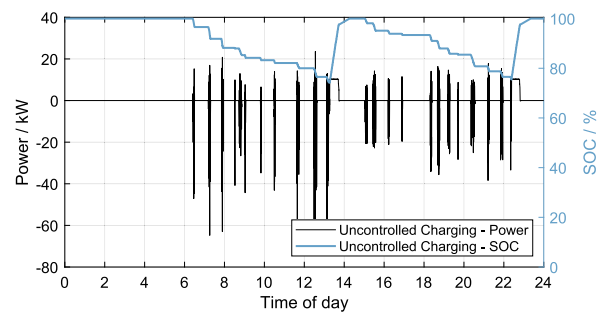


Fig. A3. Uncontrolled charging (UC) power and SOC.

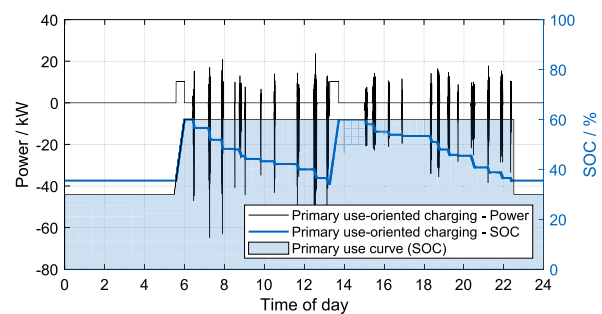


Fig. A4. Primary use-oriented charging (PUC) power and SOC.

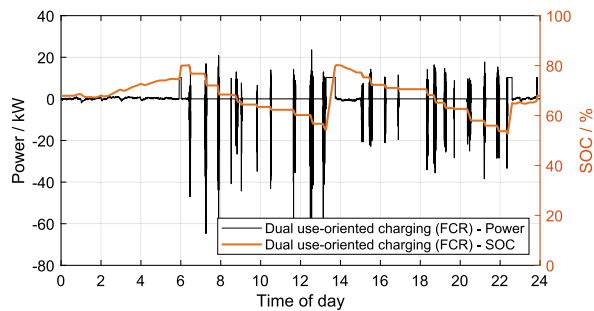


Fig. A5. Dual use-oriented charging for FCR provision (DUC-FCR) power and SOC.

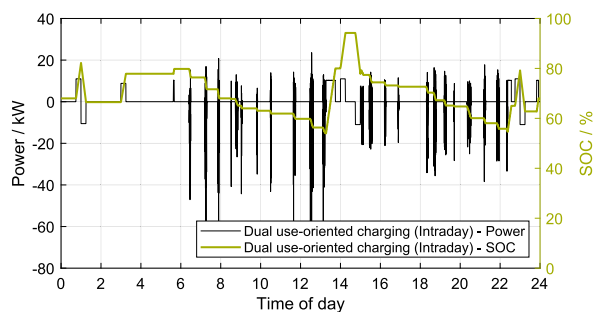


Fig. A6. Dual use-oriented charging for intraday continuous arbitrage (DUC-ID) power and SOC.

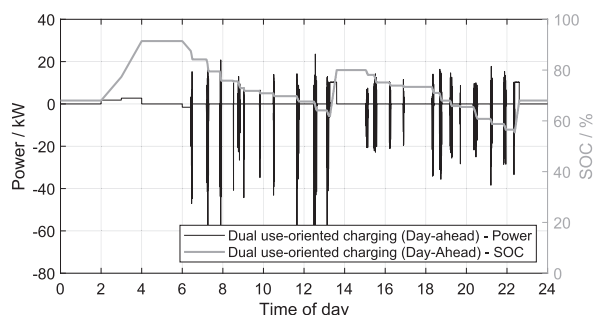


Fig. A7. Dual use-oriented charging for day-ahead auction arbitrage (DUC-DA) power and SOC.

References

- Quitrow L, Canzler W, Grundmann P, Leibenath M, Moss T, Rave T. The German Energiewende – What's happening? Introducing the special issue. *Utilities Policy* 2016;41:163–71. <https://doi.org/10.1016/j.up.2016.03.002>.
- Hake J-F, Fischer W, Venghaus S, Weckenbrock C. The German Energiewende – History and status quo. *Energy* 2015;92:532–46. <https://doi.org/10.1016/j.energy.2015.04.027>.
- International Energy Agency. *Global EV Outlook 2021*. Paris; 2021.
- Die Bundesregierung. *Key elements of the Climate Action Programme 2030*; 2019.
- Fraunhofer ISE. *Energy Charts*. [October 30, 2020]; Available from: <https://energy-charts.info/>.
- Nobis C, Kuhnimhof T. *Mobilität in Deutschland MiD. Ergebnisbericht 2018*.
- Peng C, Zou J, Lian L, Li L. An optimal dispatching strategy for V2G aggregator participating in supplementary frequency regulation considering EV driving demand and aggregator's benefits. *Appl Energy* 2017;190:591–9. <https://doi.org/10.1016/j.apenergy.2016.12.065>.
- Tarroja B, Zhang L, van Wifvat SB, Samuelsen S. Assessing the stationary energy storage equivalency of vehicle-to-grid charging battery electric vehicles. *Energy* 2016;106:673–90. <https://doi.org/10.1016/j.energy.2016.03.094>.
- Angenendt G, Zurmühlen S, Figgenger J, Kairies K-P, Sauer DU. Providing frequency control reserve with photovoltaic battery energy storage systems and power-to-heat coupling. *Energy* 2020;194:116923. <https://doi.org/10.1016/j.energy.2020.116923>.
- Figgenger J, Tepe B, Rücker F, Schoeneberger I, Hecht C, Jossen A et al. The Influence of Frequency Containment Reserve Flexibilization on the Economics of Electric Vehicle Fleet Operation. <https://arxiv.org/pdf/2107.03489v1>; 2021.
- Bessa RJ, Matos MA. The role of an aggregator agent for EV in the electricity market. In: 7th Mediterranean Conference and Exhibition on Power Generation, Transmission, Distribution and Energy Conversion (MedPower 2010). IET; 2010. p. 126.
- Han S, Han S, Sezaki K. Development of an Optimal Vehicle-to-Grid Aggregator for Frequency Regulation. *IEEE Trans. Smart Grid* 2010;1(1):65–72. <https://doi.org/10.1109/TSG.2010.2045163>.
- Guerrero JI, Personal E, García A, Parejo A, Pérez F, León C. Distributed Charging Prioritization Methodology Based on Evolutionary Computation and Virtual Power Plants to Integrate Electric Vehicle Fleets on Smart Grids. *Energies* 2019;12(12):2402. <https://doi.org/10.3390/en12122402>.
- Launger D, Vuille F, Kuhn D. A review of the state of research on vehicle-to-grid (V2G): Progress and barriers to deployment. In: *European Battery, Hybrid and Fuel Cell Electric Vehicle Congress 2017*.
- Sovacool BK, Kester J, Noel L, Zarazua de Rubens G. Actors, business models, and innovation activity systems for vehicle-to-grid (V2G) technology: A comprehensive review. *Renewable and Sustainable Energy Reviews* 2020;131:109963. <https://doi.org/10.1016/j.rser.2020.109963>.
- Irena. *Innovation outlook: Smart charging for electric vehicles*. Abu Dhabi 2019.
- Hu J, Morais H, Sousa T, Lind M. Electric vehicle fleet management in smart grids: A review of services, optimization and control aspects. *Renew Sustain Energy Rev* 2016;56:1207–26. <https://doi.org/10.1016/j.rser.2015.12.014>.
- Peterson SB, Apt J, Whitacre JF. Lithium-ion battery cell degradation resulting from realistic vehicle and vehicle-to-grid utilization. *J Power Sources* 2010;195(8):2385–92. <https://doi.org/10.1016/j.jpowsour.2009.10.010>.
- Bishop JD, Axon CJ, Bonilla D, Tran M, Banister D, McCulloch MD. Evaluating the impact of V2G services on the degradation of batteries in PHEV and EV. *Appl Energy* 2013;111:206–18. <https://doi.org/10.1016/j.apenergy.2013.04.094>.
- Petit M, Prada E, Sauvart-Moynot V. Development of an empirical aging model for Li-ion batteries and application to assess the impact of Vehicle-to-Grid strategies on battery lifetime. *Appl Energy* 2016;172:398–407. <https://doi.org/10.1016/j.apenergy.2016.03.119>.
- Geske J, Schumann D. Willing to participate in vehicle-to-grid (V2G)? Why not! *Energy Policy* 2018;120:392–401. <https://doi.org/10.1016/j.enpol.2018.05.004>.
- Sovacool BK, Axsen J, Kempton W. The Future Promise of Vehicle-to-Grid (V2G) Integration: A Sociotechnical Review and Research Agenda. *Annu. Rev. Environ. Resour.* 2017;42(1):377–406. <https://doi.org/10.1146/annurev-environ-030117-020220>.
- Irena. *Electricity storage and renewables: Costs and markets to 2030*. Abu Dhabi 2017.
- Andersen PB, Toghroljerdi SH, Meier Sørensen T, Christensen BE, Morell Lodberg Hoj JC, Zecchino A. *The Parker Project: Final Report*; 2019.
- Brooks AN. *Vehicle-to-grid demonstration project: Grid regulation ancillary service with a battery electric vehicle*. Air Resources Board, Research: California Environmental Protection Agency; 2002.
- Guo Y, Liu W, Wen F, Salam A, Mao J, Li L. Bidding Strategy for Aggregators of Electric Vehicles in Day-Ahead Electricity Markets. *Energies* 2017;10(1):144. <https://doi.org/10.3390/en10010144>.
- Giordano F, Arrigo F, Diaz-Londono C, Spertino F, Ruiz F. Forecast-Based V2G Aggregation Model for Day-Ahead and Real-Time Operations. In: 2020 IEEE Power & Energy Society Innovative Smart Grid Technologies Conference (ISGT). IEEE; 2020. p. 1–5.
- Weiller C, Shang AT, Mullen P. Market Design for Electric Vehicles. *Curr Sustainable Renewable Energy Rep* 2020. <https://doi.org/10.1007/s40518-020-00163-3>.
- Rücker F, Bremer I, Sauer DU. Development and analysis of a charging algorithm for electric vehicle fleets extending battery lifetime: 2016 IEEE Transportation Electrification Conference and Expo, Asia-Pacific (ITEC Asia-Pacific) June 1–4, 2016, BEXCO, Busan, Korea. Piscataway, NJ: IEEE.
- Lunz B, Walz H, Sauer DU. Optimizing vehicle-to-grid charging strategies using genetic algorithms under the consideration of battery aging. In: 2011 IEEE Vehicle Power and Propulsion Conference. IEEE; 2011. p. 1–7.
- Sortomme E, El-Sharkawi MA. Optimal Scheduling of Vehicle-to-Grid Energy and Ancillary Services. *IEEE Trans. Smart Grid* 2012;3(1):351–9. <https://doi.org/10.1109/TSG.2011.2164099>.
- Bañol Arias N, Hashemi S, Andersen PB, Træholt C, Romero R. Assessment of economic benefits for EV owners participating in the primary frequency regulation markets. *Int J Electr Power Energy Syst* 2020;120:105985. <https://doi.org/10.1016/j.ijepes.2020.105985>.
- Thingvad A, Ziras C, Marinelli M. Economic value of electric vehicle reserve provision in the Nordic countries under driving requirements and charger losses. *J Storage Mater* 2019;21:826–34. <https://doi.org/10.1016/j.est.2018.12.018>.
- Bessa RJ, Matos MA, Soares FJ, Lopes JAP. Optimized Bidding of a EV Aggregation Agent in the Electricity Market. *IEEE Trans. Smart Grid* 2011;3(1):443–52. <https://doi.org/10.1109/TSG.2011.2159632>.
- Schuller A, Dietz B, Flath CM, Weinhardt C. Charging Strategies for Battery Electric Vehicles: Economic Benchmark and V2G Potential. *IEEE Trans. Power Syst.* 2014;29(5):2014–22. <https://doi.org/10.1109/TPWRS.2014.2301024>.
- Kiaee M, Cruden A, Sharkh S. Estimation of cost savings from participation of electric vehicles in vehicle to grid (V2G) schemes. *J. Mod. Power Syst. Clean Energy* 2015;3(2):249–58. <https://doi.org/10.1007/s40565-015-0130-2>.

- [37] Sanchez-Martin P, Lumbreras S, Alberdi-Alen A. Stochastic Programming Applied to EV Charging Points for Energy and Reserve Service Markets. *IEEE Trans. Power Syst.* 2015;31(1):198–205. <https://doi.org/10.1109/TPWRS.2015.2405755>.
- [38] Shang D, Sun G. Electricity-price arbitrage with plug-in hybrid electric vehicle: Gain or loss? *Energy Policy* 2016;95:402–10. <https://doi.org/10.1016/j.enpol.2016.05.019>.
- [39] Zheng Y, Yu H, Shao Z, Jian L. Day-ahead bidding strategy for electric vehicle aggregator enabling multiple agent modes in uncertain electricity markets. *Appl Energy* 2020;280:115977. <https://doi.org/10.1016/j.apenergy.2020.115977>.
- [40] Krishnamurthy D, Uckun C, Zhou Z, Thimmapuram PR, Botterud A. Energy Storage Arbitrage Under Day-Ahead and Real-Time Price Uncertainty. *IEEE Trans. Power Syst.* 2018;33(1):84–93. <https://doi.org/10.1109/TPWRS.2017.2685347>.
- [41] Cao J, Harrold D, Fan Z, Morstyn T, Healey D, Li K. Deep Reinforcement Learning-Based Energy Storage Arbitrage With Accurate Lithium-Ion Battery Degradation Model. *IEEE Trans. Smart Grid* 2020;11(5):4513–21. <https://doi.org/10.1109/TSG.2020.2986333>.
- [42] Kuang Y, Wang X, Zhu Z. Optimal Bidding Strategy for a RES Virtual Power Plant in the Spot Market. In: 2019 IEEE Sustainable Power and Energy Conference (ISPEC). IEEE; 2019 - 2019, p. 1480–1485.
- [43] Bradbury K, Pratson L, Patiño-Echeverri D. Economic viability of energy storage systems based on price arbitrage potential in real-time U.S. electricity markets. *Appl Energy* 2014;114:512–9. <https://doi.org/10.1016/j.apenergy.2013.10.010>.
- [44] Wankmüller F, Thimmapuram PR, Gallagher KG, Botterud A. Impact of battery degradation on energy arbitrage revenue of grid-level energy storage. *J Storage Mater* 2017;10:56–66. <https://doi.org/10.1016/j.est.2016.12.004>.
- [45] Fares RL, Webber ME. What are the tradeoffs between battery energy storage cycle life and calendar life in the energy arbitrage application? *J Storage Mater* 2018;16:37–45. <https://doi.org/10.1016/j.est.2018.01.002>.
- [46] Zhou K, Cheng L, Lu X, Wen L. Scheduling model of electric vehicles charging considering inconvenience and dynamic electricity prices. *Appl Energy* 2020;276:115455. <https://doi.org/10.1016/j.apenergy.2020.115455>.
- [47] Tuchsitz F, Ebell N, Schlund J, Pruckner M. Development and Evaluation of a Smart Charging Strategy for an Electric Vehicle Fleet Based on Reinforcement Learning. *Appl Energy* 2021;285:116382. <https://doi.org/10.1016/j.apenergy.2020.116382>.
- [48] Agarwal L, Peng W, Goel L. Probabilistic Estimation of Aggregated Power Capacity of EVs for Vehicle-to-Grid Application. Durham, UK: IEEE; 2014.
- [49] Han S, Han S, Sezaki K. Estimation of Achievable Power Capacity From Plug-in Electric Vehicles for V2G Frequency Regulation: Case Studies for Market Participation. *IEEE Trans. Smart Grid* 2011;2(4):632–41. <https://doi.org/10.1109/TSG.2011.2160299>.
- [50] Fluhr J, Ahlert K-H, Weinhardt C. A Stochastic Model for Simulating the Availability of Electric Vehicles for Services to the Power Grid. In: In: 2010 43rd Hawaii International Conference on System Sciences. IEEE; 2010–2010, p. 1–10.
- [51] Wu Q, Nielsen AH, Ostergaard J, Cha ST, Marra F, Chen Y, et al. Driving Pattern Analysis for Electric Vehicle (EV) Grid Integration Study. In: In: 2010 IEEE PES Innovative Smart Grid Technologies Conference Europe (ISGT Europe). IEEE; 2010, p. 1–6.
- [52] Hinterstocker M, Müller M, Kern T, Ostermann A, Dossow P, Pellinger C et al. Bidirectional Charging Management - Field Trial and measurement Concept for Assessment of Novel Charging Strategies. Dublin; 2019.
- [53] Chris Randall. Renault rolling-out V2G trials across Europe. [November 04, 2020]; Available from: <https://www.electrive.com/2019/03/24/renault-kicks-off-v2g-projects-in-utrecht-porto-santos/>.
- [54] Volkswagen Newsroom. F. Outlook: the future of charging. [February 05, 2021]; Available from: <https://www.volkswagen-newsroom.com/en/quick-easy-and-convenient-charging-solutions-at-volkswagen-6599/f-outlook-the-future-of-charging-6605>.
- [55] European Network of Transmission System Operators for Electricity. Electric Vehicle Integration into Power Grids: ENTSO-E Position Paper; 2021.
- [56] Uddin K, Dubarry M, Glick MB. The viability of vehicle-to-grid operations from a battery technology and policy perspective. *Energy Policy* 2018;113:342–7. <https://doi.org/10.1016/j.enpol.2017.11.015>.
- [57] German Transmission Grid Operators: 50 Hertz, Amprion, Tennet, TransnetBW. REGELLEISTUNG.NET: Internetplattform zur Vergabe von Regelleistung. [May 05, 2020]; Available from: <https://www.regelleistung.net>.
- [58] Figgenger J, Stenzel P, Kairies K-P, Linßen J, Haberschus D, Wessels O, et al. The development of stationary battery storage systems in Germany – status 2020. *J Storage Mater* 2021;33:101982. <https://doi.org/10.1016/j.est.2020.101982>.
- [59] Fleer J, Zurmühlen S, Meyer J, Badedá J, Stenzel P, Hake J-F, et al. Price development and bidding strategies for battery energy storage systems on the primary control reserve market. *Energy Procedia* 2017;135:143–57. <https://doi.org/10.1016/j.egypro.2017.09.497>.
- [60] Spot EPEX, Se.. Trading at EPEX SPOT 2021:2021.
- [61] Kern T. European day-ahead electricity prices in 2020. <https://www.ffe.de/veroeffentlichungen/european-day-ahead-electricity-prices-in-2020/>; 2021.
- [62] Uniper Technologies GmbH, Hochschule Ruhr West, Institute for Power Generation and Storage Systems at RWTH Aachen University. Gewerblich operierende Elektro-Kleinflotten (GO-ELK) Abschlussbericht GO ELK: Berichtszeitraum: 01.2013–06.2016. Uniper Technologies GmbH; 2016.
- [63] Wietschel M. Das Innovationscluster Regional Eco Mobility (REM 2030): Systemkonzepte für die urbane Mobilität von morgen. Karlsruhe.
- [64] Funke S, Gnann T. Codebook REM 2030 driving profiles database. Karlsruhe; 2015.
- [65] The MathWorks I. MATLAB® Global Optimization Toolbox: User's Guide; 2020.
- [66] Kramer O. Genetic Algorithm Essentials. Cham: Springer International Publishing; 2017.
- [67] Man KF, Tang KS, Kwong S. Genetic algorithms: concepts and applications [in engineering design]. *IEEE Trans. Ind. Electron.* 1996;43(5):519–34. <https://doi.org/10.1109/41.538609>.
- [68] Arabali A, Ghofrani M, Etezadi-Amoli M, Fadali MS, Baghzouy Y. Genetic-Algorithm-Based Optimization Approach for Energy Management. *IEEE Trans. Power Delivery* 2013;28(1):162–70. <https://doi.org/10.1109/TPWRD.2012.2219598>.
- [69] Khatib T, Mohamed A, Sopian K. Optimization of a PV/wind micro-grid for rural housing electrification using a hybrid iterative/genetic algorithm: Case study of Kuala Terengganu. Malaysia. *Energy and Buildings* 2012;47:321–31. <https://doi.org/10.1016/j.enbuild.2011.12.006>.
- [70] Kern T, Dossow P, von Roon S. Integrating Bidirectionally Chargeable Electric Vehicles into the Electricity Markets. *Energies* 2020;13(21):5812. <https://doi.org/10.3390/en13215812>.
- [71] Bremer I, Ruecker F, Sauer DU. Investigation of li-ion battery state of health detection in electric vehicles - a comparison of simulation results and field measurement. In: 2016 IEEE Transportation Electrification Conference and Expo, Asia-Pacific (ITEC Asia-Pacific), p. 18–23.
- [72] Schmalstieg J, Käbitz S, Ecker M, Sauer DU. A holistic aging model for Li(NiMnCo)O₂ based 18650 lithium-ion batteries. *J Power Sources* 2014;257:325–34. <https://doi.org/10.1016/j.jpowsour.2014.02.012>.
- [73] Keil P, Schuster SF, Wilhelm J, Travi J, Hauser A, Karl RC, et al. Calendar Aging of Lithium-Ion Batteries: I. Impact of the Graphite Anode on Capacity Fade. *J Electrochem. Soc. (Journal of The Electrochemical Society)* 2016;163(9):A1872–80.
- [74] Kucevic D, Tepe B, Englberger S, Parlikar A, Mühlbauer M, Bohlen O, et al. Standard battery energy storage system profiles: Analysis of various applications for stationary energy storage systems using a holistic simulation framework. *J Storage Mater* 2020;28:101077. <https://doi.org/10.1016/j.est.2019.101077>.
- [75] Naumann M, Truong N, Schimpe M, Kucevic D, Jossen A, Hesse H. SimSES: Software for techno-economic Simulation of Stationary Energy Storage Systems. In: VDE-Verlag, editor. International ETG Congress 2017. Berlin und Offenbach, p. 442–447.
- [76] Möller M, Kucevic D, Collath N, Parlikar A, Dotzauer P, Tepe B, et al. SimSES: A holistic simulation framework for modeling and analyzing stationary energy storage systems. *J Energy Storage* 2022. In press.
- [77] Deutscher Wetterdienst. Annual 2020. Climate monitoring Germany. [February 12, 2021]; Available from: https://www.dwd.de/EN/climate_environment/climate_monitoring/germany/brdmap_ubr_text_aktl_jz.html?nn=519080.
- [78] BloombergNEF. Battery Pack Prices Cited Below \$100/kWh for the First Time in 2020, While Market Average Sits at \$137/kWh. [February 17, 2021]; Available from: <https://about.bnef.com/blog/battery-pack-prices-cited-below-100-kwh-for-the-first-time-in-2020-while-market-average-sits-at-137-kwh/>.
- [79] Englberger S, Jossen A, Hesse H. Unlocking the Potential of Battery Storage with the Dynamic Stacking of Multiple Applications. *Cell Reports Physical Science* 2020;1(11):100238. <https://doi.org/10.1016/j.xcrp.2020.100238>.
- [80] Englberger S, Abo Gama K, Tepe B, Schreiber M, Jossen A, Hesse H. Electric vehicle multi-use: Optimizing multiple value streams using mobile storage systems in a vehicle-to-grid context. *Appl Energy* 2021;304:117862. <https://doi.org/10.1016/j.apenergy.2021.117862>.
- [81] Gschwendtner C, Sinsel SR, Stephan A. Vehicle-to-X (V2X) implementation: An overview of predominant trial configurations and technical, social and regulatory challenges. *Renew Sustain Energy Rev* 2021;145:110977. <https://doi.org/10.1016/j.rser.2021.110977>.
- [82] Bessa RJ, Matos MA. Economic and technical management of an aggregation agent for electric vehicles: a literature survey. *Euro. Trans. Electr. Power* 2012;22(3):334–50. <https://doi.org/10.1002/etep.565>.
- [83] Kempton W, Tomic J, Letendre S, Brooks A, Lipman T. Vehicle-to-grid power: battery, hybrid, and fuel cell vehicles as resources for distributed electric power in California; 2001.

4.3 Analysis of optimally composed pools regarding battery sizes and economic sectors

This section introduces the paper named *Analysis of Optimally Composed EV Pools for the Aggregated Provision of Frequency Containment Reserve and Energy Arbitrage Trading* [7]. In general, vehicle batteries have variable capacities. While small e-Cars have capacities of around 20 kWh, larger e-Cars models have capacities of 100 kWh. Furthermore, commercial e-Cars are used in various economic sectors, which means that driving behaviour and idle times at the company's location differ greatly. After optimizing vehicle pools of different commercial e-Cars for various markets in section 4.2, this section evaluates the optimized pools in terms of EV battery capacity and economic sector of the EV. The driving style of the vehicle depends on the economic sector, so that the power and energy capability profiles vary depending on the economic sector. However, the battery capacity also determines what energy and power can be charged and discharged during idle times. This section evaluates the suitability of different battery capacities and economic sectors for the various markets. For this purpose, the optimized pools of the various markets are compared to the pool of all possible vehicles with regard to battery capacities and economic sectors.

Furthermore, as described in section 4.1, the Central European FCR market has become increasingly time flexible in recent years. The length of supply has been reduced from one week to 4 hours, which creates potential for pools of e-Cars. This section examines a further flexibilization of the FCR market in terms of minimum bid size and the impact on e-Car pool revenues. The minimum supply on the FCR market in Central Europe is currently 1 MW. Here, the revenues of optimized and random pools with reduced minimum FCR bid sizes and increments between 10 kW and 500 kW are examined. The exploitation of the possible power potential at different increments is also examined by calculating the power utilization rate.

The research questions answered in this section are:

1. Which EV battery sizes are explicitly suitable for providing balancing power or arbitrage trading in energy markets?
2. EVs of which economic sectors are to be particularly attractive for the considered markets?
3. How would an increased flexibility in the FCR market in terms of minimum bid size and bid increments affect EV pool composition and revenues?

One conclusion of this section is that small EV batteries of 20 kWh are less useful for aggregators. Optimized pools consist mostly of larger batteries of 80 kWh, especially in intraday and day-ahead trading. As there is a general trend towards larger battery capacities in EVs [27], an increasing number of vehicles are suitable for V2G provision. Regarding the economic sectors of the vehicles, the "human health and social activities" sector is particularly unsuitable for V2G-capable EV pools, as these vehicles are on the road frequently and for long periods of time. In contrast, vehicles in the "manufacturing" sector appear to be better suited for V2G use. A further study in this section shows that if the minimum bids and increments in the FCR market are reduced, revenues can be increased by 50 to 66 % due to the higher power utilization rate.

The idea of V2G provision with EVs is continued in chapter 5. There, the influence of V2X, including the BTM application PS, on battery-relevant parameters is investigated. In addition to e-Cars, e-Buses and e-Boats are also examined there.

Author contribution

Benedikt Tepe was the principle author tasked with coordinating and writing the paper and developing the methodology of the analyses. Jan Figgenger focused on data acquisition and supported the preparation of the results. Stefan Englberger assisted in the methodology of the analyses. Dirk Uwe Sauer and Andreas Jossen contributed via fruitful scientific discussions and reviewed the manuscript. Holger Hesse reviewed the manuscript and gave valuable input throughout the manuscript preparation. All authors discussed the data and commented on the results.

Analysis of optimally composed EV pools for the aggregated provision of frequency containment reserve and energy arbitrage trading

Benedikt Tepe, Jan Figgner, Stefan Englberger, Dirk Uwe Sauer, Andreas Jossen and Holger Hesse

5th E-Mobility Power System Integration Symposium (EMOB 2021), 27 September 2021, p. 175 – 180, Hybrid Conference, Germany
IET, 2021, Electronic ISBN:978-1-83953-679-3

Permanent weblink:

<https://doi.org/10.1049/icp.2021.2521>

This paper was presented at the 5th E-Mobility Power System Integration Symposium and published in the Symposium's proceedings.

Analysis of Optimally Composed EV Pools for the Aggregated Provision of Frequency Containment Reserve and Energy Arbitrage Trading

Benedikt Tepe
Institute for Electrical Energy Storage
Technology
Technical University of Munich (TUM)
Germany
benedikt.tepe@tum.de

Andreas Jossen
Institute for Electrical Energy Storage
Technology
Technical University of Munich (TUM)
Germany
andreas.jossen@tum.de

Jan Figgenger
Institute for Power Electronics and
Electrical Drives (ISEA)
RWTH Aachen University
Germany
jan.figgenger@isea.rwth-aachen.de

Dirk Uwe Sauer
Institute for Power Electronics and
Electrical Drives (ISEA)
RWTH Aachen University
Germany
dirkuwe.sauer@isea.rwth-aachen.de

Stefan Englberger
Institute for Electrical Energy Storage
Technology
Technical University of Munich (TUM)
Germany
stefan.englberger@tum.de

Holger Hesse
Institute for Electrical Energy Storage
Technology
Technical University of Munich (TUM)
Germany
holger.hesse@tum.de

Abstract— Electric vehicles (EVs) can participate in various markets through a vehicle-to-grid (V2G) interface. Aggregators can combine the individual contributions of EVs to offer them, for example, on the frequency containment reserve (FCR) market or to use them for arbitrage trading. A simple approach is combining EVs in random fashion until the pool is able to reach the threshold for a service of choice. Alternatively, aggregators can compose their pools in smart fashion and include only EVs that contribute significantly to the pool's performance. In a previous publication, we have shown that optimizing the aggregated pools of commercial vehicles for the provision of FCR or arbitrage trading can increase revenues by up to 7-fold. In this work, we analyze the optimally composed pools and show that large vehicle batteries in the order of 80 kWh are particularly useful for arbitrage trading, while FCR provision is also possible with medium-sized EV batteries in the range of 30 kWh due to the small cycle depths. The inclusion of EVs with very small vehicle batteries around 20 kWh in aggregated pools is neither economically optimal for arbitrage trading nor for FCR provision. An analysis of the economic sectors of the commercial EVs selected for the optimal EV pools shows that some economic sectors are more suitable for V2G than others: In particular EVs of the sector "human health and social work activities" are unsuitable for V2G provision due to regular and long travel times during the day. In contrast, EVs from the "manufacturing" sector are particularly well represented in all applications and the "transportation and storage" sector in the arbitrage application. In addition to these analyses of the optimized pools, we reveal that a reduction in the required minimum power and increments would make the FCR market even more attractive to EV pools by increasing revenues by 50% to 66%. It would also better exploit the potential of EVs, as increments could be better utilized than they are in the current 1 MW minimum power requirement in central Europe.

Keywords - electric vehicles, vehicle-to-grid, optimized profile combination, vehicle fleet, dual use, grid services, frequency containment reserve, intraday market, day-ahead market

I. INTRODUCTION

The climate change report of the intergovernmental panel on climate change (IPCC) in 2021 confirmed again: Climate change is present, man-made and already in 2030 we could break the 1.5 degree limit [1]. One possible measure to reduce emissions is to switch the energy used for mobility from gasoline-based fuels to electricity. This shift to electric

vehicles (EVs) is currently taking place worldwide [2]. At the same time, it is highly relevant to expand renewable energies so that no fossil-based electricity is used to charge the vehicles. Building on the general electrification of transport, the next step is to actively integrate vehicles into the electricity grid. In the future, EVs might not only be able to charge smartly at times of high renewable generation, but also feed electricity back into the grid. Bidirectional charging of EVs can generally come in different approaches: In addition to vehicle-to-building (V2B) usage in the private and commercial sector, EVs will be able to participate in electricity, balancing and flexibility markets via V2G [3,4].

One concept that is already frequently applied in research and industry is the use of vehicle batteries in second life [5]. This means that after being used for mobility, EV batteries are used in stationary storage systems, for example to provide balancing power. In contrast, in our previous work we presented the concept of dual use [6]. Here, the vehicle batteries are used alternately over periods of minutes and hours for mobility and for V2G services. Mobility has the highest priority in this concept. The EV is only used to provide grid services during the parking times.

Various markets can be considered for the use of EVs in the V2G concept: In V2B application, the EVs can take over demand charge reduction or act as an emergency back-up [3]. In grid-tied V2G, EVs can participate in frequency regulation, spot markets, or emerging flexibility markets at the distribution grid level [3,7]. The markets analyzed in this paper are the frequency containment reserve (FCR) market in the European Network of Transmission System Operators

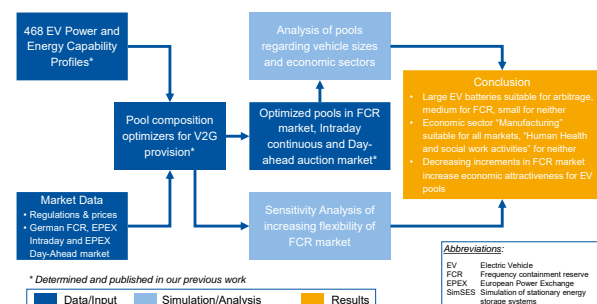


Fig. 1: Graphical Abstract

(ENTSO-E) region and the European Power Exchange (EPEX) intraday and day-ahead spot market. In these markets, individual EVs can only participate via aggregators who bundle the capacities of individual vehicles and form virtual power plants [8].

In principle, aggregators have the ability to add any EV to their pool. However, costs are to be considered for every individual EV, such as metering equipment and installation of bidirectional charging stations. For this reason, aggregators can gain competitive advantages if they only include EVs in their pool that can also make a significant contribution to the pool's energy capacity and power. To determine optimally composed pools, we have presented optimization methodologies based on the power and energy capability profiles of the EVs in a previous work [9]. The procedure for creating the profiles and determining the optimal EV pools is explained in more detail in chapter II.

Fig. 1 shows the general approach of the work and the parts created in the previous publications [6,9]. In this paper, we aim to answer three research questions:

- RQ 1) Which EV battery sizes are explicitly suitable for providing balancing power or arbitrage trading in energy markets? (section III.A)
- RQ 2) EVs of which economic sectors are to be particularly attractive for the considered markets? (section III.B)
- RQ 3) How would an increased flexibility in the FCR market in terms of minimum bid size and bid increments affect EV pool composition and revenues? (section III.C)

In the literature, the concept of V2G has been discussed since the end of the last century [10]. At the beginning of the 2000s, it was still about the theoretical general concept and potential of EVs [11,12]. Later, the focus was increasingly on the role of aggregators [8,13] and charging and bidding strategies [14,15]. Smart charging strategies can reduce the cost of charging EVs, while V2G can even lead to additional revenue [15]. Since the use of EVs in V2G concepts results in additional cycling, strategies have been developed to minimize additional battery degradation costs in addition to maximizing revenue [14]. With the global market ramp-up of EVs in recent years, an increasing number of projects testing V2G on vehicles in the field emerged from 2010 to 2021. Notable among these is the *Parker* project, which was conducted between 2016 and 2019 in a consortium of the Technical University of Denmark (DTU), Nissan, Nuvve and other partners [16]. In this project, the consortium demonstrated that EVs are capable of providing ancillary services [17]. In 2021, the authors also published an analysis of the battery degradation of V2G-providing EVs after 5 years in operation [18]. A detailed list of this and other projects on field tests can be found in the appendix of our first publication [6]. In addition we have published extensive literature reviews on FCR provision and arbitrage trading using pools of EVs [6,9].

Concerning battery sizes for V2G provision (RQ 1), Harris et al. showed in 2014 that the influence of available charging power on potential V2G capacities is greater than that of battery size [19]. However, only battery capacities between 12 kWh and 36 kWh were considered, while we investigate capacities from 19 kWh to 81 kWh in our work. We assume

11 kW as the maximum charging power, while in the aforementioned work, a maximal power range between 2.2 kW and 10 kW was investigated. Furthermore, we are not aware of any work that has used power and energy capability profiles to analyze which battery sizes of EVs or EVs of which economic sectors are particularly suitable for V2G deployment. We would like to address this research gap with the first two research questions (section III.A and III.B). Regarding the third research question, in the previous work [6] we showed that mainly by making the FCR market more flexible in provision time from months to weeks to days and to 4 hours, the potential revenue of EVs increased in 2020 although prices generally fell [6]. In this paper, we look at flexibilization in terms of minimum bid sizes and its impact on potential revenues (section III.C).

The remainder of the paper is structured as follows: Section II briefly presents the database, the previous work and related results. Subsequently, Section III presents the methodology and results in three subsections. Finally, Section IV gives a summary and an outlook.

II. DATABASE AND PREVIOUS RESULTS

This section presents the database and results of the previous two publications [6,9]. We first discuss the data basis (II.A) and the markets considered (II.B). Then we explain in subsection II.C how the power and energy capability profiles were compiled. Finally, we present the optimized EV pools (II.D).

A. Database

The data used in our work is based on the REM 2030 project and data measured at the Institute of Power Generation and Storage Systems (PGS) at RWTH Aachen University in the project "Commercially operated electric vehicle fleets (GO-ELK)" [20,21]. The REM dataset includes driving data from 630 commercial combustion vehicles over a period of a few days to a few months. We use 468 of these vehicles that included at least one week of data and made at least one trip. The trip data includes times of trip start and end, as well as distance traveled and distance to the company site after each trip. Vehicle-specific data such as vehicle size and the economic sector of the company were also published. We use these data in particular in this paper. A detailed description of the data basis including statistical evaluations can be found in [6].

B. Grid services and markets

EVs can participate in various markets through V2G. One market we analyzed is the Frequency Containment Reserve (FCR) market in the Continental European Synchronous Area (CESA) with prices from Germany in the second half of 2020. This type of balancing power is the fastest type in the German market with 30 seconds activation time and must be provided simultaneously in both positive and negative directions [22]. The market for FCR in the ENTSO-E area has undergone a number of changes in recent years [6,23]: Prior to mid-2011, FCR was marketed on a monthly basis and the minimum bid size was 5 MW. Then the service period was reduced to one week and the minimum offer was 1 MW. Since mid-2019, FCR became even more flexible in terms of time: First, FCR was tendered on a daily basis until mid-2020. Since then, FCR has even been marketed in 4h blocks. This higher temporal flexibility increases the potential for pools of EVs despite

falling FCR prices [6]. To determine the potential revenues in this market, we use the average prices of the 42 4-hour-slots of a week. For a detailed explanation and discussion of the market for FCR, including price analyses, see [6].

In addition to the application of balancing power, we also simulate arbitrage trading on the EPEX spot markets intraday continuous and day-ahead auction (1 hour). On the EPEX intraday market, energy is traded with a minimal lead time of 15 minutes in 15-minute blocks of at least 0.1 MW [24]. This market is therefore suitable for short-term trading. On the EPEX day-ahead auction market, energy can be traded in hourly blocks or more with a minimum of 0.1 MW for the following day [24]. In our simulations, we use the mean prices of 2020 for both spot markets. For the intraday continuous market, we use the weighted average pay-as-bid price of every quarter-hour of the week. For the day-ahead auction price, we use the mean market-clearing price of every hour of the week. Detailed descriptions of the markets and price diagrams can be found in [9].

C. Capability Profiles

Using the data presented in subsection II.A, we created power and energy capability profiles of the vehicles in our initial work [6]. These weekly profiles indicate which power or energy a vehicle can absorb or deliver at which time. For this purpose, we created a simulation model that uses the start probabilities, time-dependent distance and trip duration distributions to create driving profiles over arbitrary periods of time. In addition, each combustion engine is assigned a battery capacity and a consumption per kilometer driven based on its size [6].

The driving profiles and battery data are then used in a mobility model. This model checks the status of the vehicle (on the road or plugged-in) in each simulation step and decides, for example, whether to recharge. In addition, the model determines how much energy and power the EV can still charge and discharge. For this purpose, we divide the battery virtually into one part for the primary use, mobility, and one part for the secondary use, V2G provision. At times when the vehicle is frequently on the road, a large portion is reserved for mobility, since mobility always takes priority over V2G provision in our modeling approach. We assume the maximum charging power that the charging station can provide to be 11 kW. However, the available chargeable and dischargeable power of an EV may be lower depending on the provision period of the market due to energy limits of the

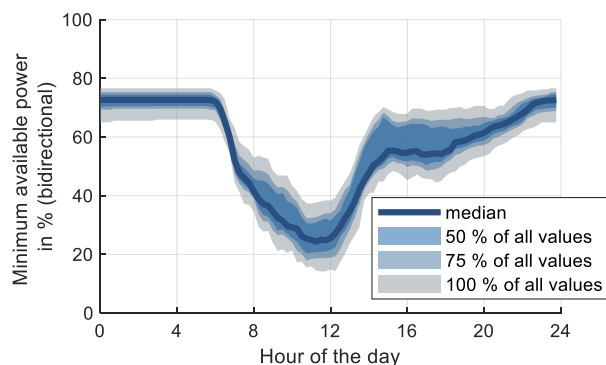


Fig. 2: Median and confidence intervals of the power capability profile of the cluster human health for all weekdays [6].

battery. For example, if the battery is almost fully charged, 11 kW can no longer be charged over 15 minutes.

In our initial work, we subsequently clustered the power capability profiles of EVs by economic sectors [6]. An example of the "Human Health" cluster is shown in Fig. 2. This shows the daily profile of the median of minimum bidirectional power of the EVs in the cluster along with confidence intervals. At night, the EVs of this cluster can charge and discharge about 70% of their maximum aggregated power. During the day, the EVs are traveling regularly, so that the median of the available power drops to about 25% of the maximum aggregated power. Other clusters have quite different curves, as we have shown in [6].

By using profiles of commercial vehicles, we achieve a certain regularity of trips and driving patterns. In addition, as described, we keep energy reserved for mobility. Nevertheless, in a worst-case scenario, a critical number of EVs could drive off contrary to the statistics. In this case, the aggregator would have to keep back-up power in stationary storage systems, for example.

D. Optimized Pools

In our previous work, we used the capability profiles of each EV to assemble different pools and perform FCR or arbitrage trading with them [9]. Aggregators can compose their EV pools in random fashion or alternatively, using the capability profiles, include only those vehicles that contribute to the pool power. For this purpose, we have developed algorithms using genetic optimization that maximize the revenue per vehicle participating in the pool. We maximize revenue per EV since the aggregator has costs per vehicle for metering equipment and bidirectional charging stations. In addition, we assume that in the future aggregators will be able to choose from an extremely large number of possible EVs and then gain competitive advantages through smarter or optimized selection.

The potential annual revenues in the three markets for random pools (mean of 10,000 pools) and the optimized pool are depicted in Table I. The optimization method chooses 243 EVs for the FCR market and much smaller pools for the spot markets. To compare pools of the same number of vehicles, equal numbers were then chosen for 10,000 random pools and the revenues were calculated. In general, the FCR market was the most attractive for EV pools in 2020, followed by arbitrage on the intraday market. Arbitrage trading on the day-ahead market can generate the least revenue. Through optimal pool composition, revenues can be increased by 72% on the FCR market, 168% on the intraday market and almost 700% on the day-ahead market. These results suggest how important pool composition might become for aggregators in the future. In the

TABLE I: COMPARISON OF REVENUES IN THE THREE MARKETS BETWEEN THE 10,000 RANDOM POOLS AND THE OPTIMIZED POOL, RESULTS FROM [9].

Market	# EVs	Annual revenue per EV	
		Optimized Pool	Mean of 10,000 random pools
FCR	243	378 €	219.6 €
Intraday	48	203.1 €	75.9 €
Day-Ahead	61	27.9 €	3.5 € ^a

^a Mean for random day-ahead pools of 61 EVs that could generate any revenue; 94% of the 10,000 pools could not generate any revenue

following, we analyze the optimized pools in terms of battery size and economic sector, and then calculate potential revenues in the FCR market if its minimum bid size were reduced.

III. METHODOLOGY AND RESULTS

The methodology and results of the analyses and optimizations are presented in the following. First, the composition of the optimized pools in terms of battery size and economic sector is discussed. Subsequently, the effects of an increased flexibility of the FCR market are presented.

A. Analysis of optimized EV pools regarding battery sizes

The determined power capability and available energy profiles are based on real driving data of commercial internal combustion vehicles [20]. For each profile, data such as the economic sector, the size of the company and the size of the vehicle exist. In this section, the optimized pools are evaluated with respect to their vehicle sizes. It should be noted that 468 vehicles were used and the optimized pools consist of 48 to 243 vehicles. The sample size is therefore relatively small and especially small deviations from the entire pool could also be of random nature.

In the published database, the internal combustion vehicles were classified in terms of their engine displacement. The categories are 'small' (<1400 cc), 'medium' (1400 to 2000 cc), 'large' (>2000 cc), 'transporter' (weight < 3,5t) and 'special vehicle' [25]. In our first work, we derived battery sizes for the electric vehicles from these vehicle sizes [6]. Different battery capacities were assumed for the respective vehicle sizes using electric car models (small: 19.1 kWh, medium: 31.4 kWh, large: 80.7 kWh, transporter: 27.9 kWh) [6]. In addition to the driving profile, the battery capacity is a factor that influences how much power a vehicle can still charge or discharge at any given time.

The share of each vehicle size category of the entire and the optimized pools are depicted in Fig. 3. The entire pool (468 EVs) consists of about one quarter small vehicles and one third medium vehicles. Transporter also make up a quarter, while large vehicles account for 13%. The three pools compiled using the optimization methods show a tendency towards larger vehicle batteries. None of the optimized pools uses small vehicles. The FCR pool, on the one hand, also uses only 16% large vehicles and instead more transporter and medium sized vehicles. The energy-intensive intraday and

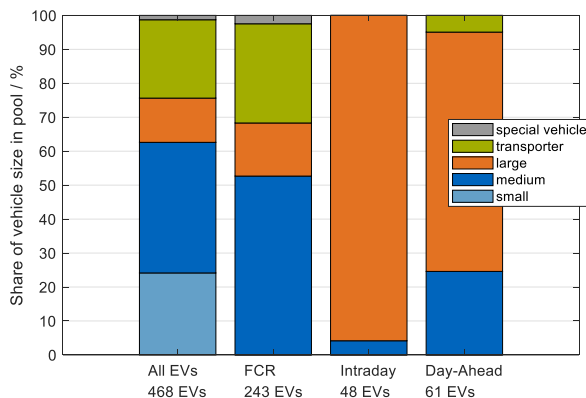


Fig. 3 Vehicle size share for all EV and the different optimized pools.

day-ahead pools, on the other hand, use over 74% large vehicles (intraday more than 95%). Here, the benefit of large vehicle batteries, with capacities assumed to be 80.7 kWh, appears to be the greatest benefit to the pool. Transporters are also only marginally represented here, as they only had a capacity of 27.9 kWh.

Overall, the analysis of vehicle sizes shows that vehicles with small battery capacities can often contribute less to the pool and are therefore filtered out by the optimization methods. Furthermore, when FCR is provided with an EV pool, it shows that all other vehicle sizes can contribute to the pool as the cycle depths in this application are relatively small [26]. Regarding the optimization of arbitrage trading at the spot markets, the battery capacity of the EVs seems to be crucial: Here, due to the larger discharge and charge cycles, mainly vehicles with large battery capacities should be used.

B. Analysis of optimized EV pools regarding economic sectors

For each of the published driving profiles, the economic sector was published in addition to the vehicle size and other categories [20]. The criteria for the economic sectors correspond to the NACE Rev. 2 classification of the EU [27]. An extract of NACE sections that exist in the database are listed in Table II. The shares of the 14 economic sectors in the four EV pools is depicted in Fig. 4 (a). In addition, Fig. 4 (b) shows the deviations of the shares in the optimized pools compared to the total pool of 468 EVs. An overweight is shown as positive and an underweight as negative.

The optimized FCR pool shows only slight deviations from the pool of all vehicles. Sectors G (+2.4 percentage points (pp)) and C (+4 pp) are slightly overweighted and sectors N (-3 pp) and Q (-6 pp) are slightly underweighted.

The intraday and day-ahead pools have significantly fewer vehicles overall, as fewer EVs are sufficient here to trade on the spot markets. The optimization method thus explicitly selects the EVs that are most suitable for arbitrage. For the spot market trading the optimization methods select 48

TABLE II: Extract of NACE sections according to [27].

Section	Description
C	Manufacturing
D	Electricity, gas, steam and air conditioning supply
E	Water supply, sewerage, waste management and remediation activities
F	Construction
G	Wholesale and retail trade; repair of motor vehicles and motorcycles
H	Transportation and storage
J	Information and communication
K	Financial and insurance activities
L	Real estate activities
M	Professional, scientific and technical activities
N	Administrative and support service activities
O	Public administration and defence; compulsory social security
Q	Human health and social work activities
S	Other service activities

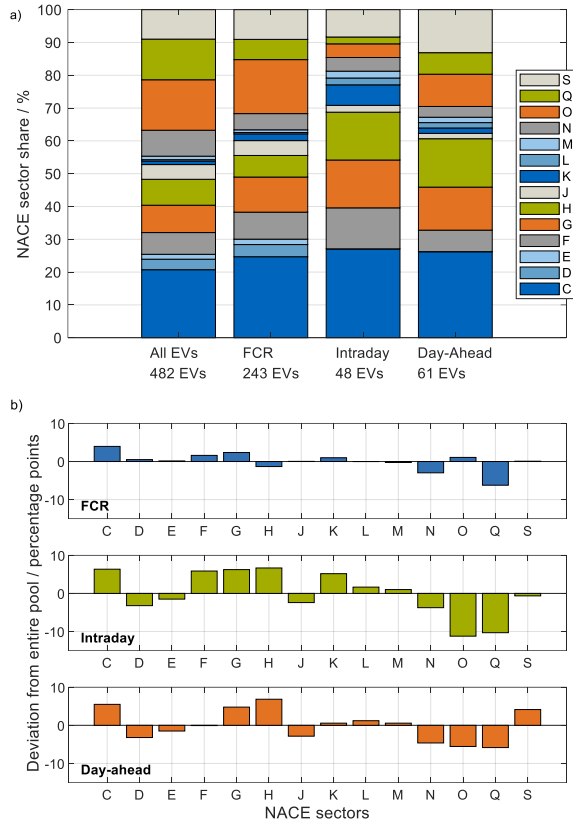


Fig. 4: NACE sector share for all EV and for the different optimized pools (a) and overweight and underweight of NACE sectors of EVs in the optimized pools compared to the entire pool in percentage points (b). Overweighing is shown positively, underweighing negatively.

(intraday) respectively 61 (day-ahead) vehicles. In both arbitrage markets, sectors C and H are more represented than in the overall pool, each at over 5 pp. In addition, sectors F, G and K are overweighed by more than 5 pp in the intraday pool. In contrast, sectors O and Q are underrepresented in both arbitrage markets, especially in the intraday pool by more than 10 pp each.

Consequently, based on the assumption that the driving behavior of the vehicles in the database is representative for the respective sectors, the sectors C, "Manufacturing", and H, "Transportation and storage", appear to be of particular interest for arbitrage trading. For the FCR pool, on the other hand, no clear tendency is discernible. However, vehicles in sector Q, "Human health and social work activities", appear unattractive in all three markets. This is because the relatively similar driving 58 EVs in this economic sector are on the road a lot, especially during the day (Fig. 2) [6]. In addition, EVs of sector O, "Public administration and defense; compulsory social security", are not very suitable for arbitrage trading. However, the 72 EVs in this sector are also 35% small vehicles, which means that the predominant non-use of this sector could be due to vehicle size in addition to the driving behavior.

C. Effects of increasing flexibility of the FCR market

This section examines the extent to which further flexibilization, i.e., downsizing, of the minimum bid size and increment in the FCR market affects the potential revenues of

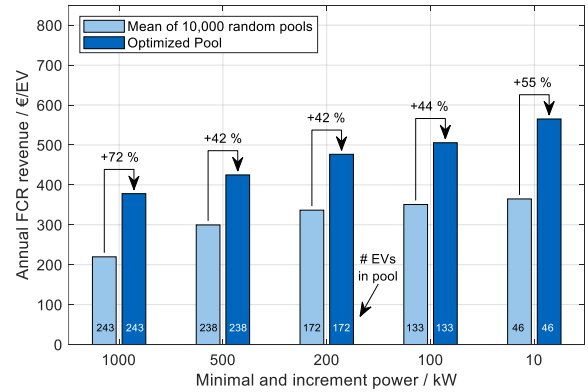


Fig. 5: Annual frequency containment reserve (FCR) revenue when decreasing the minimal and increment power for the provision of FCR random pools and optimized pools.

pools of EVs. For this purpose, the optimization with reduced minimum bid sizes was performed. In addition, for each case, 10,000 random pools were assembled and their potential revenues calculated. The minimum bid sizes used were 500 kW, 200 kW, 100 kW and 10 kW in addition to the standard of 1 MW. In the calculation of the revenues, the FCR prices for the second half of 2020 were used as in our previous works [6,9]. The results of this sensitivity analysis are depicted in Fig. 5.

If the minimum bid size and increment is reduced, pools of EVs can generate higher revenues more per vehicle. When the minimum and increment power is decreased from 1 MW to 10 kW, the revenue of the random pools increase by 66% from 220 € per EV to 365 € per EV. For the optimized pool, revenues increase by 49% from 378 € per EV to 565 € per EV for the same flexibilization. For this, the optimized pools use a reduced number of vehicles with decreasing minimum and increment power. The comparison between the random pools and the optimized pool shows that the advantage of the optimization varies between 42% and 72%. Especially with the large minimum and increment of 1 MW, the optimized pool has an advantage, since it can better utilize the large increments here.

Flexibility utilization can be calculated using the power utilization rate (τ_{PUR}) introduced in [9]. This rate indicates how much of the actual possible power could be marketed as FCR power (1). Since a buffer of 25% of the FCR power must be kept available when FCR is provided (i.e. 20% of the total power is buffer), the maximum value of τ_{PUR} is 80% [9,28].

$$\tau_{PUR} = 1 - \frac{1}{672} \sum_{t=1}^{672} \frac{\text{power capability}(t) - \text{FCR power}(t)}{\text{power capability}(t)} \quad (1)$$

The better the flexibility is used, the higher τ_{PUR} should be. The results of τ_{PUR} of the entire pool and the optimized pool as a function of minimal and increment power are shown in Table III. Therein it can be seen that the higher flexibility leads to higher τ_{PUR} . The optimization leads to slightly higher τ_{PUR} compared to the random pools of the same number. Overall, EV pools providing FCR in the future could benefit from an increase in flexibility. On the one hand, increased flexibility makes the market more financially attractive for small pools, and on the other hand, less potential power remains unused.

TABLE III: POWER UTILIZATION RATE (T_{PUR}) OF RANDOM AND OPTIMIZED POOLS WITH DECREASING MINIMAL FREQUENCY CONTAINMENT RESERVE (FCR) POWER

Min. & Increment Power	1 MW	500 kW	200 kW	100 kW	10 kW
Number of EVs	243	238	172	133	47
Mean of 10,000 random pools	39.3 %	56.7 %	65.3 %	68.3 %	71.1 %
Optimized pool	62.2 %	69.5 %	72.4 %	74.5 %	76.9 %

IV. CONCLUSION AND OUTLOOK

In this work we analyze the optimized commercial EV pools for providing FCR and arbitrage trading, and also investigate further flexibilization of the FCR market, building on our two previous publications [6] and [9]. The vehicle data published with the REM 2030 driving data is used to study the optimized pools regarding battery sizes and economic sectors [20]. In addition, we use the published optimization methods for the optimized EV pool composition in the FCR market to analyze a further flexibilization of the FCR market [9].

Regarding the EV battery size (RQ 1), we show that especially EVs with small vehicle batteries of 19.1 kWh are neither well suited for FCR provision nor for arbitrage trading. For FCR provision, all battery sizes upwards of 27.9 kWh (assumed for the transporter) are well suited, as the required depths of discharges and charges are relatively small for FCR provision [26]. For arbitrage trading, on the other hand, vehicles with large batteries should be used if possible, as the cycles are significantly deeper here. The analysis of the economic sectors (RQ 2) according to NACE criteria shows that in all scenarios considered, EVs in sector C ("Manufacturing") are well suited for the provision of V2G. Especially for arbitrage trading, EVs of sector H ("Transportation and storage") are also good candidates. Vehicles of sector Q ("Human health and social work activities") are in all scenarios considered the least suitable for V2G provision. This is because EVs of this sector are on the road every day and thus can generate less revenue [6].

In addition to the vehicle pool analyses, we also calculate further increasing flexibility in the FCR market in terms of minimum bid size and increments (RQ 3). For this purpose, the optimization algorithms from [9] are used to determine the optimized pools for the minimum and increment FCR power from 1 MW downwards to 10 kW. In addition, 10,000 random vehicle pools of the same number were compiled and the average revenues were determined. In this analysis, we find that increasing flexibility makes the FCR market more economically attractive for pools of EVs. Due to better utilization of increments, the revenues of optimized and random pools increase. Assuming increments of 10 kW instead of 1 MW, the revenues of optimized pools increase by about 50% per EV and those of random pools of the same number by about two thirds. Consequently, with smaller minimum FCR power and increment, less power potential of the EVs would remain unused.

Beyond the results presented, some research questions and issues arise regarding regulation and legislation. Verification of the results presented in this paper using more measured vehicle data of commercial (ideally electric) vehicles would be desirable. For this purpose, more field tests for V2G

provision should be conducted in research and industry projects. In addition, further analysis would be interesting on which parameters such as battery size and economic sector aggregators should compose their EV pools for maximum revenue. However, for the successful implementation of V2G, regulations also need to be simplified and new vehicle models need to be upgraded for V2G deployment. In addition, based on the revenue generation presented, the question is how much of an impact V2G will have on vehicle batteries in terms of degradation. We aim to answer these and other research questions in our following work.

ACKNOWLEDGMENT

This work was financially supported by the German Federal Ministry for Economic Affairs and Energy within the open_BEa project (Grant No. 03ET4072) and the German Federal Ministry of Education and Research within the SimBAS project (Grant No. 03XP0338A) as part of the Competence Cluster Battery Utilisation Concepts (BattNutzung), which are both managed by Project Management Jülich. The authors are responsible for the contents of this publication.

REFERENCES

- [1] IPCC. Climate Change 2021: The Physical Science Basis. Contribution of Working Group I to the Sixth Assessment Report of the Intergovernmental Panel on Climate Change: [Masson-Delmotte, V., P. Zhai, A. Pirani, S. L. Connors, C. Péan, S. Berger, N. Caud, Y. Chen, L. Goldfarb, M. I. Gomis, M. Huang, K. Leitzell, E. Lonnoy, J. B. R. Matthews, T. K. Maycock, T. Waterfield, O. Yelekçi, R. Yu and B. Zhou (eds.)]. Cambridge University Press. In Press.
- [2] International Energy Agency. Global EV Outlook 2021. Paris; 2021.
- [3] Sovacool BK, Kester J, Noel L, Zarazua de Rubens G. Actors, business models, and innovation activity systems for vehicle-to-grid (V2G) technology: A comprehensive review. *Renewable and Sustainable Energy Reviews* 2020;131:109963. <https://doi.org/10.1016/j.rser.2020.109963>.
- [4] Englberger S, Hesse H, Kucevic D, Jossen A. A Techno-Economic Analysis of Vehicle-to-Building: Battery Degradation and Efficiency Analysis in the Context of Coordinated Electric Vehicle Charging. *Energies* 2019;12(5):955. <https://doi.org/10.3390/en12050955>.
- [5] Martinez-Laserna E, Gandiaga I, Sarasketa-Zabala E, Badedo J, Stroe D-I, Swierczynski M et al. Battery second life: Hype, hope or reality? A critical review of the state of the art. *Renewable and Sustainable Energy Reviews* 2018;93:701–18. <https://doi.org/10.1016/j.rser.2018.04.035>.
- [6] Figgenger J, Tepe B, Rücker F, Schoeneberger I, Hecht C, Jossen A et al. The Influence of Frequency Containment Reserve Flexibilization on the Economics of Electric Vehicle Fleet Operation. <https://arxiv.org/pdf/2107.03489>; 2021.
- [7] Weiller C, Shang AT, Mullen P. Market Design for Electric Vehicles. *Curr Sustainable Renewable Energy Rep* 2020. <https://doi.org/10.1007/s40518-020-00163-3>.
- [8] Bessa RJ, Matos MA. The role of an aggregator agent for EV in the electricity market. In: 7th Mediterranean Conference and Exhibition on Power Generation,

- Transmission, Distribution and Energy Conversion (MedPower 2010). IET; 2010, p. 126.
- [9] Tepe B, Figgenger J, Englberger S, Sauer DU, Jossen A, Hesse H. Optimal pool composition of commercial electric vehicles in V2G fleet operation of various electricity markets. Submitted manuscript.
- [10] Kempton W, Letendre SE. Electric Vehicles as a New Power Source for Electric Utilities. Transportation Research Part D: Transport and Environment 1997(2).
- [11] Kempton W, Tomic J, Letendre S, Brooks A, Lipman T. Vehicle-to-grid power: battery, hybrid, and fuel cell vehicles as resources for distributed electric power in California 2001.
- [12] Letendre S, Perez R, Herig C. Battery-powered, electric-drive vehicles providing buffer storage for PV capacity value. In: proceedings of the solar conference; 2002, p. 105–110.
- [13] Perez-Diaz A, Gerding E, McGroarty F. Coordination and payment mechanisms for electric vehicle aggregators. Applied Energy 2018;212:185–95. <https://doi.org/10.1016/j.apenergy.2017.12.036>.
- [14] Lunz B, Walz H, Sauer DU. Optimizing vehicle-to-grid charging strategies using genetic algorithms under the consideration of battery aging. In: 2011 IEEE Vehicle Power and Propulsion Conference. IEEE; 2011 - 2011, p. 1–7.
- [15] Schuller A, Dietz B, Flath CM, Weinhardt C. Charging Strategies for Battery Electric Vehicles: Economic Benchmark and V2G Potential. IEEE Trans. Power Syst. 2014;29(5):2014–22. <https://doi.org/10.1109/TPWRS.2014.2301024>.
- [16] Bach Andersen P, Seyedmostafa Hashemi T, Meier Sørensen T, Eske Christensen B, Morell Lodberg Høj, Jens Christian, Zecchino A. The Parker Project: Final Report; 2019.
- [17] Bañol Arias N, Hashemi S, Andersen PB, Traholt C, Romero R. V2G enabled EVs providing frequency containment reserves: Field results. In: 2018 IEEE International Conference on Industrial Technology (ICIT). IEEE; 2018 - 2018, p. 1814–1819.
- [18] Thingvad A, Calearo L, Andersen PB, Marinelli M. Empirical Capacity Measurements of Electric Vehicles Subject to Battery Degradation from V2G Services. IEEE Trans. Veh. Technol. 2021;1. <https://doi.org/10.1109/TVT.2021.3093161>.
- [19] Harris CB, Webber ME. The sensitivity of vehicle-to-grid revenues to plug-in electric vehicle battery size and EVSE power rating. In: 2014 IEEE PES General Meeting | Conference & Exposition. IEEE; 2014, p. 1–5.
- [20] Fraunhofer-Institut für System- und Innovationsforschung ISI, KIT. REM 2030 Fahrprofile. Karlsruhe; 2018.
- [21] Uniper Technologies GmbH, Hochschule Ruhr West, Institute for Power Generation and Storage Systems at RWTH Aachen University. Gewerblich operierende Elektro-Kleinflotten (GO-ELK) Abschlussbericht GO ELK: Berichtszeitraum: 01.2013-06.2016. Uniper Technologies GmbH; 2016.
- [22] German Transmission Grid Operators: 50 Hertz, Amprion, Tennet, TransnetBW. REGELLEISTUNG.NET: Internetplattform zur Vergabe von Regelleistung. [May 05, 2020]; Available from: <https://www.regelleistung.net>.
- [23] Bundesnetzagentur für Elektrizität, Gas, Telekommunikation und Eisenbahnen. Beschluss BK6-18-006; 2018.
- [24] EPEX SPOT SE. Trading at EPEX SPOT 2021; 2021.
- [25] Funke S, Gnann T. Codebook REM 2030 driving profiles database. Karlsruhe; 2015.
- [26] Kucevic D, Tepe B, Englberger S, Parlikar A, Mühlbauer M, Bohlen O et al. Standard battery energy storage system profiles: Analysis of various applications for stationary energy storage systems using a holistic simulation framework. Journal of Energy Storage 2020;28:101077. <https://doi.org/10.1016/j.est.2019.101077>.
- [27] Eurostat. NACE Rev. 2: Statistical classification of economic activities in the European Community. 2nd ed. Luxembourg: Office for Official Publications of the European Communities; 2008.
- [28] Englberger S, Jossen A, Hesse H. Unlocking the Potential of Battery Storage with the Dynamic Stacking of Multiple Applications. Cell Reports Physical Science 2020;1(11):100238. <https://doi.org/10.1016/j.xcrp.2020.100238>.

5 Vehicle-to-X provision in various applications using three modes of e-transportation

This chapter presents the research paper titled *Vehicle-to-X Service Provision for various Modes of e-Transportation with Consideration of the Influence on Lithium-Ion Battery Utilization*, which was presented at the International Conference on Applied Energy in December 2023, peer-reviewed and will be published in Energy Proceedings [5]. Cars, buses and boats are purchased by private individuals and companies for the transportation of goods and people. However, the vehicles are only used a fraction of the time. The increasing electrification of vehicles now offers the potential to also use them for V2X provision during idle times. In general, vehicles are used for their primary purpose of transport with varying frequency and regularity, so the predictability of driving patterns is highly relevant for vehicle pool aggregators. Furthermore, the time availability of vehicles for V2X is essential for an analysis of potential markets and applications. If the vehicles were used for V2X, the question also arises of the additional load on the LIBs with regard to battery-relevant parameters and degradation. These are the issues addressed in this chapter.

The work combines the topics and data from the previous chapters of the thesis. From chapter 3.2, the driving profiles of e-Cars, e-Buses and e-Boats are used to simulate their driving behavior in SimSES. In addition, the storage power of stationary BSSs in typical applications is used from chapter 3.1 and scaled to the individual vehicles for V2X provision during idle times. From chapters 4.1 to 4.3, the approach of V2X provision is further elaborated and open research questions are answered. Following on from chapter 3.2, the paused charging strategy in SimSES is extended to a V2X strategy that simulates the impact on the V2X provision during idle times, i.e. when the e-Car is at home, the e-Bus is at the depot and the e-Boat is at the dock. The simulation results allow conclusions to be drawn about the additional impact on the vehicle batteries due to the V2X provision, for example the increase in EFCs. For the e-Cars, the additional battery capacity loss due to the V2X provision is also investigated. Moreover, the driving behavior of the vehicles is examined in more detail and, on the one hand, the predictability is quantified using historical data and, on the other hand, the V2X availability is determined over the course of the week.

The research questions answered in this chapter are:

1. How regular and predictable is the operation of e-Cars, e-Buses and e-Boat?
2. What is the EVs' temporal V2X-ready ratio over the week?
3. How do battery-relevant parameters change due to the provision of V2X?
4. What are the effects of V2X provision in terms of battery aging?

The analysis of the predictability of driving behavior in this chapter shows that e-Cars in particular behave predictably at night. In addition, the V2X availability of e-Cars and e-Bus is highest at night. The simulation results of V2X usage show, for example, that the EFCs of the e-Cars increase by 42 to 50 % in FCR and intraday trading. Average SoCs and C-rates are also changed by V2X provision. While the mean SoCs increase only slightly, the mean C-rates decrease significantly, as the power

during V2X provision with the assumed pool sizes is lower than the usual power during the trips. The additional capacity loss of the e-Cars batteries due to V2X provision is up to 4.5% after one year of simulation compared to the paused, unidirectional charging strategy.

Author contribution

Benedikt Tepe was the principle author tasked with coordinating and writing the paper and developing the methodologies. Sammy Jablonski contributed to the data analysis and assisted with the result visualization. Holger Hesse reviewed the manuscript and gave valuable input throughout the manuscript preparation. Andreas Jossen contributed via fruitful scientific discussions and reviewed the manuscript. All authors discussed the data and commented on the results.

Vehicle-to-X Service Provision for various Modes of e-Transportation with Consideration of the Influence on Lithium-Ion Battery Utilization

Benedikt Tepe, Sammy Jablonski, Anupam Parlikar, Holger Hesse and Andreas Jossen

15th International Conference on Applied Energy, Qatar, 2023

This paper was presented at the 15th International Conference on Applied Energy, peer-reviewed and will be published in Energy Proceedings.

Vehicle-to-X Service Provision for various Modes of e-Transportation with Consideration of the Influence on Lithium-Ion Battery Utilization

Benedikt Tepe^{1*}, Sammy Jablonski¹, Anupam Parlikar¹, Holger Hesse², Andreas Jossen¹

¹ Technical University of Munich (TUM), School of Engineering and Design, Department of Energy and Process Engineering, Chair of Electrical Energy Storage Technology, Germany

² Kempten University of Applied Sciences, Department of Mechanical Engineering, Institute for Energy and Propulsion Technologies, Germany

(*Corresponding Author: benedikt.tepe@tum.de)

ABSTRACT

The electrification of transportation modes such as cars, buses, and boats offers the potential of providing vehicle-to-X services during idle times. Pools of vehicles can provide balancing power, trade on the electricity market, or be used for load peak shaving. In this work, the usage patterns of electric cars, electric buses, and electric boats are investigated, and the provision of vehicle-to-X with these vehicles is simulated using an open-source simulation tool. A data analysis and a vehicle usage pattern assessment show that especially private electric cars behave predictably at night. It also reveals that the vehicle-to-X availability varies over the week for all vehicle types and is highest at night for cars and buses. During the day on weekdays, private cars are available for vehicle-to-X 30 to 70% of the time, the analyzed buses 5 to 50% of the time, and the availability of the boats depends on their primary use as ferries or private boats. If the three transportation modes provide vehicle-to-X during idle times, the equivalent full cycles that the lithium-ion batteries complete increase at different rates depending on the vehicle pool size, while the mean charging rates decrease. Furthermore, an exemplary aging analysis shows that the additional load of vehicle-to-X provision slightly increases the capacity loss of the car batteries compared to a paused unidirectional charging strategy.

Keywords: electric vehicles, vehicle-to-X, vehicle-to-grid, lithium-ion batteries, transportation means, battery degradation

NOMENCLATURE

Abbreviations

BSS	Battery storage system
e-Boat	Electric boat
e-Bus	Electric bus
e-Car	Electric car
EFC	Equivalent full cycle
FCR	Frequency containment reserve
LFP	Lithium iron phosphate
LIB	Lithium-ion battery
PS	Peak shaving
SOC	State of charge
V2B	Vehicle-to-building
V2G	Vehicle-to-grid
V2H	Vehicle-to-home
V2X	Vehicle-to-X

Parameters and Symbols

$b(t)$	Binary value indicating connection to electricity grid
j	Current timestep in period
m	Number of periods
n	Number of timesteps in period
$P(t)$	Power
$Pred_j$	Predictability score at current timestep
$v(t)$	Binary value of current V2X-ready ratio

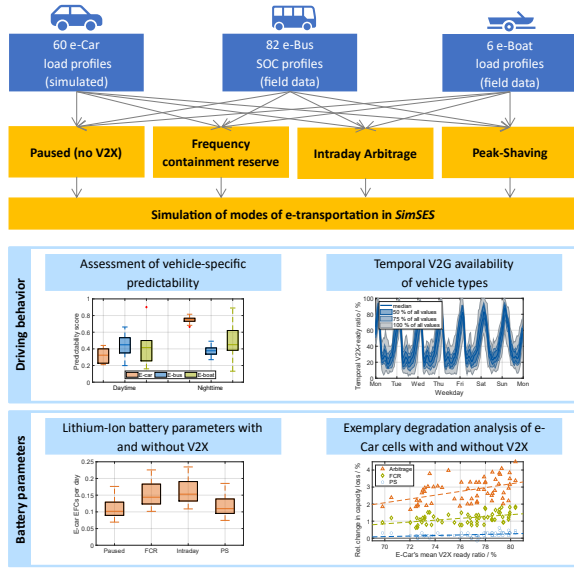


Fig. 1. Graphical overview. Three vehicle types and four charging strategies are simulated with *SimSES* to generate results on driving behavior and battery-relevant

1. INTRODUCTION

The electrification of vehicles plays an essential role in decarbonization [1]. This is one of the reasons why the number of electric cars (e-Cars), electric buses (e-Buses), and electric boats (e-Boats) increase worldwide [1–3]. These vehicles introduce relatively large storage capacities to the market through their batteries [4]. From an economic perspective, it is therefore essential to exploit the potential of vehicle batteries during idle times. When the vehicles are connected to the electricity grid, they can be used for various purposes in the future [5]: First, they can contribute behind-the-meter to consumption of photovoltaic energy via vehicle-to-home (V2H), as is done with stationary home battery storage systems (BSS) [6]. Another behind-the-meter application is peak-shaving (PS), where pools of vehicles help meet peak loads in vehicle-to-building (V2B) [6]. Second, the vehicles can participate in electricity trading or provide grid services using vehicle-to-grid (V2G), corresponding to front-the-meter applications [7,8]. For example, arbitrage trading is performed on the intraday market in the former. In the latter, pools of vehicles can provide, for example, frequency containment reserve (FCR) to compensate for frequency fluctuations in the electricity grid. Generally, the bidirectional use of electric vehicles during idle times is called vehicle-to-x (V2X) [5].

Using vehicles in V2X can generate additional revenue and bring environmental benefits by increasing battery utilization. However, it also leads to a higher load on the vehicle batteries. With suboptimal planning, the provision of V2G can increase the degradation of vehicle batteries [9]. An increased degradation of vehicle batteries when providing primary frequency regulation was also shown by Thingvad et al. in a field trial in Denmark [10].

A detailed evaluation of the impact of V2X on various battery-related parameters is part of this work. Open-access data from previous publications is used to simulate the provision of V2X in the storage simulation tool *SimSES* [11] (section 2 and section 3). The focus is on the applications FCR, intraday arbitrage trading, and PS. We use driving profiles of simulated private e-Cars and field data of city e-Buses and e-Boats. This way, various vehicle types and V2X applications are combined and analyzed. The key contributions include an analysis of the predictability of the vehicles (section 4.1), an analysis of the V2X availability of the vehicle types (section 4.2), an evaluation of the influence of V2X provision on battery-relevant parameters (section 4.3), and an exemplary degradation analysis of the e-Car batteries (section 4.4).

The innovative points of this work are enabling the simulation of V2X services in the open-source tool *SimSES*, statements on the V2X capability of various vehicle types, and the impact of V2X deployment on battery-relevant parameters.

2. DATABASE

2.1 Data of mobile BSS applications

Due to the growing electrification of vehicles, such as buses, cars, and boats, lithium-ion batteries (LIBs) are increasingly being installed in these means of transport as traction batteries. For the simulation of the three means of transportation, we rely on data published as open data in a previous work [12,13]. Based on this work, load profiles of 60 e-Cars and six e-Boats and state-of-charge (SOC) profiles of 52 e-Buses are available (see Table 1). The profiles have varying lengths, and the simulations in this work are always performed over the entire length of a vehicle profile.

2.2 Data of stationary BSS applications

Stationary BSSs are used in various applications. For example, they can perform arbitrage trading on the electricity market or provide grid services like FCR. Parked electric vehicles can also participate in these markets if they are connected to the electricity grid and

Table 1: Data on the transportation means and the stationary BSSs used for V2X provision.

Data	# of datasets	Data length	Reference
e-Cars	60	One year	Tepe et al. [13] based on Gaete-Morales et al. [16]
e-Buses	52	3 to 14 months	Tepe et al. [13]
e-Boats	6	3 to 9 months	Tepe et al. [13]
FCR	1	One year	Kucevic et al. [14]
PS	1	One year	Kucevic et al. [14]
Arbitrage	1	One year	Collath et al. [15]

combined in pools. In the following sections these applications are called V2X applications. To simulate the V2X applications in *SimSES*, we use storage load profiles that we defined in a previous work as representative load profiles for the PS and FCR applications [14]. Since the PS profile was developed with a storage system with a maximum power of 40 kW and the vehicles' charging and discharging power range from 11 to 150 kW, the PS profile was scaled up by a factor of 10 so that its maximum power now corresponds to 400 kW. For the arbitrage application, we use a load profile determined in a research work by Collath et al., who optimized arbitrage trading with a stationary BSS considering calendar and cyclic degradation [15].

3. METHODOLOGY AND SIMULATION FRAMEWORK

3.1 *SimSES: Simulation of EVs and V2X provision*

The open-access storage system simulation tool *SimSES* was developed at the Technical University of Munich and has been presented in detail in a previous publication [17]. In our work on e-transportation and their utilization of batteries, the extension of *SimSES* to mobile applications was explained [12]. The publication compared charging strategies such as uncontrolled charging versus paused charging, where charging was performed after arrival to a minimum SOC and paused until just before departure. This paused strategy was extended for this work to allow vehicles to provide V2X during the paused period. This is done by superposing a V2X load profile of one of the stationary applications FCR, PS, or arbitrage over to the load (e-Cars, e-Boats) or SOC (e-Buses) profile. As soon as the respective vehicle is at home (e-Car), in the depot (e-Bus) or at the dock (e-Boat), it is charged to a minimum SOC of 50%. Subsequently, the provision of V2X is simulated until the time when charging is required again for the vehicle to

be fully charged at departure. The e-Buses are charged to the departure SOC logged in real operation, as described in a previous publication [12]. Alternative approaches of charging strategies, for example charging only the amount of energy needed for the next trip, are not part of this work. For the estimation of the departure time, perfect foresight is assumed. To calculate the required V2X power at every point in time, the power of the V2X profile is divided by the number of currently existing vehicles in the pool and assumed to be the power to be provided by the vehicle. This means each vehicle in the pool must provide the same fraction of the total pool power. The estimation of the available number of vehicles is explained in section 4.3, as this is based on results from section 4.2. During V2X operation, the SOC of the vehicle can drop below 30%. If this is the case, the V2X operation is paused, and the vehicle is recharged to 50% so that at least 30% is always available for spontaneous trips. In a field test, users have reported an average of 34% as the minimum desired available SOC [18].

This work uses batch simulations to simulate the 60 e-Cars, 52 e-Buses, and six e-Boats in the three V2X markets FCR, arbitrage trading, and PS. *SimSES* then determines a variety of metrics that are calculated for each vehicle with each V2X market. One metric of *SimSES* is the binary quantification of whether the vehicle can be used for V2X at a point in time. The calculation of this value is shown in equation (1). This is the case when the e-Car is at home, the e-Bus at the depot, and the e-Boat at the dock ($b(t) = 1$) and not being charged ($P(t) = 0$). If the condition is met, the plugged-and-idle value $v(t)$ is 1. In contrast, if the vehicle is on the road or currently charging the plugged-and-idle value is 0. The proportion of the total time the vehicle can be used for V2G was referred to as the temporal V2G-ready ratio in [12]. Analogously, the value in this work is called V2X-ready ratio to imply that V2H and V2B could also be provided.

$$v(t) = \begin{cases} 1, & P(t) = 0 \text{ and } b(t) = 1 \\ 0, & \text{otherwise} \end{cases} \quad (1)$$

3.2 *Quantification of driving behavior predictability*

The suitability of vehicles for V2X depends on various factors. These are, for example, the driving behavior, the grid connection times, and the predictability of departures and arrivals. For electric vehicle aggregators, it is relevant to be able to predict or estimate the available pool size at any given time. Supposing that the vehicle owner does not provide the next departure or arrival time, or it cannot be determined from bus

schedules, historical data can be used to estimate when the vehicle will depart. However, for historical data, estimating the extent to which the vehicle is used according to repetitive behavior, such as a daily commute or a trip to a weekly recreational activity, is crucial. The predictability is to be quantified as explained in the next paragraph.

For the investigation of the weekly periodicity, the respective $v(t)$ vector is first decomposed into weekly segments. Figure 2 a) shows $v(t)$ for an exemplary e-Car for each hour of the week over the year. The hourly resolution is chosen here for a better visualization and results from the mean value of the 60 one-minute values. This results in values between 0 and 1 in addition to the binary values. Moreover, Figure 2 b) indicates the probability that the value for $v(t)$ is 1 at a certain time during the week. At times when the probability is close

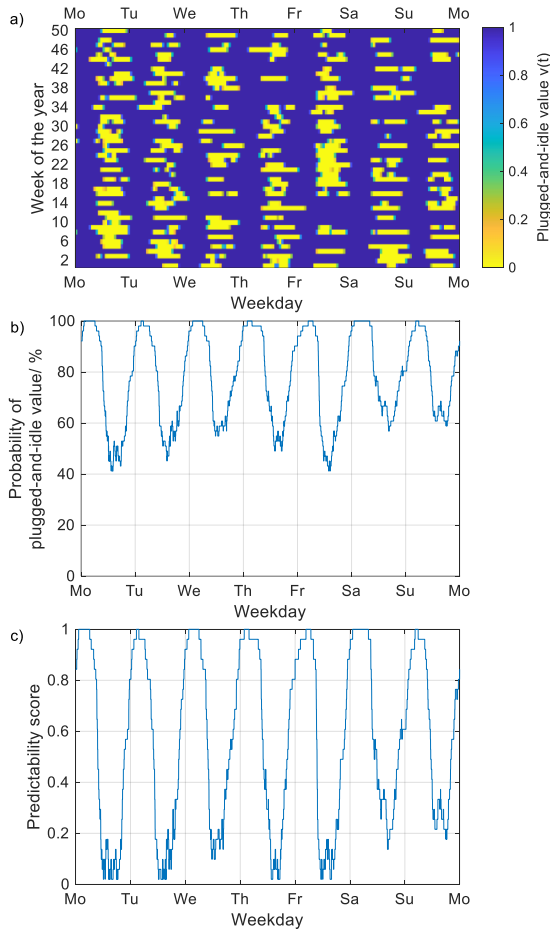


Fig. 2. Hourly plugged-and-idle values of one exemplary e-Car over the year segmented in weeks (a), probability of plugged-and-idle values of one over the week (b), and predictability score over the week (c).

to 100%, the vehicle can be used frequently for V2X. The diagrams show that there are phases during the week when the vehicle could provide V2X relatively consistently, such as Wednesday nights. Likewise, there are phases when the vehicle is often not available for V2X, such as Monday afternoons. For aggregators, these consistent phases are desirable because the vehicle is predictable. Less desirable are phases in which the vehicle is sometimes available and sometimes on the road. The worst case from the aggregator's point of view is when the vehicle is, on average, 50% available at one point in time. On the other hand, average values of 0 and 100% are desirable because the vehicle is fully predictable during these times. We now determine a predictability score at each point of time of the week using equation (2). Therefore, we subtract 0.5 from the mean value of the values at one point in the week and multiply the absolute value by two. If the mean value is 0.1, for example, this results in a predictability score ($Pred$) of 0.8. The same $Pred$ results from a mean value of 0.9. In contrast, the worst case mean value of 0.5 leads to a $Pred$ of 0.

In addition to the weekly period shown here, periods of 24 hours or 30 days, for example, can also be used. No distinction would be made between working days and weekend days in the case of daily periods. If monthly periods were used, events occurring monthly could be better captured and predicted.

$$Pred_j = \left| \frac{\sum_{k=1}^m v_j^k}{m} - 0.5 \right| \times 2 \quad (2)$$

With:

$$\mathbf{v} = \begin{bmatrix} v_1^1 & v_1^2 & \dots & v_1^m \\ v_2^1 & v_2^2 & \dots & v_2^m \\ \vdots & \vdots & \ddots & \vdots \\ v_n^1 & v_n^2 & \dots & v_n^m \end{bmatrix}$$

m : Number of periods

n : Number of timesteps per period

$$\overline{Pred} = \begin{bmatrix} Pred_1 \\ Pred_2 \\ \vdots \\ Pred_n \end{bmatrix}$$

$$Pred_j \in \{0; 1\} \quad j = 1 \dots n$$

3.3 Lithium-ion battery relevant KPIs and effects on battery degradation

LiBs are subject to degradation effects, which can be separated into calendar and cyclic aging [19]. While the former occurs permanently over time, the latter depends on the cyclization of the battery. Various parameters

influence the degradation of LIBs so that the utilization of LIBs can be quantified with respect to those parameters [12]. For example, the equivalent full cycles (EFCs) can be measured and compared with each other in various applications. For this purpose, the energy throughput is divided by the nominal energy of the battery. In general, higher cyclization, an increase in EFCs, leads to accelerated cyclic degradation. However, the extent of the increased degradation differs for different cell chemistries, as there exist more cycle-stable and less cycle-stable chemistries [20]. Another relevant parameter is the average SOC experienced by the LIB. For example, if private e-Cars are charged immediately after arriving at home, the mean SOC is relatively high because the vehicles are parked for a long time at high SOC [12]. If, in contrast, charging takes place later or with a pause, the mean SOC of the battery can be reduced [12]. The mean SOC also influences the degradation of LIBs [19]. For most LIBs, high mean SOC should be avoided because an accelerated solid electrolyte interphase growth occurs in those SOC ranges [20]. This effect amplifies the calendar degradation of the LIB. The last parameter calculated in this work is the charging rate (C-rate), which describes the current at which a battery is charged or discharged in relation to the nominal capacity of the battery [12]. The C-rate also influences cyclic degradation. If LIBs are exposed to comparatively high C-rates, cyclic degradation increases [19]. In addition, other factors play a role in degradation, such as temperature and depth of discharge [20]. The decrease of remaining capacity and the increase in resistance of a LIB then result from an interplay of the various influencing factors. In *SimSES*, for example, semi-empirical aging models are implemented for a Sony lithium iron phosphate (LFP) cell, published by Naumann et al. [21,22], and a nickel manganese cobalt (NMC) cell, published by Schmalstieg et al. [23]. Since many e-Buses and an increasing number of e-Cars have LFP batteries installed [1,24], we use the LFP model in section 4.4, which relies on a half-cycle counter.

4. RESULTS

This section presents the results of the work. First, the vehicle-specific predictability is analyzed in section 4.1. Afterwards, the V2X-ready ratio of the three vehicle types is illustrated in detail in section 4.2. Then, in section 4.3, battery-relevant parameters for V2X-providing vehicles are compared with those of unidirectional charged vehicles. Finally, in section 4.4, the influence of V2X provision on battery aging is shown using an exemplary LFP cell for the e-Cars.

4.1 Assessment of vehicle-specific predictability

The following section quantifies the driving behavior predictability of the vehicles according to the calculation from section 3.2. The presented analysis was performed for each vehicle to determine the course of the predictability score. The mean predictability scores for all vehicles are shown as boxplots in Figure 3. The periods used for the predictability scores are 24 hours (a) and seven days (b), as shown in Figure 2. Due to the significant differences in predictability scores between daytime and nighttime, Figure 3 shows the results for daytime (left) and for nighttime (right). The results for the three vehicle types are displayed and derived from the mean predictability scores of the 60 e-Cars, 52 e-Buses, and six e-Boats.

For the e-Cars, high predictability scores of 0.66 to 0.82 are achieved at night. Here, the simulated e-Cars behave relatively predictably. The e-Buses show smaller differences among themselves at night than during the day, where the scores are between 0.27 and 0.7 for the weekly pattern, for example (Figure 3 b)). At the same time, however, the median score of the buses at night is lower than the median score of the daytime. This can be explained by the fact that the required charging energy at night depends on the driving distance during the prior day, and thus the e-Buses are irregularly available for V2X at night while they are mostly on the road during the day. The e-Boats show large scatter in their predictability scores both during the day and at night. For example,

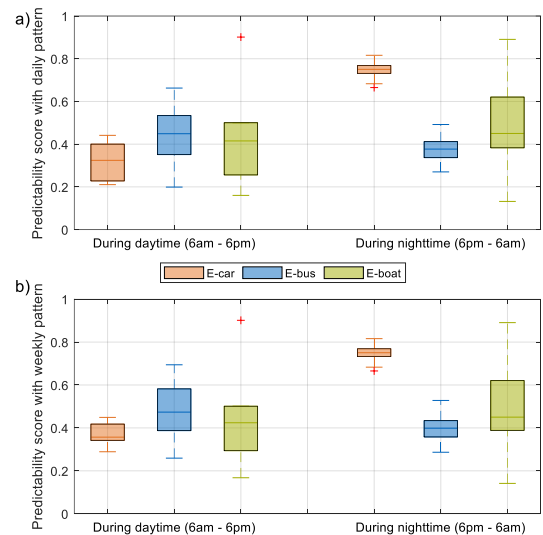


Fig. 3. Average predictability score of every vehicle during daytime (left) and during nighttime (right) using the predictability forecast for daily pattern (a) and weekly pattern (b).

there is one boat that achieves scores above 0.8. At the same time, there is another boat whose scores are below 0.2. Depending on the use of the boats as a ferry or pleasure vessel, the predictability therefore differs. Lastly, the usage of the daily pattern (Figure 3 a)) can be compared to that of the weekly pattern (Figure 3 b)). Especially for the e-Cars with their varying driving behavior between weekdays and weekends, the predictability scores increase when using a weekly pattern especially during the day. Moreover, the range of the results decreases for the e-Cars using the weekly pattern. The e-Buses also show slight improvements in predictability scores for daytime hours when changing from daily to weekly pattern and no changes at night. In contrast, no differences are observed for the e-Boats.

4.2 Temporal V2X availability of vehicle types

The V2X-ready ratio indicates the proportion of the time a vehicle can be used for V2X, as explained in section 3.1. For the e-Cars, for example, we found mean temporal V2X-ready ratios (respectively V2G-ready ratios) of 70 to 80% in a previous work [12]. At this point, the V2X-ready ratios are analyzed in more detail. Figure 4 shows the V2X-ready ratio of the three modes of transportation over a week. The dark line shows the median and the shading indicates the distributions with 50%, 75%, and 100% of all values. A value of 33% on Monday at noon means that the vehicle would be available for V2X on average every third Monday at noon. A value of 67% indicates that the vehicle would be available two out of three Monday noon times.

The private e-Cars show high temporal V2X-ready ratios of 90 to 100% at night (Figure 3 a)). On weekdays, the ratio drops to 30 to 70%, depending on the commuting behavior of the vehicle. On weekends, the ratio is also higher during the day, with 50 to 80%. E-Buses also have the highest V2X-ready ratio at night, with 50 to 100% (Figure 3 b)), although this is below the ratio of the e-Cars. During the day, the ratio drops to 5 to 50%, as the e-Buses are mostly on the road. The daytime behavior does not change much on weekends compared to weekdays. The e-Boat results are divided into two groups (Figure 4 c)): High-utilization e-Boats and low-utilization e-Boats. The high-utilization e-Boats have temporal V2X-ready ratios of mostly below 40%. The low-utilization e-Boats, in contrast, have ratios between 30 and 90%. Therefore, the e-Boats' potential differs greatly depending on how they are used. Moreover, the e-Boats do not show a typical daily pattern compared to the e-Cars and e-Buses. This is because the e-Boats are often charged at low power in the dock. In addition, low-

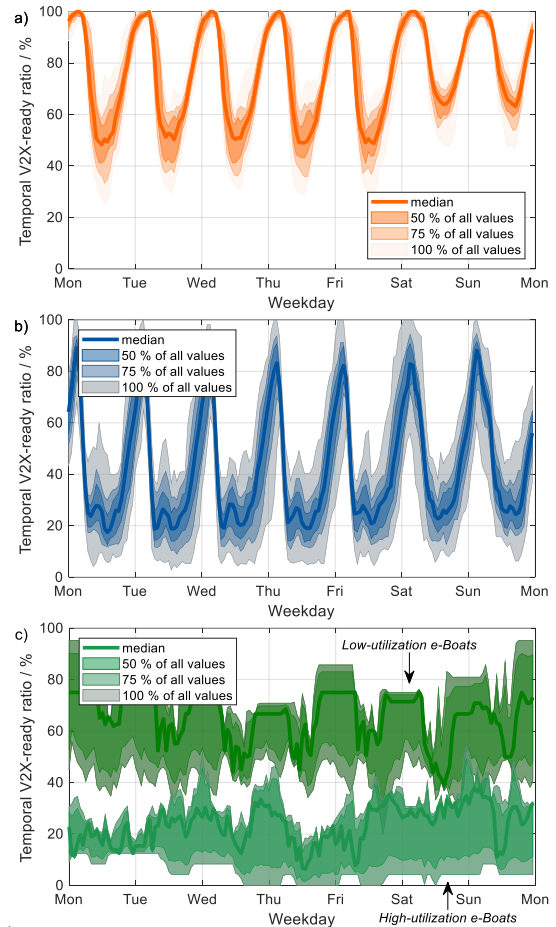


Fig. 4. Temporal V2X-ready ratio over the week using an uncontrolled charging strategy for the e-Cars (a), e-Buses (b), and e-Boats (c).

utilization e-Boats, for example, usually remain unused in the dock during the day as well as at night, resulting in no day-night rhythm as with the e-Buses and e-Cars. Overall, the evaluation shows that the temporal V2X potential of the vehicles varies over a week. Especially at night, e-Cars and e-Buses can be used for V2X. For e-Boats, the potential depends on the use of the boats.

4.3 Lithium-ion battery parameters with and without V2X

The provision of V2X changes the load on vehicle batteries. The extent of this change is examined in this section. Battery-relevant parameters considered in this work are the number of EFCs, the mean SOC, and the mean C-rates. The simulations are performed with *SimSES*, as described in section 3.1. Since the stationary applications FCR, PS, and arbitrage were generated for one large stationary BSS, the individual vehicles in the

Table 2: Pool size calculations. For determining the pool size, the maximum power required for V2X is divided by the maximum charging power (which equals the maximum discharging power) of the vehicles and by the assumed minimal temporal V2X-ready ratio.

Transportation means	e-Car			e-Bus			e-Boat		
Min. considered temporal V2X-ready ratio	40%	40%	40%	10%	10%	10%	10%	10%	10%
Max. charging power	11 kW	11 kW	11 kW	150 kW	150 kW	150 kW	11 kW	11 kW	11 kW
V2X market	FCR	Intraday	PS	FCR	Intraday	PS	FCR	Intraday	PS
Max. V2X power	1.2 MW	1 MW	400 kW	1.2 MW	1 MW	400 kW	1.2 MW	1 MW	400 kW
Required EVs in pool	273	228	91	80	67	27	1091	910	364

pool of vehicles only need to provide a fraction of the power of the original stationary storage. In general, the respective fractions depend on the current pool size. In previous works, we determined economically optimal pool sizes for commercial e-Cars to generate as much revenue as possible with as few vehicles as possible [7,25].

In this work, we estimate the total pool sizes based on the temporal V2X-ready ratio and the maximum power of the vehicle batteries and charging stations (see Table 2). For example, for the provision of FCR, a pool of 80 e-Buses is required to be able to deliver the 1.2 MW of maximum power at a minimal temporal V2X-ready ratio of 10%. The worst-case temporal V2X-ready ratio of the buses is 3% (Tuesday afternoon), according to Figure 4 b). Dimensioning the pool to this availability would significantly oversize the pool. Aggregators would likely switch to stationary backup BSS rather than sizing the pool for the annual minimum. As shown in Figure 4 b), the assumed 80 buses are not permanently available. The median temporal V2X-ready ratio fluctuates between 17% and 89% over the week. For this reason, the available number of vehicles is determined from the median temporal V2X-ready ratio at each point in time of the simulation, depending on the time of the current week. If the ratio is 17%, only 14 buses are available for FCR. If, on the other hand, the ratio is 89%, 71 buses are available. The V2X power to be provided at any given time is then divided among the currently available vehicles.

The simulation results for the three parameters daily EFCs, mean SOC and mean C-rate are shown in Figure 5. The subfigures are divided into e-Cars (left), e-Buses (center), and e-Boats (right). For each vehicle category, the boxplots of the three V2X markets are compared to the unidirectional paused charging strategy without V2X. Likewise, a comparison with an uncontrolled strategy would be possible [12]. At this point, however, we want

to compare paused charging with the V2X-providing charging strategies.

Figure 5 a) shows the daily EFCs of the 60 e-Cars as boxplots once for the paused charging strategy and once for the three V2X markets. The e-Cars encounter 0.07 to 0.18 EFCs per day in the paused charging strategy. In contrast, in the FCR and intraday arbitrage applications, the number of daily EFCs increases to a range of 0.1 to 0.23. For the median values, this corresponds to an increase of 42 to 50%. The provision of PS increases the median daily EFCs by only 8%. With unidirectional charging, the e-Buses encounter more cycles than the e-Cars due to the longer driving distances (see Figure 5 b)). As a result, the e-Buses are available for V2X less often than the e-Cars (see Figure 3). Consequently, the daily EFCs of the e-Buses increase only slightly with the additional provision of V2X. The median FCR and intraday EFCs are 7 to 13% higher than those of paused charging strategy. If PS is provided, the median daily EFCs increase by only 1%. This is because in PS operation, the BSS capacity is rarely used. The stationary BSS used to generate the PS profile performed 21 EFCs over one year, while the FCR providing BSS completed 270 EFCs [14]. The e-Boats perform 0.026 to 0.277 EFCs daily with paused charging (see Figure 5 c). This means that the least used boat makes one EFC every month, and the most used boat makes one EFC every 3.6 days. If the e-Boats are now used for FCR during idle periods, the daily EFCs increase by 1% to 40%. Similar values result in intraday trading. Accordingly, EFCs increase when e-Boats are frequently used for V2X. However, if a boat is rarely available, the number of EFCs increases only slightly. The results for PS are similar to those for e-Cars and e-Buses.

The mean SOC of vehicle batteries are also affected by the provision of V2X (Figure 5 d) - f)). Compared to the paused unidirectional charging strategy, the mean SOC change slightly as the V2X provision charges and discharges the batteries. The median mean SOC of the e-

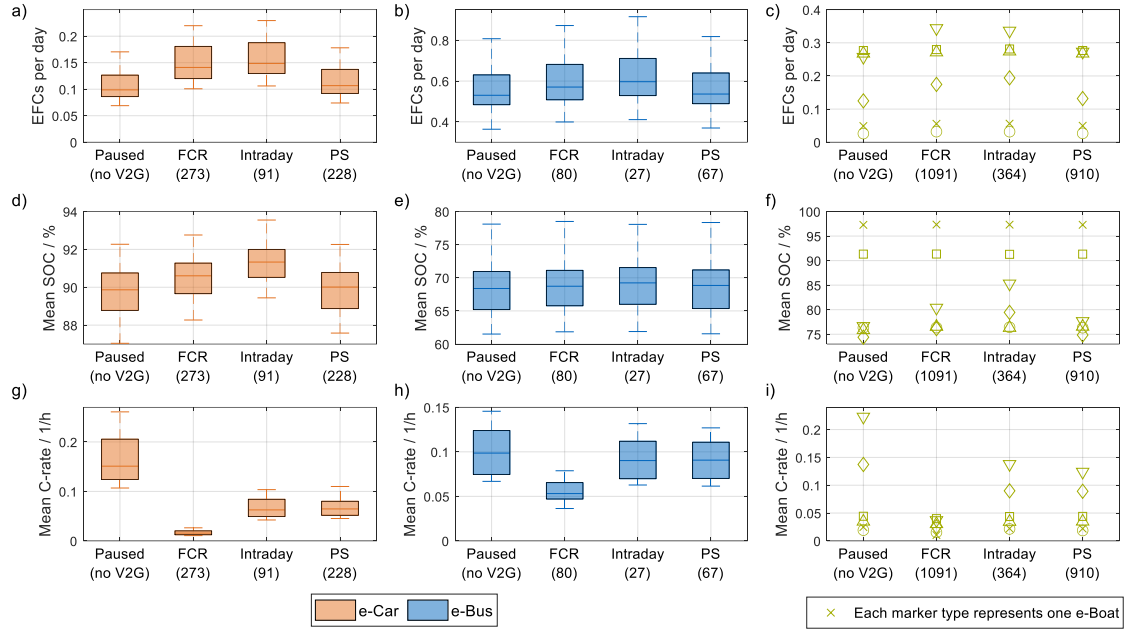


Fig. 5. Battery-related parameters of the e-Cars, e-Buses, and e-Boats. (a) EFCs per day, (b) mean SOC, and (c) mean C-rate.

Cars increases by 0.6 to 1.4 percentage points when FCR or intraday trading is performed (Figure 5 d)). For the e-Buses, the increase is 0.3 to 0.8 percentage points (Figure 5 e)). Most e-Boats also show only low rates of increase in mean SOC. Deviating from this, the mean SOC of one e-Boat (downward-pointing triangle) increases by 4 percentage points in FCR to 9 percentage points in arbitrage. This e-Boat has a mean plugged and idle time of 74.8% and can therefore often be used for V2X.

Figure 5 g) – i) present the mean C-rate of the vehicles in the paused charging and V2X strategies. In particular, the provision of FCR strongly reduces the mean C-rate experienced by the vehicle batteries. For example, the mean C-rate of the median e-Car decreases by 90% and of the median e-Bus by 46%. Providing intraday trading or PS also reduces the mean C-rates, but not as much as FCR. This is because FCR often demands low power values relative to the marketed power. In contrast, the power values provided in intraday trading and PS are higher. The fact that mean C-rates are reduced in all V2X markets shows that for the simulated pool sizes, the loads that vehicle batteries experience during V2X provision are often lower than the loads during typical driving and charging.

4.4 Exemplary degradation analysis of e-Car battery with and without V2X

In addition to quantifying parameters such as mean SOC or number of EFCs, *SimSES* can also be used to simulate the aging of vehicle batteries. As described in section 3.3, an LFP cell was simulated for this purpose over one year. The capacity losses of the e-Car batteries after one year range from 6.2% to 7.1% for all four strategies, mainly due to the calendric degradation caused by the high SOC. Figure 6 shows the change in the capacity loss of the e-Car batteries when providing V2X services relative to the paused, unidirectional strategy over each e-Car's mean V2X-ready ratio. For example, if an e-Car has lost 500 Wh of its nominal capacity in a year in the paused strategy and 505 Wh in a V2X strategy, the relative change in capacity loss corresponds to 1%.

In general, the V2X provision increases the capacity loss for the simulated cell. PS has the least influence on aging due to only slightly higher cyclization at comparatively low powers (see Figure 5). In a few cases, such as one e-Car with a mean V2X-ready ratio of 77.3%, the utilization for PS seems to reduce aging compared to the paused charging strategy (-0.15%). In these cases, the vehicle encounters only slightly more EFCs when providing PS compared to the paused charging strategy,

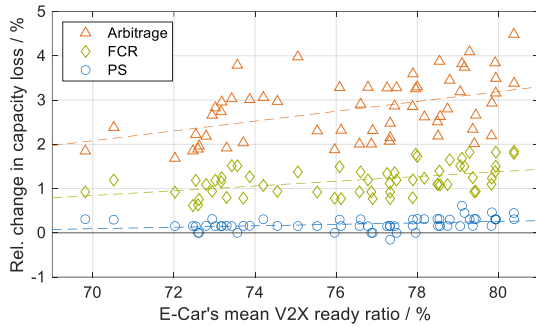


Fig. 1. Change in capacity loss of the e-Car batteries for the V2X strategies compared to the paused charging strategy without V2X over each e-Car's mean V2X-ready ratio. Each of the 60 e-Cars appears once in the diagram for each V2X strategy. The dashed lines show a linear fit for each V2X application across all cars. In the 1-year *SimSES* simulation, a Sony LFP battery with a degradation model from Naumann et al. is used [21,22].

which slightly increases cyclic battery aging. For the exemplary e-Car, the increase is 2.2 EFCs in the one-year simulation period. At the same time, providing PS decreases the mean SOC, reducing calendar aging (exemplary e-Car from 90.59% to 90.34%). The two effects subsequently overlap, which can reduce the total capacity loss of the battery despite the provision of PS in a few cases.

Providing FCR with the e-Cars results in a more significant loss of capacity in the simulations than providing PS. The aging is most severe if arbitrage trading is performed with the e-Cars. But even here, the maximum capacity loss increase compared to the paused charging strategy is 4.5%. This is because the LFP cell used is considered relatively cycle stable and can thus tolerate the increase in EFCs well.

Figure 6 also shows that e-Cars with higher mean V2X-ready ratios also lead to larger capacity loss increases due to V2X provision (dashed lines). This trend holds true for all three V2X applications. However, when individual cars are examined, it can be observed that a higher V2X-ready ratio does not always lead to a higher increase in capacity loss. This is because the mean value of the V2X-ready ratio is not the only factor of relevance, but also the times at which the car is available and the times of V2X demand. Whether the increase in capacity loss can be compensated by generated revenues on the electricity (arbitrage) and power (FCR) markets or by avoided grid charges (PS) depends on the current prices or costs of the respective location.

5. CONCLUSION AND OUTLOOK

In the present work, the V2X deployment of three means of transport was simulated and investigated. For this purpose, a dataset of 60 simulated e-Cars, 52 field-data e-Buses, and six field-data e-Boats was used on the one hand, and data from stationary BSS applications on the other. First, the vehicles were examined in terms of their predictability. It was found that in particular private e-Cars behave predictably at night. Furthermore, an analysis of idle times showed that V2X availability varies over the week, with e-Cars and e-Buses being mostly available at night. Another focus was the simulation of V2X provision in the simulation tool *SimSES*. This allowed battery-relevant parameters and the aging of the LIBs to be quantified. For example, the former showed that, compared to a paused charging strategy, the number of EFCs increases by 42% to 50% with FCR or intraday arbitrage for e-Cars and by 7% to 13% for e-Buses due to V2X deployment. The example aging simulation of the e-Car LIBs showed an increased capacity loss, especially for intraday arbitrage trading and FCR provision.

Building on the present work, further research areas can be identified. The results of section 4.3 and section 4.4 depend strongly on the pool composition and power allocation among the vehicles. Thus, pools could be formed from varying numbers of vehicles and from different vehicle types, such as a combination of e-Cars and e-Buses. Furthermore, in addition to the equal distribution of the required power to all available vehicles, a cascaded distribution or a distribution according to the remaining capacity of the batteries could also be implemented. Moreover, if the vehicles were actively discharged to 50% SOC, for example, the potential for V2X provision would increase, but the load on vehicle batteries would also rise. Additionally, more detailed analyses of battery aging could be made with further aging models and driving data over longer periods. Finally, the methodology and the results could also be used to evaluate the suitability of different battery cells for vehicles with and without V2X.

AUTHOR CONTRIBUTIONS

Benedikt Tepe: Conceptualization, Methodology, Software, Investigation, Writing - Original Draft, Visualization. **Sammy Jablonski:** Conceptualization, Methodology, Writing - Original Draft. **Anupam Parlikar:** Conceptualization, Methodology, Writing - Original Draft. **Holger Hesse:** Conceptualization, Writing - Review & Editing, Supervision. **Andreas Jossen:** Resources, Writing - Review & Editing, Supervision.

ACKNOWLEDGEMENT

This work was financially supported by the German Federal Ministry of Education and Research (BMBF) within the SimBAS project (Grant No. 03XP0338A), which is managed by Project Management Jülich. The responsibility for this publication rests with the authors.

DECLARATION OF INTEREST STATEMENT

The authors declare that they have no known competing financial interests or personal relationships that could have appeared to influence the work reported in this paper.

REFERENCE

- [1] International Energy Agency. Global EV Outlook 2023: Catching up with climate ambitions. Paris; 2023.
- [2] Bloomberg New Energy Finance. Electric Buses in Cities: Driving Towards Cleaner Air and Lower CO₂. Bloomberg Finance LP 2018.
- [3] Joshi S. Electric Boat Market Size Worth \$11.35 Billion, Globally, by 2028 at 13.7% CAGR: The Insight Partners. GlobeNewswire 2022, 8 November 2022; Available from: <https://www.globenewswire.com/en/news-release/2022/11/08/2551096/0/en/Electric-Boat-Market-Size-Worth-11-35-Billion-Globally-by-2028-at-13-7-CAGR-The-Insight-Partners.html>. [August 18, 2023].
- [4] Figgenger J, Hecht C, Haberschusz D, Bors J, Spreuer KG, Kairies K-P et al. The development of battery storage systems in Germany: A market review (status 2023); 2023.
- [5] Gschwendtner C, Sinsel SR, Stephan A. Vehicle-to-X (V2X) implementation: An overview of predominate trial configurations and technical, social and regulatory challenges. *Renewable and Sustainable Energy Reviews* 2021;145:110977. <https://doi.org/10.1016/j.rser.2021.110977>.
- [6] Borge-Diez D, Icaza D, Açıklalp E, Amaris H. Combined vehicle to building (V2B) and vehicle to home (V2H) strategy to increase electric vehicle market share. *Energy* 2021;237:121608. <https://doi.org/10.1016/j.energy.2021.121608>.
- [7] Tepe B, Figgenger J, Englberger S, Sauer DU, Jossen A, Hesse H. Optimal pool composition of commercial electric vehicles in V2G fleet operation of various electricity markets. *Applied Energy* 2022;308:118351. <https://doi.org/10.1016/j.apenergy.2021.118351>.
- [8] Kempton W, Tomic J, Letendre S, Brooks A, Lipman T. Vehicle-to-grid power: battery, hybrid, and fuel cell vehicles as resources for distributed electric power in California 2001.
- [9] Uddin K, Dubarry M, Glick MB. The viability of vehicle-to-grid operations from a battery technology and policy perspective. *Energy Policy* 2018;113:342–7. <https://doi.org/10.1016/j.enpol.2017.11.015>.
- [10] Thingvad A, Calearo L, Andersen PB, Marinelli M. Empirical Capacity Measurements of Electric Vehicles Subject to Battery Degradation from V2G Services. *IEEE Trans. Veh. Technol.* 2021:1. <https://doi.org/10.1109/TVT.2021.3093161>.
- [11] SimSES: Software for techno-economic simulation of stationary energy storage systems; 2017.
- [12] Tepe B, Jablonski S, Hesse H, Jossen A. Lithium-ion battery utilization in various modes of e-transportation. *eTransportation* 2023:100274. <https://doi.org/10.1016/j.etrans.2023.100274>.
- [13] Tepe B, Jablonski S, Hesse H, Jossen A. Lithium-Ion Battery Utilization in Various Modes of e-Transportation - Dataset. <https://doi.org/10.14459/2023mp1709192>.
- [14] Kucevic D, Tepe B, Englberger S, Parlikar A, Mühlbauer M, Bohlen O et al. Standard battery energy storage system profiles: Analysis of various applications for stationary energy storage systems using a holistic simulation framework. *Journal of Energy Storage* 2020;28:101077. <https://doi.org/10.1016/j.est.2019.101077>.
- [15] Collath N, Cornejo M, Engwerth V, Hesse H, Jossen A. Increasing the lifetime profitability of battery energy storage systems through aging aware operation. *Applied Energy* 2023;348:121531. <https://doi.org/10.1016/j.apenergy.2023.121531>.
- [16] Gaete-Morales C, Kramer H, Schill W-P, Zerrahn A. An open tool for creating battery-electric vehicle time series from empirical data, emobpy. *Sci Data* 2021;8(1):152. <https://doi.org/10.1038/s41597-021-00932-9>.
- [17] Möller M, Kucevic D, Collath N, Parlikar A, Dotzauer P, Tepe B et al. SimSES: A holistic simulation framework for modeling and analyzing stationary energy storage systems. *Journal of Energy Storage* 2022;49:103743. <https://doi.org/10.1016/j.est.2021.103743>.
- [18] Arnold G, Brandl R, Degner T, Gerhardt N, Landau M, Nestle D et al. Intelligente Netzanbindung von Elektrofahrzeugen zur Erbringung von Systemdienstleistungen—INEES. Wolfsburg,

Hamburg, Niestetal, Kassel: Volkswagen AG, LichtBlick SE, SMA Technology AG, Fraunhofer IWES 2015.

- [19] Collath N, Tepe B, Englberger S, Jossen A, Hesse H. Aging aware operation of lithium-ion battery energy storage systems: A review. *Journal of Energy Storage* 2022;55:105634. <https://doi.org/10.1016/j.est.2022.105634>.
- [20] Han X, Lu L, Zheng Y, Feng X, Li Z, Li J et al. A review on the key issues of the lithium ion battery degradation among the whole life cycle. *eTransportation* 2019;1:100005. <https://doi.org/10.1016/j.etrans.2019.100005>.
- [21] Naumann M, Schimpe M, Keil P, Hesse H, Jossen A. Analysis and modeling of calendar aging of a commercial LiFePO₄/graphite cell. *Journal of Energy Storage* 2018;17:153–69. <https://doi.org/10.1016/j.est.2018.01.019>.
- [22] Naumann M, Spingler FB, Jossen A. Analysis and modeling of cycle aging of a commercial LiFePO₄/graphite cell. *Journal of Power Sources* 2020;451:227666. <https://doi.org/10.1016/j.jpowsour.2019.227666>.
- [23] Schmalstieg J, Käbitz S, Ecker M, Sauer DU. A holistic aging model for Li(NiMnCo)O₂ based 18650 lithium-ion batteries. *Journal of Power Sources* 2014;257:325–34. <https://doi.org/10.1016/j.jpowsour.2014.02.012>.
- [24] Bibra EM, Connelly E, Dhir S, Drtil M, Henriot P, Hwang I et al. *Global EV Outlook 2022: Securing supplies for an electric future*. International Energy Agency (IEA) 2022.
- [25] Tepe B, Figgenger J, Englberger S, Jossen A, Uwe Sauer D, Hesse H. Analysis of optimally composed EV pools for the aggregated provision of frequency containment reserve and energy arbitrage trading. In: *5th E-Mobility Power System Integration Symposium (EMOB 2021)*. Institution of Engineering and Technology; 2021, p. 175–180. <https://doi.org/10.1049/icp.2021.2521>.

6 Conclusion and Outlook

6.1 Conclusion

The focus of this work is the systematic characterization of stationary and mobile BSS usage profiles and the evaluation of the possibility of using e-Cars, e-Bus and e-Boats for the provision of V2X. For this purpose, stationary and mobile applications are simulated in the SimSES simulation tool and the battery impact is examined. The simulations are extended to include V2X-providing charging strategies and the influence on battery-relevant parameters is investigated. In addition, aggregator concepts are created to optimize the composition of V2G capable EV pools. Furthermore, a method is developed to gradually anonymize load profiles in order to enable an open-source publication despite non-disclosure agreements.

First, in chapter 3.1, the stationary applications SCI, PS and FCR are examined and representative power profiles of BSSs in these applications are identified and published. For this purpose, the applications are simulated using various input profiles and system designs in SimSES. A methodology is then developed to determine representative profiles from the sets of storage profiles. Based on six key characteristics, such as the number of EFCs and efficiency, the methodology determines the BSS profile that deviates least from the median value in all characteristics. The evaluation of the three applications shows major differences in the EFCs, for example. While HSSs make around 260 EFCs per year, PS BSS make fewer than 30, depending on the industrial load profile. The identified reference profiles are published open access as part of the publication together with all other storage power and SoC profiles.

Second, in chapter 3.2, the mobile BSS applications e-Car, e-Bus and e-Boat are simulated and examined in SimSES based on simulated data (e-Car) and field data from industrial partners (e-Bus, e-Boat). For this purpose, SimSES is extended to be able to simulate not only stationary BSSs but also temporarily unavailable BSSs including various charging strategies. In addition to the extended methodology, various battery-relevant parameters that were caused by the driving behavior of the means of transport are investigated. The results show, for example, that e-Buses perform 0.4 to 1 EFCs per day, while e-Cars make less than 0.18 EFCs per day. A comparison with the stationary applications from chapter 3.1 shows that e-Buses and stationary BSSs in SCI and FCR applications are similar regarding some parameters such as EFCs. Similar to chapter 3.1, the generated data from this chapter is published open-access to enable its use in industry and research.

Following the requirement for real load profiles in chapters 3.1 and 3.2, a methodology is developed in chapter 3.3 to anonymize electrical load profiles. The methodology, which is being developed in the open-access python tool LoadPAT, segregates the load profiles into base and peak load sequences. Users of the tool can then select the desired level of anonymization. As a result, the load profile can be solely normalized or reproduced on the basis of features of the original profile. At higher levels of anonymization, the order of the base and/or peak sequences is randomly permuted. The anonymization is demonstrated using two different example load profiles. The original and synthetic load profiles are

then compared. In addition, the load profiles are used as input profiles for the simulation of two BSS applications in SimSES to investigate the effects on battery-relevant parameters. The results show that time-invariant indicators are preserved during anonymization. However, the random permutation of the order of the sequences means that in time-dependent applications such as SCI, anonymization at higher levels lead to a greater variation in battery-relevant parameters, for example, the SCR and the SSR.

Chapter 4.1 of the thesis examines the V2G use of commercial EVs in the FCR market. For this purpose, driving data from real commercial internal combustion vehicles is evaluated and EV driving profiles are created using a developed electromobility simulator. The simulator uses time-dependent probability distributions for trip start, trip duration and trip distance to determine the driving profiles. The output of the simulator are power and energy capability profiles, which indicate for each vehicle the power or energy it could charge and discharge at any time. These profiles are then used to determine the power pools of EVs could offer on the German FCR market at every time of a week. The economic attractiveness of providing FCR using EVs has increased due to the shortening of the market's service periods between 2019 and 2020. Potential annual revenues were between 450 € and 750 € per vehicle in Germany for the considered time period of July 2020 to March 2022.

The developed power and energy capability profiles of the commercial EVs are then used in chapter 4.2 to compile optimized vehicle pools. For this purpose, an optimization algorithm based on genetic algorithms is developed to maximize the revenue per EV on the FCR market and in the arbitrage application on the spot markets. Maximizing the revenue per vehicle results in only including vehicles in the pool that add value to the pool and thus increase pool revenue. The results show that by optimizing the pool composition, the revenue per EV can be multiplied in all markets by up to a factor of seven. In the FCR market, the potential annual revenue of the optimized pool in 2020 was around 380 € per EV, while randomly composed pools only achieved an average of 220 €. In 2020, the FCR market would have been more attractive than arbitrage trading on the intraday or day-ahead market.

Building on the results from chapter 4.2, the optimized vehicle pools are evaluated in chapter 4.3 with regard to battery capacity and economic sector. This analysis shows that small vehicle batteries of less than 20 kWh are not used in optimized pools and that large vehicle batteries of around 80 kWh are selected, especially in intraday and day-ahead trading. This is due to the fact that larger energy volumes are traded in arbitrage trading in particular, while smaller cycle depths are made in FCR provision. Accordingly, aggregators should give preference to larger vehicle battery capacities. With regard to the economic sectors, it is found that the "human health and social work activities" sector is underrepresented in the optimized pools, as the vehicles in this sector are often on the road for long periods of time and are not available for V2G. Vehicles from the "manufacturing" sector, on the other hand, appear to be particularly suitable for V2G, although this may also be due to larger battery capacities. In addition, a further study in the paper finds that a reduction in the minimum bid size and increments in the FCR market could increase the revenue of EVs by 50 to 66 % due to the higher power utilization rate.

Lastly, chapter 5 brings together data and approaches from the previous chapters. This involves simulating the provision of the typical stationary applications SCI, PS and FCR with the three means of transportation e-Cars, e-Buses and e-Boats. An analysis of the predictability of driving behavior shows that e-Cars in particular behave predictably at night. The investigated V2X availability varies for all vehicle types over the course of the week and is particularly high for e-Cars and e-Buses at night. The simulation results of the V2X provision show, for example, that the EFCs of e-Cars increase on

average by 42 to 50 % in FCR and intraday arbitrage trading respectively. Using an LFP battery degradation model, it is possible to show that the capacity loss of e-Car batteries increases by up to 4.5 % as a result of the V2X provision.

In summary, the thesis shows how differently BSSs are stressed in various stationary and mobile storage applications. However, there are also similarities, for example in the number of EFCs between e-Buses and stationary BSSs in SCI and FCR applications. Due to their idle times, e-Cars, e-Buses and e-Boats are able to provide V2X services. The V2X potential of commuting e-Cars and e-Buses is particularly high at night. The e-Boats investigated behave very differently, meaning that leisure boats have greater V2X potential than frequently operating ferries. The impact on the batteries increases with V2X provision compared to unidirectional charging strategies. The simulation of e-Cars shows an increased capacity loss of up to 4.5 % with intraday arbitrage trading within one year compared to the paused unidirectional strategy. Furthermore, by optimizing the composition of their pools, aggregators can gain competitive advantages if they can estimate the driving behavior of potential vehicles or select vehicles from certain economic sectors and with relatively large battery capacity. As the EVs are often idle, especially at night, they can and should make a significant contribution to the flexibility required in the electricity grid for the energy transition through V2X. In the future, V2X will play a major role in the energy system if existing regulatory barriers are removed and technologies such as LIBs, charging infrastructure and forecasting algorithms continue to improve.

6.2 Potential future research

While this thesis addressed a number of research issues related to stationary and mobile BSS applications and V2X, a number of subsequent research questions arise. These cover the topics of batteries, mobile applications, energy management, load profiles, V2X in general, V2X market related and V2X grid related.

After initial evaluations of the additional degradation of the **LIBs** due to V2X provision were carried out in this study, these could be expanded using SimSES with the aid of more up-to-date battery degradation models of different cell types. The question also arises as to which battery cell type would be particularly suitable for which V2X application. For example, a cycle-stable LFP cell could be better suited to the high cycling numbers in arbitrage than a NMC cell. New technologies like sodium-ion batteries could also be compared here. In addition, battery cells could be designed specifically for the mobile applications analyzed in this work with and without V2X provision. Furthermore, the second-life suitability of batteries used in mobile applications for stationary BSSs could also be investigated as an additional route to the V2X service provision.

With regard to **mobile applications** of LIBs, the evaluations of this thesis could be extended to a broader data basis. For example, only six e-Boats of different sizes were evaluated. Moreover, the e-Car database could be extended to field data. Other vehicle types, such as e-Trucks or electric vertical take-off and landing aircrafts, could be examined with regard to usage behavior and investigated for V2X provision. In addition to using existing open-access databases, new data could be collected and evaluated via industry partners. Furthermore, the driving and charging behavior of vehicles could be recorded using sensors, evaluated and published.

In terms of **energy management strategies and fleet management**, e-Bus and e-Truck fleet strategies could be developed and the provision of V2X with these could be investigated. Due to

the relatively large vehicle battery capacities, the predictable driving patterns and the common grid connection of those fleets, V2X use of these vehicle types is particularly interesting. These vehicle pools could also be combined with other vehicle types or stationary BSSs to compensate for periods of unavailability and reduce the uncertainty in the available power. The pool management strategies presented in this thesis could also be extended to include sub-pool formation for parallel participation in different markets.

After the anonymization of electrical **load profiles** in this thesis, the methodology of anonymization could be extended to storage power profiles that charge and discharge. In addition, the *LoadPAT* anonymization tool could be expanded to include further functionalities. For example, a new methodology could enable the extraction or creation of a representative daily load profile from a monthly or annual load profile. Moreover, an open-access database of anonymized load profiles could be developed that would make the profiles immediately available to a wide range of users.

On the subject of **V2X in general**, there are a number of other points of contact for research. V2X could be investigated with other vehicles in addition to the three vehicle types in the thesis. Moreover, the Energy System Network tool currently under development at the Technical University of Munich could be used to simulate a large number of vehicles with one SimSES instance per vehicle with a higher-level aggregator. This aggregator could simulate the applications and allocate the power to the vehicles. With regard to power allocation, further questions arise as to whether the power should be better distributed evenly or cascaded or distributed to the vehicles according to other aspects such as the batteries' SoH. Other simulation options would be agent-based simulations in which each vehicle acts independently and V2X power is gathered by an aggregator. Further work could examine the extent to which location changes need to be taken into account if a bidirectional charging station is not available at every location. There are also questions regarding DC versus AC V2X participation, as the grid codes must be in the charging station for DC charging and in the vehicle for AC charging. The regulatory requirements for V2X also differ depending on the region and country. These requirements could be collected for various countries and necessary changes could be identified. Furthermore, it would also be interesting to develop a platform that makes it possible to continuously calculate the economic V2G potential for different countries. This platform would have to take into account current prices, for example for FCR in the respective country, and include other adjustable parameters, such as commuter driving behavior versus second car driving behavior.

Regarding possible **V2X markets**, other markets in various countries could be investigated in addition to those examined in this thesis. Furthermore, markets could be designed specifically for flexible resources such as EVs in order to exploit the full power potential of the vehicles. Another interesting question would be what consequences it would have for batteries and user comfort if FCR provision with EVs was mandatory.

Following on from the thesis, there are also **grid-related V2X** research questions. One possible question would be the financial potential of enabling V2X charging in addition to smart charging and thus reducing or preventing grid expansion. In addition, the extent to which the integration of renewable energies can be improved by V2X is a relevant research topic. Finally, the risks and opportunities of V2X-enabled vehicles could be examined from the perspective of grid operators. This raises questions as to how conflicts between TSOs and DSOs can be resolved in the provision of V2X. For example, if vehicles provide FCR for the TSO level, this could lead to local congestion and curtailments at DSO level.

References

- [1] Kucevic, D., Tepe, B., Englberger, S., Parlikar, A., Mühlbauer, M., Bohlen, O., Jossen, A., and Hesse, H.: *Standard battery energy storage system profiles: Analysis of various applications for stationary energy storage systems using a holistic simulation framework*. In: *Journal of Energy Storage* 28 (2020), p. 101077. ISSN: 2352152X. DOI: [10.1016/j.est.2019.101077](https://doi.org/10.1016/j.est.2019.101077) (see pp. III, 3, 31).
- [2] Tepe, B., Figgenger, J., Englberger, S., Sauer, D. U., Jossen, A., and Hesse, H.: *Optimal pool composition of commercial electric vehicles in V2G fleet operation of various electricity markets*. In: *Applied Energy* 308 (2022), p. 118351. ISSN: 03062619. DOI: [10.1016/j.apenergy.2021.118351](https://doi.org/10.1016/j.apenergy.2021.118351) (see pp. III, 4, 121).
- [3] Tepe, B., Haberschusz, D., Figgenger, J., Hesse, H., Uwe Sauer, D., and Jossen, A.: *Feature-conserving gradual anonymization of load profiles and the impact on battery storage systems*. In: *Applied Energy* 343 (2023), p. 121191. ISSN: 03062619. DOI: [10.1016/j.apenergy.2023.121191](https://doi.org/10.1016/j.apenergy.2023.121191) (see pp. III, 3, 4, 73).
- [4] Tepe, B., Jablonski, S., Hesse, H., and Jossen, A.: *Lithium-ion battery utilization in various modes of e-transportation*. In: *eTransportation* (2023), p. 100274. ISSN: 25901168. DOI: [10.1016/j.etrans.2023.100274](https://doi.org/10.1016/j.etrans.2023.100274) (see pp. III, 3, 53).
- [5] Tepe, B., Jablonski, S., Parlikar, A., Hesse, H., and Jossen, A.: “Vehicle-to-X Service Provision for various Modes of e-Transportation with Consideration of the Influence on Lithium-Ion Battery Utilization.” In: *International Conference on Applied Energy 2023*. 2023 (see pp. III, 5, 153).
- [6] Tepe, B., Collath, N., Hesse, H., Rosenthal, M., and Windelen, U.: *Stationäre Batteriespeicher in Deutschland: Aktuelle Entwicklungen und Trends in 2021*. In: *Energiewirtschaftliche Tagesfragen* 71.3 (2021), pp. 23–27. URL: <https://mediatum.ub.tum.de/1601843> (see p. III).
- [7] Tepe, B., Figgenger, J., Englberger, S., Jossen, A., Uwe Sauer, D., and Hesse, H.: “Analysis of optimally composed EV pools for the aggregated provision of frequency containment reserve and energy arbitrage trading.” In: *5th E-Mobility Power System Integration Symposium (EMOB 2021)*. Institution of Engineering and Technology, 2021, pp. 175–180. ISBN: 978-1-83953-679-3. DOI: [10.1049/icp.2021.2521](https://doi.org/10.1049/icp.2021.2521) (see pp. III, 4, 142).
- [8] Kucevic, D., Englberger, S., Sharma, A., Trivedi, A., Tepe, B., Schachler, B., Hesse, H., Srinivasan, D., and Jossen, A.: *Reducing grid peak load through the coordinated control of battery energy storage systems located at electric vehicle charging parks*. In: *Applied Energy* 295 (2021), p. 116936. ISSN: 03062619. DOI: [10.1016/j.apenergy.2021.116936](https://doi.org/10.1016/j.apenergy.2021.116936) (see pp. III, 14).
- [9] Englberger, S., Abo Gamra, K., Tepe, B., Schreiber, M., Jossen, A., and Hesse, H.: *Electric vehicle multi-use: Optimizing multiple value streams using mobile storage systems in a vehicle-to-grid context*. In: *Applied Energy* 304 (2021), p. 117862. ISSN: 03062619. DOI: [10.1016/j.apenergy.2021.117862](https://doi.org/10.1016/j.apenergy.2021.117862) (see pp. IV, 9, 28).

- [10] Möller, M., Kucevic, D., Collath, N., Parlikar, A., Dotzauer, P., Tepe, B., Englberger, S., Jossen, A., and Hesse, H.: *SimSES: A holistic simulation framework for modeling and analyzing stationary energy storage systems*. In: *Journal of Energy Storage* 49 (2022), p. 103743. ISSN: 2352152X. DOI: [10.1016/j.est.2021.103743](https://doi.org/10.1016/j.est.2021.103743) (see pp. IV, 10).
- [11] Figgenger, J., Tepe, B., Rücker, F., Schoeneberger, I., Hecht, C., Jossen, A., and Sauer, D. U.: *The influence of frequency containment reserve flexibilization on the economics of electric vehicle fleet operation*. In: *Journal of Energy Storage* 53 (2022), p. 105138. ISSN: 2352152X. DOI: [10.1016/j.est.2022.105138](https://doi.org/10.1016/j.est.2022.105138) (see pp. IV, 4, 97).
- [12] Collath, N., Tepe, B., Englberger, S., Jossen, A., and Hesse, H.: *Aging aware operation of lithium-ion battery energy storage systems: A review*. In: *Journal of Energy Storage* 55 (2022), p. 105634. ISSN: 2352152X. DOI: [10.1016/j.est.2022.105634](https://doi.org/10.1016/j.est.2022.105634) (see pp. IV, 8, 9).
- [13] Luque, J., Tepe, B., Larios, D., León, C., and Hesse, H.: *Machine Learning Estimation of Battery Efficiency and Related Key Performance Indicators in Smart Energy Systems*. In: *Energies* 16.14 (2023), p. 5548. DOI: [10.3390/en16145548](https://doi.org/10.3390/en16145548) (see p. IV).
- [14] Moyassari, E., Li, Z., Tepe, B., Streck, L., and Jossen, A.: *Cycle Characterization of SiO-Based Lithium-Ion-Batteries Using Real Load Profiles*. In: *J. Electrochem. Soc. (Journal of The Electrochemical Society)* 170.10 (2023), p. 100510. DOI: [10.1149/1945-7111/acfe9e](https://doi.org/10.1149/1945-7111/acfe9e) (see p. IV).
- [15] Jablonski, S., Tepe, B., Zhao, Y., and Jossen, A.: “Analysis and Characterization of the Energy Consumption in an Electric Bus Fleet.” In: *NEIS - Conference on Sustainable Energy Supply and Energy Storage Systems*. 2023 (see p. IV).
- [16] European Commission: *‘Fit for 55’: delivering the EU’s 2030 climate target on the way to climate neutrality*. In: *Communication from the Commission to the European Parliament, the European Council, the Council, the European Economic and Social Committee and the Committee of the Regions* (2021). URL: <https://eur-lex.europa.eu/legal-content/EN/TXT/PDF/?uri=CELEX:52021DC0550> (see p. 1).
- [17] International Energy Agency: *World Energy Outlook 2023*. Paris, 2023. URL: <https://www.iea.org/reports/world-energy-outlook-2023> (visited on 10/25/2023) (see p. 1).
- [18] McPhie, T. and Bedini, G.: *European Green Deal: EU agrees stronger legislation to accelerate the rollout of renewable energy*. Brussels, 2023-03-30. URL: https://ec.europa.eu/commission/presscorner/detail/en/IP_23_2061 (visited on 08/17/2023) (see p. 1).
- [19] European Commission. Eurostat: *Shedding light on energy in the EU*. Publications Office, 2023. DOI: [10.2785/405482](https://doi.org/10.2785/405482). URL: <https://ec.europa.eu/eurostat/de/web/interactive-publications/energy-2023> (visited on 12/11/2023) (see p. 1).
- [20] European Parliament and Council: *Directive (EU) 2018/2001 of the European Parliament and of the Council of 11 December 2018 on the promotion of the use of energy from renewable sources*. In: *Official Journal of the European Union* (2018), pp. 82–209 (see p. 1).
- [21] Destatis - German Federal Statistical Office: *Road transport: EU-wide carbon dioxide emissions have increased by 21% since 1990*. 2023-05-31. URL: <https://www.destatis.de/Europa/EN/Topic/Environment-energy/CarbonDioxideRoadTransport.html> (visited on 12/11/2023) (see p. 1).

- [22] McPhie, T. and Crespo Parrondo, A.: *Zero emission vehicles: first ‘Fit for 55’ deal will end the sale of new CO₂ emitting cars in Europe by 2035*. Brussels, 2022-10-28. URL: https://ec.europa.eu/commission/presscorner/detail/%20en/ip_22_6462 (visited on 12/11/2023) (see p. 1).
- [23] Verma, S., Dwivedi, G., and Verma, P.: *Life cycle assessment of electric vehicles in comparison to combustion engine vehicles: A review*. In: *Materials Today: Proceedings* 49 (2022), pp. 217–222. ISSN: 22147853. DOI: [10.1016/j.matpr.2021.01.666](https://doi.org/10.1016/j.matpr.2021.01.666) (see p. 1).
- [24] Li, M., Lu, J., Chen, Z., and Amine, K.: *30 Years of Lithium-Ion Batteries*. In: *Advanced Materials* 30.33 (2018), p. 1800561. DOI: [10.1002/adma.201800561](https://doi.org/10.1002/adma.201800561) (see pp. 1, 7, 10, 17).
- [25] Chen, A. and Sen, P. K.: “Advancement in battery technology: A state-of-the-art review.” In: *2016 IEEE Industry Applications Society Annual Meeting*. IEEE, 2016, pp. 1–10. ISBN: 978-1-4799-8397-1. DOI: [10.1109/IAS.2016.7731812](https://doi.org/10.1109/IAS.2016.7731812) (see pp. 1, 7).
- [26] Sekine, Y.: *The Spectacular Energy Storage Growth: Keeping the Power On: Sparking Energy Storage Solutions in Developing Countries*. Ed. by BloombergNEF. 05/12/2021. URL: https://www.cif.org/sites/cif_enc/files/knowledge-documents/thespectacular_energy_storage_growth.pdf (visited on 08/18/2023) (see p. 1).
- [27] Figgenger, J., Hecht, C., Haberschusz, D., Bors, J., Spreuer, K. G., Kairies, K.-P., Stenzel, P., and Sauer, D. U.: *The development of battery storage systems in Germany: A market review (status 2023)*. 03/13/2023. URL: <http://arxiv.org/pdf/2203.06762v3> (see pp. 1, 10–15, 17, 18, 142).
- [28] Hesse, H., Schimpe, M., Kucevic, D., and Jossen, A.: *Lithium-Ion Battery Storage for the Grid—A Review of Stationary Battery Storage System Design Tailored for Applications in Modern Power Grids*. In: *Energies* 10.12 (2017), p. 2107. DOI: [10.3390/en10122107](https://doi.org/10.3390/en10122107) (see pp. 1, 2, 14, 16).
- [29] Wali, S. B., Hannan, M. A., Reza, M. S., Ker, P. J., Begum, R. A., Rahman, M. A., and Mansor, M.: *Battery storage systems integrated renewable energy sources: A biblio metric analysis towards future directions*. In: *Journal of Energy Storage* 35 (2021), p. 102296. ISSN: 2352152X. DOI: [10.1016/j.est.2021.102296](https://doi.org/10.1016/j.est.2021.102296) (see p. 1).
- [30] Kairies, K.-P., Figgenger, J., Haberschusz, D., Wessels, O., Tepe, B., and Sauer, D. U.: *Market and technology development of PV home storage systems in Germany*. In: *Journal of Energy Storage* 23 (2019), pp. 416–424. ISSN: 2352152X. DOI: [10.1016/j.est.2019.02.023](https://doi.org/10.1016/j.est.2019.02.023) (see p. 1).
- [31] Uddin, K., Gough, R., Radcliffe, J., Marco, J., and Jennings, P.: *Techno-economic analysis of the viability of residential photovoltaic systems using lithium-ion batteries for energy storage in the United Kingdom*. In: *Applied Energy* 206 (2017), pp. 12–21. ISSN: 03062619. DOI: [10.1016/j.apenergy.2017.08.170](https://doi.org/10.1016/j.apenergy.2017.08.170) (see pp. 1, 12).
- [32] Pimm, A. J., Cockerill, T. T., and Taylor, P. G.: *The potential for peak shaving on low voltage distribution networks using electricity storage*. In: *Journal of Energy Storage* 16 (2018), pp. 231–242. ISSN: 2352152X. DOI: [10.1016/j.est.2018.02.002](https://doi.org/10.1016/j.est.2018.02.002) (see pp. 1, 14).
- [33] Kucevic, D., Semmelmann, L., Collath, N., Jossen, A., and Hesse, H.: *Peak Shaving with Battery Energy Storage Systems in Distribution Grids: A Novel Approach to Reduce Local and Global Peak Loads*. In: *Electricity* 2.4 (2021), pp. 573–589. DOI: [10.3390/electricity2040033](https://doi.org/10.3390/electricity2040033) (see pp. 1, 14).

- [34] Colthorpe, A.: *Moss Landing: World's biggest battery storage project is now 3GWh capacity*. In: *Energy Storage News* 2023 (2023-08-02). URL: <https://www.energy-storage.news/moss-landing-worlds-biggest-battery-storage-project-is-now-3gwh-capacity/> (visited on 01/03/2024) (see p. 1).
- [35] Thien, T., Schweer, D., Vom Stein, D., Moser, A., and Sauer, D. U.: *Real-world operating strategy and sensitivity analysis of frequency containment reserve provision with battery energy storage systems in the german market*. In: *Journal of Energy Storage* 13 (2017), pp. 143–163. ISSN: 2352152X. DOI: [10.1016/j.est.2017.06.012](https://doi.org/10.1016/j.est.2017.06.012) (see pp. 1, 15).
- [36] Zeh, A., Müller, M., Naumann, M., Hesse, H., Jossen, A., and Witzmann, R.: *Fundamentals of Using Battery Energy Storage Systems to Provide Primary Control Reserves in Germany*. In: *Batteries* 2.3 (2016), p. 29. DOI: [10.3390/batteries2030029](https://doi.org/10.3390/batteries2030029) (see pp. 1, 2, 15).
- [37] Masias, A., Marcicki, J., and Paxton, W. A.: *Opportunities and Challenges of Lithium Ion Batteries in Automotive Applications*. In: *ACS Energy Letters* 6.2 (2021), pp. 621–630. ISSN: 2380-8195. DOI: [10.1021/acsenergylett.0c02584](https://doi.org/10.1021/acsenergylett.0c02584) (see pp. 1, 10).
- [38] International Energy Agency: *Global EV Outlook 2023: Catching up with climate ambitions*. Ed. by International Energy Agency. Paris, 2023. URL: <https://www.iea.org/reports/global-ev-outlook-2023> (visited on 05/10/2023) (see pp. 1, 2, 18–20).
- [39] SPD, Bündnis 90/Die Grünen, FDP: *Mehr Fortschritt wagen: Koalitionsvertrag 2021-2025 zwischen SPD, Bündnis 90/Die Grünen und FDP*. URL: https://www.spd.de/fileadmin/Dokumente/Koalitionsvertrag/Koalitionsvertrag_2021-2025.pdf (visited on 01/08/2024) (see p. 2).
- [40] Bibra, E. M. et al.: *Global EV Outlook 2022: Securing supplies for an electric future*. In: *International Energy Agency (IEA)* (2022). URL: <https://www.iea.org/reports/global-ev-outlook-2022> (visited on 07/18/2023) (see pp. 2, 19).
- [41] Bloomberg New Energy Finance: *Electric Buses in Cities: Driving Towards Cleaner Air and Lower CO₂*. In: *Bloomberg Finance LP* (2018). URL: <https://assets.bbhub.io/professional/sites/24/2018/05/Electric-Buses-in-Cities-Report-BNEF-C40-Citi.pdf> (visited on 07/18/2023) (see p. 2).
- [42] Joshi, S.: *Electric Boat Market Size Worth \$11.35 Billion, Globally, by 2028 at 13.7% CAGR: The Insight Partners*. In: *GlobeNewswire* (2022-11-08). URL: <https://www.globenewswire.com/en/news-release/2022/11/08/2551096/0/en/Electric-Boat-Market-Size-Worth-11-35-Billion-Globally-by-2028-at-13-7-CAGR-The-Insight-Partners.html> (visited on 08/18/2023) (see pp. 2, 19).
- [43] Nobis, C. and Kuhnimhof, T.: *Mobilität in Deutschland – MiD. Ergebnisbericht. Studie von infas, DLR, IVT und infas 360 im Auftrag des Bundesministers für Verkehr und digitale Infrastruktur (FE-Nr. 70.904/15). Bonn, Berlin*. In: (2018). URL: https://www.mobilitaet-in-deutschland.de/archive/pdf/MiD2017_Ergebnisbericht.pdf (visited on 11/07/2023) (see pp. 2, 18, 23).
- [44] Burger, B.: *Energy-Charts*. Ed. by Fraunhofer ISE. URL: <https://energy-charts.info/> (visited on 11/07/2023) (see pp. 2, 10).

- [45] Thingvad, A., Martinenas, S., Andersen, P. B., Marinelli, M., Olesen, O. J., and Christensen, B. E.: “Economic comparison of electric vehicles performing unidirectional and bidirectional frequency control in Denmark with practical validation.” In: *2016 51st International Universities Power Engineering Conference (UPEC)*. IEEE, 06.09.2016 - 09.09.2016, pp. 1–6. ISBN: 978-1-5090-4650-8. DOI: [10.1109/UPEC.2016.8113988](https://doi.org/10.1109/UPEC.2016.8113988) (see pp. 2, 24).
- [46] Thingvad, A., Ziras, C., and Marinelli, M.: *Economic value of electric vehicle reserve provision in the Nordic countries under driving requirements and charger losses*. In: *Journal of Energy Storage* 21 (2019), pp. 826–834. ISSN: 2352152X. DOI: [10.1016/j.est.2018.12.018](https://doi.org/10.1016/j.est.2018.12.018) (see pp. 2, 24, 28).
- [47] Gschwendtner, C., Sinsel, S. R., and Stephan, A.: *Vehicle-to-X (V2X) implementation: An overview of predominate trial configurations and technical, social and regulatory challenges*. In: *Renewable and Sustainable Energy Reviews* 145 (2021), p. 110977. ISSN: 13640321. DOI: [10.1016/j.rser.2021.110977](https://doi.org/10.1016/j.rser.2021.110977) (see pp. 2, 25, 30).
- [48] EPEX SPOT SE: *Trading at EPEX SPOT 2022*. 2022. URL: https://www.epexspot.com/sites/default/files/2023-01/22-10-25_TradingBrochure.pdf (visited on 11/07/2023) (see pp. 2, 15, 27).
- [49] Payne, G. and Cox, C.: *Understanding the true value of V2G: An analysis of the customers and valuestreams for V2G in the UK*. In: *Cenex: Leicestershire, UK* (2019). URL: <https://www.cenex.co.uk/app/uploads/2019/10/True-Value-of-V2G-Report.pdf> (visited on 08/21/2023) (see p. 2).
- [50] Gaete-Morales, C., Kramer, H., Schill, W.-P., and Zerrahn, A.: *An open tool for creating battery-electric vehicle time series from empirical data, emobpy*. In: *Scientific data* 8.1 (2021), p. 152. DOI: [10.1038/s41597-021-00932-9](https://doi.org/10.1038/s41597-021-00932-9) (see pp. 3, 28).
- [51] Šimić, Z., Topić, D., Knežević, G., and Pelin, D.: *Battery energy storage technologies overview*. In: *International journal of electrical and computer engineering systems* 12.1 (2021), pp. 53–65. ISSN: 18476996. DOI: [10.32985/ijeces.12.1.6](https://doi.org/10.32985/ijeces.12.1.6) (see p. 7).
- [52] Jung, J.: *Fundamentals of Lead-Acid Rechargeable Batteries*. In: *Lead-Acid battery technologies*. Electrochemical Energy Storage and Conversion Ser. Boca Raton, Fla.: CRC Press, 2015, pp. 14–79. ISBN: 978-1-4665-9223-0. URL: https://books.google.de/books?hl=de&lr=&id=I_c0CgAAQBAJ&oi=fnd&pg=PP1&dq=lead+acid+battery&ots=ktD1a1QoVf&sig=-hYm0i_3_s7CtR6_RwMs1bByVZ8#v=onepage&q=lead%20acid%20battery&f=false (visited on 10/12/2023) (see p. 7).
- [53] Zubi, G., Dufo-López, R., Carvalho, M., and Pasaoglu, G.: *The lithium-ion battery: State of the art and future perspectives*. In: *Renewable and Sustainable Energy Reviews* 89 (2018), pp. 292–308. ISSN: 13640321. DOI: [10.1016/j.rser.2018.03.002](https://doi.org/10.1016/j.rser.2018.03.002) (see pp. 7, 17).
- [54] Nemeth, T., Schröer, P., Kuipers, M., and Sauer, D. U.: *Lithium titanate oxide battery cells for high-power automotive applications – Electro-thermal properties, aging behavior and cost considerations*. In: *Journal of Energy Storage* 31 (2020), p. 101656. ISSN: 2352152X. DOI: [10.1016/j.est.2020.101656](https://doi.org/10.1016/j.est.2020.101656) (see p. 7).
- [55] Moyassari, E., Roth, T., Kücher, S., Chang, C.-C., Hou, S.-C., Spingler, F. B., and Jossen, A.: *The Role of Silicon in Silicon-Graphite Composite Electrodes Regarding Specific Capacity, Cycle Stability, and Expansion*. In: *J. Electrochem. Soc. (Journal of The Electrochemical Society)* 169.1 (2022), p. 010504. DOI: [10.1149/1945-7111/ac4545](https://doi.org/10.1149/1945-7111/ac4545) (see p. 7).

- [56] Hu, X., Feng, F., Liu, K., Zhang, L., Xie, J., and Liu, B.: *State estimation for advanced battery management: Key challenges and future trends*. In: *Renewable and Sustainable Energy Reviews* 114 (2019), p. 109334. ISSN: 13640321. DOI: [10.1016/j.rser.2019.109334](https://doi.org/10.1016/j.rser.2019.109334) (see pp. 7, 8).
- [57] Lin, Z., Li, D., and Zou, Y.: *Energy efficiency of lithium-ion batteries: Influential factors and long-term degradation*. In: *Journal of Energy Storage* 74 (2023), p. 109386. ISSN: 2352152X. DOI: [10.1016/j.est.2023.109386](https://doi.org/10.1016/j.est.2023.109386) (see p. 8).
- [58] Ungurean, L., Cârstoiu, G., Micea, M. V., and Groza, V.: *Battery state of health estimation: a structured review of models, methods and commercial devices*. In: *International Journal of Energy Research* 41.2 (2017), pp. 151–181. ISSN: 0363907X. DOI: [10.1002/er.3598](https://doi.org/10.1002/er.3598) (see p. 8).
- [59] Naumann, M., Spingler, F. B., and Jossen, A.: *Analysis and modeling of cycle aging of a commercial LiFePO₄/graphite cell*. In: *Journal of Power Sources* 451 (2020), p. 227666. ISSN: 03787753. DOI: [10.1016/j.jpowsour.2019.227666](https://doi.org/10.1016/j.jpowsour.2019.227666) (see pp. 8, 9).
- [60] Schmalstieg, J., Käbitz, S., Ecker, M., and Sauer, D. U.: *A holistic aging model for Li(NiMnCo)O₂ based 18650 lithium-ion batteries*. In: *Journal of Power Sources* 257 (2014), pp. 325–334. ISSN: 03787753. DOI: [10.1016/j.jpowsour.2014.02.012](https://doi.org/10.1016/j.jpowsour.2014.02.012) (see pp. 8, 9).
- [61] Lunz, B., Walz, H., and Sauer, D. U.: “Optimizing vehicle-to-grid charging strategies using genetic algorithms under the consideration of battery aging.” In: *2011 IEEE Vehicle Power and Propulsion Conference*. IEEE, 06.09.2011 - 09.09.2011, pp. 1–7. ISBN: 978-1-61284-248-6. DOI: [10.1109/VPPC.2011.6043021](https://doi.org/10.1109/VPPC.2011.6043021) (see pp. 8, 27).
- [62] Wassiliadis, N. et al.: *Quantifying the state of the art of electric powertrains in battery electric vehicles: Range, efficiency, and lifetime from component to system level of the Volkswagen ID.3*. In: *eTransportation* 12 (2022), p. 100167. ISSN: 25901168. DOI: [10.1016/j.etrans.2022.100167](https://doi.org/10.1016/j.etrans.2022.100167) (see p. 9).
- [63] Thingvad, A., Calearo, L., Andersen, P. B., and Marinelli, M.: *Empirical Capacity Measurements of Electric Vehicles Subject to Battery Degradation from V2G Services*. In: *IEEE Transactions on Vehicular Technology* (2021), p. 1. ISSN: 0018-9545. DOI: [10.1109/TVT.2021.3093161](https://doi.org/10.1109/TVT.2021.3093161) (see pp. 9, 25, 28, 98).
- [64] Parra, D. and Patel, M. K.: *The nature of combining energy storage applications for residential battery technology*. In: *Applied Energy* 239 (2019), pp. 1343–1355. ISSN: 03062619. DOI: [10.1016/j.apenergy.2019.01.218](https://doi.org/10.1016/j.apenergy.2019.01.218) (see pp. 9, 16).
- [65] Hesse, H., Martins, R., Musilek, P., Naumann, M., Truong, C. N., and Jossen, A.: *Economic Optimization of Component Sizing for Residential Battery Storage Systems*. In: *Energies* 10.7 (2017), p. 835. DOI: [10.3390/en10070835](https://doi.org/10.3390/en10070835) (see p. 9).
- [66] Ecker, M., Nieto, N., Käbitz, S., Schmalstieg, J., Blanke, H., Warnecke, A., and Sauer, D. U.: *Calendar and cycle life study of Li(NiMnCo)O₂-based 18650 lithium-ion batteries*. In: *Journal of Power Sources* 248 (2014), pp. 839–851. ISSN: 03787753. DOI: [10.1016/j.jpowsour.2013.09.143](https://doi.org/10.1016/j.jpowsour.2013.09.143) (see p. 9).
- [67] Waldmann, T., Wilka, M., Kasper, M., Fleischhammer, M., and Wohlfahrt-Mehrens, M.: *Temperature dependent ageing mechanisms in Lithium-ion batteries – A Post-Mortem study*. In: *Journal of Power Sources* 262 (2014), pp. 129–135. ISSN: 03787753. DOI: [10.1016/j.jpowsour.2014.03.112](https://doi.org/10.1016/j.jpowsour.2014.03.112) (see p. 9).

- [68] Johnen, M., Pitzen, S., Kamps, U., Kateri, M., Dechent, P., and Sauer, D. U.: *Modeling long-term capacity degradation of lithium-ion batteries*. In: *Journal of Energy Storage* 34 (2021), p. 102011. ISSN: 2352152X. DOI: [10.1016/j.est.2020.102011](https://doi.org/10.1016/j.est.2020.102011) (see p. 9).
- [69] Attia, P. M. et al.: *Review—“Knees” in Lithium-Ion Battery Aging Trajectories*. In: *J. Electrochem. Soc. (Journal of The Electrochemical Society)* 169.6 (2022), p. 060517. DOI: [10.1149/1945-7111/ac6d13](https://doi.org/10.1149/1945-7111/ac6d13) (see p. 9).
- [70] Naumann, M., Schimpe, M., Keil, P., Hesse, H., and Jossen, A.: *Analysis and modeling of calendar aging of a commercial LiFePO₄/graphite cell*. In: *Journal of Energy Storage* 17 (2018), pp. 153–169. ISSN: 2352152X. DOI: [10.1016/j.est.2018.01.019](https://doi.org/10.1016/j.est.2018.01.019) (see p. 9).
- [71] Ritchie, H., Roser, M., and Rosado, P.: *Energy: Published online at OurWorldInData.org*. 2022. URL: <https://ourworldindata.org/energy> (see p. 10).
- [72] Donalek, P. J.: *Pumped Storage Hydro: Then and Now*. In: *IEEE Power and Energy Magazine* 18.5 (2020), pp. 49–57. ISSN: 1540-7977. DOI: [10.1109/MPE.2020.3001418](https://doi.org/10.1109/MPE.2020.3001418) (see p. 10).
- [73] Eyer, J. and Corey, G.: *Energy storage for the electricity grid: Benefits and market potential assessment guide*. In: *Sandia National Laboratories* 2010.10 (2010). URL: <https://www.sandia.gov/ess-ssl/publications/SAND2010-0815.pdf> (visited on 11/07/2023) (see pp. 10, 16).
- [74] Ralon, P., Taylor, M., Ilas, A., Diaz-Bone, H., and Kairies, K.-P.: *Electricity storage and renewables: Costs and markets to 2030*. Ed. by International Renewable Energy Agency. Abu Dhabi, 2017 (see p. 10).
- [75] Anisie, A., Boshell, F., Kamath, S., Kanani, H., and Mehrotra, S.: *Utility-scale batteries – Innovation Landscape Brief*. Ed. by International Renewable Energy Agency. Abu Dhabi, 2019 (see pp. 10, 14).
- [76] Moshövel, J., Kairies, K.-P., Magnor, D., Leuthold, M., Bost, M., Gähns, S., Szczechowicz, E., Cramer, M., and Sauer, D. U.: *Analysis of the maximal possible grid relief from PV-peak-power impacts by using storage systems for increased self-consumption*. In: *Applied Energy* 137 (2015), pp. 567–575. ISSN: 03062619. DOI: [10.1016/j.apenergy.2014.07.021](https://doi.org/10.1016/j.apenergy.2014.07.021) (see pp. 11, 13).
- [77] Merei, G., Moshövel, J., Magnor, D., and Sauer, D. U.: *Optimization of self-consumption and techno-economic analysis of PV-battery systems in commercial applications*. In: *Applied Energy* 168 (2016), pp. 171–178. ISSN: 03062619. DOI: [10.1016/j.apenergy.2016.01.083](https://doi.org/10.1016/j.apenergy.2016.01.083) (see pp. 11, 13).
- [78] Truong, C. N., Viernstein, L., Schimpe, M., Witzmann, R., Jossen, A., and Hesse, H. C.: “Maximizing Solar Home Battery Systems’ Contribution to the Energy Transition of the Power System.” In: *NEIS Conference 2017*. Ed. by D. Schulz. 2017 (see pp. 11, 12).
- [79] Truong, C., Naumann, M., Karl, R., Müller, M., Jossen, A., and Hesse, H.: *Economics of Residential Photovoltaic Battery Systems in Germany: The Case of Tesla’s Powerwall*. In: *Batteries* 2.2 (2016), p. 14. DOI: [10.3390/batteries2020014](https://doi.org/10.3390/batteries2020014) (see pp. 12, 20).
- [80] Bundesnetzagentur: *EEG-Registerdaten und -Fördersätze*. Bonn, 2023. URL: https://www.bundesnetzagentur.de/DE/Fachthemen/ElektrizitaetundGas/ErneuerbareEnergien/ZahlenDatenInformationen/EEG_Registerdaten/start.html (see p. 12).
- [81] Bantle, C. and Schwencke, T.: *BDEW-Strompreisanalyse Juni 2023*. Ed. by Bundesverband der Energie- und Wasserwirtschaft e.V. Berlin, 07/24/2023 (see pp. 12, 13, 26).

- [82] Figgenger, J., Haberschusz, D., Kairies, K.-P., Wessels, O., Tepe, B., and Sauer, D. U.: *Wissenschaftliches Mess- und Evaluierungsprogramm Solarstromspeicher 2.0: Jahresbericht 2018*. In: (2018). DOI: [10.13140/RG.2.2.30057.19047](https://doi.org/10.13140/RG.2.2.30057.19047) (see p. 12).
- [83] Gorremans, J., Lits, C., Rossi, R., and Schmela, M.: *European Market Outlook for Residential Battery Storage 2022-2026*. Ed. by SolarPower Europe. 2022. URL: <https://www.solarpowereurope.org/insights/thematic-reports/european-market-outlook-for-residential-battery-storage-1> (visited on 10/02/2023) (see p. 12).
- [84] David, A.: *Residential Energy Storage: U.S. Manufacturing and Imports Grow Amid Rising Demand*. Ed. by U.S. International Trade Commission. 07/2021 (see p. 12).
- [85] Longson, M.: *Residential storage growth continues despite Covid-19 headwinds*. In: *pv magazine* 2021 (2021-02-18). URL: <https://www.pv-magazine.com/2021/02/18/residential-storage-growth-continues-despite-covid-19-headwinds/> (visited on 10/02/2023) (see p. 12).
- [86] Jansen, J.: *Energy Storage Service: Clean Technology & Renewables*. Ed. by IHS Markit. 2019. URL: <https://cdn.ihsmarkit.com/www/pdf/0620/IHSMarkit-Energy-Storage-Service-Jun2020.pdf> (visited on 10/02/2023) (see p. 12).
- [87] Schill, W.-P.: *Residual load, renewable surplus generation and storage requirements in Germany*. In: *Energy Policy* 73 (2014), pp. 65–79. ISSN: 03014215. DOI: [10.1016/j.enpol.2014.05.032](https://doi.org/10.1016/j.enpol.2014.05.032) (see p. 12).
- [88] Weniger, J., Tjaden, T., and Quaschnig, V.: *Sizing and grid integration of residential PV battery systems*. In: *8th International Renewable Energy Storage Conference and Exhibition (IRES 2013)*. Vol. 2013 (see pp. 12, 13).
- [89] Zeh, A. and Witzmann, R.: *Operational Strategies for Battery Storage Systems in Low-voltage Distribution Grids to Limit the Feed-in Power of Roof-mounted Solar Power Systems*. In: *Energy Procedia* 46 (2014), pp. 114–123. ISSN: 18766102. DOI: [10.1016/j.egypro.2014.01.164](https://doi.org/10.1016/j.egypro.2014.01.164) (see pp. 13, 20).
- [90] Li, J. and Danzer, M. A.: *Optimal charge control strategies for stationary photovoltaic battery systems*. In: *Journal of Power Sources* 258 (2014), pp. 365–373. ISSN: 03787753. DOI: [10.1016/j.jpowsour.2014.02.066](https://doi.org/10.1016/j.jpowsour.2014.02.066) (see p. 13).
- [91] Angenendt, G., Zurmühlen, S., Axelsen, H., and Sauer, D. U.: *Comparison of different operation strategies for PV battery home storage systems including forecast-based operation strategies*. In: *Applied Energy* 229 (2018), pp. 884–899. ISSN: 03062619. DOI: [10.1016/j.apenergy.2018.08.058](https://doi.org/10.1016/j.apenergy.2018.08.058) (see p. 13).
- [92] Azuatalam, D., Paridari, K., Ma, Y., Förstl, M., Chapman, A. C., and Verbič, G.: *Energy management of small-scale PV-battery systems: A systematic review considering practical implementation, computational requirements, quality of input data and battery degradation*. In: *Renewable and Sustainable Energy Reviews* 112 (2019), pp. 555–570. ISSN: 13640321. DOI: [10.1016/j.rser.2019.06.007](https://doi.org/10.1016/j.rser.2019.06.007) (see p. 13).
- [93] Paridari, K., Azuatalam, D., Chapman, A. C., Verbic, G., and Nordstrom, L.: “A plug-and-play home energy management algorithm using optimization and machine learning techniques.” In: *2018 IEEE International Conference on Communications, Control, and Computing Technologies for Smart Grids (SmartGridComm)*. IEEE, 2018, pp. 1–6. ISBN: 978-1-5386-7954-8. DOI: [10.1109/SmartGridComm.2018.8587418](https://doi.org/10.1109/SmartGridComm.2018.8587418) (see p. 13).

- [94] Haq, E. U., Lyu, C., Xie, P., Yan, S., Ahmad, F., and Jia, Y.: *Implementation of home energy management system based on reinforcement learning*. In: *Energy Reports* 8 (2022), pp. 560–566. ISSN: 23524847. DOI: [10.1016/j.egy.2021.11.170](https://doi.org/10.1016/j.egy.2021.11.170) (see p. 13).
- [95] German Federal Ministry of Justice: *Verordnung über die Entgelte für den Zugang zu Elektrizitätsversorgungsnetzen: Stromnetzentgeltverordnung StromNEV*. 2005-07-25. URL: <https://www.gesetze-im-internet.de/stromnev/StromNEV.pdf> (visited on 10/04/2023) (see p. 13).
- [96] Benetti, G., Caprino, D., Della Vedova, M. L., and Facchinetti, T.: *Electric load management approaches for peak load reduction: A systematic literature review and state of the art*. In: *Sustainable Cities and Society* 20 (2016), pp. 124–141. ISSN: 22106707. DOI: [10.1016/j.scs.2015.05.002](https://doi.org/10.1016/j.scs.2015.05.002) (see p. 13).
- [97] Mann, M., Babinex, S., and Putsche, V.: *Energy storage grand challenge: Energy storage market report*. Ed. by U.S. Department of Energy. 2020. URL: https://www.energy.gov/sites/prod/files/2020/12/f81/Energy%20Storage%20Market%20Report%202020_0.pdf (visited on 10/04/2023) (see p. 13).
- [98] Uddin, M., Romlie, M. F., Abdullah, M. F., Abd Halim, S., Abu Bakar, A. H., and Chia Kwang, T.: *A review on peak load shaving strategies*. In: *Renewable and Sustainable Energy Reviews* 82 (2018), pp. 3323–3332. ISSN: 13640321. DOI: [10.1016/j.rser.2017.10.056](https://doi.org/10.1016/j.rser.2017.10.056) (see p. 13).
- [99] Collath, N., Englberger, S., Jossen, A., and Hesse, H.: *Reduction of Battery Energy Storage Degradation in Peak Shaving Operation through Load Forecast Dependent Energy Management*. In: *NEIS 2020*. Ed. by D. Schulz. Berlin: VDE VERLAG, 2020. ISBN: 978-3-8007-5359-8 (see p. 13).
- [100] Martins, R., Hesse, H., Jungbauer, J., Vorbuchner, T., and Musilek, P.: *Optimal Component Sizing for Peak Shaving in Battery Energy Storage System for Industrial Applications*. In: *Energies* 11.8 (2018), p. 2048. DOI: [10.3390/en11082048](https://doi.org/10.3390/en11082048) (see p. 13).
- [101] European Network of Transmission System Operators for Electricity ENTSO-E: *ENTSO-E Network Code for Requirements for Grid Connection Applicable to all Generators*. 2013-03-08. URL: https://eepublicdownloads.entsoe.eu/clean-documents/pre2015/resources/RfG/130308_Final_Version_NC_RfG.pdf (visited on 10/05/2023) (see pp. 14, 26).
- [102] EU Commission Regulation: *establishing a guideline on electricity balancing*. 2017-11-23. URL: <https://eur-lex.europa.eu/legal-content/EN/TXT/PDF/?uri=CELEX:32017R2195> (visited on 10/05/2023) (see p. 14).
- [103] German Transmission Grid Operators: 50 Hertz, Amprion, Tennet, TransnetBW: *REGELLEISTUNG.NET: Platform for control energy*. URL: <https://www.regelleistung.net/en-us/> (visited on 10/05/2023) (see p. 14).
- [104] European Network of Transmission System Operators for Electricity ENTSO-E: *Electricity Balancing in Europe: An Overview of the European Balancing Market and Electricity Balancing Guideline*. 11/2018. URL: https://docstore.entsoe.eu/Documents/Network%20codes%20documents/NC%20EB/entso-e_balancing_in%20_europe_report_Nov2018_web.pdf (visited on 01/08/2024) (see p. 14).

- [105] Bundesnetzagentur für Elektrizität, Gas, Telekommunikation und Eisenbahnen: *Beschluss BK6-18-006*. 12/13/2018. URL: https://www.bundesnetzagentur.de/DE/Beschlusskammern/1_GZ/BK6-GZ/2018/BK6-18-006/beschluss_mit_anlagen.pdf?__blob=publicationFile&v=3 (visited on 11/07/2023) (see pp. 14, 27).
- [106] Bundesnetzagentur für Elektrizität, Gas, Telekommunikation und Eisenbahnen: *Beschluss BK6-10-097*. 04/12/2011. URL: https://www.bundesnetzagentur.de/DE/Beschlusskammern/1_GZ/BK6-GZ/_bis_2010/2010/BK6-10-097bis-099/BK6-10-097_Beschluss_2011_04_12.pdf?__blob=publicationFile&v=3 (visited on 11/07/2023) (see p. 14).
- [107] German Transmission Grid Operators: 50 Hertz, Amprion, Tennet, TransnetBW: *Präqualifizierte Leistung in Deutschland*. URL: [https://www.regelleistung.net/xspproxy/api/staticfiles/regelleistung/pq-leistungindeutschland\(stand01.01.2023\).pdf](https://www.regelleistung.net/xspproxy/api/staticfiles/regelleistung/pq-leistungindeutschland(stand01.01.2023).pdf) (visited on 10/05/2023) (see p. 14).
- [108] German Transmission Grid Operators: 50 Hertz, Amprion, Tennet, TransnetBW: *Prequalification Process for Balancing Service Providers (FCR, aFRR, mFRR) in Germany ("PQ conditions"): Version 1.04*. 06/03/2022 (see p. 14).
- [109] German Transmission Grid Operators: 50 Hertz, Amprion, Tennet, TransnetBW: *Eckpunkte und Freiheitsgrade bei Erbringung von Primärregelleistung*. 04/2014. URL: <https://docplayer.org/53075208-Eckpunkte-und-freiheitsgrade-bei-erbringung-von-primarregelleistung.html> (visited on 11/07/2023) (see p. 14).
- [110] Swierczynski, M., Stroe, D.-I., Stan, A.-I., Teodorescu, R., Laerke, R., and Kjaer, P. C.: "Field tests experience from 1.6MW/400kWh Li-ion battery energy storage system providing primary frequency regulation service." In: *IEEE PES ISGT Europe 2013*. IEEE, 06.10.2013 - 09.10.2013, pp. 1–5. ISBN: 978-1-4799-2984-9. DOI: [10.1109/ISGTEurope.2013.6695277](https://doi.org/10.1109/ISGTEurope.2013.6695277) (see p. 15).
- [111] Fler, J., Zurmühlen, S., Badeda, J., Stenzel, P., Hake, J.-F., and Sauer, D. U.: *Model-based Economic Assessment of Stationary Battery Systems Providing Primary Control Reserve*. In: *Energy Procedia* 99 (2016), pp. 11–24. ISSN: 18766102. DOI: [10.1016/j.egypro.2016.10.093](https://doi.org/10.1016/j.egypro.2016.10.093) (see p. 15).
- [112] Fler, J., Zurmühlen, S., Meyer, J., Badeda, J., Stenzel, P., Hake, J.-F., and Uwe Sauer, D.: *Price development and bidding strategies for battery energy storage systems on the primary control reserve market*. In: *Energy Procedia* 135 (2017), pp. 143–157. ISSN: 18766102. DOI: [10.1016/j.egypro.2017.09.497](https://doi.org/10.1016/j.egypro.2017.09.497) (see p. 15).
- [113] Cho, S.-M. and Yun, S.-Y.: *Optimal Power Assignment of Energy Storage Systems to Improve the Energy Storage Efficiency for Frequency Regulation*. In: *Energies* 10.12 (2017), p. 2092. DOI: [10.3390/en10122092](https://doi.org/10.3390/en10122092) (see p. 15).
- [114] Hollinger, R., Diazgranados, L. M., Braam, F., Erge, T., Bopp, G., and Engel, B.: *Distributed solar battery systems providing primary control reserve*. In: *IET Renewable Power Generation* 10.1 (2016), pp. 63–70. ISSN: 1752-1416. DOI: [10.1049/iet-rpg.2015.0147](https://doi.org/10.1049/iet-rpg.2015.0147) (see p. 15).
- [115] Filippa, A., Hashemi, S., and Traholt, C.: "Economic Evaluation of Frequency Reserve Provision using Battery Energy Storage." In: *2019 IEEE 2nd International Conference on Renewable Energy and Power Engineering (REPE)*. IEEE, 2019, pp. 160–165. ISBN: 978-1-7281-4562-4. DOI: [10.1109/REPE48501.2019.9025133](https://doi.org/10.1109/REPE48501.2019.9025133) (see p. 15).

- [116] Figgenger, J. et al.: *The development of stationary battery storage systems in Germany – A market review*. In: *Journal of Energy Storage* 29 (2020), p. 101153. ISSN: 2352152X. DOI: [10.1016/j.est.2019.101153](https://doi.org/10.1016/j.est.2019.101153) (see p. 15).
- [117] Figgenger, J., Stenzel, P., Kairies, K.-P., Linßen, J., Haberschusz, D., Wessels, O., Robinius, M., Stolten, D., and Sauer, D. U.: *The development of stationary battery storage systems in Germany – status 2020*. In: *Journal of Energy Storage* (2020), p. 101982. ISSN: 2352152X. DOI: [10.1016/j.est.2020.101982](https://doi.org/10.1016/j.est.2020.101982) (see p. 15).
- [118] Buttermann, H. G.: *Energieverbrauch in Deutschland im Jahr 2022: Energieverbrauch in Deutschland fällt auf niedrigsten Stand seit 1990*. Ed. by AG Energiebilanzen e.V. 03/06/2023. URL: https://ag-energiebilanzen.de/wp-content/uploads/2023/01/AGEB_Jahresbericht2022_20230413-02_dt-1.pdf (visited on 01/08/2024) (see p. 15).
- [119] Bradbury, K., Pratson, L., and Patiño-Echeverri, D.: *Economic viability of energy storage systems based on price arbitrage potential in real-time U.S. electricity markets*. In: *Applied Energy* 114 (2014), pp. 512–519. ISSN: 03062619. DOI: [10.1016/j.apenergy.2013.10.010](https://doi.org/10.1016/j.apenergy.2013.10.010) (see pp. 15, 16).
- [120] Krishnamurthy, D., Uckun, C., Zhou, Z., Thimmapuram, P. R., and Botterud, A.: *Energy Storage Arbitrage Under Day-Ahead and Real-Time Price Uncertainty*. In: *IEEE Transactions on Power Systems* 33.1 (2018), pp. 84–93. ISSN: 0885-8950. DOI: [10.1109/TPWRS.2017.2685347](https://doi.org/10.1109/TPWRS.2017.2685347) (see p. 16).
- [121] Guo, Y., Liu, W., Wen, F., Salam, A., Mao, J., and Li, L.: *Bidding Strategy for Aggregators of Electric Vehicles in Day-Ahead Electricity Markets*. In: *Energies* 10.1 (2017), p. 144. DOI: [10.3390/en10010144](https://doi.org/10.3390/en10010144) (see pp. 16, 27).
- [122] Metz, D. and Saraiva, J. T.: *Use of battery storage systems for price arbitrage operations in the 15- and 60-min German intraday markets*. In: *Electric Power Systems Research* 160 (2018), pp. 27–36. ISSN: 03787796. DOI: [10.1016/j.epsr.2018.01.020](https://doi.org/10.1016/j.epsr.2018.01.020) (see p. 16).
- [123] Wankmüller, F., Thimmapuram, P. R., Gallagher, K. G., and Botterud, A.: *Impact of battery degradation on energy arbitrage revenue of grid-level energy storage*. In: *Journal of Energy Storage* 10 (2017), pp. 56–66. ISSN: 2352152X. DOI: [10.1016/j.est.2016.12.004](https://doi.org/10.1016/j.est.2016.12.004) (see p. 16).
- [124] Collath, N., Cornejo, M., Engwerth, V., Hesse, H., and Jossen, A.: *Increasing the lifetime profitability of battery energy storage systems through aging aware operation*. In: *Applied Energy* 348 (2023), p. 121531. ISSN: 03062619. DOI: [10.1016/j.apenergy.2023.121531](https://doi.org/10.1016/j.apenergy.2023.121531) (see p. 16).
- [125] Núñez, F., Canca, D., and Arcos-Vargas, Á.: *An assessment of European electricity arbitrage using storage systems*. In: *Energy* 242 (2022), p. 122916. ISSN: 03605442. DOI: [10.1016/j.energy.2021.122916](https://doi.org/10.1016/j.energy.2021.122916) (see p. 16).
- [126] Mercier, T., Olivier, M., and Jaeger, E. de: *The value of electricity storage arbitrage on day-ahead markets across Europe*. In: *Energy Economics* 123 (2023), p. 106721. ISSN: 01409883. DOI: [10.1016/j.eneco.2023.106721](https://doi.org/10.1016/j.eneco.2023.106721) (see p. 16).
- [127] Lamp, S. and Samano, M.: *Large-scale battery storage, short-term market outcomes, and arbitrage*. In: *Energy Economics* 107 (2022), p. 105786. ISSN: 01409883. DOI: [10.1016/j.eneco.2021.105786](https://doi.org/10.1016/j.eneco.2021.105786) (see p. 16).
- [128] Ikechi Emmanuel, M. and Denholm, P.: *A market feedback framework for improved estimates of the arbitrage value of energy storage using price-taker models*. In: *Applied Energy* 310 (2022), p. 118250. ISSN: 03062619. DOI: [10.1016/j.apenergy.2021.118250](https://doi.org/10.1016/j.apenergy.2021.118250) (see p. 16).

- [129] Aamir, M., Ahmed Kalwar, K., and Mekhilef, S.: *Review: Uninterruptible Power Supply (UPS) system*. In: *Renewable and Sustainable Energy Reviews* 58 (2016), pp. 1395–1410. ISSN: 13640321. DOI: [10.1016/j.rser.2015.12.335](https://doi.org/10.1016/j.rser.2015.12.335) (see p. 16).
- [130] Khalid, M. and Savkin, A. V.: *A model predictive control approach to the problem of wind power smoothing with controlled battery storage*. In: *Renewable Energy* 35.7 (2010), pp. 1520–1526. ISSN: 09601481. DOI: [10.1016/j.renene.2009.11.030](https://doi.org/10.1016/j.renene.2009.11.030) (see p. 16).
- [131] Wang, X. Y., Mahinda Vilathgamuwa, D., and Choi, S. S.: *Determination of Battery Storage Capacity in Energy Buffer for Wind Farm*. In: *IEEE Transactions on Energy Conversion* 23.3 (2008), pp. 868–878. ISSN: 0885-8969. DOI: [10.1109/TEC.2008.921556](https://doi.org/10.1109/TEC.2008.921556) (see p. 16).
- [132] Bullich-Massagué, E., Cifuentes-García, F.-J., Glenney-Crende, I., Cheah-Mañé, M., Aragüés-Peñalba, M., Díaz-González, F., and Gomis-Bellmunt, O.: *A review of energy storage technologies for large scale photovoltaic power plants*. In: *Applied Energy* 274 (2020), p. 115213. ISSN: 03062619. DOI: [10.1016/j.apenergy.2020.115213](https://doi.org/10.1016/j.apenergy.2020.115213) (see p. 16).
- [133] Zhao, Y., Zhang, T., Sun, L., Zhao, X., Tong, L., Wang, L., Ding, J., and Ding, Y.: *Energy storage for black start services: A review*. In: *International Journal of Minerals, Metallurgy and Materials* 29.4 (2022), pp. 691–704. ISSN: 1674-4799. DOI: [10.1007/s12613-022-2445-0](https://doi.org/10.1007/s12613-022-2445-0) (see p. 16).
- [134] Ortega-Arriaga, P., Babacan, O., Nelson, J., and Gambhir, A.: *Grid versus off-grid electricity access options: A review on the economic and environmental impacts*. In: *Renewable and Sustainable Energy Reviews* 143 (2021), p. 110864. ISSN: 13640321. DOI: [10.1016/j.rser.2021.110864](https://doi.org/10.1016/j.rser.2021.110864) (see p. 16).
- [135] Veneri, O., Ferraro, L., Capasso, C., and Iannuzzi, D.: “Charging infrastructures for EV: Overview of technologies and issues.” In: *2012 Electrical Systems for Aircraft, Railway and Ship Propulsion*. IEEE, 2012, pp. 1–6. ISBN: 978-1-4673-1372-8. DOI: [10.1109/ESARS.2012.6387434](https://doi.org/10.1109/ESARS.2012.6387434) (see p. 16).
- [136] Rafi, M. A. H. and Bauman, J.: *A Comprehensive Review of DC Fast-Charging Stations With Energy Storage: Architectures, Power Converters, and Analysis*. In: *IEEE Transactions on Transportation Electrification* 7.2 (2021), pp. 345–368. DOI: [10.1109/TTE.2020.3015743](https://doi.org/10.1109/TTE.2020.3015743) (see p. 16).
- [137] Bowen, A., Engelhardt, J., Gabderakhmanova, T., Marinelli, M., and Rohde, G.: “Battery Buffered EV Fast Chargers on Bornholm: Charging Patterns and Grid Integration.” In: *2022 57th International Universities Power Engineering Conference (UPEC)*. IEEE, 2022, pp. 1–6. ISBN: 978-1-6654-5505-3. DOI: [10.1109/UPEC55022.2022.9917690](https://doi.org/10.1109/UPEC55022.2022.9917690) (see p. 16).
- [138] Stephan, A., Battke, B., Beuse, M. D., Clausdeinken, J. H., and Schmidt, T. S.: *Limiting the public cost of stationary battery deployment by combining applications*. In: *Nature Energy* 1.7 (2016), p. 334. DOI: [10.1038/nenergy.2016.79](https://doi.org/10.1038/nenergy.2016.79) (see p. 16).
- [139] Hauer, I., Balischewski, S., and Ziegler, C.: *Design and operation strategy for multi-use application of battery energy storage in wind farms*. In: *Journal of Energy Storage* 31 (2020), p. 101572. ISSN: 2352152X. DOI: [10.1016/j.est.2020.101572](https://doi.org/10.1016/j.est.2020.101572) (see p. 16).
- [140] Englberger, S., Jossen, A., and Hesse, H.: *Unlocking the Potential of Battery Storage with the Dynamic Stacking of Multiple Applications*. In: *Cell Reports Physical Science* 1.11 (2020), p. 100238. ISSN: 26663864. DOI: [10.1016/j.xcrp.2020.100238](https://doi.org/10.1016/j.xcrp.2020.100238) (see pp. 16, 17).

- [141] Englberger, S., Hesse, H., Hanselmann, N., and Jossen, A.: “SimSES Multi-Use: A simulation tool for multiple storage system applications.” In: *2019 16th International Conference on the European Energy Market (EEM)*. IEEE, 18.09.2019 - 20.09.2019, pp. 1–5. ISBN: 978-1-7281-1257-2. DOI: [10.1109/EEM.2019.8916568](https://doi.org/10.1109/EEM.2019.8916568) (see p. 16).
- [142] Fitzgerald, G., Mandel, J., Morris, J., and Touati, H.: *The economics of battery energy storage: How multi-use, customer-sited batteries deliver the most services and value to customers and the grid*. In: *Rocky Mountain Institute* (2015), p6 (see p. 17).
- [143] Truong, C. N., Schimpe, M., Bürger, U., Hesse, H. C., and Jossen, A.: *Multi-Use of Stationary Battery Storage Systems with Blockchain Based Markets*. In: *Energy Procedia* 155 (2018), pp. 3–16. ISSN: 18766102. DOI: [10.1016/j.egypro.2018.11.070](https://doi.org/10.1016/j.egypro.2018.11.070) (see p. 17).
- [144] Kraftfahrt-Bundesamt: *Der Fahrzeugbestand am 1. Januar 2023: Pressemitteilung Nr. 08/2023*. Flensburg, 2023-08. URL: https://www.kba.de/SharedDocs/Downloads/DE/Pressemitteilungen/DE/2023/pm_08_2023_bestand_01_23.pdf?__blob=publicationFile&v=7 (visited on 11/07/2023) (see p. 17).
- [145] Kraftfahrt-Bundesamt: *Entwicklung der Fahrleistungen nach Fahrzeugarten (engl. German Federal Motor Transport Authority - Development of mileage by vehicle type)*. URL: https://www.kba.de/DE/Statistik/Kraftverkehr/VerkehrKilometer/vk_inlaenderfahrleistung/2021/verkehr_in_kilometern_kurzbericht_pdf.pdf?__blob=publicationFile&v=2 (visited on 07/18/2023) (see p. 17).
- [146] Kraftfahrt-Bundesamt: *Der Fahrzeugbestand am 1. Januar 2018: Pressemitteilung Nr. 6/2018*. Flensburg, 2018-06. URL: https://www.kba.de/SharedDocs/Downloads/DE/Pressemitteilungen/DE/2018/pm_06_18_bestand_01_18_pdf.pdf?__blob=publicationFile&v=2 (visited on 10/17/2023) (see p. 17).
- [147] De Cauwer, C., Maarten, M., Heyvaert, S., Coosemans, T., and van Mierlo, J.: *Electric Vehicle Use and Energy Consumption Based on Realworld Electric Vehicle Fleet Trip and Charge Data and Its Impact on Existing EV Research Models*. In: *World Electric Vehicle Journal* 7.3 (2015), pp. 436–446. DOI: [10.3390/wevj7030436](https://doi.org/10.3390/wevj7030436) (see p. 18).
- [148] Chen, X., Li, K., Zhang, H., Yuan, Q., and Ye, Q.: “Identifying and Recognizing Usage Pattern of Electric Vehicles Using GPS and On-Board Diagnostics Data.” In: *International Conference on Transportation and Development 2020*. Ed. by G. Zhang. Reston, VA: American Society of Civil Engineers, 2020, pp. 85–97. ISBN: 9780784483138. DOI: [10.1061/9780784483138.008](https://doi.org/10.1061/9780784483138.008) (see p. 18).
- [149] Figgenger, J., Hecht, C., and Sauer, D. U.: *Battery Charts*. Ed. by RWTH Aachen University. Aachen, 2023. URL: <https://battery-charts.rwth-aachen.de/> (visited on 11/13/2023) (see p. 18).
- [150] Mao, S., Zhang, Y., Bieker, G., and Rodriguez, F.: *Zero-emission bus and truck market in China: A 2021 update*. Ed. by International Council on Clean Transportation. 2023. URL: <https://theicct.org/wp-content/uploads/2023/01/china-hvs-ze-bus-truck-market-2021-jan23.pdf> (see p. 19).
- [151] European Parliament and Council: *Directive 2013/53/EU of the European Parliament and of the Council of 20 November 2013 on recreational craft and personal watercraft and repealing Directive 94/25/EC*. In: *Official Journal of the European Union* 2013 (2013), pp. 90–131. URL: <https://eur-lex.europa.eu/legal-content/EN/TXT/?uri=CELEX%3A32013L0053> (visited on 01/08/2024) (see p. 19).

- [152] Kultanen, P.: *World's first autonomous on-demand boat in Helsinki, could turn water transport carbon-neutral*. Helsinki, 2023-09-28. URL: <https://forumvirium.fi/en/release/worlds-first-autonomous-on-demand-boat-in-helsinki-could-turn-water-transport-carbon-neutral/> (visited on 10/25/2023) (see p. 19).
- [153] Callboats, ed.: *Electric passenger boats*. URL: <https://callboats.com/> (visited on 10/25/2023) (see p. 19).
- [154] Torqeedo GmbH: *Electric mobility on the water 2023*. URL: https://media.torqeedo.com/catalogs/2023-torqeedo-catalog_EN_international.pdf (visited on 10/25/2023) (see p. 19).
- [155] Kolodziejcki, M. and Michalska-Pozoga, I.: *Battery Energy Storage Systems in Ships' Hybrid/Electric Propulsion Systems*. In: *Energies* 16.3 (2023), p. 1122. DOI: [10.3390/en16031122](https://doi.org/10.3390/en16031122) (see p. 19).
- [156] IRENA: *A pathway to decarbonise the shipping sector by 2050*. Ed. by International Renewable Energy Agency. Abu Dhabi, 2021. URL: https://www.irena.org/-/media/Files/IRENA/Agency/Publication/2021/Oct/IRENA_Decarbonising_Shipping_2021.pdf (visited on 10/25/2023) (see p. 19).
- [157] EMSA European Maritime Safety Agency, ed.: *Study on Electrical Energy Storage for Ships: Battery systems for maritime applications - technology, sustainability and safety*. 05/05/2020. URL: <https://www.emsa.europa.eu/publications/download/6186/3895/23.html> (visited on 10/25/2023) (see p. 19).
- [158] Bhardwaj, S. and Mostofi, H.: *Technical and Business Aspects of Battery Electric Trucks—A Systematic Review*. In: *Future Transportation* 2.2 (2022), pp. 382–401. DOI: [10.3390/futuretransp2020021](https://doi.org/10.3390/futuretransp2020021) (see pp. 19, 20).
- [159] International Energy Agency: *The Future of Rail: Opportunities for energy and the environment*. Ed. by International Energy Agency. Paris, 01/2019. URL: https://iea.blob.core.windows.net/assets/fb7dc9e4-d5ff-4a22-ac07-ef3ca73ac680/The_Future_of_Rail.pdf (visited on 10/26/2023) (see p. 20).
- [160] Pagenkopf, J., Schirmer, T., Boehm, M., Streuling, C., and Herwartz, S.: *Marktanalyse alternativer Antriebe im deutschen Schienenpersonennahverkehr*. 2020. URL: <https://elib.dlr.de/134615/> (see p. 20).
- [161] Reidinger, E.: *ÖBB and Siemens present battery-electric multiple unit*. In: *International Railway Journal* 2018 (2018-09-10). URL: <https://www.railjournal.com/rolling-stock/obb-and-siemens-present-battery-electric-multiple-unit/> (visited on 11/07/2023) (see p. 20).
- [162] Viswanathan, V., Epstein, A. H., Chiang, Y.-M., Takeuchi, E., Bradley, M., Langford, J., and Winter, M.: *The challenges and opportunities of battery-powered flight*. In: *Nature* 601.7894 (2022), pp. 519–525. DOI: [10.1038/s41586-021-04139-1](https://doi.org/10.1038/s41586-021-04139-1) (see p. 20).
- [163] Joshi, S.: *Growth Report: Drone Battery Market Worth \$2.45 Billion, Globally, by 2028 at 16.2% CAGR | The Insight Partners*. In: *GlobeNewswire* (2023-04-10). URL: <https://www.globenewswire.com/en/news-release/2023/04/10/2643523/0/en/Growth-Report-Drone-Battery-Market-Worth-2-45-Billion-Globally-by-2028-at-16-2-CAGR-The-Insight-Partners.html> (visited on 10/26/2023) (see p. 20).

- [164] Lineberger, R., Hussain, A., and Rutgers, V.: *Change is in the air: The elevated future of mobility: What's next on the horizon?* Ed. by Deloitte Insights. 2019. URL: <https://www2.deloitte.com/content/dam/Deloitte/us/Documents/energy-resources/di-the-elevated-future-of-mobility.pdf> (visited on 10/26/2023) (see p. 20).
- [165] Schwab, A., Thomas, A., Bennett Jesse, Robertson, E., and Cary, S.: *Electrification of aircraft: Challenges, barriers, and potential impacts*. Ed. by National Renewable Energy Lab.(NREL), Golden, CO. 2021. URL: <https://www.nrel.gov/docs/fy22osti/80220.pdf> (visited on 10/27/2023) (see p. 20).
- [166] Meier, H., Fünfgeld, C., Adam, T., and Schieferdecker, B.: *Repräsentative VDEW-Lastprofile*. Ed. by VDEW. Frankfurt (Main), 1999. URL: https://www.bdew.de/media/documents/1999_Repraesentative-VDEW-Lastprofile.pdf (visited on 01/08/2024) (see pp. 20, 31).
- [167] Anvari, M., Proedrou, E., Schäfer, B., Beck, C., Kantz, H., and Timme, M.: *Data-driven load profiles and the dynamics of residential electricity consumption*. In: *Nature communications* 13.1 (2022), p. 4593. DOI: [10.1038/s41467-022-31942-9](https://doi.org/10.1038/s41467-022-31942-9) (see p. 20).
- [168] Rascon, O. C., Schachler, B., Buhler, J., Resch, M., and Sumper, A.: “Increasing the hosting capacity of distribution grids by implementing residential PV storage systems and reactive power control.” In: *2016 13th International Conference on the European Energy Market (EEM)*. IEEE, 2016, pp. 1–5. ISBN: 978-1-5090-1298-5. DOI: [10.1109/EEM.2016.7521338](https://doi.org/10.1109/EEM.2016.7521338) (see p. 20).
- [169] Tjaden, T., Bergner, J., Weniger, J., and Quaschnig, V.: *Repräsentative elektrische Lastprofile für Wohngebäude in Deutschland auf 1-sekündiger Datenbasis: Datensatz, Hochschule für Technik und Wirtschaft HTW Berlin*. 2015. URL: <https://solar.htw-berlin.de/wp-content/uploads/HTW-Repraesentative-elektrische-Lastprofile-fuer-Wohngebaeude.pdf> (visited on 01/08/2024) (see p. 20).
- [170] Asare-Bediako, B., Kling, W. L., and Ribeiro, P. F.: *Future residential load profiles: Scenario-based analysis of high penetration of heavy loads and distributed generation*. In: *Energy and Buildings* 75 (2014), pp. 228–238. ISSN: 03787788. DOI: [10.1016/j.enbuild.2014.02.025](https://doi.org/10.1016/j.enbuild.2014.02.025) (see p. 20).
- [171] Naumann, M., Karl, R. C., Truong, C. N., Jossen, A., and Hesse, H. C.: *Lithium-ion Battery Cost Analysis in PV-household Application*. In: *Energy Procedia* 73 (2015), pp. 37–47. ISSN: 18766102. DOI: [10.1016/j.egypro.2015.07.555](https://doi.org/10.1016/j.egypro.2015.07.555) (see p. 20).
- [172] Price, P.: *Methods for Analyzing Electric Load Shape and its Variability*. Ed. by Lawrence Berkeley National Laboratory, Berkeley, CA. Lawrence Berkeley National Laboratory, California Energy Commission, 2010. DOI: [10.2172/985909](https://doi.org/10.2172/985909) (see p. 22).
- [173] Li, H., Wang, Z., Hong, T., Parker, A., and Neukomm, M.: *Characterizing patterns and variability of building electric load profiles in time and frequency domains*. In: *Applied Energy* (2021). ISSN: 03062619. DOI: [10.1016/j.apenergy.2021.116721](https://doi.org/10.1016/j.apenergy.2021.116721) (see p. 22).
- [174] Wang, Y., Chen, Q., Hong, T., and Kang, C.: *Review of Smart Meter Data Analytics: Applications, Methodologies, and Challenges*. In: *IEEE Transactions on Smart Grid* 10.3 (2019), pp. 3125–3148. ISSN: 1949-3053. DOI: [10.1109/TSG.2018.2818167](https://doi.org/10.1109/TSG.2018.2818167) (see p. 22).
- [175] Al-Otaibi, R., Jin, N., Wilcox, T., and Flach, P.: *Feature Construction and Calibration for Clustering Daily Load Curves from Smart-Meter Data*. In: *IEEE Transactions on Industrial Informatics* 12.2 (2016), pp. 645–654. ISSN: 1551-3203. DOI: [10.1109/TII.2016.2528819](https://doi.org/10.1109/TII.2016.2528819) (see p. 23).

- [176] Haben, S., Singleton, C., and Grindrod, P.: *Analysis and Clustering of Residential Customers Energy Behavioral Demand Using Smart Meter Data*. In: *IEEE Transactions on Smart Grid* 7.1 (2016), pp. 136–144. ISSN: 1949-3053. DOI: [10.1109/TSG.2015.2409786](https://doi.org/10.1109/TSG.2015.2409786) (see p. 23).
- [177] Park, J. Y., Yang, X., Miller, C., Arjunan, P., and Nagy, Z.: *Apples or oranges? Identification of fundamental load shape profiles for benchmarking buildings using a large and diverse dataset*. In: *Applied Energy* 236 (2019), pp. 1280–1295. ISSN: 03062619. DOI: [10.1016/j.apenergy.2018.12.025](https://doi.org/10.1016/j.apenergy.2018.12.025) (see p. 23).
- [178] Trotta, G.: *An empirical analysis of domestic electricity load profiles: Who consumes how much and when?* In: *Applied Energy* 275 (2020), p. 115399. ISSN: 03062619. DOI: [10.1016/j.apenergy.2020.115399](https://doi.org/10.1016/j.apenergy.2020.115399) (see p. 23).
- [179] Czétány, L., Vámos, V., Horváth, M., Szalay, Z., Mota-Babiloni, A., Deme-Bélafi, Z., and Csoknyai, T.: *Development of electricity consumption profiles of residential buildings based on smart meter data clustering*. In: *Energy and Buildings* 252 (2021), p. 111376. ISSN: 03787788. DOI: [10.1016/j.enbuild.2021.111376](https://doi.org/10.1016/j.enbuild.2021.111376) (see p. 23).
- [180] Grandjean, A., Adnot, J., and Binet, G.: *A review and an analysis of the residential electric load curve models*. In: *Renewable and Sustainable Energy Reviews* 16.9 (2012), pp. 6539–6565. ISSN: 13640321. DOI: [10.1016/j.rser.2012.08.013](https://doi.org/10.1016/j.rser.2012.08.013) (see p. 23).
- [181] Widén, J. and Wäckelgård, E.: *A high-resolution stochastic model of domestic activity patterns and electricity demand*. In: *Applied Energy* 87.6 (2010), pp. 1880–1892. ISSN: 03062619. DOI: [10.1016/j.apenergy.2009.11.006](https://doi.org/10.1016/j.apenergy.2009.11.006) (see p. 23).
- [182] Richardson, I., Thomson, M., Infield, D., and Clifford, C.: *Domestic electricity use: A high-resolution energy demand model*. In: *Energy and Buildings* 42.10 (2010), pp. 1878–1887. ISSN: 03787788. DOI: [10.1016/j.enbuild.2010.05.023](https://doi.org/10.1016/j.enbuild.2010.05.023) (see p. 23).
- [183] Müller, M., Biedenbach, F., and Reinhard, J.: *Development of an Integrated Simulation Model for Load and Mobility Profiles of Private Households*. In: *Energies* 13.15 (2020), p. 3843. DOI: [10.3390/en13153843](https://doi.org/10.3390/en13153843) (see p. 23).
- [184] Han, M., Johari, F., Huang, P., and Zhang, X.: *Generating hourly electricity demand data for large-scale single-family buildings by a decomposition-recombination method*. In: *Energy and Built Environment* (2022). ISSN: 26661233. DOI: [10.1016/j.enbenv.2022.02.011](https://doi.org/10.1016/j.enbenv.2022.02.011) (see p. 23).
- [185] Pinceti, A., Sankar, L., and Kosut, O.: “Synthetic Time-Series Load Data via Conditional Generative Adversarial Networks.” In: *2021 IEEE Power & Energy Society General Meeting (PESGM)*. IEEE, 2021, pp. 1–5. ISBN: 978-1-6654-0507-2. DOI: [10.1109/PESGM46819.2021.9637821](https://doi.org/10.1109/PESGM46819.2021.9637821) (see p. 23).
- [186] Efthymiou, C. and Kalogridis, G.: “Smart Grid Privacy via Anonymization of Smart Metering Data.” In: *2010 First IEEE International Conference on Smart Grid Communications*. IEEE, 2010, pp. 238–243. ISBN: 978-1-4244-6510-1. DOI: [10.1109/SMARTGRID.2010.5622050](https://doi.org/10.1109/SMARTGRID.2010.5622050) (see p. 23).
- [187] Pensa, R. G., Monreale, A., Pinelli, F., and Pedreschi, D.: *Pattern-preserving k-anonymization of sequences and its application to mobility data mining*. In: *International Workshop on Privacy in Location-Based Applications PiLBA’08*. Vol. 397. CEUR-WS.org, 2008, pp. 44–60. URL: https://iris.unito.it/retrieve/e27ce42b-432c-2581-e053-d805fe0acbaa/pilba2008_4aperto.pdf (see p. 23).

- [188] Machanavajjhala, A., Kifer, D., Gehrke, J., and Venkatasubramanian, M.: *L-diversity: Privacy beyond k-anonymity*. In: *ACM Transactions on Knowledge Discovery from Data* 1.1 (2007), p. 3. ISSN: 1556-4681. DOI: [10.1145/1217299.1217302](https://doi.org/10.1145/1217299.1217302) (see p. 23).
- [189] Savov, K.-K., Stoyanov, P., Stanev, R., and Stoilov, D.: “Analysis of errors in distribution networks power losses calculations with relation to the time discretization intervals.” In: *2017 15th International Conference on Electrical Machines, Drives and Power Systems (ELMA)*. IEEE, 2017, pp. 42–46. ISBN: 978-1-5090-6690-2. DOI: [10.1109/ELMA.2017.7955398](https://doi.org/10.1109/ELMA.2017.7955398) (see p. 23).
- [190] Ogasawara, E., Martinez, L. C., Oliveira, D. de, Zimbrao, G., Pap, G. L., and Mattoso, M.: “Adaptive Normalization: A novel data normalization approach for non-stationary time series.” In: *The 2010 International Joint Conference on Neural Networks (IJCNN)*. IEEE, 2010, pp. 1–8. ISBN: 978-1-4244-6916-1. DOI: [10.1109/IJCNN.2010.5596746](https://doi.org/10.1109/IJCNN.2010.5596746) (see p. 23).
- [191] Li, H., Yeo, J. H., Bornsheuer, A. L., and Overbye, T. J.: *The Creation and Validation of Load Time Series for Synthetic Electric Power Systems*. In: *IEEE Transactions on Power Systems* 36.2 (2021), pp. 961–969. ISSN: 0885-8950. DOI: [10.1109/TPWRS.2020.3018936](https://doi.org/10.1109/TPWRS.2020.3018936) (see p. 23).
- [192] Tepe, B.: *LoadPAT: Load Profile Anonymization Tool*. 2022. URL: <https://gitlab.lrz.de/open-ees-ses/loadpat> (visited on 01/08/2024) (see p. 23).
- [193] Hecht, C., Figgner, J., and Sauer, D. U.: *Vehicle-to-Grid Market Readiness in Europe with a Special Focus on Germany*. In: *Vehicles* 5.4 (2023), pp. 1452–1466. DOI: [10.3390/vehicles5040079](https://doi.org/10.3390/vehicles5040079) (see pp. 24, 26, 30).
- [194] Arnold, G. et al.: *Intelligente Netzanbindung von Elektrofahrzeugen zur Erbringung von Systemdienstleistungen—INEES*. In: *Wolfsburg, Hamburg, Niestetal, Kassel: Volkswagen AG, LichtBlick SE, SMA Technology AG, Fraunhofer IWES* (2015). URL: https://www.erneuerbar-mobil.de/sites/default/files/2016-09/INEES_Abschlussbericht.pdf (visited on 08/23/2023) (see pp. 24, 29).
- [195] Andersen, P. B., Toghroljerdi, S. H., Meier Sørensen, T., Christensen, B. E., Morell Lodberg Høj, Jens Christian, and Zecchino, A.: *The Parker Project: Final Report*. 01/31/2019. URL: https://parker-project.com/wp-content/uploads/2019/03/Parker_Final-report_v1.1_2019.pdf (visited on 11/07/2023) (see pp. 24, 29).
- [196] Element Energy Limited: *V2GB - Vehicle to Grid Britain*. United Kingdom, 07/2021. URL: <https://esc-production-2021.s3.eu-west-2.amazonaws.com/2021/07/V2GB-Public-Report.pdf> (visited on 11/03/2023) (see pp. 24, 29).
- [197] Müller, M., Kern, T., Ostermann, A., and Dossow, P.: *BDL - Bidirektionales Lademanagement - Abschlussbericht der FfE*. Ed. by Forschungsgesellschaft für Energiewirtschaft mbH. München, 03/20/2023. URL: <https://ffe.de/wp-content/uploads/2023/03/BDL-Abschlussbericht.pdf> (visited on 11/07/2023) (see pp. 24, 29).
- [198] DIN e.V.: *ISO 15118-20:2022 Road vehicles - Vehicle to grid communication interface: Part 20: 2nd generation network layer and application layer requirements*. 2022 (see p. 24).
- [199] Corchero, C. and Sanmarti, M.: “Vehicle- to- Everything (V2X): Benefits and Barriers.” In: *2018 15th International Conference on the European Energy Market (EEM)*. IEEE, 2018, pp. 1–4. ISBN: 978-1-5386-1488-4. DOI: [10.1109/EEM.2018.8469875](https://doi.org/10.1109/EEM.2018.8469875) (see pp. 24–26).

- [200] Englberger, S., Hesse, H., Kucevic, D., and Jossen, A.: *A Techno-Economic Analysis of Vehicle-to-Building: Battery Degradation and Efficiency Analysis in the Context of Coordinated Electric Vehicle Charging*. In: *Energies* 12.5 (2019), p. 955. DOI: [10.3390/en12050955](https://doi.org/10.3390/en12050955) (see p. 24).
- [201] Liu, C., Chau, K. T., Wu, D., and Gao, S.: *Opportunities and Challenges of Vehicle-to-Home, Vehicle-to-Vehicle, and Vehicle-to-Grid Technologies*. In: *Proceedings of the IEEE* 101.11 (2013), pp. 2409–2427. ISSN: 0018-9219. DOI: [10.1109/JPROC.2013.2271951](https://doi.org/10.1109/JPROC.2013.2271951) (see p. 25).
- [202] Sehim, Y., Almaksour, K., Suomalainen, E., and Robyns, B.: *Mitigating the impact of fast charging on distribution grids using vehicle-to-vehicle power transfer: A Paris city case study*. In: *IET Electrical Systems in Transportation* 13.1 (2023). ISSN: 2042-9738. DOI: [10.1049/els2.12051](https://doi.org/10.1049/els2.12051) (see p. 25).
- [203] Uddin, K., Dubarry, M., and Glick, M. B.: *The viability of vehicle-to-grid operations from a battery technology and policy perspective*. In: *Energy Policy* 113 (2018), pp. 342–347. ISSN: 03014215. DOI: [10.1016/j.enpol.2017.11.015](https://doi.org/10.1016/j.enpol.2017.11.015) (see p. 25).
- [204] Bundesnetzagentur für Elektrizität, Gas, Telekommunikation und Eisenbahnen: *Decision BK6-17-234*. 2019. URL: https://www.bundesnetzagentur.de/DE/Beschlusskammern/1_GZ/BK6-GZ/2017/BK6-17-234/BK6-17-234_beschluss_2019_05_02.pdf?__blob=publicationFile&v=2 (visited on 11/07/2023) (see p. 26).
- [205] Kern, T., Dossow, P., and Roon, S. von: *Integrating Bidirectionally Chargeable Electric Vehicles into the Electricity Markets*. In: *Energies* 13.21 (2020), p. 5812. DOI: [10.3390/en13215812](https://doi.org/10.3390/en13215812) (see p. 26).
- [206] European Union Agency for the Cooperation of Energy Regulators: *Annual Report on the Results of Monitoring the Internal Electricity and Natural Gas Markets in 2021: Energy Retail and Consumer Protection Volume*. 10/2022. URL: https://www.acer.europa.eu/Publications/MMR_2021_Energy_Retail_Consumer_Protection_Volume.pdf (visited on 11/02/2023) (see p. 26).
- [207] Bundestag: *Gesetz zum Neustart der Digitalisierung der Energiewende*. 2023-05-22. URL: <https://www.recht.bund.de/bgb1/1/2023/133/V0.html> (visited on 11/02/2023) (see p. 26).
- [208] Bessa, R. J. and Matos, M. A.: “The role of an aggregator agent for EV in the electricity market.” In: *7th Mediterranean Conference and Exhibition on Power Generation, Transmission, Distribution and Energy Conversion (MedPower 2010)*. IET, 7-10 Nov. 2010, p. 126. ISBN: 978 1 84919 319 1. DOI: [10.1049/cp.2010.0866](https://doi.org/10.1049/cp.2010.0866) (see p. 27).
- [209] Sovacool, B. K., Kester, J., Noel, L., and Zarazua de Rubens, G.: *Actors, business models, and innovation activity systems for vehicle-to-grid (V2G) technology: A comprehensive review*. In: *Renewable and Sustainable Energy Reviews* 131 (2020), p. 109963. ISSN: 13640321. DOI: [10.1016/j.rser.2020.109963](https://doi.org/10.1016/j.rser.2020.109963) (see p. 27).
- [210] Bessa, R. J., Matos, M. A., Soares, F. J., and Lopes, J. A. P.: *Optimized Bidding of a EV Aggregation Agent in the Electricity Market*. In: *IEEE Transactions on Smart Grid* 3.1 (2012), pp. 443–452. ISSN: 1949-3053. DOI: [10.1109/TSG.2011.2159632](https://doi.org/10.1109/TSG.2011.2159632) (see p. 27).
- [211] Schuller, A., Dietz, B., Flath, C. M., and Weinhardt, C.: *Charging Strategies for Battery Electric Vehicles: Economic Benchmark and V2G Potential*. In: *IEEE Transactions on Power Systems* 29.5 (2014), pp. 2014–2022. ISSN: 0885-8950. DOI: [10.1109/TPWRS.2014.2301024](https://doi.org/10.1109/TPWRS.2014.2301024) (see p. 27).

- [212] Giordano, F., Arrigo, F., Diaz-Londono, C., Spertino, F., and Ruiz, F.: “Forecast-Based V2G Aggregation Model for Day-Ahead and Real-Time Operations.” In: *2020 IEEE Power & Energy Society Innovative Smart Grid Technologies Conference (ISGT)*. IEEE, 17.02.2020 - 20.02.2020, pp. 1–5. ISBN: 978-1-7281-3103-0. DOI: [10.1109/ISGT45199.2020.9087659](https://doi.org/10.1109/ISGT45199.2020.9087659) (see p. 27).
- [213] Zheng, Y., Yu, H., Shao, Z., and Jian, L.: *Day-ahead bidding strategy for electric vehicle aggregator enabling multiple agent modes in uncertain electricity markets*. In: *Applied Energy* 280 (2020), p. 115977. ISSN: 03062619. DOI: [10.1016/j.apenergy.2020.115977](https://doi.org/10.1016/j.apenergy.2020.115977) (see p. 27).
- [214] Zhang, H., Liu, Y., Li, J., Yu, H., Xu, H., Ma, K., Liang, Y., An, X., and Hu, X.: *Influence Factors of the V2G Economic Benefits of Pure Electric Logistics Vehicles: A Case Study in Chengdu*. In: *International Journal of Automotive Technology* 24.5 (2023), pp. 1411–1422. ISSN: 1229-9138. DOI: [10.1007/s12239-023-0114-6](https://doi.org/10.1007/s12239-023-0114-6) (see p. 27).
- [215] Bessa, R. J. and Matos, M. A.: *Economic and technical management of an aggregation agent for electric vehicles: a literature survey*. In: *European Transactions on Electrical Power* 22.3 (2012), pp. 334–350. ISSN: 1430144X. DOI: [10.1002/etep.565](https://doi.org/10.1002/etep.565) (see p. 27).
- [216] The MathWorks, I., ed.: *MATLAB® Global Optimization Toolbox: User’s Guide*. 2020 (see p. 27).
- [217] Kramer, O.: *Genetic Algorithm Essentials*. Vol. 679. Cham: Springer International Publishing, 2017. ISBN: 978-3-319-52155-8. DOI: [10.1007/978-3-319-52156-5](https://doi.org/10.1007/978-3-319-52156-5) (see p. 27).
- [218] Kempton, W. and Tomić, J.: *Vehicle-to-grid power fundamentals: Calculating capacity and net revenue*. In: *Journal of Power Sources* 144.1 (2005), pp. 268–279. ISSN: 03787753. DOI: [10.1016/j.jpowsour.2004.12.025](https://doi.org/10.1016/j.jpowsour.2004.12.025) (see p. 28).
- [219] Bañol Arias, N., Hashemi, S., Andersen, P. B., Træholt, C., and Romero, R.: *Assessment of economic benefits for EV owners participating in the primary frequency regulation markets*. In: *International Journal of Electrical Power & Energy Systems* 120 (2020), p. 105985. ISSN: 01420615. DOI: [10.1016/j.ijepes.2020.105985](https://doi.org/10.1016/j.ijepes.2020.105985) (see p. 28).
- [220] Doumen, S. and Paterakis, N. G.: “Economic Viability of Smart Charging EVs in the Dutch Ancillary Service Markets.” In: *2019 International Conference on Smart Energy Systems and Technologies (SEST)*. IEEE, 2019, pp. 1–6. ISBN: 978-1-7281-1156-8. DOI: [10.1109/SEST.2019.8849122](https://doi.org/10.1109/SEST.2019.8849122) (see p. 28).
- [221] Kempton, W., Tomic, J., Letendre, S., Brooks, A., and Lipman, T.: *Vehicle-to-grid power: battery, hybrid, and fuel cell vehicles as resources for distributed electric power in California*. In: (2001) (see p. 29).
- [222] Brooks, A. N.: *Vehicle-to-grid demonstration project: Grid regulation ancillary service with a battery electric vehicle*. California Air Resources Board and California Environmental Protection Agency, 2002. URL: https://heritageproject.caltech.edu/documents/21133/Carb_V2G_project_final_report_emlP1Xu.pdf (visited on 01/08/2024) (see p. 29).
- [223] Degner, T., Arnold, G., Brandl, R., Dollichon, J., and Scheidler, A.: *Grid Impact of Electric Vehicles with Secondary Control Reserve Capability*. In: *Proceeding of the 1st E-Mobility Power System Integration Symposium*. URL: https://mobilityintegrationsymposium.org/wp-content/uploads/sites/7/2017/11/3A_4_EMob17_298_paper_Thomas_Degner.pdf (visited on 04/17/2020) (see p. 29).

- [224] Black, D., MacDonald, J. S., DeForest, N., and Gehbauer, C.: *Los Angeles Air Force Base Vehicle-To-Grid Demonstration: Final Project Report*. Ed. by California Energy Commission. 2017. URL: <https://ww2.energy.ca.gov/2018publications/CEC-500-2018-025/CEC-500-2018-025.pdf> (visited on 04/16/2020) (see p. 29).
- [225] Marinelli, M., Martinenas, S., Knezović, K., and Andersen, P. B.: *Validating a centralized approach to primary frequency control with series-produced electric vehicles*. In: *Journal of Energy Storage* 7 (2016), pp. 63–73. ISSN: 2352152X. DOI: [10.1016/j.est.2016.05.008](https://doi.org/10.1016/j.est.2016.05.008) (see p. 29).
- [226] Randall, C.: *Renault rolling-out V2G trials across Europe*. Ed. by electrive.com. 2019-03-24. URL: <https://www.electrive.com/2019/03/24/renault-kicks-off-v2g-projects-in-utrecht-porto-santos/> (visited on 11/07/2023) (see p. 29).
- [227] Aengenvoort, J.: *Next Kraftwerke and Jedlix launch initiative to use electric car batteries for grid stability*. Ed. by Next Kraftwerke GmbH. 2018-09-10. URL: <https://www.next-kraftwerke.com/news/next-kraftwerke-jedlix-launch-initiative-to-use-electric-car-batteries-for-grid-stability> (visited on 11/07/2023) (see p. 29).
- [228] Colthorpe, A.: *Renault EVs in Europe go vehicle-to-grid with The Mobility House’s technology platform*. In: *Energy Storage News* (2023-06-14). URL: <https://www.energy-storage.news/renault-evs-in-europe-go-vehicle-to-grid-with-the-mobility-houses-technology-platform/> (visited on 11/03/2023) (see p. 30).
- [229] Manzolli, J. A., Trovão, J. P., and Antunes, C. H.: *A review of electric bus vehicles research topics – Methods and trends*. In: *Renewable and Sustainable Energy Reviews* 159 (2022), p. 112211. ISSN: 13640321. DOI: [10.1016/j.rser.2022.112211](https://doi.org/10.1016/j.rser.2022.112211) (see p. 30).
- [230] Verbrugge, B., Hasan, M. M., Rasool, H., Geury, T., El Baghdadi, M., and Hegazy, O.: *Smart Integration of Electric Buses in Cities: A Technological Review*. In: *Sustainability* 13.21 (2021), p. 12189. DOI: [10.3390/su132112189](https://doi.org/10.3390/su132112189) (see p. 30).
- [231] Noel, L. and McCormack, R.: *A cost benefit analysis of a V2G-capable electric school bus compared to a traditional diesel school bus*. In: *Applied Energy* 126 (2014), pp. 246–255. ISSN: 03062619. DOI: [10.1016/j.apenergy.2014.04.009](https://doi.org/10.1016/j.apenergy.2014.04.009) (see p. 30).
- [232] Manzolli, J. A., Trovão, J. P. F., and Henggeler Antunes, C.: *Electric bus coordinated charging strategy considering V2G and battery degradation*. In: *Energy* 254 (2022), p. 124252. ISSN: 03605442. DOI: [10.1016/j.energy.2022.124252](https://doi.org/10.1016/j.energy.2022.124252) (see p. 30).
- [233] Fei, F., Sun, W., Iacobucci, R., and Schmöcker, J.-D.: *Exploring the profitability of using electric bus fleets for transport and power grid services*. In: *Transportation Research Part C: Emerging Technologies* 149 (2023), p. 104060. ISSN: 0968090X. DOI: [10.1016/j.trc.2023.104060](https://doi.org/10.1016/j.trc.2023.104060) (see p. 30).
- [234] Los Rios, A. de, Goentzel, J., Nordstrom, K. E., and Siegert, C. W.: “Economic analysis of vehicle-to-grid (V2G)-enabled fleets participating in the regulation service market.” In: *2012 IEEE PES Innovative Smart Grid Technologies (ISGT)*. IEEE, 16.01.2012 - 20.01.2012, pp. 1–8. ISBN: 978-1-4577-2159-5. DOI: [10.1109/ISGT.2012.6175658](https://doi.org/10.1109/ISGT.2012.6175658) (see p. 30).
- [235] Zhao, Y., Noori, M., and Tatari, O.: *Vehicle to Grid regulation services of electric delivery trucks: Economic and environmental benefit analysis*. In: *Applied Energy* 170 (2016), pp. 161–175. ISSN: 03062619. DOI: [10.1016/j.apenergy.2016.02.097](https://doi.org/10.1016/j.apenergy.2016.02.097) (see p. 30).

-
- [236] Mahmud, K., Rahman, M. S., Ravishankar, J., Hossain, M. J., and Guerrero, J. M.: *Real-Time Load and Ancillary Support for a Remote Island Power System Using Electric Boats*. In: *IEEE Transactions on Industrial Informatics* 16.3 (2020), pp. 1516–1528. ISSN: 1551-3203. DOI: [10.1109/TII.2019.2926511](https://doi.org/10.1109/TII.2019.2926511) (see p. 30).
- [237] Pintér, G., Vincze, A., Baranyai, N. H., and Zsiborács, H.: *Boat-to-Grid Electrical Energy Storage Potentials around the Largest Lake in Central Europe*. In: *Applied Sciences* 11.16 (2021), p. 7178. DOI: [10.3390/app11167178](https://doi.org/10.3390/app11167178) (see p. 30).
- [238] Jozwiak, D., Pillai, J. R., Ponnaganti, P., Bak-Jensen, B., and Jantzen, J.: *Optimal Charging and Discharging Strategies for Electric Cars in PV-BESS-Based Marina Energy Systems*. In: *Electronics* 12.4 (2023), p. 1033. DOI: [10.3390/electronics12041033](https://doi.org/10.3390/electronics12041033) (see p. 30).
- [239] Tutuianu, M., Bonnel, P., Ciuffo, B., Haniu, T., Ichikawa, N., Marotta, A., Pavlovic, J., and Steven, H.: *Development of the World-wide harmonized Light duty Test Cycle (WLTC) and a possible pathway for its introduction in the European legislation*. In: *Transportation Research Part D: Transport and Environment* 40 (2015), pp. 61–75. ISSN: 13619209. DOI: [10.1016/j.trd.2015.07.011](https://doi.org/10.1016/j.trd.2015.07.011) (see p. 31).

Supervised Student Theses

- a Müller, F.: *Real data analysis of large-scale storage systems (German: Realdatenanalyse von Großspeichern)*, Research Seminar, 2019
- b Niemöller, J.: *Positioning and dimensioning of stationary battery storage systems in distribution grids (German: Positionierung und Dimensionierung stationärer Batteriespeicher in Verteilnetzen)*, Bachelor's Thesis, 2019
- c Moskvina, N.: *Comparison and analysis of energy system simulation models with renewables and storage (German: Vergleich und Analyse von Energiesystem-Simulationsmodellen mit erneuerbaren Energien und Speichern)*, Advanced Seminar, 2019
- d Widmann, D.: *Potentials of Battery Storage as Buffer Storage for Electric Car Fast Charging Stations (German: Potentiale von Batteriespeichern als Pufferspeicher für Elektroauto-Schnellladestationen)*, Advanced Seminar, 2020
- e Schiefer, L.: *Analysis of potential markets for the secondary usage of virtual power plant storage systems (German: Analyse potentieller Märkte für die Sekundäranwendung von Speichern virtueller Kraftwerke)*, Research Seminar, 2020
- f Müller, F.: *Data-based determination of real cell and inverter parameters for the simulation of existing storage systems (German: Datenbasierte Bestimmung realer Zell- und Wechselrichterparameter zur Simulation von bestehenden Speichersystemen)*, Master's Thesis, 2020
- g Düsdieler, M.: *Pool composition of electric cars and home storage systems (German: Poolkomposition von Elektroautos und Heimspeichern)*, Advanced Seminar, 2020
- h Yoo, J.: *Evaluation Of Operating Strategies To Reduce Aging Of Battery Storage Systems In Microgrids (German: Analyse der Betriebsweise von Pufferspeichern an Schnellladesäulen für Elektrofahrzeuge)*, Research Seminar, 2021
- i Ziegler, M.: *Analysis and interface implementation of energy system simulation models (German: Analyse und Schnittstellenimplementierung von Energiesystem-Simulationsmodellen)*, Bachelor's Thesis, 2021
- j Precht, H.: *Analysis of the operating mode of buffer storage units at fast charging stations for electric vehicles (German: Bewertung von Betriebsstrategien zur Reduzierung der Alterung von Batteriespeichersystemen in Microgrids)*, Research Seminar, 2021
- k Pfohl, J.: *Methods of electric vehicle pool formation for participation in electricity markets (German: Methoden der Formation von Elektrofahrzeugpools zur Teilnahme an Elektrizitätsmärkten)*, Advanced Seminar, 2021
- l Röhrer, F.: *Vehicle-to-grid: Charging strategies and Degradation (German: Vehicle-to-grid: Ladestrategien und Alterung)*, Advanced Seminar, 2022
- m Zoghbi, M.: *Analysis of the life expectancy of batteries in e-buses through the use of real driving and charging profiles using the example of the Hamburger Hochbahn AG (German: Analyse der Lebenserwartung von Batterien in E-Bussen durch den Einsatz realer Fahr- und Ladeprofile am Beispiel der Hamburger Hochbahn AG)*, Research Seminar, 2022
- n Morell Vázquez, A.: *Methods of anonymization of load profiles*, Advanced Seminar, 2022
- o Krogmann, C.: *Concept Evaluation, Prototype Development and Verification of a Modular Battery Storage System for a Launch Vehicle*, Master's Thesis, 2022

- p Acevedo, O.: *Data analysis of real load profiles and design of an aging study for silicon-based LIBs (German: Datenanalyse realer Lastprofile und Aufbau einer Alterungsstudie für siliziumbasierten LIBs)*, Research Seminar, 2022
- q Matthä, A.: *Simulation of vehicle-to-grid (V2G) provision and the impact on the aging behavior of electric car batteries (German: Simulation von Vehicle-to-grid (V2G) - Erbringung und die Auswirkungen auf das Alterungsverhalten von Elektroautobatterien)*, Bachelor's Thesis, 2023
- r Reichenberger, S.: *Load on battery storage systems in mobile and stationary applications (German: Belastung von Batteriespeichern in mobilen und stationären Anwendungen)*, Advanced Seminar, 2022
- s Sampath Kumar, C.: *Feasibility in the Solution Space of the Aggregation and Disaggregation of Home Storage Systems*, Master's Thesis, 2023
- t Narayana, S.: *Implementation of a vehicle-to-grid charging strategy for a regional fleet of electric vehicles into an agent-based eMobility simulation*, Master's Thesis, 2023

Acknowledgment

This thesis originates from my time as a research associate at the Chair for Electrical Energy Storage Technology (EES) at the Technical University of Munich. A large number of people contributed to the successful completion of the thesis. First of all, I would like to thank Professor Jossen for giving me the opportunity to do my doctorate in this fascinating field. Without his support and expertise, this work would not have been possible. The second person who deserves the greatest thanks is the former team lead of our team Stationary Energy Storage Systems Holger Hesse, who in the meantime has become a professor at the University of Applied Sciences in Kempten. Thank you for all the discussions and your professional input on the research publications in this thesis.

In addition, I would like to thank all current and former team members and colleagues at the chair. I would especially like to thank my former team colleagues Daniel Kucevic and Stefan Englberger for the professional discussions and the development of exciting research papers. Through your experiences, attitudes and opinions, I have learned a lot, not only professionally but also interculturally. Interculturally, I also learned a lot from Anupam Parlikar; not only about life cycle analysis and carbon dioxide emissions, but also about India and cricket. Thanks also go to the current team lead, Nils Collath, who successfully kept our team together after several departures of graduating colleagues and acquired a large number of new projects. As a result of these new projects, our team has been able to grow again and new employees have joined us. I wish you every success with your promotion and thank you for all your input and critical questions.

Outside the team, I would especially like to thank Philipp Jocher for all the interdisciplinary talks and discussions. I would also like to thank all other members of the Chair, especially Carolin Nierwetberg, for their support with all organizational questions and uncertainties. I also particularly enjoyed supervising student theses. Thank you to all the students I was able to accompany on their way to their Bachelor's or Master's degree. You taught me how much I enjoy teaching.

Moreover, I would like to thank all the project partners in the openBEA and SimBAS research projects. Thank you for the great cooperation and the many exchanges. I would like to emphasize the ISEA of RWTH Aachen University, with whom I have always maintained contact and with whom some joint research papers have been carried out. Jan Figgenger deserves special mention here, with whom many professional and personal exchanges led to the results of this thesis. I would also like to thank the many industrial partners whose experience, opinions and data have been incorporated into this work.

Ultimately, the biggest thanks go to my family and friends who have supported me all these years. It was my parents who made this thesis possible for me in the first place through my school and university education. I would also like to thank the Murmelis, who accompanied me for a large part of my doctoral studies and thanks to whom it was possible to have both personal and scientific discussions over dinner or on hikes together. I would like to thank my girlfriend Heike from the bottom of my heart for her support, guidance and understanding during my doctoral studies. Especially since our daughter Lena was born, this dissertation would not have been completed without your help. I dedicate this thesis to both of you.